TRANSCRIPTION REGULATION - BRAIN DEVELOPMENT AND HOMEOSTASIS - A FINELY TUNED AND ORCHESTRATED SCENARIO IN PHYSIOLOGY AND PATHOLOGY

EDITED BY: Estela Maris Muñoz, Veronica Martinez Cerdeño, Flavio S. J. De Souza and Martin Fredensborg Rath

PUBLISHED IN: Frontiers in Molecular Neuroscience

frontiers Research Topics

frontiers

ISSN 1664-8714
ISBN 978-2-88974-457-2
DOI 10.3389/978-2-88974-457-2

About Frontiers

Frontiers is more than just an open-access publisher of scholarly articles: it is a pioneering approach to the world of academia, radically improving the way scholarly research is managed. The grand vision of Frontiers is a world where all people have an equal opportunity to seek, share and generate knowledge. Frontiers provides immediate and permanent online open access to all its publications, but this alone is not enough to realize our grand goals.

Frontiers Journal Series

The Frontiers Journal Series is a multi-tier and interdisciplinary set of open-access, online journals, promising a paradigm shift from the current review, selection and dissemination processes in academic publishing. All Frontiers journals are driven by researchers for researchers; therefore, they constitute a service to the scholarly community. At the same time, the Frontiers Journal Series operates on a revolutionary invention, the tiered publishing system, initially addressing specific communities of scholars, and gradually climbing up to broader public understanding, thus serving the interests of the lay society, too.

Dedication to Quality

Each Frontiers article is a landmark of the highest quality, thanks to genuinely collaborative interactions between authors and review editors, who include some of the world's best academicians. Research must be certified by peers before entering a stream of knowledge that may eventually reach the public - and shape society; therefore, Frontiers only applies the most rigorous and unbiased reviews.
Frontiers revolutionizes research publishing by freely delivering the most outstanding research, evaluated with no bias from both the academic and social point of view. By applying the most advanced information technologies, Frontiers is catapulting scholarly publishing into a new generation.

What are Frontiers Research Topics?

Frontiers Research Topics are very popular trademarks of the Frontiers Journals Series: they are collections of at least ten articles, all centered on a particular subject. With their unique mix of varied contributions from Original Research to Review Articles, Frontiers Research Topics unify the most influential researchers, the latest key findings and historical advances in a hot research area! Find out more on how to host your own Frontiers Research Topic or contribute to one as an author by contacting the Frontiers Editorial Office: frontiersin.org/about/contact

TRANSCRIPTION REGULATION - BRAIN DEVELOPMENT AND HOMEOSTASIS - A FINELY TUNED AND ORCHESTRATED SCENARIO IN PHYSIOLOGY AND PATHOLOGY

Topic Editors:
Estela Maris Muñoz, CONICET Dr. Mario H. Burgos Institute of Histology and Embryology (IHEM), Argentina
Veronica Martinez Cerdeño, University of California, United States
Flavio S. J. De Souza, CONICET Institute of Physiology, Molecular Biology and Neurosciences (IFIBYNE), Argentina
Martin Fredensborg Rath, University of Copenhagen, Denmark

Citation: Muñoz, E. M., Cerdeño, V. M., De Souza, F. S. J., Rath, M. F., eds. (2022). Transcription Regulation - Brain Development and Homeostasis - A Finely Tuned and Orchestrated Scenario in Physiology and Pathology.
Lausanne: Frontiers Media SA. doi: 10.3389/978-2-88974-457-2

Table of Contents

frontiers in Molecular Neuroscience

EDITORIAL
published: 14 January 2022
doi: 10.3389/fnmol.2021.834607

Editorial: Transcription Regulation—Brain Development and Homeostasis—A Finely Tuned and Orchestrated Scenario in Physiology and Pathology

Estela M. Muñoz[1], Flavio S. J. de Souza[2], Martin F. Rath[3] and Verónica Martínez Cerdeño[4]*

[1] Institute of Histology and Embryology of Mendoza (IHEM), National University of Cuyo (UNCuyo), National Scientific and Technical Research Council (CONICET), Mendoza, Argentina, [2] Institute of Physiology, Molecular Biology and Neurosciences (IFIBYNE), National Scientific and Technical Research Council (CONICET) and Department of Physiology, Molecular and Cellular Biology, Faculty of Exact and Natural Sciences, University of Buenos Aires (FBMC-FCEN-UBA), Buenos Aires, Argentina, [3] Department of Neuroscience, Faculty of Health and Medical Sciences, University of Copenhagen, Copenhagen, Denmark, [4] Department of Pathology and Laboratory Medicine, UC Davis School of Medicine, Institute for Pediatric Regenerative Medicine, Shriners Hospitals for Children of Northern California, and MIND Institute at the UC Davis Medical Center, Sacramento, CA, United States

Keywords: brain, transcription, transcription factor, neurogenesis, development, neurodevelopmental disorders, neurodegenerative diseases

OPEN ACCESS

Edited and reviewed by:
Clive R. Bramham,
University of Bergen, Norway

****Correspondence:***
Estela M. Muñoz
munoz.estela@fcm.uncu.edu.ar;
emunoz@mendoza-conicet.gob.ar

Specialty section:
This article was submitted to Neuroplasticity and Development, a section of the journal Frontiers in Molecular Neuroscience

Received: *13 December 2021*
Accepted: *22 December 2021*
Published: *14 January 2022*

Citation:
Muñoz EM, de Souza FSJ, Rath MF and Martínez Cerdeño V (2022) Editorial: Transcription Regulation—Brain Development and Homeostasis—A Finely Tuned and Orchestrated Scenario in Physiology and Pathology. Front. Mol. Neurosci. 14:834607. doi: 10.3389/fnmol.2021.834607

Editorial on the Research Topic

Transcription Regulation—Brain Development and Homeostasis—A Finely Tuned and Orchestrated Scenario in Physiology and Pathology

A finely tuned regulation of gene expression is essential for shaping the nervous system and for maintaining its homeostasis throughout life. Disruptions in gene regulation can impact brain development and physiology in ways that contribute to diverse pathologies. Classic and state-of-the art experimental models and technologies have advanced our knowledge of transcriptional regulators and the ways they interact in the healthy and diseased brain. Further in-depth characterization of the mechanisms of transcriptional regulation is needed to better understand how each element, from genes to cells, defines and maintains identities and functionalities in the nervous system. This Research Topic focuses on transcriptional regulation within the nervous system, with an emphasis on developmental and homeostatic processes, their dysregulation, and their association with neurodevelopmental disorders and neurodegenerative diseases. Eleven peer-reviewed manuscripts including six original articles, three reviews, one mini review, and one brief research report, encompass this special volume. Fifty-nine authors from research laboratories located in 10 countries: Argentina, Canada, China, Germany, Israel, Russia, Serbia, United Kingdom, United States, and Vietnam, took part in this initiative.

Among the interesting contributions, Oproescu et al. beautifully reviewed the regulatory intricacies of the proneuronal basic-helix-loop-helix (bHLH) transcription factors (TFs) in the cell quiescence-to-proliferation-to-differentiation continuum within the murine cerebral cortex, drawing parallels with other organisms and neural tissues. The authors discuss diverse mechanisms that govern bHLH TF expression, stability, localization, and consequent transactivation of downstream target genes, in a temporally defined and context-dependent manner. The authors conclude that further in-depth understanding of bHLH TF complexity and interactions might be useful to improve neuronal reprogramming strategies for regenerative medicine purposes.

Within the bHLH superfamily, closely related Neurod1, Neurod2, Neurod4 and Neurod6 have emerged as essential TFs for the correct functioning of cells during development and postnatal life. The Neurod family was reviewed by Tutukova et al. in the context of the developing and mature cerebral cortex, and other areas of the central nervous system such as the cerebellum, the brainstem, and the spinal cord. bHLH TFs are presented as both ubiquitous and cell-specific regulators responsible for a variety of biological functions, that range from progenitor cell proliferation and survival to neuronal differentiation, neuronal migration, fate specification, axonal navigation, dendritic elongation, and synaptic formation. The authors also present recent links between Neurod dysfunction and neurological disorders in humans, such as Alzheimer's disease, and they also discuss the Neurod family's potential use as biomarkers.

Stevanovic et al. summarize current knowledge of the roles of SOX proteins in controlling nervous system development and homeostasis in normal and pathological conditions. The SOX TFs are presented herein as a multifaceted superfamily involved in maintaining stem cell pluripotency and paradoxically, during processes that determine neuronal and glial differentiation in the developing brain. They act as both pioneer TFs and sequential regulators. SOX proteins are also key regulators of adult neurogenesis. The authors discuss regulatory mechanisms of SOX functions and the deleterious effects of deregulation of specific SOX genes in the context of neurodevelopmental disorders and neurodegenerative diseases.

Tbr2 (Eomes) is a T-box TF expressed in intermediate progenitors of the developing cerebral cortex and can be used as a molecular marker to label these cells. Bedogni and Hevner combined transcriptome profiling of cell types in the embryonic cerebral cortex of transgenic *Tbr2-GFP* mice with *in situ* hybridization, to identify genes whose expression is enriched in intermediate progenitors. They found that intermediate progenitors not only amplify neurogenesis quantitatively but also, they molecularly "prime" new projection neurons for axogenesis, guidance, and intrinsic excitability. These novel functions make intermediate precursors active participants in optimizing axon development and integration into cortical pathways, in addition to their known roles in shaping regional and laminar identity of projection neurons, and in signaling to interneurons and radial glial progenitors.

Neuronal migration is a critical process in cortical layer formation, and its dysregulation can lead to cerebral cortex malformations and neurodevelopmental disorders. The study authored by Sokpor et al., highlights the indispensable role of the ATP-dependent chromatin remodeling BAF complex in the formation of cortical layers during mouse development. This mechanism regulates multiple aspects of radial neuronal migration under the influence of Wingless/Int (WNT) signaling. Using three different mouse models, the authors applied cellular and molecular analyses of the developing cerebral cortex after temporally and cell-type specifically inactivating components of the BAF complex.

Goodwin et al. contributed to this collection with an original research article that links chromatin remodeling with neuron differentiation and brain size. The authors utilized cerebellar granule neuron precursor cultures from *Smarca1* mutant mice (Ex6DEL) to explore the influence that the nucleosome-remodeling factor subunit Snf2l has on progenitor homeostasis. They show that Ex6DEL progenitors have a transient delay in cell cycle withdrawal, but ultimately these cells do differentiate. This may account for the increased brain size in Ex6DEL mutant mice. Interestingly, Ex6DEL progenitors have a more relaxed chromatin configuration at several regions of the genome which are enriched in binding sites for Fos/Jun TFs.

MiR-184 is a highly enriched microRNA in the mammalian brain and one of the key downregulated circulating microRNAs in patients following ischemic stroke. Yang et al. show that miR-184 is crucial to alleviate damage in an ischemic stroke rat model and, in an oxygen-glucose deprivation/reoxygenation cell model. The authors propose that the targeting of the phosphatidic acid phosphatase type 2B (PPAP2B) mRNA is part of the protective molecular mechanism elicited by miR-184, and therefore they suggest that it might be a promising therapeutic option for stroke recovery.

Regarding neuronal differentiation, Sampieri et al. show that CREB3L2, a member of the CREB3 TF family, is an inhibitory downstream effector during nerve growth factor (NGF)-induced PC12 cell differentiation. CREB3L2 expression is increased upon NGF-induced differentiation, being a target shared by PKA and MAPK/ERK signaling pathways. CREB3L2 enhances Rab5 GTPase levels, a negative regulator of neuronal differentiation, and it also inhibits NGF-induced neurite growth. The authors conclude that finely tuned modulation of CREB3L2 seems to be necessary for PC12 differentiation triggered by NGF.

MANF (Mesencephalic astrocyte-derived neurotrophic factor) belongs to a novel family of secreted neurotrophic regulators. By using cell culture models in which MANF expression was altered, Wen et al. show that this factor regulates neurite outgrowth by activating Akt/mTOR and Erk/mTOR signaling pathways and protein synthesis. The authors propose that MANF may be a potential candidate to facilitate the regeneration of neuronal processes in neurodegenerative diseases.

Autism spectrum disorder is among the many neurodevelopmental disorders that show sex differences. The involved mechanisms are yet unclear, although members of the large family of nuclear receptor TFs appear to be potential candidates. In their mini review, Arnold and Saijo discuss the potential role of sex steroid hormones and their receptors, especially the estrogen receptor β, in a mouse model of maternal immune activation that is commonly used to study autism spectrum disorder. The authors hypothesize that estrogen receptor β-mediated repression of inflammation in brain myeloid-lineage cells may contribute to the male bias that they observed in the maternal immune activation model. Also, they propose new avenues of research on this subject.

Circadian clocks, as they have evolved, are excellent prototypes for studying how cellular transcription is linked to external signal. Functional circadian clocks imply interlocking transcription-translational feedback loops at the cellular level that directly or indirectly respond to external cues such as light

information. Clock genes and clock-controlled genes are key participants; among them, the *per* family. In an original research article, Ruggiero et al. show the consequences of a loss-of-function *per2* gene mutation in maintaining rhythmic expression of circadian clock genes, as well as clock-controlled genes, which consequently affects the rhythmic behavior of intact zebrafish larvae. Furthermore, they demonstrate that disruption of the *per2* gene impacts on the circadian regulation of the cell cycle *in vivo* in a tissue-specific manner.

The original research and review articles of this collection illustrate how transcription factors, chromatin remodelers, microRNAs, secreted factors, and intracellular transduction proteins are all necessary for the harmonious development and functioning of the nervous system. We expect this collection will stimulate the scientific community to continue its efforts to further understand cellular and molecular mechanisms in both healthy and diseased nervous system. Potential new biomarkers and novel treatments might emerge from this and other initiatives.

AUTHOR CONTRIBUTIONS

EM, FS, MR, and VM wrote the Research Topic proposal, edited articles, assigned reviewers, wrote the Editorial draft, and edited and approved its final version. EM contacted and invited contributors. All authors contributed to the article and approved the submitted version.

FUNDING

EM was supported by grants from ANPCyT (Argentina; PICT 2017-00499; http://www.agencia.mincyt.gob.ar), CONICET (Argentina; PUE 2017; http://www.conicet.gov.ar), NIH-CONICET (Argentina and USA; F65096), and NIH (USA; 2 R01 GM083913-41A1; https://www.nih.gov). FS was supported by grant from ANPCyT (Argentina; PICT 2018-03947). MR was supported by grants from the Lundbeck Foundation (Denmark; R344-2020-261; https://lundbeckfonden.com), the Independent Research Fund Denmark (Denmark; 1030-00045B; https://dff.dk), and the Novo Nordisk Foundation (Denmark; NNF21OC0070214; https://novonordiskfonden.dk). VM was supported by grants from NIMH and NINDS (USA; RO1 MH094681; https://www.nimh.nih.gov; RO1 NS10713; https://www.ninds.nih.gov).

ACKNOWLEDGMENTS

We thank Raymond D. Astrue for editing the manuscript.

Conflict of Interest: The authors declare that the research was conducted in the absence of any commercial or financial relationships that could be construed as a potential conflict of interest.

Publisher's Note: All claims expressed in this article are solely those of the authors and do not necessarily represent those of their affiliated organizations, or those of the publisher, the editors and the reviewers. Any product that may be evaluated in this article, or claim that may be made by its manufacturer, is not guaranteed or endorsed by the publisher.

frontiers in Molecular Neuroscience

ORIGINAL RESEARCH
published: 24 September 2020
doi: 10.3389/fnmol.2020.560020

Mesencephalic Astrocyte-Derived Neurotrophic Factor (MANF) Regulates Neurite Outgrowth Through the Activation of Akt/mTOR and Erk/mTOR Signaling Pathways

*Wen Wen[1], Yongchao Wang[2], Hui Li[1], Hong Xu[2], Mei Xu[2], Jacqueline A. Frank[3], Murong Ma[2] and Jia Luo[1]**

[1] Department of Pathology, University of Iowa, Iowa City, IA, United States, [2] Department of Pharmacology and Nutritional Sciences, University of Kentucky College of Medicine, Lexington, KY, United States, [3] Department of Neurology, University of Kentucky College of Medicine, Lexington, KY, United States

Neurite outgrowth is essential for brain development and the recovery of brain injury and neurodegenerative diseases. In this study, we examined the role of the neurotrophic factor MANF in regulating neurite outgrowth. We generated MANF knockout (KO) neuro2a (N2a) cell lines using clustered regularly interspaced short palindromic repeats (CRISPR)/Cas9 and demonstrated that MANF KO N2a cells failed to grow neurites in response to RA stimulation. Using MANF siRNA, this finding was confirmed in human SH-SY5Y neuronal cell line. Nevertheless, MANF overexpression by adenovirus transduction or addition of MANF into culture media facilitated the growth of longer neurites in RA-treated N2a cells. MANF deficiency resulted in inhibition of Akt, Erk, mTOR, and P70S6, and impaired protein synthesis. MANF overexpression on the other hand facilitated the growth of longer neurites by activating Akt, Erk, mTOR, and P70S6. Pharmacological blockade of Akt, Erk or mTOR eliminated the promoting effect of MANF on neurite outgrowth. These findings suggest that MANF positively regulated neurite outgrowth by activating Akt/mTOR and Erk/mTOR signaling pathways.

Keywords: MANF, neurotrophic factor, neurite outgrowth, neuronal differentiation, Erk/mTOR, Akt/mTOR, protein synthesis

OPEN ACCESS

Edited by:
Martin Fredensborg Rath, University of Copenhagen, Denmark

Reviewed by:
Niko Hensel, Hannover Medical School, Germany
Britta Johanna Eickholt, Charité – Universitätsmedizin Berlin, Germany
Stanislava Pankratova, University of Copenhagen, Denmark

****Correspondence:***
Jia Luo
jia-luo@uiowa.edu

Received: *07 May 2020*
Accepted: *04 September 2020*
Published: *24 September 2020*

Citation:
Wen W, Wang Y, Li H, Xu H, Xu M, Frank JA, Ma M and Luo J (2020) Mesencephalic Astrocyte-Derived Neurotrophic Factor (MANF) Regulates Neurite Outgrowth Through the Activation of Akt/mTOR and Erk/mTOR Signaling Pathways. Front. Mol. Neurosci. 13:560020. doi: 10.3389/fnmol.2020.560020

INTRODUCTION

Neurite outgrowth is the first step for the formation of axons and dendrites, which are necessary components for the development of a functional neuronal network. Proper neurite outgrowth is not only important for the normal development of the nervous system, but may also facilitate the recovery of traumatic brain injury and neurodegenerative disorders such as Parkinson's disease (PD), Alzheimer's disease (AD), and Amyotrophic lateral sclerosis (ALS) (Gouel et al., 2019; Houlton et al., 2019). Neurite outgrowth requires the synthesis and reorganization of cytoskeleton proteins including actin and microtubules (Rodriguez et al., 2003; Flynn, 2013). The dynamic of cytoskeleton elongation, branching, and retraction is regulated by various factors such as transcription factors that governs gene expression for neuron differentiation (Paolino et al., 2018) and cell adhesive molecules that interact with and remodel cytoskeleton and activate gene

expression (Missaire and Hindges, 2015; Leshchyns'ka and Sytnyk, 2016). Moreover, neurite outgrowth is also regulated by neurotrophic factors (NTF) that activate cell signaling pathways for neuron differentiation and migration, and support neuron survival and synaptic function (da Silva and Dotti, 2002; Cui, 2006).

Mesencephalic astrocyte-derived neurotrophic factor (MANF), also known as arginine-rich, mutated in early stage tumors (Armet), together with cerebral dopamine neurotrophic factor (CDNF) form a novel family of neurotrophic factors in vertebrate (Petrova et al., 2003; Lindholm et al., 2007). MANF is an endoplasmic reticulum (ER)-stress inducible protein, and its expression and secretion can be regulated by ER-stress (Mizobuchi et al., 2007; Oh-Hashi et al., 2012). MANF is broadly expressed in multiple developing and mature tissues including the central nervous system. In rodent brain, MANF is widely expressed in all brain regions during early developmental stages and declined gradually when the brain matures except for certain brain regions in the cerebral cortex, hippocampus, and cerebellar Purkinje cells, suggesting the role of MANF in neuron differentiation (Lindholm et al., 2008; Wang et al., 2014; Yang et al., 2014; Danilova et al., 2019). Increasing evidence have shown that MANF promotes the development and survival of neurons in both normal and pathological conditions (Petrova et al., 2003; Palgi et al., 2009; Voutilainen et al., 2009; Airavaara et al., 2010; Chen et al., 2012). MANF is required for dopaminergic neuron survival in *Drosophila* and zebrafish (Palgi et al., 2009; Chen et al., 2012), and selectively protects dopaminergic neuron in rat medial ventral mesencephalon cell cultures *in vitro* (Petrova et al., 2003). In rat PD model induced by 6-hydroxydopamine (6-OHDA), intrastriatally injection of MANF protects nigrostriatal dopaminergic nerves from degeneration (Voutilainen et al., 2009). Overexpression of MANF ameliorates the loss of Purkinje cells in a mouse model of spinocerebellar ataxia (Yang et al., 2014) and promotes neural progenitor cells migration and differentiation in a rat cortical stroke model (Tseng et al., 2017a). In addition, MANF is also reported to facilitate retinal ganglion cells and photoreceptor cells regeneration in the retina by regulating neuroinflammation and immune response (Neves et al., 2016; Gao et al., 2017; Lu et al., 2018). Similarly, CDNF has also been reported to be neuroprotective in animal models of PD, AD, and periphery nerve injury (Lindholm et al., 2007; Cheng et al., 2013; Kemppainen et al., 2015).

Recently, a study using conventional MANF knockout mice (Manf $^{-/-}$) revealed that MANF may be involved in neurite outgrowth (Tseng et al., 2017b). Manf $^{-/-}$ cortex showed decreased dendrite and axon length, while MANF deficient neural stem cells (NSCs) have impaired ability to grow neurites in culture. However, the mechanism and cellular signaling involved in MANF regulation neurite outgrowth remain unclear. In the present study, we used mouse neuro2a (N2a) cells to investigate the mechanisms underlying MANF regulation of neurite outgrowth. N2a cells are a neuronal cell line model widely used for studying neuronal differentiation; they differentiate into neuron-like cells in response to stimulants such as serum starvation, retinoic acid (RA), and cyclic adenosine monophosphate (cAMP) treatments (Salto et al., 2015). We demonstrated that MANF was required for RA-induced neurite outgrowth. MANF regulation of neurite outgrowth was mediated by Akt/mTOR and Erk/mTOR signaling pathways and protein synthesis.

MATERIALS AND METHODS

Materials

The following cells and materials were used: N2a (CCL-131), SH-SY5Y (CRL-2266) and HEK293 (CRL-1573) cells were from ATCC (Manassas, VA, United States); MEM (11095-080), high glucose DMEM (10569-010), L-methionine free DMEM (21013-024), FBS, antibiotic-antimycotic (15240112), GeneArt Genomic Cleavage Detection Kit (A24372), and Lipofectamine 3000 Reagent (L3000008) were from Life Technologies (Carlsbad, CA, United States); all-*trans* RA (R2625), crystal violet acetate (C5042), MTT (M5655), anhydrous DMSO (276855), DAPI (D9542), Akt activator SC79 (SML0749), and mTOR activator MHY1485 (SML0810) were from Sigma-Aldrich (St. Louis, MO, United States); PFA (15714) was from Electron Microscopy Sciences (Hatfield, PA, United States); recombinant human MANF (hMANF) (MANF-536H) was from Creative BioMart (New York, NY, United States); control CRISPR/Cas9 plasmid (sc-418922), mouse ARP double nickase plasmid (sc-428989-NIC), UltraCruz transfection reagent (sc-395739), plasmid transfection medium (sc-108062), and Akt inhibitor MK-2206 dihydrochloride (sc-364537) were from Santa Cruz Biotechnology (Dallas, TX, United States); Erk activator PDBu (12808), Erk inhibitor PD98059 (9900), and mTOR inhibitor Torin 1 (14379) were from Cell Signaling Technology (Beverly, MA, United States); pGEM-T-easy vector (A1360) was from Promega (Madison, WI, United States); 10-beta competent *E. coli* (C3019I) was from New England Biolabs (Ipswich, MA, United States); scrambled siRNA-GFP lentivector (LV015-G), Manf siRNA-GFP lentivector (279970940495), MANF-HA adenovirus (mouse) (279970540200), and CMV Null control adenovirus (000047A) were from Applied Biological Materials (Richmond, BC, Canada); PureLink Expi Endotoxin-free Maxi Plasmid Purification Kit (A31231) was from Thermo Fisher Scientific (Waltham, MA, United States); VECTASHIELD mounting medium (H-1400 and H-1500) was from Vector Laboratories (Burlingame, CA, United States); *DC* protein assay kit (5000112) was from Bio-Rad Laboratories (Hercules, CA, United States); Click-iT HPG Alexa Fluor Protein Synthesis Assay Kits (C10428) was from Invitrogen (Grand Island, NY, United States).

The following antibodies were used: anti-α-tubulin (T5168, Sigma-Aldrich); anti-ARMET/ARP (MANF) (ab67271 for C-terminus and ab67203 for N-terminus, Abcam, Cambridge, MA, United States); anti-HA-Tag (CST 3724), anti-phospho-Akt (Ser473) (CST9271), anti-Akt (CST9272), anti-phospho-Erk1/2 (CST 9101), anti-Erk1/2 antibody (CST 9102), anti-phospho-mTOR (Ser2448) (CST2971), anti-mTOR (CST2972), anti-phospho-p70 S6 (CST9204), anti-p70 S6 (CST2708), anti-Cas9 (CST 14697), and anti-β-Actin (CST3700)

antibodies were all from Cell Signaling Technology; secondary antibodies conjugated to horseradish peroxidase (NA931V and NA934V) were from GE Healthcare Life Sciences (Pittsburgh, PA, United States); Alexa-488 conjugated anti-mouse (A21202), Alexa-594 conjugated anti-mouse (A11005) and Alexa-594 conjugated anti-rabbit antibodies (A11012) were from Life Technologies.

Cell Culture and Differentiation

Neuro2a cells and HEK293 cells were cultured in MEM supplemented with 10% FBS and 1% antibiotic-antimycotic at 37°C in 5% CO_2 in a humidified incubator (Symphony 5.3A, Thermo Scientific). SH-SY5Y cells were cultured in DMEM supplemented with 10% FBS and 1% antibiotic-antimycotic. To induce neurite outgrowth, N2a or SH-SY5Y cells were plated in 6-well plates at a density of 5×10^4 cells per well for 24 h. Then growth medium was carefully removed and replaced with differentiation media of an equal volume of MEM or DMEM supplemented with 2% FBS at the present of 10 μM all-*trans* RA for 3 days unless otherwise stated. Recombinant human MANF (hMANF) was added into differentiation media at a final concentration of 100 ng/ml. Differentiation media was changed freshly every other day to ensure RA effectiveness. Neurite was defined as the extension of neuronal processes greater than two cell body diameters in length. To quantify neurite length, at least five random fields were imaged for each well using Olympus BX51 light microscope with the 40X objective. The five random fields were selected in an X manner with four fields at the corners and one field in the center of the well. Cells were either imaged alive or fixed in 4% PFA for 10 min then stained with 0.5% crystal violet for 15 min at room temperature. Neurite length was measured from the center of the cell body to the tip of the longest neurite using the CellSens imaging software (Olympus, Tokyo, Japan). Morphometrics analysis was performed independently by two or more different investigators. To quantify the percentage of cells with neurite, the total cell numbers and cells with neurite in each field were counted with ImageJ.

CRISPR Transfection and MANF Knockout Single Cell Colony Isolation

Control CRISPR/Cas9 plasmid was referred to control CRISPR thereafter and mouse ARP double nickase plasmid was referred to MANF CRISPR thereafter. Control CRISPR has a GFP marker for visually confirmation of successful transfection. MANF CRISPR consists a pair of plasmids both targeting the exon 2 of mouse Manf gene. One plasmid contains a puromycin resistance gene, the other one has a GFP marker. N2a cells were seeded onto 6-well plate to grow to 70% confluence and were transfected with 1 μg of either control or MANF CRISPR using UltraCruz transfection reagent and plasmid transfection medium according to the manufacture's protocol. GFP-positive cells were selected by flow cytometry 48 h after the transfection. MANF CRISPR transfected cells that were GFP-positive were further selected by 1 μg/ml puromycin for 5 days, then diluted and plated onto 10 cm culture dishes at 1×10^3 cells/dish to form single cell colonies. Once single cell colonies were formed and large enough, they were transferred using sterile 10 μl pipette tips to 24-well plates and then 6-well plates to expand. The presence of genomic insertions or deletions (indels) in each single cell colony were detected using the GeneArt Genomic Cleavage Detection Kit (Life Technologies) according to the manufacture's protocol. Among fourteen single cell colonies we tested, five appeared to have genomic indels. To confirm biallelic MANF knockout, we tested at genomic DNA and protein level. Genomic DNA was isolated from these five colonies. MANF was cloned by PCR using primers 5′-AGTTTTTTCCAGGGGAAATGG-3′ and 5′-ACCCACTACTTTCTCTCTCAG-3′, and then cloned into the pGEM-T-easy vector (Promega) and transformed into 10-beta competent *E. coli* (New England Biolabs) for sequencing. Protein was also extracted from each colony and subjected to immunoblot to test the presence of MANF protein. Ultimately, we confirmed 2 colonies that have biallelic MANF KO. To rule out the possibility of clonal selection, both colonies were tested in morphometric analysis in **Figure 1** and protein expression analysis in **Figures 6**, **7**. Since similar results were revealed between the two clones, we used clone 1 for all other analysis.

siRNA Transfection

Scrambled siRNA-GFP and Manf siRNA-GFP lentivector plasmids were purchased from Applied Biological Materials (Richmond, BC, Canada) with the MANF siRNA target sequence 5′-TCAAAGACAGAGATGTCACATTTTCACCA-3′ cloned into the piLenti-siRNA-GFP plasmid backbone. The siRNA is driven by the U6 promotor followed by the GFP driven by the CMV promotor. The plasmids were subcloned and amplified in 10-beta competent *E. coli* cells (New England Biolabs), and purified using PureLink Expi Endotoxin-free Maxi Plasmid Purification Kit (Thermo Fisher Scientific). Either 2.5 μg of scrambled siRNA or Manf siRNA lentivector plasmids were transfected into N2a or SH-SY5Y cells using Lipofectamine 3000 Reagent (Life Technologies) according to the manufacturer's instruction. Cells were subject to subsequent analysis.

Adenovirus Transduction

Crude viral stock of MANF-HA adenovirus (mouse), referred to AD-MANF thereafter, and CMV Null control adenovirus, referred to AD-vector thereafter (Applied Biological Materials) were prepared at titer ranging from 1×10^7 to 1×10^8 pfu/ml by manufacture and then amplified in HEK293 cells according to the manufacture's instruction. Briefly, 3×10^6 HEK293 cells were plated in 10 cm dishes and incubated with 100 μl crude viral stock until 90% of the cells were rounded up and detached. Adenovirus-containing HEK293 cells were collected with culture media and placed at −80°C for 30 min and then in 37°C water bath for 15 min to thaw. Repeat the freeze and thaw for 3 times. Cell debris were pelleted at 3000 rpm for 15 min and supernatant with viral particles were used to transduce N2a cells. N2a cells were transduced with either CMV Null control or MANF-HA adenovirus by incubating 120 μl per well in 6-well plate for 3 h. Three hours later, culture media with adenovirus were removed and replaced with fresh growth media. Cells were subject to subsequent analysis.

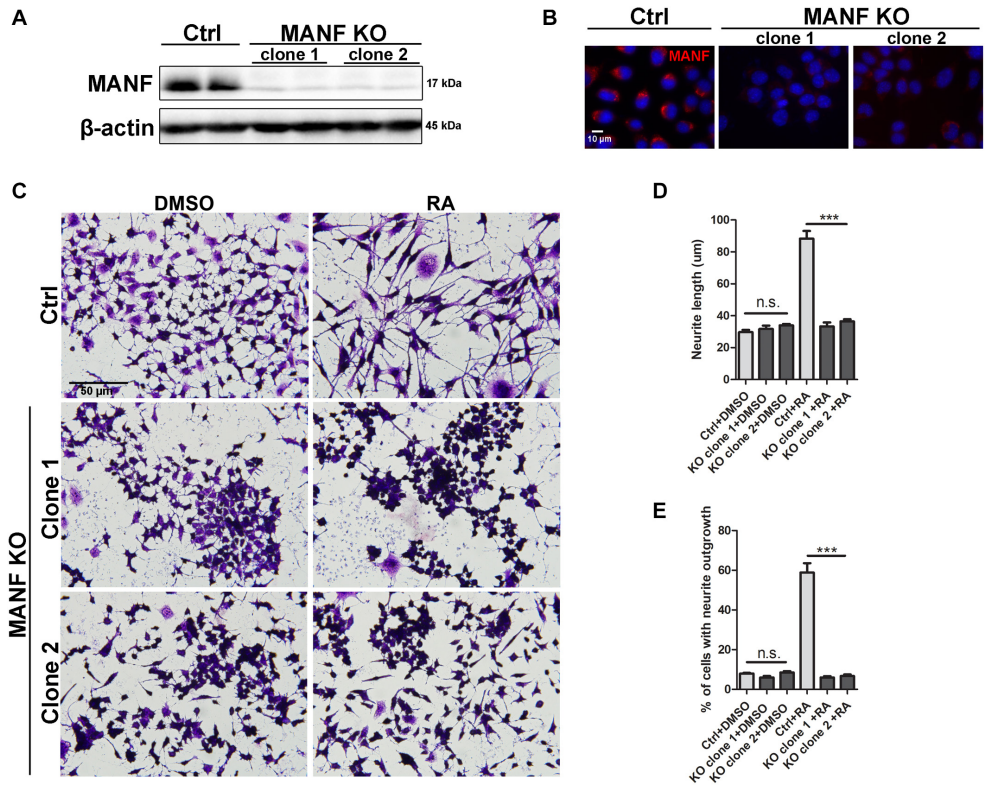

FIGURE 1 | Loss of MANF inhibits RA-induced neurite outgrowth. Stable N2a cell lines of MANF knockout (KO) were established as described in the Materials and Methods. **(A)** Protein was collected from control and MANF KO cell lysates and analyzed by immunoblotting with MANF antibody. β-actin was used as a loading control. The size of the proteins (kDa) was labeled next to each band. **(B)** Immunofluorescent staining showed MANF expression in control cells and no signal in MANF KO cells. Cell nuclei were stained by DAPI. **(C)** Representative images of control and MANF KO cells treated with DMSO or RA for 3 days. Cells were fixed and stained with crystal violet for visualization. Average neurite length **(D)** and percentage of cells that bear neurites **(E)** were measured, and analyzed by One-way ANOVA. In cases where significant differences were detected, specific *post hoc* comparisons between treatment groups were examined with the Tukey's test. ***$P < 0.0001$, n.s. not statistically significant. The data were expressed as the mean ± SEM of three independent experiments.

Immunocytochemistry

Neuro2a or SH-SY5Y cells were seeded onto 24-well plates with sterile coverslip on the bottom coated with 10 μg/ml fibronectin. After differentiation, cells were fixed with 4% PFA and permeabilized in 0.25% Triton X-100 in PBS for 10 min at room temperature. Then cells were blocked with 1% BSA/2% goat serum/PBS for 30 min and incubated with anti-α-tubulin antibody (1:1000) 1 h at room temperature. After washing with PBS, cells were incubated with Alexa fluor-conjugated secondary antibodies at a dilution of 1:200. Cells on the coverslip were counterstained with DAPI and sealed with VECTASHIELD mounting medium (Vector Laboratories). Fluorescence images were obtained using the Olympus IX81 inverted fluorescent microscope (Olympus).

Protein Extraction and Immunoblotting

Protein was extracted from N2a or SH-SY5Y cells as previously described (Xu W. et al., 2018). Briefly, cells were washed with ice cold PBS and lysed on ice for 15 min in RIPA buffer containing 150 mM NaCl, 1 mM ethylene glycol-bis(beta-aminoethyl ether)-N,N,N′,N′-tetraacetic acid (EGTA), 50 mM Tris–HCl (pH 7.5), and 0.5% Nonidet P-40 (NP-40), 0.25% sodium dodecyl sulfate (SDS), with freshly added protease inhibitors of 5 μg/ml leupeptin, 5 μg/ml aprotinin, 3 mM sodium orthovanadate, and 0.3 mg/ml phenylmethanesulfonyl fluoride (PMSF). Lysed cells were centrifuged at 10,000 × *g* for 30 min at 4°C, and the supernatant fraction was collected. Protein concentration was determined using the *DC* protein assay (Bio-Rad Laboratories) according the manufacture's instruction.

Immunoblotting was performed as previously described (Li et al., 2019; Pillai-Kastoori et al., 2020a,b). In brief, 20–30 μg protein samples were separated by SDS-PAGE on 12% polyacrylamide gels by electrophoresis. Separated proteins were then transferred to nitrocellulose membranes and blocked in 5% BSA/ 1xTBS/0.05% Tween-20 for 1 h at room temperature prior to incubation with primary antibodies at 4°C overnight. The primary antibodies used and the final dilutions were as follows: anti-ARMET/ARP (MANF), anti-HA-Tag, anti-phospho-Akt (Ser473), anti-Akt, anti-phospho-Erk1/2, anti-Erk1/2 antibody, anti-phospho-mTOR (Ser2448), anti-mTOR, anti-phospho-p70S6, anti-p70S6, anti-Cas9, and anti-β-actin (1:1000). Subsequently, membranes were washed with TBST and incubated with secondary antibodies conjugated to horseradish

peroxidase (1:5000). Blots were developed using the Amersham ECL Prime Western Blotting Detection Reagent (GE Healthcare Life Sciences). The density of immunoblotting was quantified using Image Lab software (Bio-Rad Laboratories).

MTT Assay

To examine cell metabolic activity, 3-(4,5-dimethylthiazol-2-yl)-2,5-diphenyltetrazolium bromide (MTT) assay was used. Cells were seeded on 96-well plates at 2×10^3 cells per well. At times indicated, MTT was added to each well at the final concentration of 500 μg/ml and incubated at 37°C for 2 h. After the incubation, media were carefully removed and 100 μl DMSO was added to each well to dissolve the MTT formazan. Plates were read using the Beckman Coulter DTX 880 Multimode Detector plate reader (Analytical Instruments, Golden Valley, MN, United States) at the wavelength of 595 nm.

Pharmacological Inhibition or Activation of Akt, Erk, and mTOR

Cells were preincubated with Akt activator SC79 (2.5 μM), Erk activator PDBu (2 μM), mTOR activator MHY1485 (5 μM) and Akt inhibitor MK-2206 dihydrochloride (2.5 μM), Erk inhibitor PD98059 (50 μM), mTOR inhibitor Torin 1 (50 nM) for 30 min and then treated with RA as described above.

Click-iT Homopropargylglycine (HPG) Protein Synthesis Assay

To detect the rate of protein synthesis, we utilized the Click-iT HPG Alexa Fluor Protein Synthesis Assay Kits (Invitrogen). Control and MANF KO N2a cells were seeded onto either fibronectin coated 96-well plates or fibronectin coated 24-well plates with sterile coverslip on the bottom. Protein synthesis was detected for cells treated with RA or DMSO control at 24, 48, and 72 h. An hour before the click-it reaction, media was replaced with DMEM without L-methionine (Life Technologies) to deplete methionine. Then cells were incubated with 50 μM HPG in L-methionine free DMEM media for 1 h and fixed with 4% PFA in PBS. After permeabilization in 0.5% TritonX-100 in PBS, cells were incubated in Click-iT reaction cocktail at room temperature for 30 min in dark and then cell nuclei were counter stained with DAPI. The rate of HPG incorporation in 96-well plates was examined using the Beckman Coulter DTX 880 Multimode Detector plate reader (Analytical Instruments) at the wavelength of 535 nm for the fluorescent intensity. Coverslips were removed from 24-well plates and mounted onto slides and images were taken using the Olympus IX81 inverted fluorescent microscope (Olympus). Images were analyzed using ImageJ for calculating the percentage of cells without HPG incorporation.

Statistical Analysis

All analyses were performed using the GraphPad Prism version 7 software. Data were expressed as mean ± SEM of three independent experiments in each group. Differences among experimental groups were analyzed by Student *t*-test, one-way ANOVA or two-way ANOVA with $p < 0.05$ being considered statistically significant. In cases where significant differences were detected, specific comparisons between treatment groups were examined with the Tukey's *post hoc* test for one-way ANOVA or Bonferroni's *post hoc* test for two-way ANOVA.

RESULTS

MANF Deficiency Inhibits RA-Induced Neurite Outgrowth

Mesencephalic astrocyte-derived neurotrophic factor knockout (KO) N2a cells were generated by transfection of MANF CRISPR/Cas9. Two single cell colonies with biallelic MANF knockout were isolated. Immunoblotting and immunocytochemistry revealed that MANF protein was not present in both clones of MANF KO N2a cells (**Figures 1A,B**). To examine if MANF is required for neurite outgrowth in N2a cells, control and KO cells were treated with 10 μM RA or DMSO control in media with 2% FBS for 3 days. The length of neurite and percentage of cells with neurite was analyzed. Strikingly, among 500–800 cells analyzed in three independent experiments, significantly fewer numbers of MANF KO cells have grown neurite and the length of neurite was significantly shorter compared to control cells. The treatment of RA results in about 60% control cells to grow neurites, but only ∼6% KO cells bear neurites (**Figures 1C,E**). The average neurite length after 3 days of RA treatment in KO cells was only 33.27 ± 9.95 μm for clone 1 and 36.42 ± 12.41 μm for clone 2, compared to 88.28 ± 20.59 μm for control cells (**Figures 1C,D**).

To determine whether the reduction of neurite outgrowth in MANF KO cells was a consequence of general toxicity due to MANF knockout or RA treatment, we measured the cellular metabolic activity of clone 1 by MTT assay. We observed a steady increase of viable and metabolically active cells for both DMSO treated control and KO cells, indicating that MANF knockout does not affect N2a cell metabolic activity (**Figure 2A**). Interestingly, KO cells showed higher cell metabolic activity at 48 and 72 h compared to control cells. In addition, we noticed that RA treatment slowed down cell growth and RA-treated control cells have significantly slower proliferation rate compared to other groups, which was in line with the fact that the majority of RA treated control cells ceased proliferation and underwent differentiation (**Figure 2A**).

To test the possibility that MANF KO cells may have delayed neurite outgrowth in response to RA treatment, we prolonged cells in differentiation media for 6 days and measured neurite length each day. For control cells, we observed a gradual increase in neurite length and by 6 days the neurite length reached to 154.45 ± 43.47 μm. However, for KO cells (clone 1 was used for this analysis), we only observed a subtle neurite growth to 36.94 ± 14.11 μm and it started to decline after 5 days (**Figures 2B,C**).

To confirm that the inhibition of neurite outgrowth was specific to MANF deficiency, we performed an alternative approach of using siRNA to knockdown MANF in N2a and SH-SY5Y cells and compared neurite length between MANF siRNA and scramble siRNA transfected cells. MANF siRNA sufficiently reduced about 50% MANF expression in N2a cells

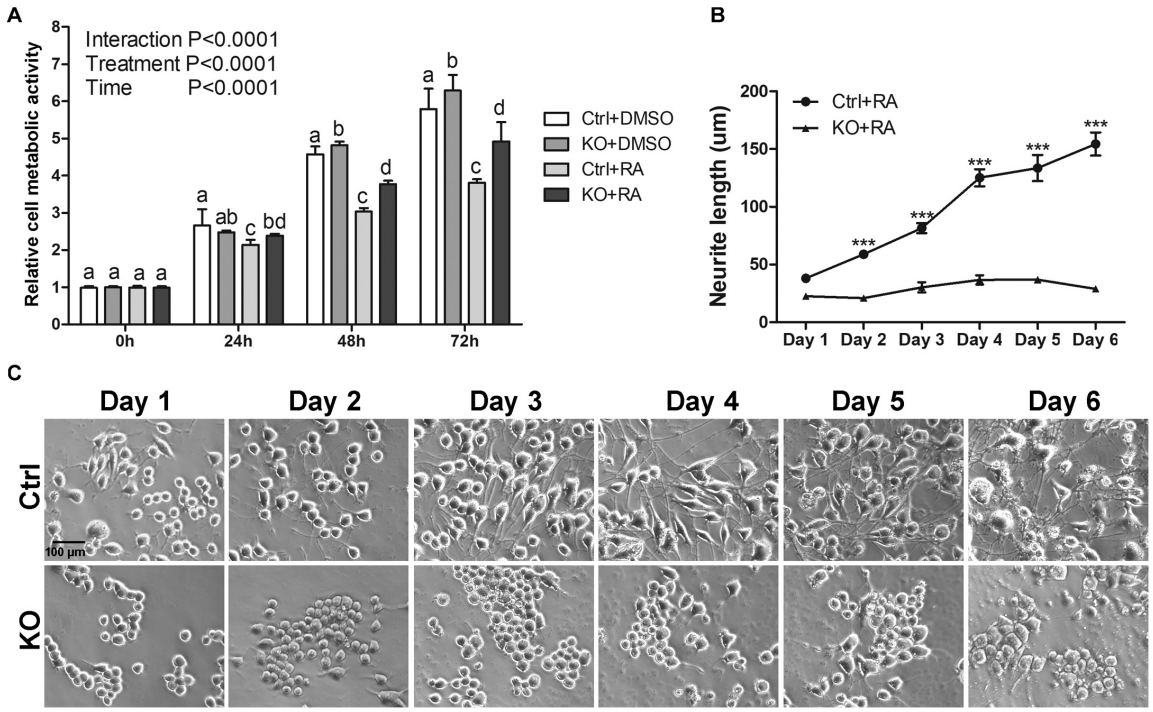

FIGURE 2 | The reduction of neurite outgrowth in MANF KO cells is neither due to toxicity nor delayed process. **(A)** Cell metabolic activity at 0, 24, 48, and 72 h of RA treatment was tested by MTT assay. Different letters above columns indicate significant differences between treatments as tested by two-way ANOVA followed with the Bonferroni's *post hoc* test ($P < 0.05$). The data were expressed as the mean ± SEM of three independent experiments. **(B)** Average neurite length of control and MANF KO cells after 6 days of RA treatment was determined and analyzed by Two-way ANOVA followed with the Bonferroni's *post hoc* test, ***$P < 0.001$. The data were expressed as the mean ± SEM of three independent experiments. **(C)** Representative images of control and MANF KO cells treated with RA.

(**Figures 3A,B**) and 30% in SH-SY5Y cells (**Figures 3E,F**). Since both scrambled siRNA and MANF siRNA plasmids contain GFP, we were able to use the expression of GFP as an indicator for successful transfection and analyze neurite length in GFP positive cells. Consistent with MANF CRISPR KO cells, siRNA MANF knockdown resulted in reduced neurite outgrowth in response to RA treatment compared to control cells as shown by α–tubulin labeling (**Figures 3C,D,G,H**). Scramble siRNA transfected N2a cells send out neurite at an average of 137.69 ± 25.06 μm in respond to RA treatment, while MANF siRNA transfected N2a cells only grow neurite at 46.25 ± 20.87 μm. Similarly, scramble siRNA transfected SH-SY5Y cells send out neurite at an average of 92.19 ± 27.55 μm in respond to RA treatment, while MANF siRNA transfected SH-SY5Y cells only grow neurite at 31.68 ± 7.71 μm. All these data above suggested that MANF deficiency inhibited neurite outgrowth.

MANF Overexpression Facilitates RA-Induced Neurite Outgrowth

Mesencephalic astrocyte-derived neurotrophic factor is mostly located in the lumen of endoplasmic reticulum (ER), but it can also be secreted under pathological conditions such as ER-stress (Apostolou et al., 2008; Glembotski et al., 2012). Since it is still unclear whether the biological function of MANF is through its intracellular form or secreted form, we performed two experiments to test whether MANF can facilitate neurite outgrowth in response to RA treatment through its intracellular or extracellular form, respectively. First, we examined whether addition of extracellular MANF in the culture media can induce neurite outgrowth in N2a cells. We found that the addition of MANF (100 ng/ml) into the culture media alone did not induce N2a cells to grow neurites (**Figures 4A,B**). However, when MANF was combined with RA, cells grow long neurites that reached 203.26 ± 71.02 μm after 3 days, which was significantly longer than cells treated with RA alone (88.28 ± 20.59 μm) (**Figures 4A,B**). This result suggested that extracellular MANF can facilitate neurite outgrowth in response to RA.

Then, we induced the overexpression of MANF intracellularly by adenovirus (AD) transduction. Adenovirus transduction did not affect endogenous MANF expression when compared to untransduced cells (**Figures 4C,D**). Immunoblotting detected that AD-MANF transduced cells show robust exogenous MANF expression which migrate slower than the endogenous MANF due to the presence of HA-tag (**Figures 4C,D**). The expression of exogenous MANF protein in AD-MANF transduced N2a cells peaked around 48 h after transduction and started to decline afterward (**Supplementary Figure S1**). Twelve hours after the transduction, cells were incubated in differentiation media for 3 days and neurite length was measured each day. We found that AD-MANF transduced N2a cells grow significantly longer neurites (173.83 ± 52.32 μm) compared

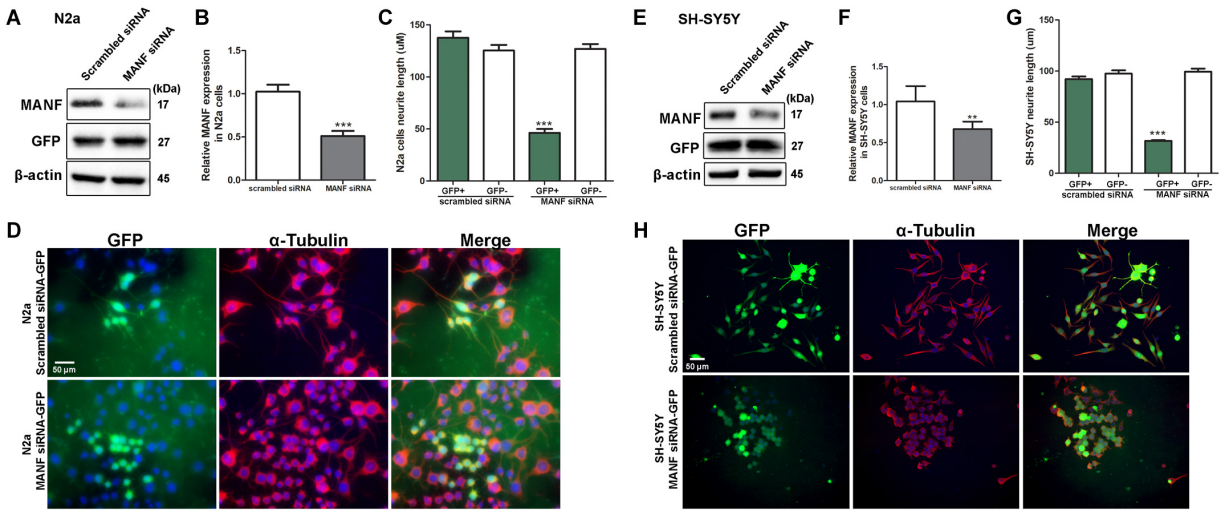

FIGURE 3 | MANF knockdown by siRNA inhibits RA-induced neurite outgrowth. N2a and SH-SY5Y cells were transfected with MANF siRNA-GFP or scramble siRNA-GFP construct as described in the section "Materials and Methods." **(A,E)** 24 h after the transfection, cells were lysed and analyzed by immunoblotting with MANF and GFP antibodies. β-actin was used as a loading control. The size of the proteins (kDa) was labeled next to each band. **(B,F)** MANF protein levels were quantified and normalized to β-actin. The data were analyzed by Student's *t* test, $^{***}P < 0.0001$. The data were expressed as the mean ± SEM of three independent experiments. **(C,G)** Average neurite length in scramble siRNA and MANF siRNA transfected GFP+ cells after 3 days of RA treatment was determined and analyzed by Student's *t* test, $^{***}P < 0.0001$. The data were expressed as the mean ± SEM of three independent experiments. **(D,H)** Representative fluorescent images revealed GFP expression in cells with successful siRNA transfection (Green). Neurites were visualized by immunofluorescent labeling of α-tubulin (Red). Cell nuclei were stained by DAPI. $^{**}P < 0.01$.

to AD-vector transduced control cells (111.20 ± 33.83 μm) starting at 2 days. By day 3, AD-MANF transduced cells still have significantly longer neurites (241.66 ± 58.16 μm) than control cells (137.82 ± 37.29 μm) (**Figures 4E,F**). As a result, we concluded that both extracellular and intracellular MANF can facilitate N2a cell neurite outgrowth in response to RA stimulation.

Addition of MANF in Culture Media Fails to Rescue Neurite Outgrowth Defects in MANF KO Cells in Response to RA Treatment

Since both intracellular and extracellular MANF facilitates RA-induced neurite outgrowth in control N2a cells, we want to test whether addition of MANF can rescue the neurite outgrowth defects in MANF KO cells. We first tried to overexpress MANF intracellularly in MANF KO cells. Unfortunately, we were unable to reintroduce MANF back into MANF KO cells by AD-MANF transduction for two possible reasons. First, the transduction efficiency was much lower in KO cells compared to control cells. As shown in **Supplementary Figure S2**, we were able to detect HA signal in 85% of control cells with correspondence strong exogenous MANF expression. However, only 31% of KO cells showed weak HA expression and no exogenous MANF was detected. The other reason why we were unable to reintroduce MANF expression in KO cells was that we still detected high level of Cas9 protein expression in KO cells (**Supplementary Figure S2D**), indicating the integration of the MANF CRISPR/Cas9 construct into the genome of the cells. Since the MANF CRISPR target sites were located within exon 2 of mouse *Manf* gene, the presence of MANF CRISPR/Cas9 in the cells was able to interfere with the expression *Manf* gene carried by AD-MANF, further inhibit the expression of exogenous MANF.

As a result, we were only able to test whether addition of extracellular MANF can rescue the neurite outgrowth defect in MANF KO cells. MANF KO cells were treated with DMSO or RA with or without addition of recombinant hMANF (100 ng/ml) in the culture media for 3 days (**Figure 5**). As before, neither RA nor hMANF can induce MANF KO cells to grow neurites. In addition, the combination of RA+hMANF also failed to induce neurite outgrowth in MANF KO cells, suggesting that addition of extracellular MANF is not sufficient to rescue the neurite outgrowth defects in MANF KO cells in response to RA.

MANF Regulates RA-Induced Neurite Outgrowth Through the Activation of Akt/mTOR and Erk/mTOR Signaling Cascades

Since Akt/mTOR and Erk/mTOR are key regulators for neurite outgrowth, we then tested whether these signaling cascades were involved in the role of MANF in regulating neurite outgrowth. We first examined changes in the expression of Akt/mTOR and Erk/mTOR cascades genes in control and MANF KO cells, and AD-vector and AD-MANF transduced cells within 12 h of RA treatment. As expected, in control and AD-vector transduced cells, the initiation of RA-induced neurite outgrowth was correlated with an upregulation of Akt/mTOR and Erk/mTOR

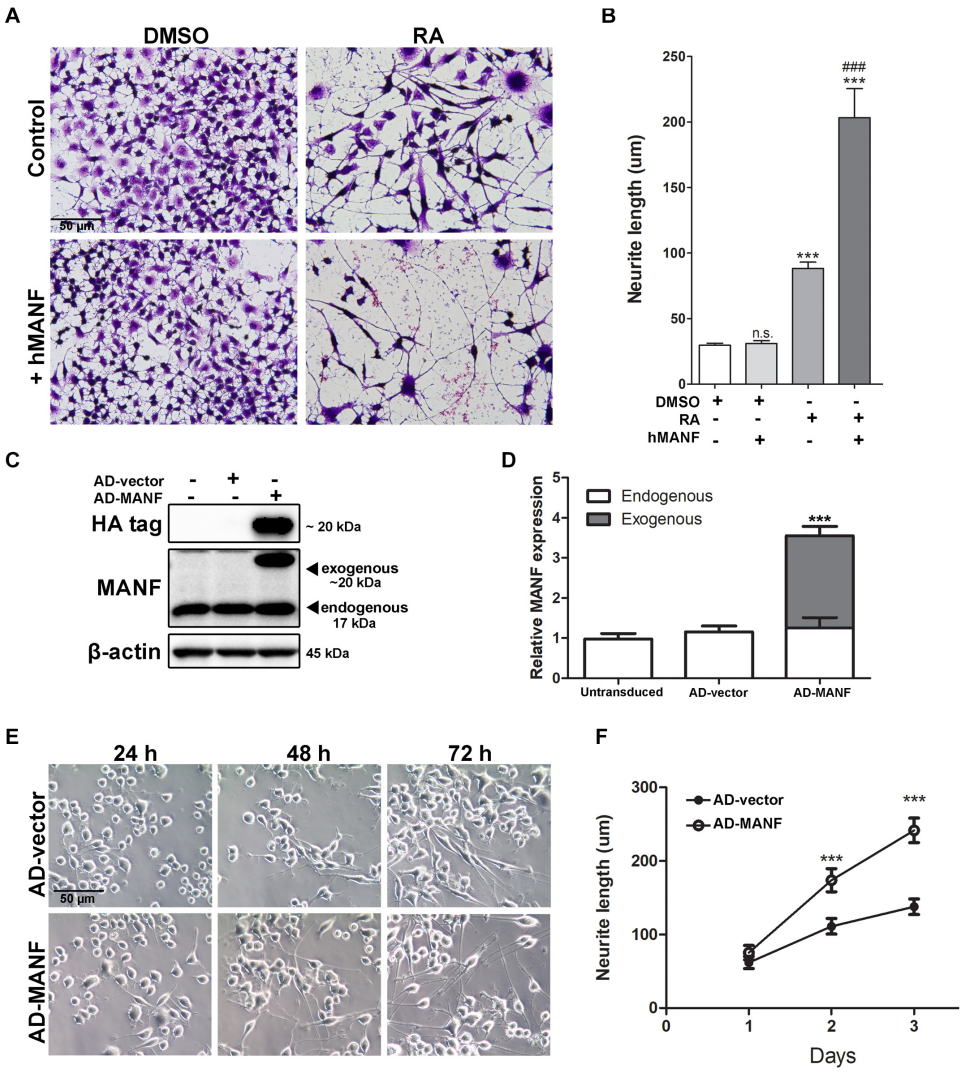

FIGURE 4 | MANF overexpression facilitates RA-induced neurite outgrowth. **(A)** Representative images of N2a cells treated with DMSO or RA for 3 days with or without addition of recombinant hMANF (100 ng/ml). Cells were fixed and stained with crystal violet for visualization. **(B)** Average neurite length was measured, and analyzed by One-way ANOVA followed with the Tukey's *post hoc* test, $^{***}P < 0.0001$ and n.s. not statistically significant compared to DMSO treated cells, $^{###}P < 0.0001$ compared to RA treated cells. The data were expressed as the mean ± SEM of three independent experiments. **(C)** Cells were lysed 48 h after adenovirus transduction and subjected to immunoblot to determine levels of MANF and HA tag expression. The size of the proteins (kDa) was labeled next to each band. **(D)** Endogenous and exogenous MANF protein levels were quantified and normalized to β-actin. The data were analyzed by Student's *t* test, $^{***}P < 0.0001$. The data were expressed as the mean ± SEM of three independent experiments. **(E)** Representative images of AD-vector and AD-MANF transduced cells treated with RA for 24, 48, and 72 h. **(F)** Average neurite length of AD-vector and AD-MANF transduced cells after RA treatment was determined, and analyzed by Two-way ANOVA followed with the Bonferroni's *post hoc* test, $^{***}P < 0.001$. The data were expressed as the mean ± SEM of three independent experiments.

signaling pathways. We observed a steady 2-fold increase of p-Akt in control cells by the end of the 12 h RA-treatment (**Figures 6A,C**). The expression of p-Erk in control cells peaked at 1–3 h to 11-fold and then started to decline (**Figures 6A,D**). Following the activation of Akt and Erk, the phosphorylation of mTOR and P70S6 in control cells was also increased to 1.4-fold at 3 h and 2-fold at 6 h, respectively, and then started to decline (**Figures 6A,E,F**). Similar Akt/mTOR and Erk/mTOR activation was observed in RA-treated AD-vector transduced cells (**Figure 7**). Strikingly, RA-treated MANF KO cells exhibit significantly less extent of Akt and Erk activation compared to control cells. RA failed to induce the phosphorylation of Akt in MANF KO cells (**Figures 6A,C**) and the induction of p-Erk was significantly reduced from 11-fold in control cells to only 6-fold in KO cells (**Figures 6A,D**). As a result, the level of p-mTOR and p-P70S6 was also reduced in MANF KO cells (**Figures 6A,E,F**). On the contrary, AD-MANF transduced cells overexpressing intracellular MANF (**Figure 7A**) showed significantly elevated expression of p-Akt and p-Erk compared to AD-vector transduced cells (**Figures 7A,C,D**). p-mTOR and p-P70S6 were also significantly upregulated in MANF overexpressed N2a cells (**Figures 7B,E,F**).

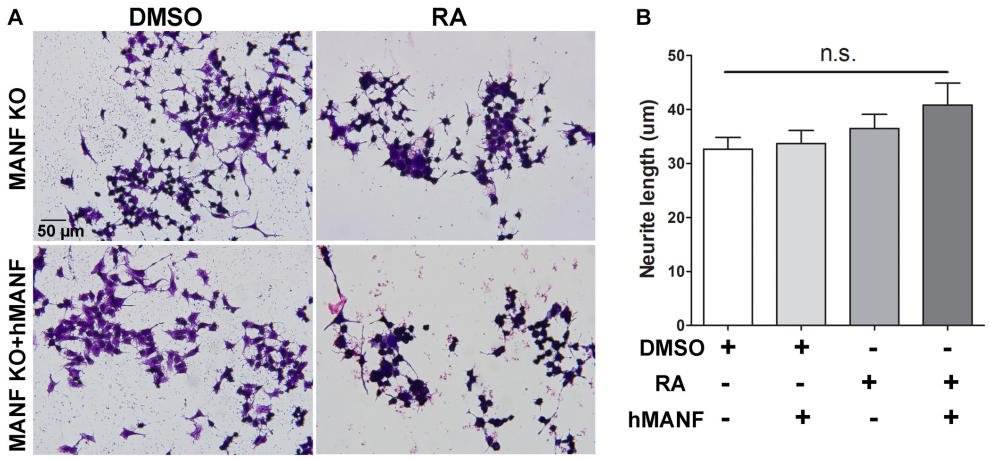

FIGURE 5 | Addition of extracellular hMANF fails to rescue the neurite outgrowth defects in MANF KO cells. **(A)** Representative images of MANF KO N2a cells treated with DMSO or RA for 3 days with or without addition of recombinant hMANF (100 ng/ml). Cells were fixed and stained with crystal violet for visualization. **(B)** Average neurite length was measured, and analyzed by One-way ANOVA followed with the Tukey's *post hoc* test, n.s. not statistically significant. The data were expressed as the mean ± SEM of three independent experiments.

To further confirm that MANF facilitates RA-induced neurite outgrowth via activating Erk/mTOR and Akt/mTOR signaling pathways, control cells were treated with RA and MANF at the presence of Erk inhibitor PD98059 (50 μM), Akt inhibitor MK2206 (2.5 μM), and mTOR inhibitor Torin 1 (50 nM), respectively. PD98059 is a highly selective MEK1 inhibitor, inhibiting the phosphorylation Erk1/2. MK2206 binds to and inhibits the phosphorylation of Thr308 and Ser 473 of Akt, resulting in the inhibition of the PI3K/Akt signaling pathway. Torin 1 is a strong inhibitor for both mTOR-containing complexes, mTORC1 and mTORC2. Treatment of either inhibitors could cause reduced cell proliferation and apoptosis. Dosages for each inhibitor were tested and the minimum dosage that was not toxic to the cells (data not shown) and showed effective inhibition of the phosphorylation of Erk, Akt, and mTOR (**Supplementary Figure S3**), respectively, was used. As expected, the neurite of RA-stimulated N2a cells reached 103.01 ± 27.63 μm after 3 days of treatment. The addition of Erk, Akt, or mTOR inhibitors significantly reduced RA-induced neurite to 34.74 ± 15.32, 36.39 ± 13.77, and 30.75 ± 9.17 μm, respectively (**Figure 8**). More importantly, the inhibitors also eliminated the effect of MANF in enhancing RA-induced neurite outgrowth. When treated with RA plus MANF, the average neurite length reached to 233.13 ± 71.71 μm; while the addition of Erk, Akt, or mTOR inhibitors reduced the average neurite length to 37.84 ± 16.46, 40.09 ± 11.16, and 31.27 ± 13.09 μm, respectively, which were significantly shorter compared to RA plus MANF alone (**Figure 8**).

Next, we tested whether treatment of Erk, Akt, and mTOR activators can rescue the neurite outgrowth defects in MANF KO cells in response to RA treatment. Erk activator PDBu (2 μM), Akt activator SC79 (2.5 μM), and mTOR activator MHY1485 (5 μM) were used at the dosage which was not toxic to the cells and showed effective activation of the phosphorylation of Erk, Akt, and mTOR, respectively (**Supplementary Figure S3**). PDBu is a potent activator of protein kinase C (PKC), which further activates Erk as a downstream PKC target. SC79 inhibits Akt membrane translocation and enhances Akt phosphorylation. MHY1485 is a cell-permeable activator of mTOR that has been shown to increase the phosphorylation of mTOR at Ser2448. We found that when treated separately, none of the activators was able to rescue the phenotype (**Figure 9B**). Considering that it might not be sufficient for the neurite to grow by activating just one of the signaling pathways, we then treated the cells with two or all three activators simultaneously. Interestingly, when treated with Erk and Akt activators together, we observed a slight but significant increase in the neurite length in some of the MANF KO cells from 30.38 ± 9.89 to 40.92 ± 18.16 μm (**Figures 9A,B**). However, none of the other combinations of treatments can rescue the defects of RA-induced neurite outgrowth in MANF KO cells (**Figure 9B**).

MANF Deficiency Impairs Protein Synthesis

Protein synthesis is critical for neurite formation and can be regulated by the activation of Akt/mTOR and Erk/mTOR signaling pathways. Since our data suggests that MANF positively regulates Akt/mTOR and Erk/mTOR signaling, we sought to further test whether protein synthesis was affected in MANF KO cells and whether it was involved in its defect in RA-induced neurite outgrowth. HPG protein synthesis assay revealed that N2a cells had robust protein synthesis. Fluorescent imaging revealed that nascent protein was mainly localized in the cell soma in DMSO treated control cells (**Figure 10A**). For RA treated control cells, fluorescent signal was also detected in the neurites, indicating that nascent protein was also present in the growing neurites (**Figure 10B**, arrowheads). MANF KO cells also exhibit robust fluorescent signal (**Figure 10C**), but it was limited to the cell soma in both DMSO and RA treated groups, indicating

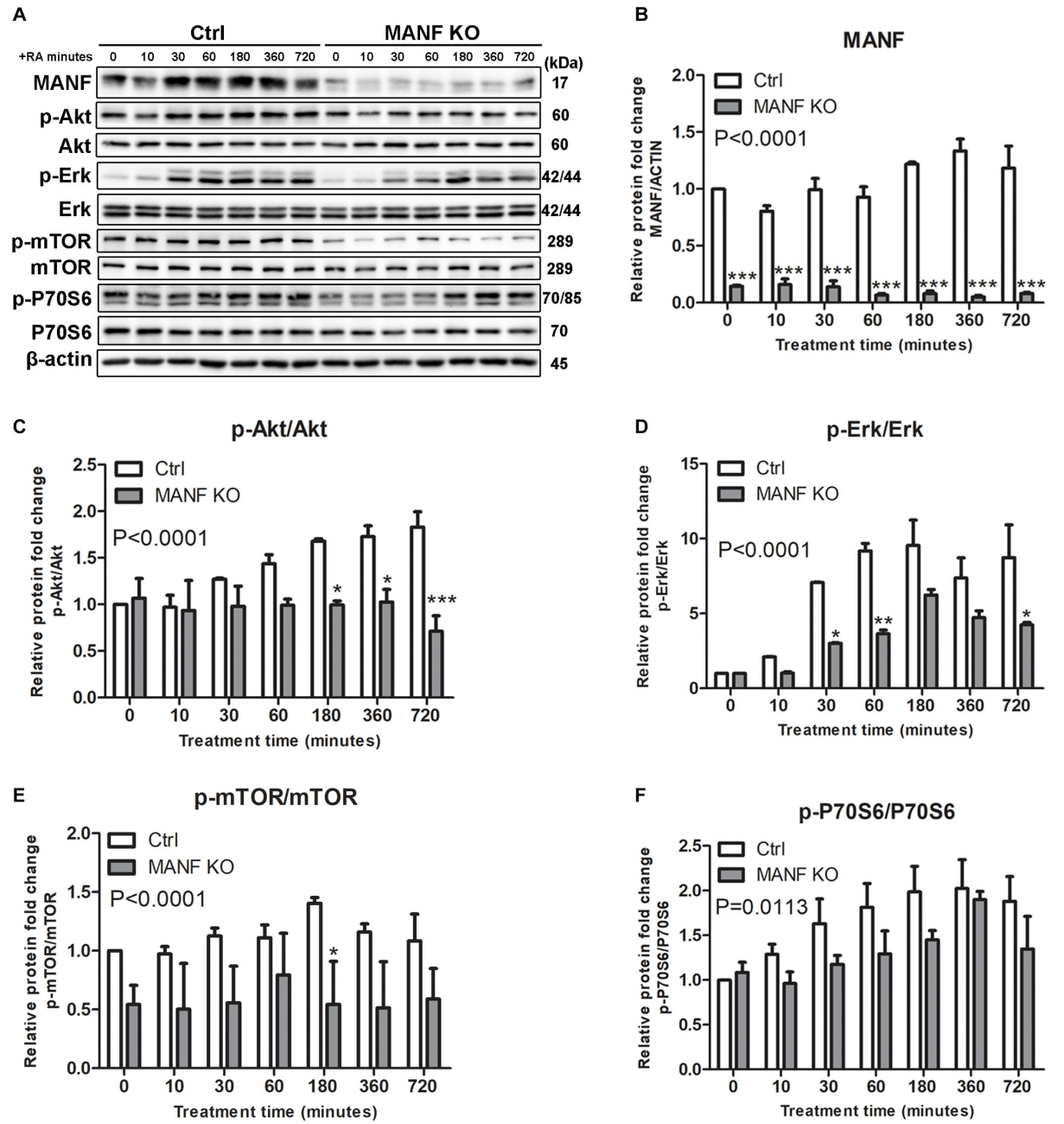

FIGURE 6 | MANF knockout reduces RA-induced activation of Akt/mTOR and Erk/mTOR signaling pathways. **(A)** Control and MANF KO cells were treated with RA for 10, 30, 60, 180, 360, and 720 min. Protein was extracted from cell lysates and subjected to immunoblot. The size of the proteins (kDa) was labeled next to each band. **(B)** MANF protein levels were quantified and normalized with β-actin. **(C)** p-Akt protein levels were quantified and normalized with total Akt. **(D)** p-Erk protein levels were quantified and normalized with total Erk. **(E)** p-mTOR protein levels were quantified and normalized with total mTOR. **(F)** p-P70S6 protein levels were quantified and normalized with total P70S6. The data were expressed as the mean ± SEM of three independent experiments and were analyzed by Two-way ANOVA followed with the Bonferroni's *post hoc* test, $^{*}P < 0.05$, $^{**}P < 0.01$, $^{***}P < 0.001$.

a lack of neurite outgrowth in response to RA (**Figure 10D**). Quantification of the fluorescent intensities revealed that for both control and KO cells, RA treatment resulted in a higher rate of protein synthesis compared to DMSO treatment, and it increased over time (**Figure 10E**). However, MANF KO cells have significantly less fluorescent signal compared to control cells. In addition, we noticed that regardless of RA treatment, a small portion (<5% at 24 and 48 h, ∼10% at 72 h) of control cells showed no nascent protein synthesis during the time of the assay (**Figures 10A,B**, arrows). MANF KO cells, on the other hand, showed significantly higher percentage of cells (∼10% at 24 h, ∼20% at 48 h, ∼35% at 72 h) that were undetectable for nascent

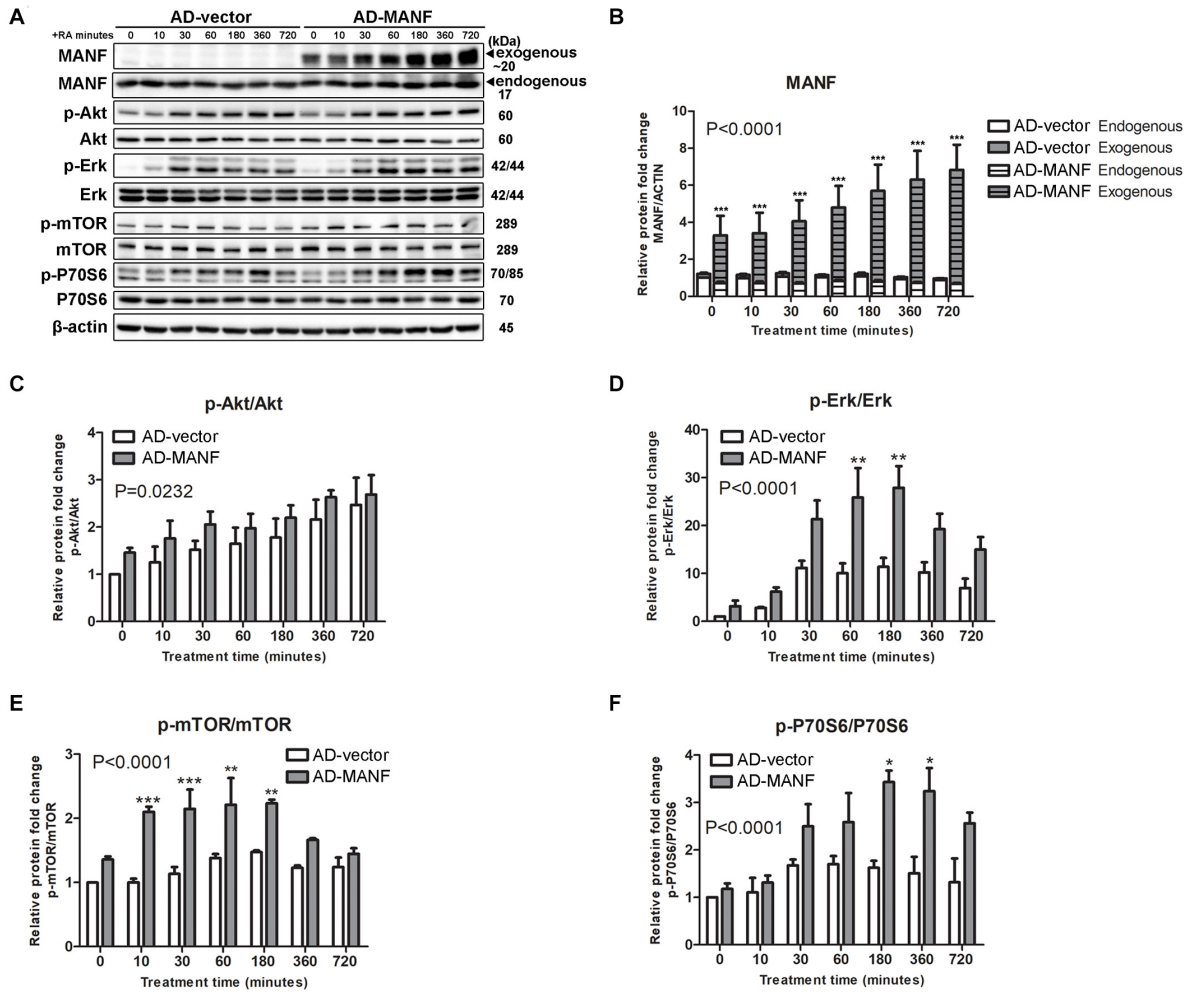

FIGURE 7 | MANF overexpression enhances RA-induced activation of Akt/mTOR and Erk/mTOR signaling pathways. **(A)** AD-vector and AD-MANF transduced cells were treated with RA for 10, 30, 60, 180, 360, and 720 min. Protein was extracted from cell lysates and subjected to immunoblot. The size of the proteins (kDa) was labeled next to each band. **(B)** Endogenous and exogenous MANF protein levels were quantified and normalized with β-actin. **(C)** p-Akt protein levels were quantified and normalized with total Akt. **(D)** p-Erk protein levels were quantified and normalized with total Erk. **(E)** p-mTOR protein levels were quantified and normalized with total mTOR. **(F)** Quantification of p-P70S6 protein levels were quantified and normalized with total P70S6. The data were expressed as the mean ± SEM of three independent experiments and were analyzed by Two-way ANOVA followed with the Bonferroni's *post hoc* test, $^{*}P < 0.05$, $^{**}P < 0.01$, $^{***}P < 0.001$.

protein (**Figure 10C,D**, arrows). These data suggest that MANF deficiency impairs N2a cell protein synthesis, which may further contribute to the neurite outgrowth defects in MANF KO cells.

DISCUSSION

Neurite outgrowth is a critical process for neuron differentiation and regeneration in neurological diseases. In this study, we demonstrated that MANF was necessary for RA-induced neurite outgrowth by positively regulating Akt/mTOR and Erk/mTOR signaling pathways. Neurite outgrowth requires protein synthesis, which is regulated by Akt/mTOR and Erk/mTOR signaling pathways (Read and Gorman, 2009; Doherty et al., 2000). We are the first to show that MANF regulates neurite outgrowth through the regulation of protein synthesis and the activation of Akt/mTOR and Erk/mTOR signaling pathways.

Neuro2a and SH-SY5Y cells are common neuronal cell line models widely used for studying neuronal differentiation *in vitro* due to their ability to proliferate and to be easily transfected compared to primary neuron. Neuronal cell lines can be induced into neuron-like cells, where they turn on the expression of neuronal cell markers and grow neuronal processes resembling axons and dendrites. However, as many neuronal cell lines were derived from immortalized neuronal tumors and have undergone numerous proliferations that could accumulate mutations and may not recapitulate the properties of normal neurons from the nervous system. We used neuronal cell lines N2a and SH-SY5Y to show that RA treatment induced neurite outgrowth and MANF deficiency attenuated this process. It is noted that a cell with longer neurites seems also to present enlarged cell

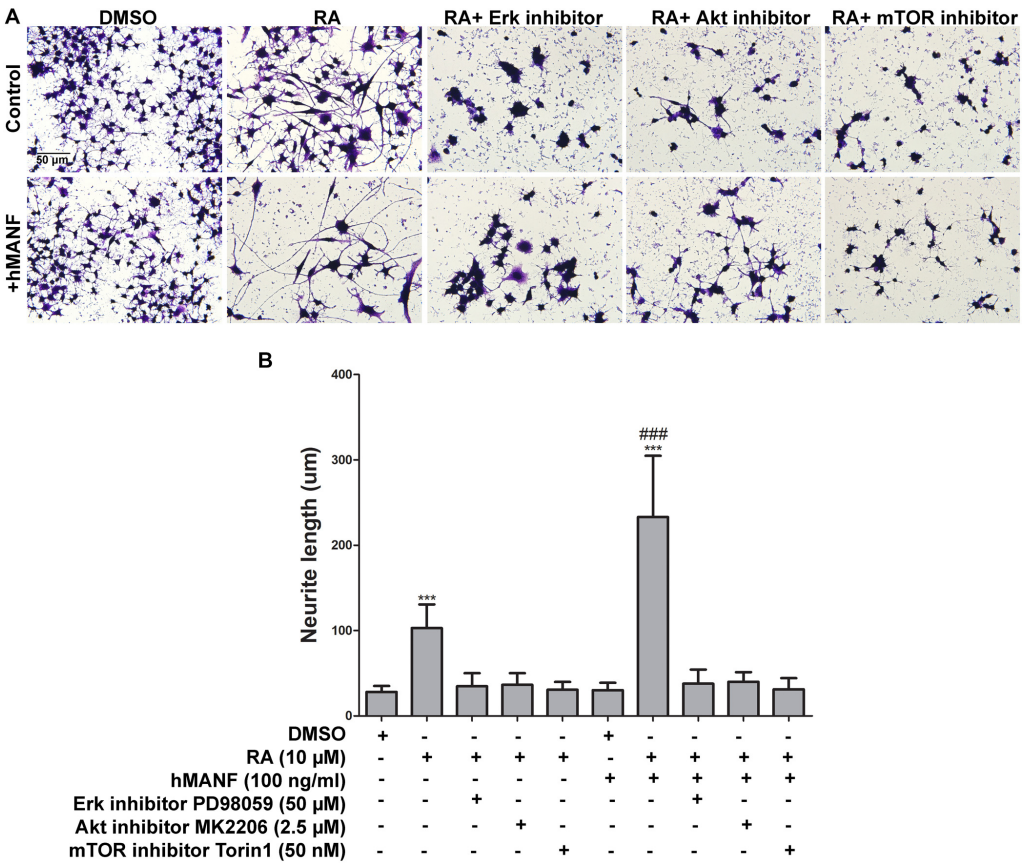

FIGURE 8 | Pharmacological inhibition of Akt, Erk, and mTOR blocks MANF-enhanced neurite outgrowth in response to RA. **(A)** Representative images of N2a cells treated with DMSO or RA or RA+inhibitors for 3 days with or without addition of recombinant hMANF (100 ng/ml). Cells were fixed and stained with crystal violet for visualization. **(B)** Average neurite length was measured, and analyzed by One-way ANOVA followed with the Tukey's *post hoc* test, $^{***}P < 0.0001$ compared to DMSO treated cells, $^{###}P < 0.0001$ compared to RA treated cells. The data were expressed as the mean ± SEM of three independent experiments.

bodies with increased neurite caliber. This suggests that RA treatment may also cause general growth and hypertrophy of the cells. It is essential to confirm cell line results with primary neurons. The role of MANF in neurite extension has been investigated in primary neurons and neural precursors as well as in animals. A study by Ko et al. reported that MANF was required for the neurite extension and maintenance in cultured retinal ganglion cells (RGCs) isolated from 3 to 5 days old rat retina (Ko et al., 2020). Another study by Tseng et al., 2017a reported that complete conventional MANF knockout mice exhibit impaired neurite outgrowth *in vivo*, and MANF-deficient neuronal stem cells isolated from the embryonic day 13.5 (E13.5) knockout mice have defect in neurite extension when cultured and differentiated *in vitro* (Tseng et al., 2017a). However, these studies did not examine the underlying cellular/molecular mechanisms. Our study used neuronal cell lines to confirm the findings and further investigate cell signaling pathways responsible for MANF's effect.

We used both siRNA and CRISPR to generate MANF deficient cells and showed that loss of MANF attenuates the ability of N2a and SH-SY5Y cells to grow neurites in response to RA-stimulation. These methods are complementary. There are two advantages of generating stable MANF knockout using CRISPR: (1) As the effectiveness of siRNA is usually diluted out around 3–4 days after transfection due to cell proliferation, the generation of stable MANF knockout cells allow us to perform experiments with a longer time span, such as the examination of neurite outgrowth with 6 days of RA treatment, which provided evidence of MANF knockout indeed attenuates but not just delays RA-induced neurite outgrowth; (2) The efficiency of siRNA transfection varies depending on the condition of cells and transfection reagents. For example, immunoblotting analysis confirmed that siRNA method only reduced MANF by 50%. MANF knockout using CRISPR had a much better efficiency. However, stable MANF knockout using CRIPSR on the other hand, may trigger compensatory expression of other UPR genes, and transient knock out of MANF by siRNA is able to overcome this shortcoming.

Different from most neurotrophic factors that are secreted, MANF is largely retained in the lumen of the ER and is secreted under pathological conditions where ER stress is elevated (Apostolou et al., 2008; Tadimalla et al., 2008; Glembotski et al., 2012; Oh-Hashi et al., 2012; Henderson et al., 2013). Under normal condition, MANF is retained in the ER via its calcium-dependent interaction with GRP78

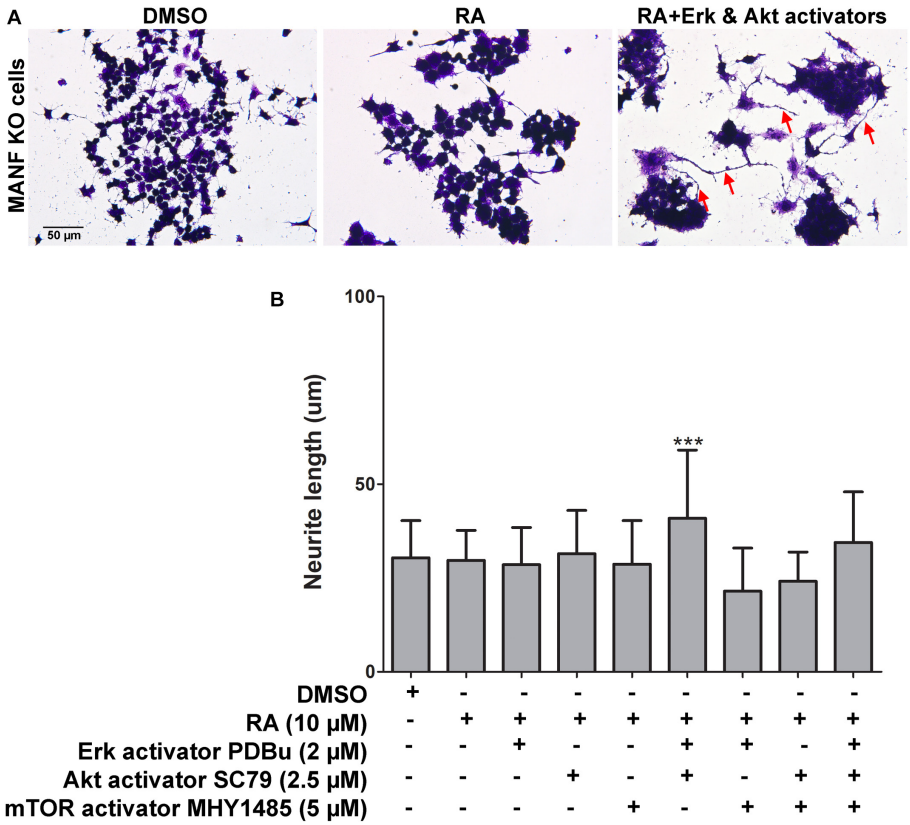

FIGURE 9 | Pharmacological activation of Akt, Erk, and mTOR partially rescues neurite outgrowth defects in MANF KO cells in response to RA. **(A)** Representative images of MANF KO cells treated with DMSO or RA or RA+Akt and Erk activators for 3 days. Cells were fixed and stained with crystal violet for visualization. Red arrows indicate cells with neurite outgrow in response to RA treatment. **(B)** Average neurite length was measured, and analyzed by One-way ANOVA followed with the Tukey's *post hoc* test, $^{***}P < 0.0001$. The data were expressed as the mean ± SEM of three independent experiments.

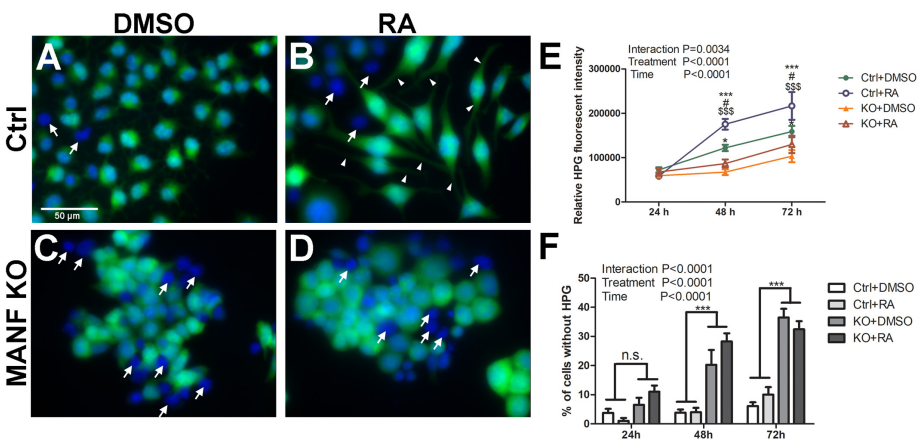

FIGURE 10 | Protein synthesis is reduced in MANF KO cells. Control cells treated with DMSO **(A)** or RA **(B)** and then incubated with HPG. MANF KO cells treated with DMSO **(C)** or RA **(D)** and then incubated with HPG. White arrows indicate cells without HPG signal (cells lacking nascent protein synthesis); white arrow heads indicate neurites with HPG signal. **(E)** HPG fluorescence intensities in control and MANF KO cells were quantified and analyzed by Two-way ANOVA followed with the Bonferroni's *post hoc* test. $^{\#}P < 0.05$ compared to Ctrl DMSO; $^{*}P < 0.05$, $^{***}P < 0.001$ compared to KO DMSO; $^{\$\$\$}P < 0.001$ compared to KO RA. The data were expressed as the mean ± SEM of three independent experiments. **(F)** Percentage of cells without HPG signal was quantified, and analyzed by Two-way ANOVA followed with the Bonferroni's *post hoc* test, $^{***}P < 0.0001$, n.s. not statistically significant. The data were expressed as the mean ± SEM of three independent experiments.

(glucose-regulated protein 78 kDa, BiP) in the lumen of the ER and the binding with endoplasmic reticulum protein retention (KDEL) receptors located on Golgi apparatus and cell surface (Glembotski et al., 2012; Henderson et al., 2013). In pathological conditions with elevated ER-stress, reduced ER calcium level interferes with the binding of MANF and GRP78. ER-stress also induces protein transportation from the ER to Golgi, resulting in an accumulation of MANF and GRP78 in the lumen of Golgi. GRP78 competes with MANF on the binding with KDEL receptors, leading to a decreased retention of MANF in the ER. MANF has been implicated as a neurotrophic factor that regulates neuron development and protects neuron from various pathological conditions (Li-Na et al., 2017; Lindahl et al., 2017). The mechanisms involved in the neuroprotective role of MANF remains unclear, although increasing evidence has suggested the involvement of MANF in ameliorating ER-stress induced apoptosis (Lindahl et al., 2017; Xu M. et al., 2018; Zhang et al., 2017a; Zhang et al., 2017b; Zhu et al., 2016). There are inconsistent reports regarding the role of intracellular and extracellular MANF in the context of neuroprotection. For example, extracellular application of MANF was reported to protect neurons and myocardial cells from ischemic injuries (Tadimalla et al., 2008; Airavaara et al., 2009; Glembotski et al., 2012), while MANF had to be injected directly into neurons to protect against Bax-dependent apoptosis or overexpressed intracellularly in Hela cells to improve cell viability under glucose-free conditions and tunicamycin treatment (Apostolou et al., 2008; Hellman et al., 2011). We showed that either overexpression of MANF intracellularly by adenovirus or addition of recombinant hMANF into cell culture can induce longer neurite outgrowth in response to RA stimulation. However, the addition of MANF in the culture media did not rescue neurite growth in MANF KO cells, indicating that the intracellular MANF plays an important role that is not compensated by MANF in the culture media. One of the limitations of this study is that we were not able to exclude the secretion of adenovirus-mediated MANF from cells, which makes it difficult to distinguish the function of intracellular and extracellular MANF. To further study the function of MANF in these two forms, we need to determine if the intracellularly overexpressed MANF can also increase the level of MANF being secreted and if blocking MANF secretion will affect the role of MANF in facilitating RA-induced neurite outgrowth.

PI3K/Akt and Ras/Erk pathways are important intracellular signal transduction cascades that are critical for fundamental cellular functions, regulating cell proliferation, growth, survival, mobility and cell death (McCubrey et al., 2007; Mendoza et al., 2011). They are often dysregulated in human cancers, leading to aberrant activation of the signaling cascades (Asati et al., 2016). Disturbed activation of the PI3K/Akt/ and Ras/Erk pathways are oncogenic, enhancing the growth, survival, and metabolism of cancer cells (Jokinen and Koivunen, 2015). PI3K/Akt and Ras/Erk signaling pathways are also key mediators for neuronal survival and several aspects of neurite outgrowth, including cell skeleton reorganization and stabilization, neurite branching and extension, and axon formation (Frebel and Wiese, 2006; Read and Gorman, 2009; Hausott and Klimaschewski, 2019). Mammalian target of rapamycin (mTOR) is one of the major downstream effectors of PI3K/Akt and Ras/Erk signaling pathways (Potter et al., 2002; Ma et al., 2005). mTOR is a serine/threonine protein kinase which is a key regulator for cell growth and metabolism by controlling protein translation and lipogenesis (Takei and Nawa, 2014). It promotes protein synthesis through the phosphorylation of P70S6 kinase, which in turn phosphoactivates the ribosomal protein S6 and lead to increased mRNA and protein synthesis (Laplante and Sabatini, 2009). Protein synthesis is essentially required for neurite outgrowth. Increased requirement of new protein synthesis is accompanied with the process of neurite initiation, branching, elongation, and stabilization (Tojima and Ito, 2004; Flynn, 2013). Protein synthesis is important for filopodia and neurite formation (Gallo, 2013; Sainath and Gallo, 2015). Local protein synthesis is critical for axon elongation and pathfinding (Twiss and van Minnen, 2006). Decreased protein synthesis has been reported in various neurodegenerative disorders, such as Alzheimer's disease (Chang et al., 2006). The activation of PI3K/Akt/mTOR and Ras/Erk/mTOR signaling cascades positively regulates protein synthesis, which is critical for cell differentiation and neurite outgrowth in neurons (Fujii et al., 1982; Takei and Nawa, 2014; Schanzenbacher et al., 2016; Rozenbaum et al., 2018).

Several studies have suggested that MANF can activate Akt and Erk signaling pathways. In an *in vitro* study, extracellular MANF was shown to protect human neuroblastoma SH-SY5Y cells from 6-hydroxydopamine (6-OHDA) induced cell death via the activation of PI3K/Akt/mTOR pathway (Hao et al., 2017). In addition to mTOR, several other downstream effectors of the PI3K/Akt signaling pathway including GSK3β, MDM2, and NF-κB have been reported to be activated by treatment of recombinant hMANF in the rodent brain, which was associated with enhanced neuron survival in neurodegenerative diseases and intracerebral hemorrhage models (Hao et al., 2017; Zhang et al., 2017b; Li et al., 2018; Xu M. et al., 2018). MANF has also been reported to activate Erk in a study showing that intracellular MANF overexpression facilitated neuron migration and activated STAT3 and Erk in mice SVZ explant (Tseng et al., 2017a). However, in the same study when NSC cultures were treated with recombinant hMANF, neither Akt nor Erk was activated, suggesting the activation of Akt and Erk by MANF may be cell type- and context-dependent.

We showed that MANF knockout in N2a cells attenuated RA-induced activation of Akt/mTOR and Erk/mTOR, leading to limited neurite outgrowth. MANF overexpression on the other hand lead to longer neurite length which was correlated with increased activation of Akt/mTOR and Erk/mTOR in response to RA. Treatment of Akt, Erk or mTOR inhibitors blocked RA-induced N2a cells neurite outgrowth. Moreover, MANF enhanced neurite outgrowth and Akt/mTOR and Erk/mTOR activation can also be blocked by inhibition of Akt, Erk or mTOR. We observed minimal toxic effect of these inhibitors

at the concentrations we used, although inhibitors appeared to slightly reduce cell density. In general, it is easier for N2a cells to extend longer neurite at lower density, however, we observed reduced neurite outgrowth in RA and RA+MANF groups after inhibitor treatments. As a result, we believe that the effect of these inhibitors on neurite outgrowth did not result from the potential toxicity and alterations in cell density, rather than through the activation of Akt/mTOR and Erk/mTOR signaling cascades.

In line with the insufficient activation of Akt/mTOR and Erk/mTOR signaling pathways, we also observed impaired protein synthesis in MANF deficient cells. Consistent with previous report that decreased protein synthesis was also observed in cultured MANF $^{-/-}$ mice NSCs (Tseng et al., 2017b), our results suggest that the impaired protein synthesis may contribute to the defect of neurite outgrowth in MANF knockout cells.

Our data indicate that MANF facilitates RA-induced neurite outgrowth by positively regulating Akt/mTOR and Erk/mTOR signaling pathways. However, the mechanisms by which MANF activates the Akt/mTOR and ERK/mTOR signaling pathways are currently unknown. In addition, in the experiment of treating MANF KO cells with RA and Akt, Erk or mTOR activators, except for a mild neurite outgrowth in Akt plus Erk activators treated group, none of the other groups showed a rescue in neurite outgrowth. This data indicates that besides Akt/mTOR and Erk/mTOR signaling pathways, there must be other signaling pathways or cellular processes that are affected by MANF knockout and are also important for RA-induced neurite outgrowth. ER stress can be one of the candidate mechanisms, as MANF is known to alleviate ER stress and elevated ER stress is associated with many neurodegenerative diseases and defects in neurite outgrowth (Kawada et al., 2018).

CONCLUSION

In conclusion, our study demonstrated that MANF deficiency attenuates RA-induced neurite outgrowth and MANF overexpression facilitates the growth of longer neurites. This is the first study to demonstrate that MANF regulate neurite outgrowth through activating Akt/mTOR and Erk/mTOR signaling pathways and protein synthesis. This study provides evidence that MANF is involved in neuronal differentiation and it may be a potential candidate to facilitate the regeneration of neuronal processes in neurodegenerative diseases.

DATA AVAILABILITY STATEMENT

All datasets presented in this study are included in the article/**Supplementary Material**.

AUTHOR CONTRIBUTIONS

WW and JL designed the study and contributed to drafting the manuscript. WW, YW, HL, HX, MX, JF, and MM performed the experiment, collated data, and carried out data analyses. All authors have read and approved the final submitted manuscript.

FUNDING

This work was supported by the National Institutes of Health (NIH) grants AA017226 and AA015407. And also supported in part by the Department of Veterans Affairs, Veterans Health Administration, Office of Research and Development [Biomedical Laboratory Research and Development: Merit Review (BX001721)].

ACKNOWLEDGMENTS

We highly appreciate all the help provided by the members of the Department of Pharmacology and Nutritional Sciences and the Center of Biomedical Research Excellence (COBRE) at University of Kentucky.

SUPPLEMENTARY MATERIAL

The Supplementary Material for this article can be found online at: https://www.frontiersin.org/articles/10.3389/fnmol.2020.560020/full#supplementary-material

Supplementary Figure S1 | Expression of exogenous MANF in N2a cells after adenovirus transduction. **(A)** Protein was extracted from cells transduced with AD-vector and AD-MANF at 24, 48, 72, 96, and 120 h after transduction, then subjected to immunoblot. The expression of HA tag and MANF was examined. β-actin was used as a loading control. The size of the proteins (kDa) was labeled next to each band. **(B)** Exogenous MANF protein levels were quantified as relative levels normalized to β-actin. Two-way ANOVA followed with the Bonferroni's *post hoc* test, $^{**}P < 0.01$, $^{***}P < 0.0001$. The data were expressed as the mean ± SEM of three independent experiments.

Supplementary Figure S2 | MANF cannot be reintroduced into MANF KO cells. **(A)** Immunofluorescent images showing control and MANF KO cells were transduced with AD-vector and AD-MANF and then immunolabeled with HA tag (green) and MANF (red). Cell nuclei were stained by DAPI. **(B)** The percentage of cells with HA tag expression was quantified. Student's *t*-test, $^{***}P < 0.0001$. The data were expressed as the mean ± SEM of three independent experiments. **(C)** Protein was extracted from cells 36 h after being incubated with AD-vector and AD-MANF for 1–4 h, and then subjected to immunoblot with HA tag and MANF antibodies. β-actin was used as a loading control. **(D)** Protein was extracted from control and MANF KO cells, and then immunoblot with Cas9 antibody. β-actin was used as a loading control. The size of the proteins (kDa) was labeled next to each band. The experiment was replicated three times.

Supplementary Figure S3 | The effect of pharmacological inhibition or activation of Akt, Erk and mTOR on the expression of p-Akt, p-Erk, and p-mTOR in response to RA treatment. **(A)** Quantification of p-Akt, p-Erk, p-mTOR, and p-P70S6 protein expression in control cells treated with DMSO, RA or RA+inhibitors. β-actin was used as a loading control. One-way ANOVA followed with the Tukey's *post hoc* test, $^{*}P < 0.05$, $^{**}P < 0.01$ compared to DMSO treated group; $^{\#}P < 0.05$, $^{\#\#}P < 0.01$, $^{\#\#\#}P < 0.001$ compared to RA treated group. The data were expressed as the mean ± SEM of three independent experiments. **(B)** Quantification of p-Akt, p-Erk, p-mTOR, and p-P70S6 protein expression in MANF KO cells treated with DMSO, RA or RA+activators. β-actin was used as a loading control. One-way ANOVA followed with the Tukey's *post hoc* test, n.s. not statistically significant, $^{*}P < 0.05$ compared to DMSO treated group; $^{\#}P < 0.05$ compared to RA treated group. The data were expressed as the mean ± SEM of three independent experiments.

REFERENCES

Airavaara, M., Chiocco, M. J., Howard, D. B., Zuchowski, K. L., Peranen, J., Liu, C., et al. (2010). Widespread cortical expression of MANF by AAV serotype 7: localization and protection against ischemic brain injury. *Exp. Neurol.* 225, 104–113. doi: 10.1016/j.expneurol.2010.05.020

Airavaara, M., Shen, H., Kuo, C.-C., Peränen, J., Saarma, M., Hoffer, B., et al. (2009). Mesencephalic astrocyte-derived neurotrophic factor reduces ischemic brain injury and promotes behavioral recovery in rats. *J. Comp. Neurol.* 515, 116–124. doi: 10.1002/cne.22039

Apostolou, A., Shen, Y., Liang, Y., Luo, J., and Fang, S. (2008). Armet, a UPR-upregulated protein, inhibits cell proliferation and ER stress-induced cell death. *Exp. Cell Res.* 314, 2454–2467. doi: 10.1016/j.yexcr.2008.05.001

Asati, V., Mahapatra, D. K., and Bharti, S. K. (2016). PI3K/Akt/mTOR and Ras/Raf/MEK/ERK signaling pathways inhibitors as anticancer agents: Structural and pharmacological perspectives. *Eur. J. Med. Chem.* 109, 314–341. doi: 10.1016/j.ejmech.2016.01.012

Chang, R. C., Yu, M. S., and Lai, C. S. (2006). Significance of molecular signaling for protein translation control in neurodegenerative diseases. *Neurosignals* 15, 249–258. doi: 10.1159/000102599

Chen, Y. C., Sundvik, M., Rozov, S., Priyadarshini, M., and Panula, P. (2012). MANF regulates dopaminergic neuron development in larval zebrafish. *Dev. Biol.* 370, 237–249. doi: 10.1016/j.ydbio.2012.07.030

Cheng, L., Liu, Y., Zhao, H., Zhang, W., Guo, Y. J., and Nie, L. (2013). Lentiviral-mediated transfer of CDNF promotes nerve regeneration and functional recovery after sciatic nerve injury in adult rats. *Biochem. Biophys. Res. Commun.* 440, 330–335. doi: 10.1016/j.bbrc.2013.09.084

Cui, Q. (2006). Actions of neurotrophic factors and their signaling pathways in neuronal survival and axonal regeneration. *Mol. Neurobiol.* 33, 155–179. doi: 10.1385/mn:33:2:155

da Silva, J. S., and Dotti, C. G. (2002). Breaking the neuronal sphere: regulation of the actin cytoskeleton in neuritogenesis. *Nat. Rev. Neurosci.* 3, 694–704. doi: 10.1038/nrn918

Danilova, T., Galli, E., Pakarinen, E., Palm, E., Lindholm, P., Saarma, M., et al. (2019). Mesencephalic Astrocyte-Derived Neurotrophic Factor (MANF) Is Highly Expressed in Mouse Tissues With Metabolic Function. *Front. Endocrinol.* 10:765. doi: 10.3389/fendo.2019.00765

Doherty, P., Williams, G., and Williams, E. J. (2000). CAMs and axonal growth: a critical evaluation of the role of calcium and the MAPK cascade. *Mol. Cell Neurosci.* 16, 283–295. doi: 10.1006/mcne.2000.0907

Flynn, K. C. (2013). The cytoskeleton and neurite initiation. *Bioarchitecture* 3, 86–109. doi: 10.4161/bioa.26259

Frebel, K., and Wiese, S. (2006). Signalling molecules essential for neuronal survival and differentiation. *Biochem. Soc. Trans.* 34, 1287–1290. doi: 10.1042/bst0341287

Fujii, D. K., Massoglia, S. L., Savion, N., and Gospodarowicz, D. (1982). Neurite outgrowth and protein synthesis by PC12 cells as a function of substratum and nerve growth factor. *J. Neurosci.* 2, 1157–1175. doi: 10.1523/jneurosci.02-08-01157.1982

Gallo, G. (2013). Mechanisms underlying the initiation and dynamics of neuronal filopodia: from neurite formation to synaptogenesis. *Int. Rev. Cell Mol. Biol.* 301, 95–156. doi: 10.1016/b978-0-12-407704-1.00003-8

Gao, F. J., Wu, J. H., Li, T. T., Du, S. S., and Wu, Q. (2017). Identification of Mesencephalic Astrocyte-Derived Neurotrophic Factor as a Novel Neuroprotective Factor for Retinal Ganglion Cells. *Front. Mol. Neurosci.* 10:76. doi: 10.3389/fnmol.2017.00076

Glembotski, C. C., Thuerauf, D. J., Huang, C., Vekich, J. A., Gottlieb, R. A., and Doroudgar, S. (2012). Mesencephalic astrocyte-derived neurotrophic factor protects the heart from ischemic damage and is selectively secreted upon sarco/endoplasmic reticulum calcium depletion. *J. Biol. Chem.* 287, 25893–25904. doi: 10.1074/jbc.m112.356345

Gouel, F., Rolland, A. S., Devedjian, J. C., Burnouf, T., and Devos, D. (2019). Past and Future of Neurotrophic Growth Factors Therapies in ALS: From Single Neurotrophic Growth Factor to Stem Cells and Human Platelet Lysates. *Front. Neurol.* 10:835. doi: 10.3389/fneur.2019.00835

Hao, F., Yang, C., Chen, S. S., Wang, Y. Y., Zhou, W., Hao, Q., et al. (2017). Long-Term Protective Effects of AAV9-Mesencephalic Astrocyte-Derived Neurotrophic Factor Gene Transfer in Parkinsonian Rats. *Exp. Neurol.* 291, 120–133. doi: 10.1016/j.expneurol.2017.01.008

Hausott, B., and Klimaschewski, L. (2019). Promotion of Peripheral Nerve Regeneration by Stimulation of the Extracellular Signal-Regulated Kinase (ERK) Pathway. *Anat. Rec.*302, 1261–1267. doi: 10.1002/ar.24126

Hellman, M., Arumäe, U., Yu, L.-Y., Lindholm, P., Peränen, J., Saarma, M., et al. (2011). Mesencephalic astrocyte-derived neurotrophic factor (MANF) has a unique mechanism to rescue apoptotic neurons. *J. Biol. Chem.* 286, 2675–2680. doi: 10.1074/jbc.M110.146738

Henderson, M. J., Richie, C. T., Airavaara, M., Wang, Y., and Harvey, B. K. (2013). Mesencephalic astrocyte-derived neurotrophic factor (MANF) secretion and cell surface binding are modulated by KDEL receptors. *J. Biol. Chem.* 288, 4209–4225. doi: 10.1074/jbc.m112.400648

Houlton, J., Abumaria, N., Hinkley, S. F. R., and Clarkson, A. N. (2019). Therapeutic Potential of Neurotrophins for Repair After Brain Injury: A Helping Hand From Biomaterials. *Front. Neurosci.* 13:790. doi: 10.3389/fnins.2019.00790

Jokinen, E., and Koivunen, J. P. (2015). MEK and PI3K inhibition in solid tumors: rationale and evidence to date. *Ther. Adv. Med. Oncol.* 7, 170–180. doi: 10.1177/1758834015571111

Kawada, K., Mimori, S., Okuma, Y., and Nomura, Y. (2018). Involvement of endoplasmic reticulum stress and neurite outgrowth in the model mice of autism spectrum disorder. *Neurochem. Int.* 119, 115–119. doi: 10.1016/j.neuint.2017.07.004

Kemppainen, S., Lindholm, P., Galli, E., Lahtinen, H. M., Koivisto, H., Hämäläinen, E., et al. (2015). Cerebral dopamine neurotrophic factor improves long-term memory in APP/PS1 transgenic mice modeling Alzheimers disease as well as in wild-type mice. *Behav. Brain Res.* 291, 1–11. doi: 10.1016/j.bbr.2015.05.002

Ko, J.-A., Komatsu, K., Okumichi, H., and Kiuchi, Y. (2020). Functional analysis of mesencephalic astrocyte-derived neurotrophic factor in retinal ganglion cells under oxidative stress. *Cell Biochem. Funct.* doi: 10.1002/cbf.3567

Laplante, M., and Sabatini, D. M. (2009). mTOR signaling at a glance. *J. Cell Sci.* 122, 3589–3594. doi: 10.1242/jcs.051011

Leshchyns'ka, I., and Sytnyk, V. (2016). Reciprocal Interactions between Cell Adhesion Molecules of the Immunoglobulin Superfamily and the Cytoskeleton in Neurons. *Front. Cell Dev. Biol.* 4:9. doi: 10.3389/fcell.2016.00009

Li, H., Wen, W., Xu, H., Wu, H., Xu, M., Frank, J. A., et al. (2019). 4-Phenylbutyric Acid Protects Against Ethanol-Induced Damage in the Developing Mouse Brain. *Alcohol. Clin. Exp. Res.* 43, 69–78.

Li, T., Xu, W., Gao, L., Guan, G., Zhang, Z., He, P., et al. (2018). Mesencephalic astrocyte-derived neurotrophic factor affords neuroprotection to early brain injury induced by subarachnoid hemorrhage via activating Akt-dependent prosurvival pathway and defending blood-brain barrier integrity. *FASEB J.* 33, 1727–1741. doi: 10.1096/fj.201800227rr

Li-Na, Z., Deng, C., Da, X., Si-Han, C., Hai-Jiao, W., and Ling, L. (2017). Mesencephalic astrocyte-derived neurotrophic factor and its role in nervous system disease. *Neurol. Sci.* 38, 1741–1746. doi: 10.1007/s10072-017-3042-2

Lindahl, M., Saarma, M., and Lindholm, P. (2017). Unconventional neurotrophic factors CDNF and MANF: Structure, physiological functions and therapeutic potential. *Neurobiol. Dis.* 97, 90–102. doi: 10.1016/j.nbd.2016.07.009

Lindholm, P., Peranen, J., Andressoo, J. O., Kalkkinen, N., Kokaia, Z., Lindvall, O., et al. (2008). MANF is widely expressed in mammalian tissues and differently regulated after ischemic and epileptic insults in rodent brain. *Mol. Cell Neurosci.* 39, 356–371. doi: 10.1016/j.mcn.2008.07.016

Lindholm, P., Voutilainen, M. H., Lauren, J., Peranen, J., Leppanen, V. M., Andressoo, J. O., et al. (2007). Novel neurotrophic factor CDNF protects and rescues midbrain dopamine neurons in vivo. *Nature* 448, 73–77. doi: 10.1038/nature05957

Lu, J., Luo, L., Huang, D., Liu, X., Xia, X., Wang, Z., et al. (2018). Photoreceptor Protection by Mesencephalic Astrocyte-Derived Neurotrophic Factor (MANF). *eNeuro* 5:29687079.

Ma, L., Chen, Z., Erdjument-Bromage, H., Tempst, P., and Pandolfi, P. P. (2005). Phosphorylation and functional inactivation of TSC2 by Erk implications for tuberous sclerosis and cancer pathogenesis. *Cell* 121, 179–193. doi: 10.1016/j.cell.2005.02.031

McCubrey, J. A., Steelman, L. S., Chappell, W. H., Abrams, S. L., Wong, E. W., Chang, F., et al. (2007). Roles of the Raf/MEK/ERK pathway in cell growth,

malignant transformation and drug resistance. *Biochim. Biophys. Acta* 1773, 1263–1284. doi: 10.1016/j.bbamcr.2006.10.001

Mendoza, M. C., Er, E. E., and Blenis, J. (2011). The Ras-ERK and PI3K-mTOR pathways: cross-talk and compensation. *Trends Biochem. Sci.* 36, 320–328. doi: 10.1016/j.tibs.2011.03.006

Missaire, M., and Hindges, R. (2015). The role of cell adhesion molecules in visual circuit formation: from neurite outgrowth to maps and synaptic specificity. *Dev. Neurobiol.* 75, 569–583. doi: 10.1002/dneu.22267

Mizobuchi, N., Hoseki, J., Kubota, H., Toyokuni, S., Nozaki, J., Naitoh, M., et al. (2007). ARMET is a soluble ER protein induced by the unfolded protein response via ERSE-II element. *Cell Struct. Funct.* 32, 41–50. doi: 10.1247/csf.07001

Neves, J., Zhu, J., Sousa-Victor, P., Konjikusic, M., Riley, R., Chew, S., et al. (2016). Immune modulation by MANF promotes tissue repair and regenerative success in the retina. *Science* 353:aaf3646. doi: 10.1126/science.aaf3646

Oh-Hashi, K., Tanaka, K., Koga, H., Hirata, Y., and Kiuchi, K. (2012). Intracellular trafficking and secretion of mouse mesencephalic astrocyte-derived neurotrophic factor. *Mol. Cell Biochem.* 363, 35–41. doi: 10.1007/s11010-011-1155-0

Palgi, M., Lindstrom, R., Peranen, J., Piepponen, T. P., Saarma, M., and Heino, T. I. (2009). Evidence that DmMANF is an invertebrate neurotrophic factor supporting dopaminergic neurons. *Proc. Natl. Acad. Sci. U S A* 106, 2429–2434. doi: 10.1073/pnas.0810996106

Paolino, A., Fenlon, L. R., Suarez, R., and Richards, L. J. (2018). Transcriptional control of long-range cortical projections. *Curr. Opin. Neurobiol.* 53, 57–65. doi: 10.1016/j.conb.2018.05.005

Petrova, P., Raibekas, A., Pevsner, J., Vigo, N., Anafi, M., Moore, M. K., et al. (2003). MANF: a new mesencephalic, astrocyte-derived neurotrophic factor with selectivity for dopaminergic neurons. *J. Mol. Neurosci.* 20, 173–188. doi: 10.1385/jmn:20:2:173

Pillai-Kastoori, L., Heaton, S., Shiflett, S. D., Roberts, A. C., Solache, A., and Schutz-Geschwender, A. R. (2020a). Antibody validation for Western blot: By the user, for the user. *J. Biol. Chem.* 295, 926–939. doi: 10.1074/jbc.ra119.010472

Pillai-Kastoori, L., Schutz-Geschwender, A. R., and Harford, J. A. (2020b). A systematic approach to quantitative Western blot analysis. *Anal. Biochem.* 593:113608. doi: 10.1016/j.ab.2020.113608

Potter, C. J., Pedraza, L. G., and Xu, T. (2002). Akt regulates growth by directly phosphorylating Tsc2. *Nat. Cell Biol.* 4, 658–665. doi: 10.1038/ncb840

Read, D. E., and Gorman, A. M. (2009). Involvement of Akt in neurite outgrowth. *Cell Mol. Life Sci.* 66, 2975–2984. doi: 10.1007/s00018-009-0057-8

Rodriguez, O. C., Schaefer, A. W., Mandato, C. A., Forscher, P., and Bement, W. M. (2003). Conserved microtubule-actin interactions in cell movement and morphogenesis. *Nat. Cell Biol.* 5, 599–609. doi: 10.1038/ncb0703-599

Rozenbaum, M., Rajman, M., Rishal, I., Koppel, I., Koley, S., Medzihradszky, K. F., et al. (2018). Translatome Regulation in Neuronal Injury and Axon Regrowth. *eNeuro* 5, ENEURO.276–217.

Sainath, R., and Gallo, G. (2015). Cytoskeletal and signaling mechanisms of neurite formation. *Cell Tissue Res.* 359, 267–278. doi: 10.1007/s00441-014-1955-0

Salto, R., Vilchez, J. D., Giron, M. D., Cabrera, E., Campos, N., Manzano, M., et al. (2015). beta-Hydroxy-beta-Methylbutyrate (HMB) Promotes Neurite Outgrowth in Neuro2a Cells. *PLoS One* 10:e0135614. doi: 10.1371/journal.pone.0135614

Schanzenbacher, C. T., Sambandan, S., Langer, J. D., and Schuman, E. M. (2016). Nascent Proteome Remodeling following Homeostatic Scaling at Hippocampal Synapses. *Neuron* 92, 358–371. doi: 10.1016/j.neuron.2016.09.058

Tadimalla, A., Belmont, P. J., Thuerauf, D. J., Glassy, M. S., Martindale, J. J., Gude, N., et al. (2008). Mesencephalic astrocyte-derived neurotrophic factor is an ischemia-inducible secreted endoplasmic reticulum stress response protein in the heart. *Circ. Res.* 103, 1249–1258. doi: 10.1161/circresaha.108.180679

Takei, N., and Nawa, H. (2014). mTOR signaling and its roles in normal and abnormal brain development. *Front. Mol. Neurosci.* 7:28. doi: 10.3389/fnmol.2014.00028

Tojima, T., and Ito, E. (2004). Signal transduction cascades underlying de novo protein synthesis required for neuronal morphogenesis in differentiating neurons. *Prog. Neurobiol.* 72, 183–193. doi: 10.1016/j.pneurobio.2004.03.002

Tseng, K. Y., Anttila, J. E., Khodosevich, K., Tuominen, R. K., Lindahl, M., Domanskyi, A., et al. (2017a). MANF Promotes Differentiation and Migration of Neural Progenitor Cells with Potential Neural Regenerative Effects in Stroke. *Mol. Ther.* 26, 238–255. doi: 10.1016/j.ymthe.2017.09.019

Tseng, K.-Y., Tatiana, D., Andrii, D., and Mart, S. (2017b). MANF Is Essential for Neurite Extension and Neuronal Migration in the Developing Cortex. *eNeuro* 4, ENEURO.214–217.

Twiss, J. L., and van Minnen, J. (2006). New insights into neuronal regeneration: the role of axonal protein synthesis in pathfinding and axonal extension. *J. Neurotrauma.* 23, 295–308. doi: 10.1089/neu.2006.23.295

Voutilainen, M. H., Back, S., Porsti, E., Toppinen, L., Lindgren, L., Lindholm, P., et al. (2009). Mesencephalic astrocyte-derived neurotrophic factor is neurorestorative in rat model of Parkinsons disease. *J. Neurosci.* 29, 9651–9659. doi: 10.1523/jneurosci.0833-09.2009

Wang, H., Ke, Z., Alimov, A., Xu, M., Frank, J. A., Fang, S., et al. (2014). Spatiotemporal expression of MANF in the developing rat brain. *PLoS One* 9:e90433. doi: 10.1371/journal.pone.0090433

Xu, M., Wang, S., Wang, Y., Wu, H., Frank, J. A., Zhang, Z., et al. (2018). Role of p38γ MAPK in regulation of EMT and cancer stem cells. *Biochim. Biophys. Acta Mol. Basis Dis.* 1864, 3605–3617. doi: 10.1016/j.bbadis.2018.08.024

Xu, W., Gao, L., Li, T., Zheng, J., Shao, A., and Zhang, J. (2018). Mesencephalic Astrocyte-Derived Neurotrophic Factor (MANF) Protects Against Neuronal Apoptosis via Activation of Akt/MDM2/p53 Signaling Pathway in a Rat Model of Intracerebral Hemorrhage. *Front. Mol. Neurosci.* 11:176. doi: 10.3389/fnmol.2018.00176

Yang, S., Huang, S., Gaertig, M. A., Li, X. J., and Li, S. (2014). Age-dependent decrease in chaperone activity impairs MANF expression, leading to Purkinje cell degeneration in inducible SCA17 mice. *Neuron* 81, 349–365. doi: 10.1016/j.neuron.2013.12.002

Zhang, J., Cai, Q., Jiang, M., Liu, Y., Gu, H., Guo, J., et al. (2017a). Mesencephalic astrocyte-derived neurotrophic factor alleviated 6-OHDA-induced cell damage via ROS-AMPK/mTOR mediated autophagic inhibition. *Exp. Gerontol.* 89, 45–56. doi: 10.1016/j.exger.2017.01.010

Zhang, J., Tong, W., Sun, H., Jiang, M., Shen, Y., Liu, Y., et al. (2017b). Nrf2-mediated neuroprotection by MANF against 6-OHDA-induced cell damage via PI3K/AKT/GSK3beta pathway. *Exp. Gerontol.* 100, 77–86. doi: 10.1016/j.exger.2017.10.021

Zhu, W., Li, J., Liu, Y., Xie, K., Wang, L., and Fang, J. (2016). Mesencephalic astrocyte-derived neurotrophic factor attenuates inflammatory responses in lipopolysaccharide-induced neural stem cells by regulating NF-kappaB and phosphorylation of p38-MAPKs pathways. *Immunophar. Immunotoxicol* 38, 205–213. doi: 10.3109/08923973.2016.1168433

Conflict of Interest: The authors declare that the research was conducted in the absence of any commercial or financial relationships that could be construed as a potential conflict of interest.

frontiers in Molecular Neuroscience

REVIEW
published: 15 February 2021
doi: 10.3389/fnmol.2021.642016

New Insights Into the Intricacies of Proneural Gene Regulation in the Embryonic and Adult Cerebral Cortex

*Ana-Maria Oproescu[1,2], Sisu Han[1,3] and Carol Schuurmans[1,2,3]**

[1] Sunnybrook Research Institute, Biological Sciences Platform, Toronto, ON, Canada, [2] Department of Laboratory Medicine and Pathobiology, University of Toronto, Toronto, ON, Canada, [3] Department of Biochemistry, University of Toronto, Toronto, ON, Canada

Historically, the mammalian brain was thought to lack stem cells as no new neurons were found to be made in adulthood. That dogma changed ∼25 years ago with the identification of neural stem cells (NSCs) in the adult rodent forebrain. However, unlike rapidly self-renewing mature tissues (e.g., blood, intestinal crypts, skin), the majority of adult NSCs are quiescent, and those that become 'activated' are restricted to a few neurogenic zones that repopulate specific brain regions. Conversely, embryonic NSCs are actively proliferating and neurogenic. Investigations into the molecular control of the quiescence-to-proliferation-to-differentiation continuum in the embryonic and adult brain have identified proneural genes encoding basic-helix-loop-helix (bHLH) transcription factors (TFs) as critical regulators. These bHLH TFs initiate genetic programs that remove NSCs from quiescence and drive daughter neural progenitor cells (NPCs) to differentiate into specific neural cell subtypes, thereby contributing to the enormous cellular diversity of the adult brain. However, new insights have revealed that proneural gene activities are context-dependent and tightly regulated. Here we review how proneural bHLH TFs are regulated, with a focus on the murine cerebral cortex, drawing parallels where appropriate to other organisms and neural tissues. We discuss upstream regulatory events, post-translational modifications (phosphorylation, ubiquitinylation), protein–protein interactions, epigenetic and metabolic mechanisms that govern bHLH TF expression, stability, localization, and consequent transactivation of downstream target genes. These tight regulatory controls help to explain paradoxical findings of changes to bHLH activity in different cellular contexts.

Keywords: *Neurog1*, *Neurog2*, *Ascl1*, phosphorylation, protein–protein interactions, protein stability, epigenetic control, translational control

OPEN ACCESS

Edited by:
Estela Maris Muñoz, CONICET Dr. Mario H. Burgos Institute of Histology and Embryology (IHEM), Argentina

Reviewed by:
Alessandro Sessa, San Raffaele Hospital (IRCCS), Italy
Itaru Imayoshi, Kyoto University, Japan
Diogo S. Castro, University of Porto, Portugal

****Correspondence:***
Carol Schuurmans
carol.schuurmans@sunnybrook.ca;
cschuurm@sri.utoronto.ca

Received: *15 December 2020*
Accepted: *26 January 2021*
Published: *15 February 2021*

Citation:
Oproescu A-M, Han S and Schuurmans C (2021) New Insights Into the Intricacies of Proneural Gene Regulation in the Embryonic and Adult Cerebral Cortex. Front. Mol. Neurosci. 14:642016. doi: 10.3389/fnmol.2021.642016

INTRODUCTION

One-hundred years ago, Santiago Ramon y Cajal likened the pyramidal cells of the cerebral cortex to "a garden filled with innumerable trees. . .which can multiply their branches thanks to intelligent cultivation, send their roots deeper, and produce more exquisite flowers and fruits every day" (Jones, 1994). In his 1942 book Man on His Nature, neurophysiologist Sir Charles Sherrington compared the electrical activity of the cortex to "an enchanted loom" (Sherrington, 2009). The field of neuroscience is ripe with such metaphors that remark upon the exquisite

architecture and cellular diversity of the cerebral cortex. It follows, then, that one of the most dominant inquiries in developmental neuroscience has been how this enormous cellular diversity is established and choreographed during brain development. Detangling this great mystery has important implications for our understanding of neurological disorders and diseases, as well as for the future design of therapeutic strategies to replace lost/dysfunctional neural cells.

This review centers on the regulatory events that govern proneural gene function in the developing and adult cerebral cortex. To provide a contextual framework, we first provide a high-level overview, not meant to be comprehensive, of the cellular context in which these genes function. The cerebral cortex, which is the seat of higher order cognitive functioning and sensory processing, is comprised of a six-layered neocortex and several three- or four-layered allocortical territories, including the hippocampal formation and paleocortex. Cortical territories are found in all mammals, but display enormous structural diversity across species, transitioning during evolution between smooth (lissencephalic) structures in smaller mammals such as rodents, to highly folded (gyrencephalic) structures in most extant primates and larger mammals (Lewitus et al., 2014). These gross structural differences arise due to species-specific differences in the regulatory events that control self-renewal, proliferation, mode of division (symmetric, asymmetric) and differentiation properties of neural stem cells (NSCs) and their daughter neural progenitor cells (NPCs). Distinguishing features of NSCs include maintenance into adulthood, the capacity to self-renew, and multipotency, which refers to their tri-lineage potential, or the capacity to give rise to neurons, astrocytes and oligodendrocytes. Conversely, NPCs do not self-renew, are more restricted in their proliferative potential, and may have reduced developmental potential as they acquire lineage biases.

To understand how the cerebral cortex acquires species-specific forms, it is essential to elucidate how NSC/NPC (hereafter NPC for simplicity) fate decisions are controlled. Proneural genes, which encode basic-helix-loop-helix (bHLH) transcription factors (TFs), are critical pieces to the puzzle as they control NPC decisions to divide or differentiate while also specifying neural subtype identities (Bertrand et al., 2002; Wilkinson et al., 2013; Guillemot and Hassan, 2017; Dennis et al., 2019). At face value, the functions of proneural genes appear simplistic, but their activities are tightly regulated by both cell intrinsic and extrinsic influences. Here we review the regulatory mechanisms that govern proneural gene function in embryonic and adult cortical domains, drawing parallels to other bHLH genes, brain regions, non-neural tissues, and non-mammalian species when comparison is informative. Of note, unless otherwise specified, the animal work cited was conducted using murine transgenic models, tissues or cells.

Introduction to Proneural Genes

Proneural genes encode type II, tissue-specific bHLH TFs that are expressed in the nervous system and have evolutionarily conserved roles in promoting neural cell fate specification and differentiation (Bertrand et al., 2002; Wilkinson et al., 2013; Guillemot and Hassan, 2017; Dennis et al., 2019). Proneural genes were first identified and characterized in *Drosophila melanogaster* where they belong to two main families that each specify distinct neural cell fates: *achaete-scute* complex (AS-C) and *atonal*-related genes (Bertrand et al., 2002; Huang et al., 2014). In the fly, bHLH genes that are defined as proneural are expressed in uncommitted ectodermal precursors and have the ability to: (1) select single ectodermal precursors within a proneural cluster to become neural by activating Notch/Delta-mediated lateral inhibition, and (2) specify neural precursor identity by activating generic and subtype-specific neuronal differentiation genes. While vertebrate and invertebrate proneural genes share several features, a major difference is that in vertebrates, proneural gene expression initiates in NPCs that are already specified as neural. With this difference in mind, vertebrate bHLH genes are defined as proneural if they: (1) are expressed in dividing NPCs, usually those at the apex of lineage hierarchies, (2) drive NPCs to differentiate into neuronal or glial cells, (3) specify neural subtype identities, and (4) activate Notch signaling in neighboring NPCs by inducing the expression of Notch ligands, such as *Dll1* and *Dll3* (Bertrand et al., 2002; Wilkinson et al., 2013; Guillemot and Hassan, 2017; Dennis et al., 2019). Based on these criteria, four proneural genes are expressed in the developing and/or adult cerebral cortex: *Neurogenin (Neurog) 1, Neurog2*, *Neurod4* (aka *Math3*), and *Achaete-scute family bHLH transcription factor 1* (*Ascl1;* aka *Mash1*) (Bertrand et al., 2002; Wilkinson et al., 2013; Guillemot and Hassan, 2017; Dennis et al., 2019). All other commonly studied neural bHLH genes, such as *Neurod1, Neurod2, Neurod6* and others are instead properly termed 'neuronal differentiation' genes because of their later expression/function in neural lineages, either in later-stage progenitors with a restricted proliferative and differentiation potential [e.g., *Neurod1* (Pleasure et al., 2000)], and/or in postmitotic neurons [e.g., *Neurod2, Neurod6* (Bormuth et al., 2013; Guzelsoy et al., 2019)]. In this review we mainly focus on the cortical functions of *Neurog1, Neurog2* and *Ascl1*, which have been most extensively studied.

To bind DNA, proneural bHLH TFs must dimerize, either with other proneural TFs or with type I bHLH factors, also known as E-proteins (Murre et al., 1989). E-proteins, which have more ubiquitous expression patterns than class II bHLH TFs, are encoded by three genes: *Tcf4* (aka *E2-2*), *Tcf12* (aka *HEB*), and *Tcf3* (aka *E2A*), the latter encoding E12 and E47 splice variants (Bertrand et al., 2002; Wang and Baker, 2015). Proneural TFs can also dimerize with HLH proteins of the Id (inhibitor of DNA-binding) family, which lack the basic DNA-binding domain and thus form non-functional heterodimers (Wang and Baker, 2015). To activate transcription, bHLH dimers bind to Ephrussi-box (E-box) sequences (CANNTG) in regulatory regions of the genome (Murre et al., 1989; Wang and Baker, 2015). ChIP-seq analyses have revealed that different proneural TF binding sites have differential enrichment of the central two E-box residues; Neurog2 favors CAKMTG motifs (K: G/T nucleotides, M: A/C nucleotides), with the CAGATG motif predominant, while Ascl1 preferentially binds sites with CAGSTG motifs (S: G/C nucleotides), with the CAGCTG motif predominant (Wapinski et al., 2013; Raposo et al., 2015; Aydin et al., 2019). Despite these known biases, the binding of proneural TF hetero- or

homo-dimers to their cognate sites is highly context-specific and tightly regulated, which is the subject of this review.

A Primer on Neocortical Development

To set the stage for the embryonic context in which proneural TFs function, we briefly outline critical developmental transitions. The neurons and macroglial cells (oligodendrocytes, astrocytes) that make up the adult cerebral cortex are derived from multipotent NPCs located in the dorsal telencephalon (cortex), with some additional contributions from ventral telencephalic (subcortical) NPCs. Telencephalic NPCs are parcellated into apical and basal compartments (Taverna et al., 2014). Apical NPCs reside in the ventricular zone (VZ), a single cell-layered neurepithelium that appears pseudostratified due to interkinetic nuclear migration, with G2/M-phase nuclei moving to the apical surface whereas S-phase nuclei move basally (Taverna et al., 2014). Apical NPCs are termed neuroepithelial cells (NECs) prior to neurogenesis and initially divide symmetrically to expand the NPC pool (Gotz and Huttner, 2005). When neurogenesis begins, at approximately embryonic day (E) 11 in mouse, NECs transform into apical radial glia (aRG), which remain in the VZ, but switch to self-renewing asymmetric neurogenic divisions to give rise to one aRG and either one new neuron (direct neurogenesis) or one basal progenitor (indirect neurogenesis) (Gotz and Huttner, 2005; Bultje et al., 2009). aRG and NECs differ at the transcriptomic level, with aRGs initiating the expression of several glial markers (Taverna et al., 2014). In rodents, basal progenitors, which form a subventricular zone (SVZ), predominantly include neuronal-committed intermediate progenitor cells (INPs) that have a limited proliferative capacity (1–2 divisions) and undergo terminal symmetric neurogenic divisions (Haubensak et al., 2004; Miyata et al., 2004; Noctor et al., 2004; Englund et al., 2005; Kowalczyk et al., 2009; Taverna et al., 2014). Further stratifications of these apical and basal NPC pools have been made based on morphological and gene expression criteria and are reviewed elsewhere (Taverna et al., 2014).

Cortical NPCs give rise in a sequential fashion to excitatory glutamatergic neurons that form the six layers of the cortical plate between E11-E17 in mouse (Caviness, 1982; Caviness et al., 1995; Takahashi et al., 1999), followed by astrocytes, beginning at E16 (Bayraktar et al., 2014), and then oligodendrocytes, beginning early postnatally (Kessaris et al., 2006). The earliest-born cortical neurons form a preplate that is later split into an overlying marginal zone (layer I) and an underlying subplate (layer VII), the latter a transient neuronal layer that nevertheless plays important roles in thalamocortical axonal pathfinding and in guiding neuronal migration (Ohtaka-Maruyama, 2020). Layer VI corticothalamic neurons are born next, followed by the sequential differentiation of layer V subcerebral and callosal neurons, layer IV internal granular layer neurons, and finally, layer II/III corticocortical neurons, two layers that are fused in mouse (Caviness, 1982; Kast and Levitt, 2019). GABAergic interneurons and oligodendrocytes also populate cortical domains, but they are born in the ventral telencephalic (subcortical) VZ/SVZ and enter the cortex via tangential migration (Peyre et al., 2015).

The progressive nature of laminar fate determination raises the question of how cortical NPCs change over time (Pearson and Doe, 2004). Seminal studies involving heterochronic transplantation experiments in ferrets revealed that early-stage cortical NPCs are multipotent, responding to new environmental signals to generate alternative laminar identities post-transplant, but only when in S-phase of the cell cycle, whereas later stage cortical NPCs lose their ability to respond to early environmental signals (McConnell and Kaznowski, 1991; Frantz and McConnell, 1996; Bohner et al., 1997; Desai and McConnell, 2000). These findings were corroborated by retroviral lineage tracing experiments, which confirmed that *early* cortical NPCs are multipotent and give rise to neuronal clones that span cortical layers, whereas *late* NPCs are fate restricted and only generate upper layer neurons (Luskin et al., 1988; Price and Thurlow, 1988; Walsh and Cepko, 1988). More recently, genetic lineage tracing experiments using various Cre drivers (Franco et al., 2012; Guo et al., 2013; Eckler et al., 2015) and Mosaic Analysis with Double Markers (MADM) (Gao et al., 2014) have confirmed that cortical NPCs are multipotent at the population and clonal level, although some fate-restricted NPCs may also exist (Franco et al., 2012; Gil-Sanz et al., 2015). How NPCs give rise to such diverse neural cell types in a stereotypically defined manner has been the subject of study for several decades now (Pearson and Doe, 2004). The importance of intrinsic factors was demonstrated by plating cortical NPCs at clonal density, which generated stereotyped lineage trees that matched those seen *in vivo* (Qian et al., 2000). Since then, revolutionary new technologies such as FlashTag and single cell (sc) RNA-seq have identified sequential transcriptional waves that successively define apical and basal NPCs and daughter neurons (Telley et al., 2016). Further studies with these techniques identified two axes of NPC transcriptional organization throughout the neurogenic period: a "birthdate axis" in which the transcriptional state varies depending on embryonic age, and a "differentiation axis," which drives NPCs to differentiate in a conserved sequence regardless of neuronal birthdate (Telley et al., 2019). Interestingly, this work showed that late-stage apical NPCs (E14/E15) have predominantly environment-sensing transcriptional properties, with activation of genetic programs related to ion transport and cell-cell or cell-matrix interaction-related processes, as opposed to the cell-intrinsic transcriptional programs in earlier apical NPCs (Telley et al., 2019).

From these pioneering studies of cortical NPCs, *Neurog2* was highlighted as a critical 'neurogenic' (actually, proneural) gene as it is expressed at high levels in apical and basal NPCs and at low levels in newborn neurons (Telley et al., 2016), consistent with earlier immunostaining studies (Hand et al., 2005). Functional assays demonstrating that *Neurog1* and *Neurog2* are true proneural genes pre-dated these studies by a decade or more and involved classical loss- and gain-of-function assays (Fode et al., 2000; Parras et al., 2002; Schuurmans et al., 2004; Mattar et al., 2008; Dixit et al., 2011, 2014; Kovach et al., 2013; Han et al., 2018). From these studies, *Neurog2* and *Neurog1* were shown to be necessary and sufficient to specify the excitatory, glutamatergic neuronal identity of early-born (layer V, VI) cortical neurons, as well as Cajal-Retzius neurons, which populate layer I (Dixit et al., 2014). In contrast, *Ascl1*, which is expressed at the highest levels in subcortical NPCs,

is necessary and sufficient to specify a GABAergic neuronal or oligodendrocyte fate in the ventral telencephalon (Casarosa et al., 1999; Horton et al., 1999; Schuurmans et al., 2004; Parras et al., 2007). Interestingly, *Ascl1* is also expressed at lower levels in cortical NPCs (Britz et al., 2006), where it also biases NPCs toward an oligodendrocyte fate (Han et al., 2020). In addition, *Ascl1* is also required for the generation of a subset of glutamatergic Cajal-Retzius neurons, as opposed to the GABAergic fates specified by this TF in ventral telencephalic domains, highlighting the importance of cell context in dictating how these proneural genes function (Dixit et al., 2011). Finally, the transient expression of *Neurog2* and *Ascl1* in newborn neurons also has functional consequences, as these genes play a role in guiding neuronal migration by regulating expression of the Rho GTPases, *Rnd2* and *Rnd3*, respectively (Heng et al., 2008; Pacary et al., 2011, 2013).

Lissencephalic Versus Gyrencephalic Cortical Development

Studies of non-human primates (NHP) and human cortices have revealed that the apical NPC pool has expanded to include both aRG and outer or basal RG (bRG), the latter forming a large outer SVZ (oSVZ) not present in rodents (Lukaszewicz et al., 2005; Zecevic et al., 2005; Bayatti et al., 2008; Martinez-Cerdeno et al., 2012; Dehay et al., 2015). Like aRG, bRG are self-renewing and generate neurons by giving rise to transit-amplifying INPs (Fietz et al., 2010; Hansen et al., 2010; Reillo et al., 2011). However, INPs divide several more times in gyrencephalic species than in rodents to generate more later-born, upper-layer or supragranular neurons that make primate cortices larger with many folds (Molnar et al., 2011; Falk and Hofman, 2012; Stahl et al., 2013; Pollen et al., 2015) (**Figure 1A**). Several genes that promote basal NPC expansion can induce cortical folding in lissencephalic mammals, such as mice, or alter folding in gyrencephalic species, such as ferrets (Hansen et al., 2010; Fietz et al., 2012; Stahl et al., 2013; de Juan Romero et al., 2015; Florio et al., 2015, 2018; Ju et al., 2016; Wang et al., 2016; Fiddes et al., 2018; Suzuki et al., 2018; Chizhikov et al., 2019). Conversion from a lissencephalic to gyrencephalic cortex is also associated with alterations of the simple radial trajectories of migrating neurons in lissencephalic species, to more circuitous, tangential routes in gyrencephalic species (Del Toro et al., 2017; Llinares-Benadero and Borrell, 2019). Recent studies have revealed an unexpected role for *Neurog2* and *Ascl1* co-expression in sustaining a lissencephalic form in the rodent cortex due to the essential role that double$^+$ NPCs play in patterning Notch signaling, which impacts the symmetry of radial glial trajectories (Han et al., 2020).

Embryonic Versus Adult Neurogenesis

While NSCs persist into adulthood, they differ from embryonic NSCs in several ways. Firstly, the adult NSC transcriptional profile is more closely related to astrocytes than to embryonic NSCs (Beckervordersandforth et al., 2010). Secondly, most embryonic NSCs are actively dividing and neurogenic, whereas adult NSCs are mainly quiescent and gliogenic (Gotz et al., 2016). Indeed, up to 90% of adult NSCs are quiescent in the adult brain at any given time, with cell cycle times ranging from 1 day to 3 months (Ponti et al., 2013; Reeve et al., 2017). Adult NSCs that become 'activated' are also restricted to a few neurogenic zones and repopulate only specific brain regions. For instance, the ventricular-subventricular zone (V-SVZ) repopulates the murine olfactory bulb and human striatum, while the subgranular zone (SGZ) repopulates the mouse/human dentate gyrus (Spalding et al., 2013; Ernst et al., 2014; Urban and Guillemot, 2014; Gotz et al., 2016; Boldrini et al., 2018; Ruddy and Morshead, 2018; Sorrells et al., 2018). Outside of these niches, the adult NSC response is limited.

Conversely, most embryonic NSCs divide rapidly *in vivo*, with cell cycle times of 8–18 h (Takahashi et al., 1995). However, a small but important pool of embryonic NSCs is slow-dividing; these are the embryonic precursors of adult NSCs, the origins of which had remained elusive until recently (Furutachi et al., 2013, 2015; Fuentealba et al., 2015). Using barcoding, a genetic lineage tracing method that can identify clonal relationships between widely distributed cells, it was revealed that a subset of E13.5-E15.5 aRG, termed 'pre-B1 cells,' are set aside as slow-dividing NPCs that will later become adult B1 cells (Fuentealba et al., 2015) (**Figure 1B**). B1 cells are adult NSCs, which when activated give rise to transit amplifying intermediate precursor cells (IPCs, C cells) that generate neuroblasts (A cells) that migrate through the rostral migratory stream (RMS) to the olfactory bulb (Li and Clevers, 2010). B1 cells retain regional identities; dorsal NSCs give rise to glutamatergic juxtaglomerular neurons (JGNs), ventral NSCs to calbindin$^+$ periglomerular cells (PGCs) and granule cells (GCs), and septal NSCs to calretinin$^+$ PGCs and GCs (Brill et al., 2009; Fuentealba et al., 2015). With respect to the focus of this review, for adult NSCs to become activated and neurogenic, neural determinants such as *Neurog2* and *Ascl1,* which are expressed at high levels in embryonic NSCs and low levels in adult NSCs, must be upregulated (Gotz et al., 2016; Guillemot and Hassan, 2017). We discuss the associated regulatory mechanisms herein.

INTERSECTION BETWEEN PRONEURAL GENES AND EXTRACELLULAR SIGNALING PATHWAYS

Notch Signaling Controls Proneural Gene Expression and Oscillations

Neurog2 and *Ascl1* are classical proneural genes, rapidly inducing NPC cell cycle exit and differentiation when misexpressed in the embryonic cortex (Britz et al., 2006; Mattar et al., 2008; Kovach et al., 2013; Wilkinson et al., 2013). Yet curiously, *Neurog2* (Hagey and Muhr, 2014) and *Ascl1* (Castro et al., 2011; Li et al., 2014) can also induce proliferation when expressed in some cellular contexts. Moreover, during normal development, *Neurog1, Neurog2* and *Ascl1* are mainly expressed in dividing NPCs (Britz et al., 2006). These findings raise the question of how proneural gene expression is compatible with both pro-proliferative and pro-differentiative NPC phenotypes. This

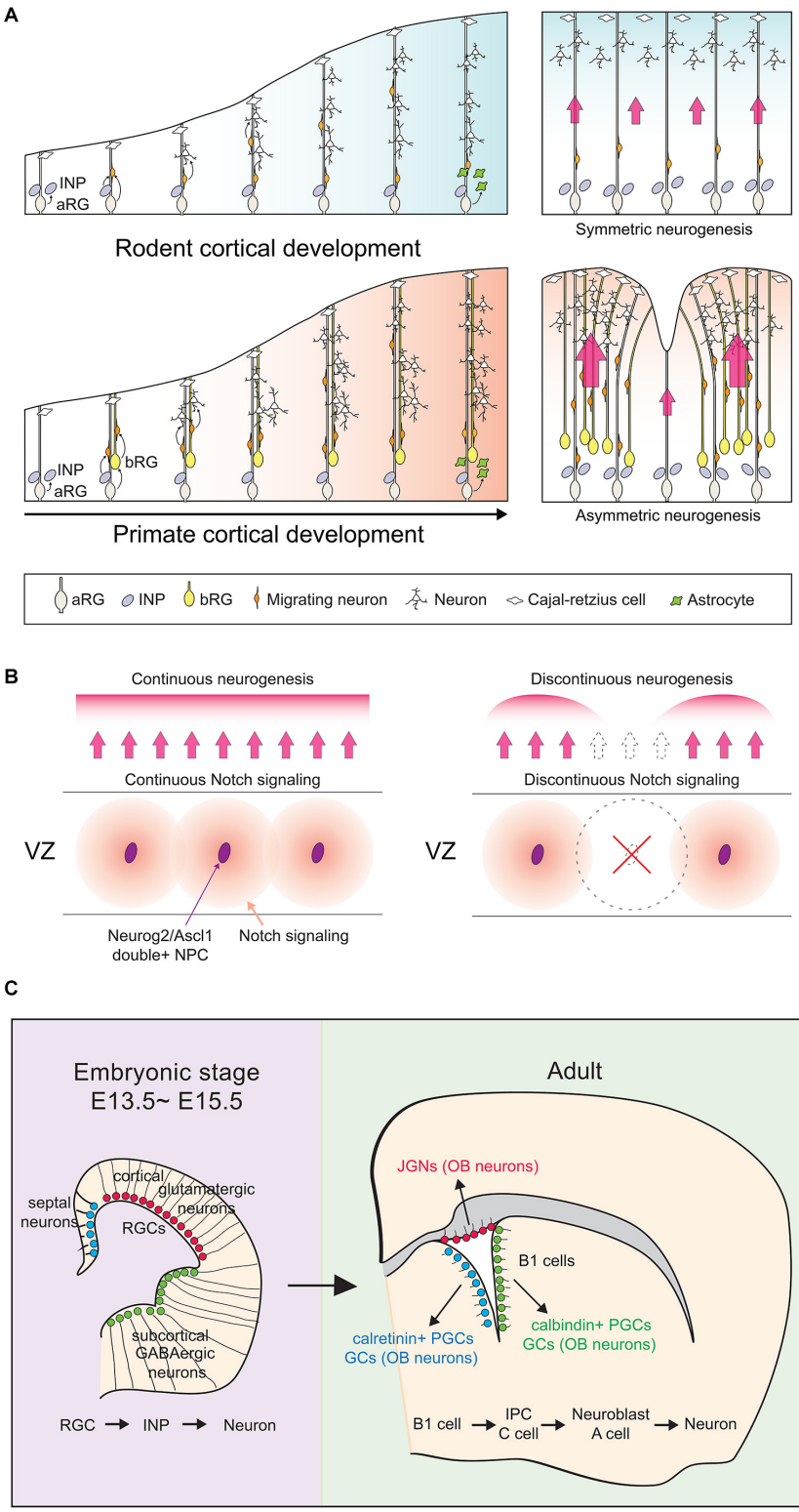

FIGURE 1 | Cortical development between species and developmental stages. **(A)** In both lissencephalic and gyrencephalic species, apical radial glial (aRG) cells can divide asymmetrically to give rise to another aRG and either a nascent neuron (direct neurogenesis) or a neuronal-committed intermediate neuronal progenitor (INP; indirect neurogenesis). Gyrencephalic species like primates have an additional population of radial glial cells, the basal RG (bRG), which contribute more dividing INP cells to in turn generate more upper layer neurons in primate cortices. In the panels on the right, red arrows signify migratory routes of nascent neurons

(Continued)

FIGURE 1 | Continued
traveling along aRG processes. Larger arrows signify cortical regions with increased neurogenesis. **(B)** *Neurog2/Ascl1* double-positive NPCs (purple ovals) act as 'niche' cells in the ventricular zone (VZ) of the rodent cortex, preventing the formation of cortical folds by maintaining continuous Notch signaling patterns. **(C)** Unlike the majority of actively dividing apical radial glia in E13.5–15.5 cortices, a subset remains quiescent and is set aside to become adult neural stem cells, the 'B1' cells. B1 cells reside in the adult cortical VZ and retain their regional identities. For adult B1 cells to exit quiescence and become neurogenic, upregulation of a cortical proneural gene like *Neurog2* or *Ascl1* must occur. aRG, apical radial glia; INP, intermediate neuronal progenitor; bRG, basal radial glia; JGN, juxtaglomerular neuron; OB, olfactory bulb; PGC, periglomerular cell; GC, granule cell.

conundrum was partially resolved in ground-breaking studies that demonstrated that *Neurog2* and *Ascl1* are expressed in 2–3 hr oscillatory cycles in dividing NPCs versus at sustained levels in NPCs that differentiate (Shimojo et al., 2008; Imayoshi et al., 2013; Ochi et al., 2020).

Notch signaling is the driving force behind oscillatory proneural gene expression (Kageyama et al., 2008, 2020) (**Figure 2**). In a process known as 'lateral inhibition,' NPCs that express high levels of the proneural TFs transactivate the expression of cell-membrane tethered Notch ligands such as *Dll1* and *Dll3* (Castro et al., 2006; Henke et al., 2009), which bind Notch receptors on neighboring NPCs. Upon ligand binding, Notch is proteolytically cleaved to form a Notch intracellular domain (NICD) that translocates to the nucleus where it binds to Rbpj, a DNA binding protein. NICD-Rbpj complexes transcribe downstream genes, including *hairy and enhancer of split* (*Hes*) *1* and *Hes5*, which encode bHLH transcriptional repressors that recruit Groucho/TLE co-repressors and bind to N-boxes (CACNAG), directly repressing proneural gene transcription to form a lateral inhibitory loop (Kageyama et al., 2007, 2008, 2020; Kovach et al., 2012; Huang et al., 2014). *Hes1* is also expressed in 2–3 h oscillatory cycles, and Hes1 protein drives its dynamic expression through direct repression of its own transcription, as well as indirectly driving oscillatory expression of the proneural genes through transcriptional repression (Shimojo et al., 2008, 2011). Consequently, *Hes* and proneural genes are expressed out-of-phase with one another in 'salt-and-pepper' expression profiles, referring to their scattered expression when captured at individual time points (Kageyama et al., 2008). Notably, while these oscillatory cycles are transcriptionally driven, proneural proteins also oscillate as they have short intracellular half-lives (< 30 min) and are rapidly degraded with each transcriptional cycle (Nguyen et al., 2006; Kovach et al., 2013; Urban et al., 2016).

While sustained proneural TF expression biases NPCs toward differentiation, it can also maintain the NPC pool by allowing neighboring NPCs with activated Notch signaling to continue to proliferate. *Hes1/5*-mediated repression of proneural genes is essential to maintain the NPC pool, with co-deletion of *Hes1/5* or *Rbpj*, their upstream regulator (Son et al., 2020), leading to precocious neurogenesis and NPC pool depletion (Ohtsuka et al., 1999; Hatakeyama et al., 2004). Strikingly, proneural genes also regulate the patterning of Notch signaling, with NPCs that co-express *Neurog2* and *Ascl1* acting as Notch-ligand expressing niche cells, the deletion of which disrupts the continuity of Notch signaling, resulting in cortical folding (Han et al., 2020) (**Figure 1B**).

Notably, there is also evidence for a Notch-independent mode of Rbpj function in regulation of bHLH TFs. While Rbpj suppresses *Neurog1* transcription in NPCs, it positively regulates *Neurog1* expression in migrating postmitotic neurons independent of Notch pathway activation (Son et al., 2020). Thus, as shown for *Neurog2* (Hand et al., 2005), *Neurog1* is expressed in dividing NPCs and newborn neurons, but distinct regulatory mechanisms drive its expression in the two cell types (Son et al., 2020). Interestingly, Rbpj also binds a conserved binding motif in the *Ascl1* promoter in the locus coeruleus (Shi et al., 2012), and Rbpj directly represses *Atoh7*, another bHLH proneural gene, in a Notch-independent fashion in the retina (Miesfeld et al., 2018). Further studies are required to elucidate the extent to which Rbpj regulates *Neurog1, Neurog2,* and *Ascl1* expression through Notch-dependent and -independent modes in the embryonic cortex.

Ras/ERK Signaling Regulates a *Neurog2-Ascl1* Toggle Switch

During embryogenesis, cortical NPCs differentiate into glutamatergic neurons and later astrocytes, but retain the potential to divert to embryonic subcortical fates (GABAergic neurons, oligodendrocytes), as revealed by the mutation of several cortical transcription factors (Theil et al., 1999; Stoykova et al., 2000; Tole et al., 2000; Muzio et al., 2002a,b; Schuurmans et al., 2004; Kroll and O'Leary, 2005), or when Ras/ERK signaling is ectopically activated (Chandran et al., 2003; Gabay et al., 2003; Hack et al., 2004; Kessaris et al., 2006; Li et al., 2014) (**Figure 2**). These events all induce a *Neurog2* to *Ascl1* transition and drive a dorsal-to-ventral re-specification of NPCs, indicating a lineage bifurcation point regulated by Neurog2 and Ascl1. While Neurog2 and Ascl1 both function as transcriptional activators themselves (Castro and Guillemot, 2011; Kovach et al., 2013), they are mutually transcriptionally cross-repressive; in *Neurog2* null mutants, *Ascl1* is upregulated and subcortical phenotypes are generated in the cortex (Fode et al., 2000; Schuurmans et al., 2004), while conversely, *Ascl1* can repress *Neurog2* expression when misexpressed in cortical NPCs (Han et al., 2020). *Neurog2* is also required to repress *Ascl1* expression in multipotent retinal progenitor cells (Hufnagel et al., 2010). Given that Neurog2 functions as a transcriptional activator, the mechanism for its repression of *Ascl1* transcript and protein expression is indirect, and remains to be fully elucidated. Partial features include that Neurog2 acts through a yet unknown transcriptional regulator to repress *Etv1* expression, which indirectly regulates *Ascl1* expression through repression of *Hes5*, a known transcriptional repressor of *Ascl1* (Kovach et al., 2013). Notably, proneural gene cross-repression in the cortex may be limited to competing lineage determinants

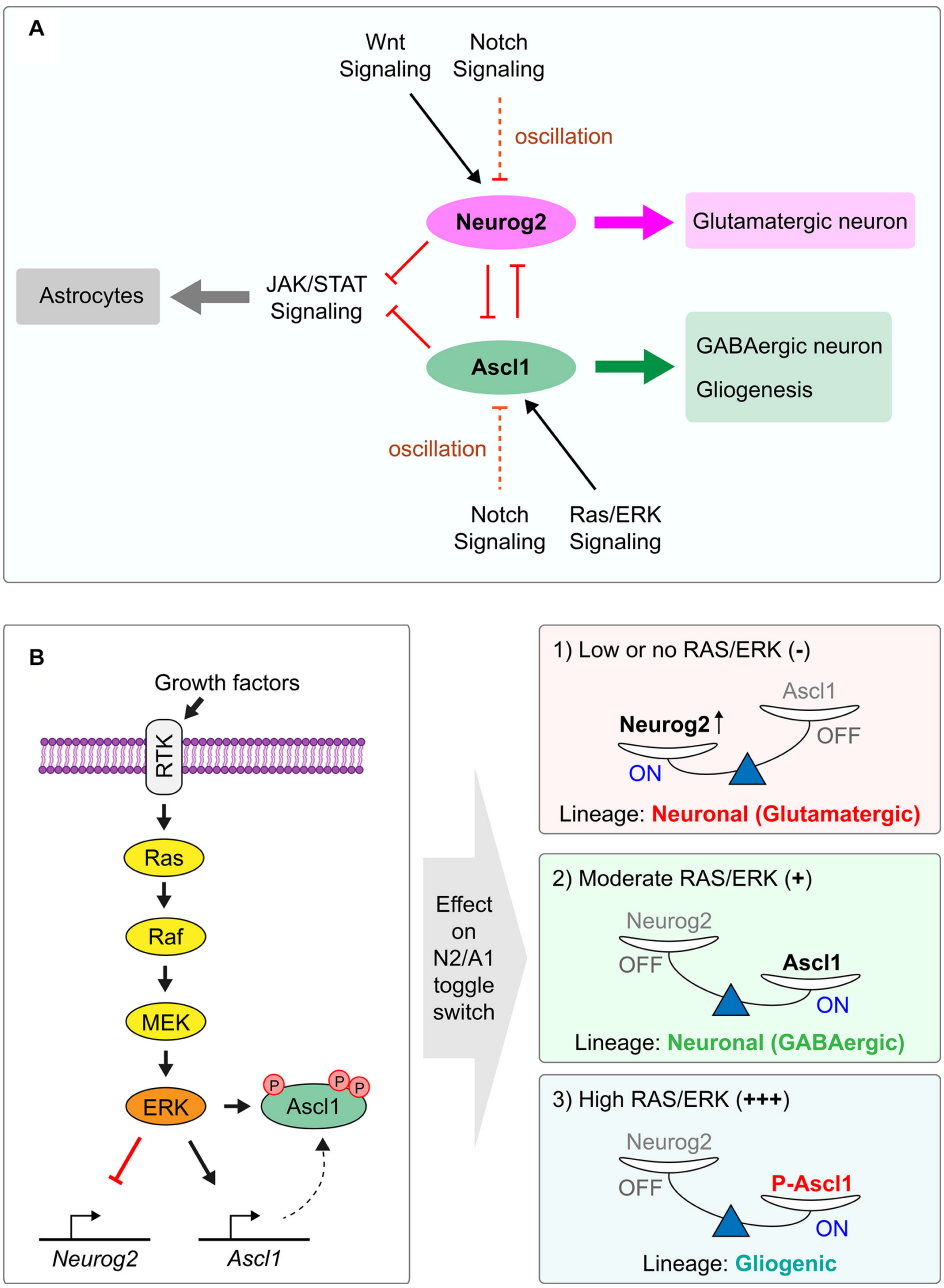

FIGURE 2 | Regulation of the *Neurog2/Ascl1* proneural gene toggle switch by extracellular signaling pathways. **(A)** Proneural TFs *Neurog2* and *Ascl1* are competing lineage determinants in the cortex, specifying glutamatergic pyramidal neurons and GABAergic interneurons, respectively. *Neurog2* and *Ascl1* have cross-repressive interactions with each other and form a bistable toggle switch, preventing lineage commitment in double-positive NPCs. Environmental signals regulate the expression of each gene to turn on the expression of one proneural TF and turn off the other. Notch signaling controls expression of both *Neurog2* and *Ascl1* through lateral inhibition, with Hes1 protein driving the 2–3 h transcriptional oscillatory cycles of the proneural genes. Extracellular Wnt promotes *Neurog2* and suppresses *Ascl1* expression, acting in early neurogenesis. Conversely, Ras/ERK signaling favors *Ascl1* over *Neurog2* expression. **(B)** Ras/ERK signaling cascade activation is achieved by ligand binding to RTK, culminating in the phosphorylation of Ascl1 protein and activation of Ascl1 expression, tipping the Neurog2/Ascl1 toggle switch in favor of Ascl1. At moderate Ras/ERK activation, this leads to GABAergic neuronal specification by Ascl1, while at higher levels of Ras/ERK activation, this leads to gliogenic specification by phosphorylated Ascl1.

such as *Neurog2* and *Ascl1* (Han et al., 2020), as *Neurog2* is instead required to positively regulate the transcription of the functionally related proneural gene, *Neurog1* (Fode et al., 2000). However, mutant analyses in the retina revealed that in the absence of *Neurog2, Ascl1* or *Neurod4*, the other two bHLH genes are upregulated (Akagi et al., 2004), indicative of cross-repressive interactions that further support context-specific functions of these genes.

Strikingly, *Neurog2* and *Ascl1* are also cross-repressive at the functional level; *Neurog2* inhibits the ability of *Ascl1* to promote a glioblast fate, while *Ascl1* inhibits the ability of *Neurog2* to specify a glutamatergic neuronal identity in cortical NPCs (Han et al., 2020) (**Figure 2**). This cross-repression at the protein level may be mediated by the formation of less transcriptionally active Neurog-Ascl1 heterodimers, reviewed in greater detail below. Taken together, these findings invoke comparisons to other stem cell systems in which pairs of TFs that specify different cell fates are in some instances co-expressed in the same progenitor cell, and their mutual cross-antagonism prevents fate specification and differentiation to maintain cellular bi- or multi-potency (Chickarmane et al., 2009; Dillon, 2012; Okawa et al., 2016; Brand and Morrissey, 2020). The co-expression of distinct lineage determinants has the added purpose of 'priming' progenitor cells for subsequent lineage selection, as downstream genes in either lineage can be readily transcribed. In the lingo of computational biologists, antagonistic TF pairs form a gene regulatory network motif known as a toggle switch (Huang et al., 2007; Chickarmane et al., 2009; Enver et al., 2009; Zandi et al., 2010; Strasser et al., 2012). Based on these operational criteria, *Neurog2* and *Ascl1* form a toggle switch to prevent lineage commitment in the embryonic cortex (Han et al., 2020).

Ras/ERK signaling is a critical regulator of the *Neurog2-Ascl1* toggle switch, and therefore it is important to understand how this signal transduction pathway is regulated in the embryonic cortex (Li et al., 2014). Ras/ERK signaling is activated by both pro-proliferative growth factors, such as epidermal growth factor (Egf) and fibroblast growth factor (Fgf) (Ghosh and Greenberg, 1995; Vaccarino et al., 1999; Raballo et al., 2000; Lukaszewicz et al., 2002; Imamura et al., 2008; Wang et al., 2009), and by pro-differentiative factors, including *platelet-derived growth factor* (*PDGF*) (Menard et al., 2002), *nerve growth factor* (*Ngf*) (Greene and Tischler, 1976; Vaudry et al., 2002), *neurotrophin 3* (*Ntf3*) (Lukaszewicz et al., 2002; Ohtsuka et al., 2009), and *brain derived neurotrophic factor* (*Bdnf*) (Barnabe-Heider and Miller, 2003; Ito et al., 2003; Medina et al., 2004; Fukumitsu et al., 2006; Bartkowska et al., 2007). Each of these signals bind receptor tyrosine kinase (RTK) receptors. The kinetics of RTK/ERK signaling is critical to its function, in that the apparently divergent effects of RTK/ERK signaling on proliferation versus differentiation are explained by the ability of Ngf/Ntrk1 to activate ERK in a sustained manner, whereas Fgf induces strong, transient ERK activation (Marshall, 1995; York et al., 1998). Mechanistic insights have also been gained into how Fgf activation biases NPCs to acquire an oligodendrocyte fate, both in the telencephalon and spinal cord (Gabay et al., 2003; Furusho et al., 2011; Li et al., 2014; Farreny et al., 2018), where Fgf acts in combination with Shh in an evolutionarily conserved manner (Esain et al., 2010). Mechanistically, downstream activation of ERK directly phosphorylates Ascl1, and higher levels of RAS/ERK activation biases this proneural TF to preferentially transactivate glioblast genes instead of promoting a GABAergic neuronal identity (Li et al., 2014).

During cortical development, activation of Ras/ERK signaling is spatially and temporally regulated, as revealed by the dynamic expression of phospho-p44/42 MAPK (Erk1/2) (Thr202/Tyr204), which is initially detected in the antihem adjacent to the lateral pallium where neurogenesis is first initiated in the cortex (Miyama et al., 1997), before spreading across the VZ by E14.5 (Li et al., 2014). Notably, the expression of pErk1/2 matches the pattern of expression of fibroblast growth factor receptor 3 (*FGFR3)* and a set of ets-domain transcription factors activated downstream of RTK signaling, including *Etv1, Etv4* and *Etv5* (Hasegawa et al., 2004; Li et al., 2014). The Etv transcription factors act as downstream effectors of FGF signaling and participate in regulating the *Neurog2-Ascl1* toggle switch; *Neurog2* indirectly represses *Etv1,* which in turn indirectly represses *Ascl1* as described above (Kovach et al., 2013). Taken together, these studies highlight the multiple points of intersection between the RAS/ERK signal transduction pathways and proneural genes.

Wnt Signaling Promotes *Neurog2* Expression in a Temporally Defined Manner

Consistent with a role for canonical Wingless/INT (Wnt) signaling in specifying a cortical identity, two transgenic reporters for this pathway, BAT-gal (Maretto et al., 2003) and TCF-lacZ (Liu et al., 2006), are both expressed at higher levels in the dorsal versus ventral telencephalon (Backman et al., 2005; Machon et al., 2005; Li et al., 2012). Upon Wnt binding to LRP/Frizzled receptor complexes, β-catenin (encoded by *Ctnnb1*) is stabilized and translocates to the nucleus where it forms active transcriptional complexes with Tcf1. Conditional knock-out (cKO) of *Ctnnb1* in early cortical NPCs, prior to neurogenesis, downregulates *Neurog2* and upregulates *Ascl1* expression (Backman et al., 2005). Conversely, the addition of exogenous Wnts allows dissociated dorsal telencephalic chick cells or murine cortical neurospheres, which normally ventralize rapidly (Gabay et al., 2003), to maintain their dorsal identity *in vitro* (Gunhaga et al., 2003; Machon et al., 2005; Watanabe et al., 2005). Similarly, misexpression of *Ctnnb1* in subcortical NPCs induces ectopic *Neurog1/2* expression and suppresses *Ascl1* (Hirabayashi et al., 2004; Backman et al., 2005). Thus, the Wnt pathway also controls the *Neurog2-Ascl1* toggle switch, biasing NPCs toward *Neurog2* expression and a cortical cell fate (**Figure 2**).

Wnt reporter activity drops off dramatically in cortical NPCs in mid-neurogenesis (E15.5-E16.5), correlating with the time when *Neurog2* function is attenuated (Backman et al., 2005; Machon et al., 2005; Li et al., 2012). In the absence of Wnts, glycogen synthase kinase (GSK) is activated, forming a destruction complex with axin, APC and other molecules that phosphorylates and targets β-catenin for degradation. GSK3 also directly phosphorylates Neurog2 during mid-late corticogenesis through phosphorylation (Li et al., 2012), which promotes the formation of Neurog2-E47 heterodimers at the expense of more transcriptionally active Neurog2-Neurog2 homodimers (Li et al., 2012). Notably, Neurog2-E47 heterodimers have longer half-lives than Neurog2-Neurog2 homodimers, so their reduced transcriptional activity is not due to enhanced degradation (Li et al., 2012), but rather due to DNA binding preferences, as discussed further below. Therefore, Wnt signaling intersects

Neurog2 function at a few levels, not only promoting Neurog2 expression, but also regulating its activity.

Intersection Between Astrocytic Signals and Proneural Genes

Several signaling pathways induce cortical NPCs to differentiate into astrocytes (Stipursky et al., 2012), including: (1) cytokines, such as cardiotrophin-1 (CT-1), leukemia inhibitory factor (LIF), and ciliary neurotrophic factor (CNTF), all of which activate JAK/STAT signaling (Bonni et al., 1997; Koblar et al., 1998; Barnabe-Heider et al., 2005; He et al., 2005); (2) bone morphogenetic proteins (BMPs) (Bonni et al., 1997) and transforming growth factor beta (Tgfb), which function through downstream Smad effector proteins to promote astrocyte maturation (Gross et al., 1996; Bonaguidi et al., 2005); and (3) Notch-Delta signaling, as described above (Gaiano et al., 2000; Ge et al., 2002; Grandbarbe et al., 2003; Kamakura et al., 2004; Wu et al., 2017).

Interestingly, cortical NPCs expressing *Neurog1/2* and/or *Ascl1* are biased against an astrocytic fate (Han et al., 2020) (**Figure 2**), with several mechanisms of action identified. Firstly, Neurog1, which declines in expression when astrocyte differentiation begins at E15.5 (He et al., 2005; Han et al., 2018), sequesters transcriptional co-activators (CBP/p300) away from Stat1/3 and Smad1 TFs, preventing the transactivation of downstream astrocytic genes such as GFAP by cytokine and BMP/Tgfb signaling (Sun et al., 2001). Secondly, Neurog1 induces the transcription of miR-9, which downregulates the expression of genes in the JAK/STAT pathway (Zhao et al., 2015). Conversely, signaling pathways promoting astrocytic fate impair the ability of proneural TFs to induce neuronal differentiation. BMP7, which is secreted from the dorsal telencephalic midline (Furuta et al., 1997) induces Id1 or Id2 expression in spinal cord and cortical NPCs (Vinals et al., 2004; Le Dreau et al., 2018). Id proteins inhibit proneural gene function by sequestering E proteins to prevent their heterodimerization with bHLH TFs (Le Dreau et al., 2018). Furthermore, Id1 induced by BMP4 promotes Ascl1 protein degradation to prevent this TF from promoting neuronal differentiation (Vinals et al., 2004).

Another important aspect of astrocyte differentiation is the timing of when NPCs switch from neurogenesis to gliogenesis. Cytokines are critical regulators of this switch (Barnabe-Heider et al., 2005), but the proneural genes are also involved, as gliogenesis occurs precociously in *Neurog2*$^{-/-}$;*Ascl1*$^{-/-}$ cortices (Nieto et al., 2001). Notably, a similar precocious differentiation of glial cells is seen in *Neurod4*$^{-/-}$;*Ascl1*$^{-/-}$ cortices in the tectum, hindbrain and spinal cord (Tomita et al., 2000), suggesting similar processes may be at play in other brain regions. One interpretation of these data is that in the absence of two proneural genes, neurogenesis cannot take place and instead, gliogenesis ensues. Another interpretation is that *Neurog2* and *Ascl1* regulate temporal identity transitions through the co-dependent activation of a unique set of downstream genes. Consistent with the latter interpretation, *Neurog2* and *Ascl1* are also together required to regulate the timing of cortical neurogenesis, as evidenced by the precocious differentiation of supragranular neurons (Dennis et al., 2017) in *Neurog2*$^{-/-}$;*Ascl1*$^{-/-}$ cortices (Dennis et al., 2017). Mechanistically, Neurog2 and Ascl1 regulate the timing of cortical neurogenesis as both proteins are required to transactivate Fezf2, a critical component of the de-repression circuit that specifies laminar identities. How these genes regulate the timing of cortical gliogenesis is less clear. A simple competitive model may explain these findings, as highlighted above, with the loss of Neurog2 and Ascl1 preventing the sequestration of transcriptional co-activators away from Stat1/3 and Smad1 TFs. However, the recent identification of a slew of transcriptional targets that are co-bound and co-regulated by Neurog2 and Ascl1 in cortical NPCs may shed new light into this process (Han et al., 2020).

REGULATION OF PRONEURAL GENE FUNCTION AT THE TRANSLATIONAL AND POST-TRANSLATIONAL LEVEL

Several studies suggest that *Neurog2* and *Ascl1* fate specification activities are temporally regulated. For example, *Neurog2* is only necessary and sufficient to specify a glutamatergic neuronal identity in cortical NPCs before E14.5 (Schuurmans et al., 2004; Li et al., 2012), whereas it promotes NPC progenitor transitions from aRG to INP (Britz et al., 2006) and neuronal migration (Heng et al., 2008) after E14.5. *Ascl1* is also normally expressed in embryonic cortical NPCs (Britz et al., 2006; Han et al., 2020), albeit at lower levels than in subcortical domains, but it does not induce the differentiation of these cells into GABAergic neurons or oligodendrocytes, although it may transactivate oligodendrocyte genes postnatally (Han et al., 2020). Temporally constrained, *Ascl1* is upregulated in *Neurog2*$^{-/-}$ cortical NPCs throughout the neurogenic period but can only respecify these cells to a GABAergic fate before E14.5 (Britz et al., 2006). Temporal changes in *Neurog2* cortical function are not surprising, considering that several differences in early and late cortical NPCs have previously been documented. For example, only early, pre-neurogenic cortices respond to the proliferative activity of Wnts (Viti et al., 2003b) and the ventralizing activity of Shh (Kohtz et al., 1998), while conversely, only late-stage NPCs respond to the gliogenic activity of CNTF (Molne et al., 2000; Takizawa et al., 2001; Viti et al., 2003a; Song and Ghosh, 2004). Several non-mutually exclusive molecular regulatory mechanisms controlling *Neurog2* and *Ascl1* functions in the cortex help explain these confounding findings.

Regulation of Proneural Gene Translation

There is a tendency to consider the presence of gene transcripts as an indication that a gene is 'active' in a particular cell type, but there are many downstream regulatory events that must also be considered. The first consideration is whether transcripts are translated into proteins. Early studies revealed that *Neurog1, Neurog2* and *Ascl1* transcripts are present in many more telencephalic cells than the proteins, but the mechanisms of translational control were not elucidated until recently. A ground-breaking study found that a large host of

transcribed neuronal differentiation genes are not translated in the developing cortex (Yang et al., 2014). This study showed that eukaryotic initiation factor 4E1 (eIF4E1) and the eIF4E-Binding Protein, 4E-T, components of the eukaryotic translational machinery, form P-body-like complexes that bind proneural bHLH mRNAs to inhibit their translation, a mechanism of translational control critical for controlling the timing of cortical neurogenesis (Yang et al., 2014) (**Figure 3A**). Since then, many additional proteins have been identified that control the translation of proneural and neural differentiation genes, including other components of the translational machinery and critical RNA binding proteins (Amadei et al., 2015; Zahr et al., 2018, 2019). Future work will be required to identify specific RNA binding proteins that control the stability and translation of proneural gene transcripts.

Protein–Protein Interactions

The requirement for dimerization presents numerous opportunities for combinatorial control of bHLH transcriptional activity (**Figure 3B**). A given bHLH dimer will have its own E-box specificity, and while a comprehensive picture of the differential binding patterns of homo- and heterodimers is not yet known, preferred binding motifs for certain proneural TFs have been discovered in mouse and fish (Seo et al., 2007; Lin et al., 2010; Wapinski et al., 2013; Raposo et al., 2015; Pfurr et al., 2017; Aydin et al., 2019) and certain bHLH dimers are less transcriptionally active than others. As mentioned earlier in this review, Ascl1 preferentially binds to CAGCTG motifs in genomic regulatory regions (Wapinski et al., 2013; Raposo et al., 2015; Aydin et al., 2019), while Neurog1 and Neurog2 preferentially bind CADATG motifs (where D = A/G/T) (Seo et al., 2007; Madelaine and Blader, 2011; Aydin et al., 2019). E47 has been shown to preferentially bind CAGSTG motifs (where S = C/G) (Lin et al., 2010; Pfurr et al., 2017). Recently it has been shown that E proteins alter the neurogenic strength of proneural TFs through physical interactions in a context-specific, E-box-dependent manner, by either synergizing with Ascl1 on CAGSTG motifs or impeding Neurog2's binding to CADATG motifs (Le Dreau et al., 2018). For example, misexpression of *E47* and *Ascl1* in spinal cord NPCs increases differentiation relative to *Ascl1* alone (Le Dreau et al., 2018), but the opposite effect is observed for co-electroporation of *E47* with *Neurog2*, either in spinal (Le Dreau et al., 2018) or cortical (Li et al., 2012) NPCs. However, there are other regulatory considerations, including that E47 heterodimerization enhances Neurog2 (Li et al., 2012) and Ascl1 (Vinals et al., 2004) protein stability, which can influence their transactivation of some target sites. The finding of E-box-dependent cooperativity of E proteins with proneural TFs leads us to the important consideration that proneural TF activity at downstream targets is modulated by the availability of appropriate dimerization partners. Indeed, in the chick spinal cord, when E protein availability is limited due to its sequestration by Id proteins, Ascl1 proneural strength is negatively impacted due to the reduction in Ascl1∼E47 heterodimers, which effectively transactivate CAGSTG E-box-containing downstream targets (Le Dreau et al., 2018). Conversely, Neurog2 transactivation of CADATG E-box-containing downstream targets is stabilized by a reduction in E47 availability due to Id sequestration (Le Dreau et al., 2018).

Heterodimers can also form between two proneural bHLH TFs. Examples include Neurog1∼Neurog2 heterodimers, which form in E12.5 cortical NPCs (Han et al., 2018) and are likely functionally important, as evidenced by the reduced *Hes5* expression (i.e., Notch signaling) and precocious neurogenesis that occurs in E12.5 *Neurog1*$^{-/-}$ cortices (Schuurmans et al., 2004; Han et al., 2018). Mechanistically, Neurog1∼Neurog2 heterodimers have a reduced capacity to induce neurogenesis compared to Neurog2∼Neurog2 homodimers, leading to the conclusion that Neurog1 slows the pace of cortical neurogenesis at early stages (∼E12.5) when there are higher levels of Neurog1/Neurog2 co-expression (Han et al., 2018). Interestingly, co-expression of *Neurog2* with *Neurod4* accelerates cortical neurogenesis (Mattar et al., 2008), and while protein–protein interactions were not assessed, it remains possible that either Neurog2∼Neurod4 heterodimers have an enhanced capacity to transactivate target genes, or these bHLH TFs form other dimers that bind to distinct E-boxes located in the same regulatory regions of a target gene. Notably, there are other examples of bHLH proneural genes and differentiation genes having co-operative functions, including in the developing retina (Akagi et al., 2004) and hippocampus (Schwab et al., 2000).

Neurog2∼Ascl1 heterodimers have also been identified (Gradwohl et al., 1996; Han et al., 2020), with evidence suggesting that they are non-functional, as predicted by the differential enrichment of bound E-box motifs for each TF identified in ChIP-seq experiments (Aydin et al., 2019). Indeed, co-expression of *Neurog2* and *Ascl1* blocks the transactivation of promoters specific to each TF *in vitro* in transcriptional reporter assays, as well as blocking the ability of *Ascl1* to induce *in vivo* proliferation and Sox9 expression (a glioblast marker in cortical NPCs) as well as the ability of *Neurog2* to induce *in vivo* glutamatergic neuron formation (Han et al., 2020). Despite the inhibitory interactions between Neurog2 and Ascl1, and while most of the genes activated by Neurog2 and Ascl1 do not overlap, there are also some commonly regulated genes (Masserdotti et al., 2015; Aydin et al., 2019). Moreover, the gene regulatory network (GRN) that is associated with Neurog2/Ascl1 double^{+} cortical NPCs is distinct from the GRNs associated with single^{+} NPCs. Neurog2 and Ascl1 could regulate a distinct repertoire of genes when in combination through two potential modes of action. Firstly, they could act on gene regulatory elements that contain both Neurog2- and Ascl1-specific binding sites, as exemplified by *Dll1,* which has two distinct enhancers that are specifically activated by Neurog2 (DeltaN) or Ascl1 (DeltaM) (Castro et al., 2006). Alternatively, enhancers may contain hybrid E-boxes that are bound equally well by Neurog2 and Ascl1, including when they form heterodimers, as exemplified by the *Dll3* promoter (Henke et al., 2009). Further studies on commonly regulated targets of Neurog2 and Ascl1 will aid our understanding of how cortical NPC fate decisions are regulated.

Finally, proneural TFs also form physical interactions with other non-bHLH TFs that play critical roles in cortical development. For example, Neurog2 synergizes with the T-box TF Tbr2, expressed in INPs, to control the radial migration

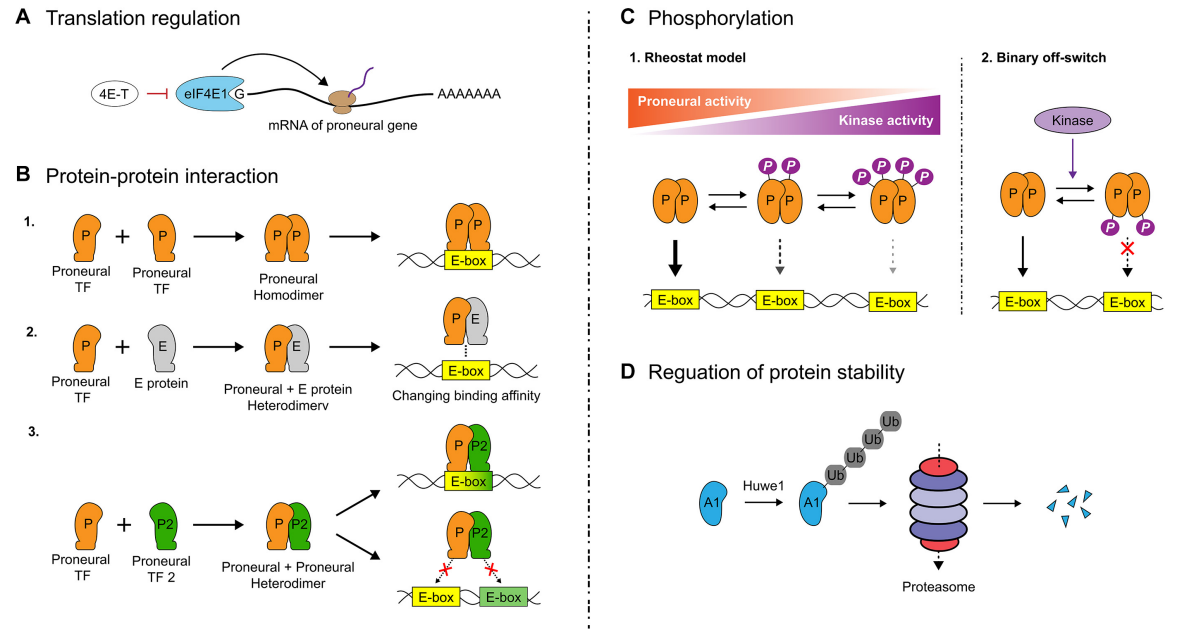

FIGURE 3 | Translational and post-translational regulation of proneural gene function. **(A)** The timing of cortical neurogenesis is controlled by eukaryotic initiation factor 4E1 (eIF4E1) and eIF4E-Binding Protein 4E-T, components of the eukaryotic translational machinery. These factors bind proneural gene transcripts, inhibiting proneural genes translation. **(B)** To bind DNA, bHLH TFs must dimerize. Proneural TF homodimers bind to regions with their cognate E-box sequences. Heterodimers with E proteins may enhance proneural TF binding to DNA if the proneural TF and E protein share a preferred E-box motif; otherwise, DNA binding is impaired. Heterodimerization between proneural TFs similarly may enhance or impede DNA binding depending on the E-box content of a target gene. **(C)** Beyond regulating proneural TF-mediated cell fate choices and neuronal migration, phosphorylation of proneural TFs generally decreases their transcriptional activity. The classical rheostat model holds that progressive phosphorylation of serines or threonines by proline directed serine-threonine kinases (e.g., Cdk, Erk, and Gsk3) at serine-proline (SP) or threonine-proline (TP) sites in proneural TFs decreases their activity depending on the number of sites phosphorylated. More recently, a single conserved residue has been discovered in proneural TFs at the loop/helix-2 junction, which when phosphorylated acts as binary off switch for proneural TF activity, with this mechanism overriding the rheostat mechanism. **(D)** Proneural TFs have short intracellular half-lives and are degraded through the ubiquitin-proteasome pathway. Recently, the E3 ligase Huwe1 was identified as a critical regulator of Ascl1 stability in the adult V-SVZ, with loss of Huwe1 leading to NPC depletion due to sustained Ascl1 expression inducing continuous neuronal differentiation.

of cortical neurons (Sessa et al., 2017). Neurog2 and Tbr2 control migration by synergistically transactivating *Rnd2*, a critical regulator of cortical neuron migration (Sessa et al., 2017). Other TFs have also been shown to associate with proneural TFs to regulate their functions. For instance, Ascl1 and the POU domain TFs Brn1 and Brn2 cooperatively bind the Dll1 promoter (Castro et al., 2006). Similarly, in the fly, senseless cooperates with atonal to regulate proneural activity (Nolo et al., 2000), and Myt1 is required for optimal Neurog2 proneural activity in Xenopus (Quan et al., 2004). The future identification of additional proneural TF binding partners in cortical NSCs/NPCs will aid in our understanding of the complex GRNs that underlie development of this brain region.

Phosphorylation of Proneural TFs

Intracellular kinases are key intermediaries between the environment and the cell nucleus, so understanding their impact on proneural TFs can reveal how environmental cues regulate cortical neurogenesis. Interestingly, DNA-binding proteins and TFs are often natively unfolded and intrinsically disordered (Ward et al., 2004), with disordered regions targeted by twice as many kinases as structured domains (Gsponer et al., 2008). Neurog2 is an example of an intrinsically disordered TF that is targeted by various kinases that modulate its activity in a context-dependent manner (McDowell et al., 2014). In general, N- and C-terminal phosphorylation outside of the bHLH domain has inhibitory effects on bHLH proneural activity, but other processes can be promoted by phosphorylation, as highlighted below.

Rheostat Model

The rheostat model holds that progressive phosphorylation of TFs results in a graded, finely tuned reduction in DNA binding and hence, transcriptional activity (Pufall et al., 2005) (**Figure 3C**). This model has garnered support with regards to proneural TFs from experimental work in mouse and xenopus (Ali et al., 2011; Hindley et al., 2012; McDowell et al., 2014; Hardwick and Philpott, 2015). Proneural TFs are phosphorylated by a host of proline-directed serine/threonine (S/T) kinases, including cyclin-dependent kinases (Cdk – on Neurog2 and Neurod4) (Ali et al., 2011; Hindley et al., 2012; McDowell et al., 2014; Hardwick and Philpott, 2015), GSK3 (on Neurog2) (Li et al., 2012) and ERK (on Ascl1) (Li et al., 2014). These S/T kinases can progressively phosphorylate nine serine-proline (SP) sites

in Neurog2, six SPs in Ascl1 and a combined seven threonine-proline (TP) and SP sites in Neurod4. In xenopus, the progressive phosphorylation of Neurog2 SP phosphoacceptor sites by Cdks limits its ability to drive neurogenesis, with the number of serine-proline sites phosphorylated more important than their location (McDowell et al., 2014). Based on the "cell cycle length hypothesis," NPCs that differentiate have a longer G_1 phase, and the prediction is that Cdk activity would be reduced in these cells so that Neurog2 would be underphosphorylated, thereby in a permissive state to initiate transcription of neurogenesis-associated target genes (Calegari and Huttner, 2003). Conversely, Cdk levels would rise in dividing NPCs, increasing proneural TF phosphorylation, and inhibiting transactivation of downstream gene (Ali et al., 2011). Notably, Cdk inhibits Neurog2-mediated transactivation of *Neurod1*, a neuronal differentiation gene, more robustly than *Dll1*, which induces neighboring NPCs to proliferate (Hindley et al., 2012), suggesting Cdk plays a critical role in regulating neural development. Accordingly, in the developing cortex, the proneural competence of Neurog2 also declines during late neurogenesis due to increasing levels of GSK3-mediated phosphorylation (Li et al., 2012).

Cell Fate Choice

Phosphorylation by SP kinases not only controls the decision to proliferate or differentiate, but also influences cell fate choices that are important in normal development but can also impact tumor formation. In the spinal cord, phosphorylation of Neurog2 S231 and S234 (SP sites) promotes the formation of TF complexes between Neurog2 and the adaptor protein Ldb1, which recruits LIM-homeodomain TFs Isl1 and Lhx3 to form a complex that transactivates motor neuron specific genes (Ma et al., 2008). Similarly, in the embryonic telencephalon, intermediate vs high RAS/ERK activation levels dictate whether *Ascl1* selects GABA vs OPC transcriptional targets, respectively (Li et al., 2014) (**Figure 2B**). Notably, there is also a correlation between higher pERK levels and more glial cells in pilocytic astrocytomas, compared to lower levels of pERK and fewer glial cells in ganglioglioma, despite these two tumor types sharing the same bRAFv600e mutation (Li et al., 2014). It is interesting to speculate that ERK-mediated phosphorylation of ASCL1 controls, at least in part, the different cellular features of these genetically similar tumors. Similarly, the tumorigenicity of bHLH TF Olig2 is driven by its phosphorylation status, with phosphomimetic mutations rendering it more tumorigenic, and phospho-dead mutations non-tumorigenic (Sun et al., 2011). In line with this, phosphorylation of a conserved triple serine motif in Olig2 promotes its unorthodox 'antineural' pro-proliferative functions, instead of the 'proneural-like' activity of inducing an oligodendrocyte fate (Sun et al., 2011). These data highlight the importance of phosphorylation events of bHLH TFs not only for normal development, but also in tumorigenesis.

Binary 'Off' Switch

A single conserved S/T residue at the Loop/Helix 2 (L-H2) junction acts as an evolutionarily conserved, binary 'off' switch for both vertebrate and invertebrate proneural TFs (Quan et al., 2016) (**Figure 3C**). 3D modeling revealed that the conserved S/T residue faces the DNA backbone such that addition of a negatively charged phosphate group would generate electrostatic repulsion between the TF and DNA, effectively rendering the TF a null mutant. At the L-H2 junction, Drosophila ato and vertebrate Atoh1 are phosphorylated on S292 by protein kinase A (PKA), while Neurog2 is phosphorylated on T149 by MARK1 and PLK1. A phosphomimetic mutation (T149D) destabilized Neurog2 binding to DNA and abolished its ability to induce neurogenesis in cortical NPCs *in vivo* (Quan et al., 2016). Strikingly, this binary off-switch essentially 'trumps' the rheostat model of control, as introduction of a single phosphomimetic mutation in the conserved L-H2 region of Ascl1 and Neurog2 prevents their proneural activities, even when 'activating' phospho-null mutations are introduced in SP and TP sites throughout the proteins (Hardwick and Philpott, 2018a,b). The speculation that these different regulatory modes may come into play at different developmental time points depending on an NPC's 'kinase environment' is interesting due to the possibility of rapidly halting proneural activity to ensure that correct neuronal numbers are generated (Hardwick and Philpott, 2018a).

Neuronal Migration

Neurog2 is also phosphorylated on Tyr241, a residue outside the bHLH domain that is dispensable for proneural activity, but required to specify a polarized neuronal phenotype and establish appropriate radial migration patterns (Hand et al., 2005). Mutation of Y241 leads to defects in neuronal migration and neuronal morphogenesis defects in the neocortex (Hand et al., 2005), in part by preventing the association between Neurog2 and CBP, a transcriptional co-activator protein that is required for Neurog2 to transactivate genes that control neuronal migration and dendritic polarity, such as Dcx (Ge et al., 2006). Notably, the ability of Neurog2 to sequester CBP is also proposed to be important for the indirect repression of RhoA, which must be downregulated for cortical neurons to migrate appropriately (Ge et al., 2006).

Regulation of Proneural TF Protein Stability

It is now well established that both fly (Kiparaki et al., 2015) and vertebrate (Nguyen et al., 2006; Ali et al., 2011; Li et al., 2012; Kovach et al., 2013) proneural TFs have very short intracellular half-lives (∼20–40 min). In the fly, two destabilizing motifs were found in the proneural TF encoded by *scute* (Sc); the transactivation domain (TAD) and an SPTSS motif, including a phosphoacceptor site for proline-directed S/T kinases (Kiparaki et al., 2015). Notably, S-A mutations in the SPTSS motif dramatically stabilized fly Sc (Kiparaki et al., 2015), and similarly, there was an ∼2-fold increase in Neurog2 stability when all 9 SP sites were mutated to SA in Xenopus (Ali et al., 2011). Removal of the C-terminal TAD domain also dramatically stabilizes murine Neurog2 (Li et al., 2012) and fly Sc (Kiparaki et al., 2015) proteins. However, while the forced tethering of mouse Neurog2 to E47 (Li et al., 2012), or E12 to human ASCL1 (Sriuranpong et al., 2002) stabilizes these proneural TFs, Sc heterodimerization with fly Daughterless (Da), the E-protein homolog, promotes further degradation (Kiparaki et al., 2015).

Thus, there are critical differences in how proneural protein stability is regulated, but nevertheless, in all species, proneural TFs have short intracellular half-lives.

There is growing evidence that proneural protein degradation is mediated by the ubiquitin-proteasome degradation system (UPS) (**Figure 3D**). Ubiquitin moieties form isopeptide bonds with lysine residues in substrate proteins that are targeted for degradation through the actions of three enzymes; ubiquitin-activating (E1), ubiquitin-conjugating (E2), and ubiquitin ligase (E3) enzymes (Komander and Rape, 2012). Polyubiquitylated substrates undergo degradation through the UPS (Johnson et al., 1995). Proneural TFs regulated by UPS include murine (Vinals et al., 2004) and human (Sriuranpong et al., 2002) Ascl1, xenopus Neurog2 (Vosper et al., 2007, 2009) and the fly protein Sc (Kiparaki et al., 2015). Recently, the E3-ligase Huwe1 (HECT, UBA and WWE domain containing 1) was identified as a critical destabilizer of Ascl1 in the postnatal hippocampus (Urban et al., 2016) (**Figure 3D**). Huwe1 maintains adult NSCs in quiescence by targeting Ascl1 for degradation, with excess NSCs entering the cell cycle upon conditional *Huwe1* deletion, resulting in a depletion of the NSC pool (Urban et al., 2016). Spatial resolution is also emerging in the picture of Ascl1 regulation by Huwe1 (Gillotin et al., 2018). Cytoplasmic Ascl1 is predominantly attached to longer polyubiquitin chains on lysines within the bHLH region and is rapidly targeted for degradation by the UPS, while chromatin-bound Ascl1 is ubiquitylated with shorter chains on N-terminal and bHLH lysines but is not targeted for degradation (Gillotin et al., 2018).

While comparable E3-ligases have yet to be identified for Neurog1 and Neurog2 in the cortex, Fbxo9 is an E3-ligase that destabilizes Neurog2 in the developing dorsal root ganglia (Liu et al., 2020). Mechanistically, in Xenopus, Neurog2 is stabilized by Cdk inhibitor p27Xic1 (Nguyen et al., 2006), and p27Xic1 promotes neurogenesis partially due to its stabilizing effect on Neurog2 (Vernon et al., 2003), but whether there is a direct involvement with UPS is not known.

EPIGENETIC REGULATION OF PRONEURAL BHLH ACTIVITY

Temporal and Spatial Restrictions on Proneural Gene Function

Transcription factors that act as cell fate determinants generally transactivate lineage-specific target genes only in certain cellular contexts (Gascon et al., 2017). For instance, the glutamatergic neuronal fate-specifying properties of *Neurog2* are temporally restricted; in the embryonic cortex, *Neurog2* only efficiently induces neurogenesis before E14.5 (Li et al., 2012). Regional restrictions also occur, with *Neurog2* efficiently able to induce neurogenesis in the dorsal and not ventral telencephalon (Mattar et al., 2008). Proneural genes have also emerged as critical architects of neuronal reprogramming (Wilkinson et al., 2013). However, in keeping with their tight contextual regulation, they are not active in all cell types; *Ascl1* is a potent neuronal reprogramming factor in fibroblasts (Vierbuchen et al., 2010; Caiazzo et al., 2011; Kim et al., 2011; Pang et al., 2011; Pfisterer et al., 2011; Son et al., 2011), hepatocytes (Marro et al., 2011), cardiomyocytes (Chuang et al., 2017), astrocytes (Rivetti di Val Cervo et al., 2017) and pluripotent stem cells (Yang et al., 2017), and not in the adult neocortex (Grande et al., 2013), hippocampus or spinal cord (Ohori et al., 2006; Jessberger et al., 2008). Conversely, *Neurog2* has a more limited ability to convert astrocytes to neurons (Grande et al., 2013; Gascon et al., 2016, 2017; Russo et al., 2020; Stricker and Gotz, 2020) and is used less often for neuronal reprogramming as it must be combined with other signals to become a potent lineage converter (Gascon et al., 2016; Russo et al., 2020).

Understanding how the lineage determination activities of *Neurog2* and *Ascl1* are restricted requires an understanding of how they interact with factors that remodel chromatin. In the field of cellular reprogramming, it is widely held that epigenetic regulators act as 'gatekeepers' to prevent cells from transiting from one cell fate to another other organisms, controlling genome accessibility to lineage-specifying TFs (Tursun et al., 2011; Cheloufi et al., 2015; Gascon et al., 2017). Notably, chromatin structure, and hence the accessibility of promoters/enhancers, changes during cortical development (Kishi et al., 2012). Moreover, even within the cortical NPC pool at a single age, there are distinct NPC populations defined as *Neurog2/Ascl1* negative, single$^+$ or double$^+$ NPCs that each have distinct chromatin landscapes (Han et al., 2020). Below we review how proneural bHLH TFs intersect with chromatin modifiers to influence the genome architecture, ultimately affecting their ability to bind and transactivate target genes.

Epigenetic and Metabolic Regulation of Proneural TF Function

Ascl1- and Neurog2 form homo- or hetero-dimers with other bHLH proteins to bind specific E-box motifs in the genome. Neurog2 and Ascl1 are termed 'pioneer factors' based on their ability to bind 'closed' (nucleosome-bound) chromatin and facilitate the opening of these sites for TF binding (Wapinski et al., 2013; Aydin et al., 2019) (**Figure 4A**). leading to the opening of distinct chromatin regions which render downstream differentiation genes accessible (Aydin et al., 2019). Several studies have begun to unravel how Neurog2 and Ascl1 influence the chromatin landscape through interactions with different epigenetic modifiers and pathways, as summarized below:

DNA Methylation

DNA hypermethylation of cytosine residues in CpG sequences, which are typically found in promoters/enhancers, represses gene expression by compacting the genome and rendering it inaccessible to TF binding. By changing DNA methylation patterns, chromatin accessibility is altered, as are downstream gene expression patterns. Notably, DNA can also be methylated on non-CpG sequences (CpH) that are prevalent throughout the genome, including in non-regulatory regions, but these modifications similarly repress gene expression (Guo et al., 2014). Strikingly, in a direct neuronal reprogramming study in which *Ascl1* was overexpressed in mouse embryonic fibroblasts (MEFs), Ascl1 induced CpH methylation of fibroblast-specific genes, but

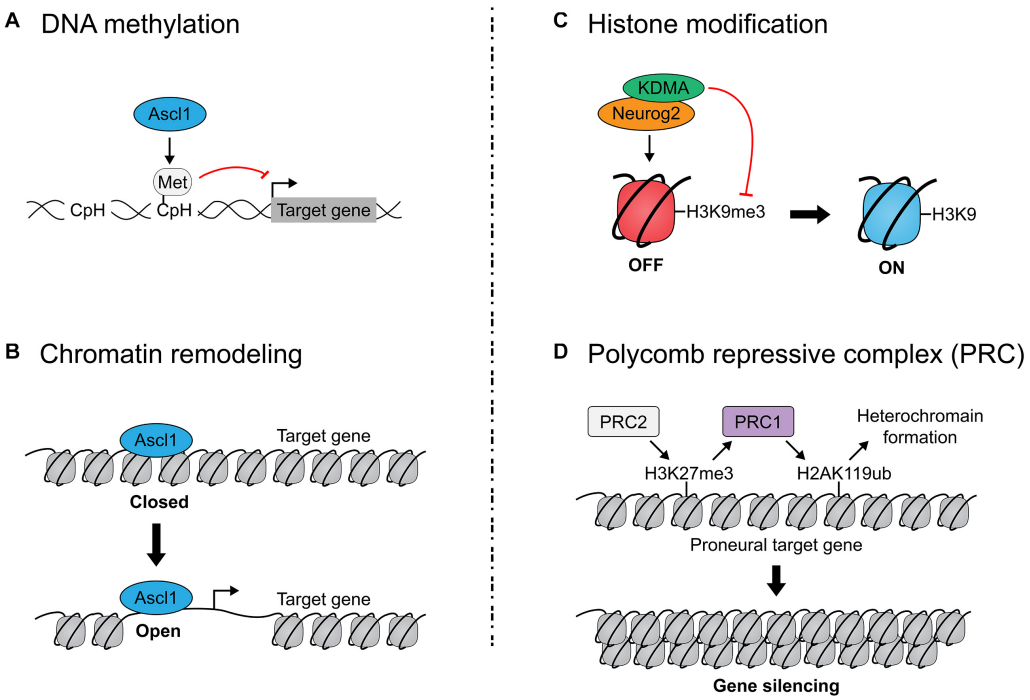

FIGURE 4 | Epigenetic regulation of proneural transcription factor activity. **(A)** Ascl1 induces non-CpG (CpH) methylation of fibroblast-specific genes during reprogramming of mouse embryonic fibroblasts to neurons. DNA methylation represses gene expression by compacting the genome and rendering it inaccessible. **(B)** Ascl1 is a pioneer factor which can bind nucleosome-bound DNA (in a 'closed' state) and facilitate the de-compacting of these sites to permit gene expression. Neurog2 has also been identified as a pioneer factor. **(C)** Neurog2 interacts with the H3K9 demethylase to open chromatin and promote neurogenesis. **(D)** Polycomb repressive complexes (PRC) close chromatin to render target genes inaccessible to proneural TFs. PRC1 ubiquitylates K119 in Histone H2A, while PRC2 methylates Lys27 in Histone H3, altogether leading to heterochromatin formation. Mutation of PRC1/2 genes prolongs proneural TF expression, implicating PRC1/2 in the temporal regulation of proneural TF activity.

cooperation with other TFs (Brn2, Myt1l) (Wapinski et al., 2013), which increase reprogramming efficiency, was required for methylation patterns to faithfully recapitulate those seen in cortical neurons (Luo et al., 2019) (**Figure 4B**).

Chromatin Remodeling

Ascl1-mediated *trans*-differentiation of MEFs to neurons showed that Ascl1 induces widespread chromatin remodeling (Wapinski et al., 2017). During this switch, there is substantial Ascl1-driven genome-wide remodeling of chromatin architecture near Ascl1 binding sites, leading to a stabilized nucleosome configuration at day 5 which facilitates the stable expression of mature neuronal genes. Notably, the presence of a swift and concerted chromatin switch in this *trans*-differentiation protocol contrasts with the classical 'step-wise' view of *in vivo* neuronal development and iPSC reprogramming, emphasizing the limitations of using direct somatic cell reprogramming to model development. In addition, Neurog1 interacts with Brg1, a SWI/SNF chromatin remodeler to aid neurogenesis (Seo et al., 2005).

Selective Transactivation of Bound E-Boxes

bHLH TFs act as lineage determinants in multiple tissues, and include Myod1, a master regulator of a skeletal muscle fate (Lee et al., 2020). Strikingly, when misexpressed in MEFs, Ascl1 and Myod1 bind very similar target genes, but to a different degree, and can only induce chromatin opening of sites involved in neuronal and muscle lineage reprogramming, respectively (Lee et al., 2020). However, when Myod1 is overexpressed with Myt1l, which inhibits the acquisition of a muscle identity, Myod1 can induce neuronal differentiation (Lee et al., 2020).

Co-activator and Co-repressor Interactions

A common property of TFs that act as transactivators is their association with co-activator proteins that function as histone acetyl transferases (HATs), as exemplified by p300/CBP (Sheikh, 2014). p300/CBP preferentially acetylates lysine residues (K) on histone H3/H4 tails (e.g., H3K27ac), and 'opens' chromatin by electrostatic repulsion between negatively charged acetyl groups and DNA. Conversely, histone deacetylases (HDACs) remove these acetyl groups and compact the chromatin. Several papers have documented associations between the proneural bHLH genes and HAT co-activators (Koyano-Nakagawa et al., 1999; Sun et al., 2001; Vojtek et al., 2003; Seo et al., 2005, 2007; Ge et al., 2006). The proneural genes are also thought to indirectly repress gliogenesis by sequestering HAT proteins away from gliogenic genes (Sun et al., 2001; Ge et al., 2006). Interestingly, the bHLH protein Hes1 switches from binding a TLE-HDAC co-repressor complex to HAT binding as neurogenesis proceeds (Ju et al., 2004), highlighting the importance of dynamic interactions between these factors in regulating the timing of neurogenesis.

Histone Methylation

Opening of the chromatin to provide access to TF binding is also associated with methylation of H3 histone tails, but here the specific lysine (K) residues are critical. For instance, while RNAPol II and trimethylation (me3) of histone H3K4 cluster at transcription start sites of actively transcribed genes, and histone H3K36me3 is in the body of actively transcribed genes, other chromatin marks are found in silenced regions of the genome (H3K9me3, H3K27me3) (Ringrose et al., 2004; Bernstein et al., 2006; Pavri et al., 2006; Sims and Reinberg, 2006; Muller and Verrijzer, 2009; Tavares et al., 2012). Notably, Neurog2 forms a complex with KDMA, an H3K9 demethylase, to open chromatin and promote neurogenesis (Lin et al., 2017) (**Figure 4C**). Additionally, Tbr2 physically interacts with JMJD3 histone demethylase, upregulating neuronal-specific genes when co-expressed, potentially by directing JMJD3 to remove repressive H3K27me3 marks (Sessa et al., 2017). Interestingly, Neurog2 physically associates with and shares a majority of its bound genomic target sequences with Tbr2 and acts synergistically on shared target genes in equimolar quantities, so perhaps Neurog2 interacts with and directs JMJD3 activity as well (Sessa et al., 2017).

Polycomb Group Proteins

Only a handful of epigenetic gatekeepers are known; most influence chromatin structure, some via interactions with Polycomb group (PcG) proteins, which close chromatin (Tursun et al., 2011; Cheloufi et al., 2015; Gascon et al., 2017). PcG proteins modify chromatin to confer transcriptional repression and exist in two repressive complexes: PRC1 (Ring1a, Ring1b, etc.) and PRC2 (Eed, Suz12, Ezh1/2, etc.). PRC1 catalyzes the ubiquitylation of K119 in Histone H2A (H2AK119ub), while PRC2 catalyzes the methylation of Lys27 in Histone H3 (H3K27me3), altogether leading to downregulation of nearby genes (**Figure 4D**).

PRC1 and PRC2 control temporal NPC fate competence by regulating proneural gene expression and proneural TF target gene availability (**Figure 5**). PRC1 controls the temporal window of *Neurog1*, but not *Neurog2*, expression, with mutation of *Ring1b* extending *Neurog1* expression into late-stage neurogenesis (e.g., E17) (Hirabayashi et al., 2009). Extending *Neurog1* gene expression and derepressing the expression of neuronal lineage genes, *Ring1B* and *Ezh2* deletions also delayed the onset of gliogenesis, indicating that PRC1 and PRC2 control the neurogenic-to-gliogenic fate switch in cortical NPCs (Hirabayashi et al., 2009). Recently, Ring1b was also shown to control the spatial expression pattern of *Neurog1*, with *Ring1b* deletion expanding *Neurog1* expression further ventrally to overlap with *Ascl1* expression in the murine E10 telencephalon (Eto et al., 2020). Surprisingly, while Neurog1/2 have been shown to repress *Ascl1* expression in the cortex, establishing mutually exclusive expression patterns, *Ring1b* deletion markedly increased *Neurog1/Ascl1* double^{+} NPCs, suggesting that PcG proteins may also regulate mutual exclusivity of proneural TF expression (Eto et al., 2020). Ring1b has also been shown to temporally limit the production of subcerebral neurons by NPCs

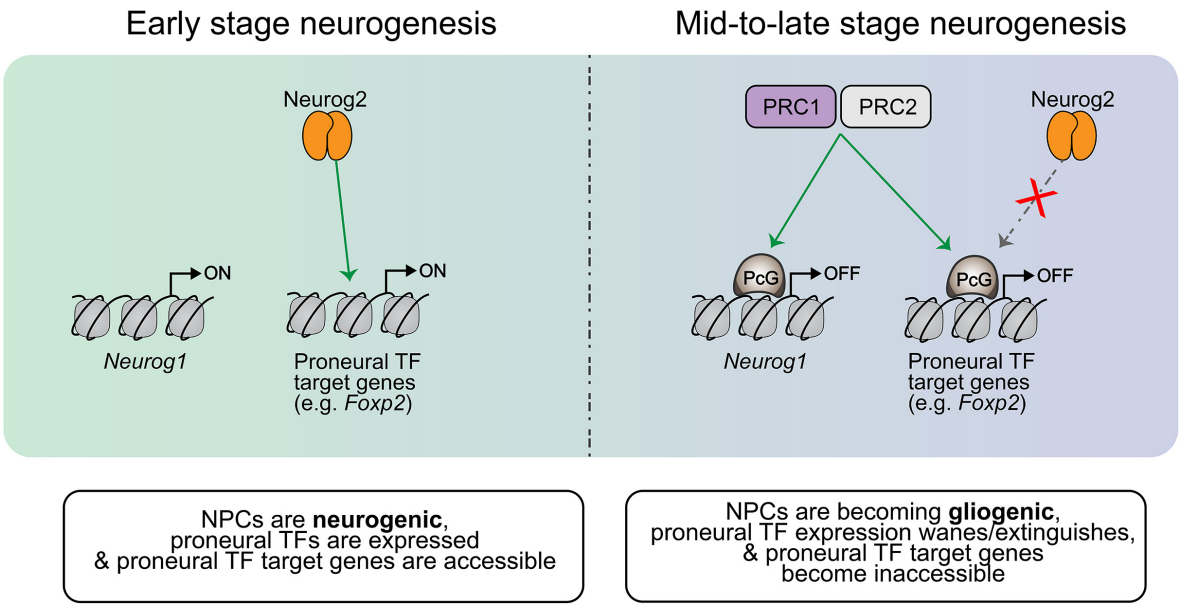

FIGURE 5 | Temporal regulation of proneural gene expression and target gene availability. In early NPCs, *Neurog1* expression is turned on and proneural TF target genes are available (not repressed). As the cortical neurogenic period progresses, PRC1/2 catalyze the addition of PcG proteins to repress certain genes which are part of the neuronal differentiation cascade. For example, PRC1/2 repress *Foxp2* in mid-neurogenesis, making it inaccessible to Neurog2 and thereby terminating the Neurog2-mediated specification of corticothalamic neurons past this period. This PRC1/2 activity thus controls the temporal competence of NPCs, dictating the differentiation programs that may be initiated at different stages of development. PRC1/2 also extinguish the expression of proneural TFs like *Neurog1* later on in the neurogenic period, and this contributes to the induction of gliogenic differentiation programs within NPCs as Neurog1 has been shown to prevent the induction of such programs.

through repression of *Fezf2* expression (Morimoto-Suzki et al., 2014), which is a known transcriptional target of Neurog2. Furthermore, PRC2 components *Eed* and *Suz12* and PRC1 components *Ring1a* and *Ring1b* suppress the ability of Neurog2 to induce a corticothalamic differentiation program by repressing downstream target, Foxp2 (Oishi et al., 2020). In this way, PRC1 and PRC2 progressively regulate targets of proneural TF-induced differentiation programs to control NPC temporal fate competence.

Recent RNA-Seq evidence from FlashTag-isolated apical NPCs further substantiates the claim that PRC2 temporally regulates NPC competence, with mutation of *Eed* (inactivation of PRC2) leading to precocious neurogenesis (Telley et al., 2019). *Eed* mutants further displayed precocious generation of typically late-born neurons and increased cell cycle exit in early neurogenesis, leading to a terminal decrease in cortical thickness (which indicates a shorter neurogenic period) (Telley et al., 2019). Similarly, the PRC2 catalytic component Ezh2 was shown to control developmental rate, with loss of Ezh2 shifting NPCs toward differentiation over proliferation as well as an earlier induction of gliogenesis (Pereira et al., 2010).

Overall, these findings implicate PcG proteins as crucial temporal regulators of proneural transcriptional programs, operating to limit the timeframe of subtype specification by proneural TFs by occluding proneural TF target genes. These critical epigenetic regulators do not act alone, though; temporal NPC fate specification is simultaneously and robustly regulated by other mechanisms such as declining proneural transcriptional activity.

Proneural TFs Are Regulated by Metabolism

The global metabolic changes associated with neuronal differentiation have only recently begun to be elucidated (Agostini et al., 2016), and new work is emerging investigating the metabolic regulators of Neurog2- or Ascl1- driven direct neuronal conversion strategies in both human and mouse cells. As we have expounded in this review, proneural TF function is context dependent, and thus the efficiency at which proneural TFs induce neuronal conversion must also be contingent on the bio-energetic differences of starting cell types in conversion protocols. Indeed, it has been shown that oxidative stress (Gascon et al., 2016) and fatty acid B-oxidation (Russo et al., 2020) impose major hurdles in the reprogramming of astrocytes, which rely on glycolytic metabolism (McKay et al., 1983; Tsacopoulos and Magistretti, 1996), to neurons, which rely on oxidative metabolism (Herrero-Mendez et al., 2009). Thus, genetic or pharmacological manipulations to reduce oxidative stress, such as Bcl-2 overexpression or the addition of forskolin, vitamin E, and calcitriol, increases the efficiency (both the speed and number of converted cells) of proneural TF-driven neuronal conversion (Gascon et al., 2016). Bcl-2 functions independently of its canonical anti-apoptotic role to reduce reactive oxygen species (ROS) and facilitate more efficient proneural TF-driven fate transitions; hence, co-transduction with Ascl1 or Neurog2 significantly improves astrocyte-to-neuron conversion efficiencies and neuronal maturation *in vitro*, as well as *in vivo* in injured mouse cortex (Gascon et al., 2016). Interestingly, microarray analysis of *Ascl1*-transduced MEFs revealed that forskolin treatment enriched BMP and Wnt signaling pathway genes (Gascon et al., 2016), both of which influence proneural TF expression, though it is unknown if the reprogramming enhancement seen in this study is caused by direct effects on proneural TF function or by creating a more permissive cellular environment for reprogramming to occur. Further underscoring the importance of bioenergetics in the regulation of proneural TF function, one-fifth of the mitochondrial proteome differs between astrocytes and cortical neurons, and CRISPRa-mediated induction of neuronal, but not astrocytic, mitochondrial proteins enhances the efficiency of Ascl1-driven reprogramming (Russo et al., 2020). The most robust enhancement of Ascl1-driven reprogramming occurs with co-transduction of neuronal-specific antioxidant protein Sod1, leading to increases in recruitment of cells for reprogramming, speed of conversion into neurons, and lifespan of converted neurons (Russo et al., 2020). These new findings add an important layer of complexity to the web of proneural TF regulation, and when considered together with the other regulatory mechanisms detailed in this review, will allow for the design of more efficient proneural TF-driven neuronal reprogramming protocols in the future.

DISCUSSION

Proneural TFs are critical regulators of neural cell differentiation and subtype specification, contributing to the enormous cellular diversity observed in the cortex. It therefore holds that proneural TFs are themselves tightly regulated, and these interplaying mechanisms of regulation are being elucidated by the scientific community. A coherent picture of robust regulation is emerging, one with overlapping mechanisms that limit proneural TF actions to certain temporal windows in development. Altogether, the current literature suggests a temporal sequence of regulation as follows. Initially, proneural gene transcript expression is induced by early morphogenetic signals and modulated in undifferentiated NPCs by antagonistic Notch signaling and by other cross-repressive proneural TFs. In NPCs where proneural gene transcript expression is permitted, translation may still be prevented by repressive eIF4E-4E-T complexes. Once proneural gene expression becomes sustained in Notch(-) NPCs, proneural TFs may then be translated into TFs which are regulated in their stability and transcriptional activity by different dimerization partners and by phosphorylation of different residues within their bHLH, N- and C-terminal domains. When the actions of a proneural TF are no longer needed, the protein may be degraded proteolytically by polyubiquitylation (for which exact enzymatic candidates are emerging), or by broader inhibition at the epigenetic level (with mechanisms like repressive PcG proteins limiting proneural TF access to downstream targets).

In the future, the ultimate application of the multifaceted picture of proneural gene regulation that we have painted in this review would aid in the refinement and improvement of neuronal

reprogramming strategies incorporating these proneural genes for regenerative medicine purposes.

AUTHOR CONTRIBUTIONS

A-MO and CS: conceptualization. A-MO, SH, and CS: writing—review and editing. A-MO and SH: artwork. CS: funding acquisition. All authors contributed to the article and approved the submitted version.

FUNDING

This work was supported by operating grants to CS from the Canadian Institutes of Health Research (CIHR PJT – 162108) and a Canada-Israel Health Research Initiative, jointly funded by the CIHR, the Israel Science Foundation, the International Development Research Centre, Canada, and the Azrieli Foundation (IDRC 108875).

ACKNOWLEDGMENTS

A-MO was supported by a Canada Graduate Scholarship – Master's NSERC Studentship. SH was supported by Scholarships from the University of Calgary Cumming School of Medicine, Ontario Graduate Scholarship, University of Toronto Vision Science Research Program (VSRP), Peterborough K.M. Hunter Charitable Foundation, and a Margaret and Howard GAMBLE Research Grant. CS holds the Dixon Family Chair in Ophthalmology Research.

REFERENCES

Agostini, M., Romeo, F., Inoue, S., Niklison-Chirou, M. V., Elia, A. J., Dinsdale, D., et al. (2016). Metabolic reprogramming during neuronal differentiation. *Cell Death Differ.* 23, 1502–1514. doi: 10.1038/cdd.2016.36

Akagi, T., Inoue, T., Miyoshi, G., Bessho, Y., Takahashi, M., Lee, J. E., et al. (2004). Requirement of multiple basic helix-loop-helix genes for retinal neuronal subtype specification. *J. Biol. Chem.* 279, 28492–28498. doi: 10.1074/jbc.m400871200

Ali, F., Hindley, C., McDowell, G., Deibler, R., Jones, A., Kirschner, M., et al. (2011). Cell cycle-regulated multi-site phosphorylation of Neurogenin 2 coordinates cell cycling with differentiation during neurogenesis. *Development* 138, 4267–4277. doi: 10.1242/dev.067900

Amadei, G., Zander, M. A., Yang, G., Dumelie, J. G., Vessey, J. P., Lipshitz, H. D., et al. (2015). A Smaug2-based translational repression complex determines the balance between precursor maintenance versus differentiation during mammalian neurogenesis. *J. Neurosci.* 35, 15666–15681. doi: 10.1523/jneurosci.2172-15.2015

Aydin, B., Kakumanu, A., Rossillo, M., Moreno-Estelles, M., Garipler, G., Ringstad, N., et al. (2019). Proneural factors Ascl1 and Neurog2 contribute to neuronal subtype identities by establishing distinct chromatin landscapes. *Nat. Neurosci.* 22, 897–908. doi: 10.1038/s41593-019-0399-y

Backman, M., Machon, O., Mygland, L., van den Bout, C. J., Zhong, W., Taketo, M. M., et al. (2005). Effects of canonical Wnt signaling on dorso-ventral specification of the mouse telencephalon. *Dev. Biol.* 279, 155–168. doi: 10.1016/j.ydbio.2004.12.010

Barnabe-Heider, F., and Miller, F. D. (2003). Endogenously produced neurotrophins regulate survival and differentiation of cortical progenitors via distinct signaling pathways. *J. Neurosci.* 23, 5149–5160. doi: 10.1523/jneurosci.23-12-05149.2003

Barnabe-Heider, F., Wasylnka, J. A., Fernandes, K. J., Porsche, C., Sendtner, M., Kaplan, D. R., et al. (2005). Evidence that embryonic neurons regulate the onset of cortical gliogenesis via cardiotrophin-1. *Neuron* 48, 253–265. doi: 10.1016/j.neuron.2005.08.037

Bartkowska, K., Paquin, A., Gauthier, A. S., Kaplan, D. R., and Miller, F. D. (2007).). Trk signaling regulates neural precursor cell proliferation and differentiation during cortical development. *Development* 134, 4369–4380. doi: 10.1242/dev.008227

Bayatti, N., Moss, J. A., Sun, L., Ambrose, P., Ward, J. F., Lindsay, S., et al. (2008). A molecular neuroanatomical study of the developing human neocortex from 8 to 17 postconceptional weeks revealing the early differentiation of the subplate and subventricular zone. *Cereb. Cortex* 18, 1536–1548. doi: 10.1093/cercor/bhm184

Bayraktar, O. A., Fuentealba, L. C., Alvarez-Buylla, A., and Rowitch, D. H. (2014). Astrocyte development and heterogeneity. *Cold Spring Harb. Perspect. Biol.* 7:a020362.

Beckervordersandforth, R., Tripathi, P., Ninkovic, J., Bayam, E., Lepier, A., Stempfhuber, B., et al. (2010). *In vivo* fate mapping and expression analysis reveals molecular hallmarks of prospectively isolated adult neural stem cells. *Cell Stem Cell* 7, 744–758. doi: 10.1016/j.stem.2010.11.017

Bernstein, B. E., Mikkelsen, T. S., Xie, X., Kamal, M., Huebert, D. J., Cuff, J., et al. (2006). A bivalent chromatin structure marks key developmental genes in embryonic stem cells. *Cell* 125, 315–326. doi: 10.1016/j.cell.2006.02.041

Bertrand, N., Castro, D. S., and Guillemot, F. (2002). Proneural genes and the specification of neural cell types. *Nat. Rev. Neurosci.* 3, 517–530. doi: 10.1038/nrn874

Bohner, A. P., Akers, R. M., and McConnell, S. K. (1997). Induction of deep layer cortical neurons *in vitro*. *Development* 124, 915–923.

Boldrini, M., Fulmore, C. A., Tartt, A. N., Simeon, L. R., Pavlova, I., Poposka, V., et al. (2018). Human hippocampal neurogenesis persists throughout aging. *Cell Stem Cell* 22, 589–599.e5.

Bonaguidi, M. A., McGuire, T., Hu, M., Kan, L., Samanta, J., and Kessler, J. A. (2005). LIF and BMP signaling generate separate and discrete types of GFAP-expressing cells. *Development* 132, 5503–5514. doi: 10.1242/dev.02166

Bonni, A., Sun, Y., Nadal-Vicens, M., Bhatt, A., Frank, D. A., Rozovsky, I., et al. (1997). Regulation of gliogenesis in the central nervous system by the JAK-STAT signaling pathway. *Science* 278, 477–483. doi: 10.1126/science.278.5337.477

Bormuth, I., Yan, K., Yonemasu, T., Gummert, M., Zhang, M., Wichert, S., et al. (2013). Neuronal basic helix-loop-helix proteins Neurod2/6 regulate cortical commissure formation before midline interactions. *J. Neurosci.* 33, 641–651. doi: 10.1523/jneurosci.0899-12.2013

Brand, M., and Morrissey, E. (2020). Single-cell fate decisions of bipotential hematopoietic progenitors. *Curr. Opin. Hematol.* 27, 232–240. doi: 10.1097/moh.0000000000000592

Brill, M. S., Ninkovic, J., Winpenny, E., Hodge, R. D., Ozen, I., Yang, R., et al. (2009). Adult generation of glutamatergic olfactory bulb interneurons. *Nat. Neurosci.* 12, 1524–1533. doi: 10.1038/nn.2416

Britz, O., Mattar, P., Nguyen, L., Langevin, L. M., Zimmer, C., Alam, S., et al. (2006). A role for proneural genes in the maturation of cortical progenitor cells. *Cereb. Cortex* 16(Suppl. 1), i138–i151.

Bultje, R. S., Castaneda-Castellanos, D. R., Jan, L. Y., Jan, Y. N., Kriegstein, A. R., and Shi, S. H. (2009). Mammalian Par3 regulates progenitor cell asymmetric division via notch signaling in the developing neocortex. *Neuron* 63, 189–202. doi: 10.1016/j.neuron.2009.07.004

Caiazzo, M., Dell'Anno, M. T., Dvoretskova, E., Lazarevic, D., Taverna, S., Leo, D., et al. (2011). Direct generation of functional dopaminergic neurons from mouse and human fibroblasts. *Nature* 476, 224–227. doi: 10.1038/nature10284

Calegari, F., and Huttner, W. B. (2003). An inhibition of cyclin-dependent kinases that lengthens, but does not arrest, neuroepithelial cell cycle induces premature neurogenesis. *J. Cell Sci.* 116, 4947–4955. doi: 10.1242/jcs.00825

Casarosa, S., Fode, C., and Guillemot, F. (1999). Mash1 regulates neurogenesis in the ventral telencephalon. *Development* 126, 525–534.

Castro, D. S., and Guillemot, F. (2011). Old and new functions of proneural factors revealed by the genome-wide characterization of their

transcriptional targets. *Cell Cycle* 10, 4026–4031. doi: 10.4161/cc.10.23.18578

Castro, D. S., Martynoga, B., Parras, C., Ramesh, V., Pacary, E., Johnston, C., et al. (2011). A novel function of the proneural factor Ascl1 in progenitor proliferation identified by genome-wide characterization of its targets. *Genes Dev.* 25, 930–945. doi: 10.1101/gad.627811

Castro, D. S., Skowronska-Krawczyk, D., Armant, O., Donaldson, I. J., Parras, C., Hunt, C., et al. (2006). Proneural bHLH and Brn proteins coregulate a neurogenic program through cooperative binding to a conserved DNA motif. *Dev. Cell* 11, 831–844. doi: 10.1016/j.devcel.2006.10.006

Caviness, V. S. Jr. (1982). Neocortical histogenesis in normal and reeler mice: a developmental study based upon [3H]thymidine autoradiography. *Brain Res.* 256, 293–302. doi: 10.1016/0165-3806(82)90141-9

Caviness, V. S. Jr., Takahashi, T., and Nowakowski, R. S. (1995). Numbers, time and neocortical neuronogenesis: a general developmental and evolutionary model. *Trends Neurosci.* 18, 379–383. doi: 10.1016/0166-2236(95)93933-o

Chandran, S., Kato, H., Gerreli, D., Compston, A., Svendsen, C. N., and Allen, N. D. (2003). FGF-dependent generation of oligodendrocytes by a hedgehog-independent pathway. *Development* 130, 6599–6609. doi: 10.1242/dev.00871

Cheloufi, S., Elling, U., Hopfgartner, B., Jung, Y. L., Murn, J., Ninova, M., et al. (2015). The histone chaperone CAF-1 safeguards somatic cell identity. *Nature* 528, 218–224. doi: 10.1038/nature15749

Chickarmane, V., Enver, T., and Peterson, C. (2009). Computational modeling of the hematopoietic erythroid-myeloid switch reveals insights into cooperativity, priming, and irreversibility. *PLoS Comput. Biol.* 5:e1000268. doi: 10.1371/journal.pcbi.1000268

Chizhikov, V. V., Iskusnykh, I. Y., Steshina, E. Y., Fattakhov, N., Lindgren, A. G., Shetty, A. S., et al. (2019). Early dorsomedial tissue interactions regulate gyrification of distal neocortex. *Nat. Commun.* 10:5192.

Chuang, W., Sharma, A., Shukla, P., Li, G., Mall, M., Rajarajan, K., et al. (2017). Partial reprogramming of pluripotent stem cell-derived cardiomyocytes into neurons. *Sci. Rep.* 7:44840.

de Juan Romero, C., Bruder, C., Tomasello, U., Sanz-Anquela, J. M., and Borrell, V. (2015). Discrete domains of gene expression in germinal layers distinguish the development of gyrencephaly. *EMBO J.* 34, 1859–1874. doi: 10.15252/embj.201591176

Dehay, C., Kennedy, H., and Kosik, K. S. (2015). The outer subventricular zone and primate-specific cortical complexification. *Neuron* 85, 683–694. doi: 10.1016/j.neuron.2014.12.060

Del Toro, D., Ruff, T., Cederfjall, E., Villalba, A., Seyit-Bremer, G., Borrell, V., et al. (2017). Regulation of cerebral cortex folding by controlling neuronal migration via FLRT adhesion molecules. *Cell* 169, 621–635.e16.

Dennis, D. J., Han, S., and Schuurmans, C. (2019). bHLH transcription factors in neural development, disease, and reprogramming. *Brain Res.* 1705, 48–65. doi: 10.1016/j.brainres.2018.03.013

Dennis, D. J., Wilkinson, G., Li, S., Dixit, R., Adnani, L., Balakrishnan, A., et al. (2017). Neurog2 and Ascl1 together regulate a postmitotic derepression circuit to govern laminar fate specification in the murine neocortex. *Proc. Natl. Acad. Sci. U.S.A.* 114, E4934–E4943.

Desai, A. R., and McConnell, S. K. (2000). Progressive restriction in fate potential by neural progenitors during cerebral cortical development. *Development* 127, 2863–2872.

Dillon, N. (2012). Factor mediated gene priming in pluripotent stem cells sets the stage for lineage specification. *Bioessays* 34, 194–204. doi: 10.1002/bies.201100137

Dixit, R., Wilkinson, G., Cancino, G. I., Shaker, T., Adnani, L., Li, S., et al. (2014). Neurog1 and Neurog2 control two waves of neuronal differentiation in the piriform cortex. *J. Neurosci.* 34, 539–553. doi: 10.1523/jneurosci.0614-13.2014

Dixit, R., Zimmer, C., Waclaw, R. R., Mattar, P., Shaker, T., Kovach, C., et al. (2011). Ascl1 participates in Cajal-Retzius cell development in the neocortex. *Cereb. Cortex* 21, 2599–2611. doi: 10.1093/cercor/bhr046

Eckler, M. J., Nguyen, T. D., McKenna, W. L., Fastow, B. L., Guo, C., Rubenstein, J. L. R., et al. (2015). Cux2-positive radial glial cells generate diverse subtypes of neocortical projection neurons and macroglia. *Neuron* 86, 1100–1108. doi: 10.1016/j.neuron.2015.04.020

Englund, C., Fink, A., Lau, C., Pham, D., Daza, R. A., Bulfone, A., et al. (2005). Pax6, Tbr2, and Tbr1 are expressed sequentially by radial glia, intermediate progenitor cells, and postmitotic neurons in developing neocortex. *J. Neurosci.* 25, 247–251. doi: 10.1523/jneurosci.2899-04.2005

Enver, T., Pera, M., Peterson, C., and Andrews, P. W. (2009). Stem cell states, fates, and the rules of attraction. *Cell Stem Cell* 4, 387–397. doi: 10.1016/j.stem.2009.04.011

Ernst, A., Alkass, K., Bernard, S., Salehpour, M., Perl, S., Tisdale, J., et al. (2014). Neurogenesis in the striatum of the adult human brain. *Cell* 156, 1072–1083. doi: 10.1016/j.cell.2014.01.044

Esain, V., Postlethwait, J. H., Charnay, P., and Ghislain, J. (2010). FGF-receptor signalling controls neural cell diversity in the zebrafish hindbrain by regulating olig2 and sox9. *Development* 137, 33–42. doi: 10.1242/dev.038026

Eto, H., Kishi, Y., Yakushiji-Kaminatsui, N., Sugishita, H., Utsunomiya, S., Koseki, H., et al. (2020). The Polycomb group protein Ring1 regulates dorsoventral patterning of the mouse telencephalon. *Nat. Commun.* 11:5709.

Falk, D., and Hofman, M. A. (2012). Evolution of the primate brain. *Preface. Prog. Brain Res.* 195, vii–ix.

Farreny, M. A., Agius, E., Bel-Vialar, S., Escalas, N., Khouri-Farah, N., Soukkarieh, C., et al. (2018). FGF signaling controls Shh-dependent oligodendroglial fate specification in the ventral spinal cord. *Neural Dev.* 13:3.

Fiddes, I. T., Lodewijk, G. A., Mooring, M., Bosworth, C. M., Ewing, A. D., Mantalas, G. L., et al. (2018). Human-specific NOTCH2NL genes affect notch signaling and cortical neurogenesis. *Cell* 173, 1356–1369.e22.

Fietz, S. A., Kelava, I., Vogt, J., Wilsch-Brauninger, M., Stenzel, D., Fish, J. L., et al. (2010). OSVZ progenitors of human and ferret neocortex are epithelial-like and expand by integrin signaling. *Nat. Neurosci.* 13, 690–699. doi: 10.1038/nn.2553

Fietz, S. A., Lachmann, R., Brandl, H., Kircher, M., Samusik, N., Schroder, R., et al. (2012). Transcriptomes of germinal zones of human and mouse fetal neocortex suggest a role of extracellular matrix in progenitor self-renewal. *Proc. Natl. Acad. Sci. U.S.A.* 109, 11836–11841. doi: 10.1073/pnas.1209647109

Florio, M., Albert, M., Taverna, E., Namba, T., Brandl, H., Lewitus, E., et al. (2015). Human-specific gene ARHGAP11B promotes basal progenitor amplification and neocortex expansion. *Science* 347, 1465–1470. doi: 10.1126/science.aaa1975

Florio, M., Heide, M., Pinson, A., Brandl, H., Albert, M., Winkler, S., et al. (2018). Evolution and cell-type specificity of human-specific genes preferentially expressed in progenitors of fetal neocortex. *eLife* 7:e32332.

Fode, C., Ma, Q., Casarosa, S., Ang, S. L., Anderson, D. J., and Guillemot, F. (2000). A role for neural determination genes in specifying the dorsoventral identity of telencephalic neurons. *Genes Dev.* 14, 67–80.

Franco, S. J., Gil-Sanz, C., Martinez-Garay, I., Espinosa, A., Harkins-Perry, S. R., Ramos, C., et al. (2012). Fate-restricted neural progenitors in the mammalian cerebral cortex. *Science* 337, 746–749. doi: 10.1126/science.1223616

Frantz, G. D., and McConnell, S. K. (1996). Restriction of late cerebral cortical progenitors to an upper-layer fate. *Neuron* 17, 55–61. doi: 10.1016/s0896-6273(00)80280-9

Fuentealba, L. C., Rompani, S. B., Parraguez, J. I., Obernier, K., Romero, R., Cepko, C. L., et al. (2015). Embryonic origin of postnatal neural stem cells. *Cell* 161, 1644–1655. doi: 10.1016/j.cell.2015.05.041

Fukumitsu, H., Ohtsuka, M., Murai, R., Nakamura, H., Itoh, K., and Furukawa, S. (2006). Brain-derived neurotrophic factor participates in determination of neuronal laminar fate in the developing mouse cerebral cortex. *J. Neurosci.* 26, 13218–13230. doi: 10.1523/jneurosci.4251-06.2006

Furusho, M., Kaga, Y., Ishii, A., Hebert, J. M., and Bansal, R. (2011). Fibroblast growth factor signaling is required for the generation of oligodendrocyte progenitors from the embryonic forebrain. *J. Neurosci.* 31, 5055–5066. doi: 10.1523/jneurosci.4800-10.2011

Furuta, Y., Piston, D. W., and Hogan, B. L. (1997). Bone morphogenetic proteins (BMPs) as regulators of dorsal forebrain development. *Development* 124, 2203–2212.

Furutachi, S., Matsumoto, A., Nakayama, K. I., and Gotoh, Y. (2013). p57 controls adult neural stem cell quiescence and modulates the pace of lifelong neurogenesis. *EMBO J.* 32, 970–981. doi: 10.1038/emboj.2013.50

Furutachi, S., Miya, H., Watanabe, T., Kawai, H., Yamasaki, N., Harada, Y., et al. (2015). Slowly dividing neural progenitors are an embryonic origin of adult neural stem cells. *Nat. Neurosci.* 18, 657–665. doi: 10.1038/nn.3989

Gabay, L., Lowell, S., Rubin, L. L., and Anderson, D. J. (2003). Deregulation of dorsoventral patterning by FGF confers trilineage differentiation capacity on

CNS stem cells *in vitro*. *Neuron* 40, 485–499. doi: 10.1016/s0896-6273(03)00637-8

Gaiano, N., Nye, J. S., and Fishell, G. (2000). Radial glial identity is promoted by Notch1 signaling in the murine forebrain. *Neuron* 26, 395–404. doi: 10.1016/s0896-6273(00)81172-1

Gao, P., Postiglione, M. P., Krieger, T. G., Hernandez, L., Wang, C., Han, Z., et al. (2014). Deterministic progenitor behavior and unitary production of neurons in the neocortex. *Cell* 159, 775–788. doi: 10.1016/j.cell.2014.10.027

Gascon, S., Masserdotti, G., Russo, G. L., and Gotz, M. (2017). Direct neuronal reprogramming: achievements, hurdles, and new roads to success. *Cell Stem Cell* 21, 18–34. doi: 10.1016/j.stem.2017.06.011

Gascon, S., Murenu, E., Masserdotti, G., Ortega, F., Russo, G. L., Petrik, D., et al. (2016). Identification and successful negotiation of a metabolic checkpoint in direct neuronal reprogramming. *Cell Stem Cell* 18, 396–409. doi: 10.1016/j.stem.2015.12.003

Ge, W., He, F., Kim, K. J., Blanchi, B., Coskun, V., Nguyen, L., et al. (2006). Coupling of cell migration with neurogenesis by proneural bHLH factors. *Proc. Natl. Acad. Sci. U.S.A.* 103, 1319–1324. doi: 10.1073/pnas.0510419103

Ge, W., Martinowich, K., Wu, X., He, F., Miyamoto, A., Fan, G., et al. (2002). Notch signaling promotes astrogliogenesis via direct CSL-mediated glial gene activation. *J. Neurosci. Res.* 69, 848–860. doi: 10.1002/jnr.10364

Ghosh, A., and Greenberg, M. E. (1995). Distinct roles for bFGF and NT-3 in the regulation of cortical neurogenesis. *Neuron* 15, 89–103. doi: 10.1016/0896-6273(95)90067-5

Gillotin, S., Davies, J. D., and Philpott, A. (2018). Subcellular localisation modulates ubiquitylation and degradation of Ascl1. *Sci. Rep.* 8:4625.

Gil-Sanz, C., Espinosa, A., Fregoso, S. P., Bluske, K. K., Cunningham, C. L., Martinez-Garay, I., et al. (2015). Lineage tracing using Cux2-Cre and Cux2-CreERT2 mice. *Neuron* 86, 1091–1099. doi: 10.1016/j.neuron.2015.04.019

Gotz, M., and Huttner, W. B. (2005). The cell biology of neurogenesis. *Nat. Rev. Mol. Cell Biol.* 6, 777–788.

Gotz, M., Nakafuku, M., and Petrik, D. (2016). Neurogenesis in the developing and adult brain-similarities and key differences. *Cold Spring Harb. Perspect. Biol.* 8:a018853. doi: 10.1101/cshperspect.a018853

Gradwohl, G., Fode, C., and Guillemot, F. (1996). Restricted expression of a novel murine atonal-related bHLH protein in undifferentiated neural precursors. *Dev. Biol.* 180, 227–241. doi: 10.1006/dbio.1996.0297

Grandbarbe, L., Bouissac, J., Rand, M., Hrabe de Angelis, M., Artavanis-Tsakonas, S., and Mohier, E. (2003). Delta-Notch signaling controls the generation of neurons/glia from neural stem cells in a stepwise process. *Development* 130, 1391–1402. doi: 10.1242/dev.00374

Grande, A., Sumiyoshi, K., Lopez-Juarez, A., Howard, J., Sakthivel, B., Aronow, B., et al. (2013). Environmental impact on direct neuronal reprogramming *in vivo* in the adult brain. *Nat. Commun.* 4:2373.

Greene, L. A., and Tischler, A. S. (1976). Establishment of a noradrenergic clonal line of rat adrenal pheochromocytoma cells which respond to nerve growth factor. *Proc. Natl. Acad. Sci. U.S.A.* 73, 2424–2428. doi: 10.1073/pnas.73.7.2424

Gross, R. E., Mehler, M. F., Mabie, P. C., Zang, Z., Santschi, L., and Kessler, J. A. (1996). Bone morphogenetic proteins promote astroglial lineage commitment by mammalian subventricular zone progenitor cells. *Neuron* 17, 595–606. doi: 10.1016/s0896-6273(00)80193-2

Gsponer, J., Futschik, M. E., Teichmann, S. A., and Babu, M. M. (2008). Tight regulation of unstructured proteins: from transcript synthesis to protein degradation. *Science* 322, 1365–1368. doi: 10.1126/science.1163581

Guillemot, F., and Hassan, B. A. (2017). Beyond proneural: emerging functions and regulations of proneural proteins. *Curr. Opin. Neurobiol.* 42, 93–101. doi: 10.1016/j.conb.2016.11.011

Gunhaga, L., Marklund, M., Sjodal, M., Hsieh, J. C., Jessell, T. M., and Edlund, T. (2003). Specification of dorsal telencephalic character by sequential Wnt and FGF signaling. *Nat. Neurosci.* 6, 701–707. doi: 10.1038/nn1068

Guo, C., Eckler, M. J., McKenna, W. L., McKinsey, G. L., Rubenstein, J. L., and Chen, B. (2013). Fezf2 expression identifies a multipotent progenitor for neocortical projection neurons, astrocytes, and oligodendrocytes. *Neuron* 80, 1167–1174. doi: 10.1016/j.neuron.2013.09.037

Guo, J. U., Su, Y., Shin, J. H., Shin, J., Li, H., Xie, B., et al. (2014). Distribution, recognition and regulation of non-CpG methylation in the adult mammalian brain. *Nat. Neurosci.* 17, 215–222. doi: 10.1038/nn.3607

Guzelsoy, G., Akkaya, C., Atak, D., Dunn, C. D., Kabakcioglu, A., Ozlu, N., et al. (2019). Terminal neuron localization to the upper cortical plate is controlled by the transcription factor NEUROD2. *Sci. Rep.* 9:19697.

Hack, M. A., Sugimori, M., Lundberg, C., Nakafuku, M., and Gotz, M. (2004). Regionalization and fate specification in neurospheres: the role of Olig2 and Pax6. *Mol. Cell. Neurosci.* 25, 664–678. doi: 10.1016/j.mcn.2003.12.012

Hagey, D. W., and Muhr, J. (2014). Sox2 acts in a dose-dependent fashion to regulate proliferation of cortical progenitors. *Cell Rep.* 9, 1908–1920. doi: 10.1016/j.celrep.2014.11.013

Han, S., Dennis, D. J., Balakrishnan, A., Dixit, R., Britz, O., Zinyk, D., et al. (2018). A non-canonical role for the proneural gene Neurog1 as a negative regulator of neocortical neurogenesis. *Development* 145:dev157719. doi: 10.1242/dev.157719

Han, S., Wilkinson, G. A., Okawa, S., Adnani, L., Dixit, R., Faisal, I., et al. (2020). Proneural genes define ground state rules to regulate neurogenic patterning and cortical folding. *bioRxiv* [Preprint]. doi: 10.1101/2020.09.22.307058

Hand, R., Bortone, D., Mattar, P., Nguyen, L., Heng, J. I., Guerrier, S., et al. (2005). Phosphorylation of Neurogenin2 specifies the migration properties and the dendritic morphology of pyramidal neurons in the neocortex. *Neuron* 48, 45–62. doi: 10.1016/j.neuron.2005.08.032

Hansen, D. V., Lui, J. H., Parker, P. R., and Kriegstein, A. R. (2010). Neurogenic radial glia in the outer subventricular zone of human neocortex. *Nature* 464, 554–561. doi: 10.1038/nature08845

Hardwick, L. J., and Philpott, A. (2015). Multi-site phosphorylation regulates NeuroD4 activity during primary neurogenesis: a conserved mechanism amongst proneural proteins. *Neural Dev.* 10:15.

Hardwick, L. J. A., and Philpott, A. (2018a). Interaction between opposing modes of phospho-regulation of the proneural proteins Ascl1 and Ngn2. *Wellcome Open Res.* 3:129. doi: 10.12688/wellcomeopenres.14848.1

Hardwick, L. J. A., and Philpott, A. (2018b). The N terminus of Ascl1 underlies differing proneural activity of mouse and *Xenopus* Ascl1 proteins. *Wellcome Open Res.* 3:125. doi: 10.12688/wellcomeopenres.14842.1

Hasegawa, H., Ashigaki, S., Takamatsu, M., Suzuki-Migishima, R., Ohbayashi, N., Itoh, N., et al. (2004). Laminar patterning in the developing neocortex by temporally coordinated fibroblast growth factor signaling. *J. Neurosci.* 24, 8711–8719. doi: 10.1523/jneurosci.3070-04.2004

Hatakeyama, J., Bessho, Y., Katoh, K., Ookawara, S., Fujioka, M., Guillemot, F., et al. (2004). Hes genes regulate size, shape and histogenesis of the nervous system by control of the timing of neural stem cell differentiation. *Development* 131, 5539–5550. doi: 10.1242/dev.01436

Haubensak, W., Attardo, A., Denk, W., and Huttner, W. B. (2004). Neurons arise in the basal neuroepithelium of the early mammalian telencephalon: a major site of neurogenesis. *Proc. Natl. Acad. Sci. U.S.A.* 101, 3196–3201. doi: 10.1073/pnas.0308600100

He, F., Ge, W., Martinowich, K., Becker-Catania, S., Coskun, V., Zhu, W., et al. (2005). A positive autoregulatory loop of Jak-STAT signaling controls the onset of astrogliogenesis. *Nat. Neurosci.* 8, 616–625. doi: 10.1038/nn1440

Heng, J. I., Nguyen, L., Castro, D. S., Zimmer, C., Wildner, H., Armant, O., et al. (2008). Neurogenin 2 controls cortical neuron migration through regulation of Rnd2. *Nature* 455, 114–118. doi: 10.1038/nature07198

Henke, R. M., Meredith, D. M., Borromeo, M. D., Savage, T. K., and Johnson, J. E. (2009). Ascl1 and Neurog2 form novel complexes and regulate Delta-like3 (Dll3) expression in the neural tube. *Dev. Biol.* 328, 529–540. doi: 10.1016/j.ydbio.2009.01.007

Herrero-Mendez, A., Almeida, A., Fernandez, E., Maestre, C., Moncada, S., and Bolanos, J. P. (2009). The bioenergetic and antioxidant status of neurons is controlled by continuous degradation of a key glycolytic enzyme by APC/C-Cdh1. *Nat. Cell Biol.* 11, 747–752. doi: 10.1038/ncb1881

Hindley, C., Ali, F., McDowell, G., Cheng, K., Jones, A., Guillemot, F., et al. (2012). Post-translational modification of Ngn2 differentially affects transcription of distinct targets to regulate the balance between progenitor maintenance and differentiation. *Development* 139, 1718–1723. doi: 10.1242/dev.077552

Hirabayashi, Y., Itoh, Y., Tabata, H., Nakajima, K., Akiyama, T., Masuyama, N., et al. (2004). The Wnt/beta-catenin pathway directs neuronal differentiation of cortical neural precursor cells. *Development* 131, 2791–2801. doi: 10.1242/dev.01165

Hirabayashi, Y., Suzki, N., Tsuboi, M., Endo, T. A., Toyoda, T., Shinga, J., et al. (2009). Polycomb limits the neurogenic competence of neural precursor cells to

promote astrogenic fate transition. *Neuron* 63, 600–613. doi: 10.1016/j.neuron.2009.08.021

Horton, S., Meredith, A., Richardson, J. A., and Johnson, J. E. (1999). Correct coordination of neuronal differentiation events in ventral forebrain requires the bHLH factor MASH1. *Mol. Cell. Neurosci.* 14, 355–369. doi: 10.1006/mcne.1999.0791

Huang, C., Chan, J. A., and Schuurmans, C. (2014). Proneural bHLH genes in development and disease. *Curr. Top. Dev. Biol.* 110, 75–127. doi: 10.1016/b978-0-12-405943-6.00002-6

Huang, S., Guo, Y. P., May, G., and Enver, T. (2007). Bifurcation dynamics in lineage-commitment in bipotent progenitor cells. *Dev. Biol.* 305, 695–713. doi: 10.1016/j.ydbio.2007.02.036

Hufnagel, R. B., Le, T. T., Riesenberg, A. L., and Brown, N. L. (2010). Neurog2 controls the leading edge of neurogenesis in the mammalian retina. *Dev. Biol.* 340, 490–503. doi: 10.1016/j.ydbio.2010.02.002

Imamura, O., Satoh, Y., Endo, S., and Takishima, K. (2008). Analysis of extracellular signal-regulated kinase 2 function in neural stem/progenitor cells via nervous system-specific gene disruption. *Stem Cells* 26, 3247–3256. doi: 10.1634/stemcells.2008-0578

Imayoshi, I., Isomura, A., Harima, Y., Kawaguchi, K., Kori, H., Miyachi, H., et al. (2013). Oscillatory control of factors determining multipotency and fate in mouse neural progenitors. *Science* 342, 1203–1208. doi: 10.1126/science.1242366

Ito, H., Nakajima, A., Nomoto, H., and Furukawa, S. (2003). Neurotrophins facilitate neuronal differentiation of cultured neural stem cells via induction of mRNA expression of basic helix-loop-helix transcription factors Mash1 and Math1. *J. Neurosci. Res.* 71, 648–658. doi: 10.1002/jnr.10532

Jessberger, S., Toni, N., Clemenson, G. D. Jr., Ray, J., and Gage, F. H. (2008). Directed differentiation of hippocampal stem/progenitor cells in the adult brain. *Nat. Neurosci.* 11, 888–893. doi: 10.1038/nn.2148

Johnson, E. S., Ma, P. C., Ota, I. M., and Varshavsky, A. (1995). A proteolytic pathway that recognizes ubiquitin as a degradation signal. *J. Biol. Chem.* 270, 17442–17456. doi: 10.1074/jbc.270.29.17442

Jones, E. G. (1994). Santiago Ramon y Cajal and the Croonian Lecture, March 1894. *Trends Neurosci.* 17, 190–192. doi: 10.1016/0166-2236(94)90100-7

Ju, B. G., Solum, D., Song, E. J., Lee, K. J., Rose, D. W., Glass, C. K., et al. (2004). Activating the PARP-1 sensor component of the groucho/ TLE1 corepressor complex mediates a CaMKinase IIdelta-dependent neurogenic gene activation pathway. *Cell* 119, 815–829. doi: 10.1016/j.cell.2004.11.017

Ju, X. C., Hou, Q. Q., Sheng, A. L., Wu, K. Y., Zhou, Y., Jin, Y., et al. (2016). The hominoid-specific gene TBC1D3 promotes generation of basal neural progenitors and induces cortical folding in mice. *eLife* 5:e18197.

Kageyama, R., Ochi, S., Sueda, R., and Shimojo, H. (2020). The significance of gene expression dynamics in neural stem cell regulation. *Proc. Jpn. Acad. Ser. B Phys. Biol. Sci.* 96, 351–363. doi: 10.2183/pjab.96.026

Kageyama, R., Ohtsuka, T., and Kobayashi, T. (2007). The Hes gene family: repressors and oscillators that orchestrate embryogenesis. *Development* 134, 1243–1251. doi: 10.1242/dev.000786

Kageyama, R., Ohtsuka, T., Shimojo, H., and Imayoshi, I. (2008). Dynamic Notch signaling in neural progenitor cells and a revised view of lateral inhibition. *Nat. Neurosci.* 11, 1247–1251. doi: 10.1038/nn.2208

Kamakura, S., Oishi, K., Yoshimatsu, T., Nakafuku, M., Masuyama, N., and Gotoh, Y. (2004). Hes binding to STAT3 mediates crosstalk between Notch and JAK-STAT signalling. *Nat. Cell Biol.* 6, 547–554. doi: 10.1038/ncb1138

Kast, R. J., and Levitt, P. (2019). Precision in the development of neocortical architecture: From progenitors to cortical networks. *Prog. Neurobiol.* 175, 77–95. doi: 10.1016/j.pneurobio.2019.01.003

Kessaris, N., Fogarty, M., Iannarelli, P., Grist, M., Wegner, M., and Richardson, W. D. (2006). Competing waves of oligodendrocytes in the forebrain and postnatal elimination of an embryonic lineage. *Nat. Neurosci.* 9, 173–179. doi: 10.1038/nn1620

Kim, J., Su, S. C., Wang, H., Cheng, A. W., Cassady, J. P., Lodato, M. A., et al. (2011). Functional integration of dopaminergic neurons directly converted from mouse fibroblasts. *Cell Stem Cell* 9, 413–419. doi: 10.1016/j.stem.2011.09.011

Kiparaki, M., Zarifi, I., and Delidakis, C. (2015). bHLH proteins involved in *Drosophil*a neurogenesis are mutually regulated at the level of stability. *Nucleic Acids Res.* 43, 2543–2559. doi: 10.1093/nar/gkv083

Kishi, Y., Fujii, Y., Hirabayashi, Y., and Gotoh, Y. (2012). HMGA regulates the global chromatin state and neurogenic potential in neocortical precursor cells. *Nat. Neurosci.* 15, 1127–1133. doi: 10.1038/nn.3165

Koblar, S. A., Turnley, A. M., Classon, B. J., Reid, K. L., Ware, C. B., Cheema, S. S., et al. (1998). Neural precursor differentiation into astrocytes requires signaling through the leukemia inhibitory factor receptor. *Proc. Natl. Acad. Sci. U.S.A.* 95, 3178–3181. doi: 10.1073/pnas.95.6.3178

Kohtz, J. D., Baker, D. P., Corte, G., and Fishell, G. (1998). Regionalization within the mammalian telencephalon is mediated by changes in responsiveness to Sonic Hedgehog. *Development* 125, 5079–5089.

Komander, D., and Rape, M. (2012). The ubiquitin code. *Annu. Rev. Biochem.* 81, 203–229.

Kovach, C., Dixit, R., Li, S., Mattar, P., Wilkinson, G., Elsen, G. E., et al. (2012). Neurog2 simultaneously activates and represses alternative gene expression programs in the developing neocortex. *Cereb. Cortex* 23, 1884–1900. doi: 10.1093/cercor/bhs176

Kovach, C., Dixit, R., Li, S., Mattar, P., Wilkinson, G., Elsen, G. E., et al. (2013). Neurog2 simultaneously activates and represses alternative gene expression programs in the developing neocortex. *Cereb. Cortex* 23, 1884–1900. doi: 10.1093/cercor/bhs176

Kowalczyk, T., Pontious, A., Englund, C., Daza, R. A., Bedogni, F., Hodge, R., et al. (2009). Intermediate neuronal progenitors (basal progenitors) produce pyramidal-projection neurons for all layers of cerebral cortex. *Cereb. Cortex* 19, 2439–2450. doi: 10.1093/cercor/bhn260

Koyano-Nakagawa, N., Wettstein, D., and Kintner, C. (1999). Activation of *Xenopus* genes required for lateral inhibition and neuronal differentiation during primary neurogenesis. *Mol. Cell. Neurosci.* 14, 327–339. doi: 10.1006/mcne.1999.0783

Kroll, T. T., and O'Leary, D. D. (2005). Ventralized dorsal telencephalic progenitors in Pax6 mutant mice generate GABA interneurons of a lateral ganglionic eminence fate. *Proc. Natl. Acad. Sci. U.S.A.* 102, 7374–7379. doi: 10.1073/pnas.0500819102

Le Dreau, G., Escalona, R., Fueyo, R., Herrera, A., Martinez, J. D., Usieto, S., et al. (2018). E proteins sharpen neurogenesis by modulating proneural bHLH transcription factors' activity in an E-box-dependent manner. *eLife* 7:e37267.

Lee, Q. Y., Mall, M., Chanda, S., Zhou, B., Sharma, K. S., Schaukowitch, K., et al. (2020). Pro-neuronal activity of Myod1 due to promiscuous binding to neuronal genes. *Nat. Cell Biol.* 22, 401–411. doi: 10.1038/s41556-020-0490-3

Lewitus, E., Kelava, I., Kalinka, A. T., Tomancak, P., and Huttner, W. B. (2014). An adaptive threshold in mammalian neocortical evolution. *PLoS Biol.* 12:e1002000. doi: 10.1371/journal.pbio.1002000

Li, L., and Clevers, H. (2010). Coexistence of quiescent and active adult stem cells in mammals. *Science* 327, 542–545. doi: 10.1126/science.1180794

Li, S., Mattar, P., Dixit, R., Lawn, S. O., Wilkinson, G., Kinch, C., et al. (2014). RAS/ERK signaling controls proneural genetic programs in cortical development and gliomagenesis. *J. Neurosci.* 34, 2169–2190. doi: 10.1523/jneurosci.4077-13.2014

Li, S., Mattar, P., Zinyk, D., Singh, K., Chaturvedi, C. P., Kovach, C., et al. (2012). GSK3 temporally regulates neurogenin 2 proneural activity in the neocortex. *J. Neurosci.* 32, 7791–7805. doi: 10.1523/jneurosci.1309-12.2012

Lin, H., Zhu, X., Chen, G., Song, L., Gao, L., Khand, A. A., et al. (2017). KDM3A-mediated demethylation of histone H3 lysine 9 facilitates the chromatin binding of Neurog2 during neurogenesis. *Development* 144, 3674–3685. doi: 10.1242/dev.144113

Lin, Y. C., Jhunjhunwala, S., Benner, C., Heinz, S., Welinder, E., Mansson, R., et al. (2010). A global network of transcription factors, involving E2A, EBF1 and Foxo1, that orchestrates B cell fate. *Nat. Immunol.* 11, 635–643. doi: 10.1038/ni.1891

Liu, H., Thurig, S., Mohamed, O., Dufort, D., and Wallace, V. A. (2006). Mapping canonical Wnt signaling in the developing and adult retina. *Invest. Ophthalmol. Vis. Sci.* 47, 5088–5097. doi: 10.1167/iovs.06-0403

Liu, J. A., Tai, A., Hong, J., Cheung, M. P. L., Sham, M. H., Cheah, K. S. E., et al. (2020). Fbxo9 functions downstream of Sox10 to determine neuron-glial fate choice in the dorsal root ganglia through Neurog2 destabilization. *Proc. Natl. Acad. Sci. U.S.A.* 117, 4199–4210. doi: 10.1073/pnas.1916164117

Llinares-Benadero, C., and Borrell, V. (2019). Deconstructing cortical folding: genetic, cellular and mechanical determinants. *Nat. Rev. Neurosci.* 20, 161–176. doi: 10.1038/s41583-018-0112-2

Lukaszewicz, A., Savatier, P., Cortay, V., Giroud, P., Huissoud, C., Berland, M., et al. (2005). G1 phase regulation, area-specific cell cycle control, and cytoarchitectonics in the primate cortex. *Neuron* 47, 353–364. doi: 10.1016/j.neuron.2005.06.032

Lukaszewicz, A., Savatier, P., Cortay, V., Kennedy, H., and Dehay, C. (2002). Contrasting effects of basic fibroblast growth factor and neurotrophin 3 on cell cycle kinetics of mouse cortical stem cells. *J. Neurosci.* 22, 6610–6622. doi: 10.1523/jneurosci.22-15-06610.2002

Luo, C., Lee, Q. Y., Wapinski, O., Castanon, R., Nery, J. R., Mall, M., et al. (2019). Global DNA methylation remodeling during direct reprogramming of fibroblasts to neurons. *eLife* 8:e40197.

Luskin, M. B., Pearlman, A. L., and Sanes, J. R. (1988). Cell lineage in the cerebral cortex of the mouse studied *in vivo* and *in vitro* with a recombinant retrovirus. *Neuron* 1, 635–647. doi: 10.1016/0896-6273(88)90163-8

Ma, Y. C., Song, M. R., Park, J. P., Henry Ho, H. Y., Hu, L., Kurtev, M. V., et al. (2008). Regulation of motor neuron specification by phosphorylation of neurogenin 2. *Neuron* 58, 65–77. doi: 10.1016/j.neuron.2008.01.037

Machon, O., Backman, M., Krauss, S., and Kozmik, Z. (2005). The cellular fate of cortical progenitors is not maintained in neurosphere cultures. *Mol. Cell. Neurosci.* 30, 388–397. doi: 10.1016/j.mcn.2005.08.003

Madelaine, R., and Blader, P. (2011). A cluster of non-redundant Ngn1 binding sites is required for regulation of deltaA expression in zebrafish. *Dev. Biol.* 350, 198–207. doi: 10.1016/j.ydbio.2010.10.025

Maretto, S., Cordenonsi, M., Dupont, S., Braghetta, P., Broccoli, V., Hassan, A. B., et al. (2003). Mapping Wnt/beta-catenin signaling during mouse development and in colorectal tumors. *Proc. Natl. Acad. Sci. U.S.A.* 100, 3299–3304. doi: 10.1073/pnas.0434590100

Marro, S., Pang, Z. P., Yang, N., Tsai, M. C., Qu, K., Chang, H. Y., et al. (2011). Direct lineage conversion of terminally differentiated hepatocytes to functional neurons. *Cell Stem Cell* 9, 374–382. doi: 10.1016/j.stem.2011.09.002

Marshall, C. J. (1995). Specificity of receptor tyrosine kinase signaling: transient versus sustained extracellular signal-regulated kinase activation. *Cell* 80, 179–185. doi: 10.1016/0092-8674(95)90401-8

Martinez-Cerdeno, V., Cunningham, C. L., Camacho, J., Antczak, J. L., Prakash, A. N., Cziep, M. E., et al. (2012). Comparative analysis of the subventricular zone in rat, ferret and macaque: evidence for an outer subventricular zone in rodents. *PLoS One* 7:e30178. doi: 10.1371/journal.pone.0030178

Masserdotti, G., Gillotin, S., Sutor, B., Drechsel, D., Irmler, M., Jorgensen, H. F., et al. (2015). Transcriptional mechanisms of proneural factors and REST in regulating neuronal reprogramming of astrocytes. *Cell Stem Cell* 17, 74–88. doi: 10.1016/j.stem.2015.05.014

Mattar, P., Langevin, L. M., Markham, K., Klenin, N., Shivji, S., Zinyk, D., et al. (2008). Basic helix-loop-helix transcription factors cooperate to specify a cortical projection neuron identity. *Mol. Cell. Biol.* 28, 1456–1469. doi: 10.1128/mcb.01510-07

McConnell, S. K., and Kaznowski, C. E. (1991). Cell cycle dependence of laminar determination in developing neocortex. *Science* 254, 282–285. doi: 10.1126/science.1925583

McDowell, G. S., Hindley, C. J., Lippens, G., Landrieu, I., and Philpott, A. (2014). Phosphorylation in intrinsically disordered regions regulates the activity of Neurogenin2. *BMC Biochem.* 15:24. doi: 10.1186/s12858-014-0024-3

McKay, N. D., Robinson, B., Brodie, R., and Rooke-Allen, N. (1983). Glucose transport and metabolism in cultured human skin fibroblasts. *Biochim. Biophys. Acta* 762, 198–204. doi: 10.1016/0167-4889(83)90071-x

Medina, D. L., Sciarretta, C., Calella, A. M., Von Bohlen Und Halbach, O., Unsicker, K., and Minichiello, L. (2004). TrkB regulates neocortex formation through the Shc/PLCgamma-mediated control of neuronal migration. *EMBO J.* 23, 3803–3814. doi: 10.1038/sj.emboj.7600399

Menard, C., Hein, P., Paquin, A., Savelson, A., Yang, X. M., Lederfein, D., et al. (2002). An essential role for a MEK-C/EBP pathway during growth factor-regulated cortical neurogenesis. *Neuron* 36, 597–610. doi: 10.1016/s0896-6273(02)01026-7

Miesfeld, J. B., Moon, M. S., Riesenberg, A. N., Contreras, A. N., Kovall, R. A., and Brown, N. L. (2018). Rbpj direct regulation of Atoh7 transcription in the embryonic mouse retina. *Sci. Rep.* 8:10195.

Miyama, S., Takahashi, T., Nowakowski, R. S., and Caviness, V. S. Jr. (1997). A gradient in the duration of the G1 phase in the murine neocortical proliferative epithelium. *Cereb. Cortex* 7, 678–689. doi: 10.1093/cercor/7.7.678

Miyata, T., Kawaguchi, A., Saito, K., Kawano, M., Muto, T., and Ogawa, M. (2004). Asymmetric production of surface-dividing and non-surface-dividing cortical progenitor cells. *Development* 131, 3133–3145. doi: 10.1242/dev.01173

Molnar, Z., Vasistha, N. A., and Garcia-Moreno, F. (2011). Hanging by the tail: progenitor populations proliferate. *Nat. Neurosci.* 14, 538–540. doi: 10.1038/nn.2817

Molne, M., Studer, L., Tabar, V., Ting, Y. T., Eiden, M. V., and McKay, R. D. (2000). Early cortical precursors do not undergo LIF-mediated astrocytic differentiation. *J. Neurosci. Res.* 59, 301–311. doi: 10.1002/(sici)1097-4547(20000201)59:3<301::aid-jnr3>3.0.co;2-h

Morimoto-Suzki, N., Hirabayashi, Y., Tyssowski, K., Shinga, J., Vidal, M., Koseki, H., et al. (2014). The polycomb component Ring1B regulates the timed termination of subcerebral projection neuron production during mouse neocortical development. *Development* 141, 4343–4353. doi: 10.1242/dev.112276

Muller, J., and Verrijzer, P. (2009). Biochemical mechanisms of gene regulation by polycomb group protein complexes. *Curr. Opin. Genet. Dev.* 19, 150–158. doi: 10.1016/j.gde.2009.03.001

Murre, C., McCaw, P. S., Vaessin, H., Caudy, M., Jan, L. Y., Jan, Y. N., et al. (1989). Interactions between heterologous helix-loop-helix proteins generate complexes that bind specifically to a common DNA sequence. *Cell* 58, 537–544. doi: 10.1016/0092-8674(89)90434-0

Muzio, L., DiBenedetto, B., Stoykova, A., Boncinelli, E., Gruss, P., and Mallamaci, A. (2002a). Emx2 and Pax6 control regionalization of the pre-neuronogenic cortical primordium. *Cereb. Cortex* 12, 129–139. doi: 10.1093/cercor/12.2.129

Muzio, L., DiBenedetto, B., Stoykova, A., Boncinelli, E., Gruss, P., and Mallamaci, A. (2002b). Conversion of cerebral cortex into basal ganglia in Emx2(-/-) Pax6(Sey/Sey) double-mutant mice. *Nat. Neurosci.* 5, 737–745. doi: 10.1038/nn892

Nguyen, L., Besson, A., Heng, J. I., Schuurmans, C., Teboul, L., Parras, C., et al. (2006). p27kip1 independently promotes neuronal differentiation and migration in the cerebral cortex. *Genes Dev.* 20, 1511–1524. doi: 10.1101/gad.377106

Nieto, M., Schuurmans, C., Britz, O., and Guillemot, F. (2001). Neural bHLH genes control the neuronal versus glial fate decision in cortical progenitors. *Neuron* 29, 401–413. doi: 10.1016/s0896-6273(01)00214-8

Noctor, S. C., Martinez-Cerdeno, V., Ivic, L., and Kriegstein, A. R. (2004). Cortical neurons arise in symmetric and asymmetric division zones and migrate through specific phases. *Nat. Neurosci.* 7, 136–144. doi: 10.1038/nn1172

Nolo, R., Abbott, L. A., and Bellen, H. J. (2000). Senseless, a Zn finger transcription factor, is necessary and sufficient for sensory organ development in Drosophila. *Cell* 102, 349–362. doi: 10.1016/s0092-8674(00)00040-4

Ochi, S., Imaizumi, Y., Shimojo, H., Miyachi, H., and Kageyama, R. (2020). Oscillatory expression of Hes1 regulates cell proliferation and neuronal differentiation in the embryonic brain. *Development* 147:dev182204. doi: 10.1242/dev.182204

Ohori, Y., Yamamoto, S., Nagao, M., Sugimori, M., Yamamoto, N., Nakamura, K., et al. (2006). Growth factor treatment and genetic manipulation stimulate neurogenesis and oligodendrogenesis by endogenous neural progenitors in the injured adult spinal cord. *J. Neurosci.* 26, 11948–11960. doi: 10.1523/jneurosci.3127-06.2006

Ohtaka-Maruyama, C. (2020). Subplate neurons as an organizer of mammalian neocortical development. *Front. Neuroanat.* 14:8. doi: 10.3389/fnana.2020.00008

Ohtsuka, M., Fukumitsu, H., and Furukawa, S. (2009). Neurotrophin-3 stimulates neurogenetic proliferation via the extracellular signal-regulated kinase pathway. *J. Neurosci. Res.* 87, 301–306. doi: 10.1002/jnr.21855

Ohtsuka, T., Ishibashi, M., Gradwohl, G., Nakanishi, S., Guillemot, F., and Kageyama, R. (1999). Hes1 and Hes5 as notch effectors in mammalian neuronal differentiation. *EMBO J.* 18, 2196–2207. doi: 10.1093/emboj/18.8.2196

Oishi, K., van den Berg, D. L. C., and Guillemot, F. (2020). Temporal control of cortico-thalamic neuron specification by regulation of Neurogenin activity and Polycomb repressive complexes. *bioRxiv* [Preprint]. doi: 10.1101/431684

Okawa, S., Nicklas, S., Zickenrott, S., Schwamborn, J. C., and Del Sol, A. (2016). A generalized gene-regulatory network model of stem cell differentiation for predicting lineage specifiers. *Stem Cell Rep.* 7, 307–315. doi: 10.1016/j.stemcr.2016.07.014

Pacary, E., Azzarelli, R., and Guillemot, F. (2013). Rnd3 coordinates early steps of cortical neurogenesis through actin-dependent and -independent mechanisms. *Nat. Commun.* 4:1635.

Pacary, E., Heng, J., Azzarelli, R., Riou, P., Castro, D., Lebel-Potter, M., et al. (2011). Proneural transcription factors regulate different steps of cortical neuron migration through Rnd-mediated inhibition of RhoA signaling. *Neuron* 69, 1069–1084. doi: 10.1016/j.neuron.2011.02.018

Pang, Z. P., Yang, N., Vierbuchen, T., Ostermeier, A., Fuentes, D. R., Yang, T. Q., et al. (2011). Induction of human neuronal cells by defined transcription factors. *Nature* 476, 220–223. doi: 10.1038/nature10202

Parras, C. M., Hunt, C., Sugimori, M., Nakafuku, M., Rowitch, D., and Guillemot, F. (2007). The proneural gene Mash1 specifies an early population of telencephalic oligodendrocytes. *J. Neurosci.* 27, 4233–4242. doi: 10.1523/jneurosci.0126-07.2007

Parras, C. M., Schuurmans, C., Scardigli, R., Kim, J., Anderson, D. J., and Guillemot, F. (2002). Divergent functions of the proneural genes Mash1 and Ngn2 in the specification of neuronal subtype identity. *Genes Dev.* 16, 324–338. doi: 10.1101/gad.940902

Pavri, R., Zhu, B., Li, G., Trojer, P., Mandal, S., Shilatifard, A., et al. (2006). Histone H2B monoubiquitination functions cooperatively with FACT to regulate elongation by RNA polymerase II. *Cell* 125, 703–717. doi: 10.1016/j.cell.2006.04.029

Pearson, B. J., and Doe, C. Q. (2004). Specification of temporal identity in the developing nervous system. *Annu. Rev. Cell Dev. Biol.* 20, 619–647. doi: 10.1146/annurev.cellbio.19.111301.115142

Pereira, J. D., Sansom, S. N., Smith, J., Dobenecker, M. W., Tarakhovsky, A., and Livesey, F. J. (2010). Ezh2, the histone methyltransferase of PRC2, regulates the balance between self-renewal and differentiation in the cerebral cortex. *Proc. Natl. Acad. Sci. U.S.A.* 107, 15957–15962. doi: 10.1073/pnas.1002530107

Peyre, E., Silva, C. G., and Nguyen, L. (2015). Crosstalk between intracellular and extracellular signals regulating interneuron production, migration and integration into the cortex. *Front. Cell. Neurosci.* 9:129. doi: 10.3389/fncel.2015.00129

Pfisterer, U., Kirkeby, A., Torper, O., Wood, J., Nelander, J., Dufour, A., et al. (2011). Direct conversion of human fibroblasts to dopaminergic neurons. *Proc. Natl. Acad. Sci. U.S.A.* 108, 10343–10348.

Pfurr, S., Chu, Y. H., Bohrer, C., Greulich, F., Beattie, R., Mammadzada, K., et al. (2017). The E2A splice variant E47 regulates the differentiation of projection neurons via p57(KIP2) during cortical development. *Development* 144, 3917–3931. doi: 10.1242/dev.145698

Pleasure, S. J., Collins, A. E., and Lowenstein, D. H. (2000). Unique expression patterns of cell fate molecules delineate sequential stages of dentate gyrus development. *J. Neurosci.* 20, 6095–6105. doi: 10.1523/jneurosci.20-16-06095.2000

Pollen, A. A., Nowakowski, T. J., Chen, J., Retallack, H., Sandoval-Espinosa, C., Nicholas, C. R., et al. (2015). Molecular identity of human outer radial glia during cortical development. *Cell* 163, 55–67. doi: 10.1016/j.cell.2015.09.004

Ponti, G., Obernier, K., Guinto, C., Jose, L., Bonfanti, L., and Alvarez-Buylla, A. (2013). Cell cycle and lineage progression of neural progenitors in the ventricular-subventricular zones of adult mice. *Proc. Natl. Acad. Sci. U.S.A.* 110, E1045–E1054.

Price, J., and Thurlow, L. (1988). Cell lineage in the rat cerebral cortex: a study using retroviral-mediated gene transfer. *Development* 104, 473–482.

Pufall, M. A., Lee, G. M., Nelson, M. L., Kang, H. S., Velyvis, A., Kay, L. E., et al. (2005). Variable control of Ets-1 DNA binding by multiple phosphates in an unstructured region. *Science* 309, 142–145. doi: 10.1126/science.1111915

Qian, X., Shen, Q., Goderie, S. K., He, W., Capela, A., Davis, A. A., et al. (2000). Timing of CNS cell generation: a programmed sequence of neuron and glial cell production from isolated murine cortical stem cells. *Neuron* 28, 69–80.

Quan, X. J., Denayer, T., Yan, J., Jafar-Nejad, H., Philippi, A., Lichtarge, O., et al. (2004). Evolution of neural precursor selection: functional divergence of proneural proteins. *Development* 131, 1679–1689. doi: 10.1242/dev.01055

Quan, X. J., Yuan, L., Tiberi, L., Claeys, A., De Geest, N., Yan, J., et al. (2016). Post-translational control of the temporal dynamics of transcription factor activity regulates neurogenesis. *Cell* 164, 460–475. doi: 10.1016/j.cell.2015.12.048

Raballo, R., Rhee, J., Lyn-Cook, R., Leckman, J. F., Schwartz, M. L., and Vaccarino, F. M. (2000). Basic fibroblast growth factor (Fgf2) is necessary for cell proliferation and neurogenesis in the developing cerebral cortex. *J. Neurosci.* 20, 5012–5023. doi: 10.1523/jneurosci.20-13-05012.2000

Raposo, A. A., Vasconcelos, F. F., Drechsel, D., Marie, C., Johnston, C., Dolle, D., et al. (2015). Ascl1 coordinately regulates gene expression and the chromatin landscape during neurogenesis. *Cell Rep.* 10, 1544–1556. doi: 10.1016/j.celrep.2015.02.025

Reeve, R. L., Yammine, S. Z., Morshead, C. M., and van der Kooy, D. (2017). Quiescent Oct4+ neural stem cells (NSCs) repopulate ablated glial fibrillary acidic protein+ NSCs in the adult mouse brain. *Stem Cells* 35, 2071–2082. doi: 10.1002/stem.2662

Reillo, I., de Juan Romero, C., Garcia-Cabezas, M. A., and Borrell, V. (2011). A role for intermediate radial glia in the tangential expansion of the mammalian cerebral cortex. *Cereb. Cortex* 21, 1674–1694. doi: 10.1093/cercor/bhq238

Ringrose, L., Ehret, H., and Paro, R. (2004). Distinct contributions of histone H3 lysine 9 and 27 methylation to locus-specific stability of polycomb complexes. *Mol. Cell* 16, 641–653. doi: 10.1016/j.molcel.2004.10.015

Rivetti di Val Cervo, P., Romanov, R. A., Spigolon, G., Masini, D., Martin-Montanez, E., Toledo, E. M., et al. (2017). Induction of functional dopamine neurons from human astrocytes *in vitro* and mouse astrocytes in a Parkinson's disease model. *Nat. Biotechnol.* 35, 444–452. doi: 10.1038/nbt.3835

Ruddy, R. M., and Morshead, C. M. (2018). Home sweet home: the neural stem cell niche throughout development and after injury. *Cell Tissue Res.* 371, 125–141. doi: 10.1007/s00441-017-2658-0

Russo, G. L., Sonsalla, G., Natarajan, P., Breunig, C. T., Bulli, G., Merl-Pham, J., et al. (2020). CRISPR-mediated induction of neuron-enriched mitochondrial proteins boosts direct glia-to-neuron conversion. *Cell Stem Cell*. doi: 10.1016/j.stem.2020.10.015 [Epub ahead of print].

Schuurmans, C., Armant, O., Nieto, M., Stenman, J. M., Britz, O., Klenin, N., et al. (2004). Sequential phases of cortical specification involve Neurogenin-dependent and -independent pathways. *EMBO J.* 23, 2892–2902. doi: 10.1038/sj.emboj.7600278

Schwab, M. H., Bartholomae, A., Heimrich, B., Feldmeyer, D., Druffel-Augustin, S., Goebbels, S., et al. (2000). Neuronal basic helix-loop-helix proteins (NEX and BETA2/Neuro D) regulate terminal granule cell differentiation in the hippocampus. *J. Neurosci.* 20, 3714–3724. doi: 10.1523/jneurosci.20-10-03714.2000

Seo, S., Lim, J. W., Yellajoshyula, D., Chang, L. W., and Kroll, K. L. (2007). Neurogenin and NeuroD direct transcriptional targets and their regulatory enhancers. *EMBO J.* 26, 5093–5108. doi: 10.1038/sj.emboj.7601923

Seo, S., Richardson, G. A., and Kroll, K. L. (2005). The SWI/SNF chromatin remodeling protein Brg1 is required for vertebrate neurogenesis and mediates transactivation of Ngn and NeuroD. *Development* 132, 105–115. doi: 10.1242/dev.01548

Sessa, A., Ciabatti, E., Drechsel, D., Massimino, L., Colasante, G., Giannelli, S., et al. (2017). The Tbr2 molecular network controls cortical neuronal differentiation through complementary genetic and epigenetic pathways. *Cereb. Cortex* 27, 3378–3396.

Sheikh, B. N. (2014). Crafting the brain - role of histone acetyltransferases in neural development and disease. *Cell Tissue Res.* 356, 553–573. doi: 10.1007/s00441-014-1835-7

Sherrington, S. C. (2009). *Man on his Nature*. Cambridge: Cambridge University Press.

Shi, M., Hu, Z. L., Zheng, M. H., Song, N. N., Huang, Y., Zhao, G., et al. (2012). Notch-Rbpj signaling is required for the development of noradrenergic neurons in the mouse locus coeruleus. *J. Cell Sci.* 125, 4320–4332. doi: 10.1242/jcs.102152

Shimojo, H., Ohtsuka, T., and Kageyama, R. (2008). Oscillations in notch signaling regulate maintenance of neural progenitors. *Neuron* 58, 52–64. doi: 10.1016/j.neuron.2008.02.014

Shimojo, H., Ohtsuka, T., and Kageyama, R. (2011). Dynamic expression of notch signaling genes in neural stem/progenitor cells. *Front. Neurosci.* 5:78. doi: 10.3389/fnins.2011.00078

Sims, R. J. III, and Reinberg, D. (2006). Histone H3 Lys 4 methylation: caught in a bind? *Genes Dev.* 20, 2779–2786. doi: 10.1101/gad.1468206

Son, A. I., Mohammad, S., Sasaki, T., Ishii, S., Yamashita, S., Hashimoto-Torii, K., et al. (2020). Dual role of Rbpj in the maintenance of neural progenitor cells and neuronal migration in cortical development. *Cereb. Cortex* 30, 6444–6457. doi: 10.1093/cercor/bhaa206

Son, E. Y., Ichida, J. K., Wainger, B. J., Toma, J. S., Rafuse, V. F., Woolf, C. J., et al. (2011). Conversion of mouse and human fibroblasts into functional spinal motor neurons. *Cell Stem Cell* 9, 205–218. doi: 10.1016/j.stem.2011.07.014

Song, M. R., and Ghosh, A. (2004). FGF2-induced chromatin remodeling regulates CNTF-mediated gene expression and astrocyte differentiation. *Nat. Neurosci.* 7, 229–235. doi: 10.1038/nn1192

Sorrells, S. F., Paredes, M. F., Cebrian-Silla, A., Sandoval, K., Qi, D., Kelley, K. W., et al. (2018). Human hippocampal neurogenesis drops sharply in children to undetectable levels in adults. *Nature* 555, 377–381. doi: 10.1038/nature25975

Spalding, K. L., Bergmann, O., Alkass, K., Bernard, S., Salehpour, M., Huttner, H. B., et al. (2013). Dynamics of hippocampal neurogenesis in adult humans. *Cell* 153, 1219–1227.

Sriuranpong, V., Borges, M. W., Strock, C. L., Nakakura, E. K., Watkins, D. N., Blaumueller, C. M., et al. (2002). Notch signaling induces rapid degradation of achaete-scute homolog 1. *Mol. Cell. Biol.* 22, 3129–3139. doi: 10.1128/mcb.22.9.3129-3139.2002

Stahl, R., Walcher, T., De Juan Romero, C., Pilz, G. A., Cappello, S., Irmler, M., et al. (2013). Trnp1 regulates expansion and folding of the mammalian cerebral cortex by control of radial glial fate. *Cell* 153, 535–549. doi: 10.1016/j.cell.2013.03.027

Stipursky, J., Spohr, T. C., Sousa, V. O., and Gomes, F. C. (2012). Neuron-astroglial interactions in cell-fate commitment and maturation in the central nervous system. *Neurochem. Res.* 37, 2402–2418. doi: 10.1007/s11064-012-0798-x

Stoykova, A., Treichel, D., Hallonet, M., and Gruss, P. (2000). Pax6 modulates the dorsoventral patterning of the mammalian telencephalon. *J. Neurosci.* 20, 8042–8050. doi: 10.1523/jneurosci.20-21-08042.2000

Strasser, M., Theis, F. J., and Marr, C. (2012). Stability and multiattractor dynamics of a toggle switch based on a two-stage model of stochastic gene expression. *Biophys. J.* 102, 19–29. doi: 10.1016/j.bpj.2011.11.4000

Stricker, S. H., and Gotz, M. (2020). Epigenetic regulation of neural lineage elaboration: Implications for therapeutic reprogramming. *Neurobiol. Dis.* 148, 105174. doi: 10.1016/j.nbd.2020.105174

Sun, Y., Meijer, D. H., Alberta, J. A., Mehta, S., Kane, M. F., Tien, A. C., et al. (2011). Phosphorylation state of Olig2 regulates proliferation of neural progenitors. *Neuron* 69, 906–917. doi: 10.1016/j.neuron.2011.02.005

Sun, Y., Nadal-Vicens, M., Misono, S., Lin, M. Z., Zubiaga, A., Hua, X., et al. (2001). Neurogenin promotes neurogenesis and inhibits glial differentiation by independent mechanisms. *Cell* 104, 365–376. doi: 10.1016/s0092-8674(01)00224-0

Suzuki, I. K., Gacquer, D., Van Heurck, R., Kumar, D., Wojno, M., Bilheu, A., et al. (2018). Human-specific NOTCH2NL genes expand cortical neurogenesis through delta/notch regulation. *Cell* 173, 1370–1384.e16.

Takahashi, T., Goto, T., Miyama, S., Nowakowski, R. S., and Caviness, V. S. Jr. (1999). Sequence of neuron origin and neocortical laminar fate: relation to cell cycle of origin in the developing murine cerebral wall. *J. Neurosci.* 19, 10357–10371. doi: 10.1523/jneurosci.19-23-10357.1999

Takahashi, T., Nowakowski, R. S., and Caviness, V. S. Jr. (1995). The cell cycle of the pseudostratified ventricular epithelium of the embryonic murine cerebral wall. *J. Neurosci.* 15, 6046–6057. doi: 10.1523/jneurosci.15-09-06046.1995

Takizawa, T., Nakashima, K., Namihira, M., Ochiai, W., Uemura, A., Yanagisawa, M., et al. (2001). DNA methylation is a critical cell-intrinsic determinant of astrocyte differentiation in the fetal brain. *Dev. Cell* 1, 749–758. doi: 10.1016/s1534-5807(01)00101-0

Tavares, L., Dimitrova, E., Oxley, D., Webster, J., Poot, R., Demmers, J., et al. (2012). RYBP-PRC1 complexes mediate H2A ubiquitylation at polycomb target sites independently of PRC2 and H3K27me3. *Cell* 148, 664–678. doi: 10.1016/j.cell.2011.12.029

Taverna, E., Gotz, M., and Huttner, W. B. (2014). The cell biology of neurogenesis: toward an understanding of the development and evolution of the neocortex. *Annu. Rev. Cell Dev. Biol.* 30, 465–502. doi: 10.1146/annurev-cellbio-101011-155801

Telley, L., Agirman, G., Prados, J., Amberg, N., Fievre, S., Oberst, P., et al. (2019). Temporal patterning of apical progenitors and their daughter neurons in the developing neocortex. *Science* 364:eaav2522. doi: 10.1126/science.aav2522

Telley, L., Govindan, S., Prados, J., Stevant, I., Nef, S., Dermitzakis, E., et al. (2016). Sequential transcriptional waves direct the differentiation of newborn neurons in the mouse neocortex. *Science* 351, 1443–1446. doi: 10.1126/science.aad8361

Theil, T., Alvarez-Bolado, G., Walter, A., and Ruther, U. (1999). Gli3 is required for Emx gene expression during dorsal telencephalon development. *Development* 126, 3561–3571.

Tole, S., Ragsdale, C. W., and Grove, E. A. (2000). Dorsoventral patterning of the telencephalon is disrupted in the mouse mutant extra-toes(J). *Dev. Biol.* 217, 254–265. doi: 10.1006/dbio.1999.9509

Tomita, K., Moriyoshi, K., Nakanishi, S., Guillemot, F., and Kageyama, R. (2000). Mammalian achaete-scute and atonal homologs regulate neuronal versus glial fate determination in the central nervous system. *EMBO J.* 19, 5460–5472. doi: 10.1093/emboj/19.20.5460

Tsacopoulos, M., and Magistretti, P. J. (1996). Metabolic coupling between glia and neurons. *J. Neurosci.* 16, 877–885. doi: 10.1523/jneurosci.16-03-00877.1996

Tursun, B., Patel, T., Kratsios, P., and Hobert, O. (2011). Direct conversion of *C. elegans* germ cells into specific neuron types. *Science* 331, 304–308. doi: 10.1126/science.1199082

Urban, N., and Guillemot, F. (2014). Neurogenesis in the embryonic and adult brain: same regulators, different roles. *Front. Cell. Neurosci.* 8:396. doi: 10.3389/fncel.2014.00396

Urban, N., van den Berg, D. L., Forget, A., Andersen, J., Demmers, J. A., Hunt, C., et al. (2016). Return to quiescence of mouse neural stem cells by degradation of a proactivation protein. *Science* 353, 292–295. doi: 10.1126/science.aaf4802

Vaccarino, F. M., Schwartz, M. L., Raballo, R., Rhee, J., and Lyn-Cook, R. (1999). Fibroblast growth factor signaling regulates growth and morphogenesis at multiple steps during brain development. *Curr. Top. Dev. Biol.* 46, 179–200. doi: 10.1016/s0070-2153(08)60329-4

Vaudry, D., Stork, P. J., Lazarovici, P., and Eiden, L. E. (2002). Signaling pathways for PC12 cell differentiation: making the right connections. *Science* 296, 1648–1649. doi: 10.1126/science.1071552

Vernon, A. E., Devine, C., and Philpott, A. (2003). The cdk inhibitor p27Xic1 is required for differentiation of primary neurones in *Xenopus*. *Development* 130, 85–92. doi: 10.1242/dev.00193

Vierbuchen, T., Ostermeier, A., Pang, Z. P., Kokubu, Y., Sudhof, T. C., and Wernig, M. (2010). Direct conversion of fibroblasts to functional neurons by defined factors. *Nature* 463, 1035–1041. doi: 10.1038/nature08797

Vinals, F., Reiriz, J., Ambrosio, S., Bartrons, R., Rosa, J. L., and Ventura, F. (2004). BMP-2 decreases Mash1 stability by increasing Id1 expression. *EMBO J.* 23, 3527–3537. doi: 10.1038/sj.emboj.7600360

Viti, J., Feathers, A., Phillips, J., and Lillien, L. (2003a). Epidermal growth factor receptors control competence to interpret leukemia inhibitory factor as an astrocyte inducer in developing cortex. *J. Neurosci.* 23, 3385–3393. doi: 10.1523/jneurosci.23-08-03385.2003

Viti, J., Gulacsi, A., and Lillien, L. (2003b). Wnt regulation of progenitor maturation in the cortex depends on Shh or fibroblast growth factor 2. *J. Neurosci.* 23, 5919–5927. doi: 10.1523/jneurosci.23-13-05919.2003

Vojtek, A. B., Taylor, J., DeRuiter, S. L., Yu, J. Y., Figueroa, C., Kwok, R. P., et al. (2003). Akt regulates basic helix-loop-helix transcription factor-coactivator complex formation and activity during neuronal differentiation. *Mol. Cell. Biol.* 23, 4417–4427. doi: 10.1128/mcb.23.13.4417-4427.2003

Vosper, J. M., Fiore-Heriche, C. S., Horan, I., Wilson, K., Wise, H., and Philpott, A. (2007). Regulation of neurogenin stability by ubiquitin-mediated proteolysis. *Biochem. J.* 407, 277–284. doi: 10.1042/bj20070064

Vosper, J. M., McDowell, G. S., Hindley, C. J., Fiore-Heriche, C. S., Kucerova, R., Horan, I., et al. (2009). Ubiquitylation on canonical and non-canonical sites targets the transcription factor neurogenin for ubiquitin-mediated proteolysis. *J. Biol. Chem.* 284, 15458–15468. doi: 10.1074/jbc.m809366200

Walsh, C., and Cepko, C. L. (1988). Clonally related cortical cells show several migration patterns. *Science* 241, 1342–1345. doi: 10.1126/science.3137660

Wang, B., Waclaw, R. R., Allen, Z. J. II, Guillemot, F., and Campbell, K. (2009). Ascl1 is a required downstream effector of Gsx gene function in the embryonic mouse telencephalon. *Neural Dev.* 4:5.

Wang, L., Hou, S., and Han, Y. G. (2016). Hedgehog signaling promotes basal progenitor expansion and the growth and folding of the neocortex. *Nat. Neurosci.* 19, 888–896. doi: 10.1038/nn.4307

Wang, L. H., and Baker, N. E. (2015). E proteins and ID proteins: helix-loop-helix partners in development and disease. *Dev. Cell* 35, 269–280. doi: 10.1016/j.devcel.2015.10.019

Wapinski, O. L., Lee, Q. Y., Chen, A. C., Li, R., Corces, M. R., Ang, C. E., et al. (2017). Rapid chromatin switch in the direct reprogramming of fibroblasts to neurons. *Cell Rep.* 20, 3236–3247. doi: 10.1016/j.celrep.2017.09.011

Wapinski, O. L., Vierbuchen, T., Qu, K., Lee, Q. Y., Chanda, S., Fuentes, D. R., et al. (2013). Hierarchical mechanisms for direct reprogramming of fibroblasts to neurons. *Cell* 155, 621–635. doi: 10.1016/j.cell.2013.09.028

Ward, J. J., Sodhi, J. S., McGuffin, L. J., Buxton, B. F., and Jones, D. T. (2004). Prediction and functional analysis of native disorder in proteins from the three kingdoms of life. *J. Mol. Biol.* 337, 635–645. doi: 10.1016/j.jmb.2004.02.002

Watanabe, K., Kamiya, D., Nishiyama, A., Katayama, T., Nozaki, S., Kawasaki, H., et al. (2005). Directed differentiation of telencephalic precursors from embryonic stem cells. *Nat. Neurosci.* 8, 288–296.

Wilkinson, G., Dennis, D., and Schuurmans, C. (2013). Proneural genes in neocortical development. *Neuroscience* 253, 256–273. doi: 10.1016/j.neuroscience.2013.08.029

Wu, Z. Q., Li, D., Huang, Y., Chen, X. P., Huang, W., Liu, C. F., et al. (2017). Caspr controls the temporal specification of neural progenitor cells through notch signaling in the developing mouse cerebral cortex. *Cereb. Cortex* 27, 1369–1385.

Yang, G., Smibert, C. A., Kaplan, D. R., and Miller, F. D. (2014). An eIF4E1/4E-T complex determines the genesis of neurons from precursors by translationally repressing a proneurogenic transcription program. *Neuron* 84, 723–739. doi: 10.1016/j.neuron.2014.10.022

Yang, N., Chanda, S., Marro, S., Ng, Y. H., Janas, J. A., Haag, D., et al. (2017). Generation of pure GABAergic neurons by transcription factor programming. *Nat. Methods* 14, 621–628. doi: 10.1038/nmeth.4291

York, R. D., Yao, H., Dillon, T., Ellig, C. L., Eckert, S. P., McCleskey, E. W., et al. (1998). Rap1 mediates sustained MAP kinase activation induced by nerve growth factor. *Nature* 392, 622–626. doi: 10.1038/33451

Zahr, S. K., Kaplan, D. R., and Miller, F. D. (2019). Translating neural stem cells to neurons in the mammalian brain. *Cell Death Differ.* 26, 2495–2512. doi: 10.1038/s41418-019-0411-9

Zahr, S. K., Yang, G., Kazan, H., Borrett, M. J., Yuzwa, S. A., Voronova, A., et al. (2018). A translational repression complex in developing mammalian neural stem cells that regulates neuronal specification. *Neuron* 97, 520-537.e6.

Zandi, S., Bryder, D., and Sigvardsson, M. (2010). Load and lock: the molecular mechanisms of B-lymphocyte commitment. *Immunol. Rev.* 238, 47–62. doi: 10.1111/j.1600-065x.2010.00950.x

Zecevic, N., Chen, Y., and Filipovic, R. (2005). Contributions of cortical subventricular zone to the development of the human cerebral cortex. *J. Comp. Neurol.* 491, 109–122. doi: 10.1002/cne.20714

Zhao, J., Lin, Q., Kim, K. J., Dardashti, F. D., Kim, J., He, F., et al. (2015). Ngn1 inhibits astrogliogenesis through induction of miR-9 during neuronal fate specification. *eLife* 4:e06885.

Conflict of Interest: The authors declare that the research was conducted in the absence of any commercial or financial relationships that could be construed as a potential conflict of interest.

frontiers in Molecular Neuroscience

ORIGINAL RESEARCH
published: 23 March 2021
doi: 10.3389/fnmol.2021.613887

Mir-184 Contributes to Brain Injury Through Targeting PPAP2B Following Ischemic Stroke in Male Rats

Huajun Yang[1,2†], Yifan Zhang[1†], Hongqun Chen[1], Yingwu Zhu[1], Yuan Li[1], Fu Ouyang[1], Lan Chu[1] and Daishun Liu[2]**

[1] Department of Neurology, Affiliated Hospital of Guizhou Medical University, Guizhou Medical University, Guiyang, China, [2] Department of Respiratory Medicine, The First People's Hospital of Zunyi, The Third Affiliated Hospital of Zunyi Medical University, Zunyi, China

Our previous study revealed that miR-184 expression is significantly altered in the brain following ischemic stroke in rats. However, it is unknown whether this alteration in miR-184 expression contributes to brain injury after ischemic stroke. Here, we aim to address the potential of miR-184 to impact nerve injury following ischemia and reperfusion. Rats received ICV injection of miR-184 adenovirus or empty vector and were subjected to right middle cerebral artery occlusion (MCAO) to establish an ischemic stroke model. We cultured SH-SY5Y cells under oxygen-glucose deprivation/reoxygenation (OGD/R) and transfected them with miR-184 lentivirus to explore the primary mechanisms. To evaluate miR-184 expression, neurological function deficits, the cerebral infarct volume, cell viability, and apoptosis, qRT-PCR analysis of miR-184 expression, the modified neurological severity score (mNSS) system, TTC staining, the CCK-8 assay, flow cytometry, and dual-luciferase reporter assays were utilized. We found that miR-184 expression was downregulated and that the cerebral infarct volume and mNSSs were increased following ischemic stroke; however, increasing the level of miR-184 alleviated brain damage. Overexpression of miR-184 resulted in increased viability and reduced apoptosis of SH-SY5Y cells following OGD/R *in vitro*. We identified the phosphatidic acid phosphatase type 2B (PPAP2B) gene as a direct target gene of miR-184. In summary, our results reveal that attenuation of miR-184 levels in ischemic stroke contributes to ischemic injury through targeting PPAP2B mRNA-mediated apoptosis, which may be a promising therapeutic target for ischemic stroke.

Keywords: ischemia stroke, mir-184, brain injury, apoptosis, type 2 phosphatidic acid phospatase gene B

OPEN ACCESS

Edited by:
Estela Maris Muñoz, CONICET Dr. Mario H. Burgos Institute of Histology and Embryology (IHEM), Argentina

Reviewed by:
Devin William McBride, University of Texas Health Science Center at Houston, United States
Kusum Sinha, Penn State College of Medicine, United States

***Correspondence:**
Lan Chu
chulan8999@yeah.net
Daishun Liu
ldsdoc@126.com

† These authors have contributed equally to this work

Received: *04 October 2020*
Accepted: *10 February 2021*
Published: *23 March 2021*

Citation:
Yang H, Zhang Y, Chen H, Zhu Y, Li Y, Ouyang F, Chu L and Liu D (2021) Mir-184 Contributes to Brain Injury Through Targeting PPAP2B Following Ischemic Stroke in Male Rats. Front. Mol. Neurosci. 14:613887. doi: 10.3389/fnmol.2021.613887

INTRODUCTION

As the most common type of stroke, ischemic stroke results from cerebral blood flow thrombosis or embolism, leading to oxygen and glucose deprivation, subsequent brain damage, and neurologic deficits (Han et al., 2014). Additionally, postischemic blood reperfusion further aggravates nerve injury (Kasdorf and Perlman, 2013). Decades of research have revealed much of the pathophysiology of cerebral ischemia and reperfusion injury. The process involves various elements, such as energy failure, oxidative stress, excitotoxicity, and ion imbalance, all of which can lead to a complex series of cellular reactions, changes in the expression patterns of genes, and subsequent brain damage and dysfunction in the ischemic brain (Cheon et al., 2018). There

are currently limited treatment options for ischemic stroke, partly due to a lack of complete understanding of the molecular mechanism responsible for neuronal damage following ischemic stroke (Khoshnam et al., 2017a).

MicroRNAs are a family of small non-coding RNAs that negatively regulate target genes at the posttranscriptional level through hybridizing to complementary sequences located in the 3'-untranslated regions of target mRNAs. It is now evident that microRNAs are region-specific. In the brains of mammals, some microRNAs are highly expressed and implicated in neurological physiological processes and diseases (Yin et al., 2015). In particular, evidence has shown that the expression levels of many microRNAs are significantly altered after ischemic stroke in the rodent and human brain (Rink and Khanna, 2011). MicroRNAs that are expressed after stroke are involved in excitotoxicity, oxidative stress, inflammatory reactions, blood-brain barrier disruption, edema after stroke, and neuronal apoptosis (Li et al., 2018). MicroRNAs have emerged as essential regulators of gene expression in the pathology of ischemic stroke (Li et al., 2018). Our previous study found that miR-184 is among the top downregulated microRNAs in the blood of patients following ischemic stroke. The expression of miR-184 is significantly altered in the brain following ischemic stroke in rats (Wang et al., 2020). MiR-184, a highly enriched microRNA in the mammalian brain, has been shown to promote oligodendrocyte differentiation and control the proliferation and differentiation of adult neural stem/progenitor cells (Liu et al., 2010; Afrang et al., 2019). It also contributes to cardiomyocyte injury during myocardial infarction (Zou et al., 2020) and cellular apoptosis in retinoblastoma (He et al., 2019). However, it is unknown whether the alteration of miR-184 expression contributes to brain injury after ischemic stroke. The present study investigation aims to address the potential of miR-184 to impact nerve injury following ischemia and reperfusion *in vivo* and *in vitro*. The results may shed new light on the underlying mechanism of poststroke brain injury and provide clues for new gene therapies for stroke recovery.

MATERIALS AND METHODS

Animals and Protocols

Male Sprague-Dawley rats weighing 250–300 g were obtained from Tianqin Biotech Co. (Changsha, China), housed in individual cages at 20 ± 3°C and 60% humidity on a 12 h light/dark cycle, and provided *ad libitum* access to standard laboratory chow and water. The experimental animal procedures were approved by the Ethics Committee of The Third Hospital Affiliated to Medical University of Zunyi and were performed according to the principles of laboratory animal use and care published by the NIH (NIH publication #85-23, revised in 2011).

We divided the rats into four groups: the middle cerebral artery occlusion (MCAO)-induced ischemic stroke, sham operation, miR-184 adenovirus-injected ischemic stroke, and empty adenovirus vector-injected ischemic stroke groups. The number of surviving animals in each group at the end of the experiment was 14/20 in the ischemic stroke group, 14/14 in the sham operation group, 15/20 in the miR-184 adenovirus-injected ischemic stroke group, and 14/20 in the empty vector-injected ischemic stroke group. A cohort of rats (n = 6 from each group) was sacrificed by decapitation after 24 h of reperfusion following MCAO. Brain tissues were carefully removed to assess the infarct volume and miR-184 expression. The remaining rats (n = 8–9 in each group) were subjected to analysis of neurological function deficits 1, 3, 7, 14, 21, and 28 days after MCAO using the mNSS system. At the end of the experimental period, the rats were euthanized by CO_2 asphyxiation.

The sample size was calculated based on the following formula:

$$n = 2.172 \times (\Sigma Si2/K)/[\Sigma(-Xi - X)2/(K - 1)]$$

with Si being the standard deviation estimated for each group, Xi being the mean value of index data estimated for each group, X being the mean value of index data for each group, K being the group number (here, K = 4), and 2.17 being the coefficient when $\alpha = 0.05$, $\beta = 0.1$, and K = 4. The inspection power was 90%.

Establishment of the Rat Model of Ischemic Stroke

Middle cerebral artery occlusion (MCAO) was used to induce ischemic stroke in rats following Lopez and Vemuganti (2018). Briefly, the rats were anesthetized with 3% isoflurane (AbbVie Inc., United States) and placed on a heating pad, and a midline incision was made in the neck. The right common, external, and internal carotid arteries were carefully separated from the surrounding tissues. The standard and external arteries were ligated. The superficial artery was cut at the distal portion. A silica gel-coated nylon monofilament (0.26 mm) was inserted into the right common carotid artery and advanced into the internal carotid artery to prevent blood flow (Dharap et al., 2009). After 2 h, the monofilament was withdrawn to restore blood circulation, and CT Imaging was performed after 24 h with a micro-CT scanner (Latheta LCT-200, Hitachi Aloka Medical) to assess the outcomes of MCAO. Ischemic stroke modeling was considered successful in rats with low-density regions in the right cerebra because of brain edema caused by the absence of flow (Heiss, 2016). Based on CT images, 2–3 rats from each group were excluded. The sham group underwent the same procedure, but the artery was not ligated and occluded.

Intracerebroventricular (ICV) Injection

To better determine the effect of miR-184 on cerebral injury after ischemia-reperfusion injury, two groups of rats were subjected to ICV injection of miR-184 adenovirus or empty vector on the right side 2 days before MCAO. In brief, the rats were anesthetized with 3% isoflurane, and a small hole was made in the skull using a hand drill (from bregma: 0.8 mm posterior, -4.8 mm dorsoventral, -1.5 mm lateral) after a sagittal skin incision was made. The coordinates were selected according to Goel et al. (2008) [10]. MiR-184 adenovirus or empty adenovirus (2.5 μl/100 g body weight) (Genechem, Shanghai, China) was microinjected into the lateral ventricles using a Hamilton microsyringe at a rate of 0.5 μl/min. Then, the hole was sealed, and the scalp was sutured.

Assessment of Neurological Function

Neurological function deficits were assessed 1, 3, 7, 14, 21, and 28 days after MCAO-induced ischemic stroke using the modified neurological severity scoring (mNSS) system by a blinded investigator. The mNSS system assesses movement, sensation, reflex, and balance. Neurological function deficits were graded from 0 to 18 (0, no deficits; 18, maximal deficits) (Germano et al., 1994).

Assessment of the Infarct Volume

The infarct volume was assessed by 2,3,5-triphenyl tetrazolium chloride (TTC) (Sigma-Aldrich, United States) staining. After the rats were sacrificed by decapitation, the brains were removed and cut into five serial coronal sections (2 mm thick). The slices were then stained with 1% TTC at 37°C for 30 min and fixed in 4% paraformaldehyde. The area of each section was quantified using ImageJ 6.0 software (NIH, Bethesda, MD, United States) following imaging. The cerebral infarct volume was estimated by the equation the infarction area × thickness/2, as described by Wei et al. (2016).

Quantitative Real-Time PCR (qRT-PCR)

Total RNA was isolated using TRIzol Reagent (Solarbio Co., Beijing, China), and cDNA synthesis was carried out using a cDNA Synthesis Kit (Solarbio Co., Beijing, China). According to the manufacturer's instructions, PCR amplification was performed with SYBR Green PCR Mix (Solarbio Co., Beijing, China). The sequences of the primers for miR-184 and U6 were as follows: miR-184, forward: 5′-AGT GCA GGG TCC GAG GTA TT-3′, reverse: 5′-CGC GTG GAC GGA GAA CTG AT-3′, stem-loop: 5′-GTC GTA TCC AGT GCA GGG TCC GAG GTA TTC GCA CTG GAT ACG ACA CCC TT; U6, forward: 5′-AGA GAA GAT TAG CAT GGC CCC TG-3′, reverse: 5′-AGT GCA GGG TCC GAG GTA TT-3′, stem-loop: 5′-GTC GTA TCC AGT GCA GGG TCC GAG GTA TTC GCA CTG GAT ACG ACA AAA TA-3′. Relative gene expression was determined by the $2^{-\Delta\Delta Ct}$ method. Gene expression levels were normalized to the level of U6.

Cell Culture and Oxygen-Glucose Deprivation

Human SH-SY5Y neuroblastoma cells [American Type Culture Collection (ATCC, Shanghai, China)] were routinely cultured in DMEM/F12 medium (HyClone, Logan, United States) supplemented with 10% fetal bovine serum (Gibco, United States), penicillin (20 U/mL) and streptomycin (20 μg/mL) (Biological Industries, Israel) at 37°C in a humid atmosphere containing 5% CO_2. Some of these cells was transfected with hsa-miR-184 lentivirus or empty vector or hsa-PPAP2B interference lentivirus or empty vector (Genechem, Shanghai, China) 30 min after polybrene (3 μl/ml) was added to the culture. Subsequently, SH-SY5Y cells with cultured with puromycin to obtain stably transfected cells. After days, cells were transferred to glucose-free DMEM (Logan, United States) in a deoxygenated environment (containing 5% CO_2 and 95% N_2) at 37°C for 4 h, and then the cells were incubated in fresh medium containing glucose (4.5 g/L) in 96-well plates at a density of 5×10^4 cells for 24 h in a 5% CO_2 and 95% O_2 incubator for oxygen-glucose deprivation/reoxygenation (OGD/R). Control cells were cultured under normal aerobic conditions.

Cell Viability Assay

Cell viability was determined using the Cell Counting Kit-8 (CCK-8) assay (Beyotime Biotechnology, China). Briefly, after OGD/R, CCK-8 solution (Dojindo, Kumamoto, Japan) was added to each well, and the cells were incubated for 4 more hours at 37°C in a 5% CO_2 atmosphere according to the manufacturer's instructions. The absorbance value was measured at 450 nm using a microplate reader (BioTek, United States).

Cell Apoptosis Assay

Cell apoptosis was assessed using fluorescein isothiocyanate (FITC)-conjugated Annexin V and propidium iodide (P.I.) dual staining. Cells were fixed in 70% ethanol after being washed in phosphate-buffered saline, stained with Annexin V-FITC-propidium iodide (P.I.) (MultiSciences Biotechnology Co., Hangzhou, China), and incubated for 1 h in the dark. then, flow cytometry was performed (3-laser FACSCanto II, B.D. Bioscience, San Jose, CA, United States). The data were analyzed using FlowJo software (Tree Star, United States).

Dual-Luciferase Reporter Assays

The wild-type 3′ UTR and mutant 3′ UTR of hsa-PPAP2B were amplified and ligated into the pGL3 vector (Promega, United States) containing the luciferase reporter gene. 293T cells (ATCC, Shanghai, China) were cotransfected with hsa-PPAP2B-3′UTR-wt, hsa-PPAP2B-3′UTR-mut, and hsa-miR-184 or its negative control mimic using Lipofectamine 2000 (Invitrogen, China). 293T cells were then incubated in Dulbecco's modified Eagle's medium supplemented with 10% fetal bovine serum, 100 U/mL penicillin, and 100 μg/mL streptomycin. After 48 h of culture, a dual-luciferase reporter assay system (Promega, United States) was used to measure luciferase activity.

Statistical Analysis

The data are expressed as the mean ± *SD*. Comparisons between multiple groups were made by one-way analysis of variance (ANOVA) followed by Tukey's *post hoc* multiple comparisons test. Neurological scores were analyzed using the Kruskal–Wallis test. $P < 0.05$ was regarded as significant.

RESULTS

Expression Levels of MiR-184 in the Brain Are Associated With Brain Injury Following Ischemic Stroke

To evaluate the expression level of miR-184 in the injured brain following ischemic stroke, MCAO was used to establish a rat model of ischemic stroke, and the rats were administered an ICV injection of miR-184 adenovirus or empty vector. We assessed neurological function deficits

1, 3, 7, 14, 21, and 28 days after MCAO using the mNSS system. We found that ischemic stroke rats had higher mNSS scores than sham operation rats, but ischemic stroke rats injected with miR-184 adenovirus had lower mNSS scores than ischemic stroke rats injected with empty vector (**Figure 1A**).

Some rats of each group were sacrificed after 24 hours, and the brain was collected. Infarct volume was assessed by staining brain tissue with TTC. Non-infarcted brain areas are red, and the infarcted regions are stained white. Consistent with other studies (Bay et al., 2018; etc.), we found that the cerebral infarct volume of ischemic stroke rats was significantly larger than that of sham-operated rats, and they accounted for about 44% of the total brain volume (**Figures 1B,C**). In contrast, rats injected with adenovirus miR-184 had smaller infarct volumes, accounting for about 35% of total brain volume, than rats injected with an empty vehicle.

Moreover, we also measured the relative expression levels of miR-184 in brain tissue from various groups. qRT-PCR analysis showed that ischemic stroke rats exhibited significantly lower expression of miR-184 than sham rats ($p < 0.05$) and that rats injected with miR-184 adenovirus had higher expression of miR-184 than rats injected with empty vector ($p < 0.05$) (**Figure 1D**). These results reveal that the expression levels of miR-184 affect nerve injury following ischemic stroke and that downregulation of miR-184 expression after ischemia-reperfusion contributes to brain damage in rats.

The Effect of MiR-184 Expression Levels on Neuronal Viability and Apoptosis *in vitro*

To investigate the primary mechanism by which miR-184 contributes to brain damage following ischemic stroke, we

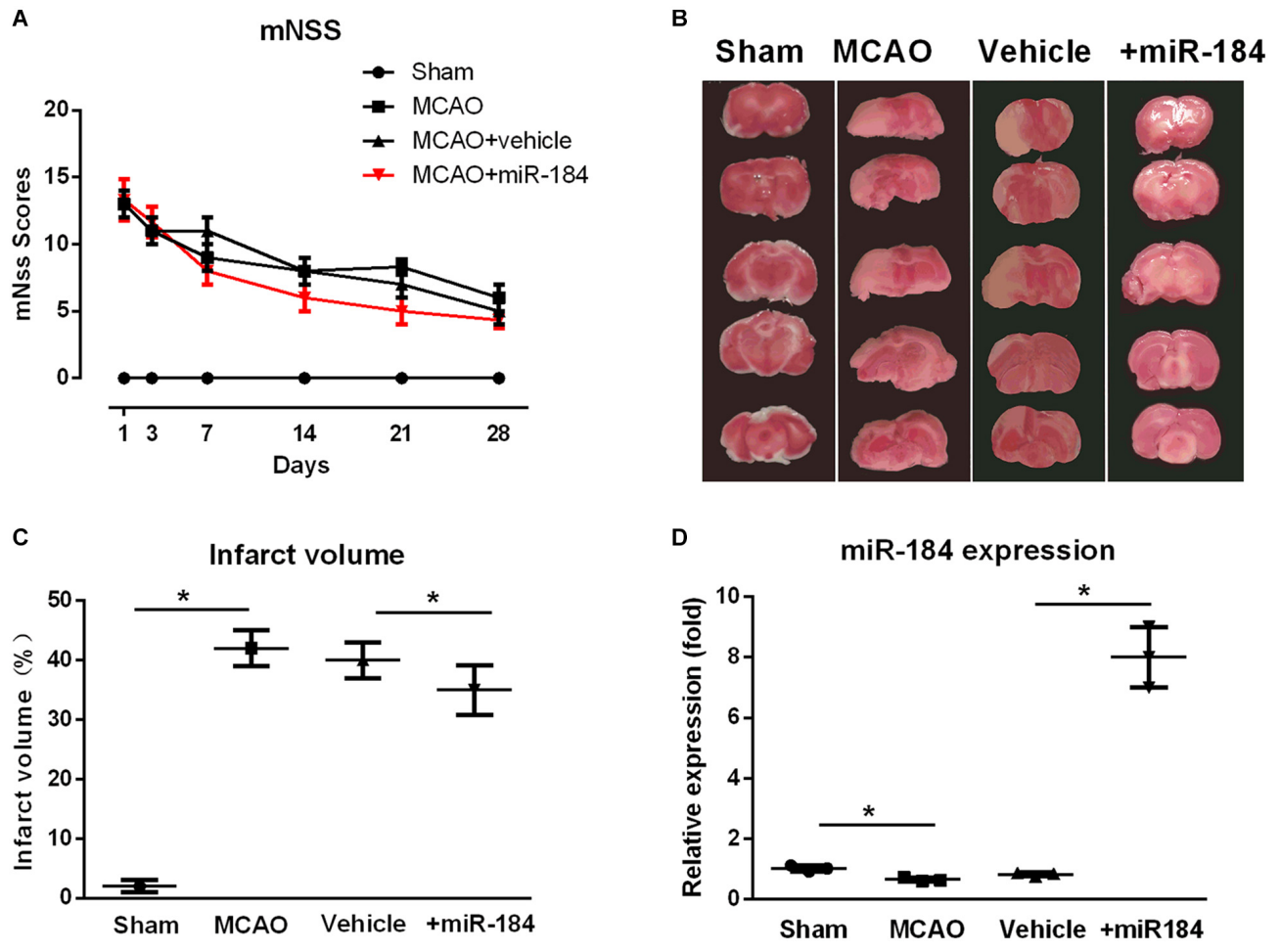

FIGURE 1 | The effect of expression levels of miR-184 in brain on the injured brain following ischemia stroke. Rats were subjected to middle cerebral artery occlusion (MCAO) operation to induce ischemic stroke model with or without intracerebroventricular injection of miR-184 adenovirus (Ad-miR-184). After 24 h following MCAO, a cohort of rats was sacrificed, and brain tissue was taken for TTC staining and qRT-PCR to evaluate the infarct volume and miR-184 expression in brain. Other rats were subjected to analysis of neurological function deficit 1, 3, 7, 14, 21, and 28 day after MCAO operation using mNSS system. **(A)** mNSS scores in various groups (n = 8–9). **(B)** TTC-stained brain slice images 24 following ischemia-reperfusion (n = 6 in each group). **(C)** Quantification analysis of the infarct volume. **(D)** Relative expression of miR-184 in the brain (n = 6 in each group). Values are mean ± *SD*. *$p < 0.05$ vs. the sham or vehicle.

cultured human SH-SY5Y neuroblastoma cells (which exhibit a neuroblast-like morphology), transfected them with or without miR-184 lentivirus, and challenged them with oxygen-glucose deprivation/reoxygenation (OGD/R) to induce ischemic stroke injury *in vitro*. After 24 h, we used qRT-PCR to analyze the relative expression of miR-184 and used the CCK-8 assay and flow cytometry to analyze cell viability and cellular apoptosis. We found that compared to normal aerobic conditions, OGD/R significantly downregulated the expression of miR-184 in SH-SY5Y cells ($p < 0.05$) (**Figure 2A**), reduced cell viability ($p < 0.05$) (**Figure 2B**), and increased cell apoptosis ($p < 0.05$) (**Figures 2C,D**). However, miR-184 lentivirus-transfected SH-SY5Y cells exhibited higher expression of miR-184 ($p < 0.05$) (**Figure 2A**), higher viability ($p < 0.05$) (**Figure 2B**), and

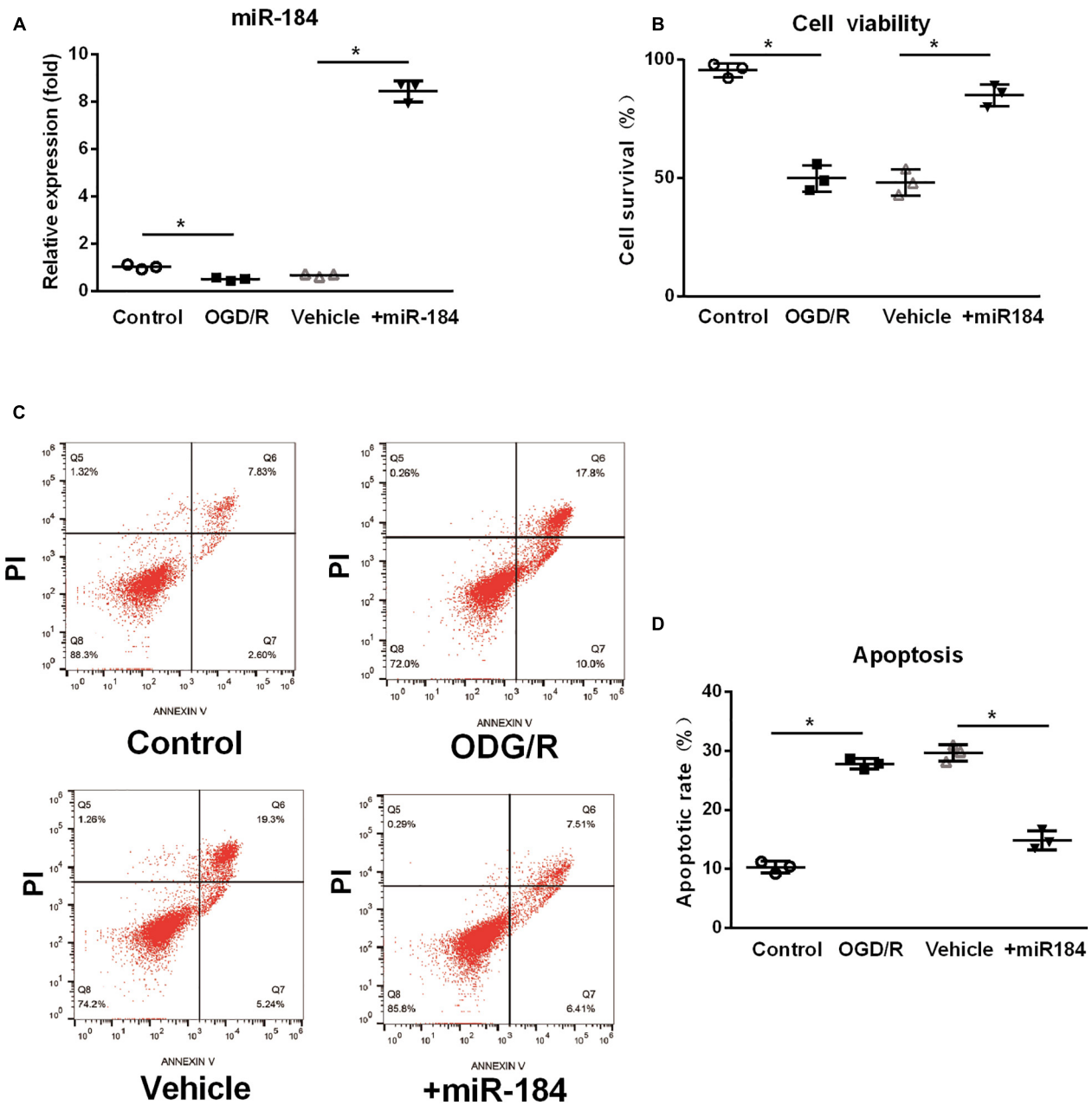

FIGURE 2 | The effect of expression levels of miR-184 on nerve cell viability and apoptosis. Human SH-SY5Y neuroblastoma cells with or without miR-184 lentivirus transduction were challenged with oxygen-glucose deprivation/reoxygenation (OGD/R) to induce ischemia-reperfusion injury *in vitro*. Cell viability, apoptosis and miR-184 expression were detected using CCK-8 assay, flow cytometry and qRT-PCR. **(A)** Relative expression of miR-184 in human SH-SY5Y neuroblastoma cells. **(B)** Cell viability. **(C)** Flow cytometry results. **(D)** Percent of cell apoptosis. Experiments were repeated in triplicate. Values are mean ± *SD*. *$p < 0.05$ vs. the control or vehicle.

lower apoptosis ($p < 0.05$) (**Figures 2C,D**) than empty vector-transduced cells following OGD/R challenge. In summary, reduced expression of miR-184 decreases neuronal viability and promotes neuronal apoptosis after ischemia-reperfusion.

PPAP2B, Target Gene of MiR-184

We further predicted the target gene of miR-184 using the starBase v.2.0 miRNA database[1]. We found that miR-184 can target the phosphatidic acid phosphatase type 2B (PPAP2B) gene, which can base-pair with miR-184 at its 3'-untranslated region (**Figure 3A**).

[1]starBase.sysu.edu.cn/

We also used dual-luciferase reporter assays to verify that the PPAP2B gene is a direct target molecule of miR-184. Hsa-PPAP2B-3′UTR-wt and hsa-PPAP2B-3′UTR-mut plasmids were constructed and cotransfected into 293T cells with hsa-miR-184 or its negative control mimic. Luciferase activity was measured using a dual-luciferase reporter assay system. The results showed that miR-184 lowered the luciferase activity of the hsa-PPAP2B-3′UTR-wt plasmid ($p < 0.05$) but no effect on the hsa-PPAP2B-3′UTR-mut plasmid (**Figure 3B**), suggesting that miR-184 targets PPAP2B mRNA and inhibits PPAP2B transcription.

Next, we evaluated the effect of suppression of PPAP2B expression on SH-SY5Y cell apoptosis following OGD/R. SH-SY5Y cells were transduced with hsa-PPAP2B interference

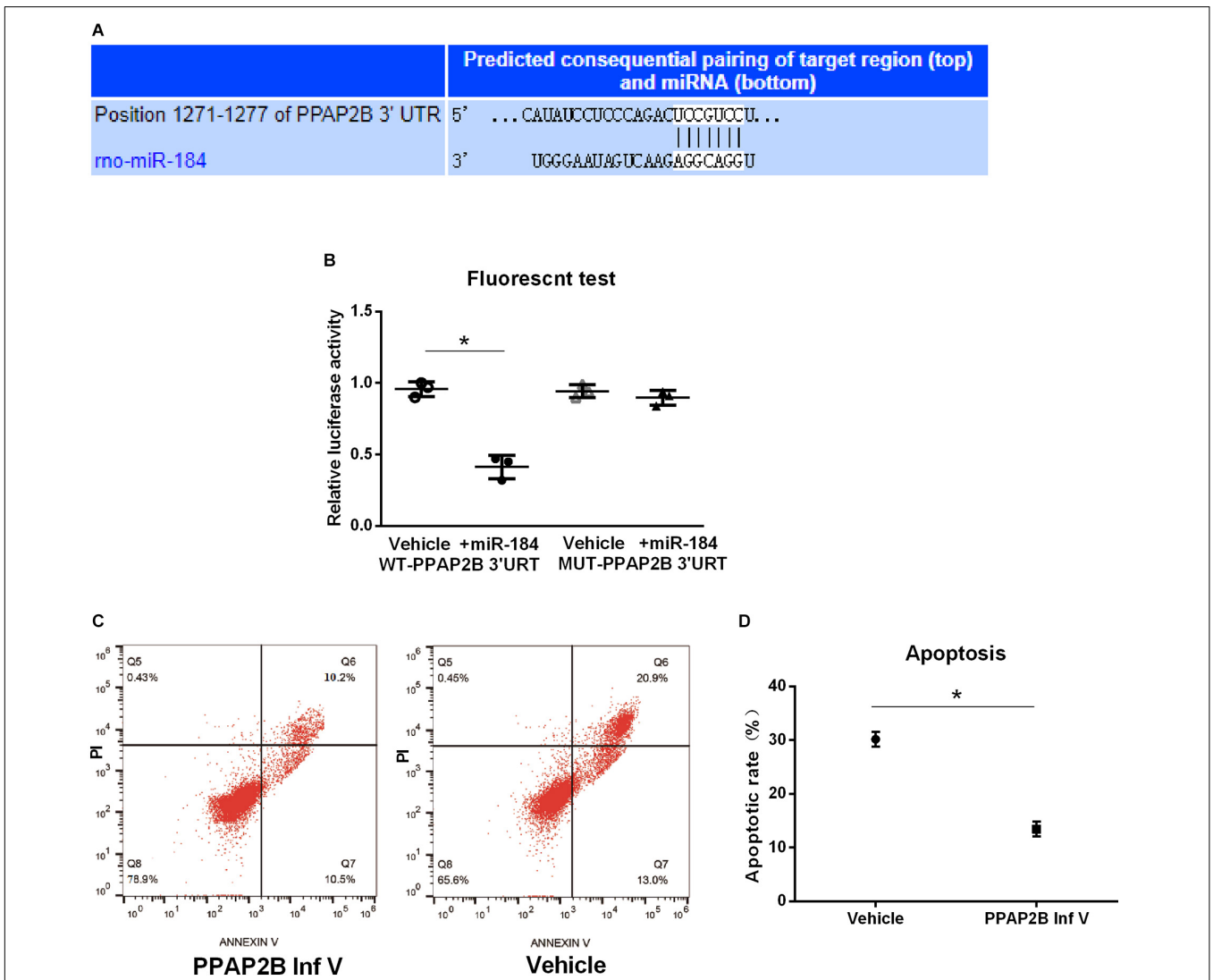

FIGURE 3 | MiR-184 target gene and verification. MiR-184 target gene was predicted using starBase v.2.0 miRNA database (starBase.sysu.edu.cn/), and was verified using dual-luciferase reporter assays. Transduction of SH-SY5Y cells with hsa-PPAP2B interference lentivirus (PPAP2B Inf V) or empty vector and attack with oxygen-glucose deprivation/reoxygenation (OGD/R). Apoptosis was analyzed by flow cytometry to evaluate the effect of the miR-184 target gene on neuronal apoptosis. **(A)** MiR-184 target is phosphatidic acid phosphatase genes type 2B (PPAP2B) mRNA, which can base-pair with miR-184 at its 3'-untranslated region sequences. **(B)** Luciferase activity. **(C)** Flow cytometry results of cell apoptosis. **(D)** Percent of cell apoptosis. Experiments were repeated in triplicate. Values are mean ± *SD*. *$p < 0.05$ vs. the control or vehicle.

lentivirus or empty vector and exposed to OGD/R, and after 24 h, cell apoptosis was analyzed by flow cytometry. The results showed that apoptosis was significantly lower ($p < 0.05$) (**Figures 3C,D**) in hsa-PPAP2B interference lentivirus-transfected SH-SY5Y cells than in empty vector-transfected cells. These results suggest that PPAP2B expression mediates miR-184-induced apoptosis in SH-SY5Y cells following ischemia-reperfusion.

DISCUSSION

In the current study, we found that MCAO-induced focal cerebral ischemia downregulated the expression of miR-184 and increased the cerebral infarct volume and neurological function deficits. We also showed that ICV injection of miR-184 adenovirus significantly alleviated the cerebral infarct area and neurological function deficits following ischemia stroke in rats. *In vitro* studies demonstrated that OGD/R-induced downregulation of miR-184 expression led to a decrease in viability and an increase in apoptosis in human neuroblastoma SH-SY5Y cells.

In our study, an ischemic stroke rat model was established using the MCAO, which is widely used in stroke-related preclinical studies in rodents. CT imaging was carried out to assess the outcomes of MCAO. Successful establishment of an ischemic stroke model in rats is indicated by the presence of low-density regions in the cerebra. This is because the interruption of blood flow results in brain edema following cerebral artery occlusion. The brain edema area in the ischemic region has a low density upon CT imaging (Heiss, 2016). MCAO commonly results in the loss of various neuronal cells and cerebral infarction (Ferrer and Planas, 2003). The infarct volume depends on multiple factors, including the duration and severity of ischemia, age and sex, and the damage is irreversible by 12 h (Liu and McCullough, 2011).

Along with cerebral infarction, MCAO also results in neurological function deficits, including sensorimotor and cognitive function impairment (DeVries et al., 2001). The extent of neurological function damage can be assessed using behavioral test(s) (DeVries et al., 2001). The mNSS system is often used to evaluate behavioral deficits in animal studies of stroke. The mNSS system can be used to functional deficits in multiple areas (motor, sensory, reflex, and balance) and can be performed within 60 days (Schaar et al., 2010).

MCAO-induced neuronal cell loss occurs through apoptosis, necrosis, autophagocytosis, necroptosis, and pyroptosis and is the core problem in ischemic stroke (Sekerdag et al., 2018). Among the types of cell death that occur after MCAO, apoptosis accounts for the loss of a significant proportion of neuronal cells and prominently occurs in the ischemic penumbra (Radak et al., 2017). Several studies have shown that apoptosis suppression decreases brain damage and behavioral abnormalities and lowers neurological deficit scores after MCAO (Graham and Chen, 2001; Wei et al., 2016; Radak et al., 2017). Postischemic apoptosis is activated by intrinsic mitochondrial signaling pathways or extrinsic apoptotic signaling cascades (Radak et al., 2017).

It has been shown that the expression levels of hundreds of microRNAs are altered following focal cerebral ischemia and reperfusion (Jeyaseelan et al., 2008). Over the past decade, accumulating evidence has identified several brain-enriched miRNAs as critical mediators in the multifaceted cascade of focal cerebral ischemia pathology, including excitotoxicity, oxidative stress, inflammatory reaction, blood-brain barrier disruption, edema after stroke, neuronal damage or death, neurogenesis, and angiogenesis (Li et al., 2018). Some microRNAs are implicated in neuronal damage or death; for example, alterations in the expression levels of miR-7a-5p, miR-9, miR-21, miR-25, miR-29b, miR-181, and miR-497 are involved in neuron apoptosis, and the miR-30 family, miR-26b, and miR-207 affect autophagocytosis in the postischemic brain and neuronal cultures under OGD/R conditions (Rink and Khanna, 2011; Wei et al., 2016; Kim et al., 2018; Li et al., 2018). Supporting the notion that microRNAs impact apoptosis, in the current study, we demonstrated that downregulation of miR-184 expression resulted in apoptosis in human neuroblastoma SH-SY5Y cells following OGD/R.

In the current study, it was confirmed that miR-184 contributes to neuronal apoptosis following ischemia and reperfusion in human neuroblastoma SH-SY5Y cells cultured under OGD/R conditions. Human neuroblastoma SH-SY5Y cells are neuroblast-like cells that are most commonly used *in vitro* cerebral ischemia-related research (Kovalevich and Langford, 2013; Liu et al., 2018). OGD/R is the most widely used *in vitro* model of ischemic stroke and can be used to model ischemia-reperfusion induced by combined oxygen and glucose deprivation (Sommer, 2017). Typically, 1 h exposure to OGD/R is sufficient to cause widespread neuronal death (Sommer, 2017). Consistent with other studies (Sommer, 2017), we found that OGD/R significantly increased the apoptosis of SH-SY5Y cells. However, overexpression of miR-184 reduced SH-SY5Y cell apoptosis.

In our study, we also found that PPAP2B is a direct target gene of miR-184. PPAP2B encodes phosphatidic acid phosphatase (also named lipid phosphate phosphatase 3), which catalyzes the dephosphorylation of various lipid phosphates into diacylglycerol and is implicated in the physiological processes of cell proliferation, differentiation, and apoptosis (Ishikawa et al., 2000; Long et al., 2005). It is well-known that diacylglycerol is an essential activator of protein kinase C. Some evidence has shown that protein kinase C plays a crucial role in mediating cerebral reperfusion injury (Zhao et al., 2016). In particular, protein kinase C delta isozyme expression is specifically upregulated and activated after ischemia and reperfusion in the perifocal cortex and has been reported to mediate apoptotic processes (Bright and Mochly-Rosen, 2005). It has been shown that protein kinase C delta isozyme can lead to mitochondrial dysfunction and the release of apoptogenic factors in the ischemic heart (Murriel et al., 2004). Identical findings have also been demonstrated in a cerebral ischemia model (Bright et al., 2004). Therefore, in our study, miR-184 downregulation-induced SH-SY5Y apoptosis may have been mediated through protein kinase C delta isozyme via phosphatidic acid phosphatase encoded by PPAP2B. Indeed, lipid phosphate phosphatase 3 has been shown to regulate the survival of other cells. For instance, the overexpression of the

PPAP2B gene significantly increases apoptosis of human primary aortic endothelial cells, and PPAP2B silencing by siRNA reduces cell apoptosis (Touat-Hamici et al., 2016). Similarly, PPAP2B-overexpressing HEK-293 cells undergo apoptosis after serum deprivation (Long et al., 2005).

MiR-184 has emerged as a highly enriched microRNA in the mammalian brain (Nomura et al., 2008). However, the exact role of miR-184 in the brain is not yet well known. Several studies have shown that miR-184 plays roles in physiological and pathophysiological processes in the brain. For example, miR-184 can promote oligodendrocyte differentiation, control the proliferation and differentiation of adult neural stem/progenitor cells, and suppress glioma proliferation, migration, and invasion (Liu et al., 2010; Cheng et al., 2015; Afrang et al., 2019), and suppression of miR-184 expression results in neuronal death after seizures in mice (McKiernan et al., 2012). Our previous study demonstrated that miR-184 expression is significantly downregulated in the rat brain and in cultured cells following ischemia and reperfusion, which modulates post-OGD/R angiogenesis *in vitro* (Wang et al., 2020). The results of the current study also revealed that downregulation of miR-184 expression contributes to neuronal cell damage and death in rats following ischemic stroke and induces SH-SY5Y cell apoptosis under OGD/R conditions. However, it is still not clear how downregulation of miR-184 expression is triggered *in vivo* and *in vitro*. A decrease in miR-184 levels appears to induce the death of SH-SY5Y cells. It has been reported that antagomir-mediated inhibition of miR-184 also results in neuronal death in the hippocampal CA1 area in mice following seizures (McKiernan et al., 2012).

Biological validation of the role of microRNAs in ischemic stroke is providing insight into the complex molecular mechanisms underlying ischemic stroke and new therapeutic strategies for ischemic stroke, such as targeting microRNAs to modulate discordant gene expression, which may represent the future of gene therapy for ischemic stroke. There have been preclinical studies on the potential of targeting microRNAs to protect against brain damage following ischemic stroke. A miR-15a/16-1 antagomir, miR-93 antagomir, miR-106b-5p antagomir, miR-181 antagomir, miR-383 antagomir, miR-497 antagomir, miR-122 mimic, and miR-1906 mimic have been proven have therapeutic potential in protecting against cerebral ischemia and reperfusion injury (Yin et al., 2010; Khoshnam et al., 2017b; Wang et al., 2018). Our study on miR-184 in ischemic brain injury suggests that targeting brain-specific miR-184 may be a promising therapeutic option for stroke recovery.

Our results revealed the critical role of miR-184 in cerebral ischemia and reperfusion injury and demonstrated that the attenuation of miR-184 following ischemia and reperfusion contributes to neuronal damage in rats and increases SH-SY5Y cell apoptosis through direct targeting of PPAP2B mRNA. Our study may provide a promising therapeutic option for stroke recovery.

DATA AVAILABILITY STATEMENT

The raw data supporting the conclusions of this article will be made available by the authors, without undue reservation.

ETHICS STATEMENT

The animal study was reviewed and approved by the Ethics Committee of The Third Hospital Affiliated to Medical University of Zunyi.

AUTHOR CONTRIBUTIONS

HY, YZ, and HC searched literatures, performed the experiments, and analyzed the data. HY, YZ, YL, and FO wrote the manuscript. LC and DL designed the experiments and revised the manuscript. All authors have approved the final article and agreed to be accountable for the content of the work.

FUNDING

This research was supported by the Guizhou Provincial Natural Science Foundation [No. (2018)5623], Science and Technology Fund Project of Guizhou Health Commission (gzwjkj2020-1-051), and Science and Technology Bureau Project of Zunyi City [Zunshi Kehe (2015)17, HZ(2019)146, HZ(2019)167, and HZ(2020)8].

SUPPLEMENTARY MATERIAL

The Supplementary Material for this article can be found online at: https://www.frontiersin.org/articles/10.3389/fnmol.2021.613887/full#supplementary-material

REFERENCES

Afrang, N., Tavakoli, R., Tasharrofi, N., Alian, A., Naderi Sohi, A., and Kabiri, M. (2019). A critical role for miR-184 in the fate determination of oligodendrocytes. *Stem Cell Res. Ther.* 10:112.

Bay, V., Kjølby, B. F., Iversen, N. K., Mikkelsen, I. K., Ardalan, M., Nyengaard, J. R., et al. (2018). Stroke infarct volume estimation in fixed tissue: comparison of diffusion kurtosis imaging to diffusion weighted imaging and histology in a rodent MCAO model. *PLoS One* 13:e0196161. doi: 10.1371/journal.pone.0196161

Bright, R., and Mochly-Rosen, D. (2005). The role of protein kinase C in cerebral ischemic and reperfusion injury. *Stroke* 36, 2781–2790. doi: 10.1161/01.str.0000189996.71237.f7

Bright, R., Raval, A. P., Dembner, J. M., Pérez-Pinzón, M. A., Steinberg, G. K., Yenari, M. A., et al. (2004). Protein kinase C delta mediates cerebral reperfusion injury in vivo. *J. Neurosci.* 24, 6880–6888. doi: 10.1523/jneurosci.4474-03.2004

Cheng, Z., Wang, H. Z., Li, X., Wu, Z., Han, Y., and Li, Y. (2015). MicroRNA-184 inhibits cell proliferation and invasion, and specifically targets TNFAIP2 in Glioma. *J. Exp. Clin. Cancer Res.* 34:27.

Cheon, S. Y., Kim, E. J., Kim, J. M., and Koo, B. N. (2018). Cell type-specific mechanisms in the pathogenesis of ischemic stroke: the role of apoptosis signal-regulating kinase 1. *Oxid. Med. Cell Longev.* 2018:2596043.

DeVries, A. C., Nelson, R. J., Traystman, R. J., and Hurn, P. D. (2001). Cognitive and behavioral assessment in experimental stroke research: will it prove useful? *Neurosci. Biobehav. Rev.* 25, 325–342. doi: 10.1016/s0149-7634(01)00017-3

Dharap, A., Bowen, K., Place, R., Li, L. C., and Vemuganti, R. (2009). Transient focal ischemia induces extensive temporal changes in rat cerebral microRNAome. *J. Cereb. Blood Flow Metab.* 29, 675–687. doi: 10.1038/jcbfm.2008.157

Ferrer, I., and Planas, A. M. (2003). Signaling of cell death and cell survival following focal cerebral ischemia: life and death struggle in the penumbra. *J. Neuropathol. Exp. Neurol.* 62, 329–339. doi: 10.1093/jnen/62.4.329

Germano, A. F., Dixon, C. E., d'Avella, D., Hayes, R. L., and Tomasello, F. (1994). Behavioral deficits following experimental subarachnoid hemorrhage in the rat. *J. Neurotrauma.* 11, 345–353. doi: 10.1089/neu.1994.11.345

Goel, R. S., Goyal, N. K., Dharap, S. B., Kumar, M., and Gore, M. A. (2008). Utility of optic nerve ultrasonography in head injury. *Injury* 39, 519–524.

Graham, S. H., and Chen, J. (2001). Programmed cell death in cerebral ischemia. *J. Cereb. Blood Flow Metab.* 21, 99–109. doi: 10.1097/00004647-200102000-00001

Han, Z., Li, L., Wang, L., Degos, V., Maze, M., and Su, H. (2014). Alpha-7 nicotinic acetylcholine receptor agonist treatment reduces neuroinflammation, oxidative stress, and brain injury in mice with ischemic stroke and bone fracture. *J. Neurochem.* 131, 498–508. doi: 10.1111/jnc.12817

He, T. G., Xiao, Z. Y., Xing, Y. Q., Yang, H. J., Qiu, H., and Chen, J. B. (2019). Tumor suppressor miR-184 enhances chemosensitivity by directly inhibiting SLC7A5 in retinoblastoma. *Front. Oncol.* 9:1163.

Heiss, W. D. (2016). Malignant MCA infarction: pathophysiology and imaging for early diagnosis and management decisions. *Cerebrovasc. Dis.* 41, 1–7. doi: 10.1159/000441627

Ishikawa, T., Kai, M., Wada, I., and Kanoh, H. (2000). Cell surface activities of the human type 2b phosphatidic acid phosphatase. *J. Biochem.* 127, 645–651. doi: 10.1093/oxfordjournals.jbchem.a022652

Jeyaseelan, K., Lim, K. Y., and Armugam, A. (2008). MicroRNA expression in the blood and brain of rats subjected to transient focal ischemia by middle cerebral artery occlusion. *Stroke* 39, 959–966. doi: 10.1161/strokeaha.107.500736

Kasdorf, E., and Perlman, J. M. (2013). Strategies to prevent reperfusion injury to the brain following intrapartum hypoxia-ischemia. *Semin. Fetal Neonatal Med.* 18, 379–384. doi: 10.1016/j.siny.2013.08.004

Khoshnam, S. E., Winlow, W., Farbood, Y., Moghaddam, H. F., and Farzaneh, M. (2017a). Emerging roles of microRNAs in ischemic stroke: as possible therapeutic agents. *J. Stroke* 19, 166–187. doi: 10.5853/jos.2016.01368

Khoshnam, S. E., Winlow, W., Farzaneh, M., Farbood, Y., and Moghaddam, H. F. (2017b). Pathogenic mechanisms following ischemic stroke. *Neurol. Sci.* 38, 1167–1186. doi: 10.1007/s10072-017-2938-1

Kim, T., Mehta, S. L., Morris-Blanco, K. C., Chokkalla, A. K., Chelluboina, B., and Lopez, M. (2018). The microRNA miR-7a-5p ameliorates ischemic brain damage by repressing α-synuclein. *Sci. Signal.* 11:eaat4285. doi: 10.1126/scisignal.aat4285

Kovalevich, J., and Langford, D. (2013). Considerations for the use of SH-SY5Y neuroblastoma cells in neurobiology. *Methods Mol. Biol.* 1078, 9–21. doi: 10.1007/978-1-62703-640-5_2

Li, G., Morris-Blanco, K. C., Lopez, M. S., Yang, T., Zhao, H., Vemuganti, R., et al. (2018). Impact of microRNAs on ischemic stroke: from pre- to post-disease. *Prog. Neurobiol.* 16, 59–78. doi: 10.1016/j.pneurobio.2017.08.002

Liu, C., Teng, Z. Q., Santistevan, N. J., Szulwach, K. E., Guo, W., Jin, P., et al. (2010). Epigenetic regulation of miR-184 by MBD1 governs neural stem cell proliferation and differentiation. *Cell Stem Cell* 6, 433–444. doi: 10.1016/j.stem.2010.02.017

Liu, F., and McCullough, L. D. (2011). Middle cerebral artery occlusion model in rodents: methods and potential pitfalls. *J. Biomed. Biotechnol.* 2011:464701.

Liu, Y., Eaton, Wills, T. E., McCann, S. K., Antonic, A., and Howells, D. W. (2018). Human ischaemic cascade studies using SH-SY5Y Cells: a systematic review and meta-analysis. *Transl. Stroke Res.* 9, 564–574. doi: 10.1007/s12975-018-0620-4

Long, J., Darroch, P., Wan, K. F., Kong, K. C., Ktistakis, N., and Pyne, N. J. (2005). Regulation of cell survival by lipid phosphate phosphatases involves the modulation of intracellular phosphatidic acid and sphingosine 1-phosphate pools. *Biochem. J.* 391(Pt 1), 25–32. doi: 10.1042/bj20050342

Lopez, M. S., and Vemuganti, R. (2018). Modeling transient focal ischemic stroke in rodents by intraluminal filament method of middle cerebral artery occlusion. *Methods Mol. Biol.* 1717, 101–113. doi: 10.1007/978-1-4939-7526-6_9

McKiernan, R. C., Jimenez-Mateos, E. M., Sano, T., Bray, I., Stallings, R. L., Simon, R. P., et al. (2012). Expression profiling the microRNA response to epileptic preconditioning identifies miR-184 as a modulator of seizure-induced neuronal death. *Exp. Neurol.* 237, 346–354. doi: 10.1016/j.expneurol.2012.06.029

Murriel, C. L., Churchill, E., Inagaki, K., Szweda, L. I., and Mochly-Rosen, D. (2004). Protein kinase Cdelta activation induces apoptosis in response to cardiac ischemia and reperfusion damage: a mechanism involving BAD and the mitochondria. *J. Biol. Chem.* 279, 47985–47991. doi: 10.1074/jbc.m405071200

Nomura, T., Kimura, M., Horii, T., Morita, S., Soejima, H., Kudo, S., et al. (2008). MeCP2-dependent repression of an imprinted miR-184 released by depolarization. *Hum. Mol. Genet.* 17, 1192–1199. doi: 10.1093/hmg/ddn011

Radak, D., Katsiki, N., Resanovic, I., Jovanovic, A., Sudar-Milovanovic, E., and Zafirovic, S. (2017). Apoptosis and acute brain ischemia in ischemic stroke. *Curr. Vasc. Pharmacol.* 15, 115–122. doi: 10.2174/1570161115666161104095522

Rink, C., and Khanna, S. (2011). MicroRNA in ischemic stroke etiology and pathology. *Physiol. Genomics.* 43, 521–528. doi: 10.1152/physiolgenomics.00158.2010

Schaar, K. L., Brenneman, M. M., and Savitz, S. I. (2010). Functional assessments in the rodent stroke model. *Exp. Transl. Stroke Med.* 2:13. doi: 10.1186/2040-7378-2-13

Sekerdag, E., Solaroglu, I., and Gursoy-Ozdemir, Y. (2018). Cell death mechanisms in stroke and novel molecular and cellular treatment options. *Curr. Neuropharmacol.* 16, 1396–1415. doi: 10.2174/1570159x16666180302115544

Sommer, C. J. (2017). Ischemic stroke: experimental models and reality. *Acta Neuropathol.* 133, 245–261. doi: 10.1007/s00401-017-1667-0

Touat-Hamici, Z., Weidmann, H., Blum, Y., Proust, C., Durand, H., and Iannacci, F. (2016). Role of lipid phosphate phosphatase 3 in human aortic endothelial cell function. *Cardiovasc. Res.* 112, 702–713. doi: 10.1093/cvr/cvw217

Wang, K., Ru, J., Zhang, H., Chen, J., Lin, X., Lin, Z., et al. (2020). Melatonin Enhances the Therapeutic Effect of Plasma Exosomes Against Cerebral Ischemia-Induced Pyroptosis Through the TLR4/NF-κB Pathway. *Front. Neurosci.* 14.

Wang, S. W., Liu, Z., and Shi, Z. S. (2018). Non-Coding RNA in acute ischemic stroke: mechanisms, biomarkers and therapeutic targets. *Cell. Transplant.* 27, 1763–1777. doi: 10.1177/0963689718806818

Wei, N., Xiao, L., Xue, R., Zhang, D., Zhou, J., and Ren, H. (2016). MicroRNA-9 mediates the cell apoptosis by targeting Bcl2l11 in ischemic stroke. *Mol. Neurobiol.* 53, 6809–6817. doi: 10.1007/s12035-015-9605-4

Yin, K. J., Deng, Z., Huang, H., Hamblin, M., Xie, C., Zhang, J., et al. (2010). miR-497 regulates neuronal death in mouse brain after transient focal cerebral ischemia. *Neurobiol. Dis.* 38, 17–26. doi: 10.1016/j.nbd.2009.12.021

Yin, K. J., Hamblin, M., and Chen, Y. E. (2015). Angiogenesis-regulating microRNAs and ischemic stroke. *Curr. Vasc. Pharmacol.* 13, 352–365. doi: 10.2174/1570161113119990016

Zhao, E. Y., Efendizade, A., Cai, L., and Ding, Y. (2016). The role of Akt (protein kinase B) and protein kinase C in ischemia-reperfusion injury. *Neurol. Res.* 38, 301–308. doi: 10.1080/01616412.2015.1133024

Zou, J. F., Wu, X. N., Shi, R. H., Sun, Y. Q., Qin, F. J., and Yang, Y. M. (2020). Inhibition of microRNA-184 reduces H2O2-mediated cardiomyocyte injury via targeting FBXO28. *Eur. Rev. Med. Pharmacol. Sci.* 24, 11251–11258.

Conflict of Interest: The authors declare that the research was conducted in the absence of any commercial or financial relationships that could be construed as a potential conflict of interest.

frontiers in Molecular Neuroscience

REVIEW
published: 31 March 2021
doi: 10.3389/fnmol.2021.654031

SOX Transcription Factors as Important Regulators of Neuronal and Glial Differentiation During Nervous System Development and Adult Neurogenesis

Milena Stevanovic[1,2,3], Danijela Drakulic[1], Andrijana Lazic[1], Danijela Stanisavljevic Ninkovic[1], Marija Schwirtlich[1] and Marija Mojsin[1]*

[1] Laboratory for Human Molecular Genetics, Institute of Molecular Genetics and Genetic Engineering, University of Belgrade, Belgrade, Serbia, [2] Faculty of Biology, University of Belgrade, Belgrade, Serbia, [3] Serbian Academy of Sciences and Arts, Belgrade, Serbia

The SOX proteins belong to the superfamily of transcription factors (TFs) that display properties of both classical TFs and architectural components of chromatin. Since the cloning of the *Sox/SOX* genes, remarkable progress has been made in illuminating their roles as key players in the regulation of multiple developmental and physiological processes. SOX TFs govern diverse cellular processes during development, such as maintaining the pluripotency of stem cells, cell proliferation, cell fate decisions/germ layer formation as well as terminal cell differentiation into tissues and organs. However, their roles are not limited to development since SOX proteins influence survival, regeneration, cell death and control homeostasis in adult tissues. This review summarized current knowledge of the roles of SOX proteins in control of central nervous system development. Some SOX TFs suspend neural progenitors in proliferative, stem-like state and prevent their differentiation. SOX proteins function as pioneer factors that occupy silenced target genes and keep them in a poised state for activation at subsequent stages of differentiation. At appropriate stage of development, SOX members that maintain stemness are down-regulated in cells that are competent to differentiate, while other SOX members take over their functions and govern the process of differentiation. Distinct SOX members determine down-stream processes of neuronal and glial differentiation. Thus, sequentially acting SOX TFs orchestrate neural lineage development defining neuronal and glial phenotypes. In line with their crucial roles in the nervous system development, deregulation of specific SOX proteins activities is associated with neurodevelopmental disorders (NDDs). The overview of the current knowledge about the link between *SOX* gene variants and NDDs is presented. We outline the roles of SOX TFs in adult neurogenesis and brain homeostasis and discuss whether impaired adult neurogenesis, detected in neurodegenerative diseases, could be associated with deregulation of SOX proteins activities. We present the current data

OPEN ACCESS

Edited by:
Veronica Martinez Cerdeño, University of California, Davis, United States

Reviewed by:
Carlos Vicario, Consejo Superior de Investigaciones Científicas (CSIC), Spain
Rebecca Hodge, Allen Institute for Brain Science, United States

***Correspondence:**
Milena Stevanovic
milenastevanovic@imgge.bg.ac.rs

Received: *15 January 2021*
Accepted: *11 March 2021*
Published: *31 March 2021*

Citation:
Stevanovic M, Drakulic D, Lazic A, Stanisavljevic Ninkovic D, Schwirtlich M and Mojsin M (2021) SOX Transcription Factors as Important Regulators of Neuronal and Glial Differentiation During Nervous System Development and Adult Neurogenesis. Front. Mol. Neurosci. 14:654031. doi: 10.3389/fnmol.2021.654031

regarding the interaction between SOX proteins and signaling pathways and microRNAs that play roles in nervous system development. Finally, future research directions that will improve the knowledge about distinct and various roles of SOX TFs in health and diseases are presented and discussed.

Keywords: SOX transcription factors, neuronal differentiation, glial differentiation, adult neurogenesis, signaling pathways, microRNA

INTRODUCTION

The development of multicellular organisms and the maintenance of homeostasis in adulthood are achieved by complex control of basic cellular processes such as the maintenance of pluripotent stem cells, cell fate decision, differentiation, proliferation, and cell death. One of the key mechanisms involved in the control of developmental processes is based on the transcriptional regulation of gene expression. Through the activation and repression of the target genes, transcription factors (TFs) determine the fate of cells within tissues, organs and organisms, controlling the development. Most TFs act within complex regulatory networks, enabling combinatorial regulation of gene expression within the cells. Numerous families of genes encoding TFs involved in the control of embryonic development have been discovered, including the *SOX* gene family.

SOX TRANSCRIPTION FACTORS

Sry (Sex-determining Region Y), a founder member of the *Sox* gene family, was discovered in 1990 as a sex-determining gene necessary and sufficient to specify the male phenotype (Gubbay et al., 1990; Sinclair et al., 1990). During the course of cloning of *Sry*, the presence of related genes was discovered sharing the homology with the HMG box of *Sry*. These newly identified genes have been named by the acronym *Sox*/*SOX* (in mammals and human, respectively) standing for *Sry*-related HMG box genes (Denny et al., 1992; Wright et al., 1993). Further, it was shown that the *SOX* family is multigenic, with new members discovered both in vertebrates and invertebrates and being assigned by numbers based on the order of their discovery. After a detailed insight, the presence of 20 *SOX* genes in human genome was identified (**Table 1**) providing the basis for their final re-numeration and classification (Schepers et al., 2002). Further research has shown that *SOX* genes encode the family of diverse and well conserved TFs.

Based on the structure, expression profiles, as well as the similarity between the proteins they encode, human *SOX* genes are divided into 8 groups, A to H (**Table 1**), with group B being further split into subgroups B1 (*SOX1*, *SOX2,* and *SOX3*) and B2 (*SOX14* and *SOX21*) (Uchikawa et al., 1999). SOX proteins within the same group show a high level of homology, both within and outside the HMG domain, while proteins from different groups show homology only within the HMG domain (Bowles et al., 2000). Apart from the genes *SRY* and *SOX3*, other family members are located on autosomes and scattered throughout the genome (**Table 1**). Majority of *SOX* family members are single exon genes, with the exception of genes *SOX5*, *SOX9*, *SOX10*, *SOX15*, *SOX17,* and *SOX18* that possess multiple exons.

The SOX proteins display properties of both classical TFs and architectural components of chromatin (reviewed in Pevny and Lovell-Badge, 1997). SOX proteins carry an HMG domain of 79 amino acids that enables their specific binding to the sequence (A/T A/T CAA A/T) (Harley et al., 1994) and additional domains involved in transcriptional regulation (reviewed in Pevny and Lovell-Badge, 1997). In contrast to the majority of DNA-binding proteins, SOX proteins interact with the minor groove and, upon binding, they introduce strong bends into DNA (reviewed in Wegner, 1999). Consequently, SOX proteins act as architectural proteins by shaping the gene regulatory regions and by enabling establishment of physical contacts between TFs bound on the same target gene promoter or enhancer (reviewed in Wegner, 2005). SOX TFs exert regulatory functions by activating or repressing gene transcription only through specific interactions with a partner factor(s) and by establishing contacts with the basic transcription machinery (Kamachi et al., 2000).

The SOX TFs perform unique functions in different cell types and regulate different events in the same cell type. Several SOX proteins are demonstrated to have the ability to pair off with various types of TFs (Kamachi et al., 2000) and their specificity is achieved via binding partners (reviewed in Bernard and Harley, 2010). Consequently, transcriptional regulatory functions of SOX proteins usually require the cooperation with interacting partner factors that bind DNA in the vicinity of the SOX site and allow specific selection of target genes (reviewed in Kamachi et al., 2000; Kondoh and Kamachi, 2010). SOX partner factor cooperation is dynamic and changes in partner factors enable SOX proteins to regulate different events in the same cell type and to drive the progression of developmental processes (reviewed in Kondoh and Kamachi, 2010).

Since discovery, essential roles have been assigned to SOX TFs. Their critical functions have been revealed by both studying naturally occurring mutations in humans, as well as, by targeted mutations introduced in animal models. Numerous studies aimed at discovery of the roles of *Sox*/*SOX* genes are often being complicated by pleiotropy and by partial or extensive functional redundancy among co-expressed members of the same groups (Kamachi and Kondoh, 2013).

Abbreviations: TFs, transcription factors; ESCs, embryonic stem cells; RA, retinoic acid; iPSCs, induced pluripotent stem cells; NPCs, neural progenitor cells; CNS, central nervous system; NSCs, neural stem cells; NDDs, neurodevelopmental disorders; SVZ, subventricular zone; SGZ, subgranular zone; TCF/LEF, T cell factor/Lymphoid enhancer factor; RARs, retinoic acid receptors; RXRs, retinoid X receptors; RAREs, *cis*-acting RA response elements; CRMs, *cis*-regulatory modules; miRNAs, microRNAs.

TABLE 1 | Classification of the human SOX genes.

Group	Gene		Gene locus	References
SOXA	*SRY*		Yp11.3	Sinclair et al., 1990
SOXB	*SOXB1*	*SOX1*	13q34	Malas et al., 1997
		SOX2	3q26.3	Stevanovic et al., 1994
		SOX3	Xq26.3	Stevanovic et al., 1993
	SOXB2	*SOX14*	3q23	Arsic et al., 1998; Malas et al., 1999
		SOX21	13q31-q32	Malas et al., 1999
SOXC	*SOX4*		6p22.3	Farr et al., 1993
	SOX11		2p25	Jay et al., 1995
	SOX12		20p13	Jay et al., 1997
	(*SOX22 is renamed as SOX12*)			
SOXD	*SOX5*		12p12.1	Wunderle et al., 1996
	SOX6		11p15.3	Cohen-Barak et al., 2001
	SOX13		1q32	Argentaro et al., 2000
SOXE	*SOX8*		16p13.3	Pfeifer et al., 2000
	SOX9		17q23	Foster et al., 1994
	SOX10		22q13	Pusch et al., 1998
SOXF	*SOX7*		8p22	Takash et al., 2001
	SOX17		8q11.23	Katoh, 2002
	SOX18		20q13.33	Stanojcic and Stevanovic, 2000
SOXG	*SOX 15*		17p13	Meyer et al., 1996;
	(SOX20 is renamed as SOX15)			Vujic et al., 1998
SOXH	*SOX30*		5q33	Osaki et al., 1999

Sox12 and SOX22, as well as, Sox15 and SOX20 denominate the same SOX proteins in mouse and human, respectively.

It has been shown that many developmental processes depend on the presence of SOX proteins, ranging from blastocyst formation, gastrulation, germ layer formation to development of adult tissues and organs (reviewed in Wegner, 2005; Lefebvre et al., 2007; Kamachi and Kondoh, 2013). SOX TFs have been implicated in preimplantation development. Expression of *Sox2* was detected from oocyte, through 2-cell to 8-cells embryo and morula to the blastocyst (Keramari et al., 2010). Study of the effects of *Sox2* knockdown in preimplantation embryo suggested that first essential function of *Sox2* is to facilitate establishment of the trophectoderm lineage (Keramari et al., 2010). Expression of *Sox2* is detected in the inner cell mass of the murine blastocyst and subsequently in primitive ectoderm, extraembryonic ectoderm (Avilion et al., 2003) and the developing nervous system (Collignon et al., 1996).

The SOX TFs govern diverse cellular processes during development, such as maintaining the pluripotency of stem cells, cell proliferation, cell fate decisions, germ layer formation as well as terminal cell differentiation into tissues and organs (reviewed in Reiprich and Wegner, 2015; She and Yang, 2015). However, their roles are not limited to development since SOX TFs influence survival, regeneration, cell death and control homeostasis in adult tissues (Pevny and Placzek, 2005; Mercurio et al., 2019). As reported in numerous publications, most cells express at least one *Sox/SOX* gene and various members of the *SOX* gene family have roles in many tissues and stages of development (reviewed in Pevny and Lovell-Badge, 1997; Wegner, 1999; Kiefer, 2007; Kamachi and Kondoh, 2013). For instance, tissues that require *Sox2* during development continue to express this factor in some adult stem and progenitor cells derived from that tissue. Thus, *Sox2* marks stem and progenitor cell populations in adult tissues that depend on *Sox2* expression during development (Sarkar and Hochedlinger, 2013).

SOX PROTEINS AND PLURIPOTENCY

A unique set of TFs is required to establish embryonic stem cells (ESCs) and to maintain their pluripotent and proliferative state. The numerous evidences reveal the roles of SOX proteins in preservation of stem cell characteristics.

As mentioned above, SOX proteins have the ability to pair off with various types of TFs and regulatory functions of SOX proteins usually require the cooperation with interacting partner factors (Kamachi et al., 2000). SOX2, together with OCT4 (octamer-binding transcription factor 4) and NANOG (named as abbreviation for the mythological Celtic land of the ever-young, "Tir nan Og") (Cavaleri and Scholer, 2003), establish the core transcriptional circuit that orchestrate self-renewal and maintenance of pluripotency of the stem cells (**Figure 1**) (Rodda et al., 2005).

This pluripotency gene regulatory network relies on direct physical interaction between SOX2, NANOG, and OCT4 (Ambrosetti et al., 2000; Gagliardi et al., 2013). Through a cooperative interaction these factors drive pluripotent-specific expression of the numerous genes and play key roles in determining the fate of ESCs, regulating two distinct and opposing functions: self-renewal and differentiation (**Figure 1**)

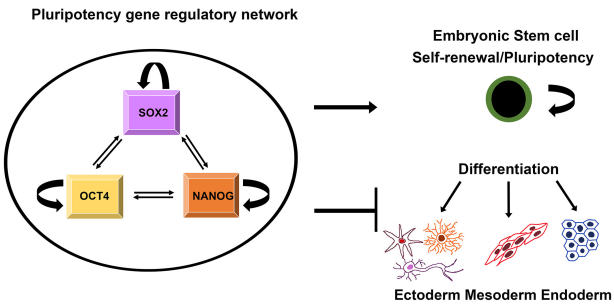

FIGURE 1 | Schematic illustration of regulatory network that controls pluripotency, self-renewal and differentiation. SOX2, NANOG, and OCT4 regulate their own expression targeting both their own promoters and those of each other. The triad contributes to maintaining pluripotency of ESCs by activating genes involved in pluripotency and by repressing genes linked to lineage commitment (Scheper and Copray, 2009).

(Rizzino, 2008). Besides directing the expression of target genes, SOX2, OCT4, and NANOG regulate their own expression via positive-feedback loops (**Figure 1**) (Boyer et al., 2005). In addition, this fully-connected triad has been implicated as recurring network motif among the transcriptional regulatory circuits that control the development and maintenance of cellular states (Faucon et al., 2014). In addition to SOX2, SOX15 is expressed in mouse ESCs and associated with Oct3/4 (Maruyama et al., 2005). It was found that SOX15 is able to replace the function of SOX2 in self-renewal of mouse ESCs (Niwa et al., 2016).

Since SOX2 is a part of integrated and self-controlling network, the level of its expression is critical to sustain the stemness phenotype. Accordingly, SOX2 overexpression reduced the level of OCT4 and NANOG in human ESCs (Adachi et al., 2010). In line with this data, we detected downregulation of *OCT4* gene expression in pluripotent embryonal carcinoma stem cells NT2/D1 with constitutive SOX2 overexpression (Drakulic et al., 2012). We also demonstrate that transition from proliferation to retinoic acid (RA) induced neural differentiation of NT2/D1 cells coincides with complete OCT4 down-regulation (Stevanović et al., 2017). However, SOX2 overexpressing NT2/D1 cells retain ability to differentiate (Drakulic et al., 2012; Klajn et al., 2014) even in the presence of elevated *SOX2* expression after 21 days of treatment with RA (Drakulic et al., 2012).

In ESCs, SOX2 overexpression rapidly induces the expression of another SOXB member – SOX21 that further influences fate of these cells (Mallanna et al., 2010). Subsequently, SOX21 acting as a repressor, disrupts ESCs self-renewal and induces differentiation (Mallanna et al., 2010).

In addition, SOX2 plays important role in reprogramming adult cells and generation of induced pluripotent stem cells (iPSCs). Reprogramming is achieved by overexpression of stem cell-associated genes in differentiated cells, such as adult fibroblasts (Takahashi et al., 2007; Wernig et al., 2007; Takahashi and Yamanaka, 2016). SOX2 is recognized as one of the "magical four" crucial TFs capable of cooperating to reprogram differentiated cells into an iPSCs (Qi and Pei, 2007). The fact that SOX2 is crucial factor for reversing the somatic cells back to their pluripotent state (Takahashi and Yamanaka, 2016) demonstrates its pivotal role in maintenance of cell pluripotency.

Apart from *Sox2*, other members of the *Sox* gene family may also be involved in the reprogramming process. *Sox1* yields iPSCs with a similar efficiency as *Sox2*, while *Sox3*, *Sox*15, and *Sox18* genes are also capable to generate iPSCs, although with decreased efficiency (Nakagawa et al., 2008).

SOX PROTEINS AS PIONEER FACTORS

The SOX proteins also function as pioneer factors that occupy silenced target genes and keep them in a poised state for activation at subsequent stages of differentiation (Bergsland et al., 2011; Zaret and Carroll, 2011).

Bergsland et al. (2011) demonstrated that binding of SOX proteins is developmental stage-specific and revealed sequential binding of SOX proteins to a common set of neural genes. Prebinding of SOX proteins to silent genes facilitates those genes to be activated at later stages of neural development. They showed that expression of many genes that are targeted by binding of SOX2 in ESCs and neural precursors is first initiated in neural precursors, while many neuronal genes that are prebound by SOX2 and SOX3 in neural precursors can only be activated by SOX11 in differentiating neurons (**Figure 2**) (Bergsland et al., 2011). By these data, the authors reveal that sequentially acting SOX TFs coordinate neural gene expression from pluripotent cells to later stages of neuronal development.

It has been demonstrated that glial-specific gene sets are extensively preselected in multipotent neural progenitor cells (NPCs) through prebinding by SOX3 (Klum et al., 2018). Further, in the subsequent lineage-restricted glial precursor cells, it was shown that SOX3 performs a negative regulation of prebound astrocyte-specific genes and efficiently hinders SOX9 from activating their expression (Klum et al., 2018). Astrocyte-specific genes become additionally targeted and activated by SOX9, while oligodendrocyte-specific genes are prebound by SOX9 only and later on they are targeted and activated by SOX10 during oligodendrocyte maturation (**Figure 2**) (Klum et al., 2018). Thus, the previous study demonstrated how sequentially expressed SOX proteins act on lineage-specific regulatory DNA elements to coordinate glial gene expression both in a temporal and in a sub-lineage-specific fashion (Klum et al., 2018).

Together these interesting data demonstrated that sequentially acting SOX TFs orchestrate neural lineage development including neuronal-, astrocyte- and oligodendrocyte-specific gene expression.

THE ROLES OF SOX TRANSCRIPTION FACTORS IN NEURONAL DIFFERENTIATION

Neuronal differentiation is a complex process that relies on a timely and spatially controlled expression of transcriptional

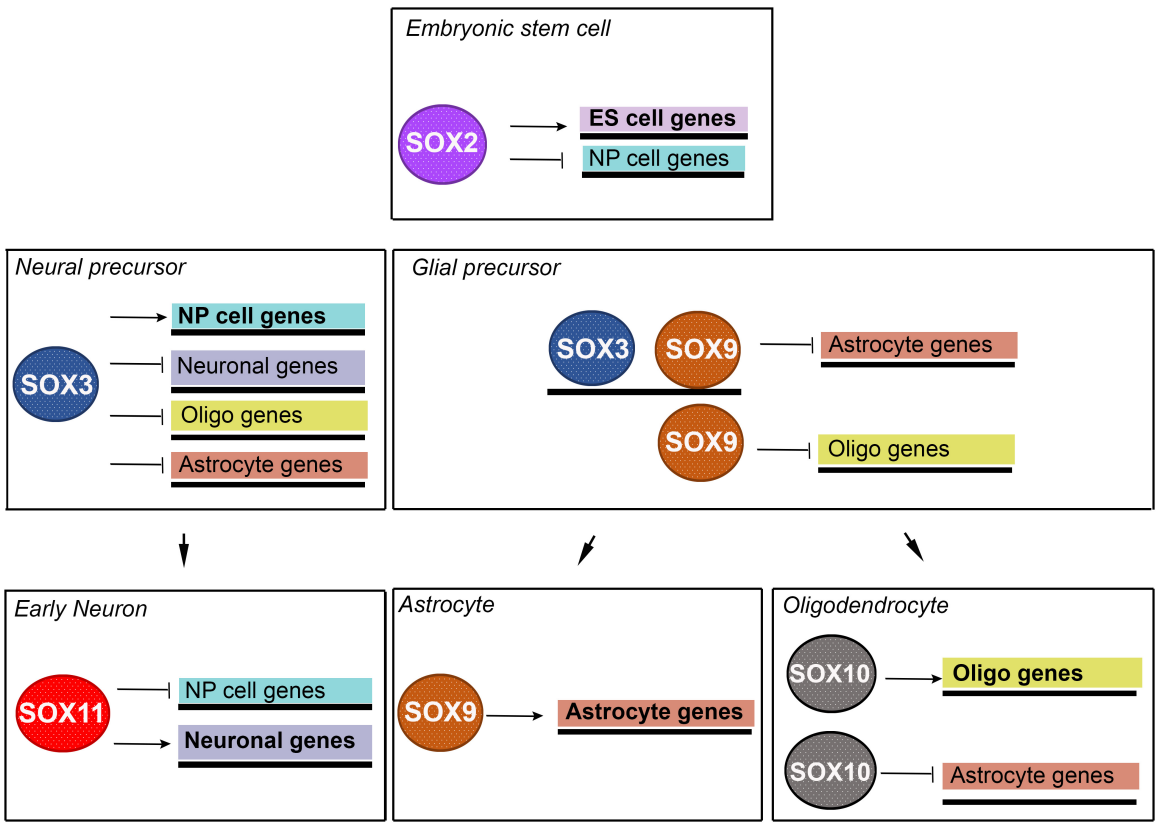

FIGURE 2 | Schematic illustration of proposed model for neuronal and glial lineage specification governed by sequentially acting SOX TFs. Neural precursor cell specific genes are repressed in ESCs by SOX2 and activated in neural precursor cells by SOX3. Neuronal specific genes are repressed in neural precursor cells by SOX3 and activated in early neurons by SOX11. Astrocyte specific genes are repressed in neural precursor cells by SOX3, in glial precursors by SOX3 and SOX9 and in oligodendrocyte by SOX10. These genes are activated in astrocytes by SOX9. Oligodendrocyte specific genes are repressed in neural precursor cells by SOX3, in glial precursor cells by SOX9 and activated in oligodendrocytes by SOX10. NP- neural precursors; Oligo – oligodendrocyte. [Modified from Bergsland et al. (2011) and Klum et al. (2018)].

regulators (Rea et al., 2020). Numerous SOX TFs play widespread roles from initial phases of differentiation until generation of mature neurons (Avilion et al., 2003; Bylund et al., 2003; Graham et al., 2003; Bergsland et al., 2006; Hoser et al., 2008). During neuronal differentiation SOXB and SOXC members act sequentially (Bergsland et al., 2011). *SoxB1* genes are expressed in the neural precursor cells, while *Sox21*, *Sox4,* and *Sox11* are mostly expressed in neural cells committed to neuronal differentiation (**Figure 3**, left panel) (Uwanogho et al., 1995; Cheung et al., 2000).

SOXB1 proteins are necessary for formation of neuroectoderm, maintenance of the neural progenitor state and suppression of neuronal differentiation (**Figure 3**, left panel) (Bylund et al., 2003). It has been revealed that forced expression of *SoxB1* genes maintains neural cells in un undifferentiated state and inhibits neuronal differentiation, whereas their suppression induces upregulation of post-mitotic neuronal markers (Bylund et al., 2003). Down-regulation of *SoxB1* gene expression by Ngn2 (Neurogenin 2) is essential for neuronal differentiation (Bylund et al., 2003).

SOX1 is one of the earliest TFs expressed in cells committed to the neural fate. Its expression correlates with the formation of neural plate, while down-regulation of *Sox1* expression in the developing neural tube correlates with the exit of cells from mitosis (Pevny et al., 1998). Overexpression of *Sox1* in NPCs is sufficient to promote neuronal lineage commitment (Kan et al., 2004) while the loss of neurons in the ventral striatum was detected in the brains of *Sox1* null mutant mice (Malas et al., 2003).

Sox2 expression is detected in the early neuroectoderm (Collignon et al., 1996) and SOX2 transcription factor is necessary to maintain neural progenitor populations throughout the developing central nervous system (CNS) (Hutton and Pevny, 2011). Constitutive *Sox2* expression kept NPCs in a precursor state and inhibited neuronal differentiation, while expression of a dominant-interfering form of *Sox2* led to exit from cell cycle, delamination of NPCs from the ventricular zone, loss of expression of progenitor markers and initiation of neuronal differentiation (Graham et al., 2003). We showed that constitutive *SOX2* overexpression altered expression of neuronal markers and reduced number of mature MAP2 (Microtubule Associated Protein 2) positive neurons upon RA induced neural differentiation of NT2/D1 cells (Drakulic et al., 2012; Klajn et al., 2014).

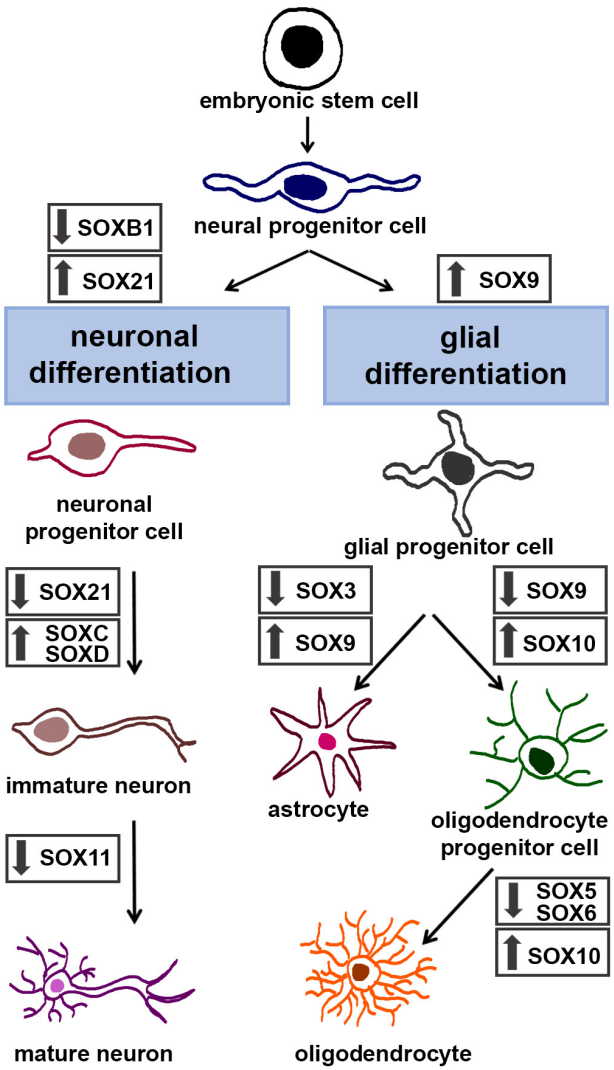

FIGURE 3 | The roles of SOX TFs in neuronal and glial differentiation. Schematic illustration of stepwise neuronal differentiation process **(left)** and glial differentiation process **(right)**. SOX TFs expression levels during specific lineage-restricted progressions are presented by down-arrows (down-regulation) and up-arrows (up-regulation). The figure summarizes following data: for neuronal differentiation – (Connor et al., 1995; Bylund et al., 2003; Stolt et al., 2003; Sandberg et al., 2005; Wang et al., 2005; Bergsland et al., 2006; Batista-Brito et al., 2009; Martinez-Morales et al., 2010; Hoshiba et al., 2016; Naudet et al., 2018); for glial differentiation – (Stolt et al., 2003, 2004, 2006; Kellerer et al., 2006; Stolt and Wegner, 2010; Kang et al., 2012; Weider et al., 2013; Klum et al., 2018).

Expression of *Sox3* is detected throughout the developing CNS (Wood and Episkopou, 1999) and activity of this gene is necessary for formation of the hypothalamo–pituitary axis (Rizzoti et al., 2004). Ectopic *Sox3* expression in zebrafish led cells of the ectoderm to acquire a neural fate, while reduction of neural ectoderm was seen in *Sox3* knocked-down study (Dee et al., 2008).

Sox21 expression is detected in NPCs (Ohba et al., 2004) while *Sox14* is expressed in limited population of neurons in the developing brain and spinal cord (Hargrave et al., 2000). The balance of *SoxB1* and *SoxB2* expression determines whether NPCs remain as progenitors or become committed to differentiation (**Figure 3**, left panel). SOX21 promotes neuronal differentiation by counteracting the activity of SOXB1 (Sandberg et al., 2005). Study conducted on *Xenopus laevis* shows that *Sox21*, like *Sox2*, functions in a dose-dependent manner and that its level of expression determines the decision between maintenance of neural progenitors and formation of neurons (Whittington et al., 2015). Namely, Whittington et al. (2015) proposed model which described how level of *Sox21* expression regulates progression of NPCs during neurogenesis. When *Sox21* expression is severely reduced, NPCs undergo cell death; with a minimal level of *Sox21* expression NPCs differentiate to become neurons while higher expression of *Sox21* inhibits neurogenesis, promotes *SoxB1* expression and progenitor maintenance (Whittington et al., 2015). On the other side, overexpression of *Sox21* in the chick neural tube led to reduction of cell proliferation, downregulation of *Sox3* expression and initiation of premature differentiation of NPCs (Sandberg et al., 2005). Furthermore, the maintenance of *Sox21* expression in NPCs disabled their terminal differentiation (Sandberg et al., 2005). Interestingly, recent study shows that both SOX21 and SOX14 have their own unique gene targets and therefore these TFs do not compete for the same target genes (Makrides et al., 2018). Thus, SOX21 is important for the maintenance, while SOX14 is necessary for terminal differentiation of the GABAergic neurons in the mouse brain (Makrides et al., 2018).

When NPCs start to differentiate into immature neurons, pro-neural proteins induce expression of SOXC TFs (**Figure 3**, left panel) (Bergsland et al., 2006). SOXC TFs are necessary to ensure survival of NPCs (Bhattaram et al., 2010) and for establishment of their neuronal properties (Bergsland et al., 2006). Overexpression of *Sox4* and *Sox11* led to premature induction of neuronal markers (Bergsland et al., 2006) while deficiency of both factors induced apoptosis in the developing nervous system (Bhattaram et al., 2010; Thein et al., 2010). Furthermore, reduced level of *Sox4* and *Sox11* resulted in reduced number of mature neurons and decreased neurite length (Chen et al., 2015). Also, results obtained by Hoshiba et al. (2016) indicate that high level of SOX11 expression, detected only in cortical neurons until birth, is necessary to suppress dendritic morphogenesis during radial migration.

As already pointed out, SOXB and SOXC members are sequentially bound to a common set of neural genes during the process of neuronal differentiation (**Figure 2**) (Bergsland et al., 2011). It has been found that 92% of the SOX3 binding sites will be targeted by SOX11 in newly formed neurons (Bergsland et al., 2011).

SOXD members are also involved in the process of neuronal differentiation (**Figure 3**, left panel). They are expressed in proliferating progenitors in the ventricular and subventricular zones and in post-mitotic neurons (Stolt et al., 2006; Azim et al., 2009; Lee et al., 2014; Quiroga et al., 2015). *Sox5* promotes exit of neural progenitors from cell cycle and downregulation of its expression is necessary for the progression of neuronal differentiation (Martinez-Morales et al., 2010).

Furthermore, SOX5 post-mitotically controls the neuronal migration, molecular identity and subcortical axonal projections of subplate and deep-layer neurons (Kwan et al., 2008). This TF is involved in the control of neurite outgrowth (Naudet et al., 2018). SOX6 is important for positioning and maturation of cortical interneurons (Connor et al., 1995; Batista-Brito et al., 2009). *Sox13* is expressed in a sub-population of post-mitotic differentiating neuronal cells and results obtained by Wang et al. (2005) suggest that this gene may have a role in the specification and/or differentiation of a specific subset of neurons in the developing CNS.

Sox9, *SoxE* member, is expressed in neural stem cells (NSCs) and gain- and loss-of-function studies indicated that *Sox9* was required for multipotentiality and maintenance of NSCs during development (Scott et al., 2010). On the other side, *Sox9* overexpression led to reduction in the number of neuronal progenitors and neurons during the spinal cord development (Vogel et al., 2020).

The majority of existing knowledge regarding the functions of *Sox* genes in the process of neuronal differentiation is obtained by conducted experiments in mice and other animal models. However, comparative transcriptome analyses point to differences in gene expression between the human and the rodent brain (Zeng et al., 2012; Silbereis et al., 2016). Thus, it would be interesting to investigate the roles of *SOX* genes in human neuronal differentiation using iPSCs and 3D brain organoids.

SOX TRANSCRIPTION FACTORS AND NEURODEVELOPMENTAL DISORDERS

Recent literature data has revealed that *SOX* gene variants are associated with neurodevelopmental disorders (NDDs), characterized by impairment of neuronal function during brain development. *SOX* gene variants associated with NDDs are listed in **Supplementary Table 1**.

Contribution of S*OX* genes to NDDs is still not clear. Both deletions and duplications of *SOX3* gene were detected in patients with intellectual disability (Stevanovic et al., 1993; Laumonnier et al., 2002; Helle et al., 2013; Stagi et al., 2014; Arya et al., 2019). Also, *SOX3* missense variant was detected in proband with mild intellectual disability (Jelsig et al., 2018). Furthermore, it was found that *SOX4* heterozygous missense variants cause neurodevelopmental disease (Zawerton et al., 2019). On the other side, *SOX5* haploinsufficiency and its loss of function variant have been found in probands with intellectual disability (Lamb et al., 2012; Schanze et al., 2013; Nesbitt et al., 2015). Also, NDDs have been detected in individuals with heterozygous *SOX6* variants (Tolchin et al., 2020). Significant down-regulation of *SOX9* expression has been revealed in neural progenitors derived from Fragile X Syndrome ESCs (Telias et al., 2015) while downregulation of *SOX10* expression is detected in brains of patients with schizophrenia (Iwamoto et al., 2005). Heterozygous missense variants within the HMG box of *SOX11* gene are associated with intellectual disability (Tsurusaki et al., 2014) while polymorphisms in distal 3′ untranslated region of this gene are associated with susceptibility for schizophrenia (Sun et al., 2020).

All these data open a new avenue of research focused on discovering the roles of SOX TFs and their gene targets in NDDs, making them promising biomarkers and potential targets for future diagnostic and therapeutic strategies.

THE ROLES OF SOX TRANSCRIPTION FACTORS IN ADULT NEUROGENESIS

In the mammalian brain, generation of neurons and astrocytes from NSCs throughout postnatal and adult life is mainly observed in the subventricular zone (SVZ) of lateral ventricle and in the subgranular zone (SGZ) of the dentate gyrus in the hippocampus (reviewed in Gage, 2000; Ming and Song, 2011; Lim and Alvarez-Buylla, 2016). NSCs that reside in the SGZ generate dentate granular cells which play roles in learning, memory and pattern separation (Kaplan and Bell, 1983, 1984; Ming and Song, 2011), whereas NSCs from the SVZ give rise to neuroblasts which migrate in the rostral migratory stream and differentiate to olfactory bulb neurons (Lois and Alvarez-Buylla, 1993).

Similar to neurogenesis in embryonic brain, the generation of new neurons from adult NSCs consists of the sequence of events including proliferation, differentiation and maturation, which are controlled by environment-derived signals and precise changes in the gene expression. However, despite many similarities between NSCs from embryonic and adult brain, emerging evidence suggests profound differences in these two cell populations, such as proliferation rates, neurogenic potential and gene expression profiles (reviewed in Gotz et al., 2016; Obernier and Alvarez-Buylla, 2019). In addition, there are important differences between NSCs from two major adult neurogenic niches, SVZ and SGZ in cellular and molecular properties which may arise as result of external signals received from different environments (reviewed in Obernier and Alvarez-Buylla, 2019).

The roles of SOX TFs in the regulation of adult neurogenesis, particularly in the hippocampus, are extensively investigated, with the main focus on SOXB, SOXC, and SOXD proteins (**Figure 4**) (reviewed in Wegner, 2011; Beckervordersandforth et al., 2015; Reiprich and Wegner, 2015). In the SGZ (**Figure 4A**) and SVZ (**Figure 4B**) of the mouse adult brain, SOX2 is mostly expressed in both, quiescent NSCs and highly proliferating multipotent neuronal progenitor cells (Ellis et al., 2004; Ferri et al., 2004; Steiner et al., 2006). Functional studies demonstrated that repression of *Sox2* gene expression impaired neurogenesis in the adult mouse brain (Ferri et al., 2004; Favaro et al., 2009; Amador-Arjona et al., 2015). SOX2 inhibits expression of pro-neurogenic TF NEUROD1 (Neuronal differentiation 1) via Wnt (Wingless-integration site)-signaling pathway, thus preventing neuronal differentiation and maintaining stem cells in a multipotent state (Kuwabara et al., 2009).

In contrast to SOX2, the expression of SOX1 has not been detected in NSCs, but it is revealed only in the highly proliferating neuronal progenitors of SGZ in the mouse adult hippocampus (Type 2a and Type 2b in the **Figure 4A**) (Venere et al., 2012). In the mouse adult brain, SOX3 protein has been detected in cells within neurogenic niches, however, with different pattern of expression. In the SGZ, its robust expression was identified

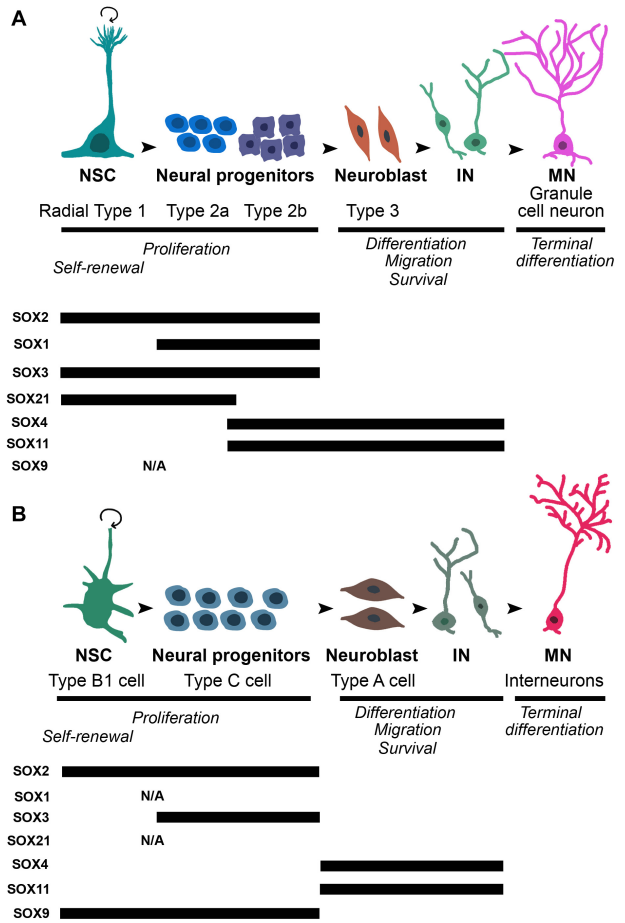

FIGURE 4 | The dynamic expression profiles of selected SOX proteins during different stages of differentiation in neurogenic regions of adult brain: SGZ of dentate gyrus of the hippocampus and SVZ in the later wall of lateral ventricles. **(A)** Upper panel: the schematic illustration of the main stages of adult neurogenesis in SGZ. Radial type 1 cells, which correspond to neural stem cells, give rise to high proliferative Type 2 cells (first 2a, followed by 2b) which further generate Type 3 neuroblasts. Neuroblasts differentiate into granule neurons that migrate into granular cell layer of dentate gyrus. Lower panel: the schematic summary of the findings regarding the expression of SOX2 (Ferri et al., 2004; Steiner et al., 2006), SOX1 (Venere et al., 2012), SOX3 (Rogers et al., 2013), SOX21 (Matsuda et al., 2012), SOX4 (Mu et al., 2012), and SOX11 (Haslinger et al., 2009; Mu et al., 2012). **(B)** Upper panel: the schematic illustration of the main stages of adult neurogenesis in the SVZ. Neural stem cells, named as Type B1 cells upon activation generate high proliferative cell population of progenitors - Type C that give rise to Type A neuroblasts. Neuroblasts migrate through rostral migratory stream of the olfactory bulb where they differentiate into interneurons. Lower panel: the schematic summary of the findings regarding expression of SOX2 (Ferri et al., 2004), SOX3 (Rogers et al., 2013), SOX4 (Pennartz et al., 2004), SOX11 (Haslinger et al., 2009), and SOX9 (Cheng et al., 2009). NSC, neural stem cell; IN, immature neuron; MN, mature neuron; N/A, data not available.

in slow dividing NSCs as well as in highly proliferating Type 2a and Type 2b neuronal progenitor cells (**Figure 4A**) (Rogers et al., 2013). In contrast, the expression of SOX3 was localized only in small population of SOX2 expressing cells in SVZ (**Figure 4B**) (Rogers et al., 2013). Despite robust expression of SOX1 and SOX3 in adult brain, their functional roles in the regulation of adult neurogenesis are yet to be determined.

In the hippocampus of adult mouse, the expression of SOX21 has been detected in NSCs (Radial Type 1) and subset of neuronal progenitor cells (Type 2a) in SGZ (**Figure 4A**). Functional study indicated that *Sox21* regulates the progression of adult neurogenesis in the hippocampus by direct repression of TF Hes5 (Hes Family bHLH Transcription Factor 5) (Matsuda et al., 2012).

In the adult mammalian brain, the expression of SOX4 and SOX11 proteins is detected prominently in the both main neurogenic niches, SGZ (**Figure 4A**) and SVZ (**Figure 4B**) (Pennartz et al., 2004; Haslinger et al., 2009; Mu et al., 2012). Similar to the expression pattern in embryonic brain, onset of SOX4 and SOX11 expression in cells coincides with the down-regulation of SOX2 and up-regulation of DCX (Doublecortin) expression, and remains throughout the period when newborn neurons migrate to their final destination (**Figure 4**). Finally, SOX4 and SOX11 expression was detected in extremely low number of mature neurons (Haslinger et al., 2009; Mu et al., 2012). Overexpression of these two TFs promoted expression of neuronal-specific genes in NPCs, whereas their repression disturbed neurogenesis, but not gliogenesis (Mu et al., 2012).

Among SOXE TFs, SOX9 expression has been detected in the NSCs and different subset of neuronal progenitor cells in the SVZ in the adult mouse brain (Type B1 and Type C neuronal progenitors in the **Figure 4B**) (Cheng et al., 2009). Functional studies provided evidence that this TF is necessary for maintaining the multipotency of NSCs in SVZ (Scott et al., 2010). Furthermore, knockdown of *miR-124*, which targets *Sox9*, increase SOX9 expression and decrease neurogenesis (Cheng et al., 2009).

SOX TRANSCRIPTION FACTORS AND IMPAIRED ADULT NEUROGENESIS

Adult neurogenesis has been implicated as a major contributor of brain homeostasis, restoring neurological functions under physiological or pathological conditions (Kempermann et al., 2004; Braun and Jessberger, 2014). Differentiation and maturation of new neurons from NSCs in adult brain are dynamically regulated by numerous intrinsic and extrinsic factors, such as neurotrophic factors, transcriptional programs, inflammatory cytokine, cell cycle regulators, neurotransmitters and hormones (Braun and Jessberger, 2014; Shohayeb et al., 2018). On the other hand, the most studied negative regulators of NSC fate during adult neurogenesis include aging, stress, inflammation and alcohol abuse (Braun and Jessberger, 2014). In addition, wide spectrum of neurological conditions is a consequence of neuron loss after injury. Although increase in neurogenesis is detected in response to injury, the capacity for restoring of neurological function in damaged areas is limited (review in Dillen et al., 2020).

Neurodegenerative diseases are heterogeneous group of deleterious conditions with multifactorial etiologies caused by progressive damage of neurons and glial cells and, consequently,

the loss of cognitive and physical functions. Recent findings provided multiple evidence for deregulated adult neurogenesis in several neurodegenerative diseases that display symptoms related to hippocampal and olfactory dysfunction, including Parkinson's, Alzheimer's, and Huntington diseases (reviewed in Deierborg et al., 2007; Winner et al., 2011; Winner and Winkler, 2015; Horgusluoglu et al., 2017).

Despite numerous data implicating the key role of *Sox*/*SOX* genes in regulation of embryonic and adult neurogenesis, their function under pathological conditions are largely unknown. Alzheimer's disease, the most common adult onset-dementia, is characterized by deteriorating hippocampus, memory impairment, and other cognitive and olfactory deficits. Recently, Briley et al. (2016) have demonstrated reduction in SOX2 positive NSCs in the hippocampus of Alzheimer's disease patients which correlated with the severity of the disease or the patient's cognitive capacity.

In our previous work, we analyzed the expression of selected members of SOXB group (SOX1, SOX2, and SOX21) in the hippocampus of 2 months old 5xFAD mice, which represent a transgenic model of Alzheimer's disease. Immunohistochemical analysis revealed a significant decrease in the number of cells expressing SOX1, SOX2, and SOX21 TFs within the SGZ of 5xFAD mice in comparison to their non-transgenic counterparts. Our comparative study also revealed, for the first time, significant difference in the number of SOX1 positive cells between genders in both, transgenic and non-transgenic animals (Zaletel et al., 2018). Considering previous findings that epigenetic-related mechanisms are involved in brain development (McCarthy and Nugent, 2015), we speculate that sex dependent level of SOX1 expression could be result of epigenetic regulation. However, further studies are needed to clarify these findings.

THE ROLES OF SOX TRANSCRIPTION FACTORS IN GLIAL DIFFERENTIATION

During embryonic development of the CNS, multipotent neural precursor cells undergo a characteristic temporal pattern of differentiation wherein neurons are generated ahead of the production of glial cells. This developmental transition consists of two distinct molecular processes: the termination of neurogenesis and the initiation of gliogenesis. This developmental interval, often named "gliogenic switch," is fundamental to the entire developing CNS and is conserved throughout all the vertebrate species (Kessaris et al., 2001; Poche et al., 2008; Subramanian et al., 2011; Kang et al., 2012). The genesis of neural cells by chronological order in vertebrates provides a good biological sense. In fact, the generated neurons create the functional neuronal circuits and, when the scaffold is formed, then the numbers and positions of glia are fitted in the preformed platform (Miller and Gauthier, 2007). The integrated glial cells further provide mechanical, metabolic and trophic support to neurons. The sequential production of neurons and glia is best characterized in the ventral region of the mouse and chick embryonic spinal cord (Kessaris et al., 2001; Rowitch, 2004; Kang et al., 2012). SOX9 TF has been reported as a crucial molecular component in triggering the switch from neurogenic to gliogenic program in the developing mouse spinal cord (Stolt et al., 2003; Kang et al., 2012). In particular, the absence of *Sox9* in NSCs caused defects in the specification of oligodendrocytes and astrocytes, the two main types of glial cells in CNS, and induced a transient increase in the number of motoneurons (Stolt et al., 2003). However, findings in the developing cerebellum indicate that the primary functional role of *Sox9* in modulating the neuron-versus-glia switch is to suppress neurogenesis, rather than to actively trigger the initiation of gliogenesis (Vong et al., 2015). The discrepancy in results obtained by studying different developmental CNS regions suggests that the importance of SOX9 transcriptional factor in orchestrating NSCs fate decision toward gliogenesis may be tissue or organ dependent (Vong et al., 2015). During gliogenic switch SOX9 actively promotes glial lineage progression by controlling a set of genes that contribute to early gliogenesis (Kang et al., 2012). As previously mentioned, an important feature of SOX proteins is that they generally display their gene regulatory functions by forming complexes with partner TFs (Kamachi and Kondoh, 2013). Thus, the NFIA (Nuclear factor-1 A) directly regulated by SOX9, has been identified as the crucial transcriptional partner of SOX9 necessary for the onset of gliogenesis. Subsequently, SOX9 and NFIA form a complex and co-activate multiple genetics programs that regulate the activities of astroglial precursors (Kang et al., 2012). It is important to note that this data has been collected from the embryonic chick and mouse spinal cord, whether the same mechanism is active in the other regions of developing CNS is still unknown. Recent findings have indicated that the synergistic activation of astrocyte genes by SOX9 and NFIA is repressed by SOX3 binding in glial precursor cells of mouse spinal cord (Klum et al., 2018). Indeed, while both astrocyte- and oligodendrocyte-specific genes are prebound by SOX9 in glial progenitor cells, a specificity of astrocyte genes is that this prebinding occurs in combination with SOX3. *Sox9* continues to be expressed in maturing astrocytes but its expression decreases during oligodendrocyte-lineage progression (**Figure 3**, right panel). At the later stages of development, maturing oligodendrocytes become fully dependent on *Sox10*, as evident from the severe disruption of both terminal oligodendrocyte differentiation and myelination in the CNS of *Sox10*-deficient mice (Stolt et al., 2002; Weider et al., 2013).

Although *Sox8* is also expressed in oligodendrocyte precursors, it performs only supportive role during oligodendrocyte development (Stolt et al., 2004; Kellerer et al., 2006; Stolt and Wegner, 2010). Despite functional redundancy, SOX8 is only able to partially rescue the compromised oligodendrocyte differentiation in *Sox10*-deficient mice (Kellerer et al., 2006). However, differentiated oligodendrocytes rely to a much greater extent on SOX8 than oligodendroglial precursors, since recent findings have indicated that SOX8 and SOX10 are jointly required for maintaining the myelinated state (Turnescu et al., 2018).

SOX10 directly controls the expression of genes encoding the major myelin proteins (Stolt and Wegner, 2010). This TF is an essential general determinant of myelination in both CNS and the peripheral nervous system (Stolt and Wegner, 2010;

Weider et al., 2013). Although both oligodendrocytes in CNS and Schwann cells in peripheral nervous system represent myelinating glia, they achieve myelination in distinct ways. However, while the interacting partners of SOX10 in Schwann cells are well described, less is known about its transcription partners in oligodendrocytes. Expression of *Sox5* and *Sox6* overlaps strongly with SOXE protein activity during oligodendrocytes specification and terminal differentiation (**Figure 3**, right panel). Nevertheless, while SOX9 and SOX10 promote oligodendrocyte lineage progression, SOX5 and SOX6 have the opposite effects as evident from both premature specification and precocious terminal differentiation of oligodendrocyte precursors in *Sox5/Sox6*-deficient mice (Stolt et al., 2006). Direct physical interaction between the SOXD and SOXE TFs during oligodendrocyte differentiation has not been reported. Actually, the SOXD proteins counteract the SOXE proteins by competition for the same binding sites and the recruitment of co-repressors to target gene promoters (Stolt and Wegner, 2010).

SOX TRANSCRIPTION FACTORS IN TISSUE HOMEOSTASIS AND REGENERATION IN THE CONTEXT OF GLIAL CELLS

Interestingly, growing evidence indicates that *Sox* genes also play additional roles in adult tissue homeostasis and regeneration (Parrinello et al., 2010; Sarkar and Hochedlinger, 2013; Chen et al., 2019). However, in comparison to the data about the roles of *Sox* genes during developmental, this research field is less explored. Unlike neurons and oligodendrocytes, which become post-mitotic and take on a distinct morphology upon terminal differentiation, astrocytes are not permanently post-mitotic. In response to injury, these cells transform from quiescent into reactive state and dedifferentiate to a progenitor cell-like state (Buffo et al., 2008), which serves as a compensatory response that modulates tissue damage and recovery (Barreto et al., 2011). The re-expression of *Sox* genes in reactivated astrocytes of adult mouse brain has been reported (Bani-Yaghoub et al., 2006; Sun et al., 2017; Chen et al., 2019), but the better understanding of their roles in this process is still needed. Peripheral nerve regeneration is a good example for the role of *Sox2* gene in tissue repair. Upon injury, mature adult Schwann cells re-express *Sox2* and re-acquire progenitor cell-like characteristics (Parrinello et al., 2010). *Sox2* re-expression seems to play a direct role in Schwann cell clustering, a key event during nerve regeneration that enables Schwann cells to form multicellular cords to guide axon re-growth across the site of injury (Parrinello et al., 2010).

The link between neural functions of *SOXE* genes and human nervous system pathologies has been reported throughout different studies. Thus, the increased number of SOX9- and SOX10-positive early glial progenitors in brains of multiple sclerosis patients has been reported (Nait-Oumesmar et al., 2007). Additionally, *SOX8* has been identified as genetic risk loci for Multiple Sclerosis in humans (International Multiple Sclerosis Genetics Consortium et al., 2011, 2013). Also, dysfunction of oligodendrocytes in patients with schizophrenia was correlated with increased DNA methylation of *SOX10* gene (Iwamoto et al., 2005). Taking together, these data imply that *SOX* genes could be considered as potential therapeutic targets. Modulation of *SOX* genes expression may change the functional properties of glial cells for more efficient remyelination of neurons or the repopulation of damaged areas upon CNS trauma. Full understanding of *SOX* genes function in nervous system development as well as homeostasis maintenance and regeneration holds the promise for development of novel therapeutic strategies.

CROSS-TALK OF SOX TRANSCRIPTION FACTORS WITH WNT/β-CATENIN AND RA SIGNALING PATHWAYS

During last decade numerous results established SOX TFs as key players in various signaling pathways. Their interplay with Wnt/β-catenin and RA signaling pathways is of particular interest since SOXB1 neural-specific interpretation of these signaling cascades are involved in the maintenance of stemness and neural differentiation (Kormish et al., 2010; Oosterveen et al., 2013; Hagey and Muhr, 2014).

SOX INTERPLAY WITH WNT/β-CATENIN SIGNALING

β-catenin is central signaling molecule in canonical Wnt pathway (Clevers, 2006). In the absence of the Wnt ligand, cytosolic β-catenin level is low due to activation of destruction complex (Orford et al., 1997; Salic et al., 2000). Wnt stimulation results in the inhibition of cytosolic β-catenin degradation and its shuttle to nucleus (Gordon and Nusse, 2006). In the nucleus β-catenin interacts with the TCF/LEF (T cell factor/Lymphoid enhancer factor) family of DNA-binding TFs on Wnt Response Elements and enhances expression of Wnt target genes (Gordon and Nusse, 2006; Fiedler et al., 2015).

Both canonical Wnt signaling and SOXB1 proteins promote self-renewal of NPCs (Kamachi et al., 1998; Pevny and Placzek, 2005; Wang et al., 2006; Kiefer, 2007). In addition, SOXB1/β-catenin interplay fine tunes the complex mechanism involved in pluripotency/differentiation switch. Activation of canonical Wnt signaling enhances self-renewal of mouse and human ESCs and embryonal carcinoma cells (Hanna et al., 2010; Hassani et al., 2012; Mojsin et al., 2015).

In neural progenitors Wnt/β-catenin signaling activates expression of the pro-neural gene *NeuroD1* by counteracting SOX2-mediated repression on DNA element containing overlapping SOX2 and TCF/LEF-binding sites (SOX/LEF) in its promoter (Van Raay et al., 2005; Kuwabara et al., 2009). We showed that lithium induced activation of Wnt/β-catenin signaling increased expression of all SOXB1 proteins in NT2/D1 cells. We also demonstrated that increase in SOX2 and SOX3 protein expression is β-catenin dependent, while overexpression

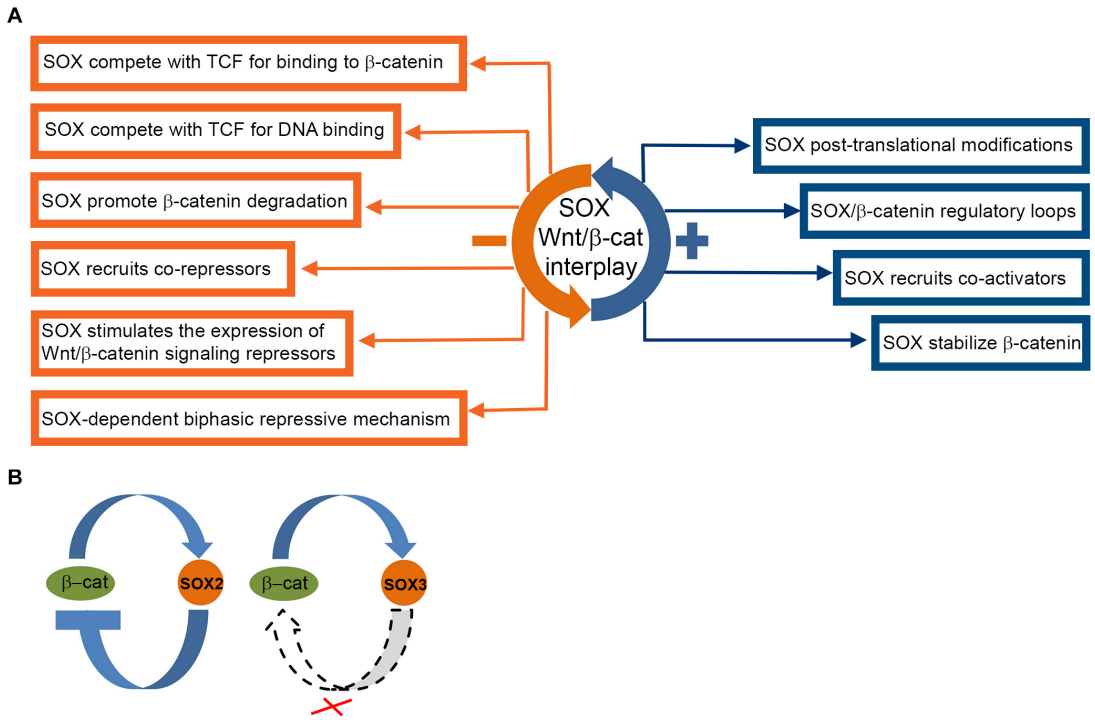

FIGURE 5 | Complex interactions of SOX proteins and Wnt/β-catenin signaling pathway. **(A)** Overview of SOX interactions with Wnt/β-catenin pathway (Bernard and Harley, 2010; Kormish et al., 2010; Hagey and Muhr, 2014). SOX protein repression and activation mechanisms are indicated by orange and blue boxes, respectively. **(B)** SOX2 and SOX3/β-catenin crosstalk in NT2/D1 cells. Proposed model of mutual regulation of SOX2 and SOX3 and β-catenin in NT2/D1 cells (Mojsin et al., 2015). Crossed dashed lines indicate absence of regulatory link.

of SOX1 is governed by β-catenin-independent manner (**Figure 5B**) (Mojsin et al., 2015).

SOX1, SOX2, and SOX3 also affect Wnt/β-catenin signaling (Zorn et al., 1999; Zhang et al., 2003; Kan et al., 2004). SOX1 binds to β-catenin via their C-terminal regions (Akiyama et al., 2004) and inhibits β-catenin/TCF transcription activity in mouse and human NPCs in the onset of neural differentiation (Kan et al., 2004). *SOX2* overexpression reduced β-catenin protein level and down-regulated Wnt/β-catenin signaling in NT2/D1 cells, suggesting negative feedback loop between β-catenin and SOX2 (**Figure 5B**) (Mojsin et al., 2015). However, overexpression of *SOX1* and *SOX3* genes has no effect on endogenous β-catenin level in NT2/D1 cells (**Figure 5B**) (Mojsin et al., 2015).

SOX3 down-regulates Wnt signaling by interactions with β-catenin or by direct binding to the regulatory regions of Wnt target genes (Zorn et al., 1999; Zhang et al., 2003). SOX21 restricts Wnt activity by interacting with β-catenin and subsequent interfering with the binding of TCF4/β-catenin complex to the *WNT8B* (Wingless-type MMTV integration site family, member 8B) enhancer (Fang et al., 2019).

The SOX proteins are considered as nuclear regulators of β-catenin/TCF activity responsible for fine tuning of transcriptional responses to Wnt signaling (Kormish et al., 2010). They regulate β-catenin/TCF activity by recruitment of various mechanisms in cell context-dependent manner (review in Kormish et al., 2010). SOX proteins can physically interact with both β-catenin (Zorn et al., 1999; Akiyama et al., 2004; Iguchi et al., 2007; Sinner et al., 2007; Bernard and Harley, 2010) and TCF/LEF (Sinner et al., 2007). SOX and TCF bind to similar DNA sequences in the DNA minor groove and induce DNA bending which enables assemble of SOX/TCF complexes regardless of distance of their binding sites (Bernard and Harley, 2010; Hou et al., 2017). Post-translational modifications of SOX, β-catenin and TCF also affect their interactions (Taylor and Labonne, 2005; Arce et al., 2006; Hattori et al., 2006). SOX proteins bind to the promoters of Wnt target genes and recruit transcriptional co-activators or co-repressors thus controlling β-catenin dependent transcriptional activity (Tsuda et al., 2003; Zhang et al., 2003; Furumatsu et al., 2005; Iguchi et al., 2007; Pan et al., 2009). SOX proteins activate the expression of Wnt signaling pathway repressors (Bastide et al., 2007). In addition, SOX proteins control endogenous β-catenin protein level by promoting either, proteosome-mediated β-catenin degradation (Preiss et al., 2001; Sinner et al., 2007; Guo et al., 2008) or its stabilization (**Figure 5A**) (Sinner et al., 2007).

Wnt and SOX interplay and mutual control led to a hypothesis pointing out that interactions between lineage-specific SOX TFs and β-catenin/TCF govern specificity of Wnt/β-catenin dependent transcription (Mukherjee et al., 2020). This idea is supported by the study conducted by Hagey and Muhr (2014). They studied the transition between stem cells and rapidly dividing progenitors in mouse cortex and proposed model of SOXB1-dependent bi-phasic repressive mechanism

(Hagey and Muhr, 2014). High level of SOXB1 in stem cells represses pro-proliferative genes, primarily *Ccnd1* (Cyclin D1), by binding to low-affinity SOX binding sites in *Ccnd1* promoter, by interactions with TCF/LEF proteins and by recruitment of GRO/TLE (Groucho/Transducin-like Enhancers) co-repressors. Upon differentiation, pro-neural proteins reduce SOXB1 level, thus only the high affinity SOX binding sites stay occupied, while loss of binding to low-affinity sites de-represses *Ccnd1* and promotes proliferation of progenitor cells (Hagey and Muhr, 2014). Proposed model provides the explanation how presence of low- and high-affinity SOX binding sites enables graded SOXB1 target gene regulation and how differences in the expression levels of SOXB1 proteins can be interpreted by determining the response of target genes.

It has been shown that complex network between Wnt/β-catenin pathway, SOX2 and proneural genes regulates the progression from progenitors to neurons and glia cells (Agathocleous et al., 2009). Lack of this coordination leads to aberrant neuronal proliferation and differentiation and contributes to the pathology of psychiatric disorders (Agathocleous et al., 2009; Santos et al., 2021). In the search for specific targets of lithium resistance in the patients with bipolar disorder, Santos et al. (2021) conducted comparative transcriptome analysis of the hippocampal dentate gyrus-like neurons derived from iPSCs of lithium-responsive and lithium-non-responsive patients. First, they have demonstrated that neurons generated from both cohorts exhibited neuronal hyperexcitability compared to control neurons that could be reversed by lithium treatment of the lithium-responsive neurons only (Santos et al., 2021). The study showed that neurons from lithium-non-responsive patients acquire distinct phenotypic characteristics, electrophysiological properties and the response to lithium during differentiation due to the severely affected function of canonic Wnt/β-catenin signaling with a significant decrease in expression of LEF1 (Lymphoid enhancer-binding factor 1) (Santos et al., 2021). Interestingly, SOX2 was also up-regulated in lithium-non-responsive neurons compared to control neurons (Santos et al., 2021).

SOX INTERPLAY WITH RA SIGNALING

Retinoic acid exerts its pleiotropic effects through binding to retinoic acid receptors (RARs), members of the nuclear receptor superfamily (reviewed by Rochette-Egly and Germain, 2009). RARs act in heterodimeric combinations with retinoid X receptors (RXRs). It was suggested that RXRs act as scaffolding proteins and facilitate DNA binding of the RAR-RXR complex (Chawla et al., 2001). In the nucleus, RAR/RXR dimers can interact with *cis*-acting RA response elements (RAREs) (Laudet and Gronemeyer, 2002), atypical RARE (Panariello et al., 1996; Brondani et al., 2002) and composite response units within the promoters of different RA-target genes (Redfern, 2004; Wang and Yen, 2004). Ligand binding induces conformational changes that lead to release of co-repressors, binding of co-activators and subsequent initiation of transcription (Balmer and Blomhoff, 2002).

Our group conducted comprehensive analyses of the SOXB1 protein expression during RA induced neural differentiation of NT2/D1 cells (Stevanovic, 2003; Klajn et al., 2014; Popovic et al., 2014; Topalovic et al., 2017). Obtained results showed dynamic changes in the expression profiles of SOX1, SOX2 and SOX3 proteins during 4-weeks course of RA induction (**Figure 6**).

Retinoic acid induced transient up-regulation of SOX1 at the day 4 of RA induction and oscillating expression followed by decrease at 3 and 4 weeks of treatment (**Figure 6**) (Popovic et al., 2014; Topalovic et al., 2017). After initial downregulation in the first 48h of induction, SOX2 was up-regulated in all time points of induction (**Figure 6**) (Stevanovic, 2003; Popovic et al., 2014; Topalovic et al., 2017). However, in mature neurons (NT2-N) expression of SOX2 is abolished (Klajn et al., 2014). Similar results were obtained in the studies of the effects of RA on *Sox2* expression in mouse P19 and F9 embryonal carcinoma cell lines (Wiebe et al., 2000; Tremblay et al., 2012; Popovic et al., 2014).

SOX3 expression was transiently up-regulated during 48h of RA treatment and then gradually decreased up to 4 weeks of RA treatment (**Figure 6**) (Stevanovic, 2003; Popovic et al., 2014; Topalovic et al., 2017). Comprehensive examination of the promoter of human *SOX3* gene revealed the presence of two RA response elements, DR-3-like RXR RE (Nikcevic et al., 2008) and atypical RA/RXR RE (Mojsin et al., 2006). In addition, we have identified numerous TFs involved in the modulation of RA induced activation of human *SOX3* promoter (Krstic et al., 2007; Nikcevic et al., 2008; Mojsin and Stevanovic, 2009).

Beside RA involvement in transcriptional regulation of SOXB proteins, SOXB1 neural-specific interpretation of signaling morphogens add an additional level of complexity to the RA/SOXB1 interplay in developing CNS (Oosterveen et al., 2013). Genome-wide characterization of *cis*-regulatory modules (CRMs) in neural-specific target genes (Oosterveen et al., 2013) showed that interpretation of pleiotropic signals is the result of integration of SOXB1 and signaling morphogens on CRMs (Oosterveen et al., 2013). CRMs of RA target genes contains RARE and SOX binding sites both required for synergistic activation of CRMs (Oosterveen et al., 2013). One of genes enriched for functions in neural development whose CRM was analyzed in the study is *Dbx1* (Developing brain homeobox 1) (Oosterveen et al., 2013). In another study conducted by Rogers et al. (2014) *Dbx1* was identified as a direct and exclusive SOX3 target gene in NPCs both *in vitro* and *in vivo*. The fact that RA regulates SOX3 expression through multiple RARE (Brunelli et al., 2003; Mojsin et al., 2006; Nikcevic et al., 2008) confirms that SOXB1/RA signaling interplay is complex and fine-tuned at multiple levels.

SOX TRANSCRIPTION FACTORS AND microRNAs IN CONTROL OF NEURONAL AND GLIAL DIFFERENTIATION

Many evolutionary conserved microRNAs (miRNAs) present key factors in fine regulation of self-renewal and proliferation of NSCs and NPCs (Meza-Sosa et al., 2014). By interaction with complementary sequence motifs in 3′ untranslated

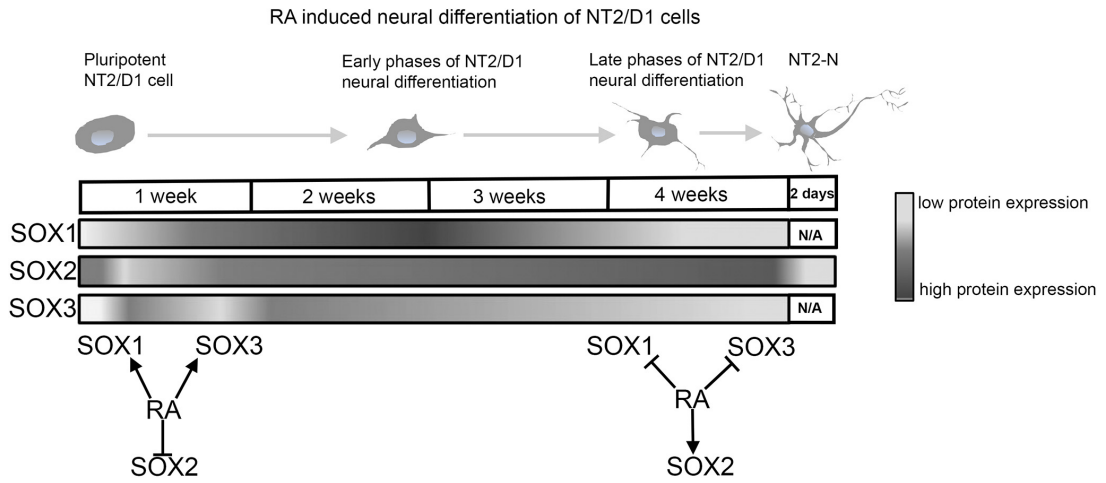

FIGURE 6 | RA modulates expression of SOXB1 proteins during neural differentiation of NT2/D1 cells. Schematic representation of SOXB1 proteins expression profiles during 4 weeks of RA induced neural differentiation of NT2/D1 cells. RA has opposite effects on SOXB1 proteins expression during early and late phases of neural differentiation of NT2/D1 cells (Stevanovic, 2003; Klajn et al., 2014; Popovic et al., 2014; Topalovic et al., 2017). N/A, not available data.

region of target genes, miRNAs regulate the gene expression during different stages of neurogenesis, thus affecting the development of nervous system (Meza-Sosa et al., 2014). Also, acting in synergy with TFs, miRNAs form regulatory networks that can influence cell fate decision (Stappert et al., 2015). Therefore, it is not surprising that miRNAs are often called "master regulators" or "fine-tuners" of gene expression orchestrating important processes during neural development (Rajman and Schratt, 2017). SOX TFs and miRNAs represent one of the most important regulatory networks that control whether NSCs will self-renew or differentiate into neurons, astrocytes or oligodendrocytes (**Figure 7**) (Reiprich and Wegner, 2015). Particularly, SOX1, SOX2, SOX4, SOX5, SOX6, SOX9, and SOX10 are shown to interact with different miRNAs and orchestrate differentiation into neurons and oligodendrocytes (**Figure 7**).

It is suggested that miR-200 family members target *Sox2*, thus regulating the transition from NSCs to postmitotic and differentiated cells (Peng et al., 2012). It turns out to be one of the most important regulatory networks during neural differentiation, whereas *Sox2* is regulated by miR-200c, forming a negative-feedback loop that further decreases expression of *Sox2* during neural differentiation (Kamachi and Kondoh, 2013). Another axis shown to be important for neuronal differentiation is miR-135a-5p/*Sox6*/CD44, where miR-135a-5p acts through *Sox*6, affecting not only differentiation of neurons, but also development of dendrites (Li et al., 2019). Moreover, it was shown that overexpression of *Sox6* could reverse miR-135a-5p-mediated neuronal differentiation and dendrite development of P19 cells (Li et al., 2019). *Sox9* is target of miR-124 during adult neurogenesis in the mouse SVZ where inhibition of *Sox*9 expression leads to differentiation into neurons (Cheng et al., 2009). Further, miR-145 is important for differentiation of neurons through regulation of *Sox2*–Lin28/let-7 signaling pathway that represents important mechanism for proliferation of NPCs (Cimadamore et al., 2013; Morgado et al., 2016). Additionally, miR-145 directly regulates *Sox2* and suppresses its expression in NPCs leading to induction of neurogenesis (Morgado et al., 2016).

Surprisingly, to the best of our knowledge, there is only one study suggesting that interaction between miRNA and SOX TFs plays role in differentiation of astrocytes. miR-124, with pivotal role in differentiation of neurons and astrocytes, can induce differentiation of NSCs to astrocytes through regulation of *Sox2* and *Sox9* expression in NSCs of amyotrophic lateral sclerosis transgenic mice (Krichevsky et al., 2006; Zhou et al., 2018).

Interestingly, it was shown that miR-184, which is one of the key miRNAs throughout all stages of oligodendrocytes differentiation, directly targets *Sox1*, leading to differentiation of NPCs to oligodendrocytes (Hoffmann et al., 2014; Afrang et al., 2019). During differentiation of NPCs the loss of *Sox2* also results in terminal differentiation of oligodendrocytes through negative regulation by miR-145 (Hoffmann et al., 2014). miR-219, miR-138 and miR-338 directly inhibit the expression of *Sox6* gene which results in reduced proliferation of oligodendrocyte progenitors and induction of oligodendrocyte differentiation and myelination (Dugas et al., 2010; Zhao et al., 2010). Further, SOX6 TF is directly regulated by miR-219 and additionally this TF represses the expression of *Sox10* in oligodendrocyte progenitor cells which results in differentiation of mature oligodendrocytes (Nazari et al., 2018). miR-204 overexpression also leads to differentiation of oligodendrocyte progenitors to mature oligodendrocytes through control of *Sox4* gene, while the expression of this miRNA is regulated by SOX9 (Wittstatt et al., 2020). SOX10 also regulates miR-338 that is important for differentiation of oligodendrocytes through inhibition of *Hes5* and *Hes6* genes and it is suggest that *Sox10* exerts its role in maturation of oligodendrocytes specifically through regulation of miR-338 (Gokey et al., 2012). Another study shows that SOX10 TF directly targets miR-338 and miR-335, and then these two

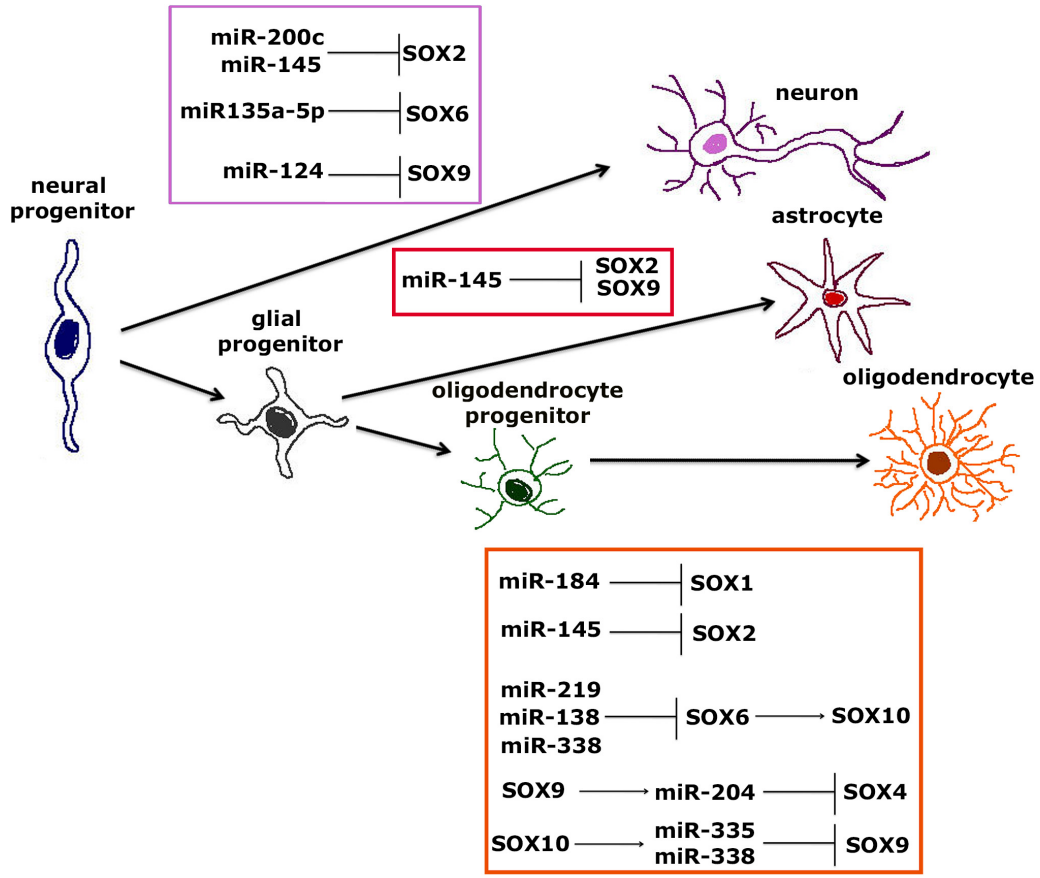

FIGURE 7 | Interaction between SOX TFs and miRNAs during neural differentiation from neural progenitors to neurons, astrocytes or oligodendrocytes. Interaction between SOX TFs and miRNAs involved in differentiation of neurons from NPCs is shown within purple frame (Cheng et al., 2009; Peng et al., 2012; Cimadamore et al., 2013; Kamachi and Kondoh, 2013; Morgado et al., 2016; Li et al., 2019). Interaction between SOX TFs and miRNAs involved in differentiation of astrocytes from NPCs is shown within red frame (Krichevsky et al., 2006; Zhou et al., 2018), while interaction between SOX TFs and miRNAs involved in differentiation of mature oligodendrocytes from oligodendrocytes progenitors is shown within orange frame (Dugas et al., 2010; Zhao et al., 2010; Gokey et al., 2012; Hoffmann et al., 2014; Reiprich et al., 2017; Nazari et al., 2018; Afrang et al., 2019; Wittstatt et al., 2020).

TABLE 2 | Main functions of SOX TFs in neural differentiation during embryonic development.

Main functions in neural differentiation during embryonic development	SOX TFs	References
Maintainance of neural progenitor cells	SOX1, SOX2, SOX3, SOX9	Bylund et al., 2003; Graham et al., 2003; Scott et al., 2010; Hutton and Pevny, 2011
Promotion of neuronal differentiation	SOX14, SOX21, SOX4, SOX11, SOX5, SOX6, SOX13	Connor et al., 1995; Hargrave et al., 2000; Sandberg et al., 2005; Wang et al., 2005; Bergsland et al., 2006; Kwan et al., 2008; Martinez-Morales et al., 2010; Chen et al., 2015; Makrides et al., 2018
Promotion of astrocytes differentiation	SOX9	Stolt et al., 2003; Kang et al., 2012
Inhibition of astrocytes differentiation	SOX3	Klum et al., 2018
Promotion of oligodendrocytes differentiation	SOX8, SOX9, SOX10	Stolt et al., 2004; Stolt and Wegner, 2010; Weider et al., 2013
Inhibition of oligodendrocytes differentiation	SOX5, SOX6	Stolt et al., 2006

miRNAs further repress *Sox9* in oligodendroglial cells (Reiprich et al., 2017). This fine tuning of *Sox9* and *Sox10* expression levels leads to terminal differentiation of oligodendrocytes.

It is evident that SOX TFs and miRNAs establish the functional interactions important for cell fate decision of NPCs during neural development. This can be achieved either through post-transcriptional regulation of *Sox* genes by miRNAs, through SOX-dependent control of miRNAs expression or by combination of both. Even though SOX3, SOX14, and SOX21 play important roles in neural differentiation, there is a lack

of data regarding their regulation by miRNAs. Although SOX TFs are involved in regulation of gliogenesis, more studies are required to clarify posttranscriptional regulation of *Sox*/*SOX* gene expression by miRNAs during this process. Additionally, we previously reported that specific *SOX* genes and miRNAs can be potentially used as biomarkers for monitoring radiation response during early phase of neural differentiation (Stanisavljevic et al., 2019). This result suggests that SOX and miRNAs have additional important roles during neural differentiation. Overall, future studies are needed in order to gain better insight into the complex interactions between miRNAs and SOX TFs during neural development.

CONCLUDING REMARKS AND FUTURE DIRECTIONS

SOX proteins belong to the family of TFs that exerts multiple important roles during nervous system development, starting from preimplantation embryo to the adulthood. Many *Sox* genes are expressed in the developing and adult nervous system in the overlapping manners, covering various cell types, beginning with the neural stem cell (NSC) stage until terminal maturation of neurons and macroglia (reviewed in Lefebvre et al., 2007). During embryonic development SOX family members are involved, both in maintaining multipotency of neural progenitors, as well as in the promotion of neuronal differentiation (**Table 2**). They are also implicated in the control of glial differentiation by promoting differentiation of astrocytes and oligodendrocytes. SOX proteins may have dual roles in the regulation of target gene expression, acting as either activators or repressors, depending on cellular and genomic context (Liu et al., 2014). For instance, SOX3 is acting as activator of genes in neural progenitors, while suppressing neuronal differentiation by repression of neuronal and glial specific genes in the same cells (**Figure 2**). It is interesting to point out that SOXB and SOXC family members are sequentially bound to the common set of neural genes during the process of neuronal differentiation, highlighting the context-dependent nature of their actions. It has been reported that majority of the SOX3 binding sites will be targeted by SOX11 in newly formed neurons (Bergsland et al., 2011). The presence of low- and high-affinity SOX binding sites enables graded control of target genes, while the levels of SOX proteins is interpreted by the corresponding response of the target gene expression (Hagey and Muhr, 2014). Thus, sequentially acting SOX TFs orchestrate neuronal-, astrocyte- and oligodendrocyte-specific gene expression defining neuronal and glial phenotypes.

The capability of SOX TFs to orchestrate the process of neural differentiation strongly relies on epigenetic regulation. We already showed that *SOXB1* genes were controlled by different epigenetic mechanisms during neural differentiation (Topalovic et al., 2017). Additional study of the differences in histone signatures will provide further insight into the epigenetic regulation of pluripotency for proper differentiation of neurons or glial cells.

The roles of SOX proteins are not limited to development since these factors influence survival, regeneration, cell death and control of homeostasis in adult tissues (Pevny and Placzek, 2005). Adult neurogenesis has been recognized as a major contributor of brain homeostasis, restoring neurological functions under physiological or pathological conditions. We provide the overview of the current data implicating at least seven SOX proteins (members of SOXB, SOXC, and SOXE groups) in control of adult neurogenesis (**Figure 4**).

The majority of current knowledge regarding the roles of *Sox*/*SOX* genes in neural development is based on research mainly conducted in mice and other animal models, and to the lesser extent, on the *in vitro* cell based models of human neural differentiation. Research based on animal models provides important information about the roles of *Sox* genes in neural development. However, significant differences in brain development between species have been revealed and evident divergence among species is discovered regarding gene expression at the earliest stages of brain development (Johnson et al., 2009; Rakic, 2009; Clowry et al., 2010).

The emerging data associates *SOX* gene variants with NDDs characterized by impairment of neuronal function during brain development (**Supplementary Table 1**). Interestingly, down-regulation of *SOX9* expression has been detected in neural progenitors derived from Fragile X Syndrome human ESCs (Telias et al., 2015). However, contribution of SOX proteins to NDDs is still not fully explored and further research is needed to clarify their roles in the underlying pathologies.

The rising field of research is devoted to study the roles of SOX TFs in neurodegenerative diseases. Neurodegenerative diseases are characterized by progressive damage of neurons and glial cells and, consequently, loss of cognitive and physical functions. Recent years provided multiple evidences of impaired adult neurogenesis in several neurodegenerative diseases (reviewed in Horgusluoglu et al., 2017). Reduction in SOX2 positive NSCs detected in the hippocampus of Alzheimer's disease patients is correlated with the severity of the disease or the patient's cognitive capacity (Briley et al., 2016).

Most of the knowledge regarding human neurodegenerative diseases has been acquired from post-mortem patient samples since human brain tissue is inaccessible and highly difficult to obtain. Although many animal models mimicking diseases have been available for the research, they have provided only limited success in identification of the molecular mechanisms underlying human brain diseases. In the recent years, generation of patient-specific iPSCs provides remarkable opportunity to recapitulate both normal and pathologic human tissue formation *in vitro*, enabling genuine disease investigation (reviewed in Park et al., 2008). Furthermore, iPSCs have potential to replace affected neurons in neurodegenerative disorders (Comella-Bolla et al., 2020). Various human brain diseases across the spectrum of neurodevelopmental, neurodegenerative and neuropsychiatric are being studying by iPSC –based disease modeling (reviewed in McKinney, 2017). Studying the differentiation of patient-specific iPSCs into neurons or glial cells provides valuable insight into the molecular mechanisms underlying brain diseases in patient-specific genetic background. In the last decades remarkable efforts have been made in developing protocols for fast and efficient differentiation of

iPSCs in specific neuronal sub-types. Recently, Comella-Bolla et al. (2020) described a fast, robust and reproducible protocol for differentiation of human iPSCs into functionally maturing forebrain neurons *in vitro*, which will facilitate studies of neurodevelopmental and neurodegenerative disorders. Obtained neurons have ability of *in vivo* integration which makes the protocol compatible with cell therapy-based strategies (Comella-Bolla et al., 2020). Apart from enabling research of disease phenotype *in vitro*, iPSCs are providing the tool for gene defect/s repair *ex vivo*. Moreover, iPSCs from healthy donors can be modified by introducing disease–specific mutation by genome editing allowing the study of the effect of specific gene defect in "healthy" background.

In an aging society, regenerative therapies based on iPSCs could provide significant potential therapeutic benefits, in particular for the patients suffering from neurodegenerative diseases including Parkinson's and Alzheimer's diseases. Study of the impacts of donor age on iPSC- derived cell functionality indicate that aging may reduce reprogramming efficiency having no significant effects on iPSCs maintenance or differentiation capacity (Strassler et al., 2018). These data suggest that donor age does not limit applications of iPSCs based methodology for modeling genetic diseases and for development of therapies for age-related diseases, especially in combination with recently developed gene-editing tools such as CRISPR/Cas9 technology (Strassler et al., 2018). The same authors indicate that burden of age-associated somatic mutations that iPSCs inherit from donor cells cannot be reduced, increasing the risk of abnormalities in iPSCs. A low number of healthy and elderly donors serving as a source of control cells present a great challenge in research and applications in the field of iPSCs (Strassler et al., 2018). Recently a collection of iPSCs derived from old male and female healthy subjects has been reported (Rodriguez-Traver et al., 2020) that can be used as controls for other disease lines derived from geriatric patients and for studying the roles of SOX TF in neurodegenerative disorders and aging.

Traditionally, brain diseases have been generally assigned to malfunction or loss of neurons. However, in the last decade, it has been shown that astrocytes play essential roles in the regulation of various brain functions. Astrocytes process and control synaptic information, modulate synaptic formation and elimination at all stages of development and in adulthood (Volterra and Meldolesi, 2005). Patient-specific iPSC-based models as human platforms for research accelerated the study of molecular mechanisms underlying neurogenesis, synapse formation, maintenance and plasticity (Oksanen et al., 2019). However, whether astrocytes contribute to the pathology of underlying brain disorders and potential contribution of SOX TFs to the pathologies is yet to be discovered. Accordingly, astrocytes became a promising target for drug discovery and the development of novel therapies.

Furthermore, wide spectrum of neurological and neurodegenerative conditions are consequence of neuron loss after ischemic injury. Although increase in neurogenesis is detected in response to injury, the capacity for restoring neurological function in damaged areas is limited (review in Dillen et al., 2020). Accordingly, iPSCs can be used for developing effective therapies aimed to increase neurogenesis by modulating *SOX* gene expression toward enhancement of regenerative potential for repair of damaged or aged neural cells.

Most recently advances in biotechnology, including stem cell propagation and novel biomaterials enable development of 3D models for studying human brain development. Brain organoids represent 3D-aggregates generated from human pluripotent cells (ESCs and iPSCs) resembling the embryonic human brain regarding the cell types, cells' architectures and maturation (Eiraku et al., 2008; Pasca et al., 2015). The 3D models, ranging from region-specific organoids to more complex whole-brain organoids, are mimicking cell interactions and interconnectivity between multiple brain regions (Lancaster and Knoblich, 2014; Xiang et al., 2020) providing novel tools for studying more complex phenotypes involving different neuronal networks, tissue architecture, and organ morphogenesis (Baldassari et al., 2020). Advances in 3D modeling including extracellular matrix composition, optimized media transitions and agitation of the tissues led to the formation of cerebral organoids with various brain region identities. These advances revealed the remarkable fidelity with which organogenesis can occur *in vitro* leading to accurate modeling of events occurring during the first half of gestation in humans (reviewed in Chiaradia and Lancaster, 2020). While cerebral organoids are capable to spontaneously acquired forebrain, midbrain and hindbrain identities, it is feasible to generate particular brain regions of interest by applying novel modified protocols for guiding and directing regional identity (Kadoshima et al., 2013; Pasca et al., 2015; Tanaka et al., 2020). Brain organoids recapitulate many features of the fetal human brain, including cytoarchitecture, cell diversity and maturation and comprise a variety of cell types comparable, to some extent, to the complex composition of the cells present in the brain (reviewed in Chiaradia and Lancaster, 2020). Importantly, spontaneous neuronal activity has been detected in brain organoids suggesting the existence of functional communication among neuronal cells (Lancaster et al., 2013). Brain organoids have been used for modeling neurological diseases and NDDs, providing remarkable advantage in studying diseases *in vitro*, in a 3D environment resembling the affected tissue (reviewed in Chiaradia and Lancaster, 2020). The position of organoids at the interface of *in vitro* and *in vivo* neurobiology makes them a unique model system that will provide further progress in understanding brain development (Chiaradia and Lancaster, 2020). Combined with single cell transcriptomics technology, the brain organoids would enable to decipher cellular heterogeneity and transcriptional landscape at single cell resolution. These novel tools will open innovative approaches for studying the roles of SOX TFs in brain development at the single cell level in physiological and pathological conditions.

In the past decade, the "omics" technologies, such as genomics, transcriptomics, miRNomics, and proteomics have become integrated parts of the research in biology and medicine, enabling progress in collecting, processing and integrating huge amounts of health-related information (D'Adamo et al., 2020).

While genomic analyses provide the insight into variation at DNA level, RNAseq data reveal transcriptome diversity in patients compared to healthy controls. For instance, integrative transcriptomic analysis may lead to the identification of key deregulated candidate genes and pathways shared between various developmental disorders. Such innovative approach may help in identifying novel roles of SOX proteins in pathology of NDDs.

Advance in proteomic technologies enables mapping of specific gene interactome providing the insights into the network of interacting partners. Thus, the study of Nanog interactome identified SOX2 as interacting factor (Gagliardi et al., 2013). Mapping the interactome of specific SOX protein will provide deeper insight into interacting factors and disruption of interactions in diverse pathological conditions. Appropriate bioinformatics analysis will reveal networks of TFs and signaling pathways differentially regulated between different cell states. Such analysis will identified position of SOX proteins within signaling cascades active in particular cell context and pinpoint their functionally relevant links in complex regulatory networks.

Although many important roles during neural development have been assigned to SOX TFs, we strongly believe that many novel functions are yet to be discovered.

AUTHOR CONTRIBUTIONS

All authors wrote the manuscript and contributed to literature collection. MiS designed the concept of the manuscript and supervised and edited the manuscript. MiS, DD, and DSN contributed to the preparation of the tables. MaS, AL, MM, and DSN designed the figures. All authors contributed to the article and approved the submitted version.

FUNDING

This work was supported by the Ministry of Education, Science and Technological Development of Republic of Serbia (Grant numbers 451-03-68/2020-14/200042 and 451-03-9/2021-14/200042).

SUPPLEMENTARY MATERIAL

The Supplementary Material for this article can be found online at: https://www.frontiersin.org/articles/10.3389/fnmol.2021.654031/full#supplementary-material

REFERENCES

Adachi, K., Suemori, H., Yasuda, S. Y., Nakatsuji, N., and Kawase, E. (2010). Role of SOX2 in maintaining pluripotency of human embryonic stem cells. *Genes Cells* 15, 455–470. doi: 10.1111/j.1365-2443.2010.01400.x

Afrang, N., Tavakoli, R., Tasharrofi, N., Alian, A., Naderi Sohi, A., Kabiri, M., et al. (2019). A critical role for miR-184 in the fate determination of oligodendrocytes. *Stem Cell Res. Ther.* 10:112. doi: 10.1186/s13287-019-1208-y

Agathocleous, M., Iordanova, I., Willardsen, M. I., Xue, X. Y., Vetter, M. L., Harris, W. A., et al. (2009). A directional Wnt/beta-catenin-Sox2-proneural pathway regulates the transition from proliferation to differentiation in the *Xenopus* retina. *Development* 136, 3289–3299. doi: 10.1242/dev.040451

Akiyama, H., Lyons, J. P., Mori-Akiyama, Y., Yang, X., Zhang, R., Zhang, Z., et al. (2004). Interactions between Sox9 and beta-catenin control chondrocyte differentiation. *Genes Dev.* 18, 1072–1087. doi: 10.1101/gad.1171104

Amador-Arjona, A., Cimadamore, F., Huang, C. T., Wright, R., Lewis, S., Gage, F. H., et al. (2015). SOX2 primes the epigenetic landscape in neural precursors enabling proper gene activation during hippocampal neurogenesis. *Proc. Natl. Acad. Sci. U.S.A.* 112, E1936–E1945. doi: 10.1073/pnas.1421480112

Ambrosetti, D. C., Scholer, H. R., Dailey, L., and Basilico, C. (2000). Modulation of the activity of multiple transcriptional activation domains by the DNA binding domains mediates the synergistic action of Sox2 and Oct-3 on the fibroblast growth factor-4 enhancer. *J. Biol. Chem.* 275, 23387–23397. doi: 10.1074/jbc.M000932200

Arce, L., Yokoyama, N. N., and Waterman, M. L. (2006). Diversity of LEF/TCF action in development and disease. *Oncogene* 25, 7492–7504. doi: 10.1038/sj.onc.1210056

Argentaro, A., Olsson, J., Critcher, R., McDowall, S. G., and Harley, V. R. (2000). Genomic characterisation and fine mapping of the human SOX13 gene. *Gene* 250, 181–189. doi: 10.1016/s0378-1119(00)00157-8

Arsic, N., Rajic, T., Stanojcic, S., Goodfellow, P. N., and Stevanovic, M. (1998). Characterisation and mapping of the human SOX14 gene. *Cytogenet. Cell Genet.* 83, 139–146. doi: 10.1159/000015149

Arya, V. B., Chawla, G., Nambisan, A. K. R., Muhi-Iddin, N., Vamvakiti, E., Ajzensztejn, M., et al. (2019). Xq27.1 duplication encompassing SOX3: variable phenotype and smallest duplication associated with hypopituitarism to date - a large case series of unrelated patients and a literature review. *Horm. Res. Paediatr.* 92, 382–389. doi: 10.1159/000503784

Avilion, A. A., Nicolis, S. K., Pevny, L. H., Perez, L., Vivian, N., and Lovell-Badge, R. (2003). Multipotent cell lineages in early mouse development depend on SOX2 function. *Genes Dev.* 17, 126–140. doi: 10.1101/gad.224503

Azim, E., Jabaudon, D., Fame, R. M., and Macklis, J. D. (2009). SOX6 controls dorsal progenitor identity and interneuron diversity during neocortical development. *Nat. Neurosci.* 12, 1238–1247. doi: 10.1038/nn.2387

Baldassari, S., Musante, I., Iacomino, M., Zara, F., Salpietro, V., and Scudieri, P. (2020). Brain organoids as model systems for genetic neurodevelopmental disorders. *Front. Cell Dev. Biol.* 8:590119. doi: 10.3389/fcell.2020.590119

Balmer, J. E., and Blomhoff, R. (2002). Gene expression regulation by retinoic acid. *J. Lipid Res.* 43, 1773–1808. doi: 10.1194/jlr.r100015-jlr200

Bani-Yaghoub, M., Tremblay, R. G., Lei, J. X., Zhang, D., Zurakowski, B., Sandhu, J. K., et al. (2006). Role of Sox2 in the development of the mouse neocortex. *Dev. Biol.* 295, 52–66. doi: 10.1016/j.ydbio.2006.03.007

Barreto, G. E., Gonzalez, J., Torres, Y., and Morales, L. (2011). Astrocytic-neuronal crosstalk: implications for neuroprotection from brain injury. *Neurosci. Res.* 71, 107–113. doi: 10.1016/j.neures.2011.06.004

Bastide, P., Darido, C., Pannequin, J., Kist, R., Robine, S., Marty-Double, C., et al. (2007). Sox9 regulates cell proliferation and is required for Paneth cell differentiation in the intestinal epithelium. *J. Cell Biol.* 178, 635–648. doi: 10.1083/jcb.200704152

Batista-Brito, R., Rossignol, E., Hjerling-Leffler, J., Denaxa, M., Wegner, M., Lefebvre, V., et al. (2009). The cell-intrinsic requirement of Sox6 for cortical interneuron development. *Neuron* 63, 466–481. doi: 10.1016/j.neuron.2009.08.005

Beckervordersandforth, R., Zhang, C. L., and Lie, D. C. (2015). Transcription-factor-dependent control of adult hippocampal neurogenesis. *Cold Spring Harb. Perspect. Biol.* 7:a018879. doi: 10.1101/cshperspect.a018879

Bergsland, M., Ramskold, D., Zaouter, C., Klum, S., Sandberg, R., and Muhr, J. (2011). Sequentially acting Sox transcription factors in neural lineage development. *Genes Dev.* 25, 2453–2464. doi: 10.1101/gad.176008.111

Bergsland, M., Werme, M., Malewicz, M., Perlmann, T., and Muhr, J. (2006). The establishment of neuronal properties is controlled by Sox4 and Sox11. *Genes Dev.* 20, 3475–3486. doi: 10.1101/gad.403406

Bernard, P., and Harley, V. R. (2010). Acquisition of SOX transcription factor specificity through protein-protein interaction, modulation of Wnt signalling and post-translational modification. *Int. J. Biochem. Cell Biol.* 42, 400–410. doi: 10.1016/j.biocel.2009.10.017

Bhattaram, P., Penzo-Mendez, A., Sock, E., Colmenares, C., Kaneko, K. J., Vassilev, A., et al. (2010). Organogenesis relies on SoxC transcription factors for the survival of neural and mesenchymal progenitors. *Nat. Commun.* 1:9. doi: 10.1038/ncomms1008

Bowles, J., Schepers, G., and Koopman, P. (2000). Phylogeny of the SOX family of developmental transcription factors based on sequence and structural indicators. *Dev. Biol.* 227, 239–255. doi: 10.1006/dbio.2000.9883

Boyer, L. A., Lee, T. I., Cole, M. F., Johnstone, S. E., Levine, S. S., Zucker, J. P., et al. (2005). Core transcriptional regulatory circuitry in human embryonic stem cells. *Cell* 122, 947–956. doi: 10.1016/j.cell.2005.08.020

Braun, S. M., and Jessberger, S. (2014). Adult neurogenesis: mechanisms and functional significance. *Development* 141, 1983–1986. doi: 10.1242/dev.104596

Briley, D., Ghirardi, V., Woltjer, R., Renck, A., Zolochevska, O., Taglialatela, G., et al. (2016). Preserved neurogenesis in non-demented individuals with AD neuropathology. *Sci. Rep.* 6:27812. doi: 10.1038/srep27812

Brondani, V., Klimkait, T., Egly, J. M., and Hamy, F. (2002). Promoter of FGF8 reveals a unique regulation by unliganded RARalpha. *J. Mol. Biol.* 319, 715–728. doi: 10.1016/S0022-2836(02)00376-5

Brunelli, S., Silva Casey, E., Bell, D., Harland, R., and Lovell-Badge, R. (2003). Expression of Sox3 throughout the developing central nervous system is dependent on the combined action of discrete, evolutionarily conserved regulatory elements. *Genesis* 36, 12–24. doi: 10.1002/gene.10193

Buffo, A., Rite, I., Tripathi, P., Lepier, A., Colak, D., Horn, A. P., et al. (2008). Origin and progeny of reactive gliosis: a source of multipotent cells in the injured brain. *Proc. Natl. Acad. Sci. U.S.A.* 105, 3581–3586. doi: 10.1073/pnas.0709002105

Bylund, M., Andersson, E., Novitch, B. G., and Muhr, J. (2003). Vertebrate neurogenesis is counteracted by Sox1-3 activity. *Nat. Neurosci.* 6, 1162–1168. doi: 10.1038/nn1131

Cavaleri, F., and Scholer, H. R. (2003). Nanog: a new recruit to the embryonic stem cell orchestra. *Cell* 113, 551–552. doi: 10.1016/s0092-8674(03)00394-5

Chawla, A., Repa, J. J., Evans, R. M., and Mangelsdorf, D. J. (2001). Nuclear receptors and lipid physiology: opening the X-files. *Science* 294, 1866–1870. doi: 10.1126/science.294.5548.1866

Chen, C., Lee, G. A., Pourmorady, A., Sock, E., and Donoghue, M. J. (2015). Orchestration of neuronal differentiation and progenitor pool expansion in the developing cortex by SoxC genes. *J. Neurosci.* 35, 10629–10642. doi: 10.1523/JNEUROSCI.1663-15.2015

Chen, C., Zhong, X., Smith, D. K., Tai, W., Yang, J., Zou, Y., et al. (2019). Astrocyte-specific deletion of Sox2 promotes functional recovery after traumatic brain injury. *Cereb. Cortex* 29, 54–69. doi: 10.1093/cercor/bhx303

Cheng, L. C., Pastrana, E., Tavazoie, M., and Doetsch, F. (2009). miR-124 regulates adult neurogenesis in the subventricular zone stem cell niche. *Nat. Neurosci.* 12, 399–408. doi: 10.1038/nn.2294

Cheung, M., Abu-Elmagd, M., Clevers, H., and Scotting, P. J. (2000). Roles of Sox4 in central nervous system development. *Brain Res. Mol. Brain Res.* 79, 180–191. doi: 10.1016/s0169-328x(00)00109-1

Chiaradia, I., and Lancaster, M. A. (2020). Brain organoids for the study of human neurobiology at the interface of in vitro and in vivo. *Nat. Neurosci.* 23, 1496–1508. doi: 10.1038/s41593-020-00730-3

Cimadamore, F., Amador-Arjona, A., Chen, C., Huang, C. T., and Terskikh, A. V. (2013). SOX2-LIN28/let-7 pathway regulates proliferation and neurogenesis in neural precursors. *Proc. Natl. Acad. Sci. U.S.A.* 110, E3017–E3026. doi: 10.1073/pnas.1220176110

Clevers, H. (2006). Wnt/beta-catenin signaling in development and disease. *Cell* 127, 469–480. doi: 10.1016/j.cell.2006.10.018

Clowry, G., Molnar, Z., and Rakic, P. (2010). Renewed focus on the developing human neocortex. *J. Anat.* 217, 276–288. doi: 10.1111/j.1469-7580.2010.01281.x

Cohen-Barak, O., Hagiwara, N., Arlt, M. F., Horton, J. P., and Brilliant, M. H. (2001). Cloning, characterization and chromosome mapping of the human SOX6 gene. *Gene* 265, 157–164. doi: 10.1016/s0378-1119(01)00346-8

Collignon, J., Sockanathan, S., Hacker, A., Cohen-Tannoudji, M., Norris, D., Rastan, S., et al. (1996). A comparison of the properties of Sox-3 with Sry and two related genes, Sox-1 and Sox-2. *Development* 122, 509–520.

Comella-Bolla, A., Orlandi, J. G., Miguez, A., Straccia, M., Garcia-Bravo, M., Bombau, G., et al. (2020). Human pluripotent stem cell-derived neurons are functionally mature in vitro and integrate into the mouse striatum following transplantation. *Mol. Neurobiol.* 57, 2766–2798. doi: 10.1007/s12035-020-01907-4

Connor, F., Wright, E., Denny, P., Koopman, P., and Ashworth, A. (1995). The Sry-related HMG box-containing gene Sox6 is expressed in the adult testis and developing nervous system of the mouse. *Nucleic Acids Res.* 23, 3365–3372. doi: 10.1093/nar/23.17.3365

D'Adamo, G. L., Widdop, J. T., and Giles, E. M. (2020). The future is now? Clinical and translational aspects of "Omics" technologies. *Immunol. Cell Biol.* 99, 168–176. doi: 10.1111/imcb.12404

Dee, C. T., Hirst, C. S., Shih, Y. H., Tripathi, V. B., Patient, R. K., and Scotting, P. J. (2008). Sox3 regulates both neural fate and differentiation in the zebrafish ectoderm. *Dev. Biol.* 320, 289–301. doi: 10.1016/j.ydbio.2008.05.542

Deierborg, T., Li, J.-Y., and Brundin, P. (2007). "Adult neurogenesis in neurodegenerative diseases," in *Interaction Between Neurons and Glia in Aging and Disease*, eds J. Malva, A. C. Rego, R. Cunha, and C. R. Oliveira (Cham: Springer), 445–460.

Denny, P., Swift, S., Brand, N., Dabhade, N., Barton, P., and Ashworth, A. (1992). A conserved family of genes related to the testis determining gene, SRY. *Nucleic Acids Res.* 20:2887. doi: 10.1093/nar/20.11.2887

Dillen, Y., Kemps, H., Gervois, P., Wolfs, E., and Bronckaers, A. (2020). Adult neurogenesis in the subventricular zone and its regulation after ischemic stroke: implications for therapeutic approaches. *Transl. Stroke Res.* 11, 60–79. doi: 10.1007/s12975-019-00717-8

Drakulic, D., Krstic, A., and Stevanovic, M. (2012). Establishment and initial characterization of SOX2-overexpressing NT2/D1 cell clones. *Genet. Mol. Res.* 11, 1385–1400. doi: 10.4238/2012.May.15.9

Dugas, J. C., Cuellar, T. L., Scholze, A., Ason, B., Ibrahim, A., Emery, B., et al. (2010). Dicer1 and miR-219 Are required for normal oligodendrocyte differentiation and myelination. *Neuron* 65, 597–611. doi: 10.1016/j.neuron.2010.01.027

Eiraku, M., Watanabe, K., Matsuo-Takasaki, M., Kawada, M., Yonemura, S., Matsumura, M., et al. (2008). Self-organized formation of polarized cortical tissues from ESCs and its active manipulation by extrinsic signals. *Cell Stem Cell* 3, 519–532. doi: 10.1016/j.stem.2008.09.002

Ellis, P., Fagan, B. M., Magness, S. T., Hutton, S., Taranova, O., Hayashi, S., et al. (2004). SOX2, a persistent marker for multipotential neural stem cells derived from embryonic stem cells, the embryo or the adult. *Dev. Neurosci.* 26, 148–165. doi: 10.1159/000082134

Fang, Z., Liu, X., Wen, J., Tang, F., Zhou, Y., Jing, N., et al. (2019). SOX21 ensures rostral forebrain identity by suppression of WNT8B during Neural regionalization of human embryonic stem cells. *Stem Cell Rep.* 13, 1038–1052. doi: 10.1016/j.stemcr.2019.10.013

Farr, C. J., Easty, D. J., Ragoussis, J., Collignon, J., Lovell-Badge, R., and Goodfellow, P. N. (1993). Characterization and mapping of the human SOX4 gene. *Mamm. Genome* 4, 577–584. doi: 10.1007/BF00361388

Faucon, P. C., Pardee, K., Kumar, R. M., Li, H., Loh, Y. H., and Wang, X. (2014). Gene networks of fully connected triads with complete auto-activation enable multistability and stepwise stochastic transitions. *PLoS One* 9:e102873. doi: 10.1371/journal.pone.0102873

Favaro, R., Valotta, M., Ferri, A. L., Latorre, E., Mariani, J., Giachino, C., et al. (2009). Hippocampal development and neural stem cell maintenance require Sox2-dependent regulation of Shh. *Nat. Neurosci.* 12, 1248–1256. doi: 10.1038/nn.2397

Ferri, A. L., Cavallaro, M., Braida, D., Di Cristofano, A., Canta, A., Vezzani, A., et al. (2004). Sox2 deficiency causes neurodegeneration and impaired neurogenesis in the adult mouse brain. *Development* 131, 3805–3819. doi: 10.1242/dev.01204

Fiedler, M., Graeb, M., Mieszczanek, J., Rutherford, T. J., Johnson, C. M., and Bienz, M. (2015). An ancient Pygo-dependent Wnt enhanceosome integrated by Chip/LDB-SSDP. *eLife* 4:e09073. doi: 10.7554/eLife.09073

Foster, J. W., Dominguez-Steglich, M. A., Guioli, S., Kwok, C., Weller, P. A., Stevanovic, M., et al. (1994). Campomelic dysplasia and autosomal sex reversal caused by mutations in an SRY-related gene. *Nature* 372, 525–530. doi: 10.1038/372525a0

Furumatsu, T., Tsuda, M., Yoshida, K., Taniguchi, N., Ito, T., Hashimoto, M., et al. (2005). Sox9 and p300 cooperatively regulate chromatin-mediated transcription. *J. Biol. Chem.* 280, 35203–35208. doi: 10.1074/jbc.M502409200

Gage, F. H. (2000). Mammalian neural stem cells. *Science* 287, 1433–1438. doi: 10.1126/science.287.5457.1433

Gagliardi, A., Mullin, N. P., Ying Tan, Z., Colby, D., Kousa, A. I., Halbritter, F., et al. (2013). A direct physical interaction between Nanog and Sox2 regulates embryonic stem cell self-renewal. *EMBO J.* 32, 2231–2247. doi: 10.1038/emboj.2013.161

Gokey, N. G., Srinivasan, R., Lopez-Anido, C., Krueger, C., and Svaren, J. (2012). Developmental regulation of microRNA expression in Schwann cells. *Mol. Cell Biol.* 32, 558–568. doi: 10.1128/MCB.06270-11

Gordon, M. D., and Nusse, R. (2006). Wnt signaling: multiple pathways, multiple receptors, and multiple transcription factors. *J. Biol. Chem.* 281, 22429–22433. doi: 10.1074/jbc.R600015200

Gotz, M., Nakafuku, M., and Petrik, D. (2016). Neurogenesis in the developing and adult brain-similarities and key differences. *Cold Spring Harb. Perspect. Biol.* 8:a018853. doi: 10.1101/cshperspect.a018853

Graham, V., Khudyakov, J., Ellis, P., and Pevny, L. (2003). SOX2 functions to maintain neural progenitor identity. *Neuron* 39, 749–765. doi: 10.1016/s0896-6273(03)00497-5

Gubbay, J., Collignon, J., Koopman, P., Capel, B., Economou, A., Munsterberg, A., et al. (1990). A gene mapping to the sex-determining region of the mouse Y chromosome is a member of a novel family of embryonically expressed genes. *Nature* 346, 245–250. doi: 10.1038/346245a0

Guo, L., Zhong, D., Lau, S., Liu, X., Dong, X. Y., Sun, X., et al. (2008). Sox7 Is an independent checkpoint for beta-catenin function in prostate and colon epithelial cells. *Mol. Cancer Res.* 6, 1421–1430. doi: 10.1158/1541-7786.MCR-07-2175

Hagey, D. W., and Muhr, J. (2014). Sox2 acts in a dose-dependent fashion to regulate proliferation of cortical progenitors. *Cell Rep.* 9, 1908–1920. doi: 10.1016/j.celrep.2014.11.013

Hanna, J., Cheng, A. W., Saha, K., Kim, J., Lengner, C. J., Soldner, F., et al. (2010). Human embryonic stem cells with biological and epigenetic characteristics similar to those of mouse ESCs. *Proc. Natl. Acad. Sci. U.S.A.* 107, 9222–9227. doi: 10.1073/pnas.1004584107

Hargrave, M., Karunaratne, A., Cox, L., Wood, S., Koopman, P., and Yamada, T. (2000). The HMG box transcription factor gene Sox14 marks a novel subset of ventral interneurons and is regulated by sonic hedgehog. *Dev. Biol.* 219, 142–153. doi: 10.1006/dbio.1999.9581

Harley, V. R., Lovell-Badge, R., and Goodfellow, P. N. (1994). Definition of a consensus DNA binding site for SRY. *Nucleic Acids Res.* 22, 1500–1501. doi: 10.1093/nar/22.8.1500

Haslinger, A., Schwarz, T. J., Covic, M., and Lie, D. C. (2009). Expression of Sox11 in adult neurogenic niches suggests a stage-specific role in adult neurogenesis. *Eur. J. Neurosci.* 29, 2103–2114. doi: 10.1111/j.1460-9568.2009.06768.x

Hassani, S. N., Totonchi, M., Farrokhi, A., Taei, A., Larijani, M. R., Gourabi, H., et al. (2012). Simultaneous suppression of TGF-beta and ERK signaling contributes to the highly efficient and reproducible generation of mouse embryonic stem cells from previously considered refractory and non-permissive strains. *Stem Cell Rev. Rep.* 8, 472–481. doi: 10.1007/s12015-011-9306-y

Hattori, T., Eberspaecher, H., Lu, J., Zhang, R., Nishida, T., Kahyo, T., et al. (2006). Interactions between PIAS proteins and SOX9 result in an increase in the cellular concentrations of SOX9. *J. Biol. Chem.* 281, 14417–14428. doi: 10.1074/jbc.M511330200

Helle, J. R., Baroy, T., Misceo, D., Braaten, O., Fannemel, M., and Frengen, E. (2013). Hyperphagia, mild developmental delay but apparently no structural brain anomalies in a boy without SOX3 expression. *Am. J. Med. Genet. A* 161A, 1137–1142. doi: 10.1002/ajmg.a.35823

Hoffmann, S. A., Hos, D., Kuspert, M., Lang, R. A., Lovell-Badge, R., Wegner, M., et al. (2014). Stem cell factor Sox2 and its close relative Sox3 have differentiation functions in oligodendrocytes. *Development* 141, 39–50. doi: 10.1242/dev.098418

Horgusluoglu, E., Nudelman, K., Nho, K., and Saykin, A. J. (2017). Adult neurogenesis and neurodegenerative diseases: a systems biology perspective. *Am. J. Med. Genet. B Neuropsychiatr. Genet.* 174, 93–112. doi: 10.1002/ajmg.b.32429

Hoser, M., Potzner, M. R., Koch, J. M., Bosl, M. R., Wegner, M., and Sock, E. (2008). Sox12 deletion in the mouse reveals nonreciprocal redundancy with the related Sox4 and Sox11 transcription factors. *Mol. Cell Biol.* 28, 4675–4687. doi: 10.1128/MCB.00338-08

Hoshiba, Y., Toda, T., Ebisu, H., Wakimoto, M., Yanagi, S., and Kawasaki, H. (2016). Sox11 balances dendritic morphogenesis with neuronal migration in the developing cerebral cortex. *J. Neurosci.* 36, 5775–5784. doi: 10.1523/JNEUROSCI.3250-15.2016

Hou, L., Srivastava, Y., and Jauch, R. (2017). Molecular basis for the genome engagement by Sox proteins. *Semin. Cell Dev. Biol.* 63, 2–12. doi: 10.1016/j.semcdb.2016.08.005

Hutton, S. R., and Pevny, L. H. (2011). SOX2 expression levels distinguish between neural progenitor populations of the developing dorsal telencephalon. *Dev. Biol.* 352, 40–47. doi: 10.1016/j.ydbio.2011.01.015

Iguchi, H., Urashima, Y., Inagaki, Y., Ikeda, Y., Okamura, M., Tanaka, T., et al. (2007). SOX6 suppresses cyclin D1 promoter activity by interacting with beta-catenin and histone deacetylase 1, and its down-regulation induces pancreatic beta-cell proliferation. *J. Biol. Chem.* 282, 19052–19061. doi: 10.1074/jbc.M700460200

International Multiple Sclerosis Genetics Consortium, Lill, C. M., Schjeide, B. M., Graetz, C., Ban, M., Alcina, A., et al. (2013). MANBA, CXCR5, SOX8, RPS6KB1 and ZBTB46 are genetic risk loci for multiple sclerosis. *Brain* 136, 1778–1782. doi: 10.1093/brain/awt101

International Multiple Sclerosis Genetics Consortium, Wellcome Trust Case Control Consortium, Sawcer, S., Hellenthal, G., Pirinen, M., Spencer, C. C., et al. (2011). Genetic risk and a primary role for cell-mediated immune mechanisms in multiple sclerosis. *Nature* 476, 214–219. doi: 10.1038/nature10251

Iwamoto, K., Bundo, M., Yamada, K., Takao, H., Iwayama-Shigeno, Y., Yoshikawa, T., et al. (2005). DNA methylation status of SOX10 correlates with its downregulation and oligodendrocyte dysfunction in schizophrenia. *J. Neurosci.* 25, 5376–5381. doi: 10.1523/JNEUROSCI.0766-05.2005

Jay, P., Goze, C., Marsollier, C., Taviaux, S., Hardelin, J. P., Koopman, P., et al. (1995). The human SOX11 gene: cloning, chromosomal assignment and tissue expression. *Genomics* 29, 541–545. doi: 10.1006/geno.1995.9970

Jay, P., Sahly, I., Goze, C., Taviaux, S., Poulat, F., Couly, G., et al. (1997). SOX22 is a new member of the SOX gene family, mainly expressed in human nervous tissue. *Hum. Mol. Genet.* 6, 1069–1077. doi: 10.1093/hmg/6.7.1069

Jelsig, A. M., Diness, B. R., Kreiborg, S., Main, K. M., Larsen, V. A., and Hove, H. (2018). A complex phenotype in a family with a pathogenic SOX3 missense variant. *Eur. J. Med. Genet.* 61, 168–172. doi: 10.1016/j.ejmg.2017.11.012

Johnson, M. B., Kawasawa, Y. I., Mason, C. E., Krsnik, Z., Coppola, G., Bogdanovic, D., et al. (2009). Functional and evolutionary insights into human brain development through global transcriptome analysis. *Neuron* 62, 494–509. doi: 10.1016/j.neuron.2009.03.027

Kadoshima, T., Sakaguchi, H., Nakano, T., Soen, M., Ando, S., Eiraku, M., et al. (2013). Self-organization of axial polarity, inside-out layer pattern, and species-specific progenitor dynamics in human ES cell-derived neocortex. *Proc. Natl. Acad. Sci. U.S.A.* 110, 20284–20289. doi: 10.1073/pnas.1315710110

Kamachi, Y., and Kondoh, H. (2013). Sox proteins: regulators of cell fate specification and differentiation. *Development* 140, 4129–4144. doi: 10.1242/dev.091793

Kamachi, Y., Uchikawa, M., Collignon, J., Lovell-Badge, R., and Kondoh, H. (1998). Involvement of Sox1, 2 and 3 in the early and subsequent molecular events of lens induction. *Development* 125, 2521–2532.

Kamachi, Y., Uchikawa, M., and Kondoh, H. (2000). Pairing SOX off: with partners in the regulation of embryonic development. *Trends Genet.* 16, 182–187. doi: 10.1016/s0168-9525(99)01955-1

Kan, L., Israsena, N., Zhang, Z., Hu, M., Zhao, L. R., Jalali, A., et al. (2004). Sox1 acts through multiple independent pathways to promote neurogenesis. *Dev. Biol.* 269, 580–594. doi: 10.1016/j.ydbio.2004.02.005

Kang, P., Lee, H. K., Glasgow, S. M., Finley, M., Donti, T., Gaber, Z. B., et al. (2012). Sox9 and NFIA coordinate a transcriptional regulatory cascade during the initiation of gliogenesis. *Neuron* 74, 79–94. doi: 10.1016/j.neuron.2012.01.024

Kaplan, M. S., and Bell, D. H. (1983). Neuronal proliferation in the 9-month-old rodent-radioautographic study of granule cells in the hippocampus. *Exp. Brain Res.* 52, 1–5. doi: 10.1007/BF00237141

Kaplan, M. S., and Bell, D. H. (1984). Mitotic neuroblasts in the 9-day-old and 11-month-old rodent hippocampus. *J. Neurosci.* 4, 1429–1441.

Katoh, M. (2002). Molecular cloning and characterization of human SOX17. *Int. J. Mol. Med.* 9, 153–157.

Kellerer, S., Schreiner, S., Stolt, C. C., Scholz, S., Bosl, M. R., and Wegner, M. (2006). Replacement of the Sox10 transcription factor by Sox8 reveals incomplete functional equivalence. *Development* 133, 2875–2886. doi: 10.1242/dev.02477

Kempermann, G., Wiskott, L., and Gage, F. H. (2004). Functional significance of adult neurogenesis. *Curr. Opin. Neurobiol.* 14, 186–191. doi: 10.1016/j.conb.2004.03.001

Keramari, M., Razavi, J., Ingman, K. A., Patsch, C., Edenhofer, F., Ward, C. M., et al. (2010). Sox2 is essential for formation of Trophectoderm in the Preimplantation embryo. *PLoS One* 5:e13952. doi: 10.1371/journal.pone.0013952

Kessaris, N., Pringle, N., and Richardson, W. D. (2001). Ventral neurogenesis and the neuron-glial switch. *Neuron* 31, 677–680. doi: 10.1016/s0896-6273(01)00430-5

Kiefer, J. C. (2007). Back to basics: sox genes. *Dev. Dyn.* 236, 2356–2366. doi: 10.1002/dvdy.21218

Klajn, A., Drakulic, D., Tosic, M., Pavkovic, Z., Schwirtlich, M., and Stevanovic, M. (2014). SOX2 overexpression affects neural differentiation of human pluripotent NT2/D1 cells. *Biochemistry* 79, 1172–1182. doi: 10.1134/S0006297914110042

Klum, S., Zaouter, C., Alekseenko, Z., Bjorklund, A. K., Hagey, D. W., Ericson, J., et al. (2018). Sequentially acting SOX proteins orchestrate astrocyte- and oligodendrocyte-specific gene expression. *EMBO Rep.* 19:e46635. doi: 10.15252/embr.201846635

Kondoh, H., and Kamachi, Y. (2010). SOX-partner code for cell specification: regulatory target selection and underlying molecular mechanisms. *Int. J. Biochem. Cell Biol.* 42, 391–399. doi: 10.1016/j.biocel.2009.09.003

Kormish, J. D., Sinner, D., and Zorn, A. M. (2010). Interactions between SOX factors and Wnt/beta-catenin signaling in development and disease. *Dev. Dyn.* 239, 56–68. doi: 10.1002/dvdy.22046

Krichevsky, A. M., Sonntag, K. C., Isacson, O., and Kosik, K. S. (2006). Specific microRNAs modulate embryonic stem cell-derived neurogenesis. *Stem Cells* 24, 857–864. doi: 10.1634/stemcells.2005-0441

Krstic, A., Mojsin, M., and Stevanovic, M. (2007). Regulation of SOX3 gene expression is driven by multiple NF-Y binding elements. *Arch. Biochem. Biophys.* 467, 163–173. doi: 10.1016/j.abb.2007.08.029

Kuwabara, T., Hsieh, J., Muotri, A., Yeo, G., Warashina, M., Lie, D. C., et al. (2009). Wnt-mediated activation of NeuroD1 and retro-elements during adult neurogenesis. *Nat. Neurosci.* 12, 1097–1105. doi: 10.1038/nn.2360

Kwan, K. Y., Lam, M. M., Krsnik, Z., Kawasawa, Y. I., Lefebvre, V., and Sestan, N. (2008). SOX5 postmitotically regulates migration, postmigratory differentiation, and projections of subplate and deep-layer neocortical neurons. *Proc. Natl. Acad. Sci. U.S.A.* 105, 16021–16026. doi: 10.1073/pnas.0806791105

Lamb, A. N., Rosenfeld, J. A., Neill, N. J., Talkowski, M. E., Blumenthal, I., Girirajan, S., et al. (2012). Haploinsufficiency of SOX5 at 12p12.1 is associated with developmental delays with prominent language delay, behavior problems, and mild dysmorphic features. *Hum. Mutat.* 33, 728–740. doi: 10.1002/humu.22037

Lancaster, M. A., and Knoblich, J. A. (2014). Organogenesis in a dish: modeling development and disease using organoid technologies. *Science* 345:1247125. doi: 10.1126/science.1247125

Lancaster, M. A., Renner, M., Martin, C. A., Wenzel, D., Bicknell, L. S., Hurles, M. E., et al. (2013). Cerebral organoids model human brain development and microcephaly. *Nature* 501, 373–379. doi: 10.1038/nature12517

Laudet, V., and Gronemeyer, H. (2002). *The Nuclear Receptor FactsBook*. Amsterdam: Elsevier, doi: 10.1016/B978-012437735-6/50026-6

Laumonnier, F., Ronce, N., Hamel, B. C., Thomas, P., Lespinasse, J., Raynaud, M., et al. (2002). Transcription factor SOX3 is involved in X-linked mental retardation with growth hormone deficiency. *Am. J. Hum. Genet.* 71, 1450–1455. doi: 10.1086/344661

Lee, K. E., Seo, J., Shin, J., Ji, E. H., Roh, J., Kim, J. Y., et al. (2014). Positive feedback loop between Sox2 and Sox6 inhibits neuronal differentiation in the developing central nervous system. *Proc. Natl. Acad. Sci. U.S.A.* 111, 2794–2799. doi: 10.1073/pnas.1308758111

Lefebvre, V., Dumitriu, B., Penzo-Mendez, A., Han, Y., and Pallavi, B. (2007). Control of cell fate and differentiation by Sry-related high-mobility-group box (Sox) transcription factors. *Int. J. Biochem. Cell Biol.* 39, 2195–2214. doi: 10.1016/j.biocel.2007.05.019

Li, W., Fang, J., Shen, J., Liu, X., Hou, J., Zhu, Y., et al. (2019). MicroRNA-135a-5p promotes neuronal differentiation of pluripotent embryonal carcinoma cells by repressing Sox6/CD44 pathway. *Biochem. Biophys. Res. Commun.* 509, 603–610. doi: 10.1016/j.bbrc.2018.12.162

Lim, D. A., and Alvarez-Buylla, A. (2016). The adult Ventricular-Subventricular Zone (V-SVZ) and Olfactory Bulb (OB) neurogenesis. *Cold Spring Harb. Perspect. Biol.* 8:a018820. doi: 10.1101/cshperspect.a018820

Liu, Y. R., Laghari, Z. A., Novoa, C. A., Hughes, J., Webster, J. R., Goodwin, P. E., et al. (2014). Sox2 acts as a transcriptional repressor in neural stem cells. *BMC Neurosci.* 15:95. doi: 10.1186/1471-2202-15-95

Lois, C., and Alvarez-Buylla, A. (1993). Proliferating subventricular zone cells in the adult mammalian forebrain can differentiate into neurons and glia. *Proc. Natl. Acad. Sci. U.S.A.* 90, 2074–2077. doi: 10.1073/pnas.90.5.2074

Makrides, N., Panayiotou, E., Fanis, P., Karaiskos, C., Lapathitis, G., and Malas, S. (2018). Sequential Role of SOXB2 Factors in GABAergic Neuron Specification of the Dorsal Midbrain. *Front. Mol. Neurosci.* 11:152. doi: 10.3389/fnmol.2018.00152

Malas, S., Duthie, S., Deloukas, P., and Episkopou, V. (1999). The isolation and high-resolution chromosomal mapping of human SOX14 and SOX21; two members of the SOX gene family related to SOX1, SOX2, and SOX3. *Mamm. Genome* 10, 934–937. doi: 10.1007/s003359901118

Malas, S., Duthie, S. M., Mohri, F., Lovell-Badge, R., and Episkopou, V. (1997). Cloning and mapping of the human SOX1: a highly conserved gene expressed in the developing brain. *Mamm. Genome* 8, 866–868. doi: 10.1007/s003359900597

Malas, S., Postlethwaite, M., Ekonomou, A., Whalley, B., Nishiguchi, S., Wood, H., et al. (2003). Sox1-deficient mice suffer from epilepsy associated with abnormal ventral forebrain development and olfactory cortex hyperexcitability. *Neuroscience* 119, 421–432. doi: 10.1016/s0306-4522(03)00158-1

Mallanna, S. K., Ormsbee, B. D., Iacovino, M., Gilmore, J. M., Cox, J. L., Kyba, M., et al. (2010). Proteomic analysis of Sox2-associated proteins during early stages of mouse embryonic stem cell differentiation identifies Sox21 as a novel regulator of stem cell fate. *Stem Cells* 28, 1715–1727. doi: 10.1002/stem.494

Martinez-Morales, P. L., Quiroga, A. C., Barbas, J. A., and Morales, A. V. (2010). SOX5 controls cell cycle progression in neural progenitors by interfering with the WNT-beta-catenin pathway. *EMBO Rep.* 11, 466–472. doi: 10.1038/embor.2010.61

Maruyama, M., Ichisaka, T., Nakagawa, M., and Yamanaka, S. (2005). Differential roles for Sox15 and Sox2 in transcriptional control in mouse embryonic stem cells. *J. Biol. Chem.* 280, 24371–24379. doi: 10.1074/jbc.M501423200

Matsuda, S., Kuwako, K., Okano, H. J., Tsutsumi, S., Aburatani, H., Saga, Y., et al. (2012). Sox21 promotes hippocampal adult neurogenesis via the transcriptional repression of the Hes5 gene. *J. Neurosci.* 32, 12543–12557. doi: 10.1523/JNEUROSCI.5803-11.2012

McCarthy, M. M., and Nugent, B. M. (2015). At the frontier of epigenetics of brain sex differences. *Front. Behav. Neurosci.* 9:221. doi: 10.3389/fnbeh.2015.00221

McKinney, C. E. (2017). Using induced pluripotent stem cells derived neurons to model brain diseases. *Neural. Regen. Res.* 12, 1062–1067. doi: 10.4103/1673-5374.211180

Mercurio, S., Serra, L., and Nicolis, S. K. (2019). More than just stem cells: functional roles of the transcription factor Sox2 in differentiated Glia and neurons. *Int. J. Mol. Sci.* 20:4540. doi: 10.3390/ijms20184540

Meyer, J., Wirth, J., Held, M., Schempp, W., and Scherer, G. (1996). SOX20, a new member of the SOX gene family, is located on chromosome 17p13. *Cytogenet. Cell Genet.* 72, 246–249. doi: 10.1159/000134200

Meza-Sosa, K. F., Pedraza-Alva, G., and Perez-Martinez, L. (2014). microRNAs: key triggers of neuronal cell fate. *Front. Cell. Neurosci.* 8:175. doi: 10.3389/fncel.2014.00175

Miller, F. D., and Gauthier, A. S. (2007). Timing is everything: making neurons versus glia in the developing cortex. *Neuron* 54, 357–369. doi: 10.1016/j.neuron.2007.04.019

Ming, G. L., and Song, H. (2011). Adult neurogenesis in the mammalian brain: significant answers and significant questions. *Neuron* 70, 687–702. doi: 10.1016/j.neuron.2011.05.001

Mojsin, M., Grujicic, N. K., Nikcevic, G., Krstic, A., Savic, T., and Stevanovic, M. (2006). Mapping of the RXRalpha binding elements involved in retinoic acid induced transcriptional activation of the human SOX3 gene. *Neurosci. Res.* 56, 409–418. doi: 10.1016/j.neures.2006.08.010

Mojsin, M., and Stevanovic, M. (2009). PBX1 and MEIS1 up-regulate SOX3 gene expression by direct interaction with a consensus binding site within the basal promoter region. *Biochem. J.* 425, 107–116. doi: 10.1042/BJ20090694

Mojsin, M., Topalovic, V., Vicentic, J. M., Schwirtlich, M., Stanisavljevic, D., Drakulic, D., et al. (2015). Crosstalk between SOXB1 proteins and WNT/beta-catenin signaling in NT2/D1 cells. *Histochem. Cell Biol.* 144, 429–441. doi: 10.1007/s00418-015-1352-0

Morgado, A. L., Rodrigues, C. M., and Sola, S. (2016). MicroRNA-145 Regulates Neural Stem Cell Differentiation Through the Sox2-Lin28/let-7 Signaling Pathway. *Stem Cells* 34, 1386–1395. doi: 10.1002/stem.2309

Mu, L., Berti, L., Masserdotti, G., Covic, M., Michaelidis, T. M., Doberauer, K., et al. (2012). SoxC transcription factors are required for neuronal differentiation in adult hippocampal neurogenesis. *J. Neurosci.* 32, 3067–3080. doi: 10.1523/JNEUROSCI.4679-11.2012

Mukherjee, S., Chaturvedi, P., Rankin, S. A., Fish, M. B., Wlizla, M., Paraiso, K. D., et al. (2020). Sox17 and beta-catenin co-occupy Wnt-responsive enhancers to govern the endoderm gene regulatory network. *eLife* 9:e58029. doi: 10.7554/eLife.58029

Nait-Oumesmar, B., Picard-Riera, N., Kerninon, C., Decker, L., Seilhean, D., Hoglinger, G. U., et al. (2007). Activation of the subventricular zone in multiple sclerosis: evidence for early glial progenitors. *Proc. Natl. Acad. Sci. U.S.A.* 104, 4694–4699. doi: 10.1073/pnas.0606835104

Nakagawa, M., Koyanagi, M., Tanabe, K., Takahashi, K., Ichisaka, T., Aoi, T., et al. (2008). Generation of induced pluripotent stem cells without Myc from mouse and human fibroblasts. *Nat. Biotechnol.* 26, 101–106. doi: 10.1038/nbt1374

Naudet, N., Moutal, A., Vu, H. N., Chounlamountri, N., Watrin, C., Cavagna, S., et al. (2018). Transcriptional regulation of CRMP5 controls neurite outgrowth through Sox5. *Cell Mol. Life Sci.* 75, 67–79. doi: 10.1007/s00018-017-2634-6

Nazari, B., Soleimani, M., Ebrahimi-Barough, S., Enderami, S. E., Kazemi, M., Negahdari, B., et al. (2018). Overexpression of miR-219 promotes differentiation of human induced pluripotent stem cells into pre-oligodendrocyte. *J. Chem. Neuroanat.* 91, 8–16. doi: 10.1016/j.jchemneu.2018.03.001

Nesbitt, A., Bhoj, E. J., McDonald Gibson, K., Yu, Z., Denenberg, E., Sarmady, M., et al. (2015). Exome sequencing expands the mechanism of SOX5-associated intellectual disability: a case presentation with review of sox-related disorders. *Am. J. Med. Genet. A* 167A, 2548–2554. doi: 10.1002/ajmg.a.37221

Nikcevic, G., Savic, T., Kovacevic-Grujicic, N., and Stevanovic, M. (2008). Up-regulation of the SOX3 gene expression by retinoic acid: characterization of the novel promoter-response element and the retinoid receptors involved. *J. Neurochem.* 107, 1206–1215. doi: 10.1111/j.1471-4159.2008.05670.x

Niwa, H., Nakamura, A., Urata, M., Shirae-Kurabayashi, M., Kuraku, S., Russell, S., et al. (2016). The evolutionally-conserved function of group B1 Sox family members confers the unique role of Sox2 in mouse ES cells. *BMC Evol. Biol.* 16:173. doi: 10.1186/s12862-016-0755-4

Obernier, K., and Alvarez-Buylla, A. (2019). Neural stem cells: origin, heterogeneity and regulation in the adult mammalian brain. *Development* 146:dev156059. doi: 10.1242/dev.156059

Ohba, H., Chiyoda, T., Endo, E., Yano, M., Hayakawa, Y., Sakaguchi, M., et al. (2004). Sox21 is a repressor of neuronal differentiation and is antagonized by YB-1. *Neurosci. Lett.* 358, 157–160. doi: 10.1016/j.neulet.2004.01.026

Oksanen, M., Lehtonen, S., Jaronen, M., Goldsteins, G., Hamalainen, R. H., and Koistinaho, J. (2019). Astrocyte alterations in neurodegenerative pathologies and their modeling in human induced pluripotent stem cell platforms. *Cell. Mol. Life Sci.* 76, 2739–2760. doi: 10.1007/s00018-019-03111-7

Oosterveen, T., Kurdija, S., Enstero, M., Uhde, C. W., Bergsland, M., Sandberg, M., et al. (2013). SoxB1-driven transcriptional network underlies neural-specific interpretation of morphogen signals. *Proc. Natl. Acad. Sci. U.S.A.* 110, 7330–7335. doi: 10.1073/pnas.1220010110

Orford, K., Crockett, C., Jensen, J. P., Weissman, A. M., and Byers, S. W. (1997). Serine phosphorylation-regulated ubiquitination and degradation of beta-catenin. *J. Biol. Chem.* 272, 24735–24738. doi: 10.1074/jbc.272.40.24735

Osaki, E., Nishina, Y., Inazawa, J., Copeland, N. G., Gilbert, D. J., Jenkins, N. A., et al. (1999). Identification of a novel Sry-related gene and its germ cell-specific expression. *Nucleic Acids Res.* 27, 2503–2510. doi: 10.1093/nar/27.12.2503

Pan, X., Zhao, J., Zhang, W. N., Li, H. Y., Mu, R., Zhou, T., et al. (2009). Induction of SOX4 by DNA damage is critical for p53 stabilization and function. *Proc. Natl. Acad. Sci. U.S.A.* 106, 3788–3793. doi: 10.1073/pnas.0810147106

Panariello, L., Quadro, L., Trematerra, S., and Colantuoni, V. (1996). Identification of a novel retinoic acid response element in the promoter region of the retinol-binding protein gene. *J. Biol. Chem.* 271, 25524–25532. doi: 10.1074/jbc.271.41.25524

Park, I. H., Arora, N., Huo, H., Maherali, N., Ahfeldt, T., Shimamura, A., et al. (2008). Disease-specific induced pluripotent stem cells. *Cell* 134, 877–886. doi: 10.1016/j.cell.2008.07.041

Parrinello, S., Napoli, I., Ribeiro, S., Wingfield Digby, P., Fedorova, M., Parkinson, D. B., et al. (2010). EphB signaling directs peripheral nerve regeneration through Sox2-dependent Schwann cell sorting. *Cell* 143, 145–155. doi: 10.1016/j.cell.2010.08.039

Pasca, A. M., Sloan, S. A., Clarke, L. E., Tian, Y., Makinson, C. D., Huber, N., et al. (2015). Functional cortical neurons and astrocytes from human pluripotent stem cells in 3D culture. *Nat. Methods* 12, 671–678. doi: 10.1038/nmeth.3415

Peng, C., Li, N., Ng, Y. K., Zhang, J., Meier, F., Theis, F. J., et al. (2012). A unilateral negative feedback loop between miR-200 microRNAs and Sox2/E2F3 controls neural progenitor cell-cycle exit and differentiation. *J. Neurosci.* 32, 13292–13308. doi: 10.1523/JNEUROSCI.2124-12.2012

Pennartz, S., Belvindrah, R., Tomiuk, S., Zimmer, C., Hofmann, K., Conradt, M., et al. (2004). Purification of neuronal precursors from the adult mouse brain: comprehensive gene expression analysis provides new insights into the control of cell migration, differentiation, and homeostasis. *Mol. Cell Neurosci.* 25, 692–706. doi: 10.1016/j.mcn.2003.12.011

Pevny, L., and Placzek, M. (2005). SOX genes and neural progenitor identity. *Curr. Opin. Neurobiol.* 15, 7–13. doi: 10.1016/j.conb.2005.01.016

Pevny, L. H., and Lovell-Badge, R. (1997). Sox genes find their feet. *Curr. Opin. Genet. Dev.* 7, 338–344. doi: 10.1016/s0959-437x(97)80147-5

Pevny, L. H., Sockanathan, S., Placzek, M., and Lovell-Badge, R. (1998). A role for SOX1 in neural determination. *Development* 125, 1967–1978.

Pfeifer, D., Poulat, F., Holinski-Feder, E., Kooy, F., and Scherer, G. (2000). The SOX8 gene is located within 700 kb of the tip of chromosome 16p and is deleted in a patient with ATR-16 syndrome. *Genomics* 63, 108–116. doi: 10.1006/geno.1999.6060

Poche, R. A., Furuta, Y., Chaboissier, M. C., Schedl, A., and Behringer, R. R. (2008). Sox9 is expressed in mouse multipotent retinal progenitor cells and functions in Muller glial cell development. *J. Comp. Neurol.* 510, 237–250. doi: 10.1002/cne.21746

Popovic, J., Stanisavljevic, D., Schwirtlich, M., Klajn, A., Marjanovic, J., and Stevanovic, M. (2014). Expression analysis of SOX14 during retinoic acid induced neural differentiation of embryonal carcinoma cells and assessment of the effect of its ectopic expression on SOXB members in HeLa cells. *PLoS One* 9:e91852. doi: 10.1371/journal.pone.0091852

Preiss, S., Argentaro, A., Clayton, A., John, A., Jans, D. A., Ogata, T., et al. (2001). Compound effects of point mutations causing campomelic dysplasia/autosomal sex reversal upon SOX9 structure, nuclear transport, DNA binding, and transcriptional activation. *J. Biol. Chem.* 276, 27864–27872. doi: 10.1074/jbc.M101278200

Pusch, C., Hustert, E., Pfeifer, D., Sudbeck, P., Kist, R., Roe, B., et al. (1998). The SOX10/Sox10 gene from human and mouse: sequence, expression, and transactivation by the encoded HMG domain transcription factor. *Hum. Genet.* 103, 115–123. doi: 10.1007/s004390050793

Qi, H., and Pei, D. (2007). The magic of four: induction of pluripotent stem cells from somatic cells by Oct4, Sox2, Myc and Klf4. *Cell Res.* 17, 578–580. doi: 10.1038/cr.2007.59

Quiroga, A. C., Stolt, C. C., Diez del Corral, R., Dimitrov, S., Perez-Alcala, S., Sock, E., et al. (2015). Sox5 controls dorsal progenitor and interneuron specification in the spinal cord. *Dev. Neurobiol.* 75, 522–538. doi: 10.1002/dneu.22240

Rajman, M., and Schratt, G. (2017). MicroRNAs in neural development: from master regulators to fine-tuners. *Development* 144, 2310–2322. doi: 10.1242/dev.144337

Rakic, P. (2009). Evolution of the neocortex: a perspective from developmental biology. *Nat. Rev. Neurosci.* 10, 724–735. doi: 10.1038/nrn2719

Rea, J., Menci, V., Tollis, P., Santini, T., Armaos, A., Garone, M. G., et al. (2020). HOTAIRM1 regulates neuronal differentiation by modulating NEUROGENIN 2 and the downstream neurogenic cascade. *Cell Death Dis.* 11:527. doi: 10.1038/s41419-020-02738-w

Redfern, C. P. (2004). Enhancing enhancers: new complexities in the retinoid regulation of gene expression. *Biochem. J.* 383, e1–e2. doi: 10.1042/BJ20041277

Reiprich, S., Cantone, M., Weider, M., Baroti, T., Wittstatt, J., Schmitt, C., et al. (2017). Transcription factor Sox10 regulates oligodendroglial Sox9 levels via microRNAs. *Glia* 65, 1089–1102. doi: 10.1002/glia.23146

Reiprich, S., and Wegner, M. (2015). From CNS stem cells to neurons and glia: sox for everyone. *Cell Tissue Res.* 359, 111–124. doi: 10.1007/s00441-014-1909-6

Rizzino, A. (2008). Transcription factors that behave as master regulators during mammalian embryogenesis function as molecular rheostats. *Biochem. J.* 411, e5–e7. doi: 10.1042/BJ20080479

Rizzoti, K., Brunelli, S., Carmignac, D., Thomas, P. Q., Robinson, I. C., and Lovell-Badge, R. (2004). SOX3 is required during the formation of the hypothalamo-pituitary axis. *Nat. Genet.* 36, 247–255. doi: 10.1038/ng1309

Rochette-Egly, C., and Germain, P. (2009). Dynamic and combinatorial control of gene expression by nuclear retinoic acid receptors (RARs). *Nucl. Recept. Signal* 7:e005. doi: 10.1621/nrs.07005

Rodda, D. J., Chew, J. L., Lim, L. H., Loh, Y. H., Wang, B., Ng, H. H., et al. (2005). Transcriptional regulation of nanog by OCT4 and SOX2. *J. Biol. Chem.* 280, 24731–24737. doi: 10.1074/jbc.M502573200

Rodriguez-Traver, E., Diaz-Guerra, E., Rodriguez, C., Arenas, F., Orera, M., Kulisevsky, J., et al. (2020). A collection of three integration-free iPSCs derived from old male and female healthy subjects. *Stem Cell Res.* 42:101663. doi: 10.1016/j.scr.2019.101663

Rogers, N., Cheah, P. S., Szarek, E., Banerjee, K., Schwartz, J., and Thomas, P. (2013). Expression of the murine transcription factor SOX3 during embryonic and adult neurogenesis. *Gene Expr. Patterns* 13, 240–248. doi: 10.1016/j.gep.2013.04.004

Rogers, N., McAninch, D., and Thomas, P. (2014). Dbx1 is a direct target of SOX3 in the spinal cord. *PLoS One* 9:e95356. doi: 10.1371/journal.pone.0095356

Rowitch, D. H. (2004). Glial specification in the vertebrate neural tube. *Nat. Rev. Neurosci.* 5, 409–419. doi: 10.1038/nrn1389

Salic, A., Lee, E., Mayer, L., and Kirschner, M. W. (2000). Control of beta-catenin stability: reconstitution of the cytoplasmic steps of the wnt pathway in *Xenopus* egg extracts. *Mol. Cell* 5, 523–532. doi: 10.1016/s1097-2765(00)80446-3

Sandberg, M., Kallstrom, M., and Muhr, J. (2005). Sox21 promotes the progression of vertebrate neurogenesis. *Nat. Neurosci.* 8, 995–1001. doi: 10.1038/nn1493

Santos, R., Linker, S. B., Stern, S., Mendes, A. P. D., Shokhirev, M. N., Erikson, G., et al. (2021). Deficient LEF1 expression is associated with lithium resistance and hyperexcitability in neurons derived from bipolar disorder patients. *Mol. Psychiatry* doi: 10.1038/s41380-020-00981-3 [Epub ahead of print].

Sarkar, A., and Hochedlinger, K. (2013). The sox family of transcription factors: versatile regulators of stem and progenitor cell fate. *Cell Stem Cell* 12, 15–30. doi: 10.1016/j.stem.2012.12.007

Schanze, I., Schanze, D., Bacino, C. A., Douzgou, S., Kerr, B., and Zenker, M. (2013). Haploinsufficiency of SOX5, a member of the SOX (SRY-related HMG-box) family of transcription factors is a cause of intellectual disability. *Eur. J. Med. Genet.* 56, 108–113. doi: 10.1016/j.ejmg.2012.11.001

Scheper, W., and Copray, S. (2009). The molecular mechanism of induced pluripotency: a two-stage switch. *Stem Cell Rev. Rep.* 5, 204–223. doi: 10.1007/s12015-009-9077-x

Schepers, G. E., Teasdale, R. D., and Koopman, P. (2002). Twenty pairs of sox: extent, homology, and nomenclature of the mouse and human sox transcription factor gene families. *Dev. Cell* 3, 167–170. doi: 10.1016/s1534-5807(02)00223-x

Scott, C. E., Wynn, S. L., Sesay, A., Cruz, C., Cheung, M., Gomez Gaviro, M. V., et al. (2010). SOX9 induces and maintains neural stem cells. *Nat. Neurosci.* 13, 1181–1189. doi: 10.1038/nn.2646

She, Z. Y., and Yang, W. X. (2015). SOX family transcription factors involved in diverse cellular events during development. *Eur. J. Cell Biol.* 94, 547–563. doi: 10.1016/j.ejcb.2015.08.002

Shohayeb, B., Diab, M., Ahmed, M., and Ng, D. C. H. (2018). Factors that influence adult neurogenesis as potential therapy. *Transl. Neurodegener.* 7:4. doi: 10.1186/s40035-018-0109-9

Silbereis, J. C., Pochareddy, S., Zhu, Y., Li, M., and Sestan, N. (2016). The cellular and molecular landscapes of the developing human central nervous system. *Neuron* 89, 248–268. doi: 10.1016/j.neuron.2015.12.008

Sinclair, A. H., Berta, P., Palmer, M. S., Hawkins, J. R., Griffiths, B. L., Smith, M. J., et al. (1990). A gene from the human sex-determining region encodes a protein with homology to a conserved DNA-binding motif. *Nature* 346, 240–244. doi: 10.1038/346240a0

Sinner, D., Kordich, J. J., Spence, J. R., Opoka, R., Rankin, S., Lin, S. C., et al. (2007). Sox17 and Sox4 differentially regulate beta-catenin/T-cell factor activity and proliferation of colon carcinoma cells. *Mol. Cell Biol.* 27, 7802–7815. doi: 10.1128/MCB.02179-06

Stagi, S., Lapi, E., Pantaleo, M., Traficante, G., Giglio, S., Seminara, S., et al. (2014). A SOX3 (Xq26.3-27.3) duplication in a boy with growth hormone deficiency, ocular dyspraxia, and intellectual disability: a long-term follow-up and literature review. *Hormones* 13, 552–560. doi: 10.14310/horm.2002.1523

Stanisavljevic, D., Popovic, J., Petrovic, I., Davidovic, S., Atkinson, M. J., Anastasov, N., et al. (2019). Radiation effects on early phase of NT2/D1 neural differentiation in vitro. *Int. J. Radiat. Biol.* 95, 1627–1639. doi: 10.1080/09553002.2019.1665207

Stanojcic, S., and Stevanovic, M. (2000). The human SOX18 gene: cDNA cloning and high resolution mapping. *Biochim. Biophys. Acta* 1492, 237–241. doi: 10.1016/s0167-4781(00)00078-6

Stappert, L., Roese-Koerner, B., and Brustle, O. (2015). The role of microRNAs in human neural stem cells, neuronal differentiation and subtype specification. *Cell Tissue Res.* 359, 47–64. doi: 10.1007/s00441-014-1981-y

Steiner, B., Klempin, F., Wang, L., Kott, M., Kettenmann, H., and Kempermann, G. (2006). Type-2 cells as link between glial and neuronal lineage in adult hippocampal neurogenesis. *Glia* 54, 805–814. doi: 10.1002/glia.20407

Stevanovic, M. (2003). Modulation of SOX2 and SOX3 gene expression during differentiation of human neuronal precursor cell line NTERA2. *Mol. Biol. Rep.* 30, 127–132. doi: 10.1023/a:1023961009869

Stevanović, M., Drakulić, D., Švirtlih, M., Stanisavljević, D., Vuković, V., Mojsin, M., et al. (2017). SOX2 gene – master regulator of numerous cellular processes. *Biol. Serb.* 39, 9–15. doi: 10.5281/zenodo.826595

Stevanovic, M., Lovell-Badge, R., Collignon, J., and Goodfellow, P. N. (1993). SOX3 is an X-linked gene related to SRY. *Hum. Mol. Genet.* 2, 2013–2018. doi: 10.1093/hmg/2.12.2013

Stevanovic, M., Zuffardi, O., Collignon, J., Lovell-Badge, R., and Goodfellow, P. (1994). The cDNA sequence and chromosomal location of the human SOX2 gene. *Mamm. Genome* 5, 640–642. doi: 10.1007/BF00411460

Stolt, C. C., Lommes, P., Friedrich, R. P., and Wegner, M. (2004). Transcription factors Sox8 and Sox10 perform non-equivalent roles during oligodendrocyte development despite functional redundancy. *Development* 131, 2349–2358. doi: 10.1242/dev.01114

Stolt, C. C., Lommes, P., Sock, E., Chaboissier, M. C., Schedl, A., and Wegner, M. (2003). The Sox9 transcription factor determines glial fate choice in the developing spinal cord. *Genes Dev.* 17, 1677–1689. doi: 10.1101/gad.259003

Stolt, C. C., Rehberg, S., Ader, M., Lommes, P., Riethmacher, D., Schachner, M., et al. (2002). Terminal differentiation of myelin-forming oligodendrocytes depends on the transcription factor Sox10. *Genes Dev.* 16, 165–170. doi: 10.1101/gad.215802

Stolt, C. C., Schlierf, A., Lommes, P., Hillgartner, S., Werner, T., Kosian, T., et al. (2006). SoxD proteins influence multiple stages of oligodendrocyte development and modulate SoxE protein function. *Dev. Cell* 11, 697–709. doi: 10.1016/j.devcel.2006.08.011

Stolt, C. C., and Wegner, M. (2010). SoxE function in vertebrate nervous system development. *Int. J. Biochem. Cell Biol.* 42, 437–440. doi: 10.1016/j.biocel.2009.07.014

Strassler, E. T., Aalto-Setala, K., Kiamehr, M., Landmesser, U., and Krankel, N. (2018). Age is relative-impact of donor age on induced pluripotent stem cell-derived cell functionality. *Front. Cardiovasc. Med.* 5:4. doi: 10.3389/fcvm.2018.00004

Subramanian, L., Sarkar, A., Shetty, A. S., Muralidharan, B., Padmanabhan, H., Piper, M., et al. (2011). Transcription factor Lhx2 is necessary and sufficient to suppress astrogliogenesis and promote neurogenesis in the developing hippocampus. *Proc. Natl. Acad. Sci. U.S.A.* 108, E265–E274. doi: 10.1073/pnas.1101109108

Sun, C. P., Sun, D., Luan, Z. L., Dai, X., Bie, X., Ming, W. H., et al. (2020). Association of SOX11 Polymorphisms in distal 3'UTR with susceptibility for schizophrenia. *J. Clin. Lab. Anal.* 34:e23306. doi: 10.1002/jcla.23306

Sun, W., Cornwell, A., Li, J., Peng, S., Osorio, M. J., Aalling, N., et al. (2017). SOX9 is an astrocyte-specific nuclear marker in the adult brain outside the neurogenic regions. *J. Neurosci.* 37, 4493–4507. doi: 10.1523/JNEUROSCI.3199-16.2017

Takahashi, K., Tanabe, K., Ohnuki, M., Narita, M., Ichisaka, T., Tomoda, K., et al. (2007). Induction of pluripotent stem cells from adult human fibroblasts by defined factors. *Cell* 131, 861–872. doi: 10.1016/j.cell.2007.11.019

Takahashi, K., and Yamanaka, S. (2016). A decade of transcription factor-mediated reprogramming to pluripotency. *Nat. Rev. Mol. Cell Biol.* 17, 183–193. doi: 10.1038/nrm.2016.8

Takash, W., Canizares, J., Bonneaud, N., Poulat, F., Mattei, M. G., Jay, P., et al. (2001). SOX7 transcription factor: sequence, chromosomal localisation, expression, transactivation and interference with Wnt signalling. *Nucleic Acids Res.* 29, 4274–4283. doi: 10.1093/nar/29.21.4274

Tanaka, Y., Cakir, B., Xiang, Y., Sullivan, G. J., and Park, I. H. (2020). Synthetic analyses of single-cell transcriptomes from multiple brain organoids and fetal brain. *Cell Rep.* 30:e1683. doi: 10.1016/j.celrep.2020.01.038

Taylor, K. M., and Labonne, C. (2005). SoxE factors function equivalently during neural crest and inner ear development and their activity is regulated by SUMOylation. *Dev. Cell* 9, 593–603. doi: 10.1016/j.devcel.2005.09.016

Telias, M., Mayshar, Y., Amit, A., and Ben-Yosef, D. (2015). Molecular mechanisms regulating impaired neurogenesis of fragile X syndrome human embryonic stem cells. *Stem Cells Dev.* 24, 2353–2365. doi: 10.1089/scd.2015.0220

Thein, D. C., Thalhammer, J. M., Hartwig, A. C., Crenshaw, E. B. III, Lefebvre, V., Wegner, M., et al. (2010). The closely related transcription factors Sox4 and Sox11 function as survival factors during spinal cord development. *J. Neurochem.* 115, 131–141. doi: 10.1111/j.1471-4159.2010.06910.x

Tolchin, D., Yeager, J. P., Prasad, P., Dorrani, N., Russi, A. S., Martinez-Agosto, J. A., et al. (2020). De Novo SOX6 variants cause a neurodevelopmental syndrome associated with ADHD, Craniosynostosis, and Osteochondromas. *Am. J. Hum. Genet.* 106, 830–845. doi: 10.1016/j.ajhg.2020.04.015

Topalovic, V., Krstic, A., Schwirtlich, M., Dolfini, D., Mantovani, R., Stevanovic, M., et al. (2017). Epigenetic regulation of human SOX3 gene expression during early phases of neural differentiation of NT2/D1 cells. *PLoS One* 12:e0184099. doi: 10.1371/journal.pone.0184099

Tremblay, R., Haukenfrers, J., Lei, J. X., Sikorska, M., and Bani-Yaghoub, M. (2012). "Retinoic acid regulates Sox2 expression during neuronal and glial differentiation in mouse P19 cells," in *Retinoic Acid: Structure, Mechanisms and Roles in Disease*, eds C. L. Hong and I. Yuto (Waltham, MA: Nova Biomedical), 165–174.

Tsuda, M., Takahashi, S., Takahashi, Y., and Asahara, H. (2003). Transcriptional co-activators CREB-binding protein and p300 regulate chondrocyte-specific gene expression via association with Sox9. *J. Biol. Chem.* 278, 27224–27229. doi: 10.1074/jbc.M303471200

Tsurusaki, Y., Koshimizu, E., Ohashi, H., Phadke, S., Kou, I., Shiina, M., et al. (2014). De novo SOX11 mutations cause Coffin-Siris syndrome. *Nat. Commun.* 5:4011. doi: 10.1038/ncomms5011

Turnescu, T., Arter, J., Reiprich, S., Tamm, E. R., Waisman, A., and Wegner, M. (2018). Sox8 and Sox10 jointly maintain myelin gene expression in oligodendrocytes. *Glia* 66, 279–294. doi: 10.1002/glia.23242

Uchikawa, M., Kamachi, Y., and Kondoh, H. (1999). Two distinct subgroups of Group B Sox genes for transcriptional activators and repressors: their expression during embryonic organogenesis of the chicken. *Mech. Dev.* 84, 103–120. doi: 10.1016/s0925-4773(99)00083-0

Uwanogho, D., Rex, M., Cartwright, E. J., Pearl, G., Healy, C., Scotting, P. J., et al. (1995). Embryonic expression of the chicken Sox2, Sox3 and Sox11 genes suggests an interactive role in neuronal development. *Mech. Dev.* 49, 23–36. doi: 10.1016/0925-4773(94)00299-3

Van Raay, T. J., Moore, K. B., Iordanova, I., Steele, M., Jamrich, M., Harris, W. A., et al. (2005). Frizzled 5 signaling governs the neural potential of progenitors in the developing *Xenopus* retina. *Neuron* 46, 23–36. doi: 10.1016/j.neuron.2005.02.023

Venere, M., Han, Y. G., Bell, R., Song, J. S., Alvarez-Buylla, A., and Blelloch, R. (2012). Sox1 marks an activated neural stem/progenitor cell in the hippocampus. *Development* 139, 3938–3949. doi: 10.1242/dev.081133

Vogel, J. K., Weider, M., Engler, L. A., Hillgartner, S., Schmitt, C., Hermans-Borgmeyer, I., et al. (2020). Sox9 overexpression exerts multiple stage-dependent effects on mouse spinal cord development. *Glia* 68, 932–946. doi: 10.1002/glia.23752

Volterra, A., and Meldolesi, J. (2005). Astrocytes, from brain glue to communication elements: the revolution continues. *Nat. Rev. Neurosci.* 6, 626–640. doi: 10.1038/nrn1722

Vong, K. I., Leung, C. K., Behringer, R. R., and Kwan, K. M. (2015). Sox9 is critical for suppression of neurogenesis but not initiation of gliogenesis in the cerebellum. *Mol. Brain* 8:25. doi: 10.1186/s13041-015-0115-0

Vujic, M., Rajic, T., Goodfellow, P. N., and Stevanovic, M. (1998). cDNA characterization and high resolution mapping of the human SOX20 gene. *Mamm. Genome* 9, 1059–1061. doi: 10.1007/s003359900925

Wang, J., and Yen, A. (2004). A novel retinoic acid-responsive element regulates retinoic acid-induced BLR1 expression. *Mol. Cell Biol.* 24, 2423–2443. doi: 10.1128/mcb.24.6.2423-2443.2004

Wang, T. W., Stromberg, G. P., Whitney, J. T., Brower, N. W., Klymkowsky, M. W., and Parent, J. M. (2006). Sox3 expression identifies neural progenitors in persistent neonatal and adult mouse forebrain germinative zones. *J. Comp. Neurol.* 497, 88–100. doi: 10.1002/cne.20984

Wang, Y., Bagheri-Fam, S., and Harley, V. R. (2005). SOX13 is up-regulated in the developing mouse neuroepithelium and identifies a sub-population of differentiating neurons. *Brain Res. Dev. Brain Res.* 157, 201–208. doi: 10.1016/j.devbrainres.2004.12.010

Wegner, M. (1999). From head to toes: the multiple facets of Sox proteins. *Nucleic Acids Res.* 27, 1409–1420. doi: 10.1093/nar/27.6.1409

Wegner, M. (2005). Secrets to a healthy Sox life: lessons for melanocytes. *Pigment Cell Res.* 18, 74–85. doi: 10.1111/j.1600-0749.2005.00218.x

Wegner, M. (2011). SOX after SOX: SOXession regulates neurogenesis. *Genes Dev.* 25, 2423–2428. doi: 10.1101/gad.181487.111

Weider, M., Reiprich, S., and Wegner, M. (2013). Sox appeal - Sox10 attracts epigenetic and transcriptional regulators in myelinating glia. *Biol. Chem.* 394, 1583–1593. doi: 10.1515/hsz-2013-0146

Wernig, M., Meissner, A., Foreman, R., Brambrink, T., Ku, M., Hochedlinger, K., et al. (2007). In vitro reprogramming of fibroblasts into a pluripotent ES-cell-like state. *Nature* 448, 318–324. doi: 10.1038/nature05944

Whittington, N., Cunningham, D., Le, T. K., De Maria, D., and Silva, E. M. (2015). Sox21 regulates the progression of neuronal differentiation in a dose-dependent manner. *Dev. Biol.* 397, 237–247. doi: 10.1016/j.ydbio.2014.11.012

Wiebe, M. S., Wilder, P. J., Kelly, D., and Rizzino, A. (2000). Isolation, characterization, and differential expression of the murine Sox-2 promoter. *Gene* 246, 383–393. doi: 10.1016/s0378-1119(00)00086-x

Winner, B., Kohl, Z., and Gage, F. H. (2011). Neurodegenerative disease and adult neurogenesis. *Eur. J. Neurosci.* 33, 1139–1151. doi: 10.1111/j.1460-9568.2011.07613.x

Winner, B., and Winkler, J. (2015). Adult neurogenesis in neurodegenerative diseases. *Cold Spring Harb. Perspect. Biol.* 7:a021287. doi: 10.1101/cshperspect.a021287

Wittstatt, J., Weider, M., Wegner, M., and Reiprich, S. (2020). MicroRNA miR-204 regulates proliferation and differentiation of oligodendroglia in culture. *Glia* 68, 2015–2027. doi: 10.1002/glia.23821

Wood, H. B., and Episkopou, V. (1999). Comparative expression of the mouse Sox1, Sox2 and Sox3 genes from pre-gastrulation to early somite stages. *Mech. Dev.* 86, 197–201. doi: 10.1016/s0925-4773(99)00116-1

Wright, E. M., Snopek, B., and Koopman, P. (1993). Seven new members of the Sox gene family expressed during mouse development. *Nucleic Acids Res.* 21, 744. doi: 10.1093/nar/21.3.744

Wunderle, V. M., Critcher, R., Ashworth, A., and Goodfellow, P. N. (1996). Cloning and characterization of SOX5, a new member of the human SOX gene family. *Genomics* 36, 354–358. doi: 10.1006/geno.1996.0474

Xiang, Y., Cakir, B., and Park, I. H. (2020). Deconstructing and reconstructing the human brain with regionally specified brain organoids. *Semin. Cell Dev. Biol.* 111, 40–51. doi: 10.1016/j.semcdb.2020.05.023

Zaletel, I., Schwirtlich, M., Perovic, M., Jovanovic, M., Stevanovic, M., Kanazir, S., et al. (2018). Early impairments of hippocampal neurogenesis in 5xFAD mouse model of Alzheimer's disease are associated with altered expression of SOXB transcription factors. *J. Alzheimers Dis.* 65, 963–976. doi: 10.3233/JAD-180277

Zaret, K. S., and Carroll, J. S. (2011). Pioneer transcription factors: establishing competence for gene expression. *Genes Dev.* 25, 2227–2241. doi: 10.1101/gad.176826.111

Zawerton, A., Yao, B., Yeager, J. P., Pippucci, T., Haseeb, A., Smith, J. D., et al. (2019). De Novo SOX4 variants cause a neurodevelopmental disease associated

with mild dysmorphism. *Am. J. Hum. Genet.* 104, 246–259. doi: 10.1016/j.ajhg.2018.12.014

Zeng, H., Shen, E. H., Hohmann, J. G., Oh, S. W., Bernard, A., Royall, J. J., et al. (2012). Large-scale cellular-resolution gene profiling in human neocortex reveals species-specific molecular signatures. *Cell* 149, 483–496. doi: 10.1016/j.cell.2012.02.052

Zhang, C., Basta, T., Jensen, E. D., and Klymkowsky, M. W. (2003). The beta-catenin/VegT-regulated early zygotic gene Xnr5 is a direct target of SOX3 regulation. *Development* 130, 5609–5624. doi: 10.1242/dev.00798

Zhao, X., He, X., Han, X., Yu, Y., Ye, F., Chen, Y., et al. (2010). MicroRNA-mediated control of oligodendrocyte differentiation. *Neuron* 65, 612–626. doi: 10.1016/j.neuron.2010.02.018

Zhou, F., Zhang, C., Guan, Y., Chen, Y., Lu, Q., Jie, L., et al. (2018). Screening the expression characteristics of several miRNAs in G93A-SOD1 transgenic mouse: altered expression of miRNA-124 is associated with astrocyte differentiation by targeting Sox2 and Sox9. *J. Neurochem.* 145, 51–67. doi: 10.1111/jnc.14229

Zorn, A. M., Barish, G. D., Williams, B. O., Lavender, P., Klymkowsky, M. W., and Varmus, H. E. (1999). Regulation of Wnt signaling by Sox proteins: XSox17 alpha/beta and XSox3 physically interact with beta-catenin. *Mol. Cell* 4, 487–498. doi: 10.1016/s1097-2765(00)80200-2

Conflict of Interest: The authors declare that the research was conducted in the absence of any commercial or financial relationships that could be construed as a potential conflict of interest.

frontiers in Molecular Neuroscience

REVIEW
published: 09 June 2021
doi: 10.3389/fnmol.2021.662774

The Role of Neurod Genes in Brain Development, Function, and Disease

Svetlana Tutukova[1,2], *Victor Tarabykin*[1,2]* *and Luis R. Hernandez-Miranda*[2]*

[1]*Institute of Neuroscience, Lobachevsky University of Nizhny Novgorod, Nizhny Novgorod, Russia,* [2]*Charité Universitätsmedizin Berlin, corporate member of Freie Universität Berlin and Humboldt-Universität zu Berlin, Institute for Cell- and Neurobiology, Berlin, Germany*

Transcriptional regulation is essential for the correct functioning of cells during development and in postnatal life. The basic Helix-loop-Helix (bHLH) superfamily of transcription factors is well conserved throughout evolution and plays critical roles in tissue development and tissue maintenance. A subgroup of this family, called neural lineage bHLH factors, is critical in the development and function of the central nervous system. In this review, we will focus on the function of one subgroup of neural lineage bHLH factors, the Neurod family. The Neurod family has four members: Neurod1, Neurod2, Neurod4, and Neurod6. Available evidence shows that these four factors are key during the development of the cerebral cortex but also in other regions of the central nervous system, such as the cerebellum, the brainstem, and the spinal cord. We will also discuss recent reports that link the dysfunction of these transcription factors to neurological disorders in humans.

Keywords: bHLH factor, neurod family, brain development, neurological diseases, transcription factors

OPEN ACCESS

Edited by:
Veronica Martinez Cerdeño, University of California, Davis, United States

Reviewed by:
Ake Liu, Changzhi University, China
Petra Wahle, Ruhr University Bochum, Germany

***Correspondence:**
Luis R. Hernandez-Miranda
luis.hernandez-miranda@charite.de
Victor Tarabykin
victor.tarabykin@charite.de

Specialty section:
This article was submitted to Neuroplasticity and Development, a section of the journal Frontiers in Molecular Neuroscience

Received: *01 February 2021*
Accepted: *11 May 2021*
Published: *09 June 2021*

Citation:
Tutukova S, Tarabykin V and Hernandez-Miranda LR (2021) The Role of Neurod Genes in Brain Development, Function, and Disease. Front. Mol. Neurosci. 14:662774. doi: 10.3389/fnmol.2021.662774

INTRODUCTION

The interest to understand the molecular mechanisms that generate our central nervous system has never been greater, as the intensive work of clinicians, neurologists, and developmental biologists demonstrate that several naturally occurring neurological disorders originate from deficits impairing brain development in humans (Ross and Walsh, 2001; Subramanian et al., 2019). This can be particularly seen in disorders affecting the development of the cerebral cortex, which are frequently associated with seizures both in childhood and in adult life (Subramanian et al., 2019). Furthermore, cognitive disorders ranging from mild to severe intellectual disability and autism are also concomitant features of cortical neurodevelopmental disorders (Guerrini and Dobyns, 2014). The advent of novel and powerful human genetics is greatly contributing to the identification of rare and common disease-causing variants disrupting the normal development of the nervous system (Ku et al., 2010; McCarthy and MacArthur, 2017; Niemi et al., 2018; Momozawa and Mizukami, 2021). Many of these underlie the elementary mechanisms acting on neurogenesis, neuronal differentiation, fate acquisition, dendritogenesis, axonal navigation, and synapse formation (Cardoso et al., 2019; Wang et al., 2019; Parenti et al., 2020).

Development of the central nervous system in humans, as in many other species, is an elaborated process that begins during an early fetal stage, for instance in the third gestational week in humans or by embryonic day 11 in mice (Bayer and Altman, 2007). It initiates with the formation of the neural tube and the differentiation and specification of neural progenitor cells that, subsequently, lead to the genesis of differentiated neurons in a process called neurogenesis that culminates in the early postnatal life in humans, but can span throughout the adult life in other species, such as rodents

(Altman and Das, 1965; Johnson, 2001; Bayer and Altman, 2007; Stiles and Jernigan, 2010; Silbereis et al., 2016; Sorrells et al., 2018; Buffalo et al., 2019; Petrik and Encinas, 2019). The specification of neural progenitor cells and their activation to self-renew and/or to differentiate in more committed progenitors and neurons is mediated by extrinsic and intrinsic molecular mechanisms (Götz and Sommer, 2005; Urbán and Guillemot, 2014; Götz et al., 2016; Oproescu et al., 2021). The intrinsic mechanisms that direct neural progenitor cell progression and differentiation rely on the coordinated function of multiple transcription factors that determine their identity and, simultaneously, the suppression of their progenitor cell programs (Schuurmans et al., 2004; Britz et al., 2006; Hevner et al., 2006; Davidson, 2010; Hodge and Hevner, 2011; Busskamp et al., 2014; Ware et al., 2016; Mall et al., 2017; Lee et al., 2019).

In the developing nervous system, proneural basic Helix-loop-Helix (bHLH) transcription factors are master regulators of cell proliferation and key in neuronal differentiation and specification (Dokucu et al., 1996; Sommer et al., 1996; Bertrand et al., 2002). Among these factors, the Neurod family stands as a critical regulator of neuronal progenitor cell differentiation and neuronal specification in the cerebral cortex, as well as in other regions of the nervous system such as the cerebellum, the brainstem, and the spinal cord. The Neurod family is composed of four members, Neurod1, Neurod2, Neurod4, and Neurod6.

In this review, we will discuss on the function of bHLH factors in neuronal development and particularly focus on the Neurod family in the development of cerebral cortex (including neuronal fate specification, dendritogenesis, and axonal navigation), as well as on the function of these factors in the development of other areas of the central nervous system. In addition, we will discuss *Neurod* disease-causing variants found in patients presenting with neurological disorders, such as Alzheimer's disease.

bHLH TRANSCRIPTION FACTORS AND THE NEUROD FAMILY

The bHLH superfamily of transcription factors contains numerous genes crucial for the regulation of gene expression in most eukaryotic organisms. These factors are classified according to the similarities in their protein structure and the characteristic presence of a basic domain that directly binds to chromatin as well as a Helix-loop-Helix (HLH) domain that comprises of a non-conserved loop region connecting to alpha-helices (Chien et al., 1996; Bertrand et al., 2002). The bHLH domain was first identified by Murre and colleagues using early, but sophisticated, oligonucleotide screening procedures on lgt11 expression clones (Murre et al., 1989). The protein sequence characteristic of the bHLH domain consists of about 60–100 amino acids. bHLH factors are known to heterodimerize with other bHLH factors, using their non-conserved loop region, to form a functional DNA binding unit. Upon forming heterodimers, bHLH transcription factors are capable to bind to E-box motifs on chromatin, which display the consensus sequence CANNTG (Longo et al., 2008). The central "NN" and flanking nucleotides are believed to confer the DNA-binding specificity shown by bHLH proteins (Ellenberger et al., 1994; Bertrand et al., 2002).

The bHLH superfamily of transcription factors is well conserved throughout evolution and was first identified in animals, although recent investigations have started to reveal their presence and function in other organisms that range from yeast to plants (Murre et al., 1994; Zhang T. et al., 2018). Phylogenetic analysis of the bHLH superfamily using seven different species (human, mouse, rat, worm, fly, yeast, and plant Arabidopsis) has revealed over 600 members belonging to this family (Stevens et al., 2008). Unsurprisingly, the number of bHLH genes increases with the complexity of the organism, for instance, the smaller number of bHLH genes, 38, is found in *Caenorhabditis elegans*, around 58 in *Drosophila melanogaster*, 117 in the *Mus musculus*, and approximately 130 in *Homo sapiens* (Ledent et al., 2002; Skinner et al., 2010).

In 1989, Murrey and others first classified bHLH transcription factors according to their expression pattern into two classes: a class A (with ubiquitous expression) and a class B (with tissue-specific expression; Murre et al., 1989). This classification has been further expanded using large–scale phylogenetic analyses comparing the bHLH domains (Sun and Baltimore, 1991; Atchley and Fitch, 1997; Meredith and Johnson, 2000; Dennis et al., 2019). A more recent phylogenetic classification done by Skinner and colleagues has related bHLH factors into five distinct clades, in which clade A contains neural lineage genes such as *Neurod*, *Neurog1*, *Ascl1*, and *Atoh1*; or clade C that contains muscle-specific genes such as *Myod1* or *Myf5* (Skinner et al., 2010).

Neural lineage bHLH transcription factors participate in the regulation of cell survival, differentiation, migration, and fate specification during neural development and in postnatal life. These factors oftentimes have overlapping functions but can be further subdivided into: (i) proneural or determination factors (usually expressed in progenitor cells) and (ii) differentiation factors [predominantly expressed in postmitotic neurons (Bertrand et al., 2002)].

(i) *Proneural factors*. They represent a small subset of the neural lineage bHLH factors which are preferentially expressed in multipotent precursor cells. They control and direct progenitor cell decisions as well as the cellular fate choices to undergo glial or neuronal differentiation. An interesting trait of these transcription factors is their pioneering function to remodel chromatin and their capacity to reprogram non-neuronal differentiated cells into neurons (Wapinski et al., 2013, 2017; Pataskar et al., 2016; Guillemot and Hassan, 2017). Members of this group include the genes *Neurod1*, *Neussrod4*, *Ascl1*, *Neurog1*, and *Neurog2*.

(ii) *Differentiation factors*. These genes encompass most of the neural lineage bHLH transcription factors and are predominantly expressed by differentiated neurons, in which they regulate fate specification and neuronal identity maintenance. Members of this group include *Neurod1*, *Neurod2*, *Neurod6*, *Bhlhe22*.

The Neurod family contains four closely related proteins: Neurod1, Neurod2, Neurod4, and Neurod6. The expression pattern of these genes is highly overlapping but not identical

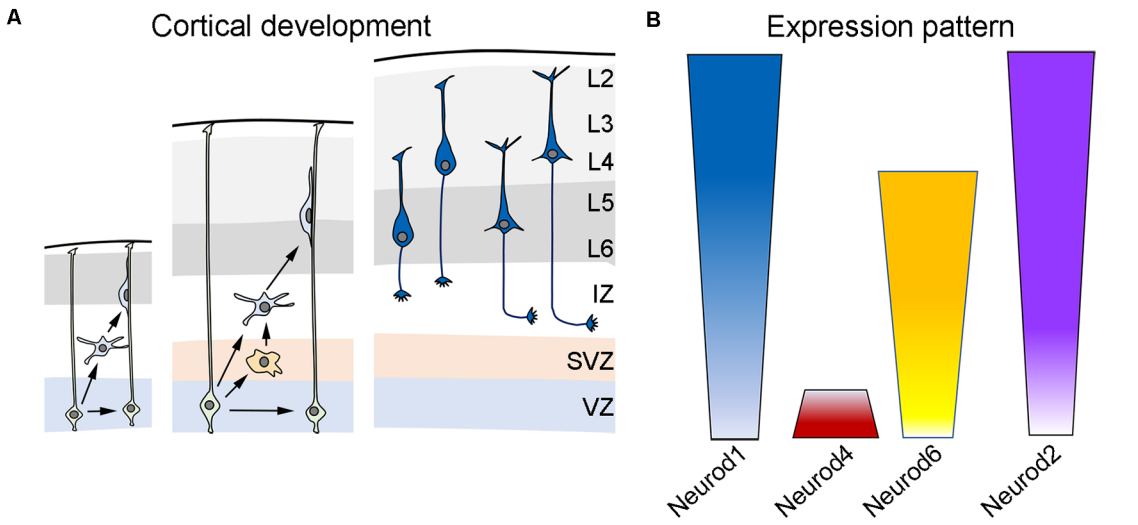

C

Neurod family function in cortical development

Function	Neurogenesis	Neuronal differentiation	Fate specification	Neuronal migration	Axonal navigation	Dendritic development
Factor	Neurod4	Neurod1 Neurod2 Neurod6	Neurod1 Neurod2	Neurod1 Neurod2	Neurod2 Neurod6	Neurod2

FIGURE 1 | Developmental expression of the Neurod family during cortical development of mice. **(A)** Schematic representation of the cortical development in mice. (Left) During early cortical development, neural progenitor cells (light green, also called radial glial cells) located in the dorsal ventricular zone (VZ) make early decisions as to self-renew or differentiate into early born neurons (light blue). (Middle) As cortical development progress, neuronal progenitor cells increase their choices and can then self-renew or differentiate into more committed progenitors (light orange) that populate an emerging subventricular zone (SVZ) or into differentiated neurons (light blue). Upon differentiation, neurons radially migrate throughout an intermediate zone (IZ) in order to populate the developing cortical plate (gray areas), using radial glial fibers as a scaffold. (Right) According to the time of birth, cortical pyramidal neurons (dark blue) settle into their appropriate cortical layer and start the elaboration of dendritic trees and the elongation or their axonal processes (see text). **(B)** Schematic display of the expression pattern exhibited by the different members of the Neurod family during cortical development (see text). **(C)** Table summarizing the known functions of the different members of the Neurod family during cortical development (see text). Panel **(A)** is inspired from Guo et al. (2015).

in the developing cerebral cortex (**Figure 1**). Expression of these genes is abundantly present in the neuroepithelium of the dorsal telencephalon in early development and is sustained in the adult neocortex, hippocampus, and cerebellum (Schwab et al., 1998). The expression of *Neurod1* can be first detected around embryonic day 12 in the dorsal ventricular zone (VZ) of mice (Bormuth et al., 2013). In the developing cerebral cortex, *Neurod1* is also expressed by mitotic and early-postmitotic neuronal cells that reside in the subventricular zone (SVZ), which contains transit-amplifying progenitors that contribute to the generation of most of the excitatory neurons that form the mature cortex. In the postnatal life, *Neurod1* expression is retained in the cerebral cortex, particularly in most excitatory pyramidal neurons that form the upper-most layers of the cortex (Lee et al., 1995; Bormuth et al., 2013; D'Amico et al., 2013). *Neurod4* expression has been reported to be confined to the ventricular zone of the dorsal telencephalon during development and can be detected around embryonic day 12/13 in mice (Mattar et al., 2008). The other two members of the Neurod family, Neurod2 and Neurod6, display a highly overlapping expression pattern that appears in the mouse cerebral cortex around embryonic day 12 (Bormuth et al., 2013). Interestingly, both transcription factors are abundantly expressed by postmitotic pyramidal neurons during embryonic development, albeit their expression levels decline in the postnatal life. *Neurod6* seems to be selectively expressed in a subset of pyramidal neurons, specifically those residing in the deeper layers of the adult mouse cortex; whereas *Neurod2* is expressed by all cortical pyramidal neurons irrespectively of their laminar position (Bormuth et al., 2013).

NEUROD FAMILY IN CORTICAL DEVELOPMENT AND CORTICAL FUNCTION

Pyramidal neurons (also known as cortical projection cells) are generated from progenitor cells located in the ventricular and subventricular zone of the dorsal telencephalon (see

Figure 1; reviewed in Götz and Sommer, 2005; Elston and Fujita, 2014; Agirman et al., 2017). Soon after leaving the cell cycle, pyramidal neurons initiate a radial migration using the fibers of neighboring radial glial cells as a scaffold and cross an intermediate zone (IZ) on their way to reach their final destination within the developing cortex (reviewed in Rakic, 1995; Kriegstein and Noctor, 2004; He et al., 2015). After completing radial migration, pyramidal neurons settle in the cortical plate (CP) and undergo terminal differentiation (Gutierrez et al., 2004; Bianchi et al., 2013; Elston and Fujita, 2014). An interesting trait in cortical development is that the distinct projection neurons that form the mature cerebral cortex do not develop simultaneously but rather they are generated and migrate in a temporal order to populate the cortical plate in an inside-first and outside-last manner (reviewed in Angevine and Sidman, 1961; Rakic, 1974; Noctor et al., 2001; Buchsbaum and Cappello, 2019). This means that neurons residing in the deepest layers of the mature cerebral cortex are generated first during development and settle in the deepest part of the developing cortex. After pyramidal neurons form the deep layers of the cortex, superficially located projection neurons are generated and radially migrate to populate their corresponding upper layers (Rakic, 1974, 1995; Noctor et al., 2001; Kriegstein and Noctor, 2004; He et al., 2015). Once in the cortical plate, pyramidal neurons initiate dendritic arborizations and the projection of their axonal processes in a stereotyped manner, that is, they start with their axon outgrowth, fasciculation, pathfinding, and targeting of their appropriated neuronal partners (**Figure 1**).

bHLH genes cooperate to control transcriptional programs that select different aspects of neural progenitor cell biology and effectively determine neuron subtype identity. Proneural bHLH genes in the telencephalon, such as Neurog1 and Neurog2, activate transcriptional cascades of gene expression in progenitor cells that eventually lead to their terminal neuronal differentiation (Ge et al., 2006). Neurog1 and Neurog2 also contribute with the dorsalization of the telencephalon by suppressing the ventralization factor Ascl1 (Fode et al., 2000). The expression of Neurog 1 and Neurog2 is primarily restricted to the dorsal ventricular zone, although a few Neurog2 expressing cells can be observed outside this area (Ge et al., 2006). An important instructive function of Neurog2 is to promote a cortical neuron identity in differentiating cells of the dorsal telencephalon. Neurod4 is a known target of Neurog2 and dimerizes with it, forming Neurog2/Neurod4 heterodimers (Mattar et al., 2008). Neurog2/Neurod4 heterodimers accelerate the expression of particular transcriptional programs in the cortex that regulate neurogenesis. Mattar et al. (2008) have also shown that NeuroD4 and Neurog2 can independently act to regulate gene expression, albeit with a temporal delay. Similarly, Neurod4 can also form heterodimers with Neurog1 which are required for habenular neurogenesis. In the habenula, Neurod4 and Neurog1 depend on Pax6 expression downstream of Sonic hedgehog (Halluin et al., 2016).

Interestingly, the phosphorylation of Neurod4 limits its ability to drive neuronal differentiation during neurogenesis, which implies that post-transcriptional modifications finely tune the activity of bHLH transcription factors, such as Neurod4 (Hardwick and Philpott, 2015; Hardwick et al., 2019). In this context, a phospho-mutant Neurod4 increases its protein stability and enhances its chromatin binding when compared to wild-type Neurod4, which results in a transcriptional up-regulation of a wide range of target genes (Hardwick and Philpott, 2015). Lastly, Neurod4 has also been reported to be capable to reprogram human and mouse astrocytes, and when it is co-expressed with *Insm1* it is capable of driving glutamatergic neuron maturation (Masserdotti et al., 2015).

In the developing neocortex, Neurod1 has been shown to promote terminal neuronal differentiation in progenitor cells, although there exists a hierarchy in the sequential activation of transcription factors that regulate the transition from precursor cells to differentiated pyramidal neurons (Hevner et al., 2001, 2006; Muzio et al., 2002a,b; Hodge et al., 2008; Hodge and Hevner, 2011). Indeed, the sequential expression of the transcription factors *Pax6* → *Neurog2* → *Tbr2* → *Neurod1* → *Tbr1* correlates with the transition from primary progenitor cells into intermediate progenitors and ultimately into the generation of newborn glutamatergic pyramidal neurons. Outside the cerebral cortex, Neurod1 has also been shown to induce terminal neuronal differentiation. For instance, Boutin et al. (2010), using the olfactory periglomerular neuron lineage *in vitro*, showed that expression of *Neurod1* alone suffices to induce terminal differentiation in olfactory periglomerular progenitor cells (Boutin et al., 2010). *In vivo*, *Neurod1* overexpression in the periventricular region leads to the rapid appearance of postmitotic cells with morphological and molecular characteristics of mature neurons both in the subventricular zone and rostral migratory stream (Boutin et al., 2010). The function of Neurod1 in promoting terminal neuronal differentiation seems to be conserved in evolution and has been reported even in lower organisms like the worm *C. teleta* (Sur et al., 2017). Environmental enrichment also seems to induce *Neurod1* expression in the forebrain and to enhance neuronal activity. For example, studies in the juvenile Atlantic salmon (*Salmo salar*) showed that environmental enrichment upregulates *Neurod1* expression in their forebrain, which greatly improves their learning abilities (Salvanes et al., 2013). In mice, environmental enrichment leads to an increase in hippocampal volume and enhances dorsal-ventral differences in DNA methylation, including binding sites recognize by Neurod1, which seem to greatly promote adult neurogenesis (Zhang T.-Y. et al., 2018). In adult humans, *NEUROD1* expression increases in the cerebral cortex after a traumatic injury, which might indicate a protective mechanism play by Neurod1 in the postnatal cerebral cortex (Zheng et al., 2013).

Neurog1 and Neurog2 play an important function in suppressing *RhoA* expression just as cortical progenitor cells are about to leave the cell cycle, and this suppression is maintained in postmitotic neurons by the direct action of Neurod1 (Ge et al., 2006). The suppression of *RhoA* is critical for the migration of pyramidal neurons into the cortical plate (Ge et al., 2006). On the way to the cortical plate, pyramidal neurons also require Reelin, a protein secreted by the Cajal-Retzius cells

that locate in the superficial marginal zone of the developing cortex. Neurod2 has been shown to control pyramidal neuron migration and Reelin signaling by direct regulation of *Cdk5r1*, *Lrp8* and the transcription factor *Cux1*, which in turn controls the differentiation of the upper layer (2/3 and 4) neurons (Bayam et al., 2015).

Neurod2 and Neurod6 are essential regulators of axonal navigation and axonal fasciculation in the mouse neocortex. For instance, the anterior commissure and the corpus callosum fiber tracts, which communicate the two cerebral hemispheres, are completely absent in *Neurod2* and *Neurod6* double mutant mice (Bormuth et al., 2013). Detailed inspections in *Neurod2* and *Neurod6* double mutant mice showed that callosal axons defasciculate in the subventricular zone during development and follow random trajectories into the ipsilateral cortex rather than growing toward the midline to contralaterally decussate (Bormuth et al., 2013). These axonal defects have been correlated with the dysregulation of the cell adhesion protein Cntn2 and the axonal receptor Robo1 (Bormuth et al., 2013). Furthermore, *Neurod2* mutant mice also exhibit deficits in their thalamocortical projections to different cortical areas, such as the somatosensory barrel cortex (Ince-Dunn et al., 2006). Furthermore, the ablation of *Neurod2* and *Neurod6* also results in reduced numbers of functional glutamatergic synapses and, consequently, in a diminished excitatory cortical network (Bormuth et al., 2013).

The development of dendrites and synapses is a fundamental process in the establishment of neuronal polarity and connectivity. In this regard, Neurod2 has been shown to regulate the structural and functional maturation of the hippocampal mossy fiber synapses *via* the regulation of the synaptic scaffolding protein PSD95 (Wilke et al., 2012). Neurod1 and Neurod2 can abrogate GABAergic differentiation directed by Ascl1, a well-known bHLH transcription factor critical for GABAergic neuron development. Furthermore, the forced expression of *Neurod2* in progenitor cells of the ventral telencephalon is sufficient to prevent their normal differentiation into GABAergic neurons (Roybon et al., 2010). In addition, Neurod2 regulates calcium signaling and homeostasis of mature neurons by controlling the expression of the *Stim1* gene that encodes for an ER calcium sensor (Guner et al., 2017). Abnormal dendritic spine remodeling and turnover from postnatal day 30, and onwards, was reported in *Neurod2* mutant mice, particularly in apical tuft dendrites of pyramidal layer 5 projection neurons of the somatosensory cortex (Runge et al., 2020a). Thus, Neurod2 is a nexus in the gene network that controls spine turnover in the postnatal cortex (Runge et al., 2020b).

Neural progenitor cells in the dorsal ventricular zone of the telencephalon also express *Neurod6*, some of which move into the subventricular zone and undergo multiple rounds of symmetrical and/or asymmetrical cell divisions to produce the set of neurons that reside in the upper cortical layers. Neurod6 positive progenitor cells in the subventricular zone are committed to generate glutamatergic neurons and might have evolved to expand the number of pyramidal neurons in the mammalian forebrain (Wu et al., 2005). Neurod6 has been shown to be central in the mitochondrial biogenesis during the early stages of neuronal differentiation. At these stages, Neurod6 appears to stimulate a maximal mitochondria mass accumulation which correlates with the onset of differentiation and lamellipodia formation in the axonal growth cone, as well as at the regions of axonal branching. This seems to be achieved by the transcriptional regulation of Neurod6 on genes encoding for cytoskeletal proteins, mitochondrial trafficking, regulators of membrane potential, and mitochondria chaperones (Uittenbogaard and Chiaramello, 2002, 2004, 2014; Kathleen Baxter et al., 2009; Uittenbogaard et al., 2010a,b; Baxter et al., 2012).

Neurod6 might also confer cellular tolerance to mitochondrial stressors and oxidative stress, which is critical to prevent neurodevelopmental disorders and neurodegenerative diseases, such as the autism spectrum disorder or Parkinson's disease. The long–term consequences of early life stress on adult pathological states are associated with significant changes in DNA methylation and deregulation of miRNAs. *miR-30a-5p* regulates hundreds of downstream targets, including *Neurod6*, which may represent an important biological signature associated with the risk to develop psychiatric disorders as a consequence of exposure to early life adversities (Cattaneo et al., 2020). Neurod1 has also been shown to be critical for neuronal plasticity and increased levels of *Neurod1* expression are triggered in the murine hippocampus after chronic or mild stress (Boulle et al., 2014). During neuronal differentiation, DNA demethylation-reprograming events are also associated with Neurod2 genome-wide binding (Hahn et al., 2019). In particular, it has been shown that highly methylated genomic regions in neuronal progenitor cells become demethylated after the onset of *Neurod2* expression, and this coincides with the transition from proliferative progenitor state to differentiated neurons (Hahn et al., 2019). Furthermore, it has also been recently reported that maternal hyperglycemia increases H3K14 acetylation levels at Neurog1 and Neurod2 binding sites. Enhanced and premature expression of Neurog1 and Neurod2 eventually leads to an earlier differentiation of progenitor cells, which accelerates the genesis of newborn neurons in the cerebral cortex (Ji et al., 2019). Therefore, Neurod factors appear to display a pioneer function in remodeling chromatin. In keeping with this, Pataskar et al. (2016) recently demonstrated the pioneer function of Neurod1 in chromatin remodeling (Pataskar et al., 2016). The pioneer function of Neurod1 seems to be responsible for the potentiation of mineralocorticoid receptor-mediated transcription in the hippocampus, which has been suggested to act as a neuronal protective mechanism against the development of psychopathologies and, in particular, mood disorders (van Weert et al., 2019). In addition, Neurod1 has also been shown to reprogram striatal non-reactive astrocytes into neurons, albeit the reprogramming function of Neurod1 seems to be less efficient in cortical non-reactive astrocytes (Agirman et al., 2017; Liu et al., 2020).

Over two decades ago, Schwab et al. demonstrated that Neurod1 and Neurod6 are required for terminal neuronal differentiation in the hippocampus (Schwab et al., 1998, 2000). In *Neurod1* and *Neurod6* double mutant mice, the granule cells that are destined to populate the hippocampal

dentate gyrus can be generated, but they fail to properly mature and display several phenotypes that include the lack of normal sodium currents, small dendritic arborization, and alterations of the entorhinal and commissural axonal projections (Schwab et al., 2000). Neurod1 has also been reported to play key functions in the survival and differentiation of newborn neurons in the subgranular and subventricular zones of the adult hippocampus (Gao et al., 2009). In keeping with this data, Roybon and others have also reported a key regulatory role for the Neurog2 and Neurod1 heterodimer complexes in controlling neuronal commitment and hippocampal neuroblast formation both in embryonic and in postnatal neurogenesis (Roybon et al., 2009). Specifically, Neurog2 and Neurod1 heterodimers control progenitor cell production and the amplification of granule neuron progenitors, but they are not required for the acquisition of their granule cell identity (Roybon et al., 2009). In the hippocampus, Neurod1 seems to induce the cell cycle exit of progenitor cells and to promote a rapid neuronal maturation of their progeny, maturation that seems to be reinforced by the expression of Neurod2 in differentiated hippocampal neurons (Roybon et al., 2009).

NEUROD FAMILY IN THE DEVELOPMENT OF THE POSTERIOR NEURAL TUBE

The Neurod family also plays critical functions in the development of the posterior nervous system, that is the cerebellum, brainstem, and the spinal cord. After the onset of neural induction, the brainstem and spinal cord adopt their posterior identity by responding to instructive patterning signals generated from specialized cell centers located within the neural tube as wells as in surrounding tissues. These patterning centers produce fibroblast growth factors, bone morphogenetic proteins, retinoids, and Wnt proteins, which are capable to diffuse over long distances to carry out their instructive function (Doniach, 1995; Lumsden and Krumlauf, 1996; Stern, 2005). The most salient outcome of this early patterning is the generation of distinct anterior-posterior segments characterized by and overlapping as well as differential expression of transcription factors, predominantly members of the Hox family (Philippidou and Dasen, 2013). In the brainstem, for example, seven units called rhombomeres (rhombomere 1–7) develop, whereas four units (cervical, thoracic, lumbar, and sacral) are specified in the spinal cord of humans and mice (Trainor and Krumlauf, 2000). Each rhombomeric and spinal cord unit is further patterned along their dorsoventral axis by the action of diffusible morphogens emanating from a dorsal and a ventral group of specialized cells that act as organizers, the roof, and floor plate. These two organizers antagonistically act and exert their function via the secretion of Sonic hedgehog (by the floor plate) and bone morphogenic proteins and Wnt proteins (by the roof plate; Roelink et al., 1995; Liem et al., 1997; Ulloa and Marti, 2010). These signals diffuse from the roof and floor plate forming concentration gradients that differentially act upon progenitor cells located at different distances from the signal source and along the dorsal-ventral axis of the neural tube. It is thus the spatial position of progenitor cells within the neural tube that determines their response to morphogenic signals. Progenitor cells then respond to these signals, in a dose-dependent manner, and differentially express particular sets of transcription factors, among these the Neurod family and several other bHLH factors.

This is the case of the cerebellum that develops from the dorsal part of rhombomere 1 (known as the cerebellar anlage), which directly receives instructive signals from the roof plate (Millet et al., 1996; Broccoli et al., 1999; Chizhikov et al., 2006; Butts et al., 2014a,b). The cerebellar anlage contains two distinct germinal zones, the ventricular zone and the rhombic lip, which produce all GABAergic and glutamatergic cerebellar neurons, respectively (Hallonet et al., 1990; Alder et al., 1996; Wingate and Hatten, 1999; Hoshino et al., 2005; Millen et al., 2014; Yamada et al., 2014). Rhombic lip progenitor cells generate three distinct neuronal populations in a stereotyped temporal order. The first generation of glutamatergic neurons occurs between embryonic days 10.5 and 13.5 (in mice), and during this period deep cerebellar neurons are generated. A subsequent generation of glutamatergic neurons occurs between embryonic day 13.5 and birth, throughout this time external granular cell layer cells become specified, these cells are the precursors of the granule cells that develop in the early postnatal life. Lastly, unipolar brush cells become specified from the rhombic lip between embryonic day 15.5 and the first day of postnatal life (Ben-Arie et al., 1997; Gazit et al., 2004; Machold and Fishell, 2005; Englund et al., 2006; Fink et al., 2006; Machold et al., 2011; Yamada et al., 2014).

The generation of deep cerebellar neurons seems to largely depend on the action of the bHLH factor Olig3 (Lowenstein et al., 2021), whereas the production of external granular layer cells and unipolar brush cells is regulated by the bHLH factor Atoh1 (Ben-Arie et al., 1997; Gazit et al., 2004; Machold and Fishell, 2005; Wang et al., 2005). Neurod1 has long been known to play a critical role in the differentiation of granule cells, mainly in postnatal life (Gao et al., 2009). Deletion of Neurod1 greatly disrupts differentiation of these cells by prolonging the proliferation of their external granular layer cell progenitors and, in parallel, by inducing apoptosis in the developing cerebellum (Miyata et al., 1999; Pan et al., 2009). The extended proliferation and lethality of Neurod1-deficient external granular layer cell progenitors might result from the loss of the pioneer and proneural function that Neurod1 exerts in these progenitor cells by mediating, among other molecular cascades, the expression of different elements of the Notch signaling pathway (Pataskar et al., 2016). Indeed, expression of Neurod1 is known to drive terminal neuronal differentiation in external granular layer cell progenitor cells both in development and in the postnatal life of mammals and other vertebrates, such as in *Xenopus* (Cho and Tsai, 2004; Boutin et al., 2010; D'Amico et al., 2013; Butts et al., 2014a; Hanzel et al., 2019). Furthermore, a recent report shows that elevated levels of *Neurod1* expression are sufficient to drive medulloblastoma cells into granule cell differentiation, which demonstrates that Neurod1 overrides oncogenic mutations present in medulloblastoma cells (Cheng et al., 2020). In spite of the substantial knowledge gained from the study of Neurod1 function in cerebellar development, less is known about the function of other members of the Neurod family in cerebellar development and cerebellar function.

However, an early study using *Neurod2* mutant mice showed that these mutants correctly develop until about the second week of postnatal life, after which they began exhibiting ataxia and the failure to thrive, which seems to be indicative of a cerebellar dysfunction (Olson et al., 2001). More recently, Pieper and colleagues (2019) reported on a critical function of Neurod2 in promoting survival of both granule cells and inhibitory neurons (particularly basket and stellate cells) that originate from the ventricular zone (Pieper et al., 2019). The analysis of *Neurod2* mutant mice seems to indicate that Neurod2 might have an important function in cerebellar inhibitory neuron function, as well as in the axonogenesis and synaptic formation of inhibitory cerebellar neurons onto Purkinje cells (Pieper et al., 2019).

Work over the last two decades has also shown the great influence of the Neurod family in other regions of the posterior nervous system, which include the midbrain, the hindbrain, and the spinal cord. Progenitor cells in the ventral midbrain express high levels of *Neurod1*, and the combinatorial expression of *Neurod1* with other bHLH factors sub-specifies different neuronal populations emanating from this area, some of which retain *Neurod1* expression (Park et al., 2006; Arimura et al., 2019; Ásgrímsdóttir and Arenas, 2020; Poulin et al., 2020). Furthermore, Neurod1 and Neurod6 have been recently reported to have a critical function in the development of particular dopaminergic midbrain neurons (Khan et al., 2017). Specifically, Khan and colleagues analyzed *Neurod6* and *Neurod1* double mutant mice, and found that these genes are required for the survival of dopaminergic midbrain neurons located in the ventral tegmental area, particularly those that project to the intermediate and dorsal regions of the septum (Khan et al., 2017).

Unlike the neurogenic function that the Neurod family has in the developing cortex, cerebellum, and the midbrain; in the hindbrain and spinal cord Neurod1, Neurod2 and Neurod6 seem to mainly regulate the correct specification of discrete subpopulations of inhibitory interneurons (Hernandez-Miranda et al., 2017). In the hindbrain and spinal cord, Ptf1a-expressing progenitor cells generate all inhibitory neurons, which are known to co-express the homeodomain proteins Lbx1, Pax2, and Lhx1/5. Interestingly, these inhibitory interneurons do not uniformly maintain the expression of these transcription factors during their maturation and greatly vary in their expression, indicating that differential expression of such factors might reflect distinct subpopulations of inhibitory neurons (Pillai et al., 2007). Indeed, available evidence illustrates that Neurod1, Neurod2, and Neurod6 secure the specification of dynorphin+ and galanin+ inhibitory interneurons, whereas Lhx1/5 instruct a NPY+ inhibitory fate (Bröhl et al., 2008).

NEUROD GENES IN HUMAN NEUROLOGICAL DISORDERS

The first report of human patients with a mutation on a gene of the Neurod family came in 2010 by Rubio-Cabezas and others (Rubio-Cabezas et al., 2010). In this study, the authors reported on two distinct homozygous mutations in *NEUROD1* that were found in two unrelated probands diagnosed with permanent neonatal diabetes and neurological abnormalities. The identified mutations correspond to frameshift mutations that predictably generate truncated proteins, without affecting their DNA-binding domain. Neurologically, both patients presented with learning difficulties, cerebellar hypoplasia, profound sensorineural deafness, and visual impairment due to severe myopia and retinal dystrophy. Thus, the deficits observed in *NEUROD1*-deficient patients resemble those seen in *Neurod1* mutant mice, which include pronounced cortical, cerebellar, brainstem, and spinal cord impairments (see above). More recently, Sega and colleagues found de novo mutations in *NEUROD2* in two unrelated children diagnosed with early infantile epileptic encephalopathy and developmental delay (Sega et al., 2019). In keeping with this, an early onset of epilepsy has also been described in *Neurod2* deficient mice (Chen et al., 2016). In this context, Chen et al. suggested that Neurod2 tightly controls the inhibition/excitation balance of neuronal transmission in the mature cortex. Furthermore, deficiencies of Neurod2 function in the mouse brain cause a decrease in the cell-intrinsic excitability of excitatory pyramidal neurons (Chen et al., 2016). There are two transcriptional targets of Neurod2 that may contribute to these processes: gastrin-releasing peptide (GRP) and the small conductance, calcium-activated potassium channel, Sk2 (Kcnn2). The expression of both genes is greatly decreased in *Neurod2* mutant mice (Chen et al., 2016). Very recently, Runge et al. (2020b) described seven families with pathogenic *NEUROD2* mutations causing a variety of neurological disorders, such as autism spectrum disorders, intellectual disability, and speech delay. The authors of this study also suggest that behavioral deficits in social behavior, which are reminiscent of autistic disorders, can be found in *Neurod2* mutant mice. In addition, Spellman et al. identified a direct association of *NEUROD2* gene polymorphisms with changes in cognitive functions present in schizophrenic patients treated with antipsychotic drugs (Spellmann et al., 2017). It has also been shown that the lateral and basolateral amygdala nuclei fail to form in *Neurod2* mutant mice, and that these mice display deficits in emotional learning (Lin et al., 2005). In particular, Lin et al., found that Neurod2 is required for amygdala development and the regulation of the AMPA receptor, the γ subunit of the GABAA receptor, and the gene *Ulip1*, which are all involved in emotional learning (Lin et al., 2005).

The most salient phenotype arising from the loss of *NEUROD1* in humans is epilepsy. In mice, the ablation of *Neurod1* produces an epileptogenic phenotype associated with a malformation of the hippocampal dentate granule cell layer, which seems to result from an excessive cell death of the neurons forming this layer (Liu et al., 2020). Impaired neurogenesis and decreased expression of *NEUROD1/Neurod1* have also been demonstrated in the hippocampus of the Huntington's disease R6/2 mouse model and in differentiated neural cultures derived from Huntington's disease patients (Fedele et al., 2011). *NEUROD6* has been recently identified as a possible biomarker for the diagnosis of Alzheimer's disease. Indeed, low expression levels of *NEUROD6/Neurod6* have been detected in postmortem Alzheimer's patients and in Alzheimer's mouse models using RNA sequencing datasets, microarray datasets,

and meta-analysis (Hokama et al., 2014; Satoh et al., 2014; Li et al., 2015).

Despite the fact that *NEUROD1* expression levels have been reported not to be significantly changed in Alzheimer's patients (Satoh et al., 2014), its overexpression into hippocampal progenitor cells increases dendritic spine density of hippocampal newborn neurons and results in a great improvement in spatial memory in the Alzheimer's disease mouse model APPxPS1 (Richetin et al., 2015). Further studies by Richetin and others have also shown that Neurod1 promotes spinogenesis and mitochondrial availability at the vicinity of mature spines, and that this improves the integration and survival of adult-generated hippocampal neurons, which are severely impaired in the APPxPS1 mouse model (Richetin et al., 2017). These results provide a potential therapeutic approach to patients affected with Alzheimer's disease. The half-life of Neurod1 can be increased by blocking its ubiquitin-dependent proteasomal degradation, which enhances the transcriptional programs mediated by Neurod1 during neuronal differentiation, but also those involved in neuronal maturation and synaptic transmission (de Wilde et al., 2016; Lee et al., 2020; Pomeshchik et al., 2020). Neurod1 has also been used to successfully reprogram reactive glial cells functional cortical neurons in stab-injured or Alzheimer's disease mouse models and in adult non-human primates after ischemic stroke, which again offers the possibility to develop new therapeutical approaches for patients affected with Alzheimer's disease (Guo et al., 2014; Ge et al., 2020).

CONCLUSION

The bHLH superfamily of transcription factors is well conserved throughout evolution and plays critical roles in tissue development and tissue maintenance. Whereas many bHLH transcription factors display ubiquitous expression, a small fraction of them has a tissue-specific expression. The question of how different members of this superfamily were selected to carry out common and divergent cellular functions remains to be elucidated. In the developing nervous system, the subfamily of neural lineage bHLH transcription factors regulates a variety of biological functions that range from progenitor cell proliferation and survival to neuronal differentiation, neuronal migration, fate specification, axonal navigation, dendritic elongation, and synaptic formation. Some members of this subfamily (called proneural, including Ascl1, Neurog1, Neurog2, Neurod1, and Neurod4) have been shown to be able to remodel chromatin and induce neuronal differentiation in progenitor cells, but they are also capable of reprogramming differentiated non-neuronal cells into neurons (Castro et al., 2011; Wapinski et al., 2013, 2017; Chanda et al., 2014; Treutlein et al., 2016; Rao et al., 2021). While Ascl1, Neurog1, Neurog2, and Neurod4 are predominantly expressed in progenitor cells, other factors like Neurod1, Neurod2, and Neurod6 are expressed both in progenitors and retained in postmitotic neurons. This raises the question of whether the function of these factors differs in progenitor cells and in differentiated neurons. Future research may elucidate whether post-transcriptional regulations, such as phosphorylation, on Neurod1, Neurod2, and Neurod6 account for their functional restriction at different points in the life of a neuron. Recent work on Ascl1 (in neurons) or Myod1 (in muscle cells) has shown that these transcription factors have an oscillatory expression which accounts for the proliferation of progenitors cells, whereas the sustained expression of these factors drives cell differentiation (Imayoshi et al., 2013; Vasconcelos and Castro, 2014; Lahmann et al., 2019; Sueda et al., 2019; Zhang et al., 2021), whether this oscillatory behavior is common for all bHLH transcription factors is unknown. However, the Neurod family offers the possibility to deepen into the expression dynamics of bHLH factors as they are expressed both in progenitors and in their progeny. An early diagnosis of neurological diseases is central in their management. Recent discoveries suggest that the expression of distinct members of the NEUROD family could serve as biomarkers at the onset of various neurological diseases, such as Alzheimer's disease, and also serve in the development of patient-oriented gene therapies.

AUTHOR CONTRIBUTIONS

ST, VT, and LH-M wrote the original draft and reviewed the literature. ST, VT, and LH-M revised the original draft. LH-M edited the final draft. All authors contributed to the article and approved the submitted final version.

FUNDING

This research work was funded by Russian Science Foundation, grant no. 19-14-00345 to VT.

REFERENCES

Agirman, G., Broix, L., and Nguyen, L. (2017). Cerebral cortex development: an outside-in perspective. *FEBS Lett.* 591, 3978–3992. doi: 10.1002/1873-3468.12924

Alder, J., Cho, N. K., and Hatten, M. E. (1996). Embryonic precursor cells from the rhombic lip are specified to a cerebellar granule neuron identity. *Neuron* 17, 389–399. doi: 10.1016/s0896-6273(00)80172-5

Altman, J., and Das, G. D. (1965). Autoradiographic and histological evidence of postnatal hippocampal neurogenesis in rats. *J. Comp. Neurol.* 124, 319–335. doi: 10.1002/cne.901240303

Angevine, J. B. Jr., and Sidman, R. L. (1961). Autoradiographic study of cell migration during histogenesis of cerebral cortex in the mouse. *Nature* 192, 766–768. doi: 10.1038/192766b0

Arimura, N., Dewa, K. I., Okada, M., Yanagawa, Y., Taya, S. I., Hoshino, M., et al. (2019). Comprehensive and cell-type-based characterization of the dorsal midbrain during development. *Genes Cells* 24, 41–59. doi: 10.1111/gtc.12656

Ásgrímsdóttir, E. S., and Arenas, E. (2020). Midbrain dopaminergic neuron development at the single cell level: *in vivo* and in stem cells. *Front. Cell. Dev. Biol.* 8:463. doi: 10.3389/fcell.2020.00463

Atchley, W. R., and Fitch, W. M. (1997). A natural classification of the basic helix-loop-helix class of transcription factors. *Proc. Natl. Acad. Sci. U S A* 94, 5172–5176. doi: 10.1073/pnas.94.10.5172

Baxter, K. K., Uittenbogaard, M., and Chiaramello, A. (2012). The neurogenic basic helix-loop-helix transcription factor NeuroD6 enhances mitochondrial biogenesis and bioenergetics to confer tolerance of neuronal PC12-NeuroD6 cells to the mitochondrial stressor rotenone. *Exp. Cell Res.* 318, 2200–2214. doi: 10.1016/j.yexcr.2012.07.004

Bayam, E., Sahin, G. S., Guzelsoy, G., Guner, G., Kabakcioglu, A., Ince-Dunn, G., et al. (2015). Genome-wide target analysis of NEUROD2 provides new insights into regulation of cortical projection neuron migration and differentiation. *BMC Genomics* 16:681. doi: 10.1186/s12864-015-1882-9

Bayer, S. A., and Altman, J. (2007). *The Human Brain During the Early First Trimester*, 1st Edn. Boca Raton, FL: CRC Press.

Ben-Arie, N., Bellen, H. J., Armstrong, D. L., McCall, A. E., Gordadze, P. R., Guo, Q., et al. (1997). Math1 is essential for genesis of cerebellar granule neurons. *Nature* 390, 169–172. doi: 10.1038/36579

Bertrand, N., Castro, D. S., and Guillemot, F. (2002). Proneural genes and the specification of neural cell types. *Nat. Rev. Neurosci.* 3, 517–530. doi: 10.1038/nrn874

Bianchi, S., Stimpson, C. D., Duka, T., Larsen, M. D., Janssen, W. G., Collins, Z., et al. (2013). Synaptogenesis and development of pyramidal neuron dendritic morphology in the chimpanzee neocortex resembles humans. *Proc. Natl. Acad. Sci. U S A* 110, 10395–10401. doi: 10.1073/pnas.1301224110

Bormuth, I., Yan, K., Yonemasu, T., Gummert, M., Zhang, M., Wichert, S., et al. (2013). Neuronal basic helix-loop-helix proteins Neurod2/6 regulate cortical commissure formation before midline interactions. *J. Neurosci.* 33, 641–651. doi: 10.1523/JNEUROSCI.0899-12.2013

Boulle, F., Massart, R., Stragier, E., Païzanis, E., Zaidan, L., Marday, S., et al. (2014). Hippocampal and behavioral dysfunctions in a mouse model of environmental stress: normalization by agomelatine. *Transl. Psychiatry* 4:e485. doi: 10.1038/tp.2014.125

Boutin, C., Hardt, O., de Chevigny, A., Coré, N., Goebbels, S., Seidenfaden, R., et al. (2010). NeuroD1 induces terminal neuronal differentiation in olfactory neurogenesis. *Proc. Natl. Acad. Sci. U S A* 107, 1201–1206. doi: 10.1073/pnas.0909015107

Britz, O., Mattar, P., Nguyen, L., Langevin, L. M., Zimmer, C., Alam, S., et al. (2006). A role for proneural genes in the maturation of cortical progenitor cells. *Cereb. Cortex* 16, i138–i151. doi: 10.1093/cercor/bhj168

Broccoli, V., Boncinelli, E., and Wurst, W. (1999). The caudal limit of Otx2 expression positions the isthmic organizer. *Nature* 401, 164–168. doi: 10.1038/43670

Bröhl, D., Strehle, M., Wende, H., Hori, K., Bormuth, I., Nave, K. A., et al. (2008). A transcriptional network coordinately determines transmitter and peptidergic fate in the dorsal spinal cord. *Dev. Biol.* 322, 381–393. doi: 10.1016/j.ydbio.2008.08.002

Buchsbaum, I. Y., and Cappello, S. (2019). Neuronal migration in the CNS during development and disease: insights from *in vivo* and *in vitro* models. *Development* 146:dev163766. doi: 10.1242/dev.163766

Buffalo, E. A., Movshon, J. A., and Wurtz, R. H. (2019). From basic brain research to treating human brain disorders. *Proc. Natl. Acad. Sci. U S A* 116, 26167–26172. doi: 10.1073/pnas.1919895116

Busskamp, V., Lewis, N. E., Guye, P., Ng, A. H., Shipman, S. L., Byrne, S. M., et al. (2014). Rapid neurogenesis through transcriptional activation in human stem cells. *Mol. Syst. Biol.* 10:760. doi: 10.15252/msb.20145508

Butts, T., Green, M. J., and Wingate, R. J. (2014a). Development of the cerebellum: simple steps to make a 'little brain'. *Development* 141, 4031–4041. doi: 10.1242/dev.106559

Butts, T., Hanzel, M., and Wingate, R. J. (2014b). Transit amplification in the amniote cerebellum evolved *via* a heterochronic shift in NeuroD1 expression. *Development* 141, 2791–2795. doi: 10.1242/dev.101758

Cardoso, A. R., Lopes-Marques, M., Silva, R. M., Serrano, C., Amorim, A., Prata, M. J., et al. (2019). Essential genetic findings in neurodevelopmental disorders. *Hum. Genomics* 13:31. doi: 10.1186/s40246-019-0216-4

Castro, D. S., Martynoga, B., Parras, C., Ramesh, V., Pacary, E., Johnston, C., et al. (2011). A novel function of the proneural factor Ascl1 in progenitor proliferation identified by genome-wide characterization of its targets. *Genes Dev.* 25, 930–945. doi: 10.1101/gad.627811

Cattaneo, A., Suderman, M., Cattane, N., Mazzelli, M., Begni, V., Maj, C., et al. (2020). Long-term effects of stress early in life on microRNA-30a and its network: preventive effects of lurasidone and potential implications for depression vulnerability. *Neurobiol. Stress* 13:100271. doi: 10.1016/j.ynstr.2020.100271

Chanda, S., Ang, C. E., Davila, J., Pak, C., Mall, M., Lee, Q. Y., et al. (2014). Generation of induced neuronal cells by the single reprogramming factor ASCL1. *Stem Cell Rep.* 3, 282–296. doi: 10.1016/j.stemcr.2014.05.020

Chen, F., Moran, J. T., Zhang, Y., Ates, K. M., Yu, D., Schrader, L. A., et al. (2016). The transcription factor NeuroD2 coordinates synaptic innervation and cell intrinsic properties to control excitability of cortical pyramidal neurons. *J. Physiol.* 594, 3729–3744. doi: 10.1113/JP271953

Cheng, Y., Liao, S., Xu, G., Hu, J., Guo, D., Du, F., et al. (2020). NeuroD1 dictates tumor cell differentiation in medulloblastoma. *Cell Rep.* 31:107782. doi: 10.1016/j.celrep.2020.107782

Chien, C. T., Hsiao, C. D., Jan, L. Y., and Jan, Y. N. (1996). Neuronal type information encoded in the basic-helix-loop-helix domain of proneural genes. *Proc. Natl. Acad. Sci. U S A* 93, 13239–13244. doi: 10.1073/pnas.93.23.13239

Chizhikov, V. V., Lindgren, A. G., Currle, D. S., Rose, M. F., Monuki, E. S., Millen, K. J., et al. (2006). The roof plate regulates cerebellar cell-type specification and proliferation. *Development* 133, 2793–2804. doi: 10.1242/dev.02441

Cho, J.-H., and Tsai, M.-J. (2004). The role of BETA2/NeuroD1 in the development of the nervous system. *Mol. Neurobiol.* 30, 35–47. doi: 10.1385/MN:30:1:035

D'Amico, L. A., Boujard, D., and Coumailleau, P. (2013). The neurogenic factor NeuroD1 is expressed in post-mitotic cells during juvenile and adult Xenopus neurogenesis and not in progenitor or radial glial cells. *PLoS One* 8:e66487. doi: 10.1371/journal.pone.0066487

Davidson, E. H. (2010). Emerging properties of animal gene regulatory networks. *Nature* 468, 911–920. doi: 10.1038/nature09645

de Wilde, M. C., Overk, C. R., Sijben, J. W., and Masliah, E. (2016). Meta-analysis of synaptic pathology in Alzheimer's disease reveals selective molecular vesicular machinery vulnerability. *Alzheimers Dement.* 12, 633–644. doi: 10.1016/j.jalz.2015.12.005

Dennis, D. J., Han, S., and Schuurmans, C. (2019). bHLH transcription factors in neural development, disease, and reprogramming. *Brain Res.* 1705, 48–65. doi: 10.1016/j.brainres.2018.03.013

Dokucu, M. E., Zipursky, S. L., and Cagan, R. L. (1996). Atonal, rough and the resolution of proneural clusters in the developing *Drosophila* retina. *Development* 122, 4139–4147. doi: 10.1242/dev.122.12.4139

Doniach, T. (1995). Basic FGF as an inducer of anteroposterior neural pattern. *Cell* 83, 1067–1070. doi: 10.1016/0092-8674(95)90133-7

Ellenberger, T., Fass, D., Arnaud, M., and Harrison, S. C. (1994). Crystal structure of transcription factor E47: E-box recognition by a basic region helix-loop-helix dimer. *Genes Dev.* 8, 970–980. doi: 10.1101/gad.8.8.970

Elston, G. N., and Fujita, I. (2014). Pyramidal cell development: postnatal spinogenesis, dendritic growth, axon growth, and electrophysiology. *Front. Neuroanat.* 8:78. doi: 10.3389/fnana.2014.00078

Englund, C., Kowalczyk, T., Daza, R. A., Dagan, A., Lau, C., Rose, M. F., et al. (2006). Unipolar brush cells of the cerebellum are produced in the rhombic lip and migrate through developing white matter. *J. Neurosci.* 26, 9184–9195. doi: 10.1523/JNEUROSCI.1610-06.2006

Fedele, V., Roybon, L., Nordstrom, U., Li, J. Y., and Brundin, P. (2011). Neurogenesis in the R6/2 mouse model of Huntington's disease is impaired at the level of NeuroD1. *Neuroscience* 173, 76–81. doi: 10.1016/j.neuroscience.2010.08.022

Fink, A. J., Englund, C., Daza, R. A., Pham, D., Lau, C., Nivison, M., et al. (2006). Development of the deep cerebellar nuclei: transcription factors and cell migration from the rhombic lip. *J. Neurosci.* 26, 3066–3076. doi: 10.1523/JNEUROSCI.5203-05.2006

Fode, C., Ma, Q., Casarosa, S., Ang, S. L., Anderson, D. J., Guillemot, F., et al. (2000). A role for neural determination genes in specifying the dorsoventral identity of telencephalic neurons. *Genes Dev.* 14, 67–80. doi: 10.1101/gad.14.1.67

Gao, Z., Ure, K., Ables, J. L., Lagace, D. C., Nave, K. A., Goebbels, S., et al. (2009). Neurod1 is essential for the survival and maturation of adult-born neurons. *Nat. Neurosci.* 12, 1090–1092. doi: 10.1038/nn.2385

Gazit, R., Krizhanovsky, V., and Ben-Arie, N. (2004). Math1 controls cerebellar granule cell differentiation by regulating multiple components of the Notch signaling pathway. *Development* 131, 903–913. doi: 10.1242/dev.00982

Ge, W., He, F., Kim, K. J., Blanchi, B., Coskun, V., Nguyen, L., et al. (2006). Coupling of cell migration with neurogenesis by proneural bHLH factors. *Proc. Natl. Acad. Sci. U S A* 103, 1319–1324. doi: 10.1073/pnas.0510419103

Ge, L. J., Yang, F. H., Li, W., Wang, T., Lin, Y., Feng, J., et al. (2020). *in vivo* neuroregeneration to treat ischemic stroke through NeuroD1 AAV-based

gene therapy in adult non-human primates. *Front. Cell. Dev. Biol.* 8:590008. doi: 10.3389/fcell.2020.590008

Götz, M., Nakafuku, M., and Petrik, D. (2016). Neurogenesis in the developing and adult brain-similarities and key differences. *Cold Spring Harb. Perspect. Biol.* 8:a018853. doi: 10.1101/cshperspect.a018853

Götz, M., and Sommer, L. (2005). Cortical development: the art of generating cell diversity. *Development* 132, 3327–3332. doi: 10.1242/dev.01931

Guerrini, R., and Dobyns, W. B. (2014). Malformations of cortical development: clinical features and genetic causes. *Lancet Neurol.* 13, 710–726. doi: 10.1016/S1474-4422(14)70040-7

Guillemot, F., and Hassan, B. A. (2017). Beyond proneural: emerging functions and regulations of proneural proteins. *Curr. Opin. Neurobiol.* 42, 93–101. doi: 10.1016/j.conb.2016.11.011

Guner, G., Guzelsoy, G., Isleyen, F. S., Sahin, G. S., Akkaya, C., Bayam, E., et al. (2017). NEUROD2 regulates *Stim1* expression and store-operated calcium entry in cortical neurons. *eNeuro* 4:ENEURO.0255-16.2017. doi: 10.1523/ENEURO.0255-16.2017

Guo, J., Higginbotham, H., Li, J., Nichols, J., Hirt, J., Ghukasyan, V., et al. (2015). Developmental disruptions underlying brain abnormalities in ciliopathies. *Nat. Commun.* 6:7857. doi: 10.1038/ncomms8857

Guo, Z., Zhang, L., Wu, Z., Chen, Y., Wang, F., Chen, G., et al. (2014). *In vivo* direct reprogramming of reactive glial cells into functional neurons after brain injury and in an Alzheimer's disease model. *Cell Stem Cell* 14, 188–202. doi: 10.1016/j.stem.2013.12.001

Gutierrez, H., Dolcet, X., Tolcos, M., and Davies, A. (2004). HGF regulates the development of cortical pyramidal dendrites. *Development* 131, 3717–3726. doi: 10.1242/dev.01209

Hahn, M. A., Jin, S.-G., Li, A. X., Liu, J., Huang, Z., Wu, X., et al. (2019). Reprogramming of DNA methylation at NEUROD2-bound sequences during cortical neuron differentiation. *Sci. Adv.* 5:eaax0080. doi: 10.1126/sciadv.aax0080

Hallonet, M. E., Teillet, M. A., and Le Douarin, N. M. (1990). A new approach to the development of the cerebellum provided by the quail-chick marker system. *Development* 108, 19–31. doi: 10.1242/dev.108.1.19

Halluin, C., Madelaine, R., Naye, F., Peers, B., Roussigne, M., Blader, P., et al. (2016). Habenular neurogenesis in zebrafish is regulated by a Hedgehog, Pax6 proneural gene cascade. *PLoS One* 11:e0158210. doi: 10.1371/journal.pone.0158210

Hanzel, M., Rook, V., and Wingate, R. J. T. (2019). Mitotic granule cell precursors undergo highly dynamic morphological transitions throughout the external germinal layer of the chick cerebellum. *Sci. Rep.* 9:15218. doi: 10.1038/s41598-019-51532-y

Hardwick, L. J. A., Davies, J. D., and Philpott, A. (2019). Multi-site phosphorylation controls the neurogenic and myogenic activity of E47. *Biochem. Biophys. Res. Commun.* 511, 111–116. doi: 10.1016/j.bbrc.2019.02.045

Hardwick, L. J., and Philpott, A. (2015). Multi-site phosphorylation regulates NeuroD4 activity during primary neurogenesis: a conserved mechanism amongst proneural proteins. *Neural. Dev.* 10:15. doi: 10.1186/s13064-015-0044-8

He, S., Li, Z., Ge, S., Yu, Y. C., and Shi, S. H. (2015). Inside-out radial migration facilitates lineage-dependent neocortical microcircuit assembly. *Neuron* 86, 1159–1166. doi: 10.1016/j.neuron.2015.05.002

Hernandez-Miranda, L. R., Müller, T., and Birchmeier, C. (2017). The dorsal spinal cord and hindbrain: from developmental mechanisms to functional circuits. *Dev. Biol.* 432, 34–42. doi: 10.1016/j.ydbio.2016.10.008

Hevner, R. F., Hodge, R. D., Daza, R. A., and Englund, C. (2006). Transcription factors in glutamatergic neurogenesis: conserved programs in neocortex, cerebellum, and adult hippocampus. *Neurosci. Res.* 55, 223–233. doi: 10.1016/j.neures.2006.03.004

Hevner, R. F., Shi, L., Justice, N., Hsueh, Y., Sheng, M., Smiga, S., et al. (2001). Tbr1 regulates differentiation of the preplate and layer 6. *Neuron* 29, 353–366. doi: 10.1016/s0896-6273(01)00211-2

Hodge, R. D., and Hevner, R. F. (2011). Expression and actions of transcription factors in adult hippocampal neurogenesis. *Dev. Neurobiol.* 71, 680–689. doi: 10.1002/dneu.20882

Hodge, R. D., Kowalczyk, T. D., Wolf, S. A., Encinas, J. M., Rippey, C., Enikolopov, G., et al. (2008). Intermediate progenitors in adult hippocampal neurogenesis: Tbr2 expression and coordinate regulation of neuronal output. *J. Neurosci.* 28, 3707–3717. doi: 10.1523/JNEUROSCI.4280-07.2008

Hokama, M., Oka, S., Leon, J., Ninomiya, T., Honda, H., Sasaki, K., et al. (2014). Altered expression of diabetes-related genes in Alzheimer's disease brains: the Hisayama study. *Cereb. Cortex* 24, 2476–2488. doi: 10.1093/cercor/bht101

Hoshino, M., Nakamura, S., Mori, K., Kawauchi, T., Terao, M., Nishimura, Y. V., et al. (2005). Ptf1a, a bHLH transcriptional gene, defines GABAergic neuronal fates in cerebellum. *Neuron* 47, 201–213. doi: 10.1016/j.neuron.2005.06.007

Imayoshi, I., Isomura, A., Harima, Y., Kawaguchi, K., Kori, H., Miyachi, H., et al. (2013). Oscillatory control of factors determining multipotency and fate in mouse neural progenitors. *Science* 342, 1203–1208. doi: 10.1126/science.1242366

Ince-Dunn, G., Hall, B. J., Hu, S.-C., Ripley, B., Huganir, R. L., Olson, J. M., et al. (2006). Regulation of thalamocortical patterning and synaptic maturation by NeuroD2. *Neuron* 49, 683–695. doi: 10.1016/j.neuron.2006.01.031

Ji, S., Zhou, W., Li, X., Liu, S., Wang, F., Li, X., et al. (2019). Maternal hyperglycemia disturbs neocortical neurogenesis *via* epigenetic regulation in C57BL/6J mice. *Cell Death Dis.* 10:211. doi: 10.1038/s41419-019-1438-z

Johnson, M. H. (2001). Functional brain development in humans. *Nat. Rev. Neurosci.* 2, 475–483. doi: 10.1038/35081509

Kathleen Baxter, K., Uittenbogaard, M., Yoon, J., and Chiaramello, A. (2009). The neurogenic basic helix-loop-helix transcription factor NeuroD6 concomitantly increases mitochondrial mass and regulates cytoskeletal organization in the early stages of neuronal differentiation. *ASN Neuro* 1:e00016. doi: 10.1042/AN20090036

Khan, S., Stott, S. R., Chabrat, A., Truckenbrodt, A. M., Spencer-Dene, B., Nave, K. A., et al. (2017). Survival of a novel subset of midbrain dopaminergic neurons projecting to the lateral septum is dependent on NeuroD proteins. *J. Neurosci.* 37, 2305–2316. doi: 10.1523/JNEUROSCI.2414-16.2016

Kriegstein, A. R., and Noctor, S. C. (2004). Patterns of neuronal migration in the embryonic cortex. *Trends Neurosci.* 27, 392–399. doi: 10.1016/j.tins.2004.05.001

Ku, C. S., Loy, E. Y., Salim, A., Pawitan, Y., and Chia, K. S. (2010). The discovery of human genetic variations and their use as disease markers: past, present and future. *J. Hum. Genet.* 55, 403–415. doi: 10.1038/jhg.2010.55

Lahmann, I., Bröhl, D., Zyrianova, T., Isomura, A., Czajkowski, M. T., Kapoor, V., et al. (2019). Oscillations of MyoD and Hes1 proteins regulate the maintenance of activated muscle stem cells. *Genes Dev.* 33, 524–535. doi: 10.1101/gad.322818.118

Ledent, V., Paquet, O., and Vervoort, M. (2002). Phylogenetic analysis of the human basic helix-loop-helix proteins. *Genome Biol.* 3:RESEARCH0030. doi: 10.1186/gb-2002-3-6-research0030

Lee, T.-Y., Cho, I.-S., Bashyal, N., Naya, F. J., Tsai, M. J., Yoon, J. S., et al. (2020). ERK regulates NeuroD1-mediated neurite outgrowth *via* proteasomal degradation. *Exp. Neurobiol.* 29, 189–206. doi: 10.5607/en20021

Lee, J. E., Hollenberg, S. M., Snider, L., Turner, D. L., Lipnick, N., Weintraub, H., et al. (1995). Conversion of Xenopus ectoderm into neurons by NeuroD, a basic helix-loop-helix protein. *Science* 268, 836–844. doi: 10.1126/science.7754368

Lee, J., Taylor, C. A., Barnes, K. M., Shen, A., Stewart, E. V., Chen, A., et al. (2019). A Myt1 family transcription factor defines neuronal fate by repressing non-neuronal genes. *eLife* 8:e46703. doi: 10.7554/eLife.46703

Li, X., Long, J., He, T., Belshaw, R., and Scott, J. (2015). Integrated genomic approaches identify major pathways and upstream regulators in late onset Alzheimer's disease. *Sci. Rep.* 5:12393. doi: 10.1038/srep12393

Liem, K. F. Jr., and Tremml, G., and Jessell, T. M. (1997). A role for the roof plate and its resident TGFbeta-related proteins in neuronal patterning in the dorsal spinal cord. *Cell* 91, 127–138. doi: 10.1016/s0092-8674(01)80015-5

Lin, C.-H., Hansen, S., Wang, Z., Storm, D. R., Tapscott, S. J., Olson, J. M., et al. (2005). The dosage of the neuroD2 transcription factor regulates amygdala development and emotional learning. *Proc. Natl. Acad. Sci. U S A* 102, 14877–14882. doi: 10.1073/pnas.0506785102

Liu, M.-H., Li, W., Zheng, J.-J., Xu, Y.-G., He, Q., Chen, G., et al. (2020). Differential neuronal reprogramming induced by NeuroD1 from astrocytes in grey matter versus white matter. *Neural Regen. Res.* 15, 342–351. doi: 10.4103/1673-5374.265185

Longo, A., Guanga, G. P., and Rose, R. B. (2008). Crystal structure of E47-NeuroD1/beta2 bHLH domain-DNA complex: heterodimer selectivity and DNA recognition. *Biochemistry* 47, 218–229. doi: 10.1021/bi701527r

Lowenstein, E. D., Rusanova, A., Stelzer, J., Hernaiz-Llorens, M., Schroer, A. E., Epifanova, E., et al. (2021). Olig3 regulates early cerebellar development. *eLife* 10:e64684. doi: 10.7554/eLife.64684

Lumsden, A., and Krumlauf, R. (1996). Patterning the vertebrate neuraxis. *Science* 274, 1109–1115. doi: 10.1126/science.274.5290.1109

Machold, R., and Fishell, G. (2005). Math1 is expressed in temporally discrete pools of cerebellar rhombic-lip neural progenitors. *Neuron* 48, 17–24. doi: 10.1016/j.neuron.2005.08.028

Machold, R., Klein, C., and Fishell, G. (2011). Genes expressed in Atoh1 neuronal lineages arising from the r1/isthmus rhombic lip. *Gene Expr. Patterns* 11, 349–359. doi: 10.1016/j.gep.2011.03.007

Mall, M., Kareta, M. S., Chanda, S., Ahlenius, H., Perotti, N., Zhou, B., et al. (2017). Myt1l safeguards neuronal identity by actively repressing many non-neuronal fates. *Nature* 544, 245–249. doi: 10.1038/nature21722

Masserdotti, G., Gillotin, S., Sutor, B., Drechsel, D., Irmler, M., Jorgensen, H. F., et al. (2015). Transcriptional mechanisms of proneural factors and REST in regulating neuronal reprogramming of astrocytes. *Cell Stem Cell* 17, 74–88. doi: 10.1016/j.stem.2015.05.014

Mattar, P., Langevin, L. M., Markham, K., Klenin, N., Shivji, S., Zinyk, D., et al. (2008). Basic helix-loop-helix transcription factors cooperate to specify a cortical projection neuron identity. *Mol. Cell. Biol.* 28, 1456–1469. doi: 10.1128/MCB.01510-07

McCarthy, M. I., and MacArthur, D. G. (2017). Human disease genomics: from variants to biology. *Genome Biol.* 18:20. doi: 10.1186/s13059-017-1160-z

Meredith, A., and Johnson, J. E. (2000). Negative autoregulation of Mash1 expression in CNS development. *Dev. Biol.* 222, 336–346. doi: 10.1006/dbio.2000.9697

Millen, K. J., Steshina, E. Y., Iskusnykh, I. Y., and Chizhikov, V. V. (2014). Transformation of the cerebellum into more ventral brainstem fates causes cerebellar agenesis in the absence of Ptf1a function. *Proc. Natl. Acad. Sci. U S A* 111, E1777–E1786. doi: 10.1073/pnas.1315024111

Millet, S., Bloch-Gallego, E., Simeone, A., and Alvarado-Mallart, R. M. (1996). The caudal limit of Otx2 gene expression as a marker of the midbrain/hindbrain boundary: a study using in situ hybridisation and chick/quail homotopic grafts. *Development* 122, 3785–3797. doi: 10.1242/dev.122.12.3785

Miyata, T., Maeda, T., and Lee, J. E. (1999). NeuroD is required for differentiation of the granule cells in the cerebellum and hippocampus. *Genes Dev.* 13, 1647–1652. doi: 10.1101/gad.13.13.1647

Momozawa, Y., and Mizukami, K. (2021). Unique roles of rare variants in the genetics of complex diseases in humans. *J. Hum. Genet.* 66, 11–23. doi: 10.1038/s10038-020-00845-2

Murre, C., Bain, G., van Dijk, M. A., Engel, I., Furnari, B. A., Massari, M. E., et al. (1994). Structure and function of helix-loop-helix proteins. *Biochim. Biophys. Acta* 1218, 129–135. doi: 10.1016/0167-4781(94)90001-9

Murre, C., McCaw, P. S., and Baltimore, D. (1989). A new DNA binding and dimerization motif in immunoglobulin enhancer binding, daughterless, MyoD, and myc proteins. *Cell* 56, 777–783. doi: 10.1016/0092-8674(89)90682-x

Muzio, L., Di Benedetto, B., Stoykova, A., Boncinelli, E., Gruss, P., Mallamaci, A., et al. (2002a). Conversion of cerebral cortex into basal ganglia in $Emx2^{-/-}$ $Pax6^{Sey/Sey}$ double-mutant mice. *Nat. Neurosci.* 5, 737–745. doi: 10.1038/nn892

Muzio, L., Di Benedetto, B., Stoykova, A., Boncinelli, E., Gruss, P., Mallamaci, A., et al. (2002b). Emx2 and Pax6 control regionalization of the pre-neuronogenic cortical primordium. *Cereb. Cortex* 12, 129–139. doi: 10.1093/cercor/12.2.129

Niemi, M. E. K., Martin, H. C., Rice, D. L., Gallone, G., Gordon, S., Kelemen, M., et al. (2018). Common genetic variants contribute to risk of rare severe neurodevelopmental disorders. *Nature* 562, 268–271. doi: 10.1038/s41586-018-0566-4

Noctor, S. C., Flint, A. C., Weissman, T. A., Dammerman, R. S., and Kriegstein, A. R. (2001). Neurons derived from radial glial cells establish radial units in neocortex. *Nature* 409, 714–720. doi: 10.1038/35055553

Olson, J. M., Asakura, A., Snider, L., Hawkes, R., Strand, A., Stoeck, J., et al. (2001). NeuroD2 is necessary for development and survival of central nervous system neurons. *Dev. Biol.* 234, 174–187. doi: 10.1006/dbio.2001.0245

Oproescu, A. M., Han, S., and Schuurmans, C. (2021). New insights into the intricacies of proneural gene regulation in the embryonic and adult cerebral cortex. *Front. Mol. Neurosci.* 14:642016. doi: 10.3389/fnmol.2021.642016

Pan, N., Jahan, I., Lee, J. E., and Fritzsch, B. (2009). Defects in the cerebella of conditional Neurod1 null mice correlate with effective Tg(Atoh1-cre) recombination and granule cell requirements for Neurod1 for differentiation. *Cell Tissue Res.* 337, 407–428. doi: 10.1007/s00441-009-0826-6

Parenti, I., Rabaneda, L. G., Schoen, H., and Novarino, G. (2020). Neurodevelopmental disorders: from genetics to functional pathways. *Trends Neurosci.* 43, 608–621. doi: 10.1016/j.tins.2020.05.004

Park, C.-H., Kang, J. S., Kim, J.-S., Chung, S., Koh, J.-Y., Yoon, E.-H., et al. (2006). Differential actions of the proneural genes encoding Mash1 and neurogenins in Nurr1-induced dopamine neuron differentiation. *J. Cell Sci.* 119, 2310–2320. doi: 10.1242/jcs.02955

Pataskar, A., Jung, J., Smialowski, P., Noack, F., Calegari, F., Straub, T., et al. (2016). NeuroD1 reprograms chromatin and transcription factor landscapes to induce the neuronal program. *EMBO J.* 35, 24–45. doi: 10.15252/embj.201591206

Petrik, D., and Encinas, J. M. (2019). Perspective: of mice and men—how widespread is adult neurogenesis? *Front. Neurosci.* 13:923. doi: 10.3389/fnins.2019.00923

Philippidou, P., and Dasen, J. S. (2013). Hox genes: choreographers in neural development, architects of circuit organization. *Neuron* 80, 12–34. doi: 10.1016/j.neuron.2013.09.020

Pieper, A., Rudolph, S., Wieser, G. L., Gotze, T., Miessner, H., Yonemasu, T., et al. (2019). NeuroD2 controls inhibitory circuit formation in the molecular layer of the cerebellum. *Sci. Rep.* 9:1448. doi: 10.1038/s41598-018-37850-7

Pillai, A., Mansouri, A., Behringer, R., Westphal, H., and Goulding, M. (2007). Lhx1 and Lhx5 maintain the inhibitory-neurotransmitter status of interneurons in the dorsal spinal cord. *Development* 134, 357–366. doi: 10.1242/dev.02717

Pomeshchik, Y., Klementieva, O., Gil, J., Martinsson, I., Hansen, M. G., de Vries, T., et al. (2020). Human iPSC-derived hippocampal spheroids: an innovative tool for stratifying Alzheimer disease patient-specific cellular phenotypes and developing therapies. *Stem Cell Rep.* 15, 256–273. doi: 10.1016/j.stemcr.2020.06.001

Poulin, J.-F., Gaertner, Z., Moreno-Ramos, O. A., and Awatramani, R. (2020). Classification of midbrain dopamine neurons using single-cell gene expression profiling approaches. *Trends Neurosci.* 43, 155–169. doi: 10.1016/j.tins.2020.01.004

Rakic, P. (1974). Neurons in rhesus monkey visual cortex: systematic relation between time of origin and eventual disposition. *Science* 183, 425–427. doi: 10.1126/science.183.4123.425

Rakic, P. (1995). Radial versus tangential migration of neuronal clones in the developing cerebral cortex. *Proc. Natl. Acad. Sci. U S A* 92, 11323–11327. doi: 10.1073/pnas.92.25.11323

Rao, Z., Wang, R., Li, S., Shi, Y., Mo, L., Han, S., et al. (2021). Molecular mechanisms underlying ascl1-mediated astrocyte-to-neuron conversion. *Stem Cell Rep.* 16, 534–547. doi: 10.1016/j.stemcr.2021.01.006

Richetin, K., Leclerc, C., Toni, N., Gallopin, T., Pech, S., Roybon, L., et al. (2015). Genetic manipulation of adult-born hippocampal neurons rescues memory in a mouse model of Alzheimer's disease. *Brain* 138, 440–455. doi: 10.1093/brain/awu354

Richetin, K., Moulis, M., Millet, A., Arrazola, M. S., Andraini, T., Hua, J., et al. (2017). Amplifying mitochondrial function rescues adult neurogenesis in a mouse model of Alzheimer's disease. *Neurobiol. Dis.* 102, 113–124. doi: 10.1016/j.nbd.2017.03.002

Roelink, H., Porter, J. A., Chiang, C., Tanabe, Y., Chang, D. T., Beachy, P. A., et al. (1995). Floor plate and motor neuron induction by different concentrations of the amino-terminal cleavage product of sonic hedgehog autoproteolysis. *Cell* 81, 445–455. doi: 10.1016/0092-8674(95)90397-6

Ross, M. E., and Walsh, C. A. (2001). Human brain malformations and their lessons for neuronal migration. *Annu. Rev. Neurosci.* 24, 1041–1070. doi: 10.1146/annurev.neuro.24.1.1041

Roybon, L., Hjalt, T., Stott, S., Guillemot, F., Li, J.-Y., Brundin, P., et al. (2009). Neurogenin2 directs granule neuroblast production and amplification while NeuroD1 specifies neuronal fate during hippocampal neurogenesis. *PLoS One* 4:e4779. doi: 10.1371/journal.pone.0004779

Roybon, L., Mastracci, T. L., Ribeiro, D., Sussel, L., Brundin, P., Li, J. Y., et al. (2010). GABAergic differentiation induced by Mash1 is compromised by the bHLH proteins Neurogenin2, NeuroD1, and NeuroD2. *Cereb. Cortex* 20, 1234–1244. doi: 10.1093/cercor/bhp187

Rubio-Cabezas, O., Minton, J. A., Kantor, I., Williams, D., Ellard, S., Hattersley, A. T., et al. (2010). Homozygous mutations in NEUROD1 are responsible for a novel syndrome of permanent neonatal diabetes and neurological abnormalities. *Diabetes* 59, 2326–2331. doi: 10.2337/db10-0011

Runge, K., Cardoso, C., and de Chevigny, A. (2020a). Dendritic spine plasticity: function and mechanisms. *Front. Synaptic Neurosci.* 12:36. doi: 10.3389/fnsyn.2020.00036

Runge, K., Mathieu, R., Bugeon, S., Lafi, S., Beurrier, C., Sahu, S., et al. (2020b). Disruption of the transcription factor NEUROD2 causes an autism syndrome *via* cell-autonomous defects in cortical projection neurons. *bioRxiv* [Preprint]. doi: 10.1101/296889

Salvanes, A. G., Moberg, O., Ebbesson, L. O., Nilsen, T. O., Jensen, K. H., Braithwaite, V. A., et al. (2013). Environmental enrichment promotes neural plasticity and cognitive ability in fish. *Proc. Biol. Sci.* 280:20131331. doi: 10.1098/rspb.2013.1331

Satoh, J.-I., Yamamoto, Y., Asahina, N., Kitano, S., and Kino, Y. (2014). RNA-Seq data mining: downregulation of NeuroD6 serves as a possible biomarker for Alzheimer's disease brains. *Dis. Markers* 2014:123165. doi: 10.1155/2014/123165

Schuurmans, C., Armant, O., Nieto, M., Stenman, J. M., Britz, O., Klenin, N., et al. (2004). Sequential phases of cortical specification involve Neurogenin-dependent and -independent pathways. *EMBO J.* 23, 2892–2902. doi: 10.1038/sj.emboj.7600278

Schwab, M. H., Bartholomae, A., Heimrich, B., Feldmeyer, D., Druffel-Augustin, S., Goebbels, S., et al. (2000). Neuronal basic helix-loop-helix proteins (NEX and BETA2/Neuro D) regulate terminal granule cell differentiation in the hippocampus. *J. Neurosci.* 20, 3714–3724. doi: 10.1523/JNEUROSCI.20-10-03714.2000

Schwab, M. H., Druffel-Augustin, S., Gass, P., Jung, M., Klugmann, M., Bartholomae, A., et al. (1998). Neuronal basic helix-loop-helix proteins (NEX, neuroD, NDRF): spatiotemporal expression and targeted disruption of the NEX gene in transgenic mice. *J. Neurosci.* 18, 1408–1418. doi: 10.1523/JNEUROSCI.18-04-01408.1998

Sega, A. G., Mis, E. K., Lindstrom, K., Mercimek-Andrews, S., Ji, W., Cho, M. T., et al. (2019). De novo pathogenic variants in neuronal differentiation factor 2 (NEUROD2) cause a form of early infantile epileptic encephalopathy. *J. Med. Genet.* 56, 113–122. doi: 10.1136/jmedgenet-2018-105322

Silbereis, J. C., Pochareddy, S., Zhu, Y., Li, M., and Sestan, N. (2016). The cellular and molecular landscapes of the developing human central nervous system. *Neuron* 89, 248–268. doi: 10.1016/j.neuron.2015.12.008

Skinner, M. K., Rawls, A., Wilson-Rawls, J., and Roalson, E. H. (2010). Basic helix-loop-helix transcription factor gene family phylogenetics and nomenclature. *Differentiation* 80, 1–8. doi: 10.1016/j.diff.2010.02.003

Sommer, L., Ma, Q., and Anderson, D. J. (1996). neurogenins, a novel family of atonal-related bHLH transcription factors, are putative mammalian neuronal determination genes that reveal progenitor cell heterogeneity in the developing CNS and PNS. *Mol. Cell. Neurosci.* 8, 221–241. doi: 10.1006/mcne.1996.0060

Sorrells, S. F., Paredes, M. F., Cebrian-Silla, A., Sandoval, K., Qi, D., Kelley, K. W., et al. (2018). Human hippocampal neurogenesis drops sharply in children to undetectable levels in adults. *Nature* 555, 377–381. doi: 10.1038/nature25975

Spellmann, I., Riedel, M., Stadtler, J., Zill, P., Obermeier, M., Cerovecki, A., et al. (2017). Associations of NEUROD2 polymorphisms and change of cognitive dysfunctions in schizophrenia and schizoaffective disorder after eight weeks of antipsychotic treatment. *Cogn. Neuropsychiatry* 22, 280–297. doi: 10.1080/13546805.2017.1322502

Stern, C. D. (2005). Neural induction: old problem, new findings, yet more questions. *Development* 132, 2007–2021. doi: 10.1242/dev.01794

Stevens, J. D., Roalson, E. H., and Skinner, M. K. (2008). Phylogenetic and expression analysis of the basic helix-loop-helix transcription factor gene family: genomic approach to cellular differentiation. *Differentiation* 76, 1006–1022. doi: 10.1111/j.1432-0436.2008.00285.x

Stiles, J., and Jernigan, T. L. (2010). The basics of brain development. *Neuropsychol. Rev.* 20, 327–348. doi: 10.1007/s11065-010-9148-4

Subramanian, L., Calcagnotto, M. E., and Paredes, M. F. (2019). Cortical malformations: lessons in human brain development. *Front. Cell. Neurosci.* 13:576. doi: 10.3389/fncel.2019.00576

Sueda, R., Imayoshi, I., Harima, Y., and Kageyama, R. (2019). High Hes1 expression and resultant Ascl1 suppression regulate quiescent vs. active neural stem cells in the adult mouse brain. *Genes Dev.* 33, 511–523. doi: 10.1101/gad.323196.118

Sun, X. H., and Baltimore, D. (1991). An inhibitory domain of E12 transcription factor prevents DNA binding in E12 homodimers but not in E12 heterodimers. *Cell* 64, 459–470. doi: 10.1016/0092-8674(91)90653-g

Sur, A., Magie, C. R., Seaver, E. C., and Meyer, N. P. (2017). Spatiotemporal regulation of nervous system development in the annelid *Capitella teleta*. *Evodevo* 8:13. doi: 10.1186/s13227-017-0076-8

Trainor, P., and Krumlauf, R. (2000). Plasticity in mouse neural crest cells reveals a new patterning role for cranial mesoderm. *Nat. Cell Biol.* 2, 96–102. doi: 10.1038/35000051

Treutlein, B., Lee, Q. Y., Camp, J. G., Mall, M., Koh, W., Shariati, S. A., et al. (2016). Dissecting direct reprogramming from fibroblast to neuron using single-cell RNA-seq. *Nature* 534, 391–395. doi: 10.1038/nature18323

Uittenbogaard, M., Baxter, K. K., and Chiaramello, A. (2010a). NeuroD6 genomic signature bridging neuronal differentiation to survival *via* the molecular chaperone network. *J. Neurosci. Res.* 88, 33–54. doi: 10.1002/jnr.22182

Uittenbogaard, M., Baxter, K. K., and Chiaramello, A. (2010b). The neurogenic basic helix-loop-helix transcription factor NeuroD6 confers tolerance to oxidative stress by triggering an antioxidant response and sustaining the mitochondrial biomass. *ASN Neuro* 2:e00034. doi: 10.1042/AN20100005

Uittenbogaard, M., and Chiaramello, A. (2002). Constitutive overexpression of the basic helix-loop-helix Nex1/MATH-2 transcription factor promotes neuronal differentiation of PC12 cells and neurite regeneration. *J. Neurosci. Res.* 67, 235–245. doi: 10.1002/jnr.10119

Uittenbogaard, M., and Chiaramello, A. (2004). Expression profiling upon Nex1/MATH-2-mediated neuritogenesis in PC12 cells and its implication in regeneration. *J. Neurochem.* 91, 1332–1343. doi: 10.1111/j.1471-4159.2004.02814.x

Uittenbogaard, M., and Chiaramello, A. (2014). Mitochondrial biogenesis: a therapeutic target for neurodevelopmental disorders and neurodegenerative diseases. *Curr. Pharm. Des.* 20, 5574–5593. doi: 10.2174/1381612820666140305224906

Ulloa, F., and Marti, E. (2010). Wnt won the war: antagonistic role of Wnt over Shh controls dorso-ventral patterning of the vertebrate neural tube. *Dev. Dyn.* 239, 69–76. doi: 10.1002/dvdy.22058

Urbán, N., and Guillemot, F. (2014). Neurogenesis in the embryonic and adult brain: same regulators, different roles. *Front. Cell. Neurosci.* 8:396. doi: 10.3389/fncel.2014.00396

van Weert, L., Buurstede, J. C., Sips, H. C. M., Mol, I. M., Puri, T., Damsteegt, R., et al. (2019). Mechanistic insights in NeuroD potentiation of mineralocorticoid receptor signaling. *Int. J. Mol. Sci.* 20:1575. doi: 10.3390/ijms20071575

Vasconcelos, F. F., and Castro, D. S. (2014). Transcriptional control of vertebrate neurogenesis by the proneural factor Ascl1. *Front. Cell. Neurosci.* 8:412. doi: 10.3389/fncel.2014.00412

Wang, W., Corominas, R., and Lin, G. N. (2019). *De novo* mutations from whole exome sequencing in neurodevelopmental and psychiatric disorders: from discovery to application. *Front. Genet.* 10:258. doi: 10.3389/fgene.2019.00258

Wang, V. Y., Rose, M. F., and Zoghbi, H. Y. (2005). Math1 expression redefines the rhombic lip derivatives and reveals novel lineages within the brainstem and cerebellum. *Neuron* 48, 31–43. doi: 10.1016/j.neuron.2005.08.024

Wapinski, O. L., Lee, Q. Y., Chen, A. C., Li, R., Corces, M. R., Ang, C. E., et al. (2017). Rapid chromatin switch in the direct reprogramming of fibroblasts to neurons. *Cell Rep.* 20, 3236–3247. doi: 10.1016/j.celrep.2017.09.011

Wapinski, O. L., Vierbuchen, T., Qu, K., Lee, Q. Y., Chanda, S., Fuentes, D. R., et al. (2013). Hierarchical mechanisms for direct reprogramming of fibroblasts to neurons. *Cell* 155, 621–635. doi: 10.1016/j.cell.2013.09.028

Ware, M., Hamdi-Roze, H., Le Friec, J., David, V., and Dupe, V. (2016). Regulation of downstream neuronal genes by proneural transcription factors during initial neurogenesis in the vertebrate brain. *Neural. Dev.* 11:22. doi: 10.1186/s13064-016-0077-7

Wilke, S. A., Hall, B. J., Antonios, J. K., Denardo, L. A., Otto, S., Yuan, B., et al. (2012). NeuroD2 regulates the development of hippocampal mossy fiber synapses. *Neural. Dev.* 7:9. doi: 10.1186/1749-8104-7-9

Wingate, R. J., and Hatten, M. E. (1999). The role of the rhombic lip in avian cerebellum development. *Development* 126, 4395–4404. doi: 10.1242/dev.126.20.4395

Wu, S. X., Goebbels, S., Nakamura, K., Nakamura, K., Kometani, K., Minato, N., et al. (2005). Pyramidal neurons of upper cortical layers generated by NEX-positive progenitor cells in the subventricular zone. *Proc. Natl. Acad. Sci. U S A* 102, 17172–17177. doi: 10.1073/pnas.0508560102

Yamada, M., Seto, Y., Taya, S., Owa, T., Inoue, Y. U., Inoue, T., et al. (2014). Specification of spatial identities of cerebellar neuron progenitors by ptf1a and atoh1 for proper production of GABAergic and glutamatergic neurons. *J. Neurosci.* 34, 4786–4800. doi: 10.1523/JNEUROSCI.2722-13.2014

Zhang, T.-Y., Keown, C. L., Wen, X., Li, J., Vousden, D. A., Anacker, C., et al. (2018). Environmental enrichment increases transcriptional and epigenetic differentiation between mouse dorsal and ventral dentate gyrus. *Nat. Commun.* 9:298. doi: 10.1038/s41467-017-02748-x

Zhang, T., Lv, W., Zhang, H., Ma, L., Li, P., Ge, L., et al. (2018). Genome-wide analysis of the basic Helix-Loop-Helix (bHLH) transcription factor family in maize. *BMC Plant Biol.* 18:235. doi: 10.1186/s12870-018-1441-z

Zhang, Y., Lahmann, I., Baum, K., Shimojo, H., Mourikis, P., Wolf, J., et al. (2021). Oscillations of Delta-like1 regulate the balance between differentiation and maintenance of muscle stem cells. *Nat. Commun.* 12:1318. doi: 10.1038/s41467-021-21631-4

Zheng, W., ZhuGe, Q., Zhong, M., Chen, G., Shao, B., Wang, H., et al. (2013). Neurogenesis in adult human brain after traumatic brain injury. *J. Neurotrauma* 30, 1872–1880. doi: 10.1089/neu.2010.1579

Conflict of Interest: The authors declare that the research was conducted in the absence of any commercial or financial relationships that could be construed as a potential conflict of interest.

frontiers in Molecular Neuroscience

ORIGINAL RESEARCH
published: 16 June 2021
doi: 10.3389/fnmol.2021.687581

Loss of BAF Complex in Developing Cortex Perturbs Radial Neuronal Migration in a WNT Signaling-Dependent Manner

Godwin Sokpor[1,2], Cemil Kerimoglu[3], Huong Nguyen[1,4], Linh Pham[1,2], Joachim Rosenbusch[1], Robin Wagener[1,5,6], Huu Phuc Nguyen[2], Andre Fischer[3,7,8], Jochen F. Staiger[1] and Tran Tuoc[1,2]**

[1] Institute for Neuroanatomy, University Medical Center Goettingen, Göttingen, Germany, [2] Department of Human Genetics, Ruhr University of Bochum, Bochum, Germany, [3] German Center for Neurodegenerative Diseases, Göttingen, Germany, [4] Faculty of Biotechnology, Thai Nguyen University of Sciences, Thai Nguyen, Vietnam, [5] Department of Neurology, University Medical Center Heidelberg, Heidelberg, Germany, [6] Neurooncology Clinical Cooperation Unit, German Cancer Research Center, Heidelberg, Germany, [7] Department for Psychiatry and Psychotherapy, University Medical Center Göttingen, Göttingen, Germany, [8] Cluster of Excellence "Multiscale Bioimaging: from Molecular Machines to Networks of Excitable Cells" (MBExC), University of Göttingen, Göttingen, Germany

Radial neuronal migration is a key neurodevelopmental event indispensable for proper cortical laminar organization. Cortical neurons mainly use glial fiber guides, cell adhesion dynamics, and cytoskeletal remodeling, among other discrete processes, to radially trek from their birthplace to final layer positions. Dysregulated radial migration can engender cortical mis-lamination, leading to neurodevelopmental disorders. Epigenetic factors, including chromatin remodelers have emerged as formidable regulators of corticogenesis. Notably, the chromatin remodeler BAF complex has been shown to regulate several aspects of cortical histogenesis. Nonetheless, our understanding of how BAF complex regulates neuronal migration is limited. Here, we report that BAF complex is required for neuron migration during cortical development. Ablation of BAF complex in the developing mouse cortex caused alteration in the cortical gene expression program, leading to loss of radial migration-related factors critical for proper cortical layer formation. Of note, BAF complex inactivation in cortex caused defective neuronal polarization resulting in diminished multipolar-to-bipolar transition and eventual disruption of radial migration of cortical neurons. The abnormal radial migration and cortical mis-lamination can be partly rescued by downregulating WNT signaling hyperactivity in the BAF complex mutant cortex. By implication, the BAF complex modulates WNT signaling to establish the gene expression program required for glial fiber-dependent neuronal migration, and cortical lamination. Overall, BAF complex has been identified to be crucial for cortical morphogenesis through instructing multiple aspects of radial neuronal migration in a WNT signaling-dependent manner.

Keywords: BAF complex, neuronal migration, cortical lamination, glial fibers, cell adhesion, Wnt signaling, cortical development

OPEN ACCESS

Edited by:
Estela Maris Muñoz, Consejo Nacional de Investigaciones Científicas y Técnicas (CONICET) Dr. Mario H. Burgos Institute of Histology and Embryology (IHEM), Argentina

Reviewed by:
Cecilia Beatriz Conde, Medical Research Institute Mercedes and Martín Ferreyra (INIMEC), Argentina
Stephen C. Noctor, University of California, Davis, United States

****Correspondence:***
Godwin Sokpor
Godwin.Sokpor@ruhr-uni-bochum.de
Tran Tuoc
Tran.Tuoc@ruhr-uni-bochum.de

Specialty section:
This article was submitted to Neuroplasticity and Development, a section of the journal Frontiers in Molecular Neuroscience

Received: *29 March 2021*
Accepted: *20 May 2021*
Published: *16 June 2021*

Citation:
Sokpor G, Kerimoglu C, Nguyen H, Pham L, Rosenbusch J, Wagener R, Nguyen HP, Fischer A, Staiger JF and Tuoc T (2021) Loss of BAF Complex in Developing Cortex Perturbs Radial Neuronal Migration in a WNT Signaling-Dependent Manner. Front. Mol. Neurosci. 14:687581. doi: 10.3389/fnmol.2021.687581

INTRODUCTION

Neuronal migration can be considered as a patterning event which affords gross and subtle anatomical and functional cortical area establishment during brain development (Silva et al., 2019). For the most part, neuronal migration is the critical process that ensures proper placement of groups of neurons into their fated cortical laminae during morphogenesis of the cortex. Hence, in the event of neuronal misplacement due to abnormal migration, the cortex is mis-laminated and the ectopic neurons become susceptible to developmental anomalies, including abnormal differentiation, incorrect neurite formation and synaptogenesis, and dysregulated cell death, which can culminate in many neurodevelopmental disorders (Valiente and Marin, 2010; Evsyukova et al., 2013; Severino et al., 2020).

The bona fide cortical excitatory neurons generated by radial glia (RG) cells in the ventricular zone (VZ) or by neurogenic progenitors in the subventricular zone (SVZ) of the developing mouse cortex make challenging radial navigations from their place of birth to reside in defined regions (layers) in the cortical plate (CP) by means of radial migration (Noctor et al., 2001, 2002; Pontious et al., 2008). Radial migration can occur in the form of somal translocation or locomotion (Nadarajah et al., 2001). During somal translocation, which is mainly used by early born neurons, the nascent neuron elaborates a long leading process anchored at the pial basement membrane. By means of progressive traction force generated by shortening of the long leading process, the soma of the neuron is continually translocated to be placed in its designated cortical lamina (Miyata et al., 2001; Nadarajah et al., 2001).

Locomotion on the other hand is a complex and multiphasic process. Unlike somal translocation, it depends on the molecular and structural guidance of RG fibers needed for radial profiles of neuronal movement that largely contribute to the formation of superficial neocortical layers (Rakic, 1972). The locomoting neuron, mainly late-born, displays striking morphological changes in the course of its trajectory. Notably, during locomotion, the newborn neuron briefly attaches to its mother glial fiber or the adjoining fiber and actively moves with a bipolar morphology into the lower part of the intermediate zone (IZ). In the IZ, the bipolar neuron disengages from the glial fiber to momentarily pause radial migration. It then transitions to or adopts a multipolar morphology with which it makes undefined micro-movements to probably collect directional cues for subsequent radial (oriented) migration. Upon adequate molecular conditioning and transient NMDA receptor-mediated glutamatergic synaptic stimulation, the multipolar neuron then switches back to bipolar morphology in the vicinity of the upper IZ and re-attaches to the glial fiber to resume locomotion to its final destination in the CP (Kriegstein and Noctor, 2004; Noctor et al., 2004; Inoue et al., 2014; Mizutani, 2018; Ohtaka-Maruyama et al., 2018). The bipolar neuron characteristically extends a pia-directed leading process, the dendrite-to-be, and a trailing process toward the VZ which becomes the future axon (Rakic et al., 1996). Adopting the appropriate neuronal morphology or polarity is a key determinate of successful radial migration and cortical layer formation, which when perturbed can lead to cortical malformation (Hakanen et al., 2019). Locomotion ends in the CP by detachment of the migrating neuron from the glial fiber to be properly positioned in its home layer via somal translocation (Nadarajah et al., 2001).

Indeed, radial neuronal migration is a complex cell biological process which must be under tight molecular regulation. As such, a myriad of factors, including transcriptional and signaling factors, have been identified to spatiotemporally regulate various aspects of cortical neuron radial migration (reviewed in Heng et al., 2007; Marin et al., 2010; Evsyukova et al., 2013). Notably, it has been shown in seminal studies that the formation and maintenance of RG fibers, and related neuronal cell adhesion dynamics are tightly regulated during radial migration (Anton et al., 1997, 1999; Elias et al., 2007; Kawauchi et al., 2010; Shikanai et al., 2011; Sild and Ruthazer, 2011; Valiente et al., 2011; Solecki, 2012; Desai et al., 2013; Evsyukova et al., 2013; Schmid et al., 2014; Tonosaki et al., 2014; Jinnou et al., 2018; Louhivuori et al., 2018; Schaffer et al., 2018; Zhang et al., 2019).

Epigenetic factors have lately been at the center stage of neurodevelopment regulation after previous underestimation of their phenomenal role in orchestrating neural development. Emerging among these epigenetic regulators are the chromatin remodelers which can redesign the epigenetic landscape to influence gene expression and related cell biological events through direct alteration of chromatin structure and/or the recruitment of other epigenetic or transcriptional cofactors during cortical development (Sokpor et al., 2018).

The Brg1/Brm-associated factor (BAF) complex, a mammalian version of the yeast SWI/SNF complex, is a multi-subunit protein complex which primarily functions as a chromatin remodeler (Clapier et al., 2017) and has been shown in recent years to be indispensable for neural development (Son and Crabtree, 2014; Sokpor et al., 2017, 2018). During cortical development, the BAF complex regulates key processes such as specification, proliferation, differentiation, and functional maturation of cortical progenitors or postmitotic neurons (Son and Crabtree, 2014; Sokpor et al., 2017, 2018). Notably, the BAF complex subunits can be reconstituted to form cell type specific variants that have unique functional effects. For example, there are some compositional and functional differences between the BAF complex in neural progenitors (npBAF) and the BAF complex in neurons (nBAF) (Lessard et al., 2007; Wu et al., 2007; Kadoch et al., 2013; Tuoc et al., 2013; Bachmann et al., 2016).

Although chromatin remodelers, including some BAF subunits, have been reported to regulate neuronal migration in the developing mammalian cortex (Nott et al., 2013; Wiegreffe et al., 2015; Nitarska et al., 2016; Xu et al., 2018) and in worm neural tissue (Weinberg et al., 2013), the mechanism involved is far from clear. In this current study, we aimed at elucidating the molecular and cellular mechanisms by which the BAF complex orchestrates migration of excitatory projection neurons in the developing cortex. To this end, we abolished the BAF complex in early and late cortical progenitors and specifically in postmitotic neurons to investigation how BAF complex(es) influence neuronal migration during corticogenesis. From our molecular and cellular analyses of the BAF complex mutant (knockout and knockdown) cortex, it was evident that neurons fail to migrate

properly in the absence of BAF complex functionality. As a result, cortical neurons are misplaced in the mutant cortex leading to abnormal cortical cytoarchitectonic and concomitant laminar malformation. The BAF complex-ablated cortical neuron is incapable of proper radial migration because of loss of glial fiber guides and cell adhesion, defective cell polarization, and abnormal Wingless/Int (WNT) signaling activity. Indeed, the said altered intrinsic and extrinsic elements are known to be vital for correct radial migration, and are tightly modulated by many regulatory factors during cortical development (reviewed in Evsyukova et al., 2013); to which we here add BAF complex as a critical component.

MATERIALS AND METHODS

Animal Handling and Generation of Transgenic Mice

We applied guidelines of the German Animal Protection Law in handling the animals. Floxed BAF155 (Choi et al., 2012), floxed BAF170 (Tuoc et al., 2013), Emx1-Cre (Gorski et al., 2002), hGFAP-Cre (Zhuo et al., 2001), and Nex-Cre (Goebbels et al., 2006) transgenic mice were used in the study. All animals were maintained in a C57BL6/J background.

To eliminate BAF155 and BAF170 in early or late cortical progenitors, and in postmitotic neurons, we crossed mice carrying floxed BAF155 and BAF170 genes with the early progenitor-active Emx1-Cre (Gorski et al., 2002) or late progenitor-active hGFAP-Cre (Zhuo et al., 2001) and neuron-specific Nex-Cre (Goebbels et al., 2006) mouse lines to generate dcKO_Emx1-Cre, dcKO_hGFAP-Cre, and dcKO_Nex-Cre mutants, respectively. Heterozygous animals (BAF155fl/+, BAF170fl/+, Cre negative) were used as controls. Emx1-Cre mutants die before birth, whereas hGFAP-Cre and Nex-Cre mutants survive early postnatal stages.

Plasmids

The following plasmids were used in the study: pCIG2-eGFP, pCIG2-Cre-ires-eGFP (gift from Prof. Francois Guillemot, NIMR London; Hand et al., 2005), and NeuroD-Cre-ires-GFP, NeuroD-GFP (gift from Prof. Laurent Nguyen, University of Liège, CHU Sart Tilman, Liège, Belgium).

Antibodies

Commercially obtained monoclonal (mAb) and polyclonal (pAb) primary antibodies used in the study: CTIP2 rat pAb (1:200; Cat. ab18465; Abcam), Cux1 rabbit pAb (1:50; Cat. sc-13024, Santa Cruz), GM130 rat mAb (1:100; Cat. 610823; BD), BAF170 rabbit pAb (1:100; Cat. HPA021213; Sigma), BAF60a mouse mAb (1:200; Cat. 611728; BD), BAF155 rabbit pAb (1:20; Cat. sc-10756; Santa Cruz), BRM rabbit pAb (1:200; Cat. ab15597; Abcam), BRG1 rabbit pAb (1:120; Cat. sc-10768X; Santa Cruz), BAF155 mouse mAb (1:100; Cat. sc-48350X; Santa Cruz), BAF250b mouse mAb (1:100; Cat. WH0057492M1; Sigma), Tbr1 rabbit pAb (1:300; Cat. ab31940; Abcam), α-Catenin rabbit pAb (1:200; Cat. C2081; Sigma), Pax6 mouse mAb (1:100; Developmental Studies Hybridoma Bank), Nestin mouse mAb (1:50; Cat. 611658, BD), Pax6 rabbit pAb (1:200; Cat. PRB-278P; Covance), GFP chicken pAb (1:500; Cat. ab13970; Abcam). Secondary antibodies used were Alexa 488-, Alexa 568-, Alexa 594- and Alexa 647-conjugated IgG (various species, 1:400; Molecular Probes).

RNA Sequencing

RNA sequencing (RNA-seq) and analyses were performed as previously described in Narayanan et al. (2015, 2018), Nguyen et al. (2018). The high throughput RNA-seq data has been deposited in the NCBI Gene Expression Omnibus and accessible via the accession number GSE106711 and also at Narayanan et al. (2015), Nguyen et al. (2018).

Immunohistology and *in situ* Hybridization

Immunohistochemical staining and *in situ* hybridization of cortical tissue sections were performed as previously described (Tuoc et al., 2013; Bachmann et al., 2016; Wagener et al., 2016). The following RNA probes were used in the *in situ* hybridization experiment: *Ndnf* (*A930038C07Rik*), *Rorb* (*Rorbeta*), *Etv1* (*Er81*), and *TC1460681* (simply designated *TC*), to label cortical layers 1, 4, 5, and 6, respectively (Wagener et al., 2016).

Imaging and Quantitative Analysis

Coronal mouse brain sections were imaged with confocal (TCS SP5, Leica) and/or widefield fluorescence (Axio Imager M2, Zeiss; fitted with Neurolucida software, MBF Bioscience) microscopes. Further image processing was done with Adobe Photoshop program.

Neuronal cell counting and distribution (bin analysis), and leading process length estimation were performed using NIH ImageJ software. Neuronal cells with nuclear or cytoplasmic labeling for specific markers with or without DAPI staining, were counted in 4–6 structurally-matched control and mutant (dcKO) or electroporated cortical sections obtained from 3 to 4 biological replicates. Fluorescent signal intensity measurement was used to quantify uncountable histological staining in confocal images using ImageJ software as previously reported (Tuoc and Stoykova, 2008; Narayanan et al., 2015).

In utero Electroporation

In utero electroporation was done as previously described (Tabata and Nakajima, 2001; Tuoc and Stoykova, 2008; Tuoc et al., 2013). In brief, the pregnant mouse was surgically operated to expose the E14.5 embryos in the intact uterus. About 3 μL of a mixture of the plasmid of interest (2 μg/μL) and 0.5% fast green, at a ratio of 1:10, was then injected into one lateral ventricle of the embryo's brain. Transfection of the cortical neuroepithelium was achieved by applying 5 pulses of current (∼30 V) across the brain, with the positive terminal of the electroporator on the injected side of the cortical hemisphere. Every other embryo was injected and electroporated for each set of embryos in the uterus. Embryos were then returned into the abdominal cavity and the surgical incision was closed. The brains of the electroporated

embryos were then harvested at E17.5 for histological processing and microscopic analysis.

Pharmacological Treatment Using WNT Inhibitor

ICG001 (Tocris Bioscience, Cat. No. 4505), was dissolved in DMSO (vehicle). Pregnant mice received daily intraperitoneal injections of vehicle (150 μL), or ICG001 (150 μL of a 1.0 mg/mL solution) from 11.5 to 16.5 days post coitum (d.p.c.). The brains of the treated embryos (control and mutant) were harvested and processed for histological analysis at Embryonic day (E) 17.5.

Statistical Analyses

Prism was used to perform statistical analyses. Statistical comparisons were carried out using Student's *t* test or its non-parametric equivalent, the Mann–Whitney *U* Test, and one-way ANOVA followed by Bonferroni's multiple comparison (*Post Hoc*) test or the non-parametric equivalent Kruskal–Wallis test followed by Dunn's multiple comparison test, where appropriate. The results are presented as means ± SEM or median and range for non-parametric data.

RESULTS

Loss of BAF Complex in Cortical Progenitors Results in Impaired Neuronal Migration Leading to Cortical Mis-Lamination

We previously identified that the BAF complex function is abolished by double deletion of its scaffolding subunits BAF155 and BAF170. In the absence of BAF155 and BAF170, the entire BAF complex stability is compromised. This leads to disassembly of other components (subunits) of the complex, making them susceptible to proteasomal degradation with attendant functional inactivation of the entire BAF complex (Narayanan et al., 2015; Bachmann et al., 2016; Nguyen et al., 2016, 2018).

Given that cortical mass is dramatically reduced when BAF complex is abolished in the neuroepithelium of early developing cortex at the onset of neurogenesis (Narayanan et al., 2015), we were unable to comprehensively study neuronal migration in the mouse cortex that has lost BAF155 and BAF170 from E10.5 onward as achieved in the dcKO_Emx1-Cre cortical model (**Supplementary Figures 1, 2**). This warranted our choice of another mutagenic strategy that allowed us to delete the BAF complex at a later stage of corticogenesis. Thus, we generated the dcKO_hGFAP-Cre mouse forebrain model in which BAF155 and BAF170 are deleted predominately in the VZ progenitors of the developing cortex to achieve ablation of the entire BAF complex (**Supplementary Figure 1**; Nguyen et al., 2018). Because the hGFAP-Cre is relatively late-acting, with the earliest activity detected around E13.5 (Zhuo et al., 2001; Nguyen et al., 2018), we were able to lessen the impact of loss of BAF complex on cortical morphogenesis compared with that caused in the dcKO_Emx1-Cre (**Figure 1** vs. **Supplementary Figure 2**). Therefore, the dcKO_hGFAP-Cre model allowed us to study neuronal migration at late embryonic and early postnatal stages of cortical development with fairly preserved cortical integrity in the absence of BAF complex.

We characterized the neuronal migration phenotype of the E17.5 cortex, by which time the knockout effect under the hGFAP-Cre activity is fully established in the entire cortex (Nguyen et al., 2018). We started by reanalyzing our previously generated RNA-seq data from the E17.5 cortex in which 1329 genes and 1195 genes were downregulated and upregulated, respectively (**Figure 1A**; Nguyen et al., 2018). We then screened for gene categories implicated in the regulation of neuron migration in the cortex. Consistent with our observations in the E12.5 dcKO_Emx1-Cre cortex (**Supplementary Figures 2A,B**), we found several gene pathways involved in neuronal cell migration, cell polarity establishment, neurite formation, and cell adhesion downregulated in the dcKO_hGFAP-Cre cortex (**Figure 1B**). Given that these categories of factors play crucial roles in oriented-neuronal migration (locomotion) to afford proper cortical lamination, we further probed the dcKO_hGFAP-Cre cortex for specific factors that can affect the radial migration of neurons therein. We selectively focused on the integrity of radial glial scaffolds and cell adhesion in the BAF complex mutant cortex due to their striking roles in radial migration (Nadarajah et al., 2001; Kriegstein and Noctor, 2004; Noctor et al., 2004; Drees et al., 2005; Elias et al., 2007; Schmid et al., 2014; Schaffer et al., 2018). Thus, immunohistochemical investigations for the adhesion protein α-Catenin and the Nestin+ RG fibers in the E17.5 control and dcKO_hGFAP-Cre cortex, which are notably downregulated in the dcKO_Emx1-Cre cortex (**Supplementary Figures 2C–E**), were performed. As expected, we found demonstrable depletion of RG fibers and reduction in the apical and intra-cortical expression of cell adhesion (α-Catenin) in the dcKO_hGFAP-Cre cortex as compared with control (**Figures 1C–E**). Alternative proteins that indicate radial glial fiber identity (BLBP, GLAST, RC2) and related cell adhesion proteins (ZO1, Occludin) were shown to be reduced in the BAF complex-ablated developing cortex (Narayanan et al., 2015; Nguyen et al., 2018). Moreover, the delamination, dispersion, and hyperproliferation of BAF155 and BAF170-deficient neural stem cells (Pax6-expressing cortical progenitors) also reflect loss of their fiber-mediated anchorage in the cortical wall (Narayanan et al., 2015, 2018; Nguyen et al., 2018; Xie et al., 2019). These observations imply that radial glial scaffolds are actually lost in the absence of BAF complex functionality.

The neuronal migration phenotype in the E17.5 dcKO_hGFAP-Cre and control developing cortex was assessed by applying antibodies against the lower layer (L5) cortical neuron marker protein Ctip2 (Arlotta et al., 2005; Gaspard et al., 2008) and the cortical layer (L2/3) neuron marker protein Cux1 (Nieto et al., 2004). It was revealed that loss of BAF complex at later-stage of embryonic corticogenesis severely disturbed migration of both lower (L5) and upper layer (L2/3) neurons in the E17.5 dcKO_hGFAP-Cre. Neurons expressing Ctip2 or Cux1 were observed to spread in the entire E17.5 dcKO_hGFAP-Cre cortex instead of forming their respective layers as outlined in the control images (**Figures 1F–H**). Because the dcKO_hGFAP-Cre

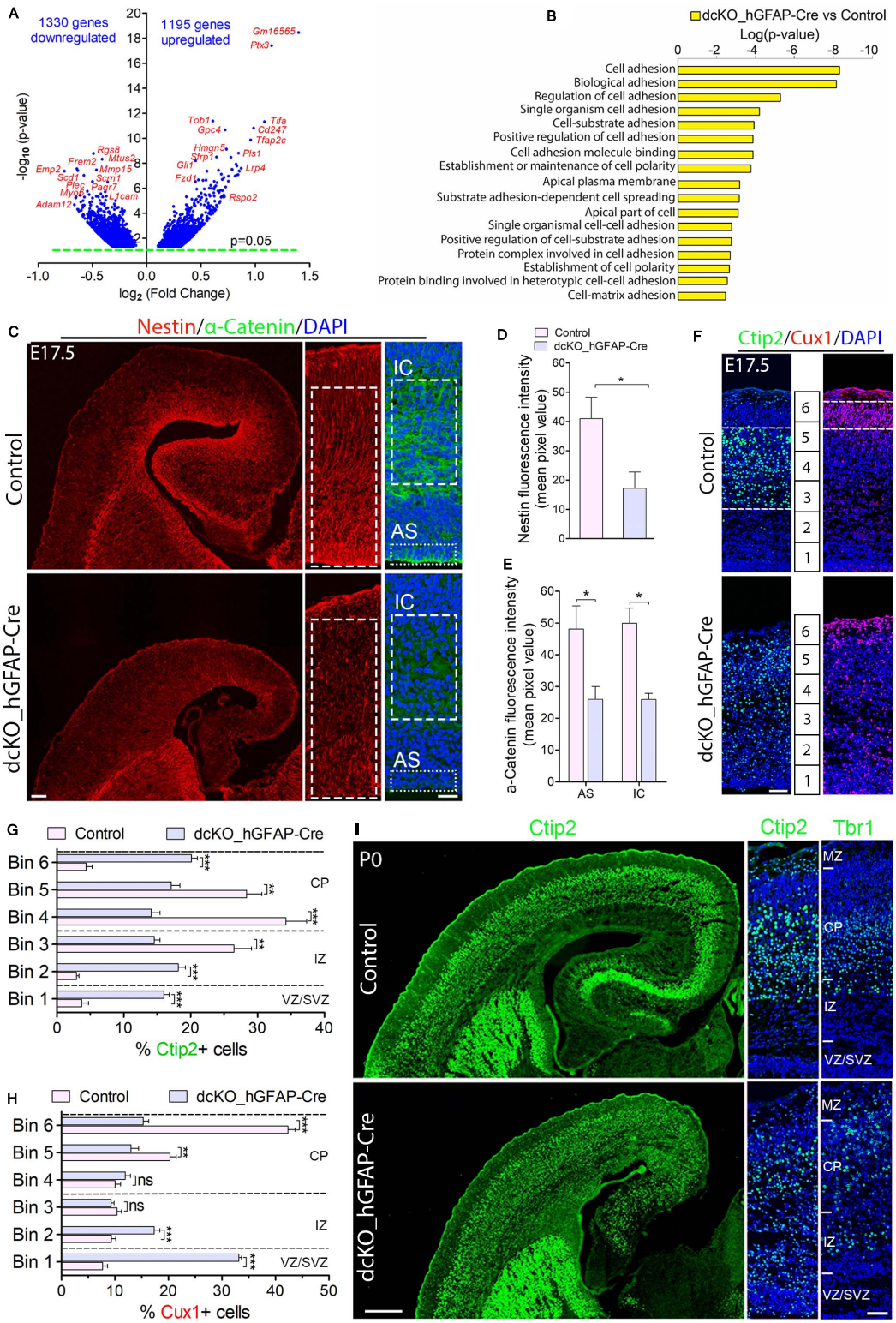

FIGURE 1 | Cortical layers are malformed in the absence of BAF complex, and attributable to loss of cell adhesion and glial fiber scaffolds. **(A)** Volcano plot showing genes downregulated and upregulated in the E17.5 dcKO_hGFAP-Cre cortex. Examples of top altered genes are indicated. **(B)** Graph showing downregulation of selected gene categories or pathways mainly related to cell adhesion and polarity formation in the E17.5 dcKO_hGFAP-Cre cortex. **(C)** Sections of E17.5 control and dcKO_hGFAP-Cre cortex immunostained for the glial fiber protein Nestin and the cell adhesion protein α-Catenin. Specifically quantified cortical areas are shown with rectangles with dashed or stippled lines. **(D,E)** Simple **(D)** and grouped **(E)** bar charts showing quantification of Nestin and α-Catenin, respectively, in the E17.5

(Continued)

FIGURE 1 | Continued
control and dcKO_hGFAP-Cre cortex. **(F)** Micrographs showing immunostaining with antibodies against Ctip2 and Cux1 to mark neurons that make the lower (deep) and upper (superficial) cortical layers, respectively, in the E17.5 control and dcKO_hGFAP-Cre cortex. White dashed lines are used to delineate the deep (Ctip2+) and superficial (Cux1+) cortical layers. Bins (1–6) for neuronal distribution analysis are indicated. **(G,H)** Bar charts showing quantitative distributions of Ctip2+ deep layer neurons and Cux1+ superficial layer neurons in the E17.5 control and dcKO_hGFAP-Cre cortical wall. Quantified cortical area = (420 μm × 170 μm). **(I)** Micrographs showing the P0 control and dcKO_hGFAP-Cre cortex with Ctip2 and Tbr1 immunostaining. Where shown, sections are counterstained with DAPI (blue). Unpaired Student's *t*-test was used to test for statistical significance: $^{*}p < 0.01$, $^{**}p < 0.001$, $^{***}p < 0.0001$; ns, not significant; $n = 6$. Scale bars: = 100 μm and 50 μm in overview and zoomed images, respectively. Results are presented as mean ± SEM. IC, intracortical; AS, apical surface; VZ, ventricular zone; SVZ, subventricular zone; IZ, intermediate zone; CP, cortical plate; MZ, marginal zone.

mutants barely survive early postnatal life, we limited the postnatal characterization of the migration phenotype to P0 (i.e., just after birth), and by which time the majority of lower layer cortical neurons [Tbr1 + (L6) and Ctip2 + (L5) neurons] have largely completed somal translocation or locomotion to properly settle in their respective layers (Nadarajah et al., 2001; Marin and Rubenstein, 2003; Molyneaux et al., 2007). Unlike Cux1 or Brn2+ neurons, Tbr1+ or Ctip2+ neuron production is minimally affected by hGFAP-Cre-mediated BAF155 and BAF170 deletion in the early postnatal cortex (Nguyen et al., 2018). Therefore, we immunohistologically compared the distribution of lower layer neurons in the P0 control and dcKO_hGFAP-Cre cortex (**Figure 1I**). Quantitative analysis indicated significant mis-distribution of Ctip2+ L5 neurons in the P0 dcKO_hGFAP-Cre cortex as compared with control (**Supplementary Figure 3A** and **Figure 1I**). Although, majority of the Tbr1 + L6 neurons migrated out of the germinal zone, they appear to have over-migrated, making them locate in the upper layer domain in the P0 dcKO_hGFAP-Cre cortex as compared with control (**Supplementary Figure 3B** and **Figure 1I**). Additional check also showed that Brn2-expressing upper layer neurons are also unable to migrate properly in the dcKO_hGFAP-Cre cortex, leading to their accumulation in the lower half of the E18.5 mutant cortical wall instead of settling in their destined upper cortical layers as in control (**Supplementary Figures 3C,D**).

Together, these results strongly implicate the role of the BAF complex in orchestrating radial migration of cortical neurons and proper cortical layer development. However, just like in the dcKO_Emx1-Cre model (**Supplementary Figure S2F**), the migration phenotype in the dcKO_hGFAP-Cre cortex co-existed with disruption in progenitor cell proliferation and differentiation consequent to BAF complex inactivation in neural stem cells (Narayanan et al., 2015; Nguyen et al., 2018). Thus, a postmitotic neuron-specific disruption of BAF complex function is necessary to exclude abnormal neurogenesis in our cortical neuron migration model.

Ablation of BAF Complex in Postmitotic Neurons Caused Abnormal Migration of Upper Cortical Layer Neurons

Specifically targeting nascent cortical neurons for BAF complex inactivation is necessary to study migration defects independent of key extrinsic factors such as glial fibers or cell adhesion elements essential for radial migration. To achieve the neuron-specific ablation of BAF complex, we resorted to the Nex-Cre line (Goebbels et al., 2006). We generated the dcKO_Nex-Cre mouse line in which BAF155 and BAF170 are deleted exclusively in the principal neurons generated in the cortex from E10.5 onward (**Supplementary Figure 1**; Goebbels et al., 2006). The dcKO_Nex-Cre cortex can be seen to have lost the expression of other core subunits of the BAF complex together with BAF155 and BAF 170, although some residuals can be seen in the mutant cortex, which are likely expressed by glia or interneurons that are not affected by the NeuroD-Cre activity (**Supplementary Figure 4**).

Characterization of the migration phenotype in the dcKO_Nex-Cre cortex was mainly done at early postnatal stage P1 due to early lethality of mutants. Generally, the gross forebrain phenotype of the dcKO_Nex-Cre cortex was less severe as compared with the dcKO_hGFAP-Cre cortex (data not shown). To identify subtle migration defects, we first performed fluorescence *in situ* hybridization (FISH) experiment in which the P1 dcKO_Nex-Cre and control cortex were riboprobed with the layer specific markers *TC*, *Etv1*, *Rorb*, and *Ndnf* which label the cortical layers 6, 5, 4, 1, respectively. Based on distribution of the aforementioned FISH probe signals, it was observed that cortical layers are much less defined in the CP of the P1 dcKO_Nex-Cre cortex compared with control (**Figure 2A**). The pattern particularly gives an impression of a wide spreading of upper layer neurons in the CP, with lower layer neurons displaying a mild form of such amorphous distribution in the P1 dcKO_Nex-Cre cortex (**Figure 2A**). Because the Ndnf-marked L1 neurons are Cajal-Retzius cell which migrate tangentially into the cortex from other cortical areas like the hem (Bielle et al., 2005), they are presumably not affected by the Nex-Cre-mediated ablation of BAF complex; hence they displayed no disturbance in their laminar fate in the P1 mutant cortex compared to control (**Figure 2A**).

At the protein level, our immunohistochemical analysis showed that loss of BAF complex led to a mild defect in the migration of Cux1+ upper layer neurons in the P1 dcKO_Nex-Cre cortex compared with control (**Figures 2B,C**), without significantly affecting the generation of such superficial cortical layer neurons (**Figure 2D**). Analysis using Brn2 immunolabeling corroborated the abnormal (mildly delayed) migration of upper layer neurons lacking BAF155 and BAF170 (**Supplementary Figure 5**). However, migration and distribution of Ctip2+ lower layer neurons, which are also normally generated in the dcKO_Nex-Cre cortex, were less obviously affected (**Figures 2C,E**). Indeed, bin analyses revealed fewer number of Cux1+ neurons reached Bins 4 and 5 in the dcKO_Nex-Cre cortex compared with control (**Figure 2F**),

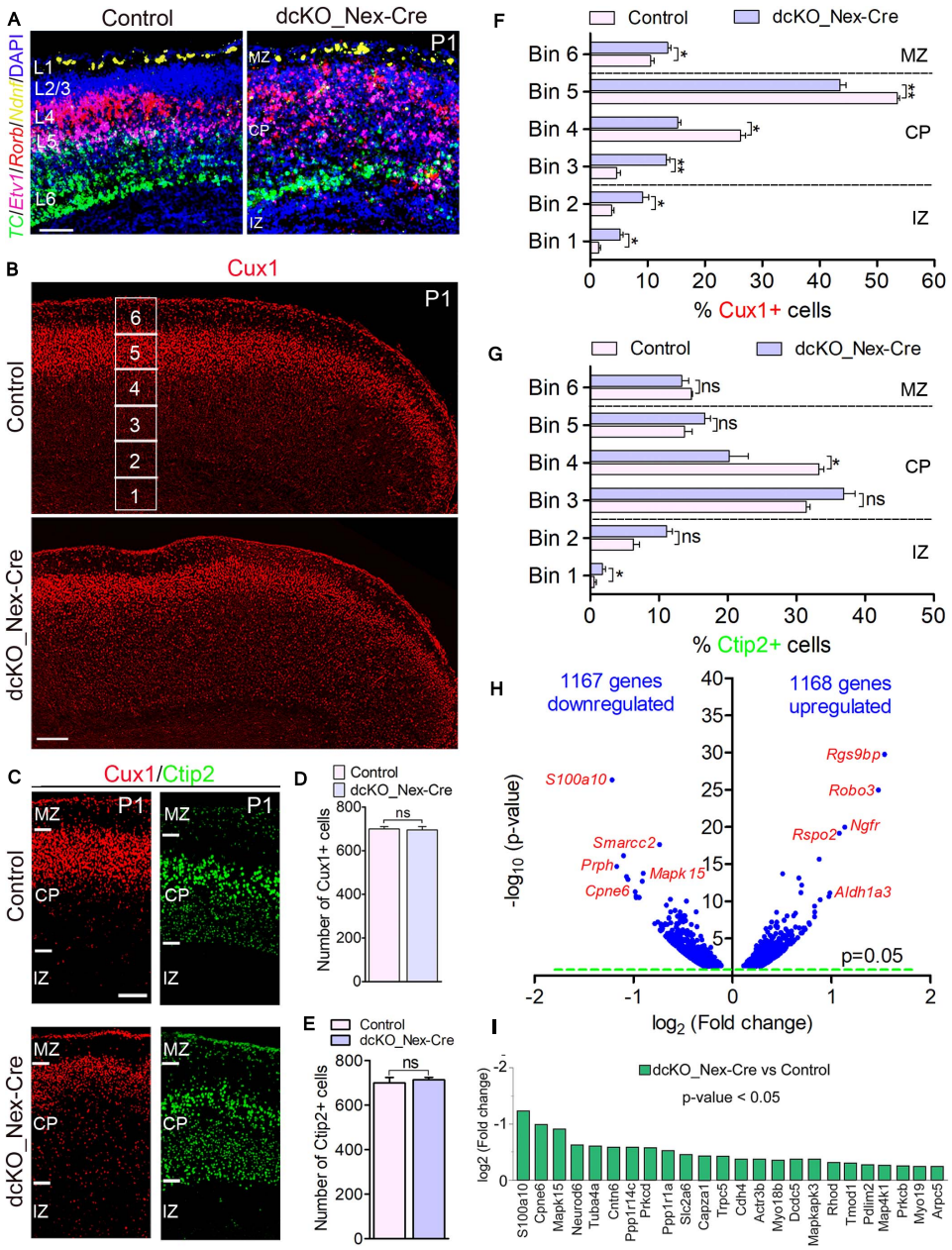

FIGURE 2 | Neuron-specific ablation of BAF complex causes downregulation of cell morphogenesis-related genes leading to delayed neuronal migration. **(A)** Micrographs showing fluorescence *in situ* hybridization in the P1 control and dcKO_Nex-Cre cortex stained with the layer-specific RNA probes *TC1460681*, *Etv1*, *Rorb*, and *Ndnf* to reveal cortical layers 6, 5, 4, and 1, respectively. **(B)** Overview micrographs showing immunostaining of the P1 control and dcKO_Nex-Cre cortex with Cux1 antibody to mainly mark cortical layer 2/3 neurons. Bins (1–6) for neuronal distribution analysis are indicated. **(C)** Micrographs with cortical regions indicated showing Cux1 and Ctip2 immunostaining of the P1 control and dcKO_Nex-Cre cortex. **(D,E)** Bar charts showing comparable number of Cux1+ **(C)** and Ctip2+ **(D)** neurons in the P1 control and dcKO_Nex-Cre cortical wall. **(F,G)** Bar graphs showing quantitative distribution (Bin analysis) of Cux1+ **(F)** and Ctip2+ **(G)** neurons in the P1 control and dcKO_Nex-Cre cortical wall. Quantified cortical area = (720 μm × 400 μm). **(H)** Volcano plot show genes downregulated and upregulated in the P1 dcKO_Nex-Cre cortex compared with control. Examples of top altered genes are shown. **(I)** Bar chart showing specific neuronal morphogenesis-related genes with reduced expression in the P1 dcKO_Nex-Cre cortex. Where shown, sections are counterstained with DAPI (blue). Unpaired Student's *t*-test was used to test for statistical significance: $*p < 0.01$, $**p < 0.001$, ns, not significant; $n = 6$. Scale bar = 100 μm. Results are presented as mean ± SEM. IZ, intermediate zone; CP, cortical plate; MZ, marginal zone.

whereas the distribution of Ctip2+ neurons is arguably fairly normal in the absence of BAF155 and BAF170 (**Figure 2G**). Of note, unlike in the dcKO_hGFAP-Cre cortex (**Figures 1C,D**), radial glial fiber density or layout seems not to be disturbed in the dcKO_Nex-Cre cortex (**Supplementary Figures 6A–D**) following the deletion of BAF155 and BAF170 in postmitotic

neurons. Therefore, the upper layer neuron migration defect observed is likely independent of problems with the radial glial scaffolds in the dcKO_Nex-Cre cortex.

Consistent with the observed phenotype, we identified pertinent abnormal alterations in gene expression program in the P1 dcKO_Nex-Cre cortex that emphasized or may have underlined the disturbed neuronal migration. We found in our RNA-seq analysis that almost equal number of genes are downregulated (1167) as upregulated (1168) in the P1 dcKO_Nex-Cre cortex compared with control (**Figure 2H**). Notably, some of the top downregulated genes include those that are associated with neuronal migration. No overt change in the expression of cell adhesion genes was observed (**Figure 2H**, see RNA-seq data sheet). Interestingly, we noticed that many of the neuronal migration-related genes downregulated in neurons lacking BAF complex are key for cytoskeletal remodeling (**Figure 2I**), and needed for cell polarization and morphogenesis critical for cell migration (de la Torre-Ubieta and Bonni, 2011). Thus, the neurons in the P1 dcKO_Nex-Cre cortex may be incapable of adopting the right morphology suitable for their radial migration.

Altogether, we have shown that exclusive deletion of BAF complex in postmitotic neurons perturbs the expression of genes crucial for neuronal morphogenesis. This can lead to improper formation of neuronal appendages necessary for oriented-neuronal migration, and which has implication for defective or sluggish locomotion of cortical neurons.

Knockdown of BAF155 and BAF170 in Cortical Progenitors Led to Disoriented Neuronal Migration in Developing Cortex

In order to refine the cortical neuron migration phenotype due to loss of BAF complex so as to identify any alteration in the cellular dynamics involved, we employed the *in utero* electroporation technique (**Figure 3A**). This focal genetic ablation strategy afforded sparse loss of BAF complex in selected/single cortical neurons, thus making the resultant migration phenotype more conspicuous. To achieve this, we electroporated the mouse cortex double floxed for BAF155 and BAF170 with control plasmid pCIG2-eGFP (CAG-eGFP/GFP-only) or effector plasmid pCIG2-Cre-ires-eGFP (CAG-Cre-eGFP) into the E14.5 cortex (**Figure 3A**). Because the CAG-Cre is active in the cortical neuroepithelium, we essentially mimicked the neuronal migration phenotype due to loss of BAF complex under the Emx1- or hGFAP-Cre promoters as observed in the dcKO_Emx1-Cre and dcKO_hGFAP-Cre cortical models reported earlier (**Supplementary Figure 2** and **Figure 1**). The electroporated embryos were allowed to develop until E17.5 and then cortical tissue was collected for immunohistological analyses.

By means of GFP immunostaining, we were able to track the progress of transfected migrating cortical neurons from the Pax6-marked VZ to the CP. We observed formation and fasciculation of the axons of the GFP-only transfected neurons, whereas the CAG_Cre-GFP transfected neurons failed to show noticeable axon formation; signifying possible differentiation defect in the neurons lacking BAF155 and BAF170 (**Figure 3B**). This can be linked to abnormal RG cell fiber-neuron contact or adhesion, which can disrupt axon formation and orientation during locomotion (Xu et al., 2015).

At higher magnification, it was evident that glial fiber-dependent (radial) migration of cortical neurons was disrupted following loss of BAF155 and BAF170. Compared with control, the BAF complex mutant (i.e., CAG_Cre-GFP-treated) neurons, presumably multipolar neurons, appeared to have accumulated in the lower regions of the cortical wall namely the Pax6-labeled VZ and SVZ, and the IZ, making the upper and lower aspects of the CP less populated with successfully migrated and/or properly migrating neurons (**Figures 3C,D**). We identified that the cortical neurons without functional BAF complex were mis-oriented with respect to their normal radial alignment and also exhibited abnormal polarity. This was revealed in our immunohistological examination of the Golgi apparatus localization and leading process length of migrating neurons in the middle and upper IZ (**Figures 3E,F**). The BAF complex-ablated bipolar neuron in the upper IZ had its GM130+ Golgi located close to the nucleus and presented a reduced leading process length (p-value = 0.0032, Mann–Whitney U Test; **Figures 3F–H**).

In further support of our assertion of defective directed-neuronal migration when BAF complex is inactivated in neurons, we observed reduced engagement of Nestin + glial fibers by the CAG_Cre-GFP-transfected migrating neurons compared with the GFP-only positive neurons in the upper IZ and lower CP (**Figure 3I**). In other words, based on neuron-glial fiber proximity (i.e., GFP and Nestin signal "colocalization"), whereas more than 80% of the control migrating neurons depend on or use the glial fiber scaffolds to radially migrate, far less proportion (16%) of CAG_Cre-GFP positive neurons seem to use glial fibers for migration—even in the presence of normal radial profiles of glial fibers (**Figures 3I,J**). Moreover, given the role of adhesion molecules in radial migration (Solecki, 2012), we inferred from the loss of cell adhesion in the developing cortex due to deletion of BAF155 and BAF170 (**Supplementary Figure 1** and **Figures 1A–E**) that it is possible the CAG_Cre-GFP positive neurons improperly attach to glial fibers (or not at all) because of loss of glial fibers and/or adhesion proteins leading to abnormal radial migration. Indeed, the decreased proportion of migrating neurons facing the pia, in mutants (CAG_Cre-GFP-transfected neurons) compared with control (GFP-only-transfected neurons) (**Figure 3K**) gives reason to abnormal radial migration seen in the BAF complex knockdown condition (**Figures 3B,C**).

In all, the reduced use of glial fibers for migration by the BAF complex-ablated cortical neurons and their defective Golgi-dependent polarization, may have contributed to their aberrant radial orientation and migration of neurons in the developing cortex.

BAF155 and BAF170-Deficient Migrating Cortical Neurons Display Defective Multipolar-to-Bipolar Transition

Applying the same logic and advantage of using the dcKO_Nex-Cre line as opposed to the dcKO_Emx1-Cre and hGFAP-Cre lines, we neuron-specifically knocked-down BAF155 and BAF170

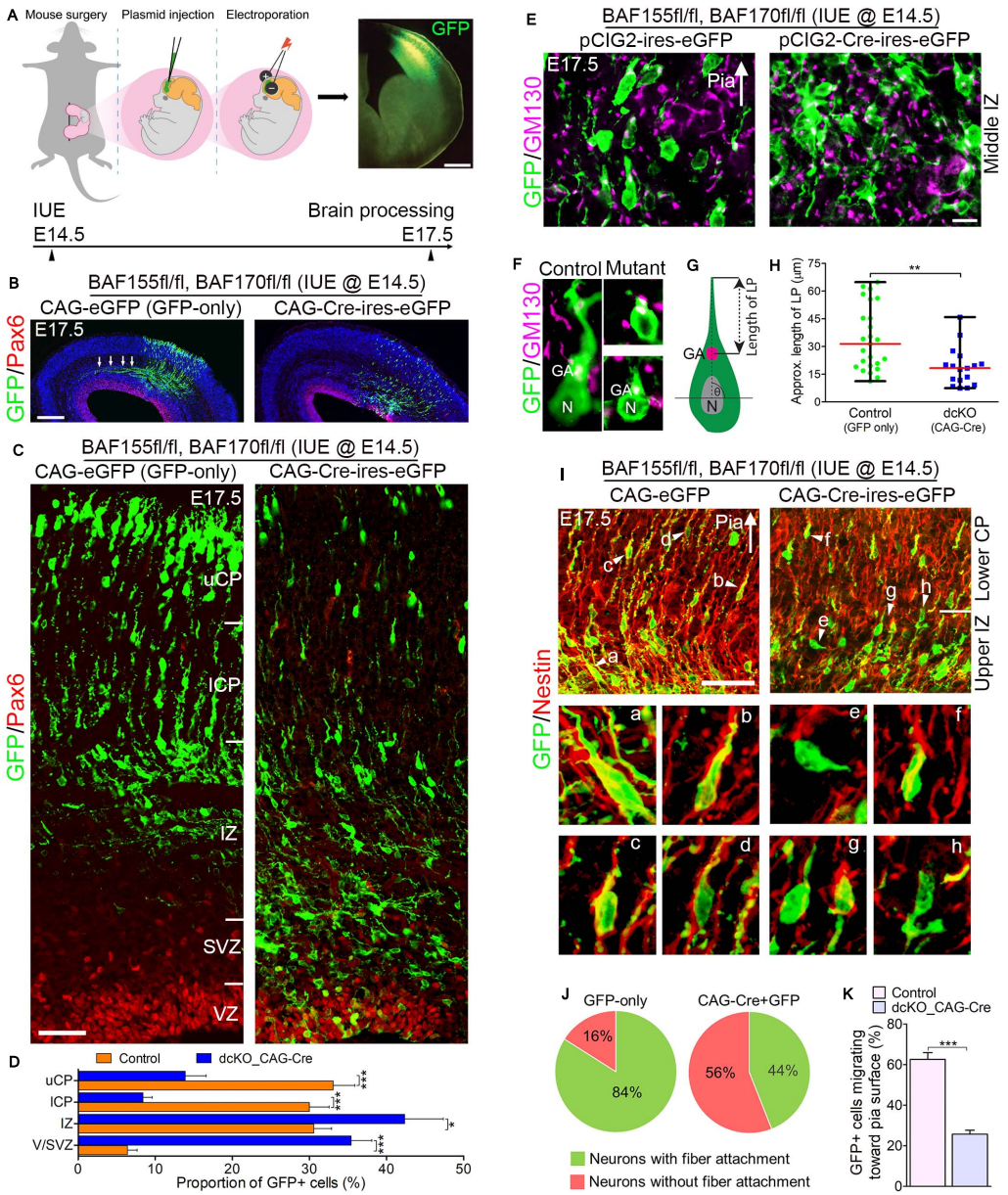

FIGURE 3 | Locomoting neurons without BAF complex exhibit abnormal polarity and radial direction mis-guidance. **(A)** Illustration of *in utero* electroporation technique used to achieve knockdown of BAF155 and BAF170. It shows a representative embryo in the uterine horn bearing double floxed BAF155 and BAF170 (BAF155fl/fl, BAF170fl/fl), and being injected in the brain with the plasmid of interest and electroporated at E14.5. Brain tissue was harvested at E17.5. A representative immunomicrograph showing GFP expression in E15.5 cortex is presented. **(B)** Immunohistochemical micrographs showing overview of Pax6 (to mark the germinal zone) and GFP staining in the E17.5 cortex (BAF155fl/fl, BAF170fl/fl) electroporated with control (GFP-only) or CAG-Cre + GFP plasmids. Arrows in control image point to outgrowth of axons. **(C)** Micrographs showing the electroporated cortical areas in **(B)** at higher magnification. Approximate cortical wall regions are shown. **(D)** Bar chart showing distribution of GFP+ cells (neurons) in the various cortical regions in the control and CAG-Cre + eGFP plasmid-injected E17.5 cortex. **(E)** Images showing the E17.5 control and mutant cortical middle intermediate zone with GFP and GM130 staining (Golgi apparatus marker). Arrow points in the direction of the pia surface. **(F–H)** Micrographs with GFP and GM130 staining **(F)** and illustration **(G)** showing estimation of the leading process (LP) length of control and BAF complex mutant cortical neurons in the lower cortical plate, which is graphically (statistically) compared in **(H)**. **(I)** Images of the E17.5 control and mutant upper intermediate zone and lower cortical plate immunostained with GFP and Nestin antibodies to reveal neuron-glial fiber colocalization. Arrow heads (a–h) indicate examples of neurons migration with (a–d) or without/abnormally with (e–h) glial fiber guide. Arrow points in the direction of the pia surface. **(J)** Pie chart depicting the quantification of the proportion of GFP+ control and BAF complex mutant neurons migrating with or without glial fiber guide in the upper intermediate zone and lower cortical plate. **(K)** Bar chart showing the proportion of GFP+ neurons with their Golgi-leading process axis oriented toward the pia in **(I)**. Arrows in **(E,I)** points in the direction of the pia surface. Where shown, sections are counterstained with DAPI (blue). Unpaired Student's *t*-test was used to test for statistical significance: $^{*}p < 0.01$, $^{***}p < 0.0001$; $n = 4$, selected in total 25 and 17 control and mutant GFP+ neurons in the upper IZ/lower CP region for leading process length estimation, respectively. Scale bars: =200 and 50 μm in overview and zoomed images, respectively. Results are presented as mean ± SEM or median and range. IUE, *in utero* electroporation; GA, Golgi apparatus; N, nucleus; VZ, ventricular zone; SVZ, subventricular zone; IZ, intermediate zone; l/uCP, lower/upper cortical plate; MZ, marginal zone.

in the E14.5 cortex using a NeuroD-Cre-ires-GFP plasmid in another *in utero* electroporation experiment as in **Figure 3A**. Thus, the NeuroD-Cre-mediated inactivation of BAF complex in postmitotic nascent cortical neurons increased the specificity of the phenotypic effect on radially migrating neuron as compared with the CAG-Cre approach, which targeted the BAF complex in neural stem or progenitor cells.

Examination of GFP immunostaining in E17.5 cortex, double floxed for BAF155/BAF170, electroporated with control (NeuroD-GFP) and NeuroD-Cre-ires-GFP plasmids at E14.5 revealed marked disruption of radial neuronal migration in the absence of BAF complex (**Figure 4A**). While the Pax6-stained VZ in the cortex transfected with NeuroD-GFP or NeuroD-Cre-ires-GFP plasmids is devoid of GFP+ cells, the IZ and lower CP of the NeuroD-Cre-ires-GFP electroporated cortex are filled with more GFP+ cells compared with the control cortex (**Figures 4A,B**). However, as an indication of successful radial migration, the control upper CP is seen to be populated with significantly more GFP+ cells as compared with the NeuroD-Cre-ires-GFP treated cortex (**Figures 4A,B**).

One of the critical cellular processes during radial migration of cortical neurons is the transient transformation from multipolar to bipolar morphology, which occurs in the upper IZ (Nadarajah et al., 2001; Noctor et al., 2004). The function of the multipolar phase is not clearly known, albeit some believe directional cues are collected by the many temporary neurites of the neurons at this stage (Mizutani, 2018; Shikanai et al., 2018). The bipolar structure on the other hand is suited for the glial fiber attachment and subsequent active locomotion to the CP (Nadarajah et al., 2001; Noctor et al., 2004). This led us to in examining the morphological integrity of migrating neurons lacking BAF complex. We sampled and grouped the diverse forms of migrating neurons in the electroporated regions of the cortical wall into three morphological categories: unipolar/bipolar, multipolar, and non-polar (neurite-lacking) neurons (**Figure 4C**). Our statistical quantification revealed a significantly smaller proportion of bipolar or unipolar neurons in the NeuroD-Cre-ires-GFP electroporated cortical area compared with the NeuroD-GFP electroporated cortical area. However, we found more multipolar neurons in the NeuroD-Cre-ires-GFP electroporated cortex compared with the cortical area electroporated with NeuroD-GFP plasmid (**Figure 4D**). Strikingly, we also found more so-called non-polar neurons in the NeuroD-Cre-ires-GFP treated cortex, particularly in the CP, as compared with that in the control cortex. Such non-polar neurons presented only with their soma (**Figures 4A,C,D**). Consistent with observations in the CAG_Cre-GFP IUE experiment, neurons transfected with NeuroD-Cre-ires-GFP plasmid display short leading process (**Figure 4E**), and many of the leading processes were also not directed toward the pia surface (**Figure 4F**).

Based on these observations and as schematized in **Figure 4G**, our findings implicate the BAF complex in the regulation of multipolar-to-bipolar transition of cortical neurons during radial migration. As such, in the event of BAF complex dysfunction (i.e., under NeuroD-Cre-ires-GFP treatment condition), this neuronal morphology conversion is hindered, leading to accumulation of multipolar neurons in the IZ at the expenses of bipolar neurons in the CP (**Figures 5A,D,G**). Moreover, it is likely that even if it occurs, the morphological transformation of the BAF complex-lacking neurons is abnormal and results in aberrantly polar neurons with truncated and mis-oriented leading processes (**Figures 4A,E,F**). Thus, it is conceivable that the BAF complex mutant neurons undergo unconventional or complicated migration other than the suitable radial (glial-guided) migration that is prerequisite for correct laminar formation in the developing cortex.

Together, we identified the BAF complex to also regulate the process of multipolar-to-bipolar neuronal morphology transition, which is a rate-determining phase in the process of radial migration permissive for correct establishment of the various cortical layers–especially upper cortical layers–during development of the mouse cortex.

BAF Complex May Repress WNT Signaling to Permit Proper Neuronal Migration and Cortical Lamination During Brain Development

In order to identify possible molecular factors or mechanism that mediate BAF complex influence on radial migration of cortical neurons, we screened the results of our RNA-seq data generated for the BAF complex mutant and control developing cortex. With reference to our previous report that BAF complex regulates cortical neurogenesis via suppression of WNT signaling in the developing mouse cortex (Nguyen et al., 2018), we asked whether the neuronal migration phenotype in the BAF complex mutant brain is dependent on WNT signaling. Interestingly, several signaling pathways, including WNT signaling, have been implicated in neuronal migration regulation during brain development (Siegenthaler and Miller, 2004; Hashimoto-Torii et al., 2008; Yi et al., 2010; Boitard et al., 2015; Bocchi et al., 2017; Martinez-Chavez et al., 2018; Saxena et al., 2018). In the case of WNT signaling, it was reported that dynamic regulation of the cascade is necessary for multipolar-to-bipolar morphology transition during radial migration of cortical neurons (Boitard et al., 2015).

Gene set enrichment analyses indicated abnormal elevation of WNT signaling activity in the BAF complex mutant cortex. Thus, WNT signaling-related or target genes were significantly upregulated in the BAF complex mutant cortex (**Figures 5A–F**). Notably, the E17.5 dcKO_hGFAP-Cre displayed more WNT signaling-related factors with increased expression (**Figures 6A,B**; Nguyen et al., 2018) compared with that observed in the E12.5 dcKO_Emx1-Cre (**Figures 5C,D**) or P1 dcKO_Nex-Cre cortex (**Figures 5E,F**). Therefore, we considered the WNT signaling pathway as a potential candidate for rescuing the neuronal migration phenotype. To this end, we designed a rescue experimental paradigm for reducing the WNT signaling hyperactivity in the mutant cortex. We chose the dcKO_hGFAP-Cre cortex for our rescue experiment. The reason being that the dcKO_Emx1-Cre cortex is not appropriate for clearly visualizing neuronal migration dynamics because of massive cortical atrophy (**Supplementary Figure 2F**), and the observation that the

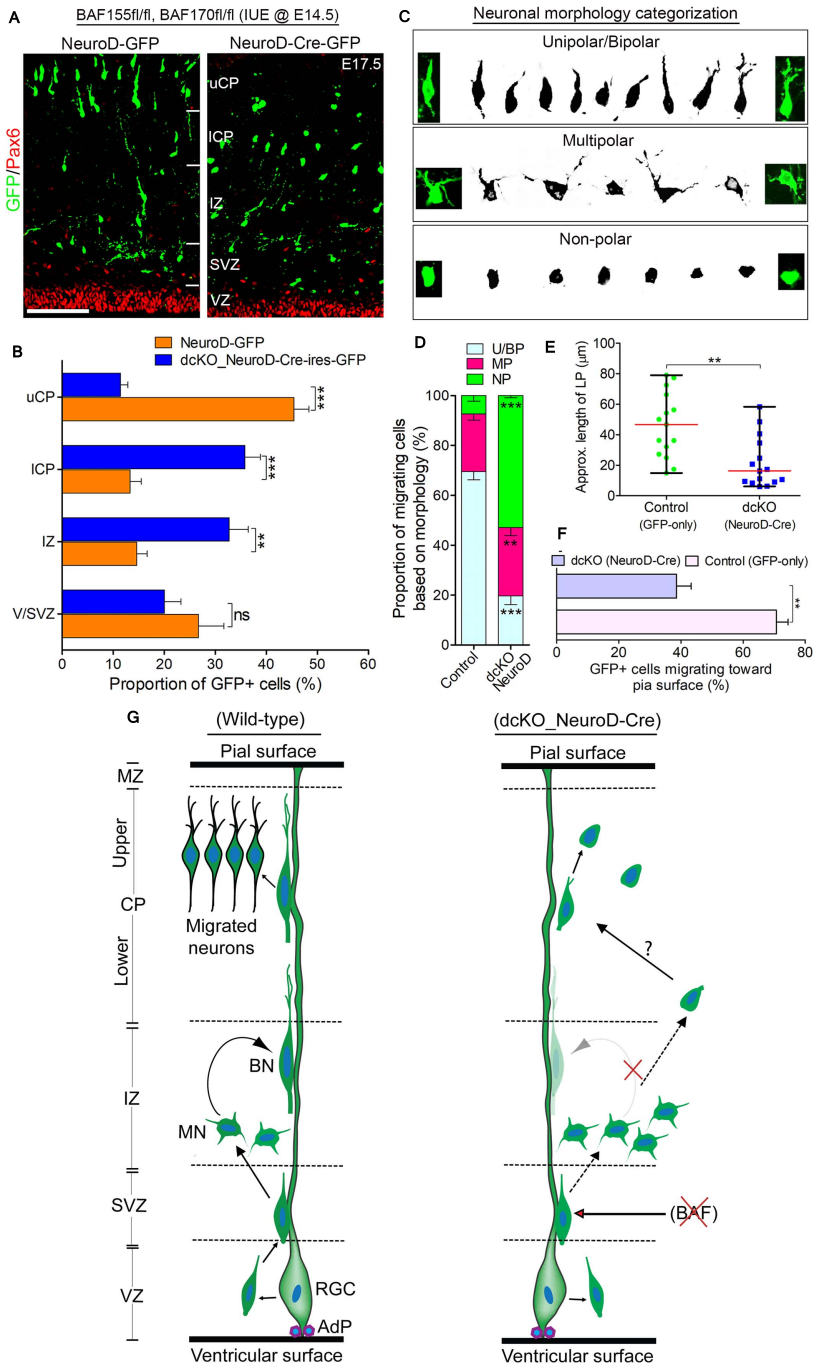

FIGURE 4 | BAF complex regulates multipolar-to-bipolar neuronal morphology transition during radial migration. **(A)** Micrographs showing Pax6 and GFP immunostaining in the E17.5 cortex (BAF155fl/fl, BAF170fl/fl) electroporated with control (NeuroD-GFP) or Cre (NeuroD-Cre-ires-GFP) plasmids. Approximate cortical regions are shown. **(B)** Bar chart showing percentage distribution of GFP+ neurons in the various cortical regions in the control (NeuroD-GFP) and NeuroD-Cre-ires-GFP plasmid-injected E17.5 cortex. **(C)** Images showing representative morphological groupings of the migrating neurons with or without BAF155/BAF170 (BAF complex) in the E17.5 cortex. **(D)** Composite bar graph showing the quantitative proportions of the various categories of neuronal morphologies (in **C**) in the E17.5 cortical areas electroporated with control (NeuroD-GFP) or NeuroD-Cre-ires-GFP plasmids. **(E)** Graph comparing the estimated leading process length of migrating neurons transfected with control or NeuroD-Cre plasmids. **(F)** Bar graph comparing the proportion of neurons migrating toward the pia surface in the cortex electroporated with control and NeuroD-Cre plasmids. **(G)** Graphical summary of the abnormal neuronal migration due to BAF complex ablation in neurons as compared with control. Solid (curved) arrows indicate normal transition, broken straight arrows denote abnormal morphology transition, and red crossed lines indicate suppression. Unpaired Student's *t*-test was used to test for statistical significance: $^{**}p < 0.001$, $^{***}p < 0.0001$; ns, not significant; $n = 4$. Results are presented as mean ± SEM or median and range. Scale bar: =50 μm. IUE, *in utero* electroporation; VZ, ventricular zone; SVZ, subventricular zone; IZ, intermediate zone; l/uCP, lower/upper cortical plate; MZ, marginal zone; U/BN, unipolar/bipolar neuron; MN, multipolar neuron; RGC, radial glial cell; AdP, adhesion protein.

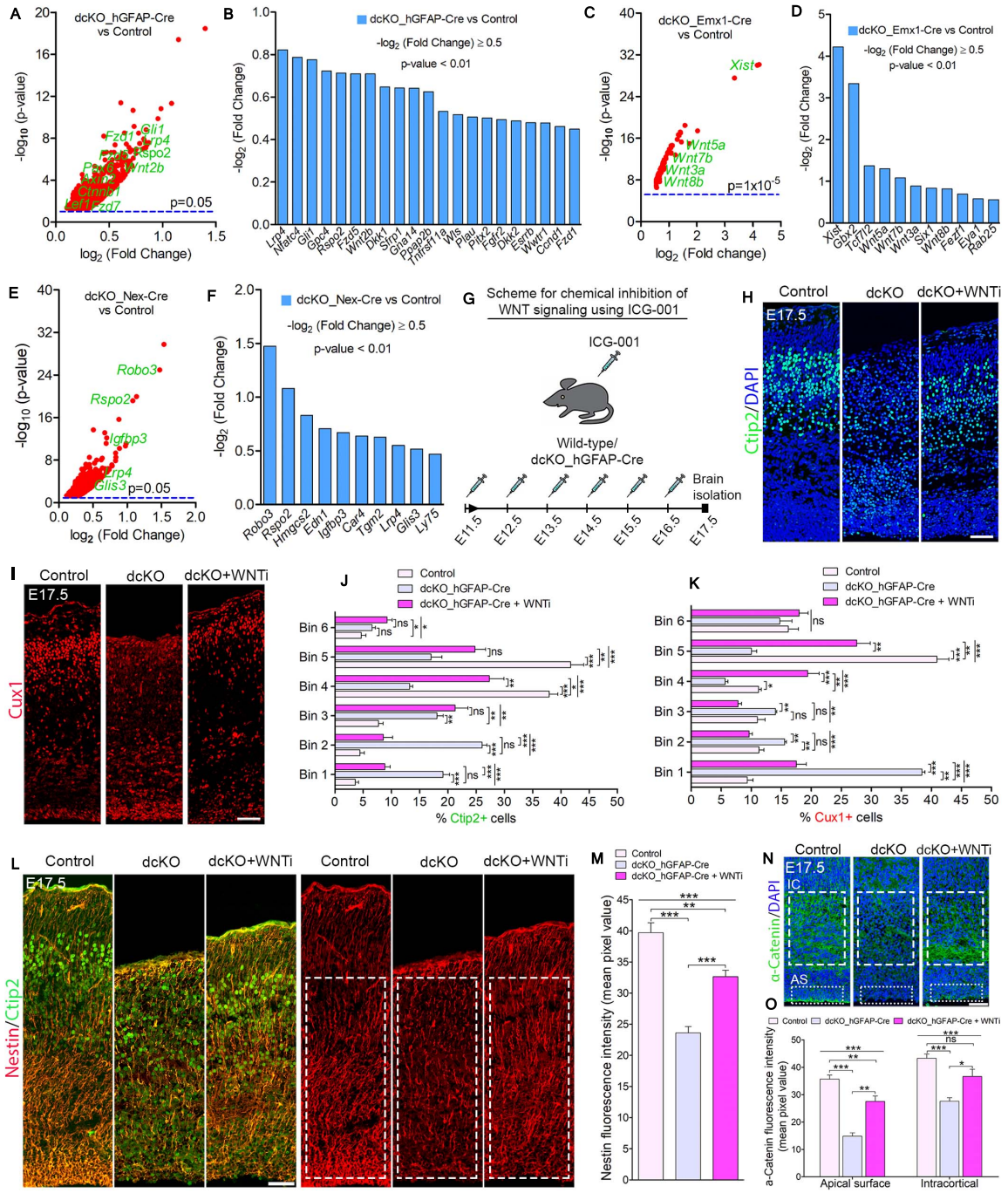

FIGURE 5 | BAF complex modulates WNT signaling to drive neuronal migration and cortical lamination. **(A–F)** Volcano plots **(A,C,E)** and bar charts **(B,D,F)** showing upregulation of WNT signaling-related or target genes in the E17.5 dcKO_hGFAP-Cre **(A,B)**, E12.5 dcKO_Emx1-Cre **(C,D)**, and P1 dcKO_Nex-Cre cortex **(E,F)**. **(G)** Illustration of the scheduled intraperitoneal injection, of pregnant mouse carrying dcKO_hGFAP-Cre embryos, with the WNT inhibitor (WNTi) ICG001. **(H,I)** Immunomicrographs showing Ctip2 **(H)** and Cux1 **(I)** – labeled neurons in the E17.5 control, dcKO_hGFAP-Cre, and WNT inhibitor-treated dcKO_hGFAP-Cre cortex. **(J,K)** Bar graphs showing quantitative bin analyses to compare the distribution of Ctip2+ **(J)** and Cux1+ **(K)** neurons in the E17.5 control, dcKO_hGFAP-Cre, and WNTi-treated dcKO_hGFAP-Cre cortex. **(L)** Immunomicrographs showing Nestin and Ctip2 (merged), and Nestin-only staining in the E17.5 control, dcKO_hGFAP-Cre, and WNT inhibitor -treated dcKO_hGFAP-Cre cortex. **(M)** Bar chart indicating quantification of Nestin+ glial fibers partial rescued in the WNT inhibitor-treated dcKO_hGFAP-Cre cortex compared with the dcKO_hGFAP-Cre and control cortex. **(N)** Images showing intracortical (IC) and apical surface (AS) expression of α-Catenin in the E17.5 control, dcKO_hGFAP-Cre, and WNT inhibitor-treated dcKO_hGFAP-Cre cortex. **(O)** Graphical representation of the quantification of α-Catenin expression following WNT inhibition in the dcKO_hGFAP-Cre cortex compared with that in the dcKO_hGFAP-Cre and control cortex. Inserted rectangles with dashed or stippled lines indicate specific cortical areas quantified. One-way ANOVA followed by Bonferroni *post hoc* analysis was used to test for significance: $^{*}p < 0.05$, $^{**}p < 0.005$, $^{***}p < 0.0005$; ns, not significant; $n = 4–6$. Scale bar: = 50 μm. Results are presented as mean ± SEM.

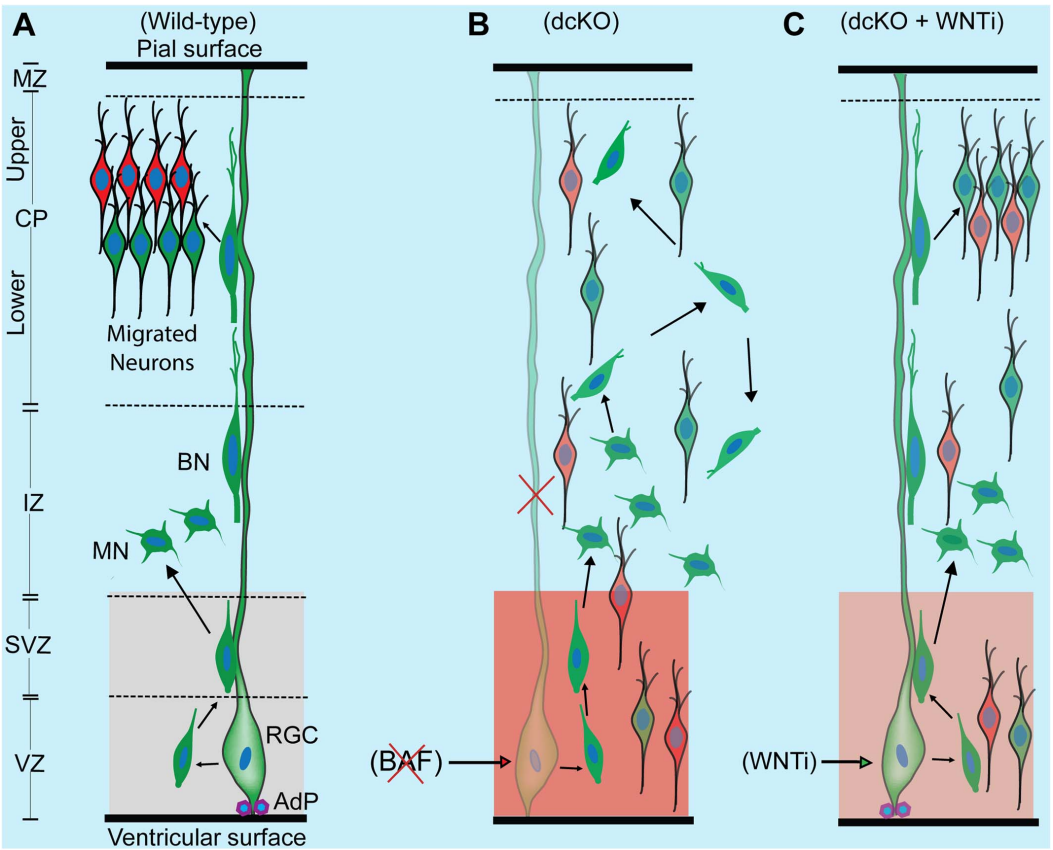

FIGURE 6 | Schematic synopsis of how BAF complex may drive radial neuronal migration. **(A)** Schema showing the normal course of radial neuronal migration in the developing wild-type cortex. The parent cortical neural progenitor that generates majority of excitatory neurons is the radial glia cell (RGC). It is typically anchored at the ventricular surface by adhesion proteins (AdP) and extends a long slender fiber that traverses the marginal zone (MZ) to be anchored at the pial surface. The fiber acts as scaffold that supports the radially migrating neurons. After the RGC gives rise to a newborn neuron in the ventricular zone (VZ), the young postmitotic neuron usually attaches to the parent glial fiber and quickly migrates into the border between the subventricular (SVZ) and intermediate zones (IZ), where it acquires a multipolar neuronal (MN) identity and briefly stops migrating to receive spatiotemporal molecular cues for further oriented migration. The MN then switches to bipolar neuron (BP) and re-attaches to the glial fiber to migrate into the cortical plate (CP). In the CP, the migrating neuron detaches from the glial fiber to undergo somal translocation leading to its correct layer placement and ensures proper cortical lamination. The optimal activity of WNT signaling in the cortical germinal zone is indicated by a light shade of red and critical for neuronal migration. **(B)** Schema showing that loss of BAF complex in neural progenitors causes loss of adhesion proteins, glial fiber, disturbance of MN-to-BN transition, and increase in WNT signaling activity (indicated with a deep shade of red). These alterations result in accumulation of nascent neurons and MNs, leading to abnormal radial migration and cortical laminar malformation. Red cross denotes deletion or loss. **(C)** Picture showing outcome of rescue experiment following inhibition of the increased WNT signaling in the BAF complex mutant (dcKO_hGFAP-Cre) cortex. WNT inhibition (WNTi) with the chemical ICG001 led to substantial preservation of neuronal polarization, glial fibers, and cell adhesion leading to partial rescue of radial neuronal migration and cortical lamination.

migration phenotype in the dcKO_Nex-Cre cortex is mild and most likely to be more of a delayed rather than stalled neuronal migration (**Figures 2A,B** and **Supplementary Figure 5**).

To perform the rescue experiment, we employed the *in vivo* chemical inhibition approach to downregulate (knockdown) the upregulated WNT signaling in the developing dcKO_hGFAP-Cre cortex. This was achieved with the chemical ICG-001, a small molecule capable of interfering with CREB-binding protein (CBP) and β-catenin complexing during WNT signaling, leading to inhibition of the pathway and its related downstream molecular and cellular effects (Emami et al., 2004; Teo et al., 2005; Wiese et al., 2017). Mice pregnant with dcKO_hGFAP-Cre embryos were thus intraperitoneally injected with daily dose of ICG-001 from E11.5 to E16.5 and the brains were harvested for histological analysis at E17.5 (**Figure 5G**). We previously established that ICG-001 treatment at the dosage applied in this study, or treatment with the vehicle (DMSO), does not affect neurogenesis or neuronal migration in the wildtype cortex. Similarly, treatment with DMSO had no effect on cortical neurogenesis or neuronal migration in the BAF mutant brain (Nguyen et al., 2018).

Intriguingly, immunostaining with Ctip2 and Cux1 antibodies revealed partial rescue of radial neuronal migration and formation of deep and superficial cortical layers in the WNT inhibitor (WNTi)-treated dcKO_hGFAP-Cre cortex compared with the dcKO_hGFAP-Cre without WNTi pharmacological treatment (**Figures 5H,I**). Our bin analysis showed that the apparent crowding of Ctip2+ lower layer neurons and Cux1+

upper layer neurons in the E17.5 dcKO_hGFAP-Cre lower cortical wall region significantly resolved due to migration of many of such neurons to populate their designated laminae in the CP upon downregulation of WNT signaling (**Figures 5J,K**). We also observed more preserved RG fibers and α-Catenin (cell adhesion) expression in the WNTi-treated dcKO_hGFAP-Cre cortex compared with dcKO_hGFAP-Cre (**Figures 5L–O**). In agreement with the migration rescue effect of WNT inhibition in the dcKO_hGFAP-Cre, we observed that more WNT inhibitor-treated mutant (dcKO_hGFAP-Cre) neurons labeled with GFP migrated out of the germinal zone and the IZ to populate the upper CP compared with neurons in the WNT inhibitor-untreated dcKO_hGFAP-Cre cortex (**Supplementary Figures 7A,B**). Furthermore, we observed slight increase in the leading process of the rescued (WNT inhibitor-treated) BAF complex mutant neurons compared with the untreated mutant neurons (**Supplementary Figure 7C**). It is probable that WNT inhibition in the dcKO_hGFAP-Cre cortex afforded maintenance of glial fibers and cell adhesion, and rescue of the defective multipolar-to-bipolar neuronal morphology transition, which culminated in a largely correct radial neuronal migration and cortical layer formation (**Figure 6**).

Put together, we have shown that the BAF complex is a critical regulator of the glial fiber-dependent and independent aspects of radial migration of cortical neurons through modulation of WNT signaling activity to allow proper cortical lamination during mouse brain development.

DISCUSSION

Laminar patterning during cortical development is fundamental to the formation of functional cortical areas during development of the cerebral cortex. Neuronal migration is a critical process in cortical layer formation, and its dysregulation can render the cortex malformed with several resultant neurodevelopmental disorders (Valiente and Marin, 2010; Evsyukova et al., 2013; Silva et al., 2019). Therefore, factors that regulate migration of cortical neurons have been of interest to many neurobiologists over the years.

In this study, we identified the ATP-dependent chromatin remodeling BAF complex to play instructional roles during radial migration of cortical neurons. We essentially inactivated the BAF complex in neurogenic cortical progenitors or in nascent postmitotic cortical neurons prior to commencement of radial migration. This was carried out using three different mouse models, in two of which the BAF complex was inactivated in cortical progenitors at early and later cortical development stages to produce the dcKO_Emx1-Cre and dcKO_hGFAP-Cre, respectively. Abrogation of the BAF complex just after generation of postmitotic cortical neurons was achieved in the dcKO_Nex-Cre model. Thus, the dcKO_Nex-Cre model offered the advantage of precluding the impact of abnormal proliferation and neurogenesis seen/reported in the dcKO_Emx1-Cre and dcKO_hGFAP-Cre cortical models (Narayanan et al., 2015; Nguyen et al., 2018). We observed that the BAF complex-deficient cortex lacks well defined cortical layers due to neuronal migration dysregulation. In principle, given that the composition and functional characteristics of the BAF complex in neural progenitors (npBAF) is different from that found in neurons (nBAF) (Lessard et al., 2007; Wu et al., 2007; Staahl et al., 2013; Bachmann et al., 2016), to a large extent, we were able to dissect the significance of BAF complexes in orchestrating neuronal migration during cortical histogenesis.

BAF Complex Orchestrates Cortical Lamination via Regulating Neuron Migration in the Developing Cortex

By temporally and cell-type specifically inactivating the BAF complex in the developing cortex, we found that the resultant mutant neurons are incapable of normal migration. As a result, the BAF complex-ablated developing cortex is improperly laminated; showing both upper and lower layer neuron misplacement in the cortical wall. The defective neuronal migration phenotype was most severe and morphogenically impactful in the dcKO_Emx1-Cre cortex followed by the dcKO_hGFAP-Cre cortex. This may be as a result of concurrent disturbance of neurogenesis due to deletion of BAF complex in the early or late cortical neural stem/progenitor cells. Indeed, neural progenitor cell proliferation and differentiation are perturbed in the absence of optimal BAF complex function (Narayanan et al., 2015; Nguyen et al., 2018). On the other hand, the migration phenotype in the dcKO_Nex-Cre cortex was mild and mainly presented as delayed locomotion of upper layer neurons because they are late-born and make the longest radial journey. This reduced impact in the dcKO_Nex-Cre cortex may have resulted from the relative stability of the BAF complex in postmitotic neurons probably because of their non-dividing nature and the non-requirement of subunit recomposition of the nBAF therein (Lessard et al., 2007; Wu et al., 2007). As such, although majority of the BAF subunits are lost, we found some subunit remnants in the P1 dcKO_Nex-Cre cortex (**Supplementary Figure 3**), which we speculate may underlie the observed mild phenotype.

Typically, abnormal neuronal migration calls forth several other neurodevelopmental perturbations (Valiente and Marin, 2010; Evsyukova et al., 2013). In our case, we found that the defective cortical neuronal migration may, in part, underscore the defective morphology of the BAF complex mutant neurons, which contributed to the diminished corticogenesis in the BAF complex mutant brain (Narayanan et al., 2015; Nguyen et al., 2016, 2018). At least, in terms of differentiation, some BAF complex subunits have been reported to be essential for axonogenesis, dendritogenesis, and spine formation during cortical neuron maturation (reviewed in Sokpor et al., 2017).

Another reason that consolidates the specific link of BAF complex dysfunction to the observed neuronal migration problem is that: it is only under the condition of entire BAF complex ablation that we disturb cortical neuron migration. Single deletion of BAF155 or BAF170 did not yield any noticeable neuronal migration anomaly in the developing cortex (Tuoc et al., 2013; Narayanan et al., 2018). That notwithstanding, a previous study reported defective neuronal migration following deletion

of Ctip1 (BAF100a), a variable subunit of the BAF complex (Wiegreffe et al., 2015). We argue, however, that BAF100a may act solitarily outside the chromatin remodeling function of the BAF complex to control aspects of cortical neuron migration. Even though the defective migration caused by deletion of BAF155 and BAF170 is more complex and severe than that resulting from BAF100a ablation alone, it would be insightful to investigate the structural and functional integrity of the BAF100a-lacking BAF complex and how it may contribute to defective neuronal migration during brain development.

Essential Cellular Mechanics in Radial Neuronal Migration Require BAF Complex Function

Classically, *in utero* electroporation is a powerful *in vivo* technique used for gene manipulation to investigate cellular processes, including neuronal migration in the developing cortex (Saito and Nakatsuji, 2001; Tabata and Nakajima, 2001; Shimogori and Ogawa, 2008). We took advantage of this method to focally ablate BAF complex in the developing cortex, so as to detail the effect on cellular mechanisms during neuronal migration. To closely reproduce loss of BAF complex in cortical progenitors as achieved in the dcKO_Emx1-Cre and dcKO_hFGAP-Cre cortex, and in postmitotic neurons as in the dcKO_Nex-Cre cortex, we used the CAG- and NeuroD-Cre plasmids to delete BAF155 and BAF170 in selected cortical areas, respectively. By this means, we identified that key steps involved in glial fiber-guided cortical neuron migration go awry in the absence of BAF complex. Notably, we found that most of the BAF complex-deficient migrating neurons "could not" locomote properly possibly because of a defect in attachment to glial fibers. The observed reduction in neuronal-glial fiber interaction may partly be due to disturbance in cell adhesion to available glial fibers as revealed in our RNA-seq analyses of the dcKO_Emx1-Cre and dcKO_hFGAP-Cre cortex. Adhesion molecules such as catenins and cadherins, play central roles in the attachment of neurons to glial guides during locomotion (Solecki, 2012). In agreement, it has been recently shown that loss of adhesion proteins in the cortex, particularly α-Catenin, can perturb radial neuronal migration leading to cortical neurodevelopmental disturbances (Schmid et al., 2014; Schaffer et al., 2018). This partly gives relevance to the link between loss of α-Catenin in the BAF complex-inactivated cortex and contribution to the defective radial migration, and cortical mis-lamination phenotype reported in this study.

Although not obviously revealed in our BAF complex knockdown investigation using *in utero* electroporation, it is conceivable that the reduced association of the BAF complex-lacking migrating cortical neurons with glial fibers may also emanate from the loss of the glial fiber layouts needed for radial migration. This is deduced from the dcKO_Emx1-Cre and dcKO_hFGAP-Cre cortex, which display dramatic loss of glial fiber scaffolds due to ablation of BAF complex (Narayanan et al., 2015; Nguyen et al., 2018). Traditionally, nascent cortical neurons use their parent glial fibers to locomote to the CP to make well-patterned radial columns, cortical laminae, and functional areas defined in the cortex (Mountcastle, 1997; Noctor et al., 2001; Torii et al., 2009). Neuronal migration may stall or deviate in the absence of such proximal glial fiber guidance, which accounts for the accumulation of Ctip2+ and Cux1+ neurons in the lower cortical wall of the dcKO_hGFAP-Cre cortex and in the germinal zones of the cortical area electroporated with the CAG-Cre-GFP plasmid. Moreover, our observation indicates that the migrating BAF complex-ablated neurons may display protracted multipolar phase leading to their accumulation in the IZ and/or may undergo excessive tangential migration in attempt to find adjoining fibers for onward radial migration (Inoue et al., 2017).

Adding to the complexity of how BAF complex regulates cortical neuron migration, we also identified its importance in controlling the multipolar-to-bipolar neuronal morphology switch during radial migration. This morphological transformation is critical for successful radial migration (Noctor et al., 2004; Ayala et al., 2007; Namba et al., 2014) and its interference or dysregulation can stifle neuronal migration (La Fata et al., 2014; Boitard et al., 2015; Chen et al., 2015; Barnat et al., 2017; Guo et al., 2017; Huang et al., 2017; Iwai et al., 2018; Kurabayashi et al., 2018; Ohtaka-Maruyama et al., 2018; Zhang et al., 2018). The BAF complex-ablated cortical neurons are unable to properly undergo multipolar-to-bipolar transition leading to their stagnation in the multipolar phase or accumulation in the IZ, and reduced success in populating the CP. In essence, we posit that neuronal polarization is fundamentally distorted in the absence of BAF complex. In support of this notion, we found downregulation of cytoskeleton-related factors in the BAF complex-deleted cortex. More so, adhesion proteins like α-catenin, which orchestrate the plastic linkage between the cell membrane and the internal cytoskeleton to afford cell (neuronal) structure remodeling (Drees et al., 2005; Desai et al., 2013), is lost in response to BAF complex inactivation in the developing cortex. Our investigation of Golgi apparatus localization, which can also indicate alteration in cell polarization, corroborates aberrant neuronal polarization and resultant disturbance of multipolar-to-bipolar morphology transition consequent to BAF complex deletion. A common outcome of improper neuronal polarization during radial migration is the disturbance of axon and dendrite formation, which in the case of the latter, we observed as truncation of the leading process (future dendrite) of the BAF complex mutant migrating neurons. Additionally, improperly polarized radially migrating neurons lacking BAF155 and BAF170 may overly adopt the non-pia surface-directed mode of radial migration, i.e., multipolar migration (Tabata and Nakajima, 2003), which can be a reason for the observed spreading of neurons and cortical mislamination. Future studies seeking to determine how the BAF complex regulates neuronal process elaboration and extension will enrich the literature on how chromatin remodelers orchestrate cortical circuitry.

Together, our investigations show that the BAF complex modulates contact guidance necessary for radial neuronal migration and cortical laminar formation. Key among them is that the BAF complex is essential for maintenance of RG fiber scaffolds, cell adhesion, and neuronal polarization that are indispensable for locomotion of cortical neurons.

BAF Complex May Suppress WNT Signaling to Drive Cortical Neuron Migration

Beyond the mechanistic cellular intricacies involved in the regulation of cortical neuron migration by the ATP-dependent chromatin remodeling BAF complex, we were interested in identifying a unified molecular mechanism through which BAF complex acts to control radial neuronal migration and cortical laminar formation in the developing brain. We started by screening for possible molecular candidates imputable to our BAF complex mutation-induced neuronal migration phenotype. The WNT signaling pathway emerged as the most plausible candidate among a complex mix of factors altered in the mutant cortex. Unlike other identified signaling pathways (e.g., BMP, SHH, Notch [data not shown]) altered in the BAF complex mutant cortex, WNT signaling appeared consistently elevated in all three dcKO models employed in the study. Moreover, the disturbance of WNT signaling and its effectors are known to cause abnormal neuronal migration (Poschl et al., 2013; Boitard et al., 2015; Bocchi et al., 2017). Admittedly, while WNT activity is markedly increased in the dcKO_Emx1-Cre and dcKO_hFGAP-Cre cortex [see RNA-seq data sheets in Narayanan et al. (2015) and Nguyen et al. (2018), respectively], the dcKO_Nex-Cre cortex displayed mild elevation in WNT signaling probably due to alteration in indirect WNT signaling effectors, including Rspo2 (Lebensohn and Rohatgi, 2018). Perhaps, the perturbation in WNT signaling in the dcKO_Nex-Cre cortex may be mild enough to allow some degree of normal cortical layer formation at later postnatal stages of cortical development, which may not be in the case of the dcKO_Emx1-Cre or dcKO_hFGAP-Cre cortex.

By downregulating the increased WNT signaling activity in the BAF mutant (dcKO_hFGAP-Cre) cortex, we were able to substantially obviate abnormal radial migration of neurons and cortical layer malformation. The neuronal migration rescue upon WNT signaling knockdown is partly due to the preservation of glial fibers, cell adhesion, and cell polarization. Thus, our rescue experiment showed that the BAF complex likely modulates WNT signaling to allow optimal establishment of the requisite molecular and cellular conditions for normal oriented neuronal migration and proper patterning of neocortical layers (**Figure 6**). A possible explanation for the WNT inhibition-mediated rescue of the migration phenotype is that BAF complex may suppress WNT signaling in neurons en route to their laminae in the CP. In support of our hypothesis, it was previously shown that BAF complex can inhibit WNT/β-catenin signaling via its subunit BAF250b (Vasileiou et al., 2015). It was also reported that WNT signaling is dynamically regulated to allow correct neuronal polarity formation and neuron-glial fiber engagement during radial migration (Boitard et al., 2015; Bocchi et al., 2017). When WNT signaling was ablated in the developing cortex, it resulted in delay of radial migration leading to cortical malformation (Boitard et al., 2015; Bocchi et al., 2017), as phenocopied in the BAF complex mutant (dcKO_Nex-Cre) cortex. We demonstrated in our previous work that BAF complex possibly modulates WNT signaling to permit the establishment of epigenetic schemes required for proper neuronal development during corticogenesis (Nguyen et al., 2018). WNT signaling is indeed a formidable regulator of cortical development as it is reported to regulate many aspects of brain development, including primary forebrain patterning, RG and neuronal precursor cell fate, cell adhesion and polarity formation, and cortical laminar patterning (reviewed in Harrison-Uy and Pleasure, 2012). Nonetheless, due to the partial rescue of the migration phenotype by WNT inhibition, we think other (signaling) factors may be involved. For instance, it could be that WNT inhibition also leads to some normalization of the other dysregulated signaling pathways in the developing BAF complex mutant cortex. As a future consideration, it would be interesting to elucidate the epiphenomenal aspect of our rescue experiment to consolidate our findings.

Altogether, this current study highlights the indispensability of the ATP-dependent chromatin remodeling BAF complex in the formation of cortical layers through regulating multiple aspects of radial neuronal migration in a WNT signaling dependent manner during mammalian cortical development.

DATA AVAILABILITY STATEMENT

The original contributions presented in the study are publicly available. These data can be found here: https://www.ncbi.nlm.nih.gov/geo/query/acc.cgi?acc=GSE175362.

ETHICS STATEMENT

The animal study was reviewed and approved by the Animal Welfare Committees of the University Medical Center Göttingen and local authority (LAVES: Niedersächsisches Landesamt für Verbraucherschutz und Lebensmittelsicherheit) under the license numbers: 14/1636 and 16/2330.

AUTHOR CONTRIBUTIONS

GS performed most of the phenotype characterization and all statistical analyses. CK generated RNA-seq data. HN, LP, and JR contributed to histological analyses. RW did FISH experiment and provided data in **Figure 2A**. HPN, AF, and JS provided research resources and contributed to discussions. GS and TT wrote the manuscript. TT conceived and supervised the work. All the authors contributed to the article and approved the submitted version.

FUNDING

This work was supported by the Universitätsmedizin Göttingen (TT), TU432/1-1, TU432/3-1, TU432/6-1 DFG grants (TT), Schram-Stiftung (TT), DFG-CNMPB (TT and JS), German Academic Exchange Service (DAAD)-MoE Ghana Scholarship (GS), and partly by the Göttingen Graduate School for

Neuroscience, Biophysics and Molecular Bioscience (DFG Grant GSC 226/4) (GS). This work was support by the Open Access Publication Funds of the Ruhr-University Bochum.

ACKNOWLEDGMENTS

We acknowledge Fett H., and Huttanus T. for their expert animal care and support. We thank Nguyen L., and Guillemot F. for sharing reagents and plasmids with us. Nave A. is also appreciated for supplying Nex-Cre transgenic mice. We are grateful to Agentur der RUB for IUE illustration.

SUPPLEMENTARY MATERIAL

The Supplementary Material for this article can be found online at: https://www.frontiersin.org/articles/10.3389/fnmol.2021.687581/full#supplementary-material

REFERENCES

Anton, E. S., Kreidberg, J. A., and Rakic, P. (1999). Distinct functions of alpha3 and alpha(v) integrin receptors in neuronal migration and laminar organization of the cerebral cortex. *Neuron* 22, 277–289.

Anton, E. S., Marchionni, M. A., Lee, K. F., and Rakic, P. (1997). Role of GGF/neuregulin signaling in interactions between migrating neurons and radial glia in the developing cerebral cortex. *Development* 124, 3501–3510.

Arlotta, P., Molyneaux, B. J., Chen, J., Inoue, J., Kominami, R., and Macklis, J. D. (2005). Neuronal subtype-specific genes that control corticospinal motor neuron development in vivo. *Neuron* 45, 207–221. doi: 10.1016/j.neuron.2004.12.036

Ayala, R., Shu, T., and Tsai, L. H. (2007). Trekking across the brain: the journey of neuronal migration. *Cell* 128, 29–43. doi: 10.1016/j.cell.2006.12.021

Bachmann, C., Nguyen, H., Rosenbusch, J., Pham, L., Rabe, T., Patwa, M., et al. (2016). mSWI/SNF (BAF) complexes are indispensable for the neurogenesis and development of embryonic olfactory epithelium. *PLoS Genet.* 12:e1006274. doi: 10.1371/journal.pgen.1006274

Barnat, M., Le Friec, J., Benstaali, C., and Humbert, S. (2017). Huntingtin-mediated multipolar-bipolar transition of newborn cortical neurons is critical for their postnatal neuronal morphology. *Neuron* 93, 99–114. doi: 10.1016/j.neuron.2016.11.035

Bielle, F., Griveau, A., Narboux-Nême, N., Vigneau, S., Sigrist, M., Arber, S., et al. (2005). Multiple origins of Cajal-Retzius cells at the borders of the developing pallium. *Nat. Neurosci.* 8, 1002–1012. doi: 10.1038/nn1511

Bocchi, R., Egervari, K., Carol-Perdiguer, L., Viale, B., Quairiaux, C., De Roo, M., et al. (2017). Perturbed Wnt signaling leads to neuronal migration delay, altered interhemispheric connections and impaired social behavior. *Nat. Commun.* 8, 1–15. doi: 10.1038/s41467-017-01046-w

Boitard, M., Bocchi, R., Egervari, K., Petrenko, V., Viale, B., Gremaud, S., et al. (2015). Wnt signaling regulates multipolar-to-bipolar transition of migrating neurons in the cerebral cortex. *Cell Rep.* 10, 1349–1361. doi: 10.1016/j.celrep.2015.01.061

Chen, T. D., Wu, Q. W., Zhang, Y., and Zhang, D. (2015). NDUFV2 regulates neuronal migration in the developing cerebral cortex through modulation of the multipolar-bipolar transition. *Brain Res.* 1625, 102–110. doi: 10.1016/j.brainres.2015.08.028

Choi, J., Ko, M., Jeon, S., Jeon, Y., Park, K., Lee, C., et al. (2012). The SWI/SNF-like BAF complex is essential for early B cell development. *J. Immunol.* 188, 3791–3803. doi: 10.4049/jimmunol.1103390

Clapier, C. R., Iwasa, J., Cairns, B. R., and Peterson, C. L. (2017). Mechanisms of action and regulation of ATP-dependent chromatin-remodelling complexes. *Nat. Rev. Mol. Cell Biol.* 18, 407–422. doi: 10.1038/nrm.2017.26

de la Torre-Ubieta, L., and Bonni, A. (2011). Transcriptional regulation of neuronal polarity and morphogenesis in the mammalian brain. *Neuron* 72, 22–40. doi: 10.1016/j.neuron.2011.09.018

Desai, R., Sarpal, R., Ishiyama, N., Pellikka, M., Ikura, M., and Tepass, U. (2013). Monomeric alpha-catenin links cadherin to the actin cytoskeleton. *Nat. Cell Biol.* 15, 261–273. doi: 10.1038/ncb2685

Drees, F., Pokutta, S., Yamada, S., Nelson, W. J., and Weis, W. I. (2005). Alpha-catenin is a molecular switch that binds E-cadherin-beta-catenin and regulates actin-filament assembly. *Cell* 123, 903–915. doi: 10.1016/j.cell.2005.09.021

Elias, L. A. B., Wang, D. D., and Kriegstein, A. R. (2007). Gap junction adhesion is necessary for radial migration in the neocortex. *Nature* 448, 901–U903. doi: 10.1038/nature06063

Emami, K. H., Nguyen, C., Ma, H., Kim, D. H., Jeong, K. W., Eguchi, M., et al. (2004). A small molecule inhibitor of beta-catenin/CREB-binding protein transcription [corrected]. *Proc. Natl. Acad. Sci. U.S.A.* 101, 12682–12687. doi: 10.1073/pnas.0404875101

Evsyukova, I., Plestant, C., and Anton, E. S. (2013). Integrative mechanisms of oriented neuronal migration in the developing brain. *Annu. Rev. Cell Dev. Biol.* 29, 299–353. doi: 10.1146/annurev-cellbio-101512-122400

Gaspard, N., Bouschet, T., Hourez, R., Dimidschstein, J., Naeije, G., van den Ameele, J., et al. (2008). An intrinsic mechanism of corticogenesis from embryonic stem cells. *Nature* 455, 351–310. doi: 10.1038/nature07287

Goebbels, S., Bormuth, I., Bode, U., Hermanson, O., Schwab, M. H., and Nave, K. A. (2006). Genetic targeting of principal neurons in neocortex and hippocampus of NEX-Cre mice. *Genesis* 44, 611–621. doi: 10.1002/dvg.20256

Gorski, J. A., Talley, T., Qiu, M., Puelles, L., Rubenstein, J. L., and Jones, K. R. (2002). Cortical excitatory neurons and glia, but not GABAergic neurons, are produced in the Emx1-expressing lineage. *J. Neurosci.* 22, 6309–6314.

Guo, Y., He, X., Zhao, L., Liu, L., Song, H., Wang, X., et al. (2017). Gβ2 regulates the multipolar-bipolar transition of newborn neurons in the developing neocortex. *Cereb. Cortex* 27, 3414–3426. doi: 10.1093/cercor/bhx042

Hakanen, J., Ruiz-Reig, N., and Tissir, F. (2019). Linking cell polarity to cortical development and malformations. *Front. Cell. Neurosci.* 13:244. doi: 10.3389/fncel.2019.00244

Hand, R., Bortone, D., Mattar, P., Nguyen, L., Heng, J. I., Guerrier, S., et al. (2005). Phosphorylation of Neurogenin2 specifies the migration properties and the dendritic morphology of pyramidal neurons in the neocortex. *Neuron* 48, 45–62. doi: 10.1016/j.neuron.2005.08.032

Harrison-Uy, S. J., and Pleasure, S. J. (2012). Wnt signaling and forebrain development. *Cold Spring Harb. Perspect. Biol.* 4:a008094. doi: 10.1101/cshperspect.a008094

Hashimoto-Torii, K., Torii, M., Sarkisian, M. R., Bartley, C. M., Shen, J., Radtke, F., et al. (2008). Interaction between reelin and notch signaling regulates neuronal migration in the cerebral cortex. *Neuron* 60, 273–284. doi: 10.1016/j.neuron.2008.09.026

Heng, J. I., Moonen, G., and Nguyen, L. (2007). Neurotransmitters regulate cell migration in the telencephalon. *Eur. J. Neurosci.* 26, 537–546. doi: 10.1111/j.1460-9568.2007.05694.x

Huang, Y. X., Li, G. H., An, L., Fan, Y. L., Cheng, X. R., Li, X. Z., et al. (2017). Fyn regulates multipolar-bipolar transition and neurite morphogenesis of migrating neurons in the developing neocortex. *Neuroscience* 352, 39–51. doi: 10.1016/j.neuroscience.2017.03.032

Inoue, M., Iwai, R., Tabata, H., Konno, D., Komabayashi-Suzuki, M., Watanabe, C., et al. (2017). Prdm16 is crucial for progression of the multipolar phase during neural differentiation of the developing neocortex. *Development* 144, 385–399. doi: 10.1242/dev.136382

Inoue, M., Kuroda, T., Honda, A., Komabayashi-Suzuki, M., Komai, T., Shinkai, Y., et al. (2014). Prdm8 regulates the morphological transition at multipolar phase during neocortical development. *PLoS One* 9:e86356. doi: 10.1371/journal.pone.0086356

Iwai, R., Tabata, H., Inoue, M., Nomura, K., Okamoto, T., Ichihashi, M., et al. (2018). A Prdm8 target gene Ebf3 regulates multipolar-to-bipolar transition in migrating neocortical cells. *Biochem. Biophys. Res. Commun.* 495, 388–394. doi: 10.1016/j.bbrc.2017.11.021

Jinnou, H., Sawada, M., Kawase, K., Kaneko, N., Herranz-Perez, V., Miyamoto, T., et al. (2018). Radial glial fibers promote neuronal migration and functional recovery after neonatal brain injury. *Cell Stem Cell* 22, 128.e9–137.e9. doi: 10.1016/j.stem.2017.11.005

Kadoch, C., Hargreaves, D. C., Hodges, C., Elias, L., Ho, L., Ranish, J., et al. (2013). Proteomic and bioinformatic analysis of mammalian SWI/SNF complexes identifies extensive roles in human malignancy. *Nat. Genet.* 45, 592–601. doi: 10.1038/ng.2628

Kawauchi, T., Sekine, K., Shikanai, M., Chihama, K., Tomita, K., Kubo, K., et al. (2010). Rab GTPases-dependent endocytic pathways regulate neuronal migration and maturation through N-cadherin trafficking. *Neuron* 67, 588–602. doi: 10.1016/j.neuron.2010.07.007

Kriegstein, A. R., and Noctor, S. C. (2004). Patterns of neuronal migration in the embryonic cortex. *Trends Neurosci.* 27, 392–399. doi: 10.1016/j.tins.2004.05.001

Kurabayashi, N., Tanaka, A., Nguyen, M. D., and Sanada, K. (2018). The LPA-LPA4 axis is required for establishment of bipolar morphology and radial migration of newborn cortical neurons. *Development* 145:dev162529. doi: 10.1242/dev.162529

La Fata, G., Gartner, A., Dominguez-Iturza, N., Dresselaers, T., Dawitz, J., Poorthuis, R. B., et al. (2014). FMRP regulates multipolar to bipolar transition affecting neuronal migration and cortical circuitry. *Nat. Neurosci.* 17, 1693–1700. doi: 10.1038/nn.3870

Lebensohn, A. M., and Rohatgi, R. (2018). R-spondins can potentiate WNT signaling without LGRs. *eLife* 7:e33126. doi: 10.7554/eLife.33126

Lessard, J., Wu, J. I., Ranish, J. A., Wan, M., Winslow, M. M., Staahl, B. T., et al. (2007). An essential switch in subunit composition of a chromatin remodeling complex during neural development. *Neuron* 55, 201–215. doi: 10.1016/j.neuron.2007.06.019

Louhivuori, L. M., Turunen, P. M., Louhivuori, V., Yellapragada, V., Nordstrom, T., Uhlen, P., et al. (2018). Regulation of radial glial process growth by glutamate via mGluR5/TRPC3 and neuregulin/ErbB4. *Glia* 66, 94–107. doi: 10.1002/glia.23230

Marin, O., and Rubenstein, J. L. (2003). Cell migration in the forebrain. *Annu. Rev. Neurosci.* 26, 441–483. doi: 10.1146/annurev.neuro.26.041002.131058

Marin, O., Valiente, M., Ge, X., and Tsai, L. H. (2010). Guiding neuronal cell migrations. *Cold Spring Harb. Perspect. Biol.* 2:a001834. doi: 10.1101/cshperspect.a001834

Martinez-Chavez, E., Scheerer, C., Wizenmann, A., and Blaess, S. (2018). The zinc-finger transcription factor GLI3 is a regulator of precerebellar neuronal migration. *Development* 145:dev166033. doi: 10.1242/dev.166033

Miyata, T., Kawaguchi, A., Okano, H., and Ogawa, M. (2001). Asymmetric inheritance of radial glial fibers by cortical neurons. *Neuron* 31, 727–741. doi: 10.1016/s0896-6273(01)00420-2

Mizutani, K. I. (2018). Physiological significance of multipolar cells generated from neural stem cells and progenitors for the establishment of neocortical cytoarchitecture. *Genes Cells* 23, 6–15. doi: 10.1111/gtc.12546

Molyneaux, B. J., Arlotta, P., Menezes, J. R., and Macklis, J. D. (2007). Neuronal subtype specification in the cerebral cortex. *Nat. Rev. Neurosci.* 8, 427–437. doi: 10.1038/nrn2151

Mountcastle, V. B. (1997). The columnar organization of the neocortex. *Brain* 120(Pt 4), 701–722. doi: 10.1093/brain/120.4.701

Nadarajah, B., Brunstrom, J. E., Grutzendler, J., Wong, R. O. L., and Pearlman, A. L. (2001). Two modes of radial migration in early development of the cerebral cortex. *Nat. Neurosci.* 4, 143–150. doi: 10.1038/83967

Namba, T., Kibe, Y., Funahashi, Y., Nakamuta, S., Takano, T., Ueno, T., et al. (2014). Pioneering axons regulate neuronal polarization in the developing cerebral cortex. *Neuron* 81, 814–829. doi: 10.1016/j.neuron.2013.12.015

Narayanan, R., Pham, L., Kerimoglu, C., Watanabe, T., Castro Hernandez, R., Sokpor, G., et al. (2018). Chromatin remodeling BAF155 subunit regulates the genesis of basal progenitors in developing cortex. *iScience* 4, 109–126. doi: 10.1016/j.isci.2018.05.014

Narayanan, R., Pirouz, M., Kerimoglu, C., Pham, L., Wagener, R. J., Kiszka, K. A., et al. (2015). Loss of BAF (mSWI/SNF) complexes causes global transcriptional and chromatin state changes in forebrain development. *Cell Rep.* 13, 1842–1854. doi: 10.1016/j.celrep.2015.10.046

Nguyen, H., Kerimoglu, C., Pirouz, M., Pham, L., Kiszka, K. A., Sokpor, G., et al. (2018). Epigenetic regulation by BAF complexes limits neural stem cell proliferation by suppressing Wnt signaling in late embryonic development. *Stem Cell Rep.* 10, 1734–1750. doi: 10.1016/j.stemcr.2018.04.014

Nguyen, H., Sokpor, G., Pham, L., Rosenbusch, J., Stoykova, A., Staiger, J. F., et al. (2016). Epigenetic regulation by BAF (mSWI/SNF) chromatin remodeling complexes is indispensable for embryonic development. *Cell Cycle* 15, 1317–1324. doi: 10.1080/15384101.2016.1160984

Nieto, M., Monuki, E. S., Tang, H., Imitola, J., Haubst, N., Khoury, S. J., et al. (2004). Expression of Cux-1 and Cux-2 in the subventricular zone and upper layers II-IV of the cerebral cortex. *J. Comp. Neurol.* 479, 168–180. doi: 10.1002/cne.20322

Nitarska, J., Smith, J. G., Sherlock, W. T., Hillege, M. M. G., Nott, A., Barshop, W. D., et al. (2016). A functional switch of NuRD chromatin remodeling complex subunits regulates mouse cortical development. *Cell Rep.* 17, 1683–1698. doi: 10.1016/j.celrep.2016.10.022

Noctor, S. C., Flint, A. C., Weissman, T. A., Dammerman, R. S., and Kriegstein, A. R. (2001). Neurons derived from radial glial cells establish radial units in neocortex. *Nature* 409, 714–720. doi: 10.1038/35055553

Noctor, S. C., Flint, A. C., Weissman, T. A., Wong, W. S., Clinton, B. K., and Kriegstein, A. R. (2002). Dividing precursor cells of the embryonic cortical ventricular zone have morphological and molecular characteristics of radial glia. *J. Neurosci.* 22, 3161–3173. doi: 10.1523/Jneurosci.22-08-03161.2002

Noctor, S. C., Martinez-Cerdeno, V., Ivic, L., and Kriegstein, A. R. (2004). Cortical neurons arise in symmetric and asymmetric division zones and migrate through specific phases. *Nat. Neurosci.* 7, 136–144. doi: 10.1038/nn1172

Nott, A., Nitarska, J., Veenvliet, J. V., Schacke, S., Derijck, A. A. H. A., Sirko, P., et al. (2013). S-nitrosylation of HDAC2 regulates the expression of the chromatin-remodeling factor Brm during radial neuron migration. *Proc. Natl. Acad. Sci. U.S.A.* 110, 3113–3118. doi: 10.1073/pnas.1218126110

Ohtaka-Maruyama, C., Okamoto, M., Endo, K., Oshima, M., Kaneko, N., Yura, K., et al. (2018). Synaptic transmission from subplate neurons controls radial migration of neocortical neurons. *Science* 360, 313–317. doi: 10.1126/science.aar2866

Pontious, A., Kowalczyk, T., Englund, C., and Hevner, R. F. (2008). Role of intermediate progenitor cells in cerebral cortex development. *Dev. Neurosci.* 30, 24–32. doi: 10.1159/000109848

Poschl, J., Grammel, D., Dorostkar, M. M., Kretzschmar, H. A., and Schuller, U. (2013). Constitutive activation of beta-catenin in neural progenitors results in disrupted proliferation and migration of neurons within the central nervous system. *Dev. Biol.* 374, 319–332. doi: 10.1016/j.ydbio.2012.12.001

Rakic, P. (1972). Mode of cell migration to the superficial layers of fetal monkey neocortex. *J. Comp. Neurol.* 145, 61–83. doi: 10.1002/cne.901450105

Rakic, P., KnyiharCsillik, E., and Csillik, B. (1996). Polarity of microtubule assemblies during neuronal cell migration. *Proc. Natl. Acad. Sci. U.S.A.* 93, 9218–9222. doi: 10.1073/pnas.93.17.9218

Saito, T., and Nakatsuji, N. (2001). Efficient gene transfer into the embryonic mouse brain using in vivo electroporation. *Dev. Biol.* 240, 237–246. doi: 10.1006/dbio.2001.0439

Saxena, M., Agnihotri, N., and Sen, J. (2018). Perturbation of canonical and non-canonical BMP signaling affects migration, polarity and dendritogenesis of mouse cortical neurons. *Development* 145:dev147157. doi: 10.1242/dev.147157

Schaffer, A. E., Breuss, M. W., Caglayan, A. O., Al-Sanaa, N., Al-Abdulwahed, H. Y., Kaymakçalan, H., et al. (2018). Biallelic loss of human CTNNA2, encoding αN-catenin, leads to ARP2/3 complex overactivity and disordered cortical neuronal migration. *Nat. Genet.* 50, 1093–1101. doi: 10.1038/s41588-018-0166-0

Schmid, M. T., Weinandy, F., Wilsch-Brauninger, M., Huttner, W. B., Cappello, S., and Gotz, M. (2014). The role of alpha-E-catenin in cerebral cortex development: radial glia specific effect on neuronal migration. *Front. Cell. Neurosci.* 8:215. doi: 10.3389/fncel.2014.00215

Severino, M., Geraldo, A. F., Utz, N., Tortora, D., Pogledic, I., Klonowski, W., et al. (2020). Definitions and classification of malformations of cortical development: practical guidelines. *Brain* 143, 2874–2894. doi: 10.1093/brain/awaa174

Shikanai, M., Nakajima, K., and Kawauchi, T. (2011). N-cadherin regulates radial glial fiber-dependent migration of cortical locomoting neurons. *Commun. Integr. Biol.* 4, 326–330. doi: 10.4161/cib.4.3.14886

Shikanai, M., Nishimura, Y. V., Sakurai, M., Nabeshima, Y. I., Yuzaki, M., and Kawauchi, T. (2018). Caveolin-1 promotes early neuronal maturation via caveolae-independent trafficking of N-Cadherin and L1. *iScience* 7, 53–67. doi: 10.1016/j.isci.2018.08.014

Shimogori, T., and Ogawa, M. (2008). Gene application with in utero electroporation in mouse embryonic brain. *Dev. Growth Differ.* 50, 499–506. doi: 10.1111/j.1440-169x.2008.01045.x

Siegenthaler, J. A., and Miller, M. W. (2004). Transforming growth factor beta1 modulates cell migration in rat cortex: effects of ethanol. *Cereb. Cortex* 14, 791–802. doi: 10.1093/cercor/bhh039

Sild, M., and Ruthazer, E. S. (2011). Radial glia: progenitor, pathway, and partner. *Neuroscientist* 17, 288–302. doi: 10.1177/1073858410385870

Silva, C. G., Peyre, E., and Nguyen, L. (2019). Cell migration promotes dynamic cellular interactions to control cerebral cortex morphogenesis. *Nat. Rev. Neurosci.* 20, 318–329. doi: 10.1038/s41583-019-0148-y

Sokpor, G., Castro-Hernandez, R., Rosenbusch, J., Staiger, J. F., and Tuoc, T. (2018). ATP-dependent chromatin remodeling during cortical neurogenesis. *Front. Neurosci.* 12:226. doi: 10.3389/fnins.2018.00226

Sokpor, G., Xie, Y., Rosenbusch, J., and Tuoc, T. (2017). Chromatin remodeling BAF (SWI/SNF) complexes in neural development and disorders. *Front. Mol. Neurosci.* 10:243. doi: 10.3389/fnmol.2017.00243

Solecki, D. J. (2012). Sticky situations: recent advances in control of cell adhesion during neuronal migration. *Curr. Opin. Neurobiol.* 22, 791–798. doi: 10.1016/j.conb.2012.04.010

Son, E. Y., and Crabtree, G. R. (2014). The role of BAF (mSWI/SNF) complexes in mammalian neural development. *Am. J. Med. Genet. C Semin. Med. Genet.* 166C, 333–349. doi: 10.1002/ajmg.c.31416

Staahl, B. T., Tang, J., Wu, W., Sun, A., Gitler, A. D., Yoo, A. S., et al. (2013). Kinetic analysis of npBAF to nBAF switching reveals exchange of SS18 with CREST and integration with neural developmental pathways. *J. Neurosci.* 33, 10348–10361. doi: 10.1523/JNEUROSCI.1258-13.2013

Tabata, H., and Nakajima, K. (2001). Efficient in utero gene transfer system to the developing mouse brain using electroporation: visualization of neuronal migration in the developing cortex. *Neuroscience* 103, 865–872. doi: 10.1016/S0306-4522(01)00016-1

Tabata, H., and Nakajima, K. (2003). Multipolar migration: the third mode of radial neuronal migration in the developing cerebral cortex. *J. Neurosci.* 23, 9996–10001. doi: 10.1523/JNEUROSCI.23-31-09996.2003

Teo, J. L., Ma, H., Nguyen, C., Lam, C., and Kahn, M. (2005). Specific inhibition of CBP/beta-catenin interaction rescues defects in neuronal differentiation caused by a presenilin-1 mutation. *Proc. Natl. Acad. Sci. U.S.A.* 102, 12171–12176. doi: 10.1073/pnas.0504600102

Tonosaki, M., Itoh, K., Umekage, M., Kishimoto, T., Yaoi, T., Lemmon, V. P., et al. (2014). L1cam is crucial for cell locomotion and terminal translocation of the soma in radial migration during murine corticogenesis. *PLoS One* 9:e086186. doi: 10.1371/journal.pone.0086186

Torii, M., Hashimoto-Torii, K., Levitt, P., and Rakic, P. (2009). Integration of neuronal clones in the radial cortical columns by EphA and ephrin-A signalling. *Nature* 461, 524–528. doi: 10.1038/nature08362

Tuoc, T. C., Boretius, S., Sansom, S. N., Pitulescu, M. E., Frahm, J., Livesey, F. J., et al. (2013). Chromatin regulation by BAF170 controls cerebral cortical size and thickness. *Dev. Cell* 25, 256–269. doi: 10.1016/j.devcel.2013.04.005

Tuoc, T. C., and Stoykova, A. (2008). Trim11 modulates the function of neurogenic transcription factor Pax6 through ubiquitin-proteosome system. *Gene Dev.* 22, 1972–1986. doi: 10.1101/gad.471708

Valiente, M., Ciceri, G., Rico, B., and Marin, O. (2011). Focal adhesion kinase modulates radial glia-dependent neuronal migration through connexin-26. *J. Neurosci.* 31, 11678–11691. doi: 10.1523/Jneurosci.2678-11.2011

Valiente, M., and Marin, O. (2010). Neuronal migration mechanisms in development and disease. *Curr. Opin. Neurobiol.* 20, 68–78. doi: 10.1016/j.conb.2009.12.003

Vasileiou, G., Ekici, A. B., Uebe, S., Zweier, C., Hoyer, J., Engels, H., et al. (2015). Chromatin-remodeling-factor ARID1B represses Wnt/beta-catenin signaling. *Am. J. Hum. Genet.* 97, 445–456. doi: 10.1016/j.ajhg.2015.08.002

Wagener, R. J., Witte, M., Guy, J., Mingo-Moreno, N., Kügler, S., and Staiger, J. F. (2016). Thalamocortical connections drive intracortical activation of functional columns in the mislaminated reeler somatosensory cortex. *Cereb. Cortex* 26, 820–837. doi: 10.1093/cercor/bhv257

Weinberg, P., Flames, N., Sawa, H., Garriga, G., and Hobert, O. (2013). The SWI/SNF chromatin remodeling complex selectively affects multiple aspects of serotonergic neuron differentiation. *Genetics* 194, 189–198. doi: 10.1534/genetics.112.148742

Wiegreffe, C., Simon, R., Peschkes, K., Kling, C., Strehle, M., Cheng, J., et al. (2015). Bcl11a (Ctip1) controls migration of cortical projection neurons through regulation of sema3c. *Neuron* 87, 311–325. doi: 10.1016/j.neuron.2015.06.023

Wiese, M., Walther, N., Diederichs, C., Schill, F., Monecke, S., Salinas, G., et al. (2017). The beta-catenin/CBP-antagonist ICG-001 inhibits pediatric glioma tumorigenicity in a Wnt-independent manner. *Oncotarget* 8, 27300–27313. doi: 10.18632/oncotarget.15934

Wu, J. I., Lessard, J., Olave, I. A., Qiu, Z., Ghosh, A., Graef, I. A., et al. (2007). Regulation of dendritic development by neuron-specific chromatin remodeling complexes. *Neuron* 56, 94–108. doi: 10.1016/j.neuron.2007.08.021

Xie, Y., Castro-Hernández, R., Sokpor, G., Pham, L., Narayanan, R., Rosenbusch, J., et al. (2019). RBM15 modulates the function of chromatin remodeling factor BAF155 through RNA methylation in developing cortex. *Mol. Neurobiol.* 56, 7305–7320. doi: 10.1007/s12035-019-1595-1

Xu, C. D., Funahashi, Y., Watanabe, T., Takano, T., Nakamuta, S., Namba, T., et al. (2015). Radial glial cell-neuron interaction directs axon formation at the opposite side of the neuron from the contact site. *J. Neurosci.* 35, 14517–14532. doi: 10.1523/Jneurosci.1266-15.2015

Xu, Q., Liu, Y. Y., Wang, X. M., Tan, G. H., Li, H. P., Hulbert, S. W., et al. (2018). Autism-associated CHD8 deficiency impairs axon development and migration of cortical neurons. *Mol. Autism* 9:65. doi: 10.1186/s13229-018-0244-2

Yi, J. J., Barnes, A. P., Hand, R., Polleux, F., and Ehlers, M. D. (2010). TGF-beta signaling specifies axons during brain development. *Cell* 142, 144–157. doi: 10.1016/j.cell.2010.06.010

Zhang, B., Wang, W. W., Zhang, Z. J., Hu, Y. L., Meng, F., Wang, F., et al. (2018). Alternative splicing of disabled-1 controls multipolar-to-bipolar transition of migrating neurons in the neocortex. *Cereb. Cortex* 28, 3457–3467. doi: 10.1093/cercor/bhx212

Zhang, T., Zhang, S., Song, X., Zhao, X., Hou, C., Li, Z., et al. (2019). Loss of Lgl1 disrupts the radial glial fiber-guided cortical neuronal migration and causes subcortical band heterotopia in mice. *Neuroscience* 400, 132–145. doi: 10.1016/j.neuroscience.2018.12.039

Zhuo, L., Theis, M., Alvarez-Maya, I., Brenner, M., Willecke, K., and Messing, A. (2001). hGFAP-cre transgenic mice for manipulation of glial and neuronal function in vivo. *Genesis* 31, 85–94.

Conflict of Interest: The authors declare that the research was conducted in the absence of any commercial or financial relationships that could be construed as a potential conflict of interest.

frontiers in Molecular Neuroscience

ORIGINAL RESEARCH
published: 06 July 2021
doi: 10.3389/fnmol.2021.680280

Impaired SNF2L Chromatin Remodeling Prolongs Accessibility at Promoters Enriched for Fos/Jun Binding Sites and Delays Granule Neuron Differentiation

*Laura R. Goodwin[1,2], Gerardo Zapata[1,2], Sara Timpano[1], Jacob Marenger[1] and David J. Picketts[1,2,3]**

[1] Regenerative Medicine Program, Ottawa Hospital Research Institute, Ottawa, ON, Canada, [2] Department of Biochemistry, Microbiology and Immunology, University of Ottawa, Ottawa, ON, Canada, [3] Cellular and Molecular Medicine, University of Ottawa, Ottawa, ON, Canada

OPEN ACCESS

Edited by:
Veronica Martinez Cerdeño, University of California, Davis, United States

Reviewed by:
Mitsuhiro Hashimoto, Fukushima Medical University, Japan
Koji Shibasaki, Nagasaki University, Japan

***Correspondence:**
David J. Picketts
dpicketts@ohri.ca

Specialty section:
This article was submitted to Neuroplasticity and Development, a section of the journal Frontiers in Molecular Neuroscience

Received: 13 March 2021
Accepted: 10 June 2021
Published: 06 July 2021

Citation:
Goodwin LR, Zapata G, Timpano S, Marenger J and Picketts DJ (2021) Impaired SNF2L Chromatin Remodeling Prolongs Accessibility at Promoters Enriched for Fos/Jun Binding Sites and Delays Granule Neuron Differentiation. Front. Mol. Neurosci. 14:680280. doi: 10.3389/fnmol.2021.680280

Chromatin remodeling proteins utilize the energy from ATP hydrolysis to mobilize nucleosomes often creating accessibility for transcription factors within gene regulatory elements. Aberrant chromatin remodeling has diverse effects on neuroprogenitor homeostasis altering progenitor competence, proliferation, survival, or cell fate. Previous work has shown that inactivation of the *ISWI* genes, *Smarca5* (encoding Snf2h) and *Smarca1* (encoding Snf2l) have dramatic effects on brain development. *Smarca5* conditional knockout mice have reduced progenitor expansion and severe forebrain hypoplasia, with a similar effect on the postnatal growth of the cerebellum. In contrast, *Smarca1* mutants exhibited enlarged forebrains with delayed progenitor differentiation and increased neuronal output. Here, we utilized cerebellar granule neuron precursor (GNP) cultures from *Smarca1* mutant mice (Ex6DEL) to explore the requirement for Snf2l on progenitor homeostasis. The Ex6DEL GNPs showed delayed differentiation upon plating that was not attributed to changes in the *Sonic Hedgehog* pathway but was associated with overexpression of numerous positive effectors of proliferation, including targets of Wnt activation. Transcriptome analysis identified increased expression of *Fosb* and *Fosl2* while ATACseq experiments identified a large increase in chromatin accessibility at promoters many enriched for Fos/Jun binding sites. Nonetheless, the elevated proliferation index was transient and the Ex6DEL cultures initiated differentiation with a high concordance in gene expression changes to the wild type cultures. Genes specific to Ex6DEL differentiation were associated with an increased activation of the ERK signaling pathway. Taken together, this data provides the first indication of how *Smarca1* mutations alter progenitor cell homeostasis and contribute to changes in brain size.

Keywords: SMARCA1, Snf2L, ISWI chromatin remodeler, cerebellar granule neuron progenitors, ATAC-seq, chromatin accessibility

INTRODUCTION

Normal brain development requires the neural progenitors to interpret external cues that are used to remodel their chromatin and modulate an intrinsic gene expression program that ultimately defines cellular competence, regulates proliferation, and/or initiates a cell fate lineage decision. Indeed, progenitor cell homeostasis is a tightly regulated process that if perturbed can affect brain size, cellular fate and lamination, and/or cause neurodevelopmental disorders. The characterization of animal models have shown that ablation of chromatin remodeling factors significantly impact neurogenesis, while human genetic studies have implicated them in numerous neurodevelopmental disorders (Bogershausen and Wollnik, 2018; Goodwin and Picketts, 2018; Sokpor et al., 2018; Timpano and Picketts, 2020).

Chromatin remodeling is catalyzed by conserved complexes containing a subunit with a SNF2-like helicase domain that binds and hydrolyzes ATP to reposition nucleosomes. These complexes can be subdivided into four classes, the switch/sucrose non-fermenting (SWI/SNF), imitation-switch (ISWI), chromodomain helicase DNA binding (CHD), and inositol requiring 80-like (INO80) families based on extended homology within the ATPase domain and the inclusion of additional motifs that facilitate chromatin interactions (Clapier et al., 2017). The mammalian ISWI family comprises the closely related *SMARCA1* and *SMARCA5* genes that are orthologs of the *Drosophila ISWI* gene and encode the SNF2L and SNF2H proteins, respectively. The mammalian ISWI proteins form heterodimers comprised of either SNF2H or SNF2L and, most often, a *BAZ* (bromodomain adjacent to zinc finger) gene family member (Goodwin and Picketts, 2018). Seven complexes have been purified including the NURF (Nucleosome remodeling factor), ACF (ATP-utilizing chromatin assembly factor) and CHRAC (chromatin assembly complex) complexes that are highly conserved across species (Tsukiyama and Wu, 1995; Ito et al., 1997; Varga-Weisz et al., 1997). In addition, four novel complexes have been purified from mammalian cells, namely the WICH (WSTF-ISWI chromatin remodeling complex), CERF (CECR2-containing remodeling factor), RSF (remodeling and spacing factor), and NoRC (Nucleolar remodeling complex) complexes (LeRoy et al., 1998; Strohner et al., 2001; Bozhenok et al., 2002; Banting et al., 2005). While it was originally reported that five complexes contained SNF2H (ACF, CHRAC, NoRC, RSF, WICH) and two comprised SNF2L (CERF, NURF), a recent study has suggested that SNF2H and SNF2L are interchangeable within all seven complexes and identified a novel eighth complex containing the protein BAZ2A (Oppikofer et al., 2017). However, most genetic and biochemical data indicate that *Smarca1* and *Smarca5* have non-redundant functions, as described below.

The ISWI proteins remodel and space nucleosome arrays *in vitro* albeit with different affinities (Corona et al., 1999; Langst et al., 1999; Tang et al., 2004; Leonard and Narlikar, 2015; Clapier et al., 2017), and have different effects on the positioning of nucleosomes at transcriptional start sites (TSS) and at CTCF and other transcription factor binding sites (Qiu et al., 2015; Kwon et al., 2016; Wiechens et al., 2016). Moreover, SNF2H containing complexes facilitate DNA repair, regulate heterochromatin maintenance and coordinate rRNA gene expression; functions not demonstrated for SNF2L complexes (as reviewed by Goodwin and Picketts, 2018). However, distinct roles seem less clear when examining mouse models. The inactivation of *Bptf*, the gene encoding the largest subunit of the Snf2l-containing NURF complex results in decreased progenitor self-renewal and impaired terminal differentiation in multiple cell types (Landry et al., 2008, 2011; Koludrovic et al., 2015; Frey et al., 2017). Similarly, inactivation of the *Smarca5* gene resulted in reduced growth and pre-implantation lethality, while tissue specific-inactivation in the developing brain resulted in mice with a striking cerebellar hypoplasia caused by a drastically reduced proportion of proliferating cells in the external granule cell layer (Stopka and Skoultchi, 2003; Alvarez-Saavedra et al., 2014). Given that Snf2l is also expressed in the granule neurons of the cerebellum, it provides the opportunity to utilize granule neuron progenitor cultures to define whether Snf2h and Snf2l act with overlapping or separate functions in progenitor cell homeostasis.

The development of the cerebellum is dependent on two distinct progenitor populations, one located in the ventricular zone (VZ) lining the fourth ventricle and one in the upper rhombic lip (Hatten and Heintz, 1995). The VZ progenitors give rise to all the inhibitory neurons, including Purkinje neurons, while some of these Nestin-expressing progenitors migrate to the external granule layer (EGL) to produce Bergmann glia (Hatten and Heintz, 1995; Hoshino et al., 2005). The progenitors from the rhombic lip give rise to all excitatory neurons including those that form the deep cerebellar nuclei and the population of granule neuron precursors (GNPs) that migrate to the EGL where they proliferate extensively in the postnatal period to produce granule neurons and promote folia growth (Hatten and Heintz, 1995; Alder et al., 1996; Machold and Fishell, 2005). *Smarca5* is expressed robustly in the rhombic lip and the VZ in the embryo but it only seems to affect GNP expansion as normal numbers of Purkinje neurons were detected in the hypoplastic cerebellum of *Smarca5* cKO mice (Alvarez-Saavedra et al., 2014). In contrast, *Smarca1* showed very weak expression in the VZ and rhombic lip appearing more prevalently after birth in differentiating granule neurons (Alvarez-Saavedra et al., 2014). In the cerebral cortex, mice with a targeted deletion of exon 6 of the *Smarca1* gene (Ex6DEL mice) that encodes the ATP-binding pocket resulted in increased proliferation of intermediate progenitor cells (IPCs) that delayed differentiation and gave rise to animals with a larger brain (Yip et al., 2012). These studies suggest that the ISWI proteins Snf2h and Snf2l play distinct and critical roles in regulating the transition of a proliferating progenitor to a differentiated neuron.

The aim of the current study was to determine the effects of *Smarca1* loss on GNP proliferation and granule neuron differentiation in the developing cerebellum. Moreover, we sought to utilize primary GNP cultures to assess the global changes to the chromatin landscape and transcriptome as a means to define the underlying function of Snf2l during neurogenesis. In this way, we established that GNPs require Snf2l to limit chromatin accessibility at key TSS to promote differentiation. Cultures from the Ex6DEL mice showed an enrichment of chromatin accessibility, particularly at the

TSS of genes containing Fos/Jun binding sites that delayed differentiation. Despite the delay in differentiation the Ex6DEL cells utilized a similar genetic program to differentiate that was characterized by increased activation of the ERK pathway.

MATERIALS AND METHODS

Animal Work

The *Smarca1* gene resides on the X chromosome and the generation of the *Smarca1*$^{Ex6DEL/Y}$ male mice have been described previously (Yip et al., 2012). Animals were maintained on an FVB/N background and housed in an animal facility under SPF (specific pathogen-free) conditions on a 12/12 light:dark cycle with water and food *ad libitum*. All animal experiments were approved by the University of Ottawa's Animal Care ethics committee, with the guidelines set out by the Canadian Council on Animal Care. *Smarca1*$^{Ex6DEL/+}$ female mice were bred with wild-type males and pups were harvested between 4 and 6 days after birth for GNP isolation, or at postnatal day 10 (P10) for RNA isolation.

GNP Cultures

GNPs were isolated from the cerebella of postnatal day (P)4-P6 pups as previously described by Lee et al. (2009). To increase GNP culture purity, GNPs were passed through a 60–35% Percoll step gradient (Sigma, cat # P4937), wherein GNPs settled at the 35–60% interphase. Cells were plated in serum-free Neurobasal^{TM}-A medium with B-27 supplement (Thermo Scientific, cat # 0080085-SA) at a density of 5.5×10^5 cells/well of a 24 well plate coated with 1 mg/ml Poly-D-lysine hydrobromide (Sigma, cat # P6407). A partial media change was performed within a day of isolation and repeated every 48 h. GNP viability was assessed using the Beckman Coulter Vi-CELLTM XR Cell Viability Analyzer default cell counting system (cell size 5–50 μM). Cell viability was assessed by trypan blue dye exclusion method.

Genotyping was performed on genomic DNA from freshly isolated GNP cultures after dissection under the following PCR conditions: a denaturing cycle at 94°C for 2 min, 39 PCR cycles (94°C for 30 s, 60°C for 30 s, 72°C for 45 s) and a final cycle at 72°C for 10 min. A three primer system was used for genotyping with two primers located in the introns flanking exon 6 (Smarca1Intron5For: 5′-CCTGGGCTGGAACCATGATC-3′ and Smarca1Intron6Rev: 5′-GTATGGACAAGTGTGTGAAGCC-3′) and a third primer located within Exon 6 (Smarca1Exon6Rev: 5′-CCATGTGGGGTCCAGGAATG-3′). PCR conditions result in the amplification of only the smaller WT product of 509 bp (Intron5-Exon6; the larger 1108 bp Intron5-Intron6 product is undetectable). The Ex6DEL product is 450 bp and the PCR reactions were electrophoresed on a 1.5–2% agarose gel for genotype analysis.

BrdU-Pulse Labeling and Immunostaining

Granule neuron precursors cultured on coverslips ($n = 4$) were pulse labeled by adding BrdU (50 μM; Sigma, cat # B-5002) directly to the culture for 2 h. For BrdU immunodetection, cells were fixed (2% PFA, 10 min, RT) and permeabilized (PBS with 0.03% triton-X 100, 10 min at RT) and then were subjected to a DNA hydrolysis incubation (2.5 N HCl, 10 min, RT) prior to immunostaining. For immunostaining, cells were fixed to coverslips and permeabilized as described above. Cells were blocked in 10% horse serum (Life Technologies, cat # 26050-088) in TBST with BSA for 1 hr at RT. Primary antibodies rabbit anti-NF200 (1:500, Sigma, N4142); rabbit anti-Ki67 (1:500, Abcam, ab16667); mouse anti-BrdU (1:500, BD Bioscience, 347580); or rabbit anti-GFAP (1:500, Stem Cell Technologies, 01415) were diluted 1:500 in blocking solution and incubated on the coverslips overnight at 4°C. Secondary Alexa Fluor® (Jackson Immunoresearch) antibody was diluted 1:4000 in PBS and applied for 30 min RT prior to 5 min in a 1:10000 bis-benzimide-Hoescht 33342 (Sigma, United States, cat#B2261) solution in PBS. Coverslips were mounted onto slides with mounting medium (Agilent Technologies, cat # S3023). Coverslips were imaged with an Axio Imager M1 microscope (Zeiss) using either 20X or 40X objectives. Images (6 per time point for each replicate) were prepared with Fiji software[1] (version 2.0.0). All BrdU-positive cell counts were performed relative to DAPI-labeled nuclei and statistically analyzed by two-way ANOVA from 3-replicate experiments using Excel software. Statistical significance was assumed when the p-value was less than 0.05. p-values were annotated on the figures as follows: $^{*}p < 0.05$; $^{**}p < 0.01$; $^{***}p < 0.001$.

Immunoblotting

Cerebellar extracts were quickly dissected from individual pups and then homogenized in ice-cold lysis buffer supplemented with protease inhibitor cocktail (Sigma, United States; P8340) and phosphatase inhibitor cocktail (Fisher, cat # 78441), and then incubated for 10 min at 4°C with gentle mixing. Cultured GNP cell lysates were prepared similarly following resuspension in PBS with a cell scraper. After pre-clearing by centrifugation (5 min at 17,000 × g), proteins were quantified by the Bradford method (BioRad, cat # 500-00006). Protein samples were resolved on sodium dodecyl sulfate polyacrylamide gels under denaturing conditions or using Bis-Tris 4–12% gradient gels (NuPage, Invitrogen, United States; cat # NP0007) and blotted onto PVDF membranes (BioRad, cat # 162-0177) by wet transfer for 1 hr at 90V. Membranes were blocked (45 min, room temperature) with 5% skim milk in TBST and incubated (4°C, overnight) in primary antibody [rabbit anti-Snf2l (1:2000, Abcam, ab37003); rabbit anti-Snf2h (1:2000, Abcam, ab72499); rabbit anti-vinculin (1:2000, Abcam, ab129002); rabbit anti-Ki67 (1:2000, Abcam, ab16667); mouse anti-NeuN (1:2000, Millipore, MAB377); mouse anti-Tuj1 (1:2000, Stem Cell Technologies, 01409); rabbit anti-CECR2 (1:1000; gift from Dr. Heather McDermid, uAlberta); rabbit anti-ERK (1:2000, Santa Cruz, sc154); or mouse anti-pERK (1:500, Santa Cruz, sc7383)]. Membranes were incubated (1 h, RT) with ImmunoPure® HRP-conjugated goat anti-rabbit or goat anti-mouse IgG (H + L) secondary antibodies (1:25000; Pierce, Rockford, IL, United States). Membranes were

[1] http://gtrd.biouml.org/#!

washed 3 × 10 min in TBST after antibody incubations, and the signal was detected using the Pierce Supersignal West Fempto chemiluminescence substrate (ThermoFisher Scientific, cat # 34095). At least 2 separate Western blots were quantified using ImageJ software for quantitation (Schneider et al., 2012).

Co-immunoprecipitation (co-IP)

Each co-IP was prepared with 500 μg of P21 cerebellar protein lysate (described above), 1 μg antibody, protease inhibitors and lysis buffer to bring the final co-IP volume to 500 μL, which was then rocked overnight at 4°C. Protein A/G magnetic beads (Bioclone Inc, #MA-102) was rinsed twice on a magnetized stand (Thermo Fisher) with two volumes of non-denaturing lysis buffer. Thirty μL bead slurry was then added to each co-IP reaction for capture on a rocking platform at 4°C for 1 h. Beads were washed 5 times in 1 mL 0.3% triton-X in PBS, with each wash being performed on a rocking platform at 4°C for 5 min. Beads were resuspended in 0.1M glycine (pH 2.5) elution buffer and incubated for 10 min RT prior to recovering eluate. Elution was repeated 3 additional times. Samples were prepared in 1:3 in 1X NuPAGE LDS Sample Buffer and 1.5% β-mercaptoethanol (Sigma, #M7522) prior to immunoblotting.

qRT-PCR

RNA was isolated from P10 cerebella or cultured GNPs using TRIzol Reagent (Life Technologies, #15596018) according to manufacturer's instructions. RNA was purified using DNA-*free* kit (ThermoFisher Scientific, AM1906) according to the manufacturer's instructions. Complementary DNA (cDNA) was generated with the RevertAid First Strand cDNA Synthesis Kit (Thermo Fisher, #K1621) and was carried out in a thermocycler for 5 min at 25°C, 1 h at 42°C followed by 5 min at 70°C. qPCR reactions were prepared by mixing 10 μL Lo-ROX 2X SYBR Master Mix (FroggaBio Inc, #BIO-94020) with 0.5 μM of primers and 200 ng of cDNA. Primer used in this study are listed in **Table 1**. All reactions were performed in technical triplicates. qPCR was carried out on MicroAmp® Fast Optical 96-well Reaction Plate (Life Technologies, #4346906) and run on 7500 Applied Biosystems® Fast Real-Time PCR System [95°C 5 min, 40 cycles (95°C for 5 s, 60°C for 15 s, 72°C for 20 s), and 72°C for 5 min]. Relative fold change was normalized using two controls (18S rRNA and GAPDH) and calculated using ΔΔCt method. Statistical significance was determined using Student's *t*-test.

TABLE 1 | List of qPCR primers used for validation of differential gene expression.

BDNF	F: 5′-AGCCTCCTCTTCTCTTTCTGCTGGA-3′ R: 5′-CTTTTGTTGTCTATGCCCCTGCCTT-3′
Sox2	F: 5′-TGCTCAAGATCAAATGGC-3′ R: 5′-GGACTTTTGACCCAGTG-3′
TH	F: 5′-TCCCCAAGGTTCATTGGACG-3′ R: 5′-GGTACCCTATGCATTTAGCT-3′
c-Fos	F: 5′-GGGGACAGCCTTTCCTACTA-3′ R: 5′-CTGTCACCGTGGGGATAAAG-3′
FosB	F: 5′-AAGTGTGCTGTGGAGTTC-3′ R: 5′-ATGTTGGAAGTGGTCGA-3′
Fosl2	F: 5′-CCAGCAGAAGTTCCGGGTAG-3′ R: 5′-GTAGGGATGTGAGCGTGGATA-3′
JunB	F: 5′-TCACGACGACTCTTACGCAG-3′ R: 5′-CCTTGAGACCCCGATAGGGA-3′
Jun	F: 5′-CCTTCTACGACGATGCCCTC-3′ R: 5′-GGTTCAAGGTCATGCTCTGTTT-3′
c-Jun	F: 5′-ACGACCTTCTACGACGATGC-3′ R: 5′-CCAGGTTCAAGGTCATGCTC-3′
JunD	F: 5′-CCAGGTTCAAGGTCATGCTC-3′ R: 5′-AGCCCGTTGGACTGGATGA-3′
Ets-1	F: 5′-AAAGAGTGCTTCCTCGAGCT-3′ R: 5′-AGGCTGTTGAAGGATGACTG-3′
Edn-1	F: 5′-TTTTTCCCCACTCTTCTGACCC-3′ R: 5′-AGTCCATACGGTACGACG-3′
Ednra	F: 5′-CAACTGTGTCTAGGAGGTGGGG-3′ R: 5′-ATGGTCAGCCAAAAGTATGCCG-3′
Ednrb	F: 5′-TTGCTCGCAGAGGACTGGCCA-3′ R: 5′-AAGCATGCAGACCCTTAGGGG-3′
Fgf-3	F: 5′-TCCACAAACTCACACTCTGC-3′ R: 5′-GAACAGCGCCTATAGCATCC-3′
Fgf-5	F: 5′-AACTCCTCGTATTCCTACAATCC-3′ R: 5′-CGGATGGCAAAGTCAATGG-3′
18S	F: 5′-TGTCTCAAAGATTAAGCCATGC-3′ R: 5′-GCGACCAAAGAAACCATAAC-3′
Gapdh	F: 5′-ATCCACGACGGACACATTGG-3′ R: 5′ -CAACGACCCCTTCATTGACCTC-3′

RNA-seq Analysis

RNA was isolated from GNPs (∼3 × 10^6 cells) using TRIzol (Life Technologies, #15596018) according to manufacturer's instructions. RNA cleanup was performed with PureLink RNA Mini Kit (Thermo Fisher, #12183020) with in-column DNaseI digestion (Thermo Fisher, AM1906). RNA samples (n = 3) were sequenced at GenomeQuébec (Montréal). RNA integrity was confirmed upon arrival by Bioanalyzer prior to cDNA library generation. Paired RNA-seq was performed on HiSeq4000 PE 100 bp lane and a minimum of 35 million reads was obtained per sample. Quality control (QC) on raw.fastq files was carried out with FastQC (version 0.11.5). Reads were pseudoaligned to GRCm38 (release 88) by kallisto (version 0.44.0; bootstraps = 50) and quantified with Sleuth (version 0.29.0). Differentially expressed genes (DEGs) set a fold-change threshold of ±1.5 with qval ≤0.05. Heatmaps were generated with pheatmap (version 1.0.10) and RColorBrewer (version 1.1-2). Gene Ontology (GO) enrichment analysis[2] established enriched biological process terms (significant enrichment set at fold enrichment ≥ 1.5 and FDR ≤ 0.05). oPOSSUM was used to identify the transcription factor binding sites within promoter sequences of the differentially expressed genes (Kwon et al., 2012). RNA-seq data was deposited into the GEO database with the accession number GSE122173.

ATAC-seq Sample Preparation

Samples from WT and Ex6DEL GNP cultures [1 days *in vitro* (DIV) and 3DIV; n = 2] were prepared according to Buenrostro et al. (2013, 2015) with modification in transposase reaction conditions. Briefly, 50,000 cells were pelleted, resuspended in

[2]http://www.geneontology.org/

50 μL lysis buffer and centrifuged (500 × *g* for 10 min at 4°C). Transposition mix was prepared by combining 25 μL Nextera TD 2X reaction buffer and 5 μL Nextera TDE1 Tn5 Transposase (Illumina, #FC-121- 1030) to 20 μL nuclease free H2O. Nuclei pellet was resuspended in transposition mix and incubated for 40 min at 37°C. Transposed DNA was purified and eluted using Qiagen MinElute PCR Purification Kit (Qiagen, #28004). The PCR reaction was prepared with 10 μL eluted tagmented DNA, 10 μL nuclease-free H2O, 2.5 μL 25 μM ATAC PCR primers and 2X NEBNext High-Fidelity 2X PCR master mix (New England Biolabs, #M0541S). Amplification and qPCR side reaction was carried out as previously described by Buenrostro et al. (2013, 2015). The amplified library was cleaned with Qiagen MinElute PCR Purification Kit and verified by Bioanalyzer prior to sequencing (Stemcore, Ottawa Hospital Research Institute). Sequencing was performed with Illumina NextSeq500 (PE 75 bp) and an average of 100 million reads were obtained per sample (Stemcore, Ottawa Hospital Research Institute).

ATAC-seq Analysis

Quality control on raw fastq files was carried out with FastQC (version 0.11.6). Adapters were trimmed using atactk (version 0.1.5) and aligned to mm10 with Bowtie 2 (version 2.3.4). Duplicates were removed with Picard tools (version 2.17.0) and peaks were called using macs2 –shift −100, –ext size 200 in –broad mode (qval < 0.1). BigWig files were prepared for visualization with deepTools2 bamCoverage command and normalized to reads per kilobase per million mapped reads (RPKM) and visualized with IGV (Thorvaldsdottir et al., 2013). DeepTools2 was used to plot read abundance over scaled gene and accessibility heatmaps (Ramirez et al., 2016). Differentially accessible regions (DARs) were established from consensus peaks of merged replicates without summits with DiffBind (version 2.8.0; Ross-Innes et al., 2012). Distribution over genomic features was plotted with ChIPpeakAnno (version 3.14.0; Zhu et al., 2010). ATACseqQC (version 1.2.9; Ou et al., 2018) was used to separate reads based on length. HOMER was used to annotate peaks, as well as to identify and quantify differential motif binding sites on accessible peaks (Heinz et al., 2010). SeqPlots was used to quantify and compare accessible TSS (Stempor and Ahringer, 2016). mESC E14 merged control ATACseq dataset (GEO number GSE98390) was retrieved and analyzed similarly using deepTools2. DAVID was used to identify the biological process, Gene Ontology (GO) functional annotation of ATAC peaks alongside the 0 and 72 h DEGs (Huang da et al., 2009). Dplyr[3], ggplot2[4], and Vennerable[5] were then used to organize and plot results in R (RStudio Team., 2020). Gene Transcription Regulation Database (GRTD) was used to identify the overlap of Fos/Jun/AP-1 binding sites between the DAR and DEG list of the granule neuron progenitor cell population[5]. The ATAC-seq data was deposited into the GEO database with the accession number GSE122172.

[3]https://dplyr.tidyverse.org//

[4]https://ggplot2.tidyverse.org

[5]https://github.com/js229/Vennerable

RESULTS

During forebrain development, the *ISWI* homologs *Smarca5* and *Smarca1* (encoding Snf2h and Snf2l proteins, respectively) play essential non-redundant roles. When *Smarca5* is inactivated progenitor expansion is compromised leading to cortical hypoplasia (Alvarez-Saavedra et al., 2019). In contrast, the Ex6DEL mice, containing an internal deletion in the *Smarca1* gene and lacking a functional Snf2l protein present with an enlarged brain due to hyperproliferation of the IPCs (Yip et al., 2012). Taken together, this data suggests that Snf2l and Snf2h have differential effects on progenitor cell homeostasis. *Smarca5* and *Smarca1* are both expressed in the developing postnatal cerebellum, with the early loss of expression of *Smarca5* causing a severe reduction in cerebellar granule neuron progenitor expansion and cerebellar growth (Alvarez-Saavedra et al., 2014). To determine whether the ISWI proteins have antagonistic roles in the cerebellum, we isolated primary cultures of GNPs from WT and Ex6DEL mice to study the role of the Snf2l protein (**Figure 1A**; Oliver et al., 2005; Bassett et al., 2016). Freshly isolated GNPs from WT spontaneously differentiate over 3 days in culture into granule neurons (GNs) in the absence of Sonic hedgehog protein (Shh) or agonist (Wechsler-Reya and Scott, 1999). The GNP cultures had a high level of purity as we observed < 5% of cells positive for glial acidic fibrillary protein (GFAP; **Supplementary Figure 1A**). Immunostaining for neurofilament 200 (NF200) of the GNPs from WT suggested a neuronal identity and, by 3 DIV, highlighted the growth of neurite extensions (**Figure 1B**) that were also readily visible by phase-contrast microscopy (WT, **Figure 1E**). Immunoblot analysis at 1 DIV and at 3 DIV from WT GNP cultures indicated that Snf2l protein levels increased 3.6-fold with differentiation while Snf2h protein levels decreased by 11-fold (**Figure 1C**), consistent with our observations in murine cerebellar extracts (Alvarez-Saavedra et al., 2014). The WT cells were also immunoblotted for two pan-neuronal markers (NeuN, Tuj1) and a protein characteristic of cycling cells (Ki67). These blots indicated that GNPs of WT had exited the cell cycle and obtained neuronal identity by 3 DIV (**Figure 1C**). Next, we isolated GNPs from the Ex6DEL mice to compare their differentiation properties. Immunoblot and PCR genotyping analysis (WT band 508 bp; Ex6DEL band 450 bp) confirmed that the cells were deleted for exon 6 and expressed the internally truncated Snf2l protein (WT protein 122 kDa; Ex6DEL protein 115 kDa; **Figure 1D**). While the cultures were very similar at 1 DIV, we observed that the majority of the Ex6DEL GNPs had not extended neurites by 3 DIV (**Figure 1E**) despite insignificant differences in cell viability (**Supplementary Figure 1B**).

Ex6DEL GNP Cultures Show Delayed Differentiation Upon Plating

Within the developing forebrain of Ex6DEL mice we had previously demonstrated that an increased proportion of IPCs underwent self-renewal and that this in turn delayed cell differentiation (Yip et al., 2012). To assess whether GNPs had a similar fate, we initially immunostained 1 and 3 DIV cultures for Ki67 (**Supplementary Figure 2A**). GNPs require Shh as a

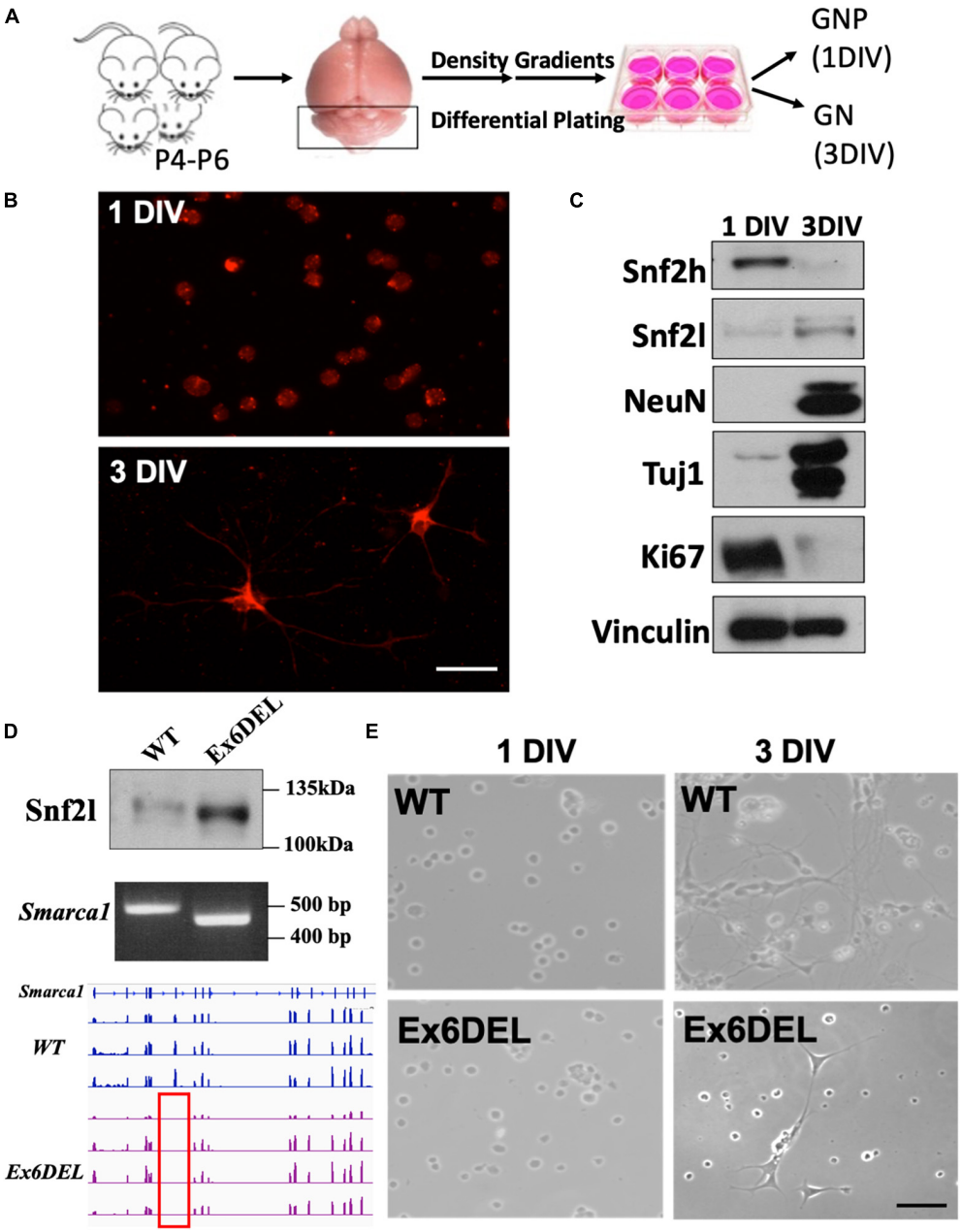

FIGURE 1 | Generation of GNP cultures from the Ex6DEL mice. **(A)** Schematic diagram of the procedure for generating GNP and granule neuron cultures. **(B)** Representative images of WT cultures 1 DIV (top image) and 3 DIV (bottom image) stained with neurofilament-200 (red). Scale bar, 25 μM. **(C)** Protein extracts of primary GNP cultures at I and 3 DIV were immunoblotted for the ISWI proteins (Snf2h, Snf2l), neuronal (Tuj, NeuN) and proliferation (Ki67) markers. Vinculin was used as a loading control. **(D)** Immunoblot (top panel), *Smarca1* genotyping (middle panel), and RNAseq analysis (bottom panel) from WT and Ex6DEL GNP cultures confirmed the loss of exon 6 in the GNP cultures isolated from Ex6DEL mice. The red rectangle outlines the absence of RNAseq reads corresponding to the position of exon 6. **(E)** Phase contrast images of GNP cultures from WT and Ex6DEL mice. Scale bar, 50 μM.

growth mitogen which is released from Purkinje neurons, and since it is not present in the culture media the GNPs typically complete a final mitotic cycle and initiate differentiation upon plating (Wechsler-Reya and Scott, 1999). At 1 DIV, $Ki67^{+}$ cells were present in both WT GNP and Ex6DEL GNP cultures but $Ki67^{+}$ cells were only detected in the Ex6DEL GNP cultures at 3 DIV (**Supplementary Figure 2A**) suggesting that cell cycle exit was delayed. As such, we incubated GNP cultures with BrdU 2 h before harvesting them at 2 h, 1 DIV, 2 DIV, and 3 DIV after plating to quantify the proportion of cells in S-phase as a second measure of cell proliferation (four independent experiments per timepoint analyzed, five images quantified per coverslip). As expected, the short BrdU pulse labeled 25–30% of cells at 2 h and incorporation of BrdU decreased in the GNPs from WT

to less than 10% after 1 DIV (**Figure 2A**). In contrast, BrdU incorporation in the GNPs from Ex6DEL mice remained at or above 25% at the 1 DIV and 2 DIV timepoints before dropping below 10% at 3 DIV (**Figure 2A**). This suggests that the Ex6DEL GNPs are delayed in their ability to exit the cell cycle, which is consistent with what we observed *in vivo* in the developing forebrain of Ex6DEL mice (Yip et al., 2012). In the postnatal developing cerebellum, $Pax6^+$ GNPs proliferate in the EGL then the postmitotic granule neurons migrate through the molecular layer to complete their maturation in the IGL. We reasoned that the Ex6DEL cerebellum should contain fewer $Pax6^+$ cells migrating through the molecular layer at P10 if cell cycle exit was delayed. P10 cerebellar sections from WT and Ex6DEL mice were stained for Pax6 and the number of $Pax6^+$ cells within the molecular layer was quantified. This experiment showed a 25% reduction in the number of migrating $Pax6^+$ granule neurons in the molecular layer of Ex6DEL mice compared to WT mice (**Figures 2B,C**). Taken together, these results suggest that Snf2l is required for timely cell cycle exit that delayed but does not impair granule neuron differentiation as indicated by NeuN and Tuj1 staining in both GNP and cortical neuron cultures (**Supplementary Figures 2B–D**).

The removal of exon 6 maintains the Snf2l open reading frame (ORF) resulting in an internally truncated protein that renders the enzyme unable to bind and hydrolyze ATP, thereby impairing chromatin remodeling activity (Yip et al., 2012). Nonetheless, it remains possible that the Ex6DEL Snf2l protein is incorporated into ISWI complexes such as CERF. These complexes may then maintain their ability to bind chromatin without catalytic remodeling activity, which could contribute to the delayed differentiation of the GNPs. To assess whether the truncated Snf2l protein in Ex6DEL mice can incorporate into an ISWI complex we performed co-immunoprecipitation (co-IP) experiments with CECR2, the partner protein associated with Snf2l in the CERF complex and abundant in the cerebellum (Banting et al., 2005). Cerebellar lysates from WT and Ex6DEL mice isolated at P21 were used for co-IP with anti-Snf2l and anti-Cecr2 antibodies. As indicated in **Figure 2D**, we detected the intact CERF complex in both WT and Ex6DEL lysates suggesting that the internally truncated Snf2l protein was incorporated into the CERF complex.

Increased Proliferation Linked to Edn1/Ednra-MAPK-Fos/Jun Pathway

We next performed RNAseq analysis of WT and Ex6DEL cerebellar GNP cultures ($\sim 3 \times 10^6$ cells) at 1 and 3 DIV to identify transcriptome differences that might contribute to the delay in cell cycle exit and differentiation. At 1 DIV, we observed 126 downregulated and 403 upregulated genes in Ex6DEL GNPs as compared with WT GNPs ($\log_2$fold-change threshold $\pm$ 0.5 with qval $\leq$ 0.05; **Figure 3A** and **Supplementary Table 1**). GO term analysis of the differentially expressed genes (DEGs) indicated that angiogenesis was the biological process with the most significant change (**Figure 3B**). It also highlighted a number of biological processes that could mediate GNP homeostasis and contribute to the delayed differentiation including transcriptional regulation, cell signaling, cell adhesion, and cell proliferation (**Figure 3B**). The specific gene changes we observed that are associated with these four GO terms are highlighted in **Figure 3C**. It is well known that Shh signaling mediates GNP proliferation (Wechsler-Reya and Scott, 1999), but we did not observe any changes at 1 DIV to the pathway components or downstream effectors (*Gli1*, *N-Myc*, *Math1*, or *Ccnd1*; **Supplementary Table 1**), except for an increase in *Stox1* ($\text{Log}_2\text{FC} = 0.80$), a gene normally repressed by Shh signaling (**Figure 3C**). Of note, two members of the mitogenic fibroblast growth factor family (*Fgf3*, $\text{Log}_2\text{FC} = -1.04$; *Fgf5*, $\text{Log}_2\text{FC} = -1.02$) were decreased in expression (**Figure 3C**). Despite the lack of change in mitogenic pathways affecting GNP proliferation (e.g., Shh and Fgf), we observed altered expression of many genes with known roles in cancer and the epithelial-to-mesenchyme transition (e.g., *Acer2,* $\text{Log}_2\text{FC} = 0.59$; *Apln*, $\text{Log}_2\text{FC} = 1.20$; *Chp2*, $\text{Log}_2\text{FC} = 1.21$; *Cntfr*, $\text{Log}_2\text{FC} = -0.66$; *Pak1*, $\text{Log}_2\text{FC} = -0.62$; and *Wwtr1*, $\text{Log}_2\text{FC} = 0.89$; **Figure 3C**). In addition, the Wnt receptor *Fzd6* was upregulated ($\text{Log}_2\text{FC} = 0.84$) as were multiple downstream targets of the WNT/β-catenin signaling pathway (*Flt4,* $\text{Log}_2\text{FC} = 1.00$; *Kdr*, $\text{Log}_2\text{FC} = 0.89$; *Lef1*, $\text{Log}_2\text{FC} = 0.84$), including endothelin 1 (*Edn1*, $\text{Log}_2\text{FC} = 0.93$) and its receptor (*Ednra*, $\text{Log}_2\text{FC} = 0.79$) (**Figure 3C**; Eckey et al., 2012; Katoh, 2018; Adams et al., 2020). The observation suggested that the prolonged proliferative phenotype of the Ex6DEL GNP cultures could arise from activation of the Wnt signaling pathway or dysregulation of genes associated with cancer.

Aside from the genes linked to the GO term Cell Proliferation, we examined our DEG list for changes in *Wnt* and β-catenin (*Ctnnb1*) gene expression but did not observe any changes suggesting that they are not direct transcriptional targets of Snf2l (**Figure 3C** and **Supplementary Table 1**). Comparison of our DEG list with known direct and indirect Wnt target genes from two sources (The Wnt Homepage; Boonekamp et al., 2021) revealed increased expression in seven additional Wnt target genes (*Abcb1a*, $\text{Log}_2\text{FC} = 0.97$; *Neurod1*, $\text{Log}_2\text{FC} = -0.61$; *Ptgs2*, $\text{Log}_2\text{FC} = 0.89$; *Fn1*, $\text{Log}_2\text{FC} = 0.77$; and *Plaur*, $\text{Log}_2\text{FC} = 1.12$; *Abcc4*, $\text{Log}_2\text{FC} = 0.74$; *Nes*, $\text{Log}_2\text{FC} = 0.63$) suggesting activation of the Wnt signaling cascade in Ex6DEL cultures. Moreover, several downstream signaling components of the Edn1/Ednra pathway showed increased expression including *Mapk15* ($\text{Log}_2\text{FC} = 0.87$), *Map3k8* ($\text{Log}_2\text{FC} = 0.61$), and *Fos* gene expression (*Fosb*, $\text{Log}_2\text{FC} = 0.64$; *Fosl2*, $\text{Log}_2\text{FC} = 0.74$) suggesting further involvement of this effector pathway (**Supplementary Table 1**). To assess the Edn1/Ednra-MAPK-Fos/Jun pathway in the Ex6DEL mice we first validated that *Edn1* and both receptors (*Ednra* and *Ednrb*) were upregulated in P10 cerebellum from mutant animals (**Supplementary Figure 3A**). Similarly, we confirmed a ∼3-fold increase in expression of the *Fosb* (FC = 3.16, $p = 0.035$) and *Fosl2* (FC = 2.79, $p = 0.39$) genes, although Fosl2 did not reach statistical significance (**Figure 3D**) in the Ex6DEL P10 cerebella, suggesting that the pathway was active both *in vitro* (isolated GNPs) and *in vivo*. However, in the Ex6DEL mice we observed that the expression of *Jun*, *Junb*, and *Jund* were also upregulated in the cerebella, but this was not observed in the Ex6DEL GNP cultures. Taken together, this data suggested that activation of Wnt signaling and dysregulation of the *Edn1*/*Ednra*-MAPK-*Fos*/*Jun* signaling pathway might be

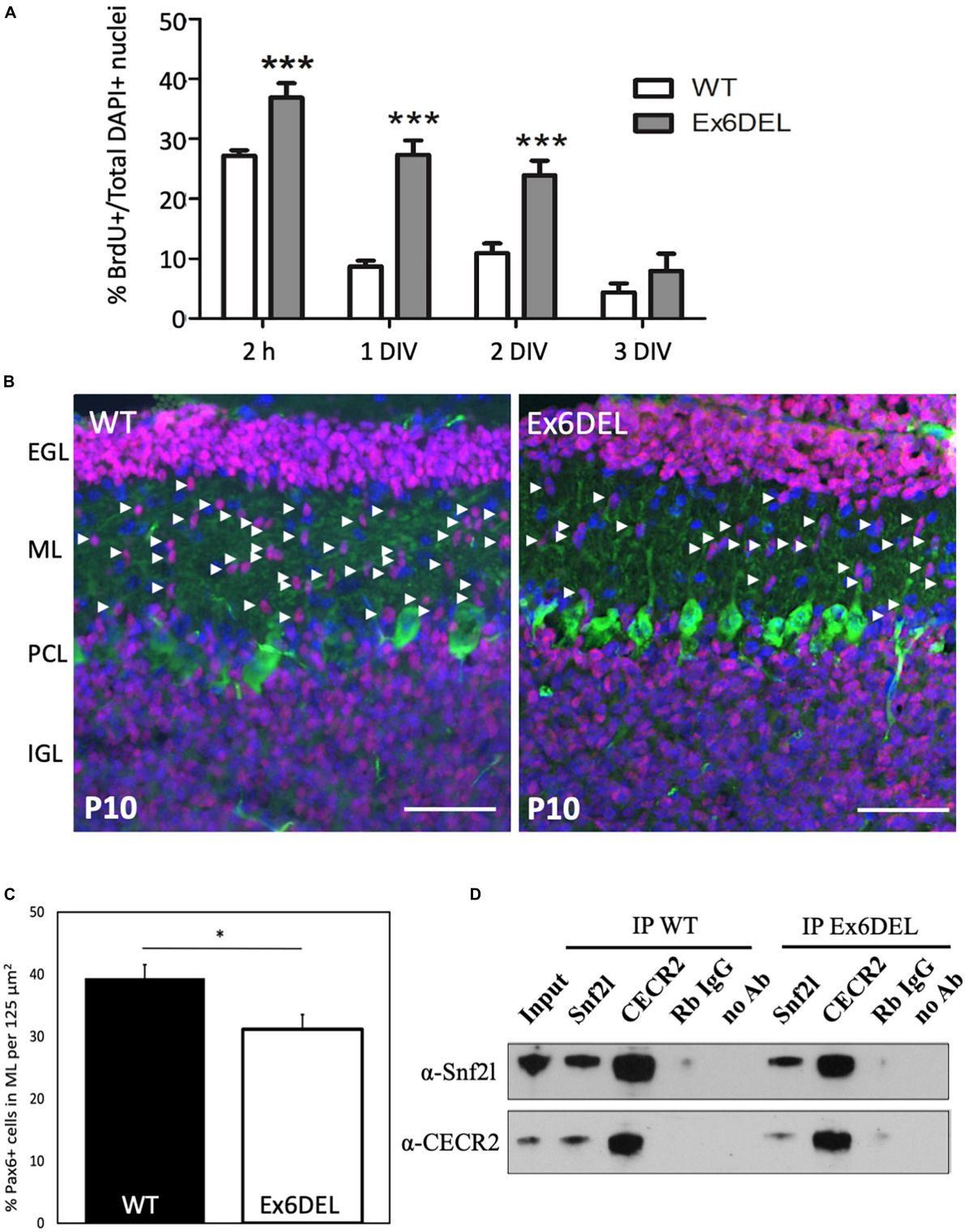

FIGURE 2 | Ex6DEL cultures show delayed differentiation. **(A)** Graph depicting the fraction of BrdU + cells in WT (white bars) and Ex6DEL (gray bars) GNP cultures at the specified times. Cultures were pulsed with BrdU for 2 h prior to harvesting cells for analysis. ($n = 4$ independent experiments; five images per coverslip used for quantification). ***$p < 0.001$. **(B)** P10 cerebellar sections from WT and Ex6DEL mice stained for committed granule neurons (Pax6, magenta), Purkinje neurons (Calbindin, green) or all cell nuclei (DAPI, blue). Arrowheads indicate the migrating postmitotic granule neurons. EGL, external granule layer; ML, molecular layer; PCL, Purkinje cell layer; IGL, inner granule layer. Scale bar, 50 μM. **(C)** Plot of the percentage of $Pax6^+$ cells within the ML. *$p < 0.05$. **(D)** Immunoblot analysis of cerebellar extracts from WT and Ex6DEL mice co-immunoprecipitated for Snf2l, Cecr2, or a control rabbit antibody (Rb IgG).

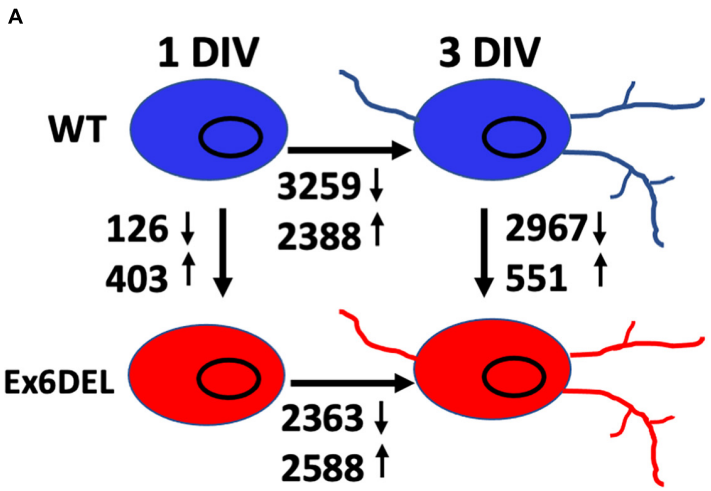

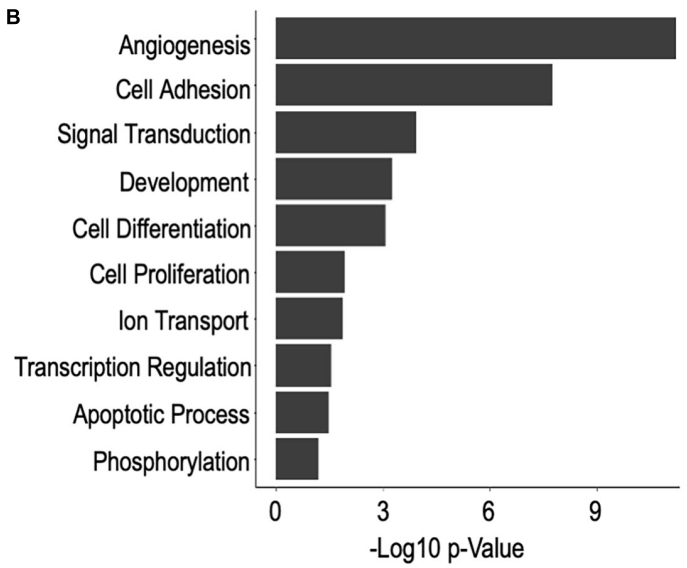

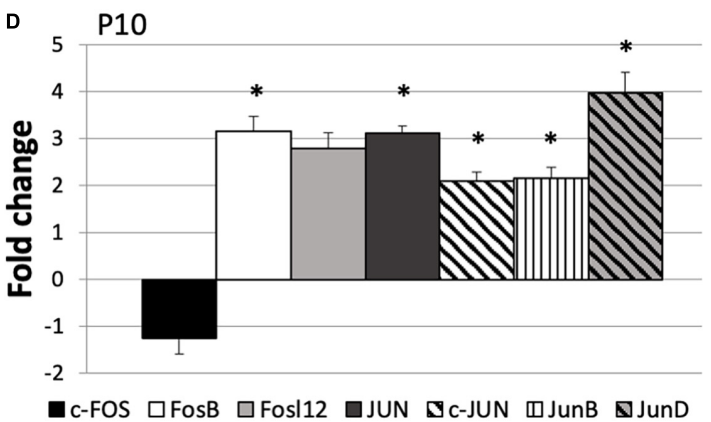

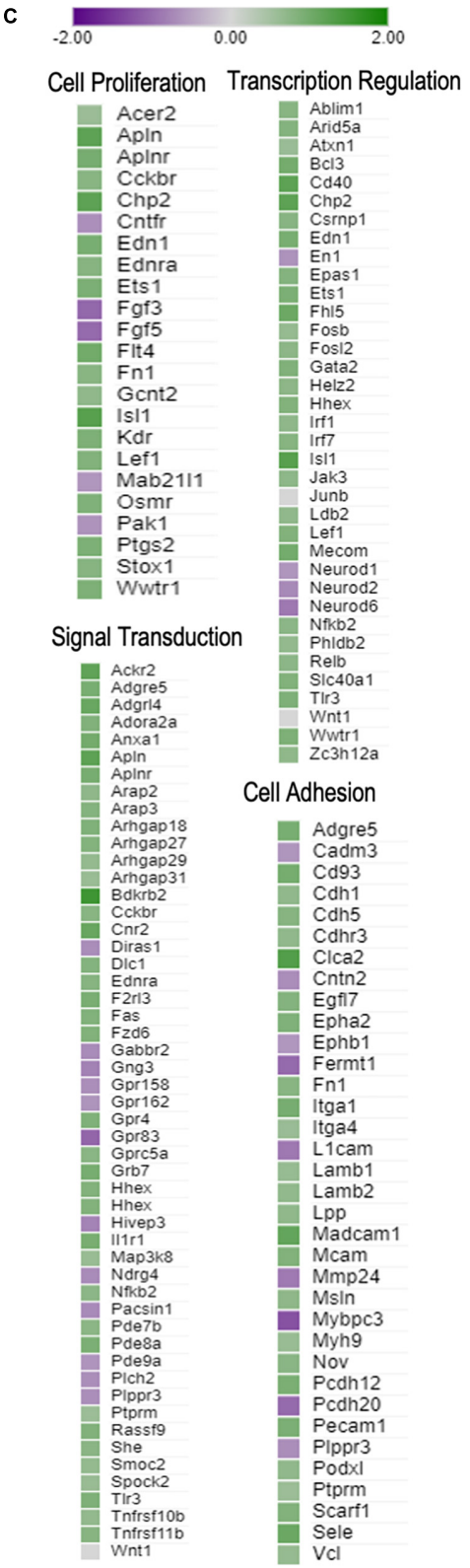

FIGURE 3 | RNAseq analysis of WT and Ex6DEL cultures. **(A)** Schematic diagram showing the numbers of differentially expressed genes (DEGs) between different samples (WT and Ex6DEL) and days in culture. **(B)** GO term analysis of the DEGs observed at 1 DIV. **(C)** DEG lists for some of the top GO terms. **(D)** RT-qPCR validation of Fos/Jun genes from RNA isolated from P10 cerebella. $*p < 0.05$.

a key contributor to the prolonged proliferation of the GNPs isolated from the Ex6DEL mice.

Increased Promoter Accessibility Associated With Fos/Jun Binding Sites

The *Drosophila* ISWI protein has been shown to bind near promoters and affect nucleosome positioning adjacent to the transcription start site (TSS) of genes (Sala et al., 2011; Morris et al., 2014). In HeLa cells, both SNF2H and SNF2L were important for organizing nucleosomes adjacent to transcription factor binding sites (Wiechens et al., 2016). As such, we reasoned that loss of Snf2l remodeling activity in GNP cultures would alter the chromatin landscape, particularly at gene regulatory regions. Since we were not able to confirm the validity of the commercial Snf2l antibodies for chromatin immunoprecipitation, it prompted us to employ ATAC-seq to map modifications in chromatin accessibility. ATAC-seq takes advantage of a hyperactive Tn5 transposase which can insert itself and add sequencing primers to sufficiently accessible DNA from nucleosome free regions (NFR) to polynucleosomes (Buenrostro et al., 2013, 2015). We performed ATAC-seq on WT and Ex6DEL GNPs (1 DIV) and GNs (3 DIV) and binned reads according to size, categorizing them as either nucleosome-free (NFR), mono-, di-, or tri-nucleosome reads. Normalized accessibility of WT and Ex6DEL cultures aligned over an averaged gene showed an increased number of reads at the TSS in Ex6DEL samples compared to WT cultures (**Figure 4A**), most notably corresponding to NFR reads (both time points) and for mono- and di-nucleosome reads at 1 DIV that suggests there is increased accessibility and reduced nucleosome density at the TSS (**Supplementary Figure 3B**). Progressive chromatin condensation accompanies progenitor cell commitment toward a specialized cell fate. The increased accessibility observed at the TSS in the Ex6DEL progenitors compared to the WT cultures at 1 DIV led us to explore whether the Ex6DEL chromatin accessibility was similar to that of an earlier lineage cell type. To this end, we added a publicly available ATAC-seq E14 mouse embryonic stem cell (mESC) dataset (GEO GSE98390) to our analysis. Interestingly, the mESC ATAC-seq accessibility reads aligned most closely to those of the Ex6DEL GNPs (**Figure 4B** and **Supplementary Figure 4**).

We next compared the number of differentially accessible regions (DARs; FDR < 0.05) between WT and Ex6DEL cultures, identifying 3231 DARs at 1 DIV and 860 DARs at 3 DIV (**Figure 4C**). We focused on the large number of DARs at 1 DIV to determine if these might contribute to the delay in cell differentiation that we observed in the Ex6DEL cultures. Initially, we examined whether the DARs were associated with an increase or a decrease in accessibility. We observed a large increase in the number of accessible chromatin domains (3118), while far fewer DARs (113) showed a reduced level of accessibility within the Ex6DEL cultures compared to the WT cultures (**Figure 4D**). Overall, the distribution of DARs demonstrated that the majority of accessible regions were located in introns (44%) and intergenic regions (39%) (**Figure 4E**). The significance of these accessible regions remains to be determined. Nonetheless, an enrichment of 315 DARs was observed at promoter/TSS regions, which were defined as peaks mapped between −1 kb and + 100 bp of a TSS (**Figure 4E** and **Supplementary Table 1**); a finding consistent with previous studies (Sala et al., 2011; Morris et al., 2014). Since previous work has indicated that SNF2H and SNF2L organize nucleosomes adjacent to transcription factor binding sites (Wiechens et al., 2016), we examined the 315 promoter/TSS DARs for enrichment of transcription factor binding sites. We first examined CTCF since SNF2H but not SNF2L was required to maintain CTCF occupancy at its binding sites (Wiechens et al., 2016). Similar to that study, we did not observe an enrichment in CTCF motifs in the promoter DARs (**Figure 5A**). However, we did observe enrichment of 38 transcription factor motifs including Fos-binding motifs (**Figure 5B** and **Supplementary Table 1**), which is interesting given the upregulation of *Fosb* and *Fosl2* that we observed at the 1 DIV time point. Indeed, 97 of the 315 promoter DARs contained a Fos/Jun/AP-1 transcription factor binding site within the accessible region (**Supplementary Table 1**).

Next, we examined the frequency of DARs associated with the DEGs at 1 DIV. All DARs were linked to a gene based on map position to the nearest gene. Overall, 79% of the upregulated genes contained an open DAR associated with them, although only 25 DEGs had a DAR located within the promoter/TSS region (**Figure 5C** and **Supplementary Table 1**). Of the 25 genes with a promoter/TSS DAR, thirteen genes (*Akap2*, *Arap2*, *Arc*, *Bhlhe40*, *Col4a2*, *Csrnp1*, *Emp1*, *Ets1*, *Gcnt2*, *P2rx6*, *Wnt9a*, *Wwtr1*, and *Zc3h12a*) also contained a Fos/Jun/AP-1 binding site and were increased in expression (**Supplementary Table 1**). These genes also contained binding motifs for *Mzf1*, *Klf4*, and *Sp1* transcription factors within the promoter DAR (**Supplementary Figure 5**).

Analysis of mapped IGV (integrated genome viewer) tracks showed a clear increase in ATAC peaks and RNAseq reads for the 13 genes with a Fos/Jun binding site in the promoter/TSS DAR, as shown for the *Arc* gene (**Figure 5D**; additional genes shown in **Supplementary Figures 6A,B**). However, *Fosb* and *Fosl2* upregulation was not associated with a promoter/TSS DAR despite an apparent increase in chromatin accessibility (**Figure 5E** and **Supplementary Figure 6C**). Similarly, the IGV tracks for *Mapk15*, *Edn1* and *Ednra* showed increased expression in the Ex6DEL cultures but the increased chromatin accessibility at the promoter/TSS region did not reach the statistical threshold cutoff for a DAR (**Supplementary Figures 6D–F**). Taken together, we observed a good correlation between increased chromatin accessibility and upregulated gene expression with a subset of genes displaying *Fos*/*Jun* dysregulation.

In contrast to the upregulated genes, 38% of the downregulated DEGs were associated with a DAR that had reduced accessibility or showed no change in chromatin accessibility (**Figure 5C**). In addition, for genes that showed reduced accessibility we did not observe any overlap with the promoter/TSS DAR list suggesting that downregulation was not associated with altered chromatin structure at the promoter. Surprisingly, 61% of DARs linked to downregulated genes showed enhanced accessibility, which reflects the large number

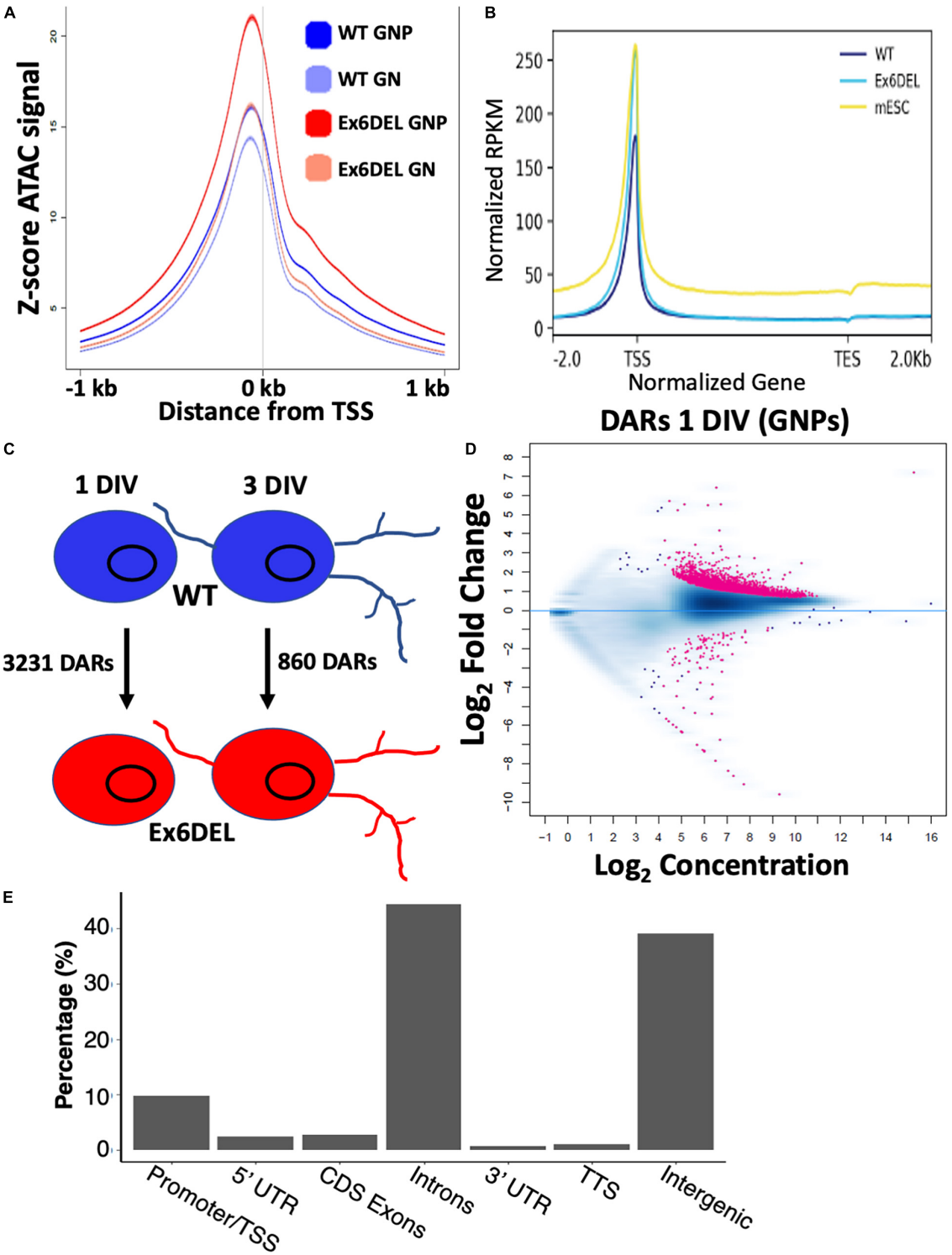

FIGURE 4 | ATACseq analysis of WT and Ex6DEL cultures. **(A)** Compilation of all ATACseq peaks showing enrichment at the TSS under all culture conditions. Mutant cultures at 1 DIV (Ex6DEL GNP) showed the greatest enrichment of peaks at the TSS, followed by Ex6DEL GN (3 DIV), WT GNPs and WT GNs. **(B)** Peaks aligned to a normalized genes showed that Ex6DEL chromatin (light blue) was more accessible than WT chromatin (dark blue) and more similar to the profile of ESCs (yellow). TSS, transcriptional start site; TES, transcriptional end site. **(C)** Schematic diagram showing the numbers of differentially accessible regions (DARs) between WT and Ex6DEL samples at 1 and 3 days in culture. **(D)** MA plot of the 3231 differentially accessible regions. Pink dots represent significant changes in accessibility, with dots above the line representing increased accessibility and below the line decreased accessible regions. **(E)** Plot showing the frequency of DARs at different genomic positions. Promoter/TSS, −1KB to +100 bp; 5′UTR, >100 bp from TSS; TTS, transcriptional termination sites.

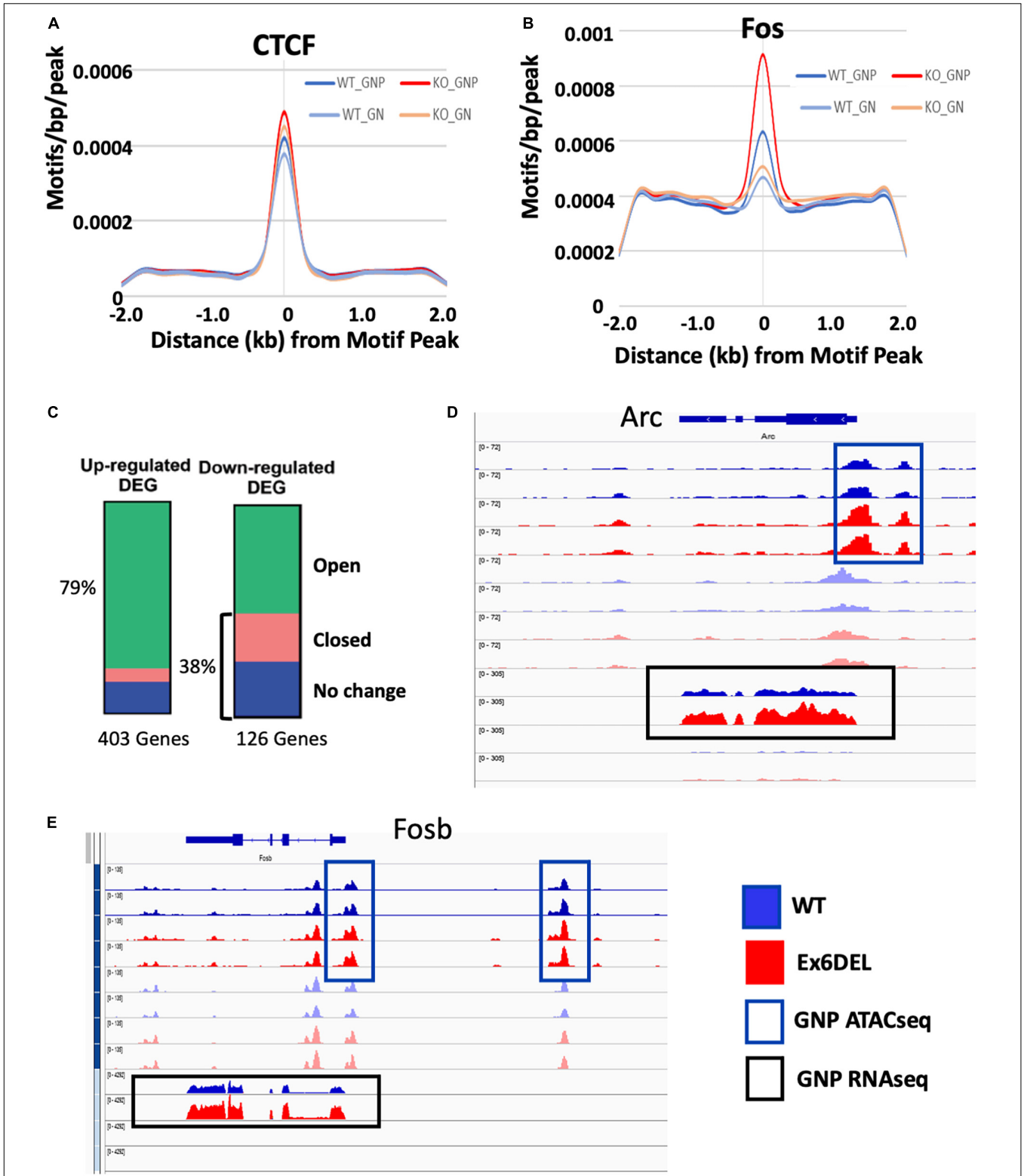

FIGURE 5 | Accessible regions are enriched for Fos/Jun binding sites. ATACseq peak alignment with binding sites for CTCF **(A)** or Fos **(B)** showed enrichment in the Ex6DEL samples for Fos binding sites but not CTCF. **(C)** ATACseq peaks at 1 DIV were assigned to the nearest gene and then cross referenced to the up- and down-regulated genes to generate the bar graphs. Open (green) closed (pink) or chromatin regions showing no change (blue) are shown. **(D,E)** ATACseq and RNAseq reads shown in IGV browser format for the *Arc* **(D)** and *Fosb* **(E)** genes. The GNP ATACseq tracks are shown in the blue box. The GNP RNAseq is shown in the black box. The unboxed tracks correspond to ATACseq and RNAseq from GNs.

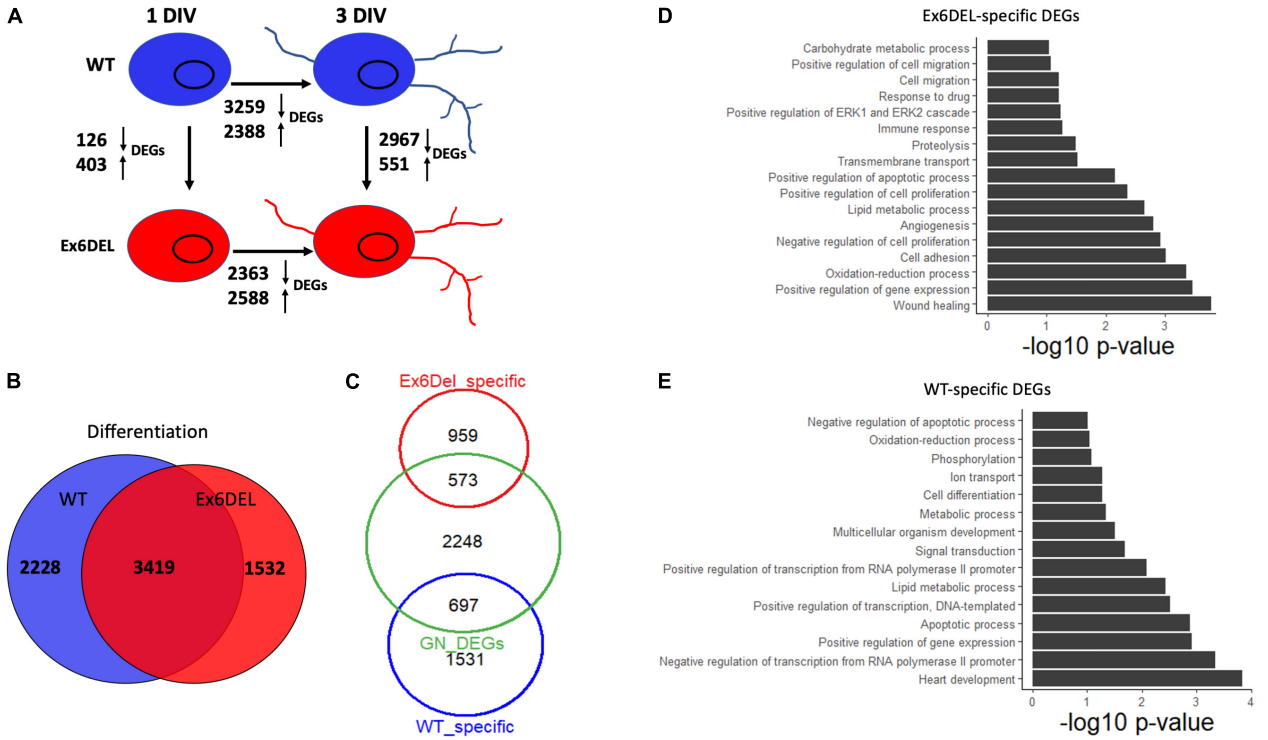

FIGURE 6 | Ex6DEL cultures are delayed in differentiation. **(A)** Schematic diagram showing the numbers of differentially expressed genes (DEGs) between different samples (WT and Ex6DEL) and days in culture (same as **Figure 3A**). **(B)** Venn diagram showing overlapping differentially expressed genes in WT or Ex6DEL cultures during differentiation (gene expression comparison between I and 3 DIV). **(C)** Venn diagram highlighting that only 1/3 of the uniquely expressed genes from **(B)** (Ex6DEL specific: 1532; WT-specific: 2228) remain differentially expressed at 3 DIV. Green circle comprises the 2967 down- and 551 up-regulated DEGs between WT and Ex6DEL cultures. **(D,E)** GO term analysis of the DEGs at # DIV that were specific to the Ex6DEL **(D)** or WT **(E)** cultures.

of accessible DARs in introns although the significance of these chromatin changes remains to be determined.

Ex6DEL Cultures Show Increased Activation of Erk Signaling

Despite the delay exiting the cell cycle, GNPs from the Ex6DEL cultures initiate the differentiation program. We compared the differential gene expression between 1 DIV and 3 DIV timepoints for both WT and Ex6DEL cultures to determine whether the process of differentiation results in similar gene set changes. In this regard, we observed a similar number of genes differentially expressed from 1 DIV to 3 DIV, with 5647 DEGs changing in WT cultures and 4951 DEGs altered in the Ex6DEL cultures (**Figure 6A**). Moreover, 3419 genes were common to both cultures (WT: 60.5% of DEGs; Ex6DEL: 69% of DEGs) suggesting that the differentiation program proceeds along a similar path regardless of Snf2l status (**Figure 6B**). There were 2228 and 1532 genes in WT and Ex6DEL cultures, respectively, that were specific to the differentiation of the individual cultures. We reasoned that many of these gene expression differences could reflect the overall lag in differentiation occurring in the Ex6DEL cultures while others could represent Snf2l-specific changes.

Next, we examined the differences in gene expression at 3 DIV to determine how similar or different the GNP cultures were 3 days after plating. This analysis demonstrated 3518 DEGs between the WT GNs and Ex6DEL GNs at 3 DIV (**Figure 6A**). Given the lag in differentiation of the Ex6DEL cultures, we compared how many of the DEGs between 1 DIV and 3 DIV were resolved by the third day in culture. In both sets of cultures approximately 2/3 of DEGs were resolved (60%, 1531/2228 WT DEGs; 63%, 959/1532 Ex6DEL DEGs; **Figure 6C**). Alternatively, one-third of the Ex6DEL (573 DEGs) and WT (697 DEGs) remain altered in the 3 DIV cultures, while 2248 "new" genes (GN DEGs) become differentially expressed (**Figure 6C**). Finally, we performed GO analysis on these clusters of DEGs identified at 3 DIV (i.e., Ex6DEL-specific, WT-specific, GN DEGs). Of the 573 DEGs that were considered to be specific for Ex6DEL 3 DIV cultures, notable GO terms showed changes in cell proliferation, cell migration, cell adhesion, and regulation of the ERK1/ERK2 pathway (**Figure 6D**). Notable GO terms for the 697 DEGs specific for WT 3 DIV cultures included positive regulation of transcription & gene expression, cell differentiation, multicellular organism development (**Figure 6E**). Very similar GO terms were also identified for the novel 2248 DEGs at the 3 DIV timepoint suggesting that these latter gene sets are representative of a more mature differentiated state (**Supplementary Figure 7**).

As such, we focused on the Ex6DEL-specific dataset and, more specifically, the DEGs within the GO term "regulation of ERK1/ERK2 pathway" to identify a potential pathway critical for GN differentiation of the Ex6DEL cells. In this regard,

we performed immunoblots for the Erk1/2 proteins and their phosphorylated isoforms. GNPs were cultured from WT and Ex6DEL mice and protein extracts isolated at 1 DIV and 3 DIV for analysis. Since Erk1 and Erk2 exhibit functional redundancy we quantified global Erk phosphorylation (normalized pErk1 and pErk2/Erk1 and Erk2 levels) and not isoform specificity as a measure of pathway activation (Busca et al., 2016). In the WT samples the total Erk protein level dropped by 40% in the 3 DIV sample compared to the 1 DIV sample, but the activation increased ∼3-fold (3.6% at 1 DIV; 10.4% at 3 DIV). It should be noted that the activation was primarily through phosphorylation of Erk2 (**Figures 7A,B**). In the Ex6DEL cultures we observed a similar drop in total Erk protein levels (∼50%) at 3 DIV but pathway activation was significantly increased (24-fold; 2.6% 1 DIV; 63.4% 3 DIV; **Figures 7A,B**).

To determine if the Erk pathway is altered in the Ex6DEL mice, we performed RT-qPCR for three downstream Erk target genes, using RNA isolated from cerebellar tissue at P10 from Ex6DEL mice and control littermates. Consistent with increased activation of the Erk1/2 pathway in Ex6DEL 3 DIV cultures we observed increased expression of all three downstream target genes, namely *Sox2*, *Bdnf*, and *Th* in the Ex6DEL cerebellum (**Figure 7C**). We also examined whether the transcriptional changes in the mice were duplicated in the cultures by assessing the chromatin accessibility and transcript reads of these target genes. For both *Sox2* and *Bdnf* we observed a slight increase in accessibility although none of the accessible regions reached the significant threshold to be considered a DAR (**Figures 7D,E**). Moreover, increased transcript reads were only observed for *Sox2* (**Figure 7D**) but not for *Bdnf* (**Figure 7E**) in the culture experiments.

DISCUSSION

The Ex6DEL mice contain an internally truncated Snf2l protein that lacks the ability to bind and hydrolyze ATP thereby rendering it unable to remodel nucleosomes. We have shown that the truncated Snf2l protein can assemble into ISWI complexes (e.g., CERF) and thus, it likely retains some ability to be recruited to its genomic targets (e.g., promoter/TSS sites). GNPs isolated from the Ex6DEL mice were mildly impaired in their ability to exit the cell cycle, thus delaying differentiation when plated in culture. The chromatin landscape of the Ex6DEL GNP cultures showed a general increase in accessibility at TSS that was more similar to that of mESCs than to control GNP cultures. Over 96% of the DARs between WT and Ex6DEL GNP cultures showed increased accessibility. Of those located in promoter/TSS regions we identified an enrichment for Fos/Jun binding sites suggesting that Snf2l remodeling normally decreases accessibility at these sites to facilitate differentiation. The increased accessibility was correlated with increased gene expression with ∼80% of the 529 DEGs, consistent with a role for Snf2l in repressing gene expression during cerebellar development. Collectively, the Ex6DEL cultures either represent a "less differentiated" or committed GNP that does not immediately exit the cell cycle upon plating, or alternatively, the culture contains a greater proportion of a distinct progenitor cell type that alters the differentiation kinetics of the culture. Regardless, the enhanced proliferation index was transient and the Ex6DEL cultures underwent differentiation showing a 69% concordance with WT cultures in the DEGs associated with this process (i.e., 1 DIV vs. 3 DIV expression changes). Expression differences at 3 DIV highlighted the importance of the ERK signaling cascade for GNP differentiation.

Granule neuron precursors migrate to the EGL from the upper rhombic lip, one of two germinal zones in the developing cerebellum. Within the EGL they respond to Shh released from Purkinje cells to proliferate during the early postnatal period which is critical for cerebellar folia growth. Dysregulation of GNP expansion can result in a hypoplastic cerebellum, as was observed for *Smarca5* cKO mice (Alvarez-Saavedra et al., 2014), or conversely, cause some subtypes of medulloblastoma as shown for activating hedgehog (HH) mutations. We observed a transient maintenance of proliferation in the Ex6DEL cultures that was not associated with alterations in HH signaling suggesting that other mitogenic pathways were active. A previous study demonstrated increased proliferation of HeLa cells after siRNA knockdown of *Smarca1* through the activation of the Wnt signaling cascade (Eckey et al., 2012). The study demonstrated activation of β-catenin using the TOP/FOP flash assay but determined that this was a post-transcriptional effect ruling out SNF2L remodeling of the *CTNNB1* gene. Three of the Wnt target genes upregulated in that study (*EDN1*, *FN1*, *PLAUR*) were similarly altered in our study as were an additional 9 Wnt responsive genes (*Fzd6*, *Flt4*, *Kdr*, *Lef1*, *Abcc4*, *Abcb1a*, *Neurod1*, *Ptgs2*, *Nes*) and the receptor for *Edn1* (*Ednra*). The significance of these changes to proliferation, however, remain to be fully determined. Another similarity between our study and the one by Eckey et al. (2012) was that the GO term analysis indicated that angiogenesis was the biological process with the most significant change. While further work is required to delineate the significance of the specific gene changes, one possibility is that Snf2l is required to maintain repression of genes critical for blood vessel formation.

One of the dysregulated Wnt target genes of interest was the endothelin-1 gene, *Edn1* because it has been shown to be critical for autocrine-mediated neuroprogenitor proliferation within the postnatal subventricular zone of mice (Adams et al., 2020). A similar decrease in proliferation was obtained when one of the endothelin receptors, endothelin b receptor (*Ednrb*) was deleted in mice. Further studies revealed that endothelin signaling activated the Notch pathway to maintain proliferation of the radial glia progenitors (Adams et al., 2020). While a similar Edn1-Ednra autocrine effect could be occurring in the Ex6DEL GNP cultures, we did not observe transcriptional activation of Notch signaling components (e.g., *Jag1*, *Hey1*) as shown in the Adams et al. (2020) study. Despite this difference, endothelin-1 signaling can be transduced through phosphatidylinositol 3-kinase (PI3-K), Wnt, and mitogen-activated protein kinase (MAPK) signaling pathways (Bouallegue et al., 2007; Kristianto et al., 2017), the latter two for which we observed several gene expression differences in the Ex6DEL cultures.

Given the incidence of Wnt activation in medulloblastoma, several studies have examined the requirement for Wnt in GNP

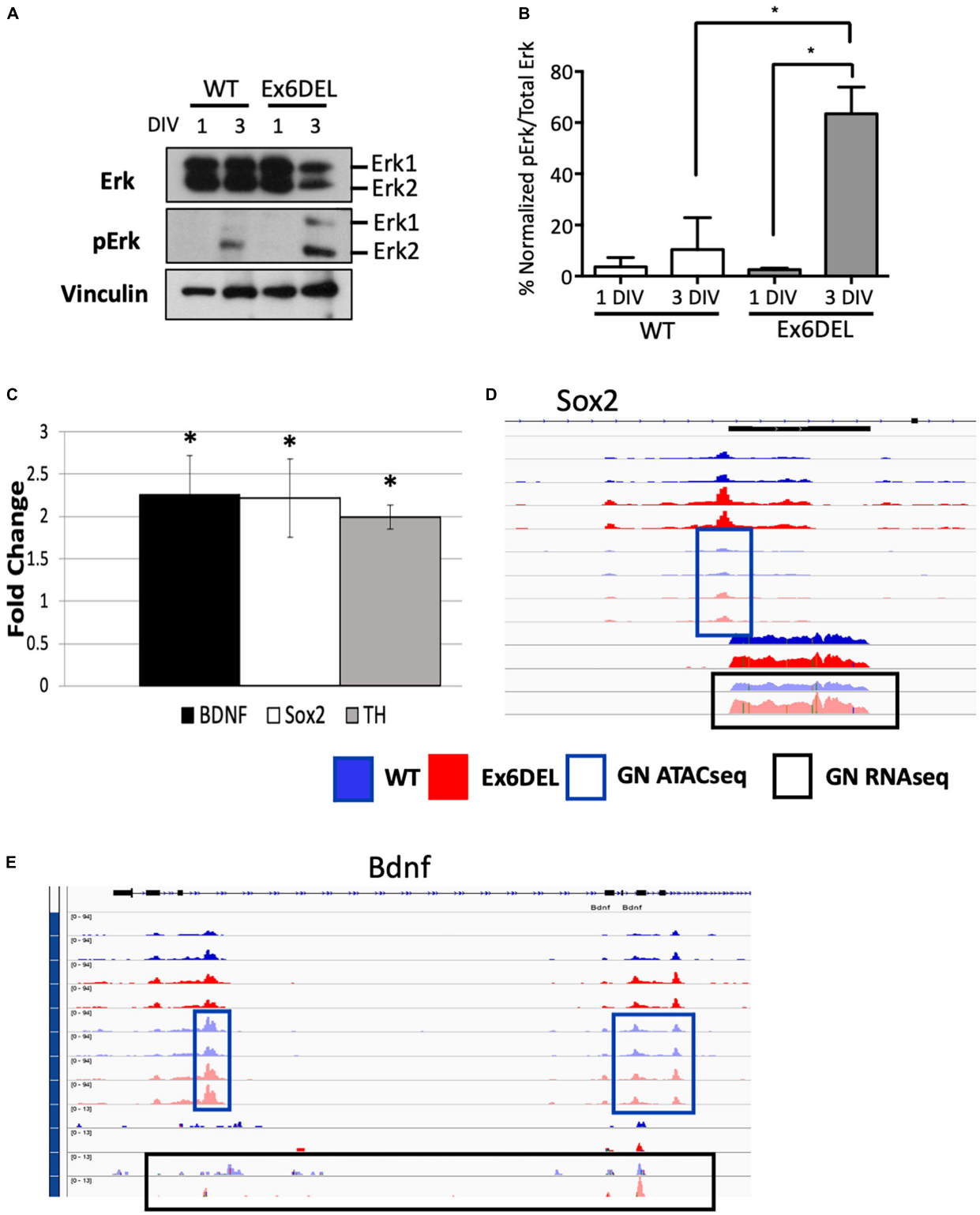

FIGURE 7 | Granule neuron precursor differentiation is associated with ERK signaling activation. **(A)** Immunoblots from WT and Ex6DEL GNP cultures (1 and 3 DIV) for Erk and phospho-Erk (pErk). Vinculin serves as a protein loading control. **(B)** Quantification of the immunoblots in A showing the normalized change in Erk activation (pErk1 + pErk2 level) to total Erk protein level. *$p < 0.05$. **(C)** RT-qPCR validation of the expression of downstream target genes of ERK/Fos/Jun signaling. *$p < 0.05$. **(D)** Genome browser views of the *Sox2* **(D)** and *Bdnf* **(E)** genes. The blue boxes highlight the ATACseq peaks and the black boxes mark the RNAseq reads at 3 DIV. All unboxed tracks correspond to the I DIV time.

proliferation (Lorenz et al., 2011; Pei et al., 2012; Yang et al., 2019). Using different methods to activate Wnt signaling, each study came to the same conclusion, namely that Wnt activation was not mitogenic for GNPs but actually promoted their differentiation. This is opposite to the effect of Wnt signaling in the developing forebrain where b-catenin stabilization resulted in a dramatic increase in progenitor proliferation (Chenn and Walsh, 2002). As such, it seems difficult to reconcile that Wnt activation in the Ex6DEL GNPs is driving their proliferation unless perhaps, we are observing an increased level of a second progenitor subtype in the Ex6DEL cultures. In this regard, a rare population of Nestin-expressing progenitor cells (NEPs) that migrate from the second germinal zone (VZ lining the fourth ventricle) and reside in the deep part of the EGL could be affected by loss of Snf2l function. These NEPs are typically quiescent but can be activated to replenish granule neurons following injury in the postnatal period (Li et al., 2013; Wojcinski et al., 2017, 2019). In such a scenario, the lack of Snf2l in this cell population would alleviate their quiescence and activate their proliferation. As we observed increased *Nes* gene expression, it remains possible that both the activated Wnt signaling signature and the enhanced BrdU incorporation observed in the Ex6DEL cultures result from inappropriate NEP proliferation. Future analyses using a scRNAseq approach should help define progenitor cell type differences within the GNP cultures.

An essential marker of GNPs is the bHLH transcription factor *Atoh1/Math1* which is required for their generation in the rhombic lip, and later for the regulation of primary cilia formation that facilitates proliferation in response to Shh (Ben-Arie et al., 1997; Dahmane and Ruiz i Altaba, 1999; Wallace, 1999; Chang et al., 2019). *Atoh1* also induces the expression of *Zic1*, *En1*, and *Neurod1* to facilitate differentiation, the latter of which has been shown in other experiments to be required for granule neuron differentiation (Miyata et al., 1999; Pan et al., 2009; Iulianella et al., 2019). Examination of the 1 DIV transcriptome indicated that *Neurod1* expression is reduced ($Log_2FC = -0.61$) compared to control cultures but at 3 DIV it is differentially increased ($Log_2FC = 0.725$) supporting the argument that differentiation is transiently delayed in the Ex6DEL cultures. *Zic1* was increased at the 3 DIV timepoint ($Log_2FC = 0.625$) only, while *En1* and *En2* were not altered compared to control cultures.

We also analyzed the gene expression profiles during (1 DIV vs. 3 DIV) and after differentiation (WT vs. Ex6DEL 3 DIV). In this way, we observed that differentiation was associated with similar expression profiles regardless of Snf2l status. This data suggests that Snf2l is not required to initiate GNP differentiation. When we compared expression profiles at 3 DIV we observed activation of the ERK1/2 pathway which we confirmed by immunoblots of the protein extracts from the cultures. Multiple studies have previously shown that a wide range of soluble factors (Glucose, IGF-1, Wnt3) can promote cerebellar granule differentiation through MAPK-ERK1/2 activation (Torres-Aleman et al., 1998; Petersen et al., 2002; Anne et al., 2013; Kronenberg et al., 2020). Our finding that this was specific to the Ex6DEL cultures may simply reflect the delayed differentiation of these cultures. Several of these studies have also linked MAPK-ERK1/2 activation directly to *Neurod1* activity which we mentioned above was upregulated (Petersen et al., 2002; Kronenberg et al., 2020). One study of particular interest demonstrated that Wnt3 promoted GNP differentiation through a non-canonical Wnt signaling pathway that activated the MAPK-ERK1/2 pathway instead of the β-catenin canonical pathway (Anne et al., 2013). Wnt3 ($Log_2FC = 0.690$) was also upregulated in the DEGs linked to Ex6DEL differentiation. Regardless, it is clear that GNP cultures isolated from Ex6DEL mice undergo differentiation utilizing a common MAPK-ERK1/2-*Neurod1* pathway previously shown to be important for granule neuron differentiation.

Analysis of *Drosophila* ISWI protein binding sites by ChIPseq showed that the majority of sites mapped to ∼300 bp after the TSS with fewer binding sites located at exons, introns and the 3′-end of several genes (Sala et al., 2011). The role of ISWI binding near the TSS is important for positioning the downstream nucleosomes, particularly the +1 and +2 nucleosome positions (Sala et al., 2011; Wiechens et al., 2016). In mammals, the nucleosome positioning by SNF2H facilitated binding at CTCF binding sites while depletion of SNF2L had minor effects on nucleosome organization at CTCF sites (Wiechens et al., 2016). In addition to CTCF, the authors observed that SNF2H and SNF2L depletion altered the +1 and −1 nucleosome spacing adjacent to 49 different TF binding sites often with contrasting effects on nucleosome spacing, suggesting that they likely have antagonistic effects on TF occupancy (Wiechens et al., 2016). Using an ATACseq approach to define accessible chromatin in GNPs we observed that depletion of Snf2l resulted in increased accessibility at 3118 sites suggesting that Snf2l normally represses access to chromatin. However, the large majority of differentially accessible sites were located in introns and intergenic regions with a smaller fraction (10%) at promoter/TSS regions, which is different than the ChIPseq experiment in *Drosophila* (Sala et al., 2011) and may reflect additional indirect changes in chromatin accessibility. While the nature of the non-coding sites was not examined, a high proportion (30%) of the promoter/TSS DARs contained binding sites for the Fos/Jun transcription factor. This data suggests that Snf2l may have an important role in regulating TF occupancy at Fos/Jun target genes during GNP differentiation. Consistent with this, we found that 25 of the DEGs contained a promoter/TSS DAR and that half of these had Fos/Jun binding sites. Many of the upregulated DEGs showed minor increases in promoter accessibility that did not reach the significance threshold for a DAR (compare *Arc* vs. *Fosb*). It suggests that these genes may contain additional inter- or intra-genic accessible regions that alter access at distal regulatory elements or, change topological chromatin domains to affect expression. Certainly, such changes were underappreciated in the type of analysis performed here but would also represent a unique ISWI function.

In summary, we have shown that the Ex6DEL GNP cultures have a transient delay in cell cycle withdrawal that was also found in the intermediate progenitors of the developing forebrain. GNPs undergo an average of eight divisions during postnatal cerebellar growth producing an average of 250 granule neurons (Iulianella et al., 2019). An extra cycle of proliferation within the GNPs (or IPCs) are more than sufficient to account for the increased brain size observed in the Ex6DEL

mice. We suggest that the delay results from a less-restricted chromatin configuration in the Ex6DEL progenitors, allowing continued access to transcription factors such as Fos/Jun. Despite the alterations to the chromatin landscape the Ex6DEL GNPs maintain the ability to differentiate using previously defined pathways.

DATA AVAILABILITY STATEMENT

The datasets presented in this study can be found in online repositories. The names of the repository/repositories and accession number(s) can be found below: https://www.ncbi.nlm.nih.gov/geo/query/acc.cgi?acc=GSE122172, https://www.ncbi.nlm.nih.gov/geo/query/acc.cgi?acc=GSE122173.

ETHICS STATEMENT

The animal study was reviewed and approved by the University of Ottawa's Animal Care ethics committee.

AUTHOR CONTRIBUTIONS

LG executed all experiments with the technical support of JM, unless stated otherwise. GZ and LG performed the bioinformatic analysis. ST performed the RT-qPCR validation experiments and cerebellar IF staining. DP designed, supervised, and provided funding for the project. LG, GZ, ST, and DJP wrote the manuscript. All the authors contributed to the article and approved the submitted version.

FUNDING

This work was funded by CIHR grants MOP97764 and MOP84412 to DJP.

ACKNOWLEDGMENTS

We thank V. Wallace and P. Mattar for critical reading of the manuscript. We also thank Nicholas Tokarew for showing us how to establish GNP cultures.

SUPPLEMENTARY MATERIAL

The Supplementary Material for this article can be found online at: https://www.frontiersin.org/articles/10.3389/fnmol.2021.680280/full#supplementary-material

REFERENCES

Adams, K. L., Riparini, G., Banerjee, P., Breur, M., Bugiani, M., and Gallo, V. (2020). Endothelin-1 signaling maintains glial progenitor proliferation in the postnatal subventricular zone. *Nat. Commun.* 11:2138.

Alder, J., Cho, N. K., and Hatten, M. E. (1996). Embryonic precursor cells from the rhombic lip are specified to a cerebellar granule neuron identity. *Neuron* 17, 389–399. doi: 10.1016/s0896-6273(00)80172-5

Alvarez-Saavedra, M., De Repentigny, Y., Lagali, P. S., Raghu Ram, E. V., Yan, K., Hashem, E., et al. (2014). Snf2h-mediated chromatin organization and histone H1 dynamics govern cerebellar morphogenesis and neural maturation. *Nat. Commun.* 5:4181.

Alvarez-Saavedra, M., Yan, K., De Repentigny, Y., Hashem, L. E., Chaudary, N., Sarwar, S., et al. (2019). Snf2h Drives Chromatin Remodeling to Prime Upper Layer Cortical Neuron Development. *Front. Mol. Neurosci.* 12:243. doi: 10.3389/fnmol.2019.00243

Anne, S. L., Govek, E. E., Ayrault, O., Kim, J. H., Zhu, X., Murphy, D. A., et al. (2013). WNT3 inhibits cerebellar granule neuron progenitor proliferation and medulloblastoma formation via MAPK activation. *PLoS One* 8:e81769. doi: 10.1371/journal.pone.0081769

Banting, G. S., Barak, O., Ames, T. M., Burnham, A. C., Kardel, M. D., Cooch, N. S., et al. (2005). CECR2, a protein involved in neurulation, forms a novel chromatin remodeling complex with SNF2L. *Hum. Mol. Genet.* 14, 513–524. doi: 10.1093/hmg/ddi048

Bassett, E. A., Tokarew, N., Allemano, E. A., Mazerolle, C., Morin, K., Mears, A. J., et al. (2016). Norrin/Frizzled4 signalling in the preneoplastic niche blocks medulloblastoma initiation. *Elife* 5:e16764.

Ben-Arie, N., Bellen, H. J., Armstrong, D. L., McCall, A. E., Gordadze, P. R., Guo, Q., et al. (1997). Math1 is essential for genesis of cerebellar granule neurons. *Nature* 390, 169–172. doi: 10.1038/36579

Bogershausen, N., and Wollnik, B. (2018). Mutational Landscapes and Phenotypic Spectrum of SWI/SNF-Related Intellectual Disability Disorders. *Front. Mol. Neurosci.* 11:252. doi: 10.3389/fnmol.2018.00252

Boonekamp, K. E., Heo, I., Artegiani, B., Asra, P., van Son, G., de Ligt, J., et al. (2021). Identification of novel human Wnt target genes using adult endodermal tissue-derived organoids. *Dev. Biol.* 474, 37–47. doi: 10.1016/j.ydbio.2021.01.009

Bouallegue, A., Daou, G. B., and Srivastava, A. K. (2007). Endothelin-1-induced signaling pathways in vascular smooth muscle cells. *Curr. Vasc. Pharmacol.* 5, 45–52. doi: 10.2174/157016107779317161

Bozhenok, L., Wade, P. A., and Varga-Weisz, P. (2002). WSTF-ISWI chromatin remodeling complex targets heterochromatic replication foci. *EMBO J.* 21, 2231–2241. doi: 10.1093/emboj/21.9.2231

Buenrostro, J. D., Giresi, P. G., Zaba, L. C., Chang, H. Y., and Greenleaf, W. J. (2013). Transposition of native chromatin for fast and sensitive epigenomic profiling of open chromatin, DNA-binding proteins and nucleosome position. *Nat. Methods* 10, 1213–1218. doi: 10.1038/nmeth.2688

Buenrostro, J. D., Wu, B., Chang, H. Y., and Greenleaf, W. J. (2015). ATAC-seq: a method for assaying chromatin accessibility genome-wide. *Curr. Protoc. Mol. Biol.* 109, 21.29.21–29.

Busca, R., Pouyssegur, J., and Lenormand, P. (2016). ERK1 and ERK2 map kinases: specific roles or functional redundancy? *Front. Cell Dev. Biol.* 4:53. doi: 10.3389/fcell.2016.00053

Chang, C. H., Zanini, M., Shirvani, H., Cheng, J. S., Yu, H., Feng, C. H., et al. (2019). Atoh1 Controls Primary Cilia Formation to Allow for SHH-Triggered Granule Neuron Progenitor Proliferation. *Dev. cell* 48, 184–199.e5.

Chenn, A., and Walsh, C. A. (2002). Regulation of cerebral cortical size by control of cell cycle exit in neural precursors. *Science* 297, 365–369. doi: 10.1126/science.1074192

Clapier, C. R., Iwasa, J., Cairns, B. R., and Peterson, C. L. (2017). Mechanisms of action and regulation of ATP-dependent chromatin-remodelling complexes. *Nat. Rev. Mol. Cell Biol.* 18, 407–422. doi: 10.1038/nrm.2017.26

Corona, D. F., Langst, G., Clapier, C. R., Bonte, E. J., Ferrari, S., Tamkun, J. W., et al. (1999). ISWI is an ATP-dependent nucleosome remodeling factor. *Mol. Cell* 3, 239–245. doi: 10.1016/s1097-2765(00)80314-7

Dahmane, N., and Ruiz i Altaba, A. (1999). Sonic hedgehog regulates the growth and patterning of the cerebellum. *Development* 126, 3089–3100. doi: 10.1242/dev.126.14.3089

Eckey, M., Kuphal, S., Straub, T., Rummele, P., Kremmer, E., Bosserhoff, A. K., et al. (2012). Nucleosome remodeler SNF2L suppresses cell proliferation and

migration and attenuates Wnt signaling. *Mol. Cell Biol.* 32, 2359–2371. doi: 10.1128/mcb.06619-11

Frey, W. D., Chaudhry, A., Slepicka, P. F., Ouellette, A. M., Kirberger, S. E., Pomerantz, W. C. K., et al. (2017). BPTF Maintains Chromatin Accessibility and the Self-Renewal Capacity of Mammary Gland Stem Cells. *Stem Cell Rep.* 9, 23–31. doi: 10.1016/j.stemcr.2017.04.031

Goodwin, L. R., and Picketts, D. J. (2018). The role of ISWI chromatin remodeling complexes in brain development and neurodevelopmental disorders. *Mol. Cell. Neurosci.* 87, 55–64. doi: 10.1016/j.mcn.2017.10.008

Hatten, M. E., and Heintz, N. (1995). Mechanisms of neural patterning and specification in the developing cerebellum. *Annu. Rev. Neurosci.* 18, 385–408. doi: 10.1146/annurev.ne.18.030195.002125

Heinz, S., Benner, C., Spann, N., Bertolino, E., Lin, Y. C., Laslo, P., et al. (2010). Simple combinations of lineage-determining transcription factors prime cis-regulatory elements required for macrophage and B cell identities. *Mol. Cell* 38, 576–589. doi: 10.1016/j.molcel.2010.05.004

Hoshino, M., Nakamura, S., Mori, K., Kawauchi, T., Terao, M., Nishimura, Y. V., et al. (2005). Ptf1a, a bHLH transcriptional gene, defines GABAergic neuronal fates in cerebellum. *Neuron* 47, 201–213. doi: 10.1016/j.neuron.2005.06.007

Huang da, W., Sherman, B. T., and Lempicki, R. A. (2009). Systematic and integrative analysis of large gene lists using DAVID bioinformatics resources. *Nat. Protoc.* 4, 44–57. doi: 10.1038/nprot.2008.211

Ito, T., Bulger, M., Pazin, M. J., Kobayashi, R., and Kadonaga, J. T. (1997). ACF, an ISWI-containing and ATP-utilizing chromatin assembly and remodeling factor. *Cell* 90, 145–155. doi: 10.1016/s0092-8674(00)80321-9

Iulianella, A., Wingate, R. J., Moens, C. B., and Capaldo, E. (2019). The generation of granule cells during the development and evolution of the cerebellum. *Dev. Dyn.* 248, 506–513. doi: 10.1002/dvdy.64

Katoh, M. (2018). Multilayered prevention and treatment of chronic inflammation, organ fibrosis and cancer associated with canonical WNT/betacatenin signaling activation (Review). *Int. J. Mol. Med.* 42, 713–725.

Koludrovic, D., Laurette, P., Strub, T., Keime, C., Le Coz, M., Coassolo, S., et al. (2015). Chromatin-Remodelling Complex NURF Is Essential for Differentiation of Adult Melanocyte Stem Cells. *PLoS Genet.* 11:e1005555. doi: 10.1371/journal.pgen.1005555

Kristianto, J., Johnson, M. G., Afzal, R., and Blank, R. D. (2017). Endothelin Signaling in Bone. *Endocrinol. Metab. Clin. North Am.* 46, 51–62.

Kronenberg, N. M., Tilston-Lunel, A., Thompson, F. E., Chen, D., Yu, W., Dholakia, K., et al. (2020). Willin/FRMD6 Influences Mechanical Phenotype and Neuronal Differentiation in Mammalian Cells by Regulating ERK1/2 Activity. *Front. Cell. Neurosci.* 14:552213. doi: 10.3389/fncel.2020.552213

Kwon, A. T., Arenillas, D. J., Worsley Hunt, R., and Wasserman, W. W. (2012). oPOSSUM-3: advanced analysis of regulatory motif over-representation across genes or ChIP-Seq datasets. *G3 (Bethesda)* 2, 987–1002. doi: 10.1534/g3.112.003202

Kwon, S. Y., Grisan, V., Jang, B., Herbert, J., and Badenhorst, P. (2016). Genome-Wide Mapping Targets of the Metazoan Chromatin Remodeling Factor NURF Reveals Nucleosome Remodeling at Enhancers, Core Promoters and Gene Insulators. *PLoS Genet.* 12:e1005969. doi: 10.1371/journal.pgen.1005969

Landry, J., Sharov, A. A., Piao, Y., Sharova, L. V., Xiao, H., Southon, E., et al. (2008). Essential role of chromatin remodeling protein Bptf in early mouse embryos and embryonic stem cells. *PLoS Genet.* 4:e1000241. doi: 10.1371/journal.pgen.1000241

Landry, J. W., Banerjee, S., Taylor, B., Aplan, P. D., Singer, A., and Wu, C. (2011). Chromatin remodeling complex NURF regulates thymocyte maturation. *Genes Dev.* 25, 275–286. doi: 10.1101/gad.2007311

Langst, G., Bonte, E. J., Corona, D. F., and Becker, P. B. (1999). Nucleosome movement by CHRAC and ISWI without disruption or trans- displacement of the histone octamer. *Cell* 97, 843–852. doi: 10.1016/s0092-8674(00)80797-7

Lee, H. Y., Greene, L. A., Mason, C. A., and Manzini, M. C. (2009). Isolation and culture of post-natal mouse cerebellar granule neuron progenitor cells and neurons. *J. Vis. Exp.* 23:990.

Leonard, J. D., and Narlikar, G. J. (2015). A nucleotide-driven switch regulates flanking DNA length sensing by a dimeric chromatin remodeler. *Mol. Cell* 57, 850–859. doi: 10.1016/j.molcel.2015.01.008

LeRoy, G., Orphanides, G., Lane, W. S., and Reinberg, D. (1998). Requirement of RSF and FACT for transcription of chromatin templates in vitro. *Science* 282, 1900–1904. doi: 10.1126/science.282.5395.1900

Li, P., Du, F., Yuelling, L. W., Lin, T., Muradimova, R. E., Tricarico, R., et al. (2013). A population of Nestin-expressing progenitors in the cerebellum exhibits increased tumorigenicity. *Nat. Neurosci.* 16, 1737–1744. doi: 10.1038/nn.3553

Lorenz, A., Deutschmann, M., Ahlfeld, J., Prix, C., Koch, A., Smits, R., et al. (2011). Severe alterations of cerebellar cortical development after constitutive activation of Wnt signaling in granule neuron precursors. *Mol. Cell. Biol.* 31, 3326–3338. doi: 10.1128/mcb.05718-11

Machold, R., and Fishell, G. (2005). Math1 is expressed in temporally discrete pools of cerebellar rhombic-lip neural progenitors. *Neuron* 48, 17–24. doi: 10.1016/j.neuron.2005.08.028

Miyata, T., Maeda, T., and Lee, J. E. (1999). NeuroD is required for differentiation of the granule cells in the cerebellum and hippocampus. *Genes Dev.* 13, 1647–1652. doi: 10.1101/gad.13.13.1647

Morris, S. A., Baek, S., Sung, M. H., John, S., Wiench, M., Johnson, T. A., et al. (2014). Overlapping chromatin-remodeling systems collaborate genome wide at dynamic chromatin transitions. *Nat. Struct. Mol. Biol.* 21, 73–81. doi: 10.1038/nsmb.2718

Oliver, T. G., Read, T. A., Kessler, J. D., Mehmeti, A., Wells, J. F., Huynh, T. T., et al. (2005). Loss of patched and disruption of granule cell development in a pre-neoplastic stage of medulloblastoma. *Development* 132, 2425–2439. doi: 10.1242/dev.01793

Oppikofer, M., Bai, T., Gan, Y., Haley, B., Liu, P., Sandoval, W., et al. (2017). Expansion of the ISWI chromatin remodeler family with new active complexes. *EMBO Rep.* 18, 1697–1706. doi: 10.15252/embr.201744011

Ou, J., Liu, H., Yu, J., Kelliher, M. A., Castilla, L. H., Lawson, N. D., et al. (2018). ATACseqQC: a Bioconductor package for post-alignment quality assessment of ATAC-seq data. *BMC Genomics* 19:169. doi: 10.1186/s12864-018-4559-3

Pan, N., Jahan, I., Lee, J. E., and Fritzsch, B. (2009). Defects in the cerebella of conditional Neurod1 null mice correlate with effective Tg(Atoh1-cre) recombination and granule cell requirements for Neurod1 for differentiation. *Cell Tissue Res.* 337, 407–428. doi: 10.1007/s00441-009-0826-6

Pei, Y., Brun, S. N., Markant, S. L., Lento, W., Gibson, P., Taketo, M. M., et al. (2012). WNT signaling increases proliferation and impairs differentiation of stem cells in the developing cerebellum. *Development* 139, 1724–1733. doi: 10.1242/dev.050104

Petersen, H. V., Jensen, J. N., Stein, R., and Serup, P. (2002). Glucose induced MAPK signalling influences NeuroD1-mediated activation and nuclear localization. *FEBS Lett.* 528, 241–245. doi: 10.1016/s0014-5793(02)03318-5

Qiu, Z., Song, C., Malakouti, N., Murray, D., Hariz, A., Zimmerman, M., et al. (2015). Functional interactions between NURF and Ctcf regulate gene expression. *Mol. Cell. Biol.* 35, 224–237. doi: 10.1128/mcb.00553-14

Ramirez, F., Ryan, D. P., Gruning, B., Bhardwaj, V., Kilpert, F., Richter, A. S., et al. (2016). deepTools2: a next generation web server for deep-sequencing data analysis. *Nucleic Acids Res.* 44, W160–W165.

Ross-Innes, C. S., Stark, R., Teschendorff, A. E., Holmes, K. A., Ali, H. R., Dunning, M. J., et al. (2012). Differential oestrogen receptor binding is associated with clinical outcome in breast cancer. *Nature* 481, 389–393.

RStudio Team. (2020). *RStudio: Integrated Devolpment for R*. Boston: RStudio.

Sala, A., Toto, M., Pinello, L., Gabriele, A., Di Benedetto, V., Ingrassia, A. M., et al. (2011). Genome-wide characterization of chromatin binding and nucleosome spacing activity of the nucleosome remodelling ATPase ISWI. *EMBO J.* 30, 1766–1777. doi: 10.1038/emboj.2011.98

Schneider, C. A., Rasband, W. S., and Eliceiri, K. W. (2012). NIH Image to ImageJ: 25 years of image analysis. *Nat. Methods* 9, 671–675. doi: 10.1038/nmeth.2089

Sokpor, G., Castro-Hernandez, R., Rosenbusch, J., Staiger, J. F., and Tuoc, T. (2018). ATP-Dependent Chromatin Remodeling During Cortical Neurogenesis. *Front. Neurosci.* 12:226. doi: 10.3389/fnins.2018.00226

Stempor, P., and Ahringer, J. (2016). SeqPlots - Interactive software for exploratory data analyses, pattern discovery and visualization in genomics. *Wellcome Open Res.* 1:14. doi: 10.12688/wellcomeopenres.10004.1

Stopka, T., and Skoultchi, A. I. (2003). The ISWI ATPase Snf2h is required for early mouse development. *Proc. Natl. Acad. Sci. U. S. A.* 100, 14097–14102. doi: 10.1073/pnas.2336105100

Strohner, R., Nemeth, A., Jansa, P., Hofmann-Rohrer, U., Santoro, R., Langst, G., et al. (2001). NoRC–a novel member of mammalian ISWI-containing chromatin remodeling machines. *EMBO J.* 20, 4892–4900. doi: 10.1093/emboj/20.17.4892

Tang, J., Wu, S., Liu, H., Stratt, R., Barak, O. G., Shiekhattar, R., et al. (2004). A novel transcription regulatory complex containing Daxx and the ATR-X syndrome protein. *J. Biol. Chem.* 279, 20369–20377. doi: 10.1074/jbc.m401321200

Thorvaldsdottir, H., Robinson, J. T., and Mesirov, J. P. (2013). Integrative Genomics Viewer (IGV): high-performance genomics data visualization and exploration. *Brief. Bioinform.* 14, 178–192. doi: 10.1093/bib/bbs017

Timpano, S., and Picketts, D. J. (2020). Neurodevelopmental disorders caused by defective chromatin remodeling: phenotypic complexity is highlighted by a review of atrx function. *Front. Genet.* 11:885. doi: 10.3389/fgene.2020.00885

Torres-Aleman, I., Villalba, M., and Nieto-Bona, M. P. (1998). Insulin-like growth factor-I modulation of cerebellar cell populations is developmentally stage-dependent and mediated by specific intracellular pathways. *Neuroscience* 83, 321–334. doi: 10.1016/s0306-4522(97)00367-9

Tsukiyama, T., and Wu, C. (1995). Purification and properties of an ATP-dependent nucleosome remodeling factor. *Cell* 83, 1011–1020. doi: 10.1016/0092-8674(95)90216-3

Varga-Weisz, P. D., Wilm, M., Bonte, E., Dumas, K., Mann, M., and Becker, P. B. (1997). Chromatin-remodelling factor CHRAC contains the ATPases ISWI and topoisomerase II. *Nature* 388, 598–602. doi: 10.1038/41587

Wallace, V. A. (1999). Purkinje-cell-derived Sonic hedgehog regulates granule neuron precursor cell proliferation in the developing mouse cerebellum. *Curr. Biol.* 9, 445–448. doi: 10.1016/s0960-9822(99)80195-x

Wechsler-Reya, R. J., and Scott, M. P. (1999). Control of neuronal precursor proliferation in the cerebellum by Sonic Hedgehog. *Neuron* 22, 103–114. doi: 10.1016/s0896-6273(00)80682-0

Wiechens, N., Singh, V., Gkikopoulos, T., Schofield, P., Rocha, S., and Owen-Hughes, T. (2016). The Chromatin Remodelling Enzymes SNF2H and SNF2L Position Nucleosomes adjacent to CTCF and Other Transcription Factors. *PLoS Genet.* 12:e1005940. doi: 10.1371/journal.pgen.1005940

Wojcinski, A., Lawton, A. K., Bayin, N. S., Lao, Z., Stephen, D. N., and Joyner, A. L. (2017). Cerebellar granule cell replenishment postinjury by adaptive reprogramming of Nestin(+) progenitors. *Nat. Neurosci.* 20, 1361–1370. doi: 10.1038/nn.4621

Wojcinski, A., Morabito, M., Lawton, A. K., Stephen, D. N., and Joyner, A. L. (2019). Genetic deletion of genes in the cerebellar rhombic lip lineage can stimulate compensation through adaptive reprogramming of ventricular zone-derived progenitors. *Neural Dev.* 14:4.

Yang, H., Zhu, Q., Cheng, J., Wu, Y., Fan, M., Zhang, J., et al. (2019). Opposite regulation of Wnt/beta-catenin and Shh signaling pathways by Rack1 controls mammalian cerebellar development. *Proc. Natl. Acad. Sci. U. S. A.* 116, 4661–4670. doi: 10.1073/pnas.1813244116

Yip, D. J., Corcoran, C. P., Alvarez-Saavedra, M., DeMaria, A., Rennick, S., Mears, A. J., et al. (2012). Snf2l regulates Foxg1-dependent progenitor cell expansion in the developing brain. *Dev. Cell* 22, 871–878. doi: 10.1016/j.devcel.2012.01.020

Zhu, L. J., Gazin, C., Lawson, N. D., Pages, H., Lin, S. M., Lapointe, D. S., et al. (2010). ChIPpeakAnno: a Bioconductor package to annotate ChIP-seq and ChIP-chip data. *BMC Bioinformatics* 11:237. doi: 10.1186/1471-2105-11-237

Conflict of Interest: The authors declare that the research was conducted in the absence of any commercial or financial relationships that could be construed as a potential conflict of interest.

frontiers in Molecular Neuroscience

ORIGINAL RESEARCH
published: 12 July 2021
doi: 10.3389/fnmol.2021.686034

Cell-Type-Specific Gene Expression in Developing Mouse Neocortex: Intermediate Progenitors Implicated in Axon Development

Francesco Bedogni[1]* *and Robert F. Hevner*[2]*

[1] School of Biosciences, Cardiff University, Cardiff, United Kingdom, [2] Department of Pathology, University of California, San Diego, La Jolla, CA, United States

Cerebral cortex projection neurons (PNs) are generated from intermediate progenitors (IPs), which are in turn derived from radial glial progenitors (RGPs). To investigate developmental processes in IPs, we profiled IP transcriptomes in embryonic mouse neocortex, using transgenic *Tbr2*-GFP mice, cell sorting, and microarrays. These data were used in combination with *in situ* hybridization to ascertain gene sets specific for IPs, RGPs, PNs, interneurons, and other neural and non-neural cell types. RGP-selective transcripts (n = 419) included molecules for Notch receptor signaling, proliferation, neural stem cell identity, apical junctions, necroptosis, hippo pathway, and NF-κB pathway. RGPs also expressed specific genes for critical interactions with meningeal and vascular cells. In contrast, IP-selective genes (n = 136) encoded molecules for activated Delta ligand presentation, epithelial-mesenchymal transition, core planar cell polarity (PCP), axon genesis, and intrinsic excitability. Interestingly, IPs expressed several "dependence receptors" (*Unc5d*, *Dcc*, *Ntrk3*, and *Epha4*) that induce apoptosis in the absence of ligand, suggesting a competitive mechanism for IPs and new PNs to detect key environmental cues or die. Overall, our results imply a novel role for IPs in the patterning of neuronal polarization, axon differentiation, and intrinsic excitability prior to mitosis. Significantly, IPs highly express Wnt-PCP, netrin, and semaphorin pathway molecules known to regulate axon polarization in other systems. In sum, IPs not only amplify neurogenesis quantitatively, but also molecularly "prime" new PNs for axogenesis, guidance, and excitability.

Keywords: radial glia, intermediate progenitors, epithelial-mesenchymal transition, planar cell polarity, Wnt-PCP, cortical development, touch-and-go

OPEN ACCESS

Edited by:
Martin Fredensborg Rath, University of Copenhagen, Denmark

Reviewed by:
Takashi Namba, University of Helsinki, Finland
Julien Ferent, Institut National de la Santé et de la Recherche Médicale (INSERM), France

***Correspondence:**
Francesco Bedogni
bedognif@cardiff.ac.uk
Robert F. Hevner
rhevner@ucsd.edu

Specialty section:
This article was submitted to Neuroplasticity and Development, a section of the journal Frontiers in Molecular Neuroscience

Received: *26 March 2021*
Accepted: *03 June 2021*
Published: *12 July 2021*

Citation:
Bedogni F and Hevner RF (2021) Cell-Type-Specific Gene Expression in Developing Mouse Neocortex: Intermediate Progenitors Implicated in Axon Development. Front. Mol. Neurosci. 14:686034. doi: 10.3389/fnmol.2021.686034

INTRODUCTION

Intermediate progenitors (IPs) are a type of cortical progenitors "intermediate" in the lineage from radial glial progenitors (RGPs), which produce IPs, and projection neurons (PNs), which are generated from IPs (Haubensak et al., 2004; Miyata et al., 2004; Noctor et al., 2004). RGPs have high self-renewal capacity and multilineage differentiation potential, and are thus considered to be a class of neural stem cells (NSCs) (Taverna et al., 2014). In contrast, IPs have low proliferative capacity and single lineage commitment to produce only glutamatergic PNs, and thus are neural progenitor cells

but not NSCs (Mihalas and Hevner, 2018). In mice, RGPs and IPs are further distinguished by morphology, expression of transcription factors (TFs) such as Sox9 and Tbr2 (respectively); and by cell body location in the ventricular zone (VZ) for RGPs, or VZ and subventricular zone (SVZ) for IPs (Kowalczyk et al., 2009; Hevner, 2019). In mice, IPs generate the vast majority (possibly all) of the PNs in all cortical layers, including Cajal-Retzius cells and subplate neurons (Haubensak et al., 2004; Kowalczyk et al., 2009; Mihalas et al., 2016).

Cortical IPs are a unique cell type in vertebrate neurogenesis, but their significance in development remains uncertain. One proposed advantage of IPs is that they can divide away from the ventricular surface, to reduce crowding and increase neurogenic output per VZ surface area (Taverna et al., 2014). Also, IPs play a crucial role in Delta-Notch signaling as the major source of Delta-like signals that activate Notch and prevent premature RGP differentiation (Yoon et al., 2008; Nelson et al., 2013). In addition, IPs interact with migrating interneurons (INs) by secreting chemokine *Cxcl12* (SDF-1), which binds to *Cxcr4* and *Ackr3* receptors on INs to guide their tangential migration (Sessa et al., 2010; Saaber et al., 2019). Previously, it was suggested that IPs are specialized to amplify upper layer neurons; however, IPs were found to produce the majority of PNs in lower as well as upper layers (reviewed by Hevner, 2019). Evolutionarily, IPs are thought to serve as a cellular substrate for development of gyral folds (Kriegstein et al., 2006; Hevner, 2016; Toda et al., 2016).

In the present study, we hypothesized that IPs may play additional, unknown roles in cortical development, which might be revealed by transcriptome analysis. Our goals were: (1) to identify genes that are selectively expressed in IPs; (2) to analyze the pathways of IP-specific genes, using context-specific annotations from previous studies of neocortex; and (3) to identify developmental processes that are selectively activated in IPs, and compare them to those in RGPs and PNs. As part of this analysis, we ascertained gene sets for other cell types and features of E14.5 mouse neocortex, including neocortex-specific properties such as rostrocaudal patterning and PN laminar fate.

Previous studies of mouse IP transcriptomes, using different approaches, have produced distinct perspectives. An early single-cell transcriptome study using microarrays and unbiased cluster analysis distinguished RGPs, two types of IPs, and new PNs as cell types in the embryonic mouse VZ and SVZ (Kawaguchi et al., 2008). That study divided IPs into "type II" or apical IPs (aIPs), and "type III" or basal IPs (bIPs). ("Type I" cells were RGPs, and "type IV" were new PNs). The aIPs and bIPs were found to share expression of many genes, including *Tbr2* (MGI: *Eomes*), but also exhibited some transcriptome differences. That transcriptome study accorded with histological results showing that Tbr2+ IPs occupy distinct bands in the VZ and SVZ (Englund et al., 2005; Kowalczyk et al., 2009). Subsequently, a different study used cells sorted from *Tbr2*-GFP mouse neocortex to compare IP gene expression across embryonic ages (Cameron et al., 2012); however, due to the study design, general markers of IPs (such as *Tbr2*) were not ascertained. More recently, single-cell analyses of temporally defined RGP-IP-PN lineages reported transcriptional waves associated with PN differentiation (Telley et al., 2016, 2019). However, those single-cell results were not all validated by *in situ* hybridization (ISH), and we have found that many putative markers of RGPs, IPs, and PNs from that study do not show expected patterns on ISH. For example, some proposed IP markers (such as *Dbt*, *Pfkm*, and *Rprm*) show strong expression in the CP on ISH, consistent with postmitotic PNs. In the present study, we hypothesized that a new approach and analysis of IP transcriptomes could improve our knowledge of IP-selective genes and developmental mechanisms.

To profile IP gene expression, we sorted GFP+ cells and GFP− cells from embryonic day (E) 14.5 *Tbr2*-GFP mouse neocortex, then compared their transcriptomes using microarrays. Partial analyses of these data have been published previously (Bedogni et al., 2010; Nelson et al., 2013; Elsen et al., 2018), but this is the first comprehensive analysis to ascertain cell-type-specific gene sets. Genes (transcripts) that were highly enriched in either GFP+ cells or GFP− cells were further evaluated by ISH and literature search. Using known correlations between histological zone, gene expression, and cell identity in embryonic neocortex (Kawaguchi et al., 2008; Ayoub et al., 2011), we determined that gene expression was cell-type-selective only if microarray and ISH criteria met specific criteria (see section "Materials and Methods"). This approach enabled us to identify gene sets for all known cell types (neural and non-neural) in E14.5 mouse neocortex.

Non-neural cell types in developing neocortex are known to include microglia, leptomeninges, vascular, and blood cells. The vascular and blood elements are each further divided into multiple types: endothelium and pericytes for vascular; erythrocytes, monocytes, T lymphocytes, and B lymphocytes for blood. The gene sets for these cell types were useful to evaluate interactions between neural and non-neural cells during cortical development, such as those between RGPs and meningeal cells (Myshrall et al., 2012; Dasgupta and Jeong, 2019), and between RGPs and blood vessels (Biswas et al., 2020).

Our results demonstrate: (1) that each cell type in E14.5 mouse neocortex is characterized by the expression of specific gene sets; (2) that different cell types activate distinct signaling pathways; (3) that IPs likely play previously unsuspected roles in defining neuronal polarity and axogenesis; and (4) that extensive interactions occur between diverse cell types to coordinately regulate the growth, organization, and homeostasis of this complex brain region.

RESULTS

Cell-Type-Specific Gene Expression Determined by Microarray and *in situ* Hybridization

To identify genes expressed selectively by IPs and other cell types, we correlated microarray transcriptome profiling of lineage-sorted cells with ISH expression patterns in embryonic neocortex (**Figure 1**). *Tbr2*-GFP neocortex (E14.5) was dissociated, and cells were sorted into GFP+ and GFP− bins, after first enriching for progenitor cells on the basis of DNA

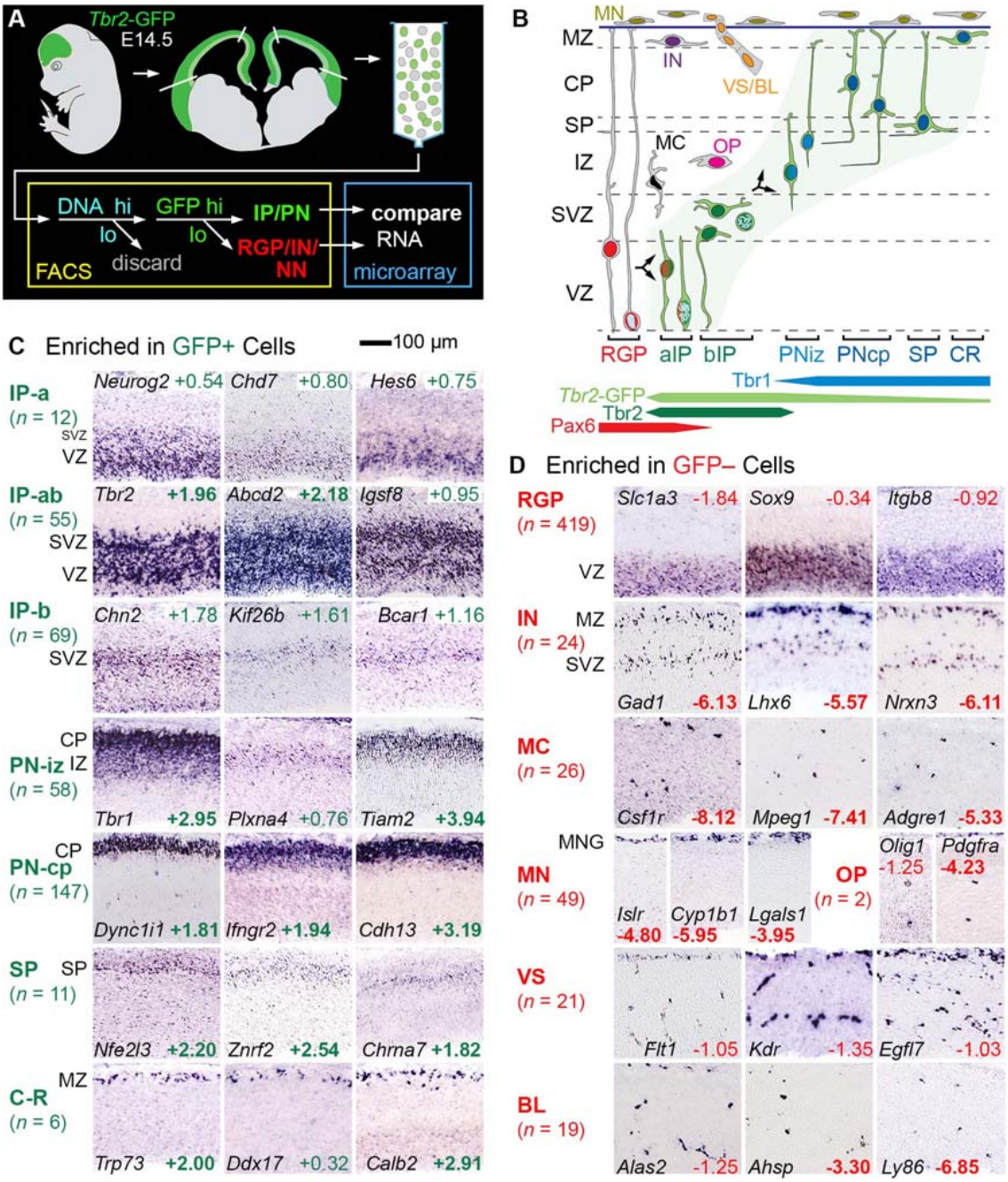

FIGURE 1 | Determination of cell type-selective gene expression in E14.5 mouse neocortex. **(A)** Cells from E14.5 *Tbr2*-GFP neocortex were sorted into GFP+ and GFP– cells, each profiled with transcriptome microarrays. Genes enriched in either group were studied by ISH. Note that sorting by DNA content evidently did not exclude postmitotic cells (see test for details). **(B)** Schematic of cell types and TF expression in E14.5 neocortex. **(C)** GFP+ cell types included IPs and PNs in various stages of differentiation, as indicated by typical ISH patterns. Some IP genes were expressed in the VZ and SVZ, indicating apical and basal IPs (IP-ab); others selectively in VZ or SVZ, indicating enrichment in aIP or bIP cells, respectively. **(D)** GFP– cell types showed characteristic ISH patterns. Numbers are $\log_2$FC values, in colored text if significant ($p < 0.05$), and bold if in the top 300 positively or negatively enriched genes. ISH: Genepaint. Abbreviations: see text.

content (**Figure 1A**). Importantly, despite sorting by DNA content, postmitotic cells were evidently not excluded, as they were well represented in the transcriptome results; the most likely explanation is that cell dissociation was incomplete, with doublets sorted as high-DNA cells.

RNA was amplified from GFP+ and GFP− cells for hybridization on Affymetrix Mouse Gene 430 2.0 microarrays (Nelson et al., 2013). In this experiment, GFP+ cells were significantly enriched (unadjusted $p < 0.05$) in 4,685 genes, and GFP− cells were significantly enriched in 3,262 genes.

Gene enrichment was expressed quantitatively as $\log_2$ of the fold change ($\log_2$FC), which was positive for genes enriched in GFP+ cells, and negative for genes enriched in GFP− cells. The raw microarray results are presented in **Supplementary Table 1**. Consolidated microarray results are presented along with other information about each gene (ISH expression pattern, literature references, etc.) in **Supplementary Table 2** (the primary integrated resource for this paper). Gene sets for all of the cell types and other features ascertained here are presented in **Supplementary Tables 3–10**.

Since GFP fluorescence in *Tbr2*-GFP neocortex labels not only IPs, but also postmitotic PNs (due to passive GFP inheritance), GFP+ cells encompassed the entire IP-PN lineage, including Cajal-Retzius and subplate neurons. Conversely, GFP– cells included RGPs and other non-*Tbr2*-expressing cell types, including all non-neural lineages. We evaluated the top 300 enriched genes in GFP+ cells and GFP− cells by ISH, using online databases and previous studies as described (Bedogni et al., 2010). Genes that met both criteria of (1) enrichment in GFP+ cells or GFP− cells, and (2) characteristic ISH expression patterns, were ascertained as cell-type-selective (**Figure 1** and **Supplementary Table 2** column I). (Genes are called "cell-type-selective" rather than "cell-type-specific" because very few genes are truly specific for one cell type).

Thus, cell-type-selectivity was strictly defined by criteria from both microarray and ISH data (**Figures 1C,D**; see section "Materials and Methods" for details). For example, IP-selective genes were (1) significantly enriched in GFP+ cells, and (2) expressed mainly in VZ (aIPs), VZ and SVZ (all IPs), or SVZ (bIPs) (**Figure 1C**). Genes that were expressed in all IPs, such as *Tbr2*, were classified as IP-ab genes (n = 55). Genes expressed mainly in aIPs were designated IP-a (n = 12), and genes mainly in bIP cells were designated IP-b (n = 69). Thus, genes expressed in aIPs included IP-a and IP-ab genes, while genes expressed in bIPs included IP-b and IP-ab genes. The standard for determining localization in VZ and SVZ was *Tbr2* (**Figure 1C**). Detailed analyses of IP- and RGP-selective are given below, following brief descriptions of additional features captured in our analysis.

Pallial Identity, Rostrocaudal Patterning, and Laminar/Axonal Projection Subtypes

Among genes enriched in GFP+ cells (IP-PN lineage), some were expressed predominantly in the pallium (cortical primordium) on ISH, with little expression in subpallial forebrain. These pallial-selective genes, which may be important in cortex-specific differentiation, were designated PN-cp, PN-iz, PN-svz, or PN-vz, according to zonal expression patterns (**Figure 2A**, upper row "PN"). Other genes enriched in GFP+ cells were more broadly expressed in pallial and subpallial differentiation zones on ISH. These genes, representing general neuronal differentiation, were designated N-cp, N-iz, N-svz, or N-vz (**Figure 2A**, lower row "N"). Interestingly, many markers of PN or general neuronal differentiation, such as *Elavl2*, were initially expressed in the VZ of cortex and were maintained in more superficial zones, suggesting they are initially activated in aIPs (**Figure 2A**). Gene sets for the IP-PN lineage are listed in **Supplementary Table 3**, and for general neuronal differentiation in **Supplementary Table 4**.

Rostrocaudal expression gradients were noted for some genes (**Figures 2B,C**). For most such genes, expression was confined within one or two adjacent zones (VZ, SVZ, IZ, and CP) rather than spanning multiple zones (Elsen et al., 2013). Markers of the cortical hem and antihem, which serve as cortical patterning centers (Subramanian et al., 2009), were also noted (**Supplementary Figure 1**), as were some genes with hippocampal-restricted expression. Gene sets for rostrocaudal markers, hem, antihem, and hippocampus are given in **Supplementary Table 5**.

Laminar fates and axonal projection-defined subtypes of PNs could not be inferred directly from gene expression data, but candidate gene sets for these features were assembled from previous studies (see section "Materials and Methods"). Genes were confirmed as PN laminar fate or axon target markers if they were enriched in GFP+ cells, and exhibited zonal expression consistent with the proposed identity (**Figure 2D**). For example, early-born corticothalamic (CTh) PNs are expected to reside in the cortical plate on E14.5, while late-born upper layers 2-4 (L2-4) neuron precursors are expected mainly in the SVZ and IZ. Since callosal projection neurons (CPNs) are found in all neocortical layers (although enriched in upper layers), CPN-selective genes could be expressed in any zone. Gene sets for PN laminar fate and axonal target identity are presented in **Supplementary Table 6**.

Proliferation Markers and Neural Stem Cell Identity

Transcriptional markers of proliferative activity have been established in previous studies (Whitfield et al., 2006). These were screened against our microarray and ISH results (**Supplementary Figure 2A**). The vast majority of proliferation markers were enriched in GFP− cells, and were localized in the VZ on ISH, thus satisfying criteria for RGP-selective genes. Additional markers of proliferative activity were ascertained by annotating known cell cycle functions. In contrast to proliferation genes, molecules linked to cell cycle exit or quiescence were enriched in GFP+ cells, and exhibited various expression patterns on ISH (**Supplementary Figure 2B**). Gene sets for proliferation and cell cycle exit are listed in **Supplementary Table 7**.

Proposed markers of neural stem cell (NSC) and progenitor (NSPC) identity (Easterday et al., 2003; Andreotti et al., 2019) were screened in the context of developing neocortex, using our microarray and ISH data. Since RGPs exhibit properties of NSCs while IPs do not (Taverna et al., 2014; Hevner, 2019), candidate NSC marker genes were confirmed only if RGP-selective (n = 15; **Supplementary Figure 2C**). Some candidate NSC or NSPC genes were expressed in the VZ/SVZ, but were not RGP-selective by microarray criteria. Such genes (n = 9; **Supplementary Figure 2D**) were identified as markers of neural stem and progenitor cells (NSPCs), likely expressed in both RGPs and IPs. Indeed, this expression pattern has been reported for *Nes* (Mignone et al., 2004) and *Msi1* (Kawase et al., 2011). Gene sets for cortical NSCs and NSPCs are listed in **Supplementary Table 7**. Since Notch signaling is critical for NSC maintenance,

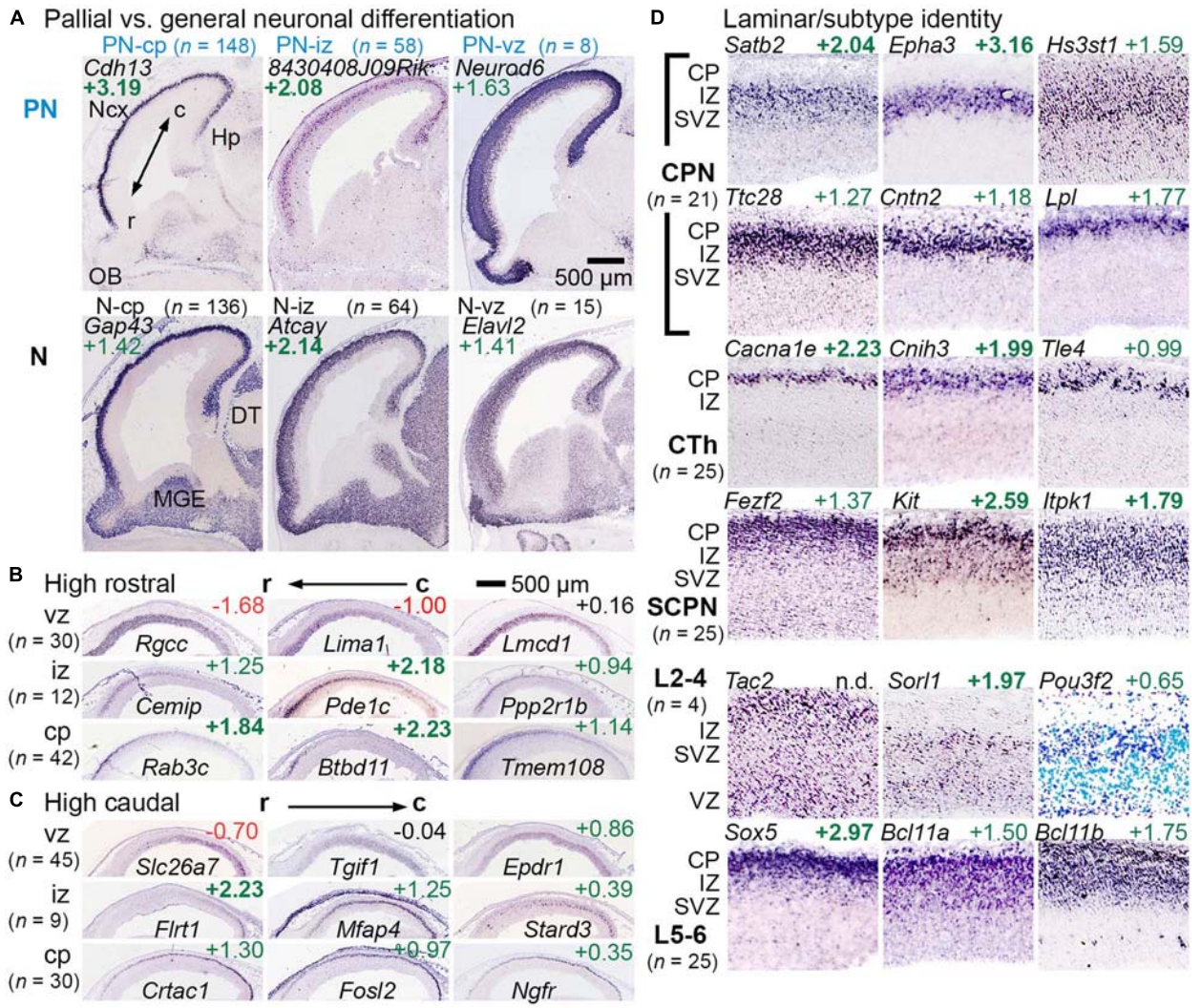

FIGURE 2 | Gene sets for regional, laminar, and axonal projection identity or fate. **(A)** Genes that were expressed mainly in pallium but not ventral forebrain were categorized as PN genes, while genes expressed widely expressed in differentiation zones were categorized as general neuronal (N). PN and N genes were found in each histologic zone, categorized according to the deepest zone of expression. Not shown: PN-svz (n = 14) and N-svz (n = 48). R-C indicates the rostrocaudal axis. **(B,C)** Rostrocaudal expression gradients were typically found within 1–2 contiguous zones. **(D)** Genes linked to specific laminar and axonal projection fates were categorized (see section "Materials and Methods"). Abbreviations: CPN, callosal projection neuron; CTh, corticothalamic; SCPN, subcerebral projection neuron. n.d., not detected.

genes for Notch signaling are also listed in **Supplementary Table 7** (and are further discussed below).

Radial Glial Progenitor Identity

RGP-Selective Transcripts

Radial glial progenitor-selective genes (n = 419; **Supplementary Table 8**) were significantly enriched in GFP− cells, and were expressed mainly in the VZ (**Figures 1D**, **3**). Our analysis confirmed classic markers of RG identity including *Slc1a3* (GLAST), *Notch1*, *Glul* (glutamine synthetase), *Sox9*, and *Vim* (vimentin) (**Supplementary Table 2** column I). Many RGP-selective genes were devoted to gene regulation, including 46 TFs, 10 non-TF epigenetic factors (Elsen et al., 2018), 6 RNA-binding proteins (RBPs), and 5 lncRNAs, for a total of 67 RGP-selective regulators of gene expression. Among the RGP-specific TFs were four Sox (*Sox1*, *Sox2*, *Sox9*, and *Sox21*), two Spalt (*Sall1* and *Sall3*), and two Tcf/Lef (*Tcf7l1* and *Tcf7l2*) family TFs, all linked to NSC maintenance and/or repression of neuronal differentiation. *Pax6*, previously characterized as a possible marker of RGPs (Götz et al., 1998), did not qualify as RGP-selective in the present analysis because microarray probes were discrepant. Indeed, Pax6 is expressed in many Tbr2+ IPs, especially aIPs, as well as RGPs (Englund et al., 2005). Other TFs, such as *Sox9*, are more specific RGP markers (Kaplan et al., 2017). Interestingly, among the RGP-selective RBPs, *Ngdn* (neuroguidin) regulates mRNA translation spatially and in response to signaling activity (Jung et al., 2006). Presumably, *Ngdn* may play a part in regulating local RGP translation, linked to rapid RNA transport (Pilaz et al., 2016).

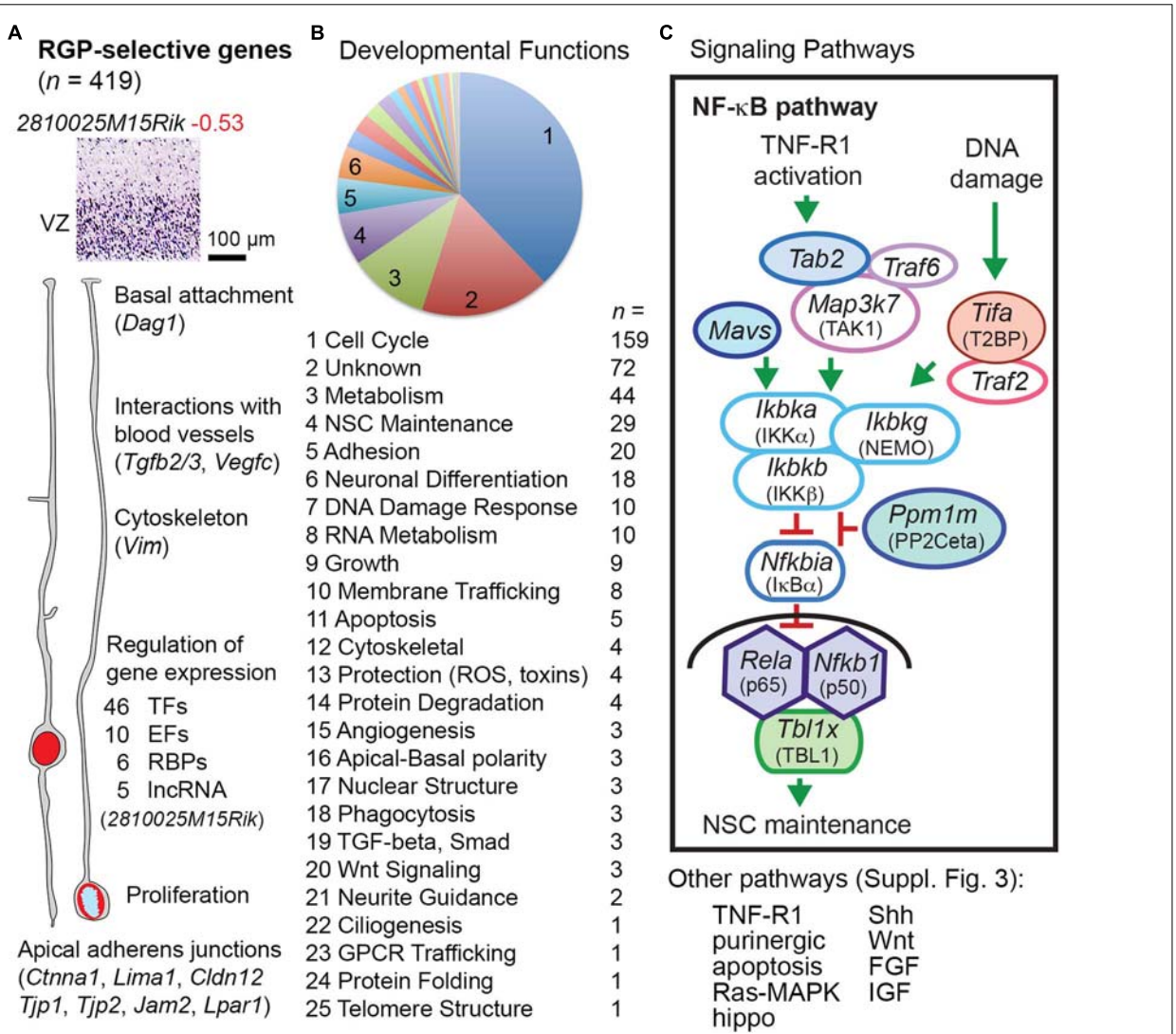

FIGURE 3 | RGP-selective genes. **(A)** The example transcript (*2810025M15Rik*) is a ncRNA of unknown function. Some key functions of RGP-selective genes and examples are indicated. **(B)** Developmental function categories of RGP-selective genes. **(C)** RGP-selective genes (indicated by colored shading) were highly linked to certain signaling pathways such as NF-κB. Components of the transcription complex (p65, p50, and TBL1) were all RGP-selective, as were upstream activators and repressors of the pathway. Shapes with white fill represent genes expressed in multiple cell types.

Among molecules for RNA degradation, *Pnrc2*, an adaptor in nonsense-mediated decay, was also RGP-selective.

RGP-Selective Signaling

Pathways were inferred from gene expression, with the caveat that protein signaling activity may not reflect mRNA expression. With this caveat in mind, pathway data (**Figure 3B**) showed that large numbers of RGP-selective genes were linked to cell cycle activity ($n = 159$) or DNA damage response ($n = 10$), the latter also active during the mitotic cycle (Petsalaki and Zachos, 2020). Genes that control NSC self-renewal ($n = 29$) or IP/neuronal differentiation ($n = 18$) were also numerous among RGP-selective genes. Other RGP-selective transcripts indicated functions such as membrane trafficking ($n = 8$), phagocytosis ($n = 3$), and GPCR trafficking ($n = 1$; *Cnih4*).

Several important intercellular and intracellular signaling pathways had one or more key components with RGP-selective expression. For example, multiple molecules in the NF-κB signaling pathway (Mitchell et al., 2016) showed RGP-selective expression (**Figure 3C**). The NF-κB transcriptional effectors p65 (*Rela*), p50 (*Nfkb1*), and TBL1 (*Tbl1x*) were all RGP-selective, as were several upstream positive and negative regulators. These findings indicate that the p65/p50-dependent NF-κB pathway is largely RGP-selective in developing neocortex. The function of NF-κB signaling in RGPs is primarily to maintain NSC identity and block IP genesis (Methot et al., 2013; Yamanishi et al., 2015). While the essential upstream activators of NF-κB signaling in developing cortex are unknown, this pathway can be engaged by TNF-R1 (*Tnfrsf1a*) activation or DNA damage (Fu et al., 2018; Van Quickelberghe et al., 2018). Activation of

TNF-R1 (for example, by TNF-α, potentially released from activated microglia) may lead to NF-κB signaling or necroptosis (Khoury et al., 2020), the latter a type of apoptosis mediated by RIPK (*Ripk1*) (**Supplementary Figure 3**).

Additional pathways with RGP-selective components included Shh, Wnt, Ras-MAPK, hippo, IGF, FGF, and purinergic signaling (**Supplementary Figure 3**). The Shh signaling pathway functions in RGPs primarily to promote symmetric proliferative divisions (Dave et al., 2011), but must be modulated to prevent acquisition of ventral forebrain properties (Yabut et al., 2020). RGP-selective components of Shh signaling included *Gas1*, a Shh co-receptor that binds Shh and potentiates its activity; *Gli3*, a downstream effector of Shh that promotes proliferation and represses IP genesis; and *Tulp3*, an intracellular repressor of Shh signaling. The coordinated RGP-selective expression of both activators and inhibitors of signaling pathways was a theme observed with not only NF-κB and Shh, but also apoptosis, canonical Wnt, and hippo pathways (**Supplementary Figure 3**). In addition, RGPs were selectively enriched in components of the ephrin-B1 (*Efnb1*) signaling pathway, which represses neuronal differentiation (Qiu et al., 2008; Wu et al., 2009). *Efnb1*, its signaling partner *Rgs3*, and proposed target gene *Gpsm2* (LGN/Pins), were all RGP-selective. Moreover, we observed that *Ephb6*, a ligand for ephrin-B1, is highly expressed by IPs and PNs. Potentially, *Ephb6* from IPs and PNs might provide feedback to repress neuronal differentiation of RGPs. Since EphB6 lacks an intracellular kinase domain, its feedback to *Efnb1* could be an example of pure reverse signaling.

RGPs and Junctional Complexes

Near the apical (ventricular) surface, RGPs have robust adherens junctions (AJs) that form a belt-like zonula adherens (Taverna et al., 2014). But unlike most classic epithelial cells, RGPs do not form tight junction (TJ) barriers (Aaku-Saraste et al., 1996; Taverna et al., 2014; Veeraval et al., 2020). However, some TJ related proteins (TJRPs) are expressed in RGPs, such as ZO-1 (*Tjp1*) (Aaku-Saraste et al., 1996). IPs and neurons link to surrounding cells with AJ patches that are smaller and molecularly distinct from RGP AJs (Wilsch-Bräuninger et al., 2012). In RGPs, the zonula adherens is linked to a contractile ring of F-actin and non-muscle myosin type II (NM-II). RGPs and migrating neurons have gap junctions, which may be important for PN radial migration (Elias et al., 2007), but no gap junction genes were RGP-selective in our analysis.

Unique Molecular Composition of RGP AJs

We found that a large number of AJ and TJRP molecules are selectively expressed in RGPs (**Figure 4A**). Interestingly, RGPs expressed both "epithelial" (*Ctnna1*; αE-catenin) and "neural" (*Cdh2*; N-cadherin) AJ molecules (**Figure 4A** and **Supplementary Table 2** column I). RGP-selective TJRPs included *Tjp1*, *Tjp2*, *Jam2*, and *Cldn12* (**Figure 4A**). The latter is an atypical claudin that promotes paracellular diffusion of calcium ions (Plain et al., 2020). Thus, although RGPs lack functional TJs and do not express *Ocln* (occludin), they express several TJRPs for enhanced adhesion and paracellular calcium diffusion. In addition, RGPs selectively expressed *Fat1*, which associates with AJs and promotes F-actin; *Rhoa*, a key regulator of AJ integrity; *Efhd2*, which stabilizes F-actin; *Lima1* (eplin), which promotes formation of the zonula adherens (Taguchi et al., 2011); and *Plekha7*, a zonula adherens-specific AJ adaptor that is repressed by *Insm1* to initiate IP delamination (Tavano et al., 2018). In addition, *Adgrv1*, an adhesion GPCR, is also selectively expressed by RGPs, but whether this molecule localizes in AJs is unknown. In sum, at least nine RGP-selective AJ molecules (shaded in **Figure 4A**) are down-regulated in the transition from RGP to aIP.

Apicobasal properties of RGPs such as the location of AJs are regulated in part by the apical polarity complexes PAR, CRB, and Mals/Pals. The PAR complex is composed of Pard3, Par6, atypical protein kinase C (aPKC), and Cdc42 (Kohjima et al., 2002). Some components of PAR complexes, such as *Prkci* (aPKCλ) and *Cdc42*, are essential to maintain AJs and apical surface integrity of the neocortex (Cappello et al., 2006; Imai et al., 2006). Perhaps surprisingly, then, none of the PAR complex molecules were RGP-selective. The CRB complex contains Crb, Pals1, and Patj proteins. Among these, only *Crb2* was RGP-selective. Indeed, previous studies have shown that *Crb2* is essential to maintain AJs and prevent premature RGP to IP differentiation (Dudok et al., 2016). No Mals/Pals molecules were RGP-selective.

The plasma membrane at the ventricular surface of RGPs, known as the apical plasma membrane, gives rise to the RGP primary cilium, and contains specific proteins for functions such as endocytic uptake and membrane remodeling. Among these, *Lrp2* (megalin) was RGP-selective, but *Prom1* was not (Our data suggest that *Prom1* is a marker of NSPCs, not NSCs). Among many dozens of known primary cilium molecules, only one (*Ift74*) was RGP-selective.

The Basal Surface and RGP Interactions With Leptomeninges

At the basal surface, RGPs attach to the basement membrane produced mainly by leptomeningeal cells (**Supplementary Figure 4A**) (Radner et al., 2012). Leptomeningeal-selective basement membrane genes included many isoforms of laminins (such as *Lama2*, *Lamb1*, and *Lamb2*) and collagens (such as *Col3a1*). RGPs selectively produced only a few ECM molecules, including *Vit*, *Ccdc80*, and *Bcan*. To attach to the basement membrane, RGPs require three basal attachment complexes built around dystroglycan (*Dag1*), which binds *Lama2*; GPR56 (*Adgrg1*), which binds *Col3a1*; and integrin-$\alpha_6\beta_1$ (*Itga6*, *Itgb1*), which binds laminins and promotes focal adhesions. Of these, only *Dag1* showed RGP-selective expression, while *Adgrg1* and the integrin genes were also expressed in other cell types (**Supplementary Figure 4A**). Mutations in these basal attachment genes (such as *Dag1*) or their signaling pathways cause cobblestone-like cortical malformations (Myshrall et al., 2012; Radner et al., 2012). Meningeal cells also send an essential signal by producing *Bmp7*, which is necessary to maintain RGP attachment to the basement membrane (Segklia et al., 2012). Our analysis of ISH and microarray data indicates that RGPs express BMP7 receptor subunits ALK3 (*Bmpr1a*) and *Bmpr2*, although not RGP-specifically (Saxena et al., 2018) (**Supplementary Figure 4A**).

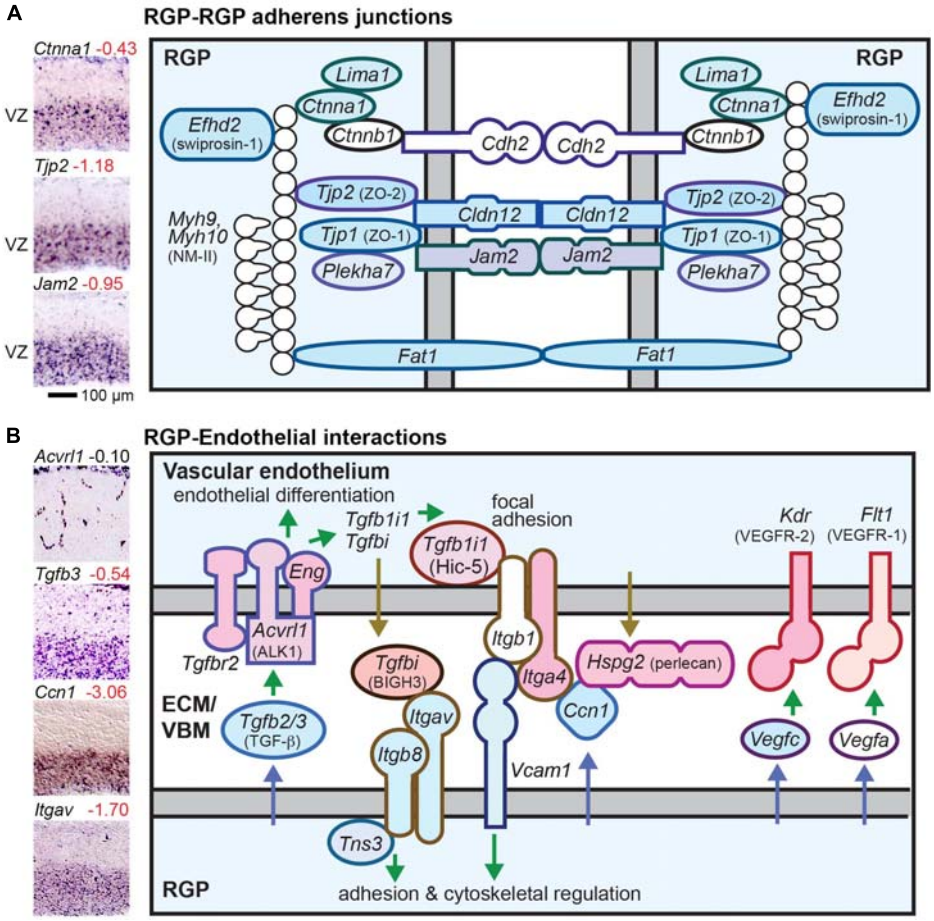

FIGURE 4 | RGP adherens junctions and vascular interactions. **(A)** The RGP adherens junction includes many tight junction related proteins (TJRPs) encoded by genes such as *Tjp1*, *Tjp2*, and *Jam2*. The junctions form a continuous band around the RGP apical region, called the zonula adherens, which is promoted by Lima1. The adherens junction is linked to the actin cytoskeleton with a contractile ring of F-actin and NMII. *Cldn12* promotes paracellular calcium diffusion, and *Fat1* is a giant cadherin. **(B)** RGP interactions with endothelial cells. Key pathways for cortical vascular development include TGFβ, Integrin ($\alpha_v\beta_8$), and VEGF produced by RGPs. Colored shapes indicate cell-type-specific genes; white fill indicates widely expressed genes.

The basal plasma membrane of RGPs, which covers 99% of the RGP surface, expresses a basal polarity complex consisting of DLG, LGL, and SCRIB. This complex, together with endocytic adaptors *Numb* and *Numbl*, contribute to regulating the location of AJs; however, none of these molecules were expressed selectively in RGPs.

Notch Signaling

Activation of Notch receptors is essential for RGP self-renewal, and is driven by presentation of Delta-like 1 (*Dll1*), mostly from aIPs (Kawaguchi et al., 2008; Yoon et al., 2008; Nelson et al., 2013). Notch signaling occurs predominantly near the apical surface, and during mitosis is organized by the PAR complex. We found that *Notch1*, *Notch2*, and *Notch3* were selectively expressed by RGPs, along with *Hes5*, a downstream target gene that is activated by Notch signaling (**Supplementary Figure 4B**). On the IP side, we observed that *Dll1*, *Mib1* (an essential activator of *Dll1*), *Mfng* (a glycosyltransferase that modifies Dll1 and Notch), as well as *Hes6* and *Hey1* TFs, were IP-selective. Dll3 was bIP-selective, and acts cell autonomously to dampen Notch signaling. The Delta-Notch signaling interaction between IPs and RGPs is illustrated in **Supplementary Figure 4B**.

Mitochondria and Metabolism

Several mitochondrial molecules, including *Mrpl13*, *Mrpl35*, *Mrpl39*, *Ndufaf8*, *Timm44*, and others, were RGP-selective. Mitochondria are important in cortical development and their distribution within RGPs is regulated (Rash et al., 2018). Also, many molecules important in intermediary metabolism were RGP-selective ($n = 44$).

RGP Interactions With Endothelial Cells

Radial glial progenitors are known to play essential roles in cerebral cortex vascular development (**Figure 4B**) (Tata and Ruhrberg, 2018). For example, production of integrin-$\alpha_v\beta_8$ (*Itgav* and *Itgb8*) by RGPs is essential for cortical vasculature development. Also, TGF-β and VEGF signals

from RGPs promote vascular development. Many molecules that mediate RGP-endothelial interactions were selectively expressed by RGPs or endothelial cells, illustrating the extensive, highly specific interactions between these cell types (**Figure 4B**). Gene sets for vascular cell types are listed in **Supplementary Table 9**.

Intermediate Progenitor Identity

IP-selective molecules were defined by significant enrichment in GFP+ cells on microarray, and predominant expression in the VZ/SVZ on ISH. Previous studies have reported that aIPs and bIPs have partially overlapping gene expression (Kawaguchi et al., 2008). To capture the distinct transcriptome profiles of aIPs and bIPs, we assessed IP-selective gene as "IP-a" if they were enriched predominantly in the VZ; "IP-ab" if in VZ and SVZ; or "IP-b" if mainly in the SVZ (**Figure 1C**). Accordingly, the aIP transcriptome consists of the union of IP-a and IP-ab genes, while the bIP transcriptome consists of IP-b plus IP-ab genes.

IP-Specific Transcripts

Among 136 total IP-selective molecules, 12 were IP-a, 55 were IP-ab, and 69 were IP-b (**Figures 5A–C** and **Supplementary Table 2**). The largest functional category in each group was neuronal differentiation, consistent with previous evidence that Tbr2+ IPs are committed neurogenic progenitors that produce glutamatergic PNs (Hevner et al., 2006; Hevner, 2019). For gene regulation, each group of IP-selective genes included multiple TFs, such as *Neurog2* among IP-a genes, *Tbr2* in IP-ab genes, and *Neurod1* in IP-b genes (**Figure 5D**). These TFs illustrate that transcripts were ascertained for selective, but not absolutely specific expression. *Neurog2*, for example, fit criteria for IP-a enrichment, but is also expressed to some extent in RGPs (Kawaguchi et al., 2008). In contrast, *Tbr2* appears to be completely IP-specific, while *Neurod1* is expressed in bIPs and, to some extent, postmitotic neurons (Hevner et al., 2006). Other interesting regulators of gene expression selectively expressed in IPs included a microRNA (miR) host gene, *Mir17hg*, in aIPs; *Ago1*, an RBP that mediates mRNA silencing, in abIPs (**Figure 5A**); and multiple lncRNAs in bIPs. The epigenetic factors selectively expressed by IPs have been described (Elsen et al., 2018).

TF Regulation in IPs

The transitions between RGPs, IPs, and PNs appear to be highly discrete. In accordance with this view, regulatory mechanisms that rapidly control the expression of key TFs in IPs have been identified. While *Pax6* is crucial to IP genesis and *Tbr2* expression (Quinn et al., 2007), *Pax6* is downregulated and deactivated in IPs, in part by feedback repression from *Tbr2* (Elsen et al., 2018), and in part due to dephosphorylation by protein phosphatase-1 (Yan et al., 2007). Similarly, *Neurog2*, another driver of IP genesis and *Tbr2* expression (Ochiai et al., 2009), is rapidly downregulated in IPs by *Cbfa2t2* (MTGR1), an IP-specific transcriptional coregulator that is first induced by *Neurog2*, then binds and inactivates *Neurog2* (Aaker et al., 2009). Indeed, decreased *Neurog2* activity is essential for further differentiation from IPs to PNs (Aaker et al., 2009). These examples illustrate the principle that differentiation in the RGP-IP-PN lineage requires rapid, active up- and downregulation of critical genes.

Adhesion and Apoptosis Pathways in IPs

Compared to RGPs, IPs markedly down-regulated proliferation, AJ components, and RGP-specific pathways such as NF-κB, hippo, and necroptosis. Not only were AJ components overall downregulated in IPs, but the isoform of α-catenin also changed from *Ctnna1* (αE-catenin) in RGPs, to *Ctnna2* (αN-catenin) in IPs and differentiating PNs. Conversely, aIPs and bIPs selectively expressed *Ptprk*, a homophilic adhesion molecule. These data revealed a rapid, profound change in both the strength and quality of AJs occurs concomitantly with RGP-IP differentiation. Interestingly, while necroptosis pathways were reduced in IPs, apoptosis of IPs may occur by other pathways, mediated by "dependence receptors" that promote apoptosis if ligand is not bound (see below). Consistent with this idea, IPs and neurons express *Ppp2r2b*, which drives apoptosis in response to growth factor deficiency.

Shh and Wnt Signaling Pathways in IPs

Shh co-receptor *Boc* was selectively expressed in aIPs (**Figure 5A**), rather than *Gas1* as in RGPs (**Supplementary Figure 3B**). The canonical Wnt signaling pathway (involving regulation of β-catenin signaling) was likewise modified in IPs, for example, by selective upregulation of *Fzd1* in the PN lineage. Previous studies have shown that in multipolar bIPs, canonical Wnt signaling is transiently downregulated (Boitard et al., 2015). Our molecular analysis suggested that this change might be mediated by *Bcl6* (Bonnefont et al., 2019), expressed selectively in the IP-PN lineage; and by *Shisa2*, a bIP-selective, cell-autonomous inhibitor of Wnt and FGF signaling (Furushima et al., 2007). However, non-canonical Wnt signaling, especially the Wnt-PCP pathway, appears massively upregulated in IPs (see below).

Delta-Notch Signaling in IPs

Notch pathway molecules were differentially and selectively expressed between not only RGPs and IPs, but also between aIPs and bIPs. Expression of *Dll1* was aIP-selective (**Supplementary Figure 4B**), while *Dll3* was bIP-selective. Like *Dll1*, *Dll3* is a Delta-like ligand that is fucosylated by *Mfng*, but *Dll3* functions cell-autonomously to block Notch activation and thus consolidate neuronal differentiation of bIP cells (Serth et al., 2015). At the same time, *Bcl6* (which is selectively expressed in the IP-PN lineage, beginning in aIPs) functions to repress Notch signaling and, together with *Bcor* (an abIP-selective gene), represses *Hes5* (Tiberi et al., 2012). *Hey1* (abIP-selective) represses *Hes1* and *Gas1*, while promoting self-renewal of NSPCs (Heisig et al., 2012; Weber et al., 2014). Thus, *Hey1*, together with *Boc* (replacing *Gas1*) in the Shh pathway, may support IP division despite overall reduced proliferative activity of IPs compared to RGPs.

Extracellular Matrix and Vascular Interactions

Intermediate progenitors do not interact with the meningeal basement membrane, but do associate with blood vessels, especially in the SVZ (Javaherian and Kriegstein, 2009;

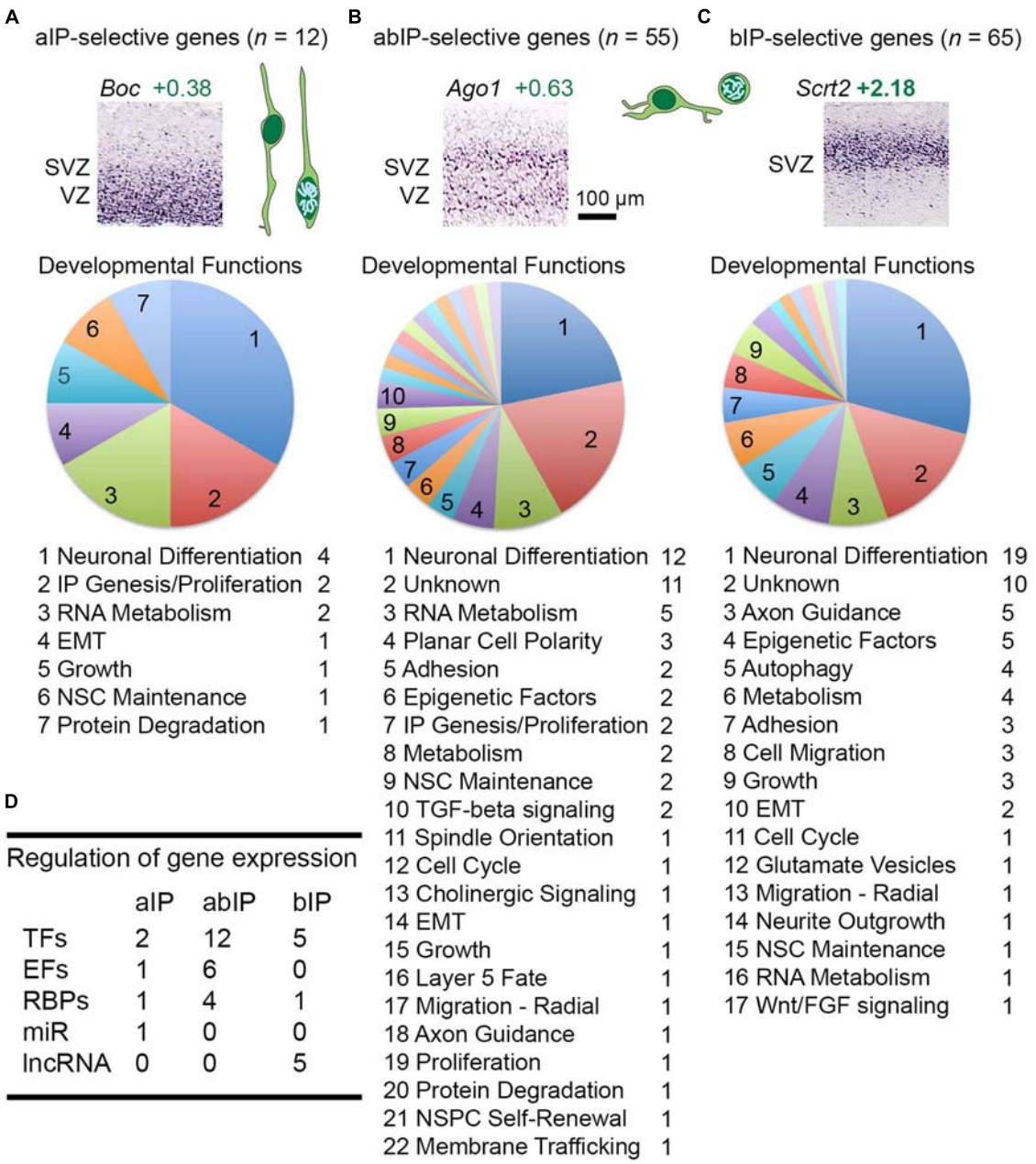

FIGURE 5 | (A–C) IP-selective genes included those expressed mainly in VZ (IP-a genes), in VZ and SVZ (IP-ab), and in SVZ (IP-b), with examples for each. Neuronal development functions were highly represented in each category. **(D)** Table showing the number of gene regulatory molecules in each IP type.

Stubbs et al., 2009). Interestingly, we observed that bIPs selectively express *Mfap4*, an RGD-containing ECM component that may be a ligand for integrins and collagen. We found that *Adgrg1* (GPR56), although best known for mediating RGP interactions with the meninges (**Supplementary Figure 4A**), is enriched in abIPs. We speculate that *Adgrg1* and/or *Mfap4* may mediate the association of IPs with blood vessels. Also, abIPs selectively expressed *Ltbp3* and *Mfap2* (MAGP-1), both of which stabilize TGF-β, and thus potentially enhance TGF-β signaling from RGPs to blood vessels (**Figure 4B**).

IP Cell Migration

Previous studies have shown that as IPs differentiate from aIP to bIP subtype, they migrate from the VZ where they have "short radial" (Gal et al., 2006) or "pin-like" (Ochiai et al., 2009) morphology, to the SVZ where bIPs remodel to multipolar morphology. The aIPs initially maintain contact with RGPs at apical AJs (Taverna et al., 2014), which are lost in the transition to bIP. After final mitosis, new PNs exhibit multipolar morphology, select an axonal process, convert to bipolar morphology, then migrate into the cortical plate. During the multipolar phase,

bIPs and new PNs undergo "multipolar migration" characterized by frequent extension and retraction of short processes, and short-range slow tangential migration in the SVZ and IZ (Tabata and Nakajima, 2003).

Epithelial-Mesenchymal Transition

One proposed mechanism for neural precursor migration from the VZ is epithelial-mesenchymal transition (EMT) (Itoh et al., 2013). Consistent with this idea, we observed that several critical genes for EMT (Nieto et al., 2016; Aznar et al., 2018) are selectively expressed in IPs, including *Srsf2* in aIPs, *Akna* in abIPs, and *Scrt2* and *Ccdc88c* (Daple) in bIPs (**Supplementary Table 2**). By ISH, scattered *Scrt2*-expressing cells were observed in the VZ, likely indicating cells in transition from aIP to bIP (**Figure 5C**). In addition, *Serpini1* (neuroserpin), which is expressed in the IP-PN lineage beginning in the SVZ, may contribute to EMT (Matsuda et al., 2016). Partial or specialized forms of EMT are common in biology (Nieto et al., 2016). In addition, ATP and Ca(2+) signaling may also regulate migration from VZ to SVZ (Liu et al., 2008).

Multipolar Migration

During the multipolar phase, we found that bIPs selectively expressed *Chn2* (β2-chimerin; **Figure 1C**), a Rac-GAP, as well as *Prex1* (P-Rex-1), a Rac-GEF. Both *Chn2* and *Prex1* have been linked to regulation of multipolar migration, indicating the importance of *Rac1* (which is widely expressed) in this process. Interestingly, *Chn2* links EphA receptor signaling with Rac1 inactivation to suppress migration (Takeuchi et al., 2009), while *Prex1* activates Rac1 and stimulates migration (Li et al., 2019). Since several EphA molecules (such as *Epha4*, *Epha5*) are expressed in the SVZ and IZ, our data suggest that EphA activation restricts migration. Lateral dispersion of PN clones away from source RGPs is also regulated by EphA signaling (Torii et al., 2009). Interestingly, lateral dispersion of neural precursors thus occurs before axogenesis and bipolar migration.

Other known regulators of bIP and new PN migration include *Rnd3* (Pacary et al., 2011), which we found was selectively expressed by bIPs; and *Rnd2*, which was expressed by new PNs (Heng et al., 2008). Another factor that may regulate IP migration is the peptide CCK. The receptor CCK-1R (*Cckar*), reported to mediate repulsive responses to CCK (Giacobini et al., 2004), was selectively expressed on bIPs. The *Cck* ligand was the expressed by PNs in the cortical plate (CP). Potentially, CCK signaling may restrict IPs from entering the CP.

Cholinergic Signaling

Intermediate progenitors express cholinergic receptor subunits, including *Chrna3* selectively in abIPs, and *Chrnb2* in IPs and new neurons beginning in the SVZ. Cholinergic receptors can be activated *in vivo* to provoke inward Ca(2+) currents (Atluri et al., 2001). However, the functional significance of cholinergic signaling remains unknown.

Wnt-PCP Pathway

Planar cell polarity is a conserved mechanism to polarize sheets of cells in the tangential plane, for example, to orient bristles on the fly body (Butler and Wallingford, 2017). The molecular components of PCP include "core" and "Fat–Dachsous–Four-jointed" (Ft–Ds–Fj) modules, which may interact concurrently or sequentially. Arising by asymmetric endocytosis and endosomal trafficking, PCP ultimately reorganizes the actin cytoskeleton to control cellular morphology. One key mechanism that can orient PCP is Wnt signaling gradients (Yang and Mlodzik, 2015).

Core PCP is implemented by six molecules (*Fzd*, *Vangl*, *Celsr*, *Dvl*, *Prickle*, and *Ankrd6*), some of which have multiple gene isoforms. We found that a suite of three core PCP molecules were expressed selectively in abIPs: *Celsr1*, *Vangl2*, and *Ankrd6*. Together with broadly expressed isoforms of other core PCP components — including *Fzd3*, *Prickle2*, and *Dvl2* — IPs thus uniquely acquire a full complement of core PCP components (**Figures 6A,B**). Notably, *Fzd3* is the isoform most frequently implicated in core PCP, although other *Fzd* isoforms can be involved as well.

While several mechanisms may contribute to orienting the directionality of PCP, one is by response to Wnt gradients, known as Wnt-PCP signaling (Yang and Mlodzik, 2015). In developing cortex, Wnt signaling gradients (Machon et al., 2007) are established by caudomedial expression of multiple Wnts and *Rspo2* (which potentiates Wnts) in the cortical hem and hippocampus; and by *Sfrp2* (a Wnt antagonist) from the rostrolateral antihem (**Supplementary Figure 1**). The Wnt most associated with PCP signaling in mammals is *Wnt5a*, expressed in the hem (**Figure 6A**). Other Wnts and Fzds show diverse expression patterns that demonstrate the complexity of Wnt signaling in developing cortex (**Supplementary Figure 5**).

Our findings suggest that concurrent with EMT, IPs undergo a profound change in polarity, from apicobasal to planar (**Figure 6D**). In PNs, no *Ankrd6* or *Vangl* isoforms were detected, and instead of *Celsr1* as in IPs, *Celsr2* and *Celsr3* were expressed in PNs (**Figure 6A**). These molecular data suggest that PNs may express a minimal "maintenance" form of PCP, initially oriented in IPs, to promote axon fasciculation (**Figure 6C**). Importantly, mutations in core PCP molecules have been associated with defects of axon growth and connectivity in the forebrain (Hakanen et al., 2019).

Axogenesis and Excitability

Axon selection by cortical PNs is thought to occur shortly after they are generated from IPs, concurrently with the transition from multipolar to bipolar morphology (Namba et al., 2014). Interestingly, we observed that multiple genes associated with axogenesis, neurite growth, and excitability were expressed by bIPs (**Figure 6E**).

Among the bIP-selective genes for axogenesis were *Pcdh7*, which initiates axon outgrowth in retina; *Arhgef25*, which drives axon formation and growth; *Nrn1* (neuritin-1), an activity-induced cell surface protein that promotes axon growth; *Sstr2*, which stimulates axon outgrowth upon activation by somatostatin (Le Verche et al., 2009); *Bcar1*, an adaptor protein linked to neurite outgrowth; *Igfs8*, a cell surface protein associated with neurite outgrowth; *Ppp2r3c*, a regulatory component of protein phosphatase 2A (PP2A), which is linked to axogenesis; and *Dusp14*, a phosphatase that inhibits MAPK signaling and negatively regulates axon growth (references in

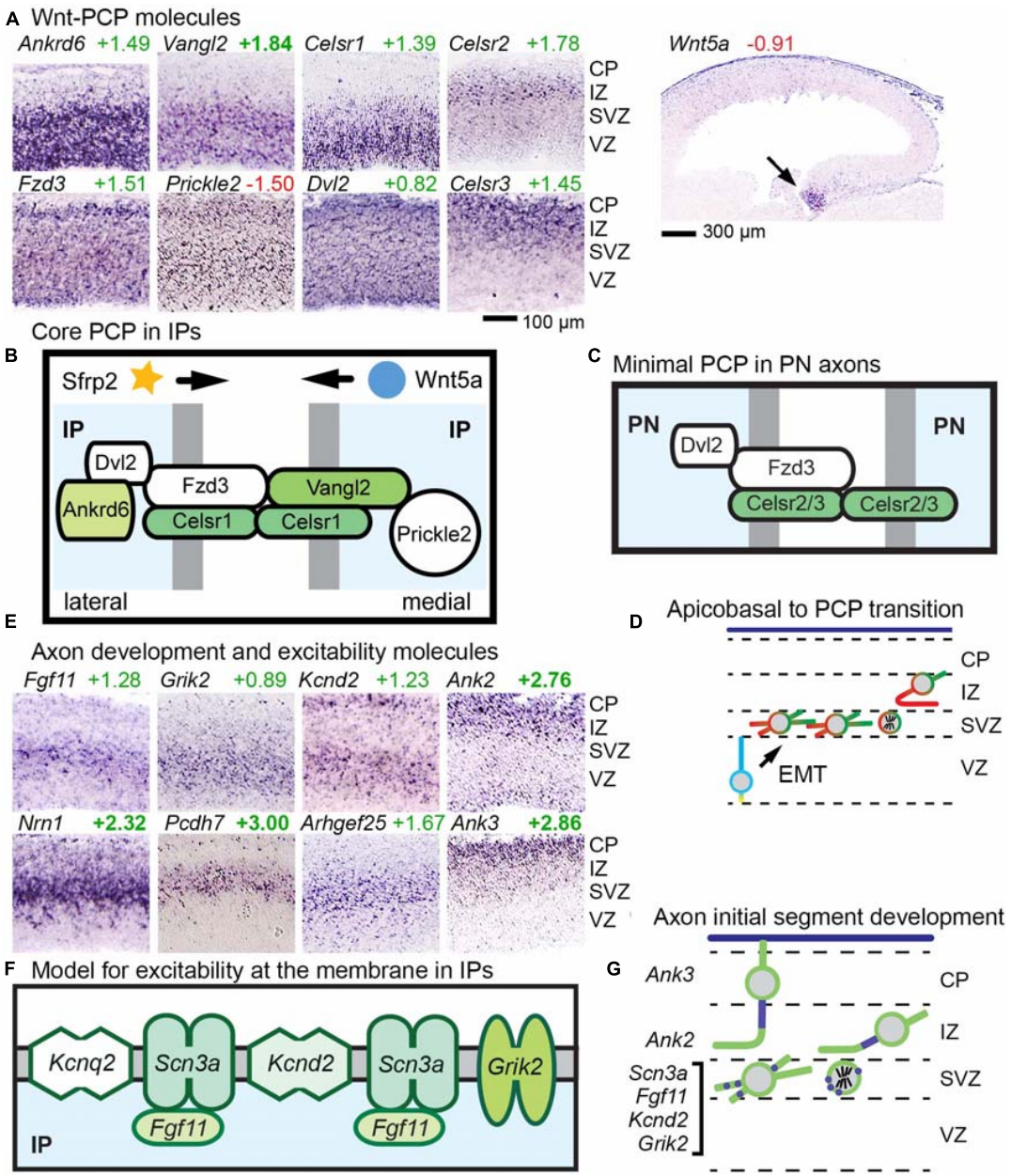

FIGURE 6 | Wnt-PCP and axon differentiation pathways in IPs. **(A)** *Ankrd6*, *Vangl2*, and *Celsr1* showed IP-specific expression; *Fzd3*, *Prickle2*, and *Dvl2* were broadly expressed; *Celsr2* and *Celsr3* were expressed in postmitotic PNs. **(B)** Proposed model of Wnt-PCP signaling complexes in IPs, possibly patterned by gradients of Wnt signaling, such as *Wnt5a* from the hem. *Sfrp2* from the antihem might also shape Wnt gradients. Colored shapes indicate IP-selective genes, and white fill indicates widely expressed molecules. **(C)** Proposed model of "minimal PCP" in PNs. Unlike IPs, PNs do not produce a full complement of core PCP molecules, but do express *Fzd3*, *Celsr2/3*, and *Dvl2*. **(D)** Proposed model of transition from apicobasal polarity (blue–yellow) to PCP (red–green) in aIP to bIP differentiation. In this model, PCP is initially patterned in IPs, and transmitted to postmitotic neurons in the IZ. **(E)** Molecules for axon development and excitability were expressed in the SVZ (including *Fgf11*, *Grik2*, *Kcnd2*, *Nrn1*, *Pcdh7*, and *Arhgef25* as shown), while genes for axon initial segment stabilization were expressed in postmitotic PNs (*Ank2* and *Ank3*) of the IZ and CP. **(F)** Proposed model of axon-like excitability patch in IPs. **(G)** Proposed model for the development of excitability beginning in IPs. Patches of excitable membrane may be produced in IPs, and rapidly assembled into axon initial segments in new postmitotic PNs.

Supplementary Table 2, column Z). Another critical regulator of axon formation in neocortex, *Rapgef1*, was expressed in the IP-PN lineage beginning in bIPs. The selective expression of not only activators, but also an inhibitor of axon growth suggests that axogenesis is a regulated process that begins in bIPs.

Intrinsic Excitability

A recent study unexpectedly found that voltage-gated sodium channel *SCN3A* ($Na_V1.3$) is expressed by Tbr2+ IPs in developing human cortex (Smith et al., 2018). In the present study, *Scn3a* could not be evaluated because *Scn3a* ISH data are

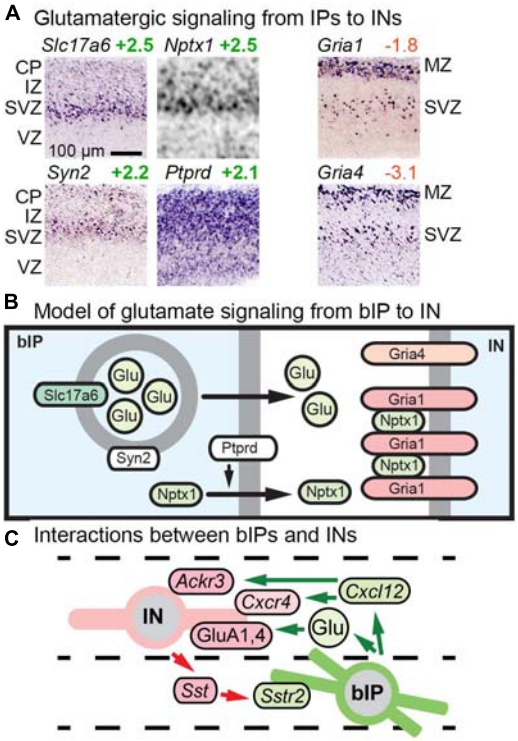

FIGURE 7 | Glutamate signaling and other bIP-IN interactions. **(A)** bIPs in the SVZ express molecules for glutamatergic signaling including *Slc17a6* (VGLUT2), *Nptx1*, *Syn2*, and *Ptprd*; while migrating INs express AMPA receptors (*Gria1*, *Gria4*). **(B)** Proposed model for glutamatergic signaling from bIPs to INs. Interestingly, bIPs produce *Nptx1*, a secreted protein that clusters AMPA receptors. **(C)** Glutamate signaling is one of several interactions between IPs and INs.

not available for embryonic mouse. Nevertheless, we did find other excitability molecules expressed selectively in bIPs (**Figure 6E**). These included *Grik2* (GluK2/GluR6), which causes membrane depolarization upon glutamate binding; *Kcnd2* (K_V4.2), which mediates repolarization; and *Fgf11*, a member of the FGF-homologous factor family, whose members function as intracellular modulators of voltage-gated sodium channels, and may localize with them to the AIS (Goldfarb et al., 2007; Pablo and Pitt, 2016). In addition, *Kcnq2* (K_V7.2) was also expressed in IPs, albeit not selectively. Molecular markers of stabilized axon initial segments, such as *Ank2*, *Ank3*, and *Cacna2d1*, were not expressed until PNs reach the IZ and CP (**Figure 6E**). Thus, despite the fact that IPs lack axons or initial segments, IPs may function to promote excitability even before the axon is formed (**Figures 6F,G**). We speculate that together, IP-expressed ion channels and *Fgf11* may form excitable membrane patches (**Figure 6F**), with properties similar to the *Ank3*-independent, immature AIS which accumulates voltage-gated sodium channels and K_V7.2 (Sánchez-Ponce et al., 2012; Yamada and Kuba, 2016). Also, *Nfasc* (neurofascin), another molecule linked to axon initial segment stabilization, was expressed in bIPs; but this function of *Nfasc* is thought to be *Ank3*-dependent.

Glutamatergic Signaling in IPs

Previous studies reported that bIPs express *Slc17a6* (VGLUT2), a vesicular glutamate transporter that packages glutamate for release as a neurotransmitter (Kawaguchi et al., 2008). Our analysis confirmed that bIPs selectively express *Slc17a6*, and further revealed that bIPs also express *Syn2* (synapsin II), a synaptic vesicle molecule enriched in the IP-PN lineage beginning in bIPs (**Figure 7A**). Thus, IPs may be prepared to release glutamate vesicles. In addition, we found that bIPs selectively express *Nptx1*, a secreted clustering factor for GluA1-type glutamate receptors (**Figure 7A**). Moreover, bIPs express *Ptprd* (RPTPδ), a tyrosine phosphatase that functions to promote release of *Nptx1*. Interestingly, GluA1 (*Gria1*), as well as GluA4 (*Gria4*), are selectively expressed by migrating INs (**Figure 7A**). Thus, bIPs have some properties of glutamate-releasing neurons, along with the capacity to promote glutamate receptor clustering on adjacent cells, in this case INs (**Figure 7B**). Overall, glutamate signaling may be another mechanism of interaction between IPs and INs, along with *Cxcl12* and *Sstr2* (**Figure 7C**).

Axon Guidance Molecules in IPs

Previous studies also reported that IPs express axon guidance receptors, including *Unc5d* (same gene as *Svet1*) and *Plxna2* (Kawaguchi et al., 2008). Our analysis confirmed and expanded this repertoire, finding that IPs also selectively express *Sema3c*, *Sema5a*, and *Nrp2*. These molecules belong to netrin and semaphorin guidance pathways (**Figure 8**).

Netrin Signaling and IPs

Netrins are secreted factors that attract or repel axons, depending on the receptor: For *Ntn1*, the most studied netrin, *Dcc* and *Neo1* are attractive, while *Unc5* family molecules interact with *Dcc* to form repulsive receptors (Boyer and Gupton, 2018; Yamagishi et al., 2021). Other molecules that interact with the netrin system include *Dscam*, a netrin co-receptor with *Dcc*; and *Draxin*, a secreted factor that binds *Dcc* to modulate thalamocortical axon guidance. In addition, *Flrt2* and *Flrt3* secreted ligands can bind *Unc5d* and *Unc5b* receptors, respectively, to mediate repulsive cues for cell migration (Yamagishi et al., 2021).

Among netrins, *Ntn1* and *Ntn4* have similar receptor binding and interactions (Qin et al., 2007). *Ntn1* is not expressed in embryonic neocortex, but *Ntn4* expression has been reported in E14.5 VZ (Yin et al., 2000; Ayoub et al., 2011). We confirmed expression of *Ntn4* in the VZ on ISH, and furthermore observed a high rostrocaudal to low caudomedial gradient (**Figure 8G**). (*Ntn4* was not detected at significant levels on microarray, presumably for technical reasons). These findings suggested that *Ntn4* may be important in cortical development. Indeed, *Ntn4* deficient rats show reduced thalamocortical innervation (Hayano et al., 2014).

Dcc was highly enriched in the IP-PN lineage ($\log_2$FC =+2.57), and was expressed in the SVZ, IZ, and CP, consistent with bIPs and PNs (**Figure 8D**). Since bIPs also express *Unc5d* (**Figure 8F**), they presumably respond to *Ntn4* as a repulsive guidance cue. This repulsive response is likely maintained for

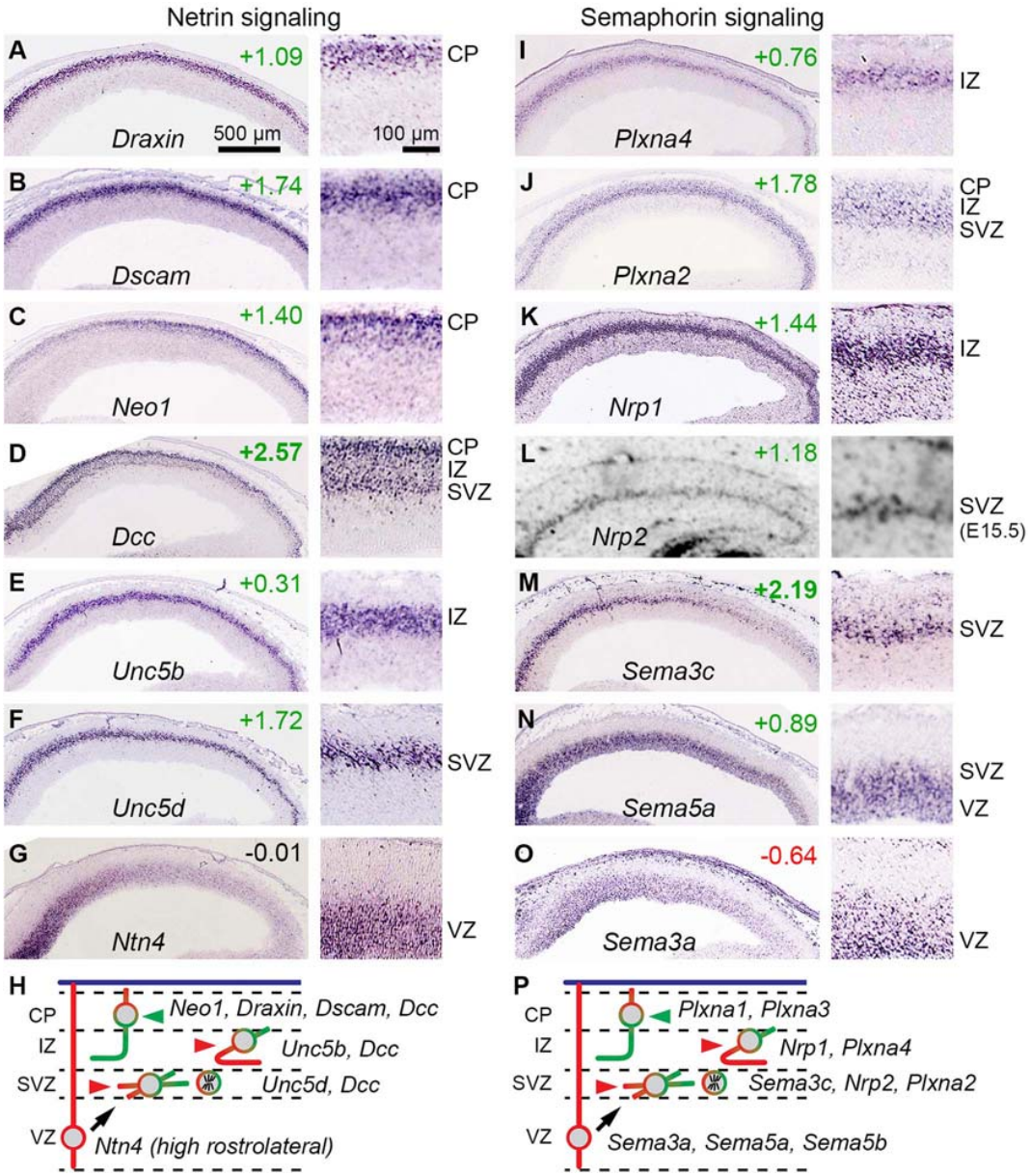

FIGURE 8 | Netrin and semaphorin signaling involving IPs. **(A–G)** Expression of selected netrin signaling molecules, including bIP-selective *Unc5d* **(F)**. Each panel shows low **(left)** and high **(right)** magnification views of cortex; rostral is to the left. **(H)** Proposed model for netrin signaling involving *Ntn4* from RGPs in a high rostral gradient, and responsive PNs in each histologic zone. **(I–O)** Expression of selected semaphorin signaling molecules, including bIP-selective genes *Plxna2* **(J)**, *Nrp2* **(L)**, and *Sema3c* **(M)**; and abIP-selective *Sema5a* **(N)**. **(P)** Proposed model for semaphorin signaling among cell types.

new PNs in the IZ, which express *Unc5b* (**Figure 8E**). In contrast, PNs in the CP did not express *Unc5* molecules, except for very low levels of *Unc5a* in the most superficial CP cells (not shown). PNs in the CP did, however, express high levels of *Dcc*, *Neo1* (in a high caudal gradient), *Dscam*, and *Draxin* (**Figures 8A–D**), suggesting that axons from PNs already in the CP on E14.5 (early-born PNs) respond to *Ntn4* as an attractive cue (**Figure 8H**). These findings suggest that netrin signaling may play an important early role in bIP polarization and axon guidance.

Semaphorin Signaling and IPs

In this repulsive signaling system, semaphorins are ligands, neuropilins are ligand-binding receptors, and plexins are signal-transducing co-receptors (reviewed by Alto and Terman, 2017; Toledano et al., 2019). Previous studies have shown that this system is important in the development of callosal axons, which are repelled toward the midline by graded expression of rostrolateral factors, including *Sema3a*, a secreted semaphorin. We confirmed that *Sema3a* is expressed in a high rostrolateral gradient in the VZ, and further found that *Sema3a* is selectively

expressed by RGPs (**Figure 8O**). The *Sema3a* receptor, *Nrp1* (Hossain et al., 2019), and the co-receptor *Plxna4*, were both expressed by new PNs in the IZ (**Figures 8I,K**). Thus, many new PNs in the IZ on E14.5 express *Nrp1*/*Plxna4* repulsive receptors for *Sema3a*, consistent with callosal axon phenotype (**Figure 8P**).

Many additional semaphorins and receptors were expressed by specific cell types. Interestingly, like *Sema3a* in RGPs, other semaphorins were expressed in high rostrolateral gradients, including *Sema5a* in abIPs (**Figure 8N**) and *Sema3c* in bIPs (**Figure 8M**). Also, *Sema5b* was expressed specifically by RGPs, but no gradient was apparent (not shown). The receptor for *Sema5a* consists of *Nrp2* with *Plxna2*, both expressed selectively by bIPs (**Figures 8J,L**); signaling through this receptor may be further potentiated by *Ranbp9*, a bIP-selective scaffold protein that augments plexin-A activity. *Sema3c* has multiple potential receptors. *Sema5b*, a transmembrane semaphorin, functions as a repulsive cue for *Nrp1*+/*Plxna1*+ corticofugal axons to prevent their entry into the VZ. While the complexity of signaling using multiple semaphorins (each with multiple receptors) defies simple predictions about effects on axon guidance, it seems clear at least that the high rostrocaudal gradients of secreted semaphorins (*Sema3a*, *Sema3c*, and *Sema5a*) may have additive or redundant effects, especially on cortical axons destined to cross the midline (Suárez et al., 2014; Ku and Torii, 2020).

Molecules in the Robo-Slit system are also extremely important in neocortical axon guidance, but were not selectively expressed in IPs or RGPs, only in postmitotic neurons.

Apoptosis-Inducing Dependence Receptors

Previous studies have reported high levels of apoptosis in the SVZ (Blaschke et al., 1996; Thomaidou et al., 1997), recently attributed to asymmetric apoptosis of IP daughter cells (Mihalas and Hevner, 2018). In contrast to RGPs, which were specifically enriched in necroptosis pathways (**Supplementary Figure 3A**), IPs showed no selective enrichment for apoptosis effectors. However, we noted that IPs and new PNs in the IZ express multiple dependence receptors, defined as transmembrane receptors that trigger cell death if not bound by ligand (Negulescu and Mehlen, 2018). Dependence receptors in bIPs included *Unc5d*, *Dcc*, *Ntrk3*, and *Epha4*. As noted above, *Unc5d* and *Dcc* are netrin receptors. *Ntrk3*, which is highly (but not selectively) expressed in bIPs in the SVZ, is the receptor for *Ntf3*, and is part of a neurogenic feedback mechanism from PNs to progenitor cells that promotes a switch to upper layer fates (Parthasarathy et al., 2014). *Epha4* is a significant driver of cortical progenitor cell proliferation (North et al., 2009). These findings suggest that PN numbers are regulated by competitive mechanisms that utilize dependence receptors.

Gene Sets for Other Cell Types

Gene sets for all neural and non-neural cell types in E14.5 mouse neocortex are presented in **Supplementary Tables 3–10**. The criteria for assignment of each cell type, and the specific **Supplementary Table**, are given in the "Materials and Methods" section.

DISCUSSION

In the present study, we produced cell-type-specific gene sets for E14.5 mouse neocortex, and analyzed the transcriptomes of RGPs and IPs in detail. We found that IPs express suites of genes for processes such as EMT, PCP, neuron polarization, axogenesis, excitability, and glutamate signaling. Since IPs are still dividing and do not have axons, our findings raise new questions about how processes such as neuron polarization and axogenesis could begin in progenitor cells. In addition, it is important to recognize the limitations of our approach to assigning IP-selective genes, and question whether the combination of transcriptomes and ISH assigns genes to specific cell types accurately. Also, it is important to keep in mind that mRNA expression does not always correlate with protein abundance and post-translational regulation.

Compared to previous studies, our approach identified relatively large numbers of cell-type-selective genes, especially for IPs (Kawaguchi et al., 2008; Cameron et al., 2012; Telley et al., 2016). This outcome likely reflected the robust quantities of RNA used for our bulk analysis. One pitfall was the interpretation of ISH images to distinguish between bIPs in the SVZ, and new PNs in the IZ: the SVZ and IZ overlap histologically, and some genes are expressed in both cell types. In particular, genes involved in neuron polarization, axon guidance, and excitability, might seem more likely to be neuron-selective, rather than IP-selective. On the other hand, other studies have independently substantiated IP expression of some axon guidance and excitability genes. Axon guidance molecules *Plxna2* and *Unc5d* were reported in IPs by single-cell analysis (Kawaguchi et al., 2008). Also, core PCP molecule *Celsr1* was confirmed as an IP gene (Telley et al., 2016). And most significantly, *SCN3A* was previously colocalized with Tbr2 in IPs of developing human neocortex (Smith et al., 2018). Overall, the coherence of our results and independent confirmations increase confidence in the conclusions.

Epithelial-Mesenchymal Transition (EMT)

Epithelial-mesenchymal transition is a flexible process, usually involving some or most of the same key EMT molecules, such as *Scrt2* (Nieto et al., 2016). In a previous study, EMT of new neocortical neurons was attributed to the activity of *Scrt1* and *Scrt2*, and was proposed to occur by transcriptional repression of *Cdh1* (E-cadherin) (Itoh et al., 2013). In the present study, we found that EMT begins at the step when aIPs delaminate from the ventricular surface to become bIPs (**Figure 6D**). Also, we did not detect *Cdh1* expression in E14.5 mouse neocortex by microarray or ISH, making *Cdh1* an unlikely target of EMT-related transcriptional repression. Furthermore, we identified *Scrt2* selectively in bIPs, with some expression in aIPs (**Figure 5C**), consistent with EMT occurring mainly in IPs, not RGPs. These findings imply that bIPs have some mesenchymal-like properties.

Core PCP in IPs and Minimal PCP in PNs

Our results revealed coordinate abIP-selective expression of *Celsr1*, *Ankrd6*, and *Vangl2*, completing, along with more broadly expressed molecules, a core PCP program in IPs (**Figures 6A,B**).

In contrast, postmitotic PNs apparently expressed only a rudimentary set of core PCP molecules, including *Fzd3* (the *Fzd* most often linked to PCP) along with *Celsr2* or *Celsr3* instead of *Celsr1* (**Figure 6C**). The PCP polarization of IPs is consistent with previous studies showing that, although PCP was originally described in epithelia, mesenchymal-like cells can also have PCP, for example, in convergent extension during gastrulation and neurulation, and in limb bud morphogenesis (Yang and Mlodzik, 2015). Our findings raise the following questions: (1) What is the function of core PCP in IPs? (2) What mechanisms orient PCP in IPs? (3) Can PCP that is established in IPs be transmitted to daughter PNs?

The functions of core PCP in developing neocortex have previously been linked mainly to directional growth of axons (reviewed by Hakanen et al., 2019). The most severe axon phenotypes are seen in mice lacking *Fzd3* (Wang et al., 2002; Hua et al., 2014), or *Celsr2* and *Celsr3* (Qu et al., 2014). Striking similarities between the *Fzd3* and *Celsr2/Celsr3* knockout phenotypes suggest an interaction between these molecules, consistent with our model for "minimal" PCP in PN axons (**Figure 6C**). On this basis, we propose that *Celsr* molecules are plausible candidates for mediating "touch and go" interactions between new PN axons and established tracts (Namba et al., 2014). The original "touch and go" model (Namba et al., 2014) proposed that TAG1 (*Cntn2*) and *Lyn* mediate axon interactions; however, *Cntn2* null mice have no significant axonal defects, and in our assays, *Lyn* was detected only in non-neural cells of E14.5 neocortex.

Of the IP-enriched PCP genes, mice lacking *Celsr1* have microcephaly, due to reduced numbers of IPs and PNs (Boucherie et al., 2018). This phenotype was previously attributed to RGP defects, but as *Celsr1* expression is IP-selective, defects in IPs would seem more likely. For example, it could be that PCP is required in IPs for axon orientation, and axon failure causes apoptosis. Deficiency of *Vangl2* in mice (*Lp*/*Lp*) caused severe cortical thinning (Lake and Sokol, 2009), but cortex-specific *Vangl2* knockout caused a much different phenotype, with partial agenesis of the corpus callosum and hippocampal commissure (Dos-Santos Carvalho et al., 2020). Mice lacking *Ankrd6* have no reported defects of cortical development, although subtle changes of PCP were reported in the inner ear (Jones et al., 2014). Together, the data suggest that in IPs, core PCP is important to maintain IP numbers, and to facilitate growth of axon pathways. These phenotypes may be related because, if core PCP serves to polarize IPs, then it is possible that "a failure to correctly polarize the budding axon leads to abortive axonal outgrowth" (Wang et al., 2002) and cell death.

We propose that PCP polarization of IPs serves to pre-orient and thereby optimize polarization of PNs, improving the efficiency of axon selection and growth. Previously, PCP has been shown to regulate progenitor cell activities in flies, fish, and mammals. In flies and zebrafish, PCP can orient cell divisions, which is interesting because IPs divide with mostly horizontal cleavage planes, while RGPs divide with vertical cleavage planes (Smart, 1973; Englund et al., 2005; Kowalczyk et al., 2009). In mammals, progenitor cells in developing epidermis express PCP components that are internalized and redistributed during mitosis, in a process that is important for patterning of the skin and hair follicles (Devenport et al., 2011).

Wnt-PCP Signaling in IPs

Wnt-PCP is a signaling pathway conserved from flies to mammals, in which Wnt gradients orient tissue polarity by binding to *Fzd* receptors that are part of PCP complexes (Yang and Mlodzik, 2015; Humphries and Mlodzik, 2018). In developing neocortex, high caudomedial gradients of canonical Wnt signaling have been documented (Machon et al., 2007), and *Wnt5a* (a non-canonical Wnt frequently associated with PCP) is, like several other Wnts (**Supplementary Figures 1**, **5**), expressed mainly in the cortical hem, a caudomedial patterning center (**Figure 6A**). Also, *Rspo1* and *Rspo2*, which bind Wnts to enhance signaling potency, are likewise expressed in the hem. Conversely, *Sfrp2*, a secreted molecule that binds Wnts to inhibit their signaling, is highly expressed in the antihem (rostrolateral patterning center) (**Supplementary Figure 1A**) and may sharpen Wnt gradients (Humphries and Mlodzik, 2018). Moreover, "transient downregulation of canonical Wnt/β-catenin signaling during the multipolar stage" may facilitate a switch to non-canonical, Wnt-PCP signaling in bIPs (Boitard et al., 2015).

Overall, the data suggest that an intracortical gradient of *Wnt5a* and other Wnts could potentially orient PCP in IPs by Wnt-PCP signaling. But could this system orient axons? Previous studies have demonstrated that Wnt-PCP signaling can specify axon orientation and steer axon growth in diverse species (Onishi et al., 2014). For example, Wnt-PCP polarizes and guides axons in *Caenorhabditis elegans* (Ackley, 2014) and zebrafish (Sun et al., 2016). Together with the genetic evidence implicating PCP in cortical axon development, these observations suggest that Wnt-PCP signaling in IPs may orient the future growth of PN axons, possibly in conjunction with axon guidance molecules.

IPs and Netrin Signaling

We (**Figure 8F**) and Tarabykin et al. (2001) and Kawaguchi et al. (2008) found that bIPs selectively express *Unc5d* (*Svet1*), a netrin receptor transducing repulsive responses. One proposed function of *Unc5d* is to regulate cell migration through interactions with *Flrt2*; however, *Unc5d* null mice exhibit no histological defects in cortical layer formation (Yamagishi et al., 2011). Moreover, *Ntn4* produced by RGPs in a high rostrocaudal gradient (**Figure 8G**; see also Yin et al., 2000) would be expected to bind *Unc5d* and repel IP processes. Interestingly, *Ntn4* deficient rats show aberrant thalamocortical innervation (Hayano et al., 2014), but it remains unclear how the guidance of PN axons is affected.

Axon Polarity Can Be Regulated Prior to Mitosis

Previous studies have shown that axon polarity can be oriented in neural progenitor cells prior to mitosis and

axon outgrowth. In *C. elegans*, multiple guidance molecules function to regulate polarity coordinates that are inherited by daughter neurons (Killeen and Sybingco, 2008; Adler et al., 2014). In chick neural crest, polarity generated prior to mitosis can be inherited by dorsal root ganglia neurons through a mechanism involving *Septin7*, which labels sites for re-initiation of process growth following mitosis (Boubakar et al., 2017). In neocortex, *Septin7* is essential for callosal and corticospinal axon growth (Ageta-Ishihara et al., 2013). Together, these observations support the possibility that PN axon polarization is initiated in IPs prior to final mitosis.

Excitability in IPs

Surprisingly, several genes linked to neuronal excitability are expressed in IPs (**Figures 6E–G**). This finding intersects with a recent report that *SCN3A*, a voltage-gated sodium channel, is expressed in IPs and is required for cortical morphogenesis (Smith et al., 2018). What role might IP excitability play in cortical development? One possibility is that IPs express excitability genes to enhance interactions with migrating INs (**Figure 7**). A second possibility is that IPs accumulate excitability molecules in order to "prime" PNs for rapid development of excitability after mitosis. Third, excitability may enhance survival and differentiation of IPs and new PNs. For example, it has been shown that depolarization recruits *Dcc* to the plasma membrane and enhances axon growth (Bouchard et al., 2008).

Polarization of IPs as a Mechanism to Enhance PN Axon Development

Recent observations suggest that new PNs become polarized and accelerate axon growth upon contacting a pre-existing PN axon, prompting the "touch and go" model (Namba et al., 2014). In our modification of this model (**Figures 6B,C**), we propose that *Celsr* genes make contact at the axon surface, while *Fzd3* transduces the signal as a form of Wnt-PCP signaling for axon fasciculation. In addition, *Ntn4-Unc5d* might also orient the axon prior to IP mitosis. In sum, we propose that IPs are oriented by Wnt-PCP and netrin signaling, start to become excitable upon reaching the SVZ as bIPs, and produce "pre-polarized" PNs that interact with adjacent existing axons to rapidly integrate into cortical circuitry.

CONCLUSION

We have ascertained gene sets for cell types in E14.5 mouse cortex, and found that IPs selectively express genes involved in core PCP, axogenesis, axon guidance, excitability, and glutamate signaling. On this basis, we propose new neurodevelopmental functions for IPs, in optimizing axon development and integration into cortical pathways. These novel functions add to previously known IP roles in amplifying neurogenesis, shaping regional and laminar identity of PNs, and signaling to INs and RGPs.

MATERIALS AND METHODS

Animals

No new mice were used for this study; only data from previous microarrays and ISH were analyzed. The *Tbr2*-GFP mice for cell sorting and microarrays were described previously (Bedogni et al., 2010; Nelson et al., 2013; Elsen et al., 2018).

Identification of Differentially Expressed Genes (DEGs) in Microarray Experiments

Genes from the microarray experiment (**Supplementary Table 1**) were selected as DEGs if they showed significantly different expression (unadjusted $p < 0.05$) between sorted cell populations (GFP+ and GFP−), and were expressed above a minimal detection threshold (2.279), determined empirically to accord with ISH detection. For genes with multiple probes, the gene was excluded if different probes conflicted by indicating significant enrichment in both GFP+ and GFP− cells. If multiple probes were differentially expressed and in agreement, the probe with highest absolute value of $\log_2$FC was used to represent the gene for integrated analysis (**Supplementary Table 2**).

Selection of Cell-Type-Selective Genes by Microarray and ISH Criteria

For each cell type, specific criteria of expression on microarray and by ISH were utilized. The ISH data were from public open databases, or previous studies. The public databases were Genepaint (Visel et al., 2004), Allen Brain Atlas Developing Mouse Brain[1], and BGEM (Magdaleno et al., 2006). If no ISH data were available, the zonal expression data of Ayoub et al. (2011) were used.

Cajal-Retzius (C-R) Neurons

C-R neuron-selective genes (**Supplementary Table 3**) were significantly enriched in GFP+ cells, and were expressed exclusively or predominantly in the marginal zone on ISH. Established markers of C-R neurons (*Trp73*, *Calb2*, and *Reln*) were confirmed as C-R markers. Additional genes were also screened from candidate C-R neuron markers (Yamazaki et al., 2004), of which two (*Cacna2d2* and *Rcan2*) were included.

Choroid Plexus

Genes (**Supplementary Table 8**) were selected on the basis of enrichment in *Tbr2*-GFP− cells on microarray, and predominant expression in choroid plexus epithelium (not fibrovascular core) on ISH. *Ttr*, a known marker of choroid plexus, met these criteria and was included.

Interneurons (INs) and Subtypes

Interneurons (**Supplementary Table 8**) were enriched in *Tbr2*-GFP− cells on microarray, and showed expression predominantly in the marginal zone and SVZ. Although most IN subtypes do not differentiate until postnatal ages, we also assessed peptide markers of IN subtypes (*Calb1*, *Npy*, *Pvalb*,

[1] http://developingmouse.brain-map.org/

Sst, and *Tac1*). All except *Pvalb* (which was below the detection threshold) were significantly expressed and enriched in Tbr2-GFP− cells. Putative IN genes from previous studies were also screened (Batista-Brito et al., 2008; Marsh et al., 2008).

Intermediate Progenitors

IP genes (**Supplementary Table 3**) were assessed as listed below for each subtype. Putative IP genes from previous studies were also screened (Kawaguchi et al., 2008; Cameron et al., 2012; Telley et al., 2016) along with novel targets.

Apical Intermediate Progenitor Enriched Genes (IP-a)

These genes (**Supplementary Table 3**) were selected on the basis of significant enrichment in Tbr2-GFP+ cells on microarray, and expression predominantly in the VZ on ISH.

Apical and Basal Intermediate Progenitor Enriched Genes (IP-ab)

Genes for this set (**Supplementary Table 3**) were selected on the basis of significant enrichment in Tbr2-GFP+ cells on microarray, and largely balanced expression predominantly in the VZ and SVZ on ISH.

Basal Intermediate Progenitor Enriched Genes (IP-b)

These (**Supplementary Table 3**) were selected for significant enrichment in Tbr2-GFP+ cells on microarray, and expression primarily in the SVZ on ISH.

Microglia

Genes (**Supplementary Table 10**) were selected on the basis of enrichment in Tbr2-GFP− cells, expression in cells scattered in all cortical zones, and literature linking the gene to microglia. Widely used microglial markers *Aif1* (Iba-1 gene), *Cx3cr1*, and *Cd68* met these criteria and were among the included genes.

Meninges (Leptomeninges)

Meningeal genes (**Supplementary Table 9**) were enriched in Tbr2-GFP− cells on microarray, and showed predominantly leptomeningeal expression on ISH. Putative meningeal markers were also screened (DeSisto et al., 2020).

Neuronal Differentiation in the Cortical Plate (N-cp)

These genes (**Supplementary Table 4**), representing general neuronal differentiation in the CP, were selected by significant enrichment in Tbr2-GFP+ cells on microarray, and expression predominantly in the CP on ISH. They were also expressed in neuronal differentiation zones of other forebrain areas besides cortex.

Neuronal Differentiation in the Intermediate Zone (N-iz)

These genes (**Supplementary Table 4**), representing general neuronal differentiation beginning in the IZ, were selected by significant enrichment in Tbr2-GFP+ cells on microarray, and expression predominantly in the IZ, or IZ and CP, on ISH. They were also expressed in neuronal differentiation zones in other forebrain areas besides cortex.

Neuronal Differentiation in the Subventricular Zone (N-svz)

These genes (**Supplementary Table 4**) were highly enriched in Tbr2-GFP+ cells on microarray, and were expressed in the SVZ and IZ, or SVZ, IZ, and CP on ISH. They were also expressed in similar zones in other forebrain areas.

Neuronal Differentiation in the Ventricular Zone (N-vz)

These markers of general neuronal differentiation (**Supplementary Table 4**) were enriched in Tbr2-GFP+ cells on microarray, and showed expression in the VZ, SVZ, IZ, and CP on ISH. They were also expressed in differentiating neurons in other forebrain areas.

Oligodendroglial Progenitor Cells

Oligodendrocytes do not differentiate until postnatal ages. the possibilities that oligogenic lineages might exist in E14.5 cortex, or might differentiate prematurely in mutant mice, prompted us to select markers of oligodendroglia in postnatal cortex as candidate oligodendrocyte identity genes (**Supplementary Table 8**). Two genes (*Olig1* and *Pdgfra*) were significantly enriched in Tbr2-GFP− cells on microarray, and were expressed by scattered cells in progenitor and differentiation compartments (mainly rostrolateral), suggesting that a few immature oligodendrocyte precursors are present in E14.5 neocortex.

Projection Neuron Differentiation in the Cortical Plate (PN-cp)

These genes (**Supplementary Table 3**), representing relatively specific differentiation of projection neurons in the CP, were selected by significant enrichment in Tbr2-GFP+ cells on microarray, and expression predominantly in the CP on ISH. They were not highly expressed in other areas of the telencephalon besides cortex, such as the striatum.

Projection Neuron Differentiation in the Intermediate Zone (PN-iz)

These genes (**Supplementary Table 3**), representing specific differentiation of projection neurons beginning in the IZ, were selected by significant enrichment in Tbr2-GFP+ cells on microarray, and expression predominantly in the IZ, or IZ and CP, on ISH. They were not expressed in other areas of the telencephalon besides cortex, such as the striatum.

Projection Neuron Differentiation in the Subventricular Zone (PN-svz)

These genes (**Supplementary Table 3**), representing specific differentiation of projection neurons beginning in the SVZ, were selected by significant enrichment in Tbr2-GFP+ cells on

microarray, and expression predominantly in the SVZ and IZ, or SVZ, IZ, and CP, on ISH. They were not highly expressed in other areas of the telencephalon besides cortex.

Projection Neuron Differentiation in the Ventricular Zone (PN-vz)

These genes (**Supplementary Table 3**), representing relatively specific differentiation of projection neurons beginning in the VZ, were selected by significant enrichment in Tbr2-GFP+ cells on microarray, with expression in the VZ, SVZ, IZ, and CP on ISH. These genes were not expressed at high levels in the VZ of subcortical areas of the telencephalon.

Subplate

The goal was to identify glutamatergic pioneer neurons in the histological subplate. Accordingly, genes (**Supplementary Table 3**) were selected by significant enrichment in *Tbr2*-GFP+ cells on microarray, and predominant expression in the subplate on ISH. Proposed markers of the embryonic subplate (Hoerder-Suabedissen et al., 2013) were also screened.

Vascular Cells

These genes (**Supplementary Table 9**) were enriched in Tbr2-GFP− cells on microarray, and were expressed by cells lining vascular spaces. They were further annotated by reference to literature for each gene, and divided into endothelial and pericyte groups.

Vascular Endothelial Cells

These genes (**Supplementary Table 9**) were significantly enriched in Tbr2-GFP− cells on microarray, were expressed in elongated cells of the vascular endothelium, and were confirmed as endothelial markers by literature references.

Vascular Pericytes

These genes (**Supplementary Table 9**) were significantly enriched in Tbr2-GFP− cells on microarray, were expressed in scattered cells along blood vessels, and were confirmed as pericyte markers by literature references.

Blood Cells

These genes (**Supplementary Table 10**) were enriched in Tbr2-GFP− cells on microarray, and were expressed by cells within vascular spaces. They were further annotated by reference to literature for each gene, and divided into erythrocyte, lymphocyte, and monocyte groups where possible from available literature.

Neural Stem Cells

Candidate NSC markers were screened from previous studies (Easterday et al., 2003; Andreotti et al., 2019). NSC markers (**Supplementary Table 7**) met criteria for RGPs (enriched in GFP− cells on microarray, and localized predominantly in the VZ).

Callosal Projection Neurons

Genes in CPN Signature clusters (Molyneaux et al., 2015) were screened. Genes (**Supplementary Table 6**) were selected if they demonstrated enrichment in Tbr2-GFP+ cells, regardless of ISH localization.

Corticothalamic Neurons

Genes in CThN Signature clusters (Molyneaux et al., 2015) were selected for evaluation, and were included (**Supplementary Table 6**) if they demonstrated significant enrichment in *Tbr2*-GFP+ cells, and were localized mainly in the cortical plate. Genes with predominant expression in progenitor zones were excluded.

Subcerebral Projection Neurons

Genes in SCPN Signature clusters (Molyneaux et al., 2015) were screened, were included (**Supplementary Table 6**) if they showed enrichment in Tbr2-GFP+ cells, and were expressed mainly in the IZ and CP. Notable excluded genes were *Sox5* and *Bcl11b*, which were classified as Mixed cell-type genes by Molyneaux et al. (2015).

Upper Layers 2–4

Genes previously implicated in genesis of upper layers in publications were selected (**Supplementary Table 6**) if they showed significant expression and enrichment in *Tbr2*-GFP+ cells, and were expressed predominantly in progenitor zones (VZ and SVZ) and/or IZ, possibly extending into the upper CP. Notable exclusions were *Cux1* and *Cux2*, due to non-enrichment in *Tbr2*-GFP + cells (possibly reflecting expression in INs). *Tac2* (**Figure 2D**) was below the detection threshold on microarray, presumably for technical reasons, but was retained as an upper layer marker.

Lower Layers 5–6

Lower layers are comprised of mainly corticothalamic and subcerebral projection neurons. Genes were selected (**Supplementary Table 6**) if they met criteria for either of those cell types.

Hem and Antihem

Genes (**Supplementary Table 5**) were selected if they showed predominant expression in the patterning center by ISH. No microarray criteria were applied.

Rostral and Caudal Identity

These gene sets (**Supplementary Table 5**) have been developed and expanded from previous studies (Bedogni et al., 2010; Elsen et al., 2013). Most recently, we have stratified rostral and caudal gene sets into CP, IZ, SVZ, and VZ subsets, to precisely evaluate rostrocaudal patterning of differentiating neurons and progenitors in different zones. The criteria for each subset are described next.

Rostral Identity in the Cortical Plate (R-cp)

By ISH, these genes (**Supplementary Table 5**) were expressed predominantly in the CP and subplate, at higher levels in rostral than in caudal neocortex. On microarray, genes were enriched in GFP+ cells, or were not enriched in either cell group.

Rostral Identity in the Intermediate Zone (R-iz)

By ISH, these genes (**Supplementary Table 5**) were expressed predominantly in the IZ, or IZ and CP, at higher levels in rostral than in caudal neocortex. On microarray, these genes were enriched in GFP+ cells, or were not enriched in either cell group.

Rostral Identity in the SVZ (R-svz)

By ISH, these genes (**Supplementary Table 5**) were expressed predominantly in the SVZ, at higher levels in rostral than in caudal neocortex. On microarray, these genes were enriched in GFP+ cells, or were not enriched in either cell group.

Rostral Identity in the VZ (R-vz)

By ISH, these genes (**Supplementary Table 5**) were expressed predominantly in the VZ, at higher levels in rostral than in caudal neocortex. No microarray criteria were used, because these genes could theoretically be expressed in RGPs, RGPs and aIPs, or aIPs.

Caudal Identity

Caudal identity in each zone (**Supplementary Table 5**) was assessed using the same criteria as for rostral identity, except that the gene was expressed at higher levels in caudal than in rostral cortex.

Proliferation Genes

Genes (**Supplementary Table 7**) were first evaluated from known proliferation markers across cell types (Whitfield et al., 2006). Additional proliferation markers were selected if they were functionally linked primarily to cell cycle, and matched the expression of validated markers (Whitfield et al., 2006) in mainly RGPs.

Quiescence Genes

These (**Supplementary Table 7**) were aggregated from multiple previous studies.

RBPs

These were designated according to McKee et al. (2005), or more recent studies documenting RNA-binding activity, as cited for individual genes.

TFs

These were designated according to Gray et al. (2004), or more recent studies documenting TF function, as cited for individual genes.

DATA AVAILABILITY STATEMENT

Publicly available datasets were generated for this study. This data can be found here: NCBI GEO accession number GSE22371 (GPL1261) at www.ncbi.nlm.nih.gov/geo/query/acc.cgi?acc=GPL1261.

ETHICS STATEMENT

The animal study was reviewed and approved by The University of Washington Institutional Animal Care and Use Committee (where the original animal experiments were done).

AUTHOR CONTRIBUTIONS

FB and RH: study conception and design, acquisition of data, analysis and interpretation of data, critical revision, and final approval of the version to be published. RH: drafting of manuscript. Both authors contributed to the article and approved the submitted version.

FUNDING

This work was funded by NIH grants R01NS092339, R01NS085081, R21MH087070, and K02NS045018 to RH.

ACKNOWLEDGMENTS

We thank Ray A. M. Daza for technical assistance, Rebecca Hodge for mice, and other members of the Hevner lab for discussions about the genes and signaling pathways mentioned in this manuscript.

SUPPLEMENTARY MATERIAL

The Supplementary Material for this article can be found online at: https://www.frontiersin.org/articles/10.3389/fnmol.2021.686034/full#supplementary-material

REFERENCES

Aaker, J. D., Patineau, A. L., Yang, H. J., Ewart, D. T., Gong, W., Li, T., et al. (2009). Feedback regulation of NEUROG2 activity by MTGR1 is required for progression of neurogenesis. *Mol. Cell. Neurosci.* 42, 267–277. doi: 10.1016/j.mcn.2009.07.011

Aaku-Saraste, E., Hellwig, A., and Huttner, W. B. (1996). Loss of occludin and functional tight junctions, but not ZO-1, during neural tube closure–remodeling of the neuroepithelium prior to neurogenesis. *Dev. Biol.* 180, 664–679. doi: 10.1006/dbio.1996.0336

Ackley, B. D. (2014). Wnt-signaling and planar cell polarity genes regulate axon guidance along the anteroposterior axis in C. elegans. *Dev. Neurobiol.* 74, 781–796. doi: 10.1002/dneu.22146

Adler, C. E., Fetter, R. D., and Bargmann, C. I. (2014). UNC-6/Netrin induces neuronal asymmetry and defines the site of axon formation. *Nat. Neurosci.* 9, 511–518. doi: 10.1038/nn1666

Ageta-Ishihara, N., Miyata, T., Ohshima, C., Watanabe, M., Sato, Y., Hamamura, Y., et al. (2013). Septins promote dendrite and axon development by negatively regulating microtubule stability via HDAC6-mediated deacetylation. *Nat. Commun.* 4:2532. doi: 10.1038/ncomms3532

Alto, L. T., and Terman, J. R. (2017). Semaphorins and their signaling mechanisms. *Methods Mol. Biol.* 1493, 1–25.

Andreotti, J. P., Silva, W. N., Costa, A. C., Picoli, C. C., Bitencourt, F. C. O., Coimbra-Campos, L. M. C., et al. (2019). Neural stem cell niche heterogeneity. *Semin. Cell Dev. Biol.* 95, 42–53.

Atluri, P., Fleck, M. W., Shen, Q., Mah, S. J., Stadfelt, D., Barnes, W., et al. (2001). Functional nicotinic acetylcholine receptor expression in stem and progenitor cells of the early embryonic mouse cerebral cortex. *Dev. Biol.* 240, 143–156. doi: 10.1006/dbio.2001.0453

Ayoub, A. E., Oh, S., Xie, Y., Leng, J., Cotney, J., Dominguez, M. H., et al. (2011). Transcriptional programs in transient embryonic zones of the cerebral cortex defined by high-resolution mRNA sequencing. *Proc. Natl. Acad. Sci. U.S.A.* 108, 14950–14955. doi: 10.1073/pnas.1112213108

Aznar, N., Ear, J., Dunkel, Y., Sun, N., Satterfield, K., He, F., et al. (2018). Convergence of Wnt, growth factor, and heterotrimeric G protein signals on the guanine nucleotide exchange factor Daple. *Sci. Signal.* 11:eaao4220. doi: 10.1126/scisignal.aao4220

Batista-Brito, R., Machold, R., Klein, C., and Fishell, G. (2008). Gene expression in cortical interneuron precursors is prescient of their mature function. *Cereb. Cortex* 18, 2306–2317. doi: 10.1093/cercor/bhm258

Bedogni, F., Hodge, R. D., Elsen, G. E., Nelson, B. R., Daza, R. A., Beyer, R. P., et al. (2010). Tbr1 regulates regional and laminar identity of postmitotic neurons in developing neocortex. *Proc. Natl. Acad. Sci. U.S.A.* 107, 13129–13134. doi: 10.1073/pnas.1002285107

Biswas, S., Cottarelli, A., and Agalliu, D. (2020). Neuronal and glial regulation of CNS angiogenesis and barriergenesis. *Development* 147:dev182279. doi: 10.1242/dev.182279

Blaschke, A. J., Staley, K., and Chun, J. (1996). Widespread programmed cell death in proliferative and postmitotic regions of the fetal cerebral cortex. *Development* 122, 1165–1174. doi: 10.1242/dev.122.4.1165

Boitard, M., Bocchi, R., Egervari, K., Petrenko, V., Viale, B., Gremaud, S., et al. (2015). Wnt signaling regulates multipolar-to-bipolar transition of migrating neurons in the cerebral cortex. *Cell Rep.* 10, 1349–1361. doi: 10.1016/j.celrep.2015.01.061

Bonnefont, J., Tiberi, L., van den Ameele, J., Potier, D., Gaber, Z. B., Lin, X., et al. (2019). Cortical neurogenesis requires Bcl6-mediated transcriptional repression of multiple self-renewal-promoting extrinsic pathways. *Neuron* 103, 1096–1108.e4.

Boubakar, L., Falk, J., Ducuing, H., Thoinet, K., Reynaud, F., Derrington, E., et al. (2017). Molecular memory of morphologies by septins during neuron generation allows early polarity inheritance. *Neuron* 95, 834–851.e5

Bouchard, J.-F., Horn, K. E., Stroh, T., and Kennedy, T. E. (2008). Depolarization recruits DCC to the plasma membrane of embryonic cortical neurons and enhances axon extension in response to netrin-1. *J. Neurochem.* 107, 398–417. doi: 10.1111/j.1471-4159.2008.05609.x

Boucherie, C., Boutin, C., Jossin, Y., Schakman, O., Goffinet, A. M., Ris, L., et al. (2018). Neural progenitor fate decision defects, cortical hypoplasia and behavioral impairment in Celsr1-deficient mice. *Mol. Psychiatry* 23, 723–734. doi: 10.1038/mp.2017.236

Boyer, N. P., and Gupton, S. L. (2018). Revisiting netrin-1: one who guides (axons). *Front. Cell. Neurosci.* 12:221. doi: 10.3389/fncel.2018.00221

Butler, M. T., and Wallingford, J. B. (2017). Planar cell polarity in development and disease. *Nat. Rev. Mol. Cell. Biol.* 18, 375–388.

Cameron, D. A., Middleton, F. A., Chenn, A., and Olson, E. C. (2012). Hierarchical clustering of gene expression patterns in the Eomes + lineage of excitatory neurons during early neocortical development. *BMC Neurosci.* 13:90. doi: 10.1186/1471-2202-13-90

Cappello, S., Attardo, A., Wu, X., Iwasato, T., Itohara, S., Wilsch-Bräuninger, M., et al. (2006). The Rho-GTPase cdc42 regulates neural progenitor fate at the apical surface. *Nat. Neurosci.* 9, 1099–1107. doi: 10.1038/nn1744

Dasgupta, K., and Jeong, J. (2019). Developmental biology of the meninges. *Genesis* 57:e23288. doi: 10.1002/dvg.23288

Dave, R. K., Ellis, T., Toumpas, M. C., Robson, J. P., Julian, E., Adolphe, C., et al. (2011). Sonic hedgehog and notch signaling can cooperate to regulate neurogenic divisions of neocortical progenitors. *PLoS One* 6:e14680. doi: 10.1371/journal.pone.0014680

DeSisto, J., O'Rourke, R., Jones, H. E., Pawlikowski, B., Malek, A. D., Bonney, S., et al. (2020). Single-cell transcriptomic analyses of the developing meninges reveal meningeal fibroblast diversity and function. *Dev. Cell.* 54, 43–59.e4.

Devenport, D., Oristian, D., Heller, E., and Fuchs, E. (2011). Mitotic internalization of planar cell polarity proteins preserves tissue polarity. *Nat. Cell Biol.* 13, 893–902. doi: 10.1038/ncb2284

Dos-Santos Carvalho, S., Moreau, M. M., Hien, Y. E., Garcia, M., Aubailly, N., Henderson, D. J., et al. (2020). Vangl2 acts at the interface between actin and N-cadherin to modulate mammalian neuronal outgrowth. *Elife* 9:e51822. doi: 10.7554/eLife.51822

Dudok, J. J., Murtaza, M., Henrique Alves, C., Rashbass, P., and Wijnholds, J. (2016). Crumbs 2 prevents cortical abnormalities in mouse dorsal telencephalon. *Neurosci. Res.* 108, 12–23. doi: 10.1016/j.neures.2016.01.001

Easterday, M. C., Dougherty, J. D., Jackson, R. L., Ou, J., Nakano, I., Paucar, A. A., et al. (2003). Neural progenitor genes. germinal zone expression and analysis of genetic overlap in stem cell populations. *Dev. Biol.* 264, 309–322.

Elias, L. A., Wang, D. D., and Kriegstein, A. R. (2007). Gap junction adhesion is necessary for radial migration in the neocortex. *Nature* 448, 901–907. doi: 10.1038/nature06063

Elsen, G. E., Bedogni, F., Hodge, R. D., Bammler, T. K., MacDonald, J. W., Lindtner, S., et al. (2018). The epigenetic factor landscape of developing neocortex is regulated by transcription factors Pax6→ Tbr2→ Tbr1. *Front. Neurosci.* 12:571. doi: 10.3389/fnins.2018.00571

Elsen, G. E., Hodge, R. D., Bedogni, F., Daza, R. A., Nelson, B. R., Shiba, N., et al. (2013). The protomap is propagated to cortical plate neurons through an Eomes-dependent intermediate map. *Proc. Natl. Acad. Sci. U.S.A.* 110, 4081–4086. doi: 10.1073/pnas.1209076110

Englund, C., Fink, A., Lau, C., Pham, D., Daza, R. A., Bulfone, A., et al. (2005). Pax6, Tbr2, and Tbr1 are expressed sequentially by radial glia, intermediate progenitor cells, and postmitotic neurons in developing neocortex. *J. Neurosci.* 25, 247–251. doi: 10.1523/jneurosci.2899-04.2005

Fu, J., Huang, D., Yuan, F., Xie, N., Li, Q., Sun, X., et al. (2018). TRAF-interacting protein with forkhead-associated domain (TIFA) transduces DNA damage-induced activation of NF-κB. *J. Biol. Chem.* 293, 7268–7280. doi: 10.1074/jbc.ra117.001684

Furushima, K., Yamamoto, A., Nagano, T., Shibata, M., Miyachi, H., Abe, T., et al. (2007). Mouse homologues of Shisa antagonistic to Wnt and Fgf signalings. *Dev. Biol.* 306, 480–492. doi: 10.1016/j.ydbio.2007.03.028

Gal, J. S., Morozov, Y. M., Ayoub, A. E., Chatterjee, M., Rakic, P., and Haydar, T. F. (2006). Molecular and morphological heterogeneity of neural precursors in the mouse neocortical proliferative zones. *J. Neurosci.* 26, 1045–1056. doi: 10.1523/jneurosci.4499-05.2006

Giacobini, P., Kopin, A. S., Beart, P. M., Mercer, L. D., Fasolo, A., and Wray, S. (2004). Cholecystokinin modulates migration of gonadotropin-releasing hormone-1 neurons. *J. Neurosci.* 24, 4737–4748. doi: 10.1523/jneurosci.0649-04.2004

Goldfarb, M., Schoorlemmer, J., Williams, A., Diwakar, S., Wang, Q., Huang, X., et al. (2007). Fibroblast growth factor homologous factors control neuronal excitability through modulation of voltage-gated sodium channels. *Neuron* 55, 449–463. doi: 10.1016/j.neuron.2007.07.006

Götz, M., Stoykova, A., and Gruss, P. (1998). Pax6 controls radial glia differentiation in the cerebral cortex. *Neuron* 21, 1031–1044. doi: 10.1016/s0896-6273(00)80621-2

Gray, P. A., Fu, H., Luo, P., Zhao, Q., Yu, J., Ferrari, A., et al. (2004). Mouse brain organization revealed through direct genome-scale TF expression analysis. *Science* 306, 2255–2257. doi: 10.1126/science.1104935

Hakanen, J., Ruiz-Reig, N., and Tissir, F. (2019). Linking cell polarity to cortical development and malformations. *Front. Cell. Neurosci.* 13:244. doi: 10.3389/fncel.2019.00244

Haubensak, W., Attardo, A., Denk, W., and Huttner, W. B. (2004). Neurons arise in the basal neuroepithelium of the early mammalian telencephalon: a major site of neurogenesis. *Proc. Natl. Acad. Sci. U.S.A.* 101, 3196–3201. doi: 10.1073/pnas.0308600100

Hayano, Y., Sasaki, K., Ohmura, N., Takemoto, M., Maeda, Y., Yamashita, T., et al. (2014). Netrin-4 regulates thalamocortical axon branching in an

activity-dependent fashion. *Proc. Natl. Acad. Sci. U.S.A.* 111, 15226–15231. doi: 10.1073/pnas.1402095111

Heisig, J., Weber, D., Englberger, E., Winkler, A., Kneitz, S., Sung, W. K., et al. (2012). Target gene analysis by microarrays and chromatin immunoprecipitation identifies HEY proteins as highly redundant bHLH repressors. *PLoS Genet.* 8:e1002728. doi: 10.1371/journal.pgen.1002728

Heng, J. I., Nguyen, L., Castro, D. S., Zimmer, C., Wildner, H., Armant, O., et al. (2008). Neurogenin 2 controls cortical neuron migration through regulation of Rnd2. *Nature* 455, 114–118. doi: 10.1038/nature07198

Hevner, R. F. (2016). Evolution of the mammalian dentate gyrus. *J. Comp. Neurol.* 524, 578–594. doi: 10.1002/cne.23851

Hevner, R. F. (2019). Intermediate progenitors and Tbr2 in cortical development. *J. Anat.* 235, 616–625. doi: 10.1111/joa.12939

Hevner, R. F., Hodge, R. D., Daza, R. A., and Englund, C. (2006). Transcription factors in glutamatergic neurogenesis: conserved programs in neocortex, cerebellum, and adult hippocampus. *Neurosci. Res.* 55, 223–233. doi: 10.1016/j.neures.2006.03.004

Hoerder-Suabedissen, A., Oeschger, F. M., Krishnan, M. L., Belgard, T. G., Wang, W. Z., Lee, S., et al. (2013). Expression profiling of mouse subplate reveals a dynamic gene network and disease association with autism and schizophrenia. *Proc. Natl. Acad. Sci. U.S.A.* 110, 3555–3560. doi: 10.1073/pnas.1218510110

Hossain, M. M., Tsuzuki, T., Sakakibara, K., Imaizumi, F., Ikegaya, A., Inagaki, M., et al. (2019). PlexinA1 is crucial for the midline crossing of callosal axons during corpus callosum development in BALB/cAJ mice. *PLoS One* 14:e0221440. doi: 10.1371/journal.pone.0221440

Hua, Z. L., Jeon, S., Caterina, M. J., and Nathans, J. (2014). Frizzled3 is required for the development of multiple axon tracts in the mouse central nervous system. *Proc. Natl. Acad. Sci. U.S.A.* 111, E3005–E3014.

Humphries, A. C., and Mlodzik, M. (2018). From instruction to output: Wnt/PCP signaling in development and cancer. *Curr. Opin. Cell Biol.* 51, 110–116. doi: 10.1016/j.ceb.2017.12.005

Imai, F., Hirai, S., Akimoto, K., Koyama, H., Miyata, T., Ogawa, M., et al. (2006). Inactivation of aPKClambda results in the loss of adherens junctions in neuroepithelial cells without affecting neurogenesis in mouse neocortex. *Development* 133, 1735–1744. doi: 10.1242/dev.02330

Itoh, Y., Moriyama, Y., Hasegawa, T., Endo, T. A., Toyoda, T., and Gotoh, Y. (2013). Scratch regulates neuronal migration onset via an epithelial-mesenchymal transition-like mechanism. *Nat. Neurosci.* 16, 416–425. doi: 10.1038/nn.3336

Javaherian, A., and Kriegstein, A. (2009). A stem cell niche for intermediate progenitor cells of the embryonic cortex. *Cereb. Cortex* 19(Suppl. 1), i70–i77.

Jones, C., Qian, D., Kim, S. M., Li, S., Ren, D., Knapp, L., et al. (2014). Ankrd6 is a mammalian functional homolog of Drosophila planar cell polarity gene diego and regulates coordinated cellular orientation in the mouse inner ear. *Dev. Biol.* 395, 62–72. doi: 10.1016/j.ydbio.2014.08.029

Jung, M. Y., Lorenz, L., and Richter, J. D. (2006). Translational control by neuroguidin, a eukaryotic initiation factor 4E and CPEB binding protein. *Mol. Cell Biol.* 26, 4277–4287. doi: 10.1128/mcb.02470-05

Kaplan, E. S., Ramos-Laguna, K. A., Mihalas, A. B., Daza, R. A. M., and Hevner, R. F. (2017). Neocortical Sox9+ radial glia generate glutamatergic neurons for all layers, but lack discernible evidence of early laminar fate restriction. *Neural Dev.* 12:14. doi: 10.1186/s13064-017-0091-4

Kawaguchi, A., Ikawa, T., Kasukawa, T., Ueda, H. R., Kurimoto, K., Saitou, M., et al. (2008). Single-cell gene profiling defines differential progenitor subclasses in mammalian neurogenesis. *Development* 135, 3113–3124. doi: 10.1242/dev.022616

Kawase, S., Imai, T., Miyauchi-Hara, C., Yaguchi, K., Nishimoto, Y., Fukami, S., et al. (2011). Identification of a novel intronic enhancer responsible for the transcriptional regulation of musashi1 in neural stem/progenitor cells. *Mol. Brain* 4:14. doi: 10.1186/1756-6606-4-14

Khoury, M. K., Gupta, K., Franco, S. R., and Liu, B. (2020). Necroptosis in the pathophysiology of disease. *Am. J. Pathol.* 190, 272–285. doi: 10.1016/j.ajpath.2019.10.012

Killeen, M. T., and Sybingco, S. S. (2008). Netrin, Slit and Wnt receptors allow axons to choose the axis of migration. *Dev. Biol.* 323, 143–151. doi: 10.1016/j.ydbio.2008.08.027

Kohjima, M., Noda, Y., Takeya, R., Saito, N., Takeuchi, K., and Sumimoto, H. (2002). PAR3beta, a novel homologue of the cell polarity protein PAR3, localizes to tight junctions. *Biochem. Biophys. Res. Commun.* 299, 641–646. doi: 10.1016/s0006-291x(02)02698-0

Kowalczyk, T., Pontious, A., Englund, C., Daza, R. A., Bedogni, F., Hodge, R., et al. (2009). Intermediate neuronal progenitors (basal progenitors) produce pyramidal-projection neurons for all layers of cerebral cortex. *Cereb. Cortex* 19, 2439–2450. doi: 10.1093/cercor/bhn260

Kriegstein, A., Noctor, S., and Martínez-Cerdeño, V. (2006). Patterns of neural stem and progenitor cell division may underlie evolutionary cortical expansion. *Nat. Rev. Neurosci.* 7, 883–890. doi: 10.1038/nrn2008

Ku, R. Y., and Torii, M. (2020). New molecular players in the development of callosal projections. *Cells* 10:29. doi: 10.3390/cells10010029

Lake, B. B., and Sokol, S. Y. (2009). Strabismus regulates asymmetric cell divisions and cell fate determination in the mouse brain. *J. Cell Biol.* 185, 59–66. doi: 10.1083/jcb.200807073

Le Verche, V., Kaindl, A. M., Verney, C., Csaba, Z., Peineau, S., Olivier, P., et al. (2009). The somatostatin 2A receptor is enriched in migrating neurons during rat and human brain development and stimulates migration and axonal outgrowth. *PLoS One* 4:e5509. doi: 10.1371/journal.pone.0005509

Li, Q., Wang, L., Ma, Y., Yue, W., Zhang, D., and Li, J. (2019). P-Rex1 overexpression results in aberrant neuronal polarity and psychosis-related behaviors. *Neurosci. Bull.* 35, 1011–1023. doi: 10.1007/s12264-019-00408-2

Liu, X., Hashimoto-Torii, K., Torii, M., Haydar, T. F., and Rakic, P. (2008). The role of ATP signaling in the migration of intermediate neuronal progenitors to the neocortical subventricular zone. *Proc. Natl. Acad. Sci. U.S.A.* 105, 11802–11807. doi: 10.1073/pnas.0805180105

Machon, O., Backman, M., Machonova, O., Kozmik, Z., Vacik, T., Andersen, L., et al. (2007). A dynamic gradient of Wnt signaling controls initiation of neurogenesis in the mammalian cortex and cellular specification in the hippocampus. *Dev. Biol.* 311, 223–237. doi: 10.1016/j.ydbio.2007.08.038

Magdaleno, S., Jensen, P., Brumwell, C. L., Seal, A., Lehman, K., Asbury, A., et al. (2006). BGEM: an in situ hybridization database of gene expression in the embryonic and adult mouse nervous system. *PLoS Biol.* 4:e86. doi: 10.1371/journal.pbio.0040086

Marsh, E. D., Minarcik, J., Campbell, K., Brooks-Kayal, A. R., and Golden, J. A. (2008). FACS-array gene expression analysis during early development of mouse telencephalic interneurons. *Dev. Neurobiol.* 68, 434–445. doi: 10.1002/dneu.20602

Matsuda, Y., Miura, K., Yamane, J., Shima, H., Fujibuchi, W., Ishida, K., et al. (2016). SERPINI1 regulates epithelial-mesenchymal transition in an orthotopic implantation model of colorectal cancer. *Cancer Sci.* 107, 619–628. doi: 10.1111/cas.12909

McKee, A. E., Minet, E., Stern, C., Riahi, S., Stiles, C. D., and Silver, P. A. (2005). A genome-wide in situ hybridization map of RNA-binding proteins reveals anatomically restricted expression in the developing mouse brain. *BMC Dev. Biol.* 5:14. doi: 10.1186/1471-213X-5-14

Methot, L., Hermann, R., Tang, Y., Lo, R., Al-Jehani, H., Jhas, S., et al. (2013). Interaction and antagonistic roles of NF-κB and Hes6 in the regulation of cortical neurogenesis. *Mol. Cell Biol.* 33, 2797–2808. doi: 10.1128/mcb.01610-12

Mignone, J. L., Kukekov, V., Chiang, A.-S., Steindler, D., and Enikolopov, G. (2004). Neural stem and progenitor cells in nestin-GFP transgenic mice. *J. Comp. Neurol.* 469, 311–324. doi: 10.1002/cne.10964

Mihalas, A. B., and Hevner, R. F. (2018). Clonal analysis reveals laminar fate multipotency and daughter cell apoptosis of mouse cortical intermediate progenitors. *Development* 145:dev164335. doi: 10.1242/dev.164335

Mihalas, A. B., Elsen, G. E., Bedogni, F., Daza, R. A. M., Ramos-Laguna, K. A., Arnold, S. J., et al. (2016). Intermediate progenitor cohorts differentially generate cortical layers and require Tbr2 for timely acquisition of neuronal subtype identity. *Cell Rep.* 16, 92–105. doi: 10.1016/j.celrep.2016.05.072

Mitchell, S., Vargas, J., and Hoffmann, A. (2016). Signaling via the NFkappaB system. *Wiley Interdiscip. Rev. Syst. Biol. Med.* 8, 227–241. doi: 10.1002/wsbm.1331

Miyata, T., Kawaguchi, A., Saito, K., Kawano, M., Muto, T., and Ogawa, M. (2004). Asymmetric production of surface-dividing and non-surface-dividing cortical progenitor cells. *Development* 131, 3133–3145. doi: 10.1242/dev.01173

Molyneaux, B. J., Goff, L. A., Brettler, A. C., Chen, H. H., Hrvatin, S., Rinn, J. L., et al. (2015). DeCoN: genome-wide analysis of in vivo transcriptional dynamics

during pyramidal neuron fate selection in neocortex. *Neuron* 85, 275–288. doi: 10.1016/j.neuron.2014.12.024

Myshrall, T. D., Moore, S. A., Ostendorf, A. P., Satz, J. S., Kowalczyk, T., Nguyen, H., et al. (2012). Dystroglycan on radial glia end feet is required for pial basement membrane integrity and columnar organization of the developing cerebral cortex. *J. Neuropathol. Exp. Neurol.* 71, 1047–1063. doi: 10.1097/nen.0b013e318274a128

Namba, T., Kibe, Y., Funahashi, Y., Nakamuta, S., Takano, T., Ueno, T., et al. (2014). Pioneering axons regulate neuronal polarization in the developing cerebral cortex. *Neuron* 81, 814–829. doi: 10.1016/j.neuron.2013.12.015

Negulescu, A.-M., and Mehlen, P. (2018). Dependence receptors - the dark side awakens. *FEBS J.* 285, 3909–3924. doi: 10.1111/febs.14507

Nelson, B. R., Hodge, R. D., Bedogni, F., and Hevner, R. F. (2013). Dynamic interactions between intermediate neurogenic progenitors and radial glia in embryonic mouse neocortex: potential role in Dll1-Notch signaling. *J. Neurosci.* 33, 9122–9139. doi: 10.1523/jneurosci.0791-13.2013

Nieto, M. A., Huang, R. Y., Jackson, R. A., and Thiery, J. P. (2016). EMT: 2016. *Cell* 166, 21–45.

Noctor, S. C., Martínez-Cerdeño, V., Ivic, L., and Kriegstein, A. R. (2004). Cortical neurons arise in symmetric and asymmetric division zones and migrate through specific phases. *Nat. Neurosci.* 7, 136–144. doi: 10.1038/nn1172

North, H. A., Zhao, X., Kolk, S. M., Clifford, M. A., Ziskind, D. M., and Donoghue, M. J. (2009). Promotion of proliferation in the developing cerebral cortex by EphA4 forward signaling. *Development* 136, 2467–2476. doi: 10.1242/dev.034405

Ochiai, W., Nakatani, S., Takahara, T., Kainuma, M., Masaoka, M., Minobe, S., et al. (2009). Periventricular notch activation and asymmetric Ngn2 and Tbr2 expression in pair-generated neocortical daughter cells. *Mol. Cell. Neurosci.* 40, 225–233. doi: 10.1016/j.mcn.2008.10.007

Onishi, K., Hollis, E., and Zou, Y. (2014). Axon guidance and injury-lessons from Wnts and Wnt signaling. *Curr. Opin. Neurobiol.* 27, 232–240. doi: 10.1016/j.conb.2014.05.005

Pablo, J. L., and Pitt, G. S. (2016). Fibroblast growth factor homologous factors: new roles in neuronal health and disease. *Neuroscientist* 22, 19–25. doi: 10.1177/1073858414562217

Pacary, E., Heng, J., Azzarelli, R., Riou, P., Castro, D., Lebel-Potter, M., et al. (2011). Proneural transcription factors regulate different steps of cortical neuron migration through Rnd-mediated inhibition of RhoA signaling. *Neuron* 69, 1069–1084. doi: 10.1016/j.neuron.2011.02.018

Parthasarathy, S., Srivatsa, S., Nityanandam, A., and Tarabykin, V. (2014). Ntf3 acts downstream of Sip1 in cortical postmitotic neurons to control progenitor cell fate through feedback signaling. *Development* 141, 3324–3330. doi: 10.1242/dev.114173

Petsalaki, E., and Zachos, G. (2020). DNA damage response proteins regulating mitotic cell division: double agents preserving genome stability. *FEBS J.* 287, 1700–1721. doi: 10.1111/febs.15240

Pilaz, L. J., Lennox, A. L., Rouanet, J. P., and Silver, D. L. (2016). Dynamic mRNA transport and local translation in radial glial progenitors of the developing brain. *Curr. Biol.* 26, 3383–3392. doi: 10.1016/j.cub.2016.10.040

Plain, A., Pan, W., O'Neill, D., Ure, M., Beggs, M. R., Farhan, M., et al. (2020). Claudin-12 knockout mice demonstrate reduced proximal tubule calcium permeability. *Int. J. Mol. Sci.* 21:2074. doi: 10.3390/ijms21062074

Qin, S., Yu, L., Gao, Y., Zhou, R., and Zhang, C. (2007). Characterization of the receptors for axon guidance factor netrin-4 and identification of the binding domains. *Mol. Cell. Neurosci.* 34, 243–250. doi: 10.1016/j.mcn.2006.11.002

Qiu, R., Wang, X., Davy, A., Wu, C., Murai, K., Zhang, H., et al. (2008). Regulation of neural progenitor cell state by ephrin-B. *J. Cell Biol.* 181, 973–983. doi: 10.1083/jcb.200708091

Qu, Y., Huang, Y., Feng, J., Alvarez-Bolado, G., Grove, E. A., Yang, Y., et al. (2014). Genetic evidence that Celsr3 and Celsr2, together with Fzd3, regulate forebrain wiring in a Vangl-independent manner. *Proc. Natl. Acad. Sci. U.S.A.* 111, E2996–E3004.

Quinn, J. C., Molinek, M., Martynoga, B. S., Zaki, P. A., Faedo, A., Bulfone, A., et al. (2007). Pax6 controls cerebral cortical cell number by regulating exit from the cell cycle and specifies cortical cell identity by a cell autonomous mechanism. *Dev. Biol.* 302, 50–65. doi: 10.1016/j.ydbio.2006.08.035

Radner, S., Banos, C., Bachay, G., Li, Y. N., Hunter, D. D., Brunken, W. J., et al. (2012). β2 and γ3 laminins are critical cortical basement membrane components: ablation of Lamb2 and Lamc3 genes disrupts cortical lamination and produces dysplasia. *Dev. Neurobiol.* 73, 209–229. doi: 10.1002/dneu.22057

Rash, B. G., Micali, N., Huttner, A. J., Morozov, Y. M., Horvath, T. L., and Rakic, P. (2018). Metabolic regulation and glucose sensitivity of cortical radial glial cells. *Proc. Natl. Acad. Sci. U.S.A.* 115, 10142–10147. doi: 10.1073/pnas.1808066115

Saaber, F., Schütz, D., Miess, E., Abe, P., Desikan, S., Kumar, P. A., et al. (2019). ACKR3 regulation of neuronal migration requires ACKR3 phosphorylation, but not β-arrestin. *Cell Rep.* 26, 1473–1488. doi: 10.1016/j.celrep.2019.01.049

Sánchez-Ponce, D., DeFelipe, J., Garrido, J. J., and Muñoz, A. (2012). Developmental expression of Kv potassium channels at the axon initial segment of cultured hippocampal neurons. *PLoS One* 7:e48557. doi: 10.1371/journal.pone.0048557

Saxena, M., Agnihotri, N., and Sen, J. (2018). Perturbation of canonical and non-canonical BMP signaling affects migration, polarity and dendritogenesis of mouse cortical neurons. *Development* 145:dev147157. doi: 10.1242/dev.147157

Segklia, A., Seuntjens, E., Elkouris, M., Tsalavos, S., Stappers, E., Mitsiadis, T. A., et al. (2012). Bmp7 regulates the survival, proliferation, and neurogenic properties of neural progenitor cells during corticogenesis in the mouse. *PLoS One* 7:e34088. doi: 10.1371/journal.pone.0034088

Serth, K., Schuster-Gossler, K., Kremmer, E., Hansen, B., Marohn-Köhn, B., and Gossler, A. (2015). O-fucosylation of DLL3 is required for its function during somitogenesis. *PLoS One* 10:e0123776. doi: 10.1371/journal.pone.0123776

Sessa, A., Mao, C. A., Colasante, G., Nini, A., Klein, W. H., and Broccoli, V. (2010). Tbr2-positive intermediate (basal) neuronal progenitors safeguard cerebral cortex expansion by controlling amplification of pallial glutamatergic neurons and attraction of subpallial GABAergic interneurons. *Genes Dev.* 24, 1816–1826. doi: 10.1101/gad.575410

Smart, I. H. M. (1973). Proliferative characteristics of the ependymal layer during the early development of the mouse neocortex: a pilot study based on recording the number, location and plane of cleavage of mitotic figures. *J. Anat.* 116, 67–91.

Smith, R. S., Kenny, C. J., Ganesh, V., Jang, A., Borges-Monroy, R., Partlow, J. N., et al. (2018). Sodium channel SCN3A (NaV1.3) regulation of human cerebral cortical folding and oral motor development. *Neuron* 99, 905–913.e7.

Stubbs, D., DeProto, J., Nie, K., Englund, C., Mahmud, I., Hevner, R., et al. (2009). Neurovascular congruence during cerebral cortical development. *Cereb. Cortex* 19(Suppl._1), i32–i41.

Suárez, R., Gobius, I., and Richards, L. J. (2014). Evolution and development of interhemispheric connections in the vertebrate forebrain. *Front. Hum. Neurosci.* 8:497. doi: 10.3389/fnhum.2014.00497

Subramanian, L., Remedios, R., Shetty, A., and Tole, S. (2009). Signals from the edges: the cortical hem and antihem in telencephalic development. *Semin. Cell Dev. Biol.* 20, 712–718. doi: 10.1016/j.semcdb.2009.04.001

Sun, S. D., Purdy, A. M., and Walsh, G. S. (2016). Planar cell polarity genes Frizzled3a, Vangl2, and Scribble are required for spinal commissural axon guidance. *BMC Neurosci.* 17:83. doi: 10.1186/s12868-016-0318-z

Tabata, H., and Nakajima, K. (2003). Multipolar migration: the third mode of radial neuronal migration in the developing cerebral cortex. *J. Neurosci.* 23, 9996–10001. doi: 10.1523/jneurosci.23-31-09996.2003

Taguchi, K., Ishiuchi, T., and Takeichi, M. (2011). Mechanosensitive EPLIN-dependent remodeling of adherens junctions regulates epithelial reshaping. *J. Cell Biol.* 194, 643–656. doi: 10.1083/jcb.201104124

Takeuchi, S., Yamaki, N., Iwasato, T., Negishi, M., and Katoh, H. (2009). Beta2-chimaerin binds to EphA receptors and regulates cell migration. *FEBS Lett.* 583, 1237–1242. doi: 10.1016/j.febslet.2009.03.032

Tarabykin, V., Stoykova, A., Usman, N., and Gruss, P. (2001). Cortical upper layer neurons derive from the subventricular zone as indicated by Svet1 gene expression. *Development* 128, 1983–1993. doi: 10.1242/dev.128.11.1983

Tata, M., and Ruhrberg, C. (2018). Cross-talk between blood vessels and neural progenitors in the developing brain. *Neuronal Signal.* 2:NS20170139. doi: 10.1042/NS20170139

Tavano, S., Taverna, E., Kalebic, N., Haffner, C., Namba, T., Dahl, A., et al. (2018). Insm1 induces neural progenitor delamination in developing neocortex via downregulation of the adherens junction belt-specific protein Plekha7. *Neuron* 97, 1299–1314.e8.

Taverna, E., Götz, M., and Huttner, W. B. (2014). The cell biology of neurogenesis: toward an understanding of the development and evolution of the neocortex.

Annu. Rev. Cell Dev. Biol. 30, 465–502. doi: 10.1146/annurev-cellbio-101011-155801

Telley, L., Agirman, G., Prados, J., Amberg, N., Fièvre, S., Oberst, P., et al. (2019). Temporal patterning of apical progenitors and their daughter neurons in the developing neocortex. *Science* 364:eaav2522. doi: 10.1126/science.aav2522

Telley, L., Govindan, S., Prados, J., Stevant, I., Nef, S., Dermitzakis, E., et al. (2016). Sequential transcriptional waves direct the differentiation of newborn neurons in the mouse neocortex. *Science* 351, 1443–1446. doi: 10.1126/science.aad8361

Thomaidou, D., Mione, M. C., Cavanagh, J. F., and Parnavelas, J. G. (1997). Apoptosis and its relation to the cell cycle in the developing cerebral cortex. *J. Neurosci.* 17, 1075–1085. doi: 10.1523/jneurosci.17-03-01075.1997

Tiberi, L., van den Ameele, J., Dimidschstein, J., Piccirilli, J., Gall, D., Herpoel, A., et al. (2012). BCL6 controls neurogenesis through Sirt1-dependent epigenetic repression of selective Notch targets. *Nat. Neurosci.* 15, 1627–1635. doi: 10.1038/nn.3264

Toda, T., Shinmyo, Y., Dinh Duong, T. A., Masuda, K., and Kawasaki, H. (2016). An essential role of SVZ progenitors in cortical folding in gyrencephalic mammals. *Sci. Rep.* 6:29578. doi: 10.1038/srep29578

Toledano, S., Nir-Zvi, I., Engelman, R., Kessler, O., and Neufeld, G. (2019). Class-3 semaphorins and their receptors: potent multifunctional modulators of tumor progression. *Int. J. Mol. Sci.* 20:556. doi: 10.3390/ijms20030556

Torii, M., Hashimoto-Torii, K., Levitt, P., and Rakic, P. (2009). Integration of neuronal clones in the radial cortical columns by EphA and ephrin-A signalling. *Nature* 461, 524–528. doi: 10.1038/nature08362

Van Quickelberghe, E., De Sutter, D., van Loo, G., Eyckerman, S., and Gevaert, K. (2018). A protein-protein interaction map of the TNF-induced NF-κB signal transduction pathway. *Sci. Data* 5:180289. doi: 10.1038/sdata.2018.289

Veeraval, L., O'Leary, C. J., and Cooper, H. M. (2020). Adherens junctions: guardians of cortical development. *Front. Cell. Dev. Biol.* 8:6. doi: 10.3389/fcell.2020.00006

Visel, A., Thaller, C., and Eichele, G. (2004). GenePaint.org: an atlas of gene expression patterns in the mouse embryo. *Nucleic Acids Res.* 32, D552–D556.

Wang, Y., Thekdi, N., Smallwood, P. M., Macke, J. P., and Nathans, J. (2002). Frizzled-3 is required for the development of major fiber tracts in the rostral CNS. *J. Neurosci.* 22, 8563–8573. doi: 10.1523/jneurosci.22-19-08563.2002

Weber, D., Wiese, C., and Gessler, M. (2014). Hey bHLH transcription factors. *Curr. Top. Dev. Biol.* 110, 285–315. doi: 10.1016/b978-0-12-405943-6.00008-7

Whitfield, M. L., George, L. K., Grant, G. D., and Perou, C. M. (2006). Common markers of proliferation. *Nat. Rev. Cancer* 6, 99–106. doi: 10.1038/nrc1802

Wilsch-Bräuninger, M., Peters, J., Paridaen, J. T., and Huttner, W. B. (2012). Basolateral rather than apical primary cilia on neuroepithelial cells committed to delamination. *Development* 139, 95–105. doi: 10.1242/dev.069294

Wu, C., Qiu, R., Wang, J., Zhang, H., Murai, K., and Lu, Q. (2009). ZHX2 Interacts with Ephrin-B and regulates neural progenitor maintenance in the developing cerebral cortex. *J. Neurosci.* 29, 7404–7412. doi: 10.1523/jneurosci.5841-08.2009

Yabut, O. R., Ng, H. X., Yoon, K., Arela, J. C., Ngo, T., and Pleasure, S. J. (2020). The neocortical progenitor specification program is established through combined modulation of SHH and FGF signaling. *J. Neurosci.* 40, 6872–6887. doi: 10.1523/jneurosci.2888-19.2020

Yamada, R., and Kuba, H. (2016). Structural and functional plasticity at the axon initial segment. *Front. Cell. Neurosci.* 10:250. doi: 10.3389/fncel.2016.00250

Yamagishi, S., Bando, Y., and Sato, K. (2021). Involvement of netrins and their receptors in neuronal migration in the cerebral cortex. *Front. Cell. Dev. Biol.* 8:590009. doi: 10.3389/fcell.2020.590009

Yamagishi, S., Hampel, F., Hata, K., Del Toro, D., Schwark, M., Kvachnina, E., et al. (2011). FLRT2 and FLRT3 act as repulsive guidance cues for Unc5-positive neurons. *EMBO J.* 30, 2920–2933. doi: 10.1038/emboj.2011.189

Yamanishi, E., Yoon, K., Alberi, L., Gaiano, N., and Mizutani, K. (2015). NF-κB signaling regulates the generation of intermediate progenitors in the developing neocortex. *Genes Cells* 20, 706–719. doi: 10.1111/gtc.12267

Yamazaki, H., Sekiguchi, M., Takamatsu, M., Tanabe, Y., and Nakanishi, S. (2004). Distinct ontogenic and regional expressions of newly identified Cajal-Retzius cell-specific genes during neocorticogenesis. *Proc. Natl. Acad. Sci. U.S.A.* 101, 14509–14514. doi: 10.1073/pnas.0406295101

Yan, Q., Liu, W. B., Qin, J., Liu, J., Chen, H. G., Huang, X., et al. (2007). Protein phosphatase-1 modulates the function of Pax-6, a transcription factor controlling brain and eye development. *J. Biol. Chem.* 282, 13954–13965. doi: 10.1074/jbc.m611476200

Yang, Y., and Mlodzik, M. (2015). Wnt-Frizzled/planar cell polarity signaling: cellular orientation by facing the wind (Wnt). *Annu. Rev. Cell. Dev. Biol.* 31, 623–646. doi: 10.1146/annurev-cellbio-100814-125315

Yin, Y., Sanes, J. R., and Miner, J. H. (2000). Identification and expression of mouse netrin-4. *Mech. Dev.* 96, 115–119. doi: 10.1016/s0925-4773(00)00369-5

Yoon, K. J., Koo, B. K., Im, S. K., Jeong, H. W., Ghim, J., Kwon, M. C., et al. (2008). Mind bomb 1-expressing intermediate progenitors generate notch signaling to maintain radial glial cells. *Neuron* 58, 519–531. doi: 10.1016/j.neuron.2008.03.018

Conflict of Interest: The authors declare that the research was conducted in the absence of any commercial or financial relationships that could be construed as a potential conflict of interest.

frontiers in Molecular Neuroscience

BRIEF RESEARCH REPORT
published: 03 August 2021
doi: 10.3389/fnmol.2021.650338

CREB3L2 Modulates Nerve Growth Factor-Induced Cell Differentiation

Luciana Sampieri[1,2†], Macarena Funes Chabán[1,2†], Pablo Di Giusto[1,2], Victoria Rozés-Salvador[3] and Cecilia Alvarez[1,2]*

[1] Centro de Investigaciones en Bioquímica Clínica e Inmunología (CIBICI-CONICET), Córdoba, Argentina, [2] Departamento de Bioquímica Clínica, Facultad de Ciencias Químicas, Universidad Nacional de Córdoba, Córdoba, Argentina, [3] Instituto de Investigación Médica Mercedes y Martín Ferreyra, INIMEC-CONICET-Universidad Nacional de Córdoba, Córdoba, Argentina

Nerve growth factor (NGF) stimulates numerous cellular physiological processes, including growth, differentiation, and survival, and maintains the phenotype of several neuronal types. Most of these NGF-induced processes require adaptation of the secretory pathway since they involve extensive remodeling of membranes and protein redistribution along newly formed neuritic processes. CREB3 transcription factors have emerged as signaling hubs for the regulation of numerous genes involved in the secretory pathway and Golgi homeostasis, integrating stimuli from multiple sources to control secretion, posttranslational modifications and trafficking of proteins. Although recent studies have focused on their role in the central nervous system, little is known about their participation in cell differentiation. Therefore, we aimed to analyze the expression and signaling mechanism of CREB3 transcription factor family members, using the NGF-induced PC12 cell differentiation model. Results show that NGF treatment causes Golgi enlargement and a parallel increased expression of proteins and mRNAs encoding for proteins required for membrane transport (transport factors). Additionally, a significant increase in CREB3L2 protein and mRNA levels is detected in response to NGF. Both MAPK and cAMP signaling pathways are required for this response. Interestingly, CREB3L2 overexpression hampers the NGF-induced neurite outgrowth while its inhibition enhances the morphological changes driven by NGF. In agreement, CREB3L2 overexpressing cells display higher immunofluorescence intensity of Rab5 GTPase (a negative regulator of PC12 differentiation) than control cells. Also, Rab5 immunofluorescence levels decrease in CREB3L2-depleted cells. Taken together, our findings imply that CREB3L2 is an important downstream effector of NGF-activated pathways, leading to neuronal differentiation.

Keywords: neuronal differentiation, Golgi complex, CREB3L2, CREB3, PC12, Rab5

OPEN ACCESS

Edited by:
Estela Maris Muñoz, CONICET Dr. Mario H. Burgos Institute of Histology and Embryology (IHEM), Argentina

Reviewed by:
Kazunori Imaizumi, Hiroshima University, Japan
Angelika Hausser, University of Stuttgart, Germany
Suzanne Scarlata, Worcester Polytechnic Institute, United States

***Correspondence:**
Cecilia Alvarez
ceci.alvarez@unc.edu.ar; calvarez@fcq.unc.edu.ar

† These authors have contributed equally to this work

Specialty section:
This article was submitted to Molecular Signalling and Pathways, a section of the journal Frontiers in Molecular Neuroscience

Received: *07 January 2021*
Accepted: *24 June 2021*
Published: *03 August 2021*

Citation:
Sampieri L, Funes Chabán M, Di Giusto P, Rozés-Salvador V and Alvarez C (2021) CREB3L2 Modulates Nerve Growth Factor-Induced Cell Differentiation. Front. Mol. Neurosci. 14:650338. doi: 10.3389/fnmol.2021.650338

INTRODUCTION

Members of the CREB3 family of transcription factors (CREB3, CREB3L1, CREB3L2, CREB3L3, and CREB3L4) modulate a broad range of cellular processes. They are critical for development, metabolism, secretion, survival, and cell division, among others, and show clear cell-specific expression patterns (Chan et al., 2011). CREB3 members have been implicated in the ER and Golgi stress responses as regulators of the cell secretory capacity and expression of cell specific cargos (Fox and Andrew, 2015; Sampieri et al., 2019). They are ER-localized transmembrane proteins that,

in response to the appropriate stimulus, are transported from the ER to the Golgi, cleaved by S1P and S2P proteases; and the released N-terminal cytosolic domains are translocated to the nucleus to regulate transcription of specific target genes (Fox and Andrew, 2015).

CREB3 transcription factors have been also implicated in cell differentiation processes, such as osteoblast differentiation (Murakami et al., 2009) and during human B-cell transition to antibody secreting cells (Al-Maskari et al., 2018). Furthermore, CREB3, CREB3L1, and CREB3L2 are expressed in different cell types of the central nervous system (CNS), where they perform important functions. For instance, CREB3 and CREB3L1 contribute to neuroendocrine regulation of the hypothalamic/pituitary/adrenal axis by modulating the glucocorticoid receptor activity and the arginine vasopressin gene transcription (Greenwood et al., 2017; Penney et al., 2018). Also, in hippocampal cells, CREB3 regulates gene expression of several components of Golgi outposts and, therefore, their formation (Chung et al., 2017). Furthermore, CREB3L2 levels are positively regulated during oligodendrocyte maturation (He et al., 2016), and, in dorsal root ganglia neurons, the C-terminal domain of CREB3L2 is secreted and promotes axon growth (McCurdy et al., 2019). Interestingly, CREB3 has been identified as an NGF-sensitive transcription factor in a comprehensive time-course microarray study performed in PC12 cells (Dijkmans et al., 2008). Despite the advances in the knowledge of CREB3 factors in the CNS, their participation during neuronal differentiation has been poorly explored. In this work, we aim to study the modifications in organelles and proteins associated with the secretory pathway as well as the response and participation of CREB3 transcription factors in the NGF-induced PC12 cell differentiation model (Greene and Tischler, 1976). In this model, NGF activates the Ras/Raf/MEK/ERK signaling pathway (Cowley et al., 1994), which, in turn, triggers a transcriptional program, leading to upregulation of neuronal genes as well as a neurite outgrowth.

In summary, our data indicate that (a) the differentiation process goes along with an increase in proteins and mRNAs encoding for proteins of membrane trafficking pathways; (b) although CREB3, CREB3L1, and CREB3L2 are co-expressed in PC12 cells, only CREB3L2 increases significantly at an early time point of differentiation (6 h); (c) both ERK and PKA signaling pathways associated with NGF-dependent neuritogenesis regulate CREB3L2 expression; (d) a CREB3L2 knockdown affects Golgi phenotype and neuronal differentiation, acting as a negative regulator of this process; and (e) Rab5 levels change after CREB3L2 inhibition or overexpression. Considering our results and the existing literature, we assume that CREB3L2 is a downstream effector of NGF-activated pathways important to neuronal differentiation of PC12 cells.

MATERIALS AND METHODS

DNA Constructs and Antibodies

A CREB3L2FL construct (cloned in pTRE2hyg plasmid) was a kind gift from Dr. Kazunori Imaizumi (Saito et al., 2014). Rab5WT and Rab5S34N, cloned in pEGFP plasmid (Gomez and Daniotti, 2005), were kindly provided by Dr. Alejandro Vilcaes (Universidad Nacional de Córdoba), and Rab1b WT and Rab1b N121I were available in our laboratory (Slavin et al., 2011). shRNA pGFP-C-shLenti vectors were obtained from OriGene (OriGene Technologies, Inc., Rockville, MD, United States).

The following primary antibodies were used: Rab1b (catalog No. SC-599, Santa Cruz Biotechnology, Santa Cruz, CA, United States), MAP2 (catalog No. M2320, Sigma-Aldrich, St. Louis, MO, United States), KAP1 (catalog No. A300-274A, Bethyl Laboratories, Montgomery, TX, United States), GM130 (catalog No. 610823, BD Biosciences, San José, CA, United States), Calreticulin (catalog No. PA3-900, Thermo Fisher Scientific, Waltham, MA, United States), SRP54 (catalog No. 610941, BD Biosciences, San José, CA, United States), GalNAc-T2 (catalog No. HPA011222, Sigma-Aldrich, St. Louis, MO, United States), rabbit polyclonal antibodies to StarD7 [a gift from Dr. Susana Genti-Raimondi, CIBICI-CONICET, National University of Córdoba, Argentina (Angeletti et al., 2008)], Rab5 (catalog No. 46692, Santa Cruz Biotechnology, Santa Cruz, CA, United States), β-actin (catalog No. A2228, Sigma-Aldrich, St. Louis, MO, United States), α-tubulin (catalog No. T9026, Sigma-Aldrich, St. Louis, MO, United States), and CREB3L2 (catalog No. PA5-40951, Thermo Fisher Scientific, Waltham, MA, United States and catalog No. HPA015534, Atlas Antibodies, Stockholm, Sweden). CREB3L2 antibodies were raised against N-terminal residues.

Cell Culture and Treatments

The rat pheochromocytoma cell line PC12 [ATCC® CRL-1721™ (Greene and Tischler, 1976)] was grown in a normal growing medium, containing Dulbecco's modified Eagle's medium (DMEM), 5% fetal bovine serum, 5% of horse serum, and penicillin-streptomycin (Thermo Fisher Scientific, Waltham, MA, United States). For differentiation, cells were grown in the DMEM medium, containing 1.5% horse serum, 1.5% fetal bovine serum, penicillin-streptomycin, and 100 ng/ml nerve growth factor (NGF, catalog No. B.5017, ENVIGO, Indianapolis, IN, United States) for different periods of time. Alternatively, cells were treated with 15 μM forskolin (FSK, catalog No. ab120058, Abcam, Cambridge, United Kingdom). Differentiation conditions include growth onto poly-L-lysine (catalog No. P8920, Sigma-Aldrich, St. Louis, MO, United States), coated plates and coverslips. A MAPK signaling cascade was blocked with 10 μM U0126 (catalog No. 9903, Cell Signaling Technology, Danvers, MA, United States) for 2 h before NGF addition. For transfection, PC12 cells were transiently transfected with Lipofectamine 2000 (Thermo Fisher Scientific, Waltham, MA, United States), following the instructions of the manufacturer. Complexes containing different DNA constructs plus Lipofectamine 2000 were resuspended in Opti-MEM (Thermo Fisher Scientific, Waltham, MA, United States) and mixed with 10% of fetal bovine serum; after 4 h, the medium was replaced for a normal growing medium. After 24 h of transfection, cells were NGF differentiated. For shRNA experiments, transfections were performed for 48 h before NGF differentiation.

Immunofluorescence Analysis

Cells grown on poly-L-lysine (catalog No. P8920, Sigma-Aldrich, St. Louis, MO, United States) were fixed, blocked, and immunolabeled as described previously (Gil et al., 2004). Primary antibodies were diluted as follows: anti-GM130 at 1:200; anti-CREB3L2 at 1:200; anti-Rab5 at 1:75. Secondary antibodies were diluted at 1:1000. Nuclei were stained, using Hoechst 33258 (catalog No. H-3569, Molecular Probes, Eugene, OR, United States) at 1:1000.

Image Acquisition and Quantification

Image acquisition was performed for 2D images, using the Leica DMi8 epifluorescence microscope (lasers: 488; resolution X = 1024 and Y = 1024; objectives: 40× and 63×) and for 3D images, using either a spectral (Olympus Fluoview 1200) or LSM 800 (Zeiss) (lasers: 488, 533, and 633; resolution X = 1024; Y = 1024 and Z = 0.3–0.5 μm; objectives: 63×: plan-apochromat 63×/1.40 Oil DICM27 and 20×: objective 20× LD apochromat 20×/0.40, both inverted confocal microscopes). Image quantification was performed, using Fiji-ImageJ software (Schindelin et al., 2012), pixel by pixel, and data were used to calculate the average of Golgi volume. To quantify GM130, GalNAc-T2, CREB3L2, and Rab5 levels, total fluorescence intensity was calculated throughout the z-axis, using the "z-project/sum slices" plug-in of Fiji-ImageJ. Then, the soma was measured as previously described (Siri et al., 2020). The results were normalized with the control condition of each experiment. Fire-LUTs are shown to clearly visualize the fluorescence levels of each epitope.

Morphometric Analysis

Images of differentiated PC12 cells were processed, using a Fiji-ImageJ software macro. After image processing, total neurite length and the longest neurite of each cell were measured. Sholl analysis was performed to quantify the number of intersections in the neurite outgrowth of the cells [Sholl analysis v3.4.10 plug-in for ImageJ (Sholl, 1953)]. For measurements, a straight line was traced from the center of the cell body to the end of the neurites; intersections were analyzed, defining five shells, starting at 30 μm of the cell soma to the last shell at 150 μm.

Protein Analysis

Cell processing and Western blot assays were performed as described previously (Garcia et al., 2017). Detection and quantification of the near-infrared fluorescence on the membranes were performed, using the Odyssey CLx Imaging System (LI-COR Biosciences, Lincoln, NE, United States) through the Image Studio Software. Images were acquired on the auto intensity at high resolution. The following primary antibody dilutions were used: anti-MAP2 at 1:1000, anti-KAP1 at 1:1000, anti-SRP54 at 1:500, anti-GalNAc-T2 at 1:500, anti-StarD7 at 1:500, anti-Rab1b at 1:100; anti-GM130 at 1:400; anti-CREB3L2 at 1:500; anti-calreticulin at 1:2000; anti-α-tubulin at 1:2000 and anti-β-actin at 1:1000.

For Western blot quantification, the intensity of each band normalized to β-actin or to KAP1 (loading controls) was measured, and the fold change was calculated as the ratio of the normalized values in the differentiated (D2 to D6) versus control cells (D0). Unless indicated otherwise, three independent experiments were performed, and each sample was run in duplicate. The normalized value of one control was set as one, the other values of the controls were calculated relative to these values, and average values are shown in the bar graphs. Therefore, the values in the different control conditions are close to one, and their error bars represent ± SEM.

RNA Isolation and RT-qPCR

Total RNA was purified from PC12 cells by using TRI Reagent (catalog No. T9424, Sigma-Aldrich, St. Louis, MO, United States) according to the protocol of the manufacturer. Synthesis of cDNA was performed from 1 μg of total RNA in a total volume of 20 μl, using random primers (catalog No. C118A, Promega, Madison, WI, United States) and 50 U M-MLV reverse transcriptase (catalog No. M1705, Promega, Madison, WI, United States). Primers were designed with the assistance of the NetPrimer software (PREMIER Biosoft International, Palo Alto, CA, United States). Primers were from Sigma-Aldrich (Houston, TX, United States) or Macrogen (Seoul, South Korea), and their concentrations and sequences (5′–3′) are: Sec31a (150 nM), ATTCGGAGGGAAGTTGGTGAC (F), TCTGAGC GGCTGAGGAAGTC (R); GM130 (150 nM), CGGGA TGTCGGAAGAAAC (F), GTGTGGTCTGTGGGCACATT (R), Rab1b (250 nM) AACGGTTCAGGACCATCACTTC (F) TCTCACTGGCGTAGCGATCTATT (R); KDELR3 (100 nM), GGCATCTCTGGGAAGAGTCAG (F), ATAGGCACACAGGA GGAAAACC (R); CREB3L1 (300 nM), GTGAAAGA AGACCCCGTCGC (F), CTCCACAGGCAGTAGAGCACC (R); CREB3L2 (300 nm), CGGGCTCAGTCACCATTTACC (F), CCATTTCTCACTCTCCACCTCC (R); CREB3 (200 nM), GGAAAGTGGAGATTTGTGGGC (F), GCACGGAGTTCTCG GAAG (R); Rab7a (100 nM forward primer and 75 nM reverse primer), GGAGGTGATGGTGGATGACAG (F), GG GTTTTGAATGTGTTGGGG (R), Rab5a (250 nM forward primer and 150 nM reverse primer), TTCTTCTAGGAGA GTCTGCTGTTGG (F), CATCAAGACACACAGTTTGGGTT (R), MAP2 (300 nM), GACGGACCACCAGGTCAGAA (F), ACGTGAAGAGTAGCTTGGAGGAGT (R), TBP (300 nM), GCACAGGAGCCAAGAGTGAA (F), CACATCACAGCTCCC CACC (R). qPCR analysis was performed, using an ABI Prism 7500 detection system (Applied Biosystems, Foster City, CA, United States) and SYBR Green chemistry. Reactions were carried out in triplicate, using 1X SYBR Green PCR Master Mix (catalog No. 4309155, Thermo Fisher Scientific, Waltham, MA, United States) in a total volume of 15 μl. Specificity was verified by melting curve analysis and agarose gel electrophoresis. The fold change in gene expression was calculated according to the $2^{-\Delta\Delta Ct}$ method, using TBP as the internal control (Livak and Schmittgen, 2001).

shRNA

CREB3L2 expression was inhibited by using a commercial pEGFP-C-shLenti vector (OriGene Technologies, Inc., Rockville, MD, United States). This vector was designed to

specifically inhibit CREB3L2 expression (shCREB3L2 I: 5′-AAC CTCAAGGTTGTAGAACTGGAGAGGA-3′; shCREB3L2 II: 5′-AGCACCTCTCATCCAGGCTGAACACAGCT-3′) and encodes GFP protein as a marker of transfection. Lentiviral particles were obtained by co-transfecting the HEK293T cell line with pEGFP-C-shLenti, psPAX2, and pMD2.G plasmids. PC12 cells were then transduced, and, after 3 days of puromycin selection, quantification of neurite length and number, following NGF-differentiation, was carried out. Lentiviral particles expressing scrambled shRNA (shScramble: 5′-GCACTACCAGAGCTAACTCAGATAGTACT-3′) were used as control.

Statistical Analysis

Results are presented as the mean ± SEM of at least three independent experiments performed in duplicates or triplicates. Comparisons between two groups were made by using an unpaired Student's *T*-test. Multiple group analysis was conducted by one-way ANOVA. As a post-test, the Bonferroni multiple-comparison test was used. Statistical analysis was performed by using GraphPad Prism 5.0 software (GraphPad Software, San Diego, CA, United States). Differences were considered significant at $p < 0.05$.

RESULTS

NGF-Induced Cell Differentiation Promotes Changes in the Secretory Pathway

To investigate changes in the secretory pathway during NGF-induced PC12 cell differentiation, cells were treated with NGF during 6 days as previously reported (Galbiati et al., 1998; Vanhoutte et al., 2001). The differentiated phenotype was determined by analyzing the neurite outgrowth, morphological transformations, as well as the changes in the expression levels of the neuron-specific protein MAP2 (∼8-fold relative to the control, **Supplementary Figures 1A,B**). Next, we evaluated the effect of NGF induction on Golgi morphology by the immunostaining of *cis*-Golgi marker GM130, using confocal microscopy and acquiring Z-stack images. As shown in **Figures 1A,C**, the fluorescence intensity of GM130 signal increases in response to NGF, being evidently visible between days 4 and 6. Thus, to further analyze changes induced by NGF differentiation, Golgi volume was assessed by 3D reconstruction of Z-stacks, and a set of transport proteins was analyzed. In agreement with the increase of fluorescence intensity, Golgi volume increases ∼1.5- to 2-fold after 4 and 6 days of NGF treatment (**Figure 1B**). Moreover, we analyzed the fluorescence intensity of other proteins associated with membrane trafficking, such as the GTPase Rab1b, essential for ER to Golgi transport, localized at the ER-Golgi-Intermediate compartment (Garcia et al., 2011; Slavin et al., 2011) and the *medial*- and *trans*-Golgi marker GalNAc-T2 (Rottger et al., 1998). As shown in **Figures 1C–E**, the fluorescence intensity of both protein markers correlates with the increase of the GM130 signal. In agreement with the confocal examination, Western blot analysis (**Figures 1F,G**) indicated that GM130, GalNAc-T2, and Rab1b levels increased more than 2 times relative to untreated cells (D0). Additionally, the expression levels of the ER markers calreticulin and SRP54, and of the phosphatidylcholine transfer protein StarD7 [one of the main lipid transfer proteins associated with membrane expansion in NGF-treatment of PC12 cells (Durand et al., 2004; Yang et al., 2017)] increase up to 1.5 times relative to control. To verify that increased protein levels are associated with transcriptional changes, quantitative real-time reverse transcription-polymerase chain reaction assays (qRT-PCR) were performed at different times after NGF treatment (**Figure 1H**), and the relative mRNA levels of undifferentiated (0 h) and NGF-differentiated PC12 cells (6, 24, and 96 h) were evaluated. We analyzed MAP2 transcript levels as a positive control of NGF treatment (Fischer et al., 1991), as well as mRNAs encoding for Rab1b, GM130, and two endocytic pathway proteins, Rab5 and Rab7. NGF induced a progressive increase in MAP2 and Rab1b mRNA levels during the analyzed time, reaching 3-fold and ∼2.5-fold increase relative to the control for 96 h. GM130 displays a slight increase after 6 h of NFG treatment and remains stable throughout the analyzed times. Rab5a and Rab7 also increase significantly during differentiation with NGF (**Figure 1H**). Taken together, these results suggest that the homeostatic cellular response to NGF involves transcriptional regulation of multiple genes-encoding proteins of different compartments of the membrane trafficking pathway.

NGF-Induced PC12 Differentiation Strongly Increases CREB3L2 Expression

CREB3 factors have been characterized as regulators of genes-encoding components of the secretory pathway (Fox et al., 2010; Sampieri et al., 2019). In addition, CREB3, CREB3L1, and CREB3L2 are expressed in different cell types of the CNS (MacGillavry et al., 2011; Okuda et al., 2014; Ying et al., 2014; Sumida et al., 2018). We hypothesize that levels of the CREB3 family members could be modified during PC12 cell differentiation, and, therefore, mRNA levels of all were quantified by qRT-PCR assays (**Figure 2A**). The results indicated that CREB3 levels slightly increased ∼1.5- and 1.8-fold after 24 and 96 h of NGF treatment, respectively. On the other hand, CREB3L1 levels remained constant during the evaluated times, and CREB3L2 levels increased rapidly and noticeably at 6 h after NGF treatment (∼6-fold), followed by a gradual decline after 24 and 96 h of NGF treatment. Interestingly, the response of CREB3L2 to NGF is fast, at 6 h, whereas CREB3 does not show a significant increase at the same time. Furthermore, at later times (24 and 96 h), CREB3 mRNA levels slightly increase, while those of CREB3L2 decrease, suggesting that CREB3L2 leads an early homeostatic cellular response. In contrast to CREB3, CREB3L1 and CREB3L2, the transcript levels of CREB3L3 and CREB3L4 were extremely low, making it difficult to quantify their changes during differentiation (data not shown). Additionally, we analyzed the CREB3L2 protein expression changes by immunofluorescence and Western blot assays. As shown in

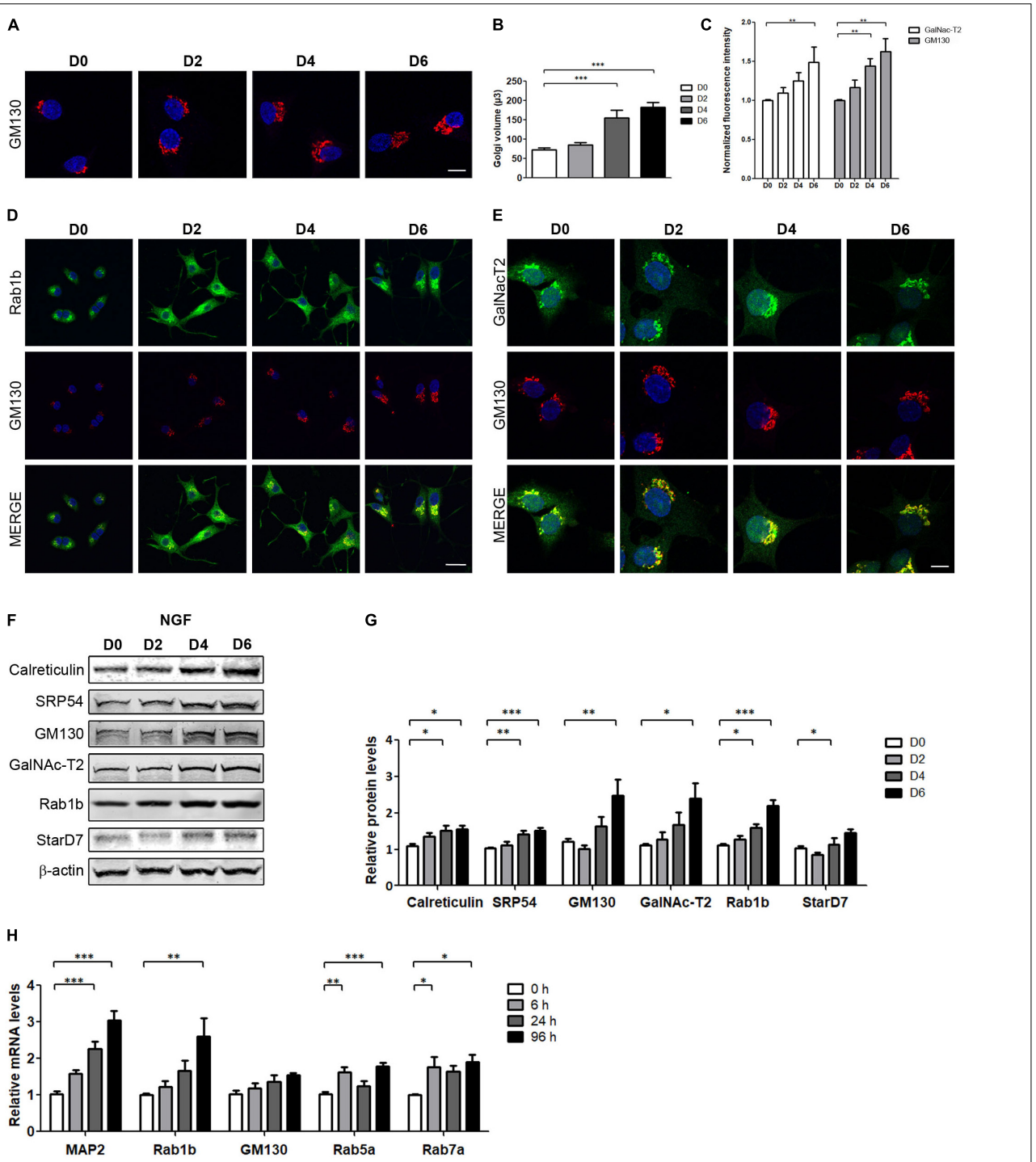

FIGURE 1 | NGF-induced PC12 cell differentiation increases Golgi volume and transport proteins. **(A,D,E)** Immunofluorescence performed in PC12 cells differentiated with NGF (100 ng/ml) during the indicated days and stained with the specified markers. Nuclei were stained with Hoechst (blue). **(A,C)** The Golgi complex was labeled with GM130 (red, Bar: 8 μm) and the normalized fluorescence intensity was plotted (a total of 60 cells were analyzed). **(B)** Golgi volume was quantified on the indicated days. Fiji-ImageJ software was used to perform three-dimensional reconstruction and quantification of the images. **(D,E)** Rab1b, GM130, and GalNAc-T2 staining. Scale bars: 20 and 8 μm, respectively. **(F)** Representative Western blot assays performed with cell lysates obtained from PC12 cells differentiated with NGF during the indicated days (D2, D4, and D6). **(G)** Densitometric quantification of proteins shown in **(F)** normalized to β-actin. Values represent fold change relative to protein levels in untreated cells (D0). **(H)** Quantification of the indicated genes by qRT-PCR performed with total RNA during the indicated times. Results were normalized to the levels of TBP and expressed according to the $2^{-\Delta\Delta Ct}$ method relative to the expression level of each gene in untreated cells (0 h, set as 1). Bars represent the mean ± SEM of three independent experiments carried out in triplicates. **(B,C,G,H)** Statistical data analysis were performed using ANOVA test, followed by Bonferroni multiple comparison post-test, considering statistically significant a value of $p < 0.05$ (*$p < 0.05$; **$p < 0.001$; ***$p < 0.0001$).

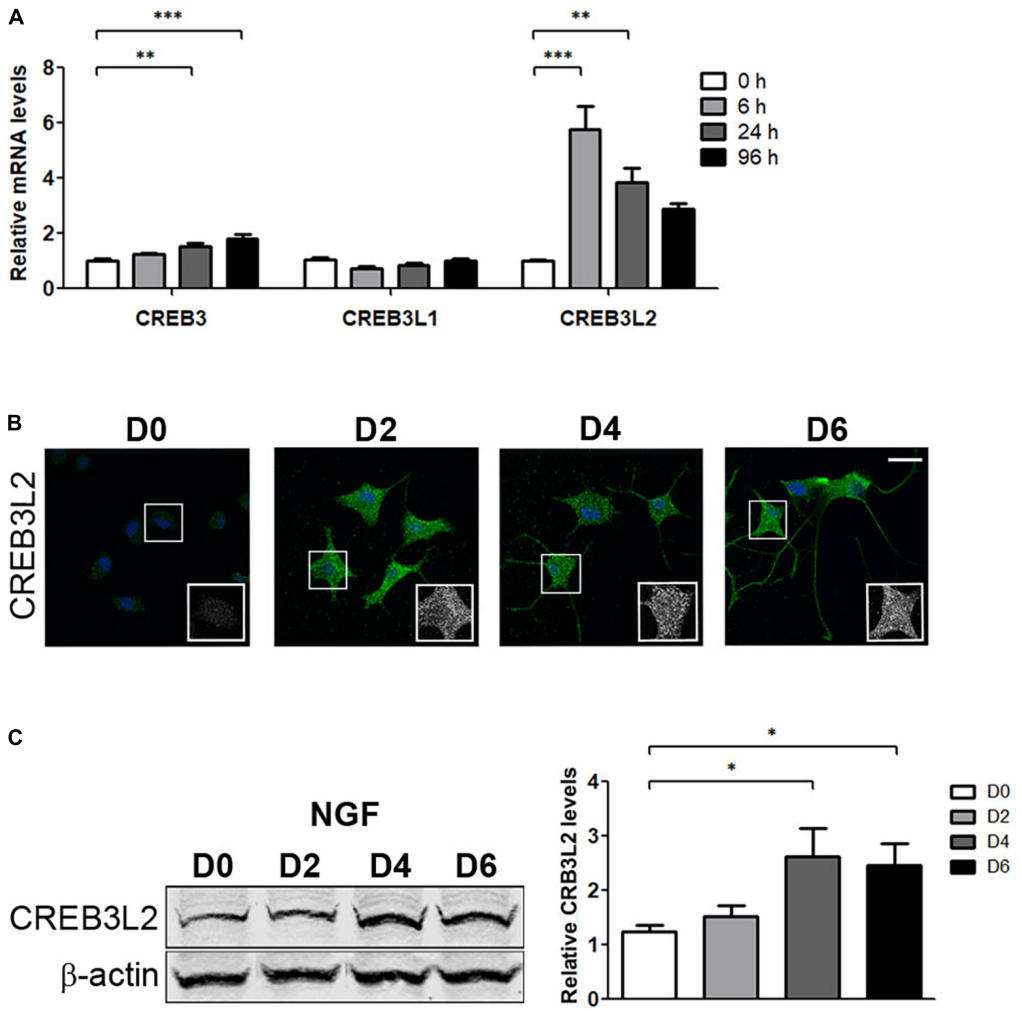

FIGURE 2 | Effect of NGF on CREB3 transcription factor expression. PC12 cells differentiated with NGF at the indicated times. **(A)** Quantification of CREB3, CREB3L1, and CREB3L2 mRNA levels by qRT-PCR performed with total RNA. The results were normalized to the levels of TBP and expressed according to the $2^{-\Delta\Delta Ct}$ method relative to the expression level of each gene in untreated cells (0 h, set as 1). **(B)** Representative immunofluorescence staining of CREB3L2 in PC12 cells at the indicated times of NGF incubation. Nuclei were stained with Hoechst (blue). Insets show the ROI (white square) magnification from each image. Scale bar: 20 μm. **(C)** Left panel: Representative Western blot assays (detecting the CREB3L2 N-terminal domain or cleaved fragment) performed with cell extracts obtained from PC12 cells treated with NGF during the indicated times. Right panel: Densitometric quantification of CREB3L2 protein shown in left normalized to β-actin. Values represent fold change relative to protein levels in untreated cells (D0). Bars represent the mean ± SEM of three independent experiments carried out in triplicates. Statistical data analysis was performed using ANOVA test, followed by Bonferroni multiple comparison post-test, considering statistically significant a value of $p < 0.05$ (*$p < 0.05$; **$p < 0.001$; ***$p < 0.0001$).

Figures 2B,C, the immunofluorescence signal of CREB3L2 increased during NGF differentiation: full length CREB3L2 is localized at the ER as indicated by its reticular pattern, and the N-terminal domain (or cleaved fraction) colocalizes with Hoechst in the nucleus (Murakami et al., 2009; Saito et al., 2014). Taken together, these findings indicate that NGF induces an important upregulation of CREB3L2 expression.

CREB3L2 Expression Requires MAPK and cAMP Signaling Pathways

It has been shown that PC12 differentiation induced by NGF is mediated by its interaction with the tyrosine kinase receptor type 1, TrkA (Kaplan et al., 1991; Klein et al., 1991). Upon interaction with NGF, TrkA is phosphorylated and triggers the Ras/Raf/MEK/ERK signaling pathway to stimulate CREB phosphorylation. Furthermore, in PC12 cells, the second messenger cyclic AMP (cAMP) also mediates the action of NGF in a calcium-dependent manner (Stessin et al., 2006) *via* the PKA-CREB-dependent signaling pathway (**Figure 3A**).

To determine whether the Ras/Raf/MEK/Erk pathway was associated with the effect of NGF on CREB3L2 expression, CREB3L2 mRNA levels were evaluated after treatment with U0126 (**Figure 3A**), a pharmacological inhibitor of MAP kinases MEK1 and MEK2 (Duncia et al., 1998). As shown in **Figure 3B**, the inhibitor was effective and blocked differentiation even after

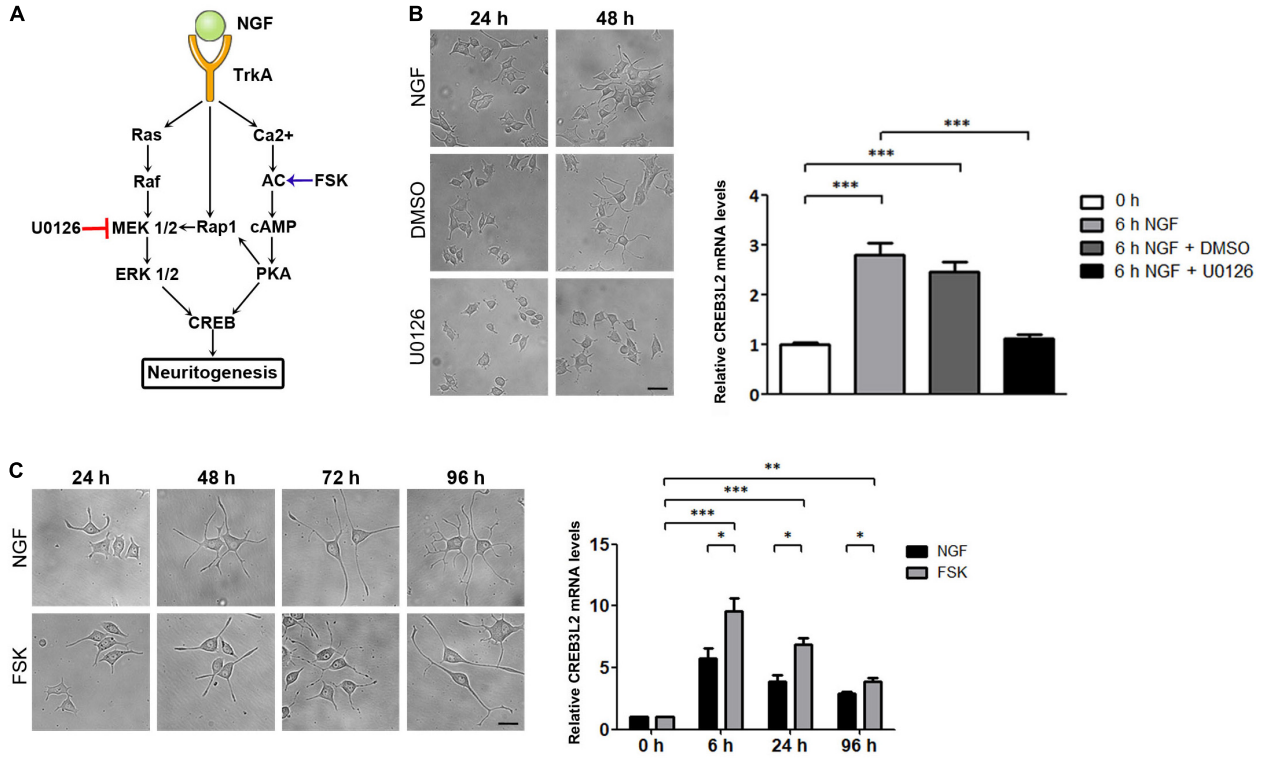

FIGURE 3 | Effect of U0126 and Forskolin on neuritogenesis and CREB3L2 expression. PC12 cells differentiated with NGF during the indicated times in the presence of vehicle (DMSO), U0126 (10 μM), or Forskolin (FSK, 15 μM). DMSO and U0126 were added 2 h before NGF induction. **(A)** Schematic representation of NGF-activated signaling pathways in PC12 cells with the site of action of U0126 and FSK. **(B)** Left panel: Representative images of cells incubated with NGF, or with NGF and either DMSO or the MAPK/ERK 1/2 inhibitor, U0126, during the indicated times. Scale bar: 10 μm. Right panel: qRT-PCR of CREB3L2 transcript levels performed with total RNA extracted from cells incubated with NGF at the indicated times. **(C)** Left panel: Representative images of cells incubated with NGF or Forskolin during the indicated times. Scale bar: 10 μm. Right panel: qRT-PCR of CREB3L2 transcript levels performed with total RNA extracted from cells incubated with Forskolin; mRNA values **(B,C)** were normalized to the levels of TBP and expressed according to the $2^{-\Delta\Delta Ct}$ method relative to the expression level of CREB3L2 in untreated cells (0 h, set as 1). Bars represent the mean ± SEM of three independent experiments carried out in triplicates. Statistical data analysis was performed using ANOVA test followed by Bonferroni multiple comparison post-test, considering statistically significant a value of $p < 0.05$ (**$p < 0.001$, ***$p < 0.0001$).

48 h of NGF incubation. Also, quantification of CREB3L2 mRNA performed after 6 h of NGF addition indicates that U0126 inhibited the increase of mRNA CREB3L2 levels induced by NGF.

To analyze the influence of the cAMP pathway in the NGF-induced increase of CREB3L2, the effect of the adenylate cyclase activator forskolin (FSK, **Figure 3A**) was tested (Seamon et al., 1981). PC12 cells were incubated with FSK (15 μM), and as performed with U0126, its effect on the neurite outgrowth was first confirmed microscopically (**Figure 3C**). As previously shown (Richter-Landsberg and Jastorff, 1986), the increase in the number and length of neurites in response to FSK was similar or slightly lower to that induced by NGF. FSK also increased CREB3L2 mRNA levels with the same kinetics as NGF, reaching a maximum value at 6 h after treatment (**Figure 3C**). Remarkably, CREB3L2 transcript levels increased up to 10 times at 6 h of FSK treatment relative to the untreated cells (0 h), whereas the maximum CREB3L2 mRNA increase after 6 h of NGF addition was 6 times with respect to untreated cells.

Taken together, the data indicate that both MAPK and cAMP signaling pathways are associated with neurite formation as well as with the upregulation of CREB3L2 expression and highlight a key role of CREB3L2 as a common effector of ERK and cAMP pathways.

CREB3L2 shRNA-Mediated Knockdown and CREB3L2 Overexpression Modify the NGF-Induced Neuronal Differentiation Phenotype of PC12 Cells and Rab5 Protein Levels

To analyze the role of CREB3L2 during PC12 cells differentiation, loss- and gain-of-function experiments were performed. Loss of function was achieved by using a specific shRNA sequence to selectively decrease CREB3L2 expression (see section "Materials and Methods"). PC12 cells were transduced with lentiviral particles-encoding shRNA against CREB3L2 (shCREB3L2 I) or a non-specific shRNA used as control (shScramble), and after puromycin selection, cells were differentiated with NGF (**Figure 4A**). CREB3L2 levels in cells expressing shCREB3L2 were ∼50% less than in control cells (**Figure 4B**). Total neurite length and extension of the longest neurite were quantified at days 1,

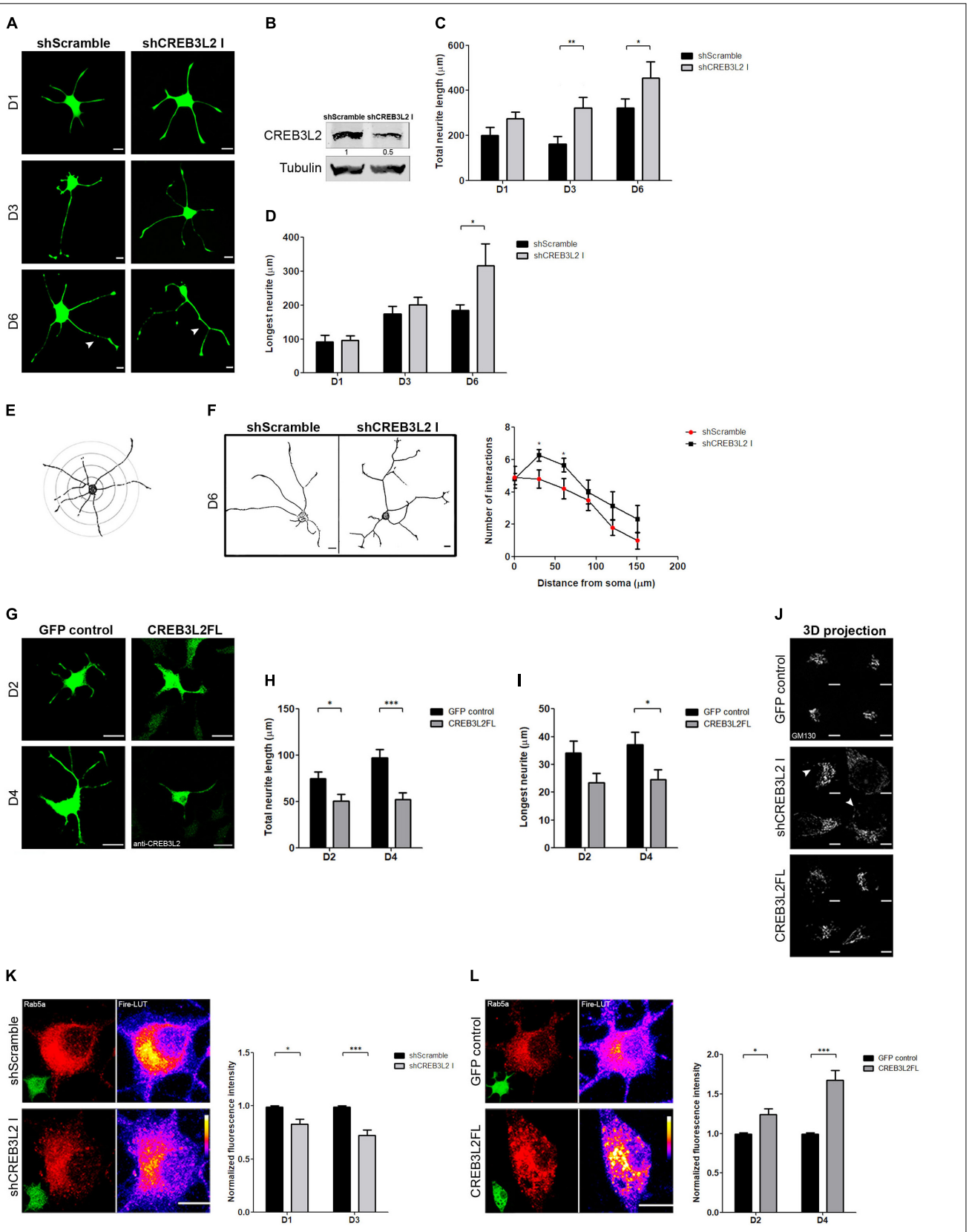

FIGURE 4 | The suppression of CREB3L2 alters the correct neuronal differentiated phenotype of PC12 cells. **(A)** Representative images of differentiated PC12 cells transduced with shScramble-EGFP (shScramble) or shCREB3L2-EGFP (shCREB3L2 I) and fixed at the indicated time after NGF induction. Arrowheads indicate the

(Continued)

FIGURE 4 | Continued
longest neurite. **(B)** Representative Western blot assays performed with cell lysates obtained from differentiated PC12 cells transduced with shScramble or shCREB3L2 I and blotted against CREB3L2 (detecting the N-terminal domain or cleaved fragment) and α-tubulin. Quantification of the total neurite length **(C)** and the longest neurite **(D)**. **(E)** Schematic representation of the Sholl analysis performed in the cells. **(F)** Left panel: Representative images of differentiated PC12 cells transduced with shScramble or shCREB3L2 I and fixed at 6 days post NGF induction. Acquired images were inverted for morphometric analysis. Right panel: Quantification of the number of intersections crossing the shells. **(G)** Representative images of differentiated PC12 cells transfected with control EGFP or CREB3L2FL plasmids and fixed at 2 and 4 days post NGF induction. Quantification of the total neurite length **(H)** and the longest neurite **(I)**. **(J)** 3D projection of GM130 immunostaining in cells transduced with shCREB3L2 I or transfected with control EGFP or CREB3L2 FL plasmids. Arrowheads indicate punctate structures labeled with GM130. **(K)** Left panel: Representative images of differentiated PC12 cells transfected with shScramble or shCREB3L2 I and fixed at 3 days post NGF induction and immunostained for Rab5. Fire-LUTs are shown to clearly visualize IF levels. Right panel: Quantification of Rab5 fluorescence intensity normalized with the control. **(L)** Left panel: Representative images of differentiated PC12 cells transfected with control-EGFP or CREB3L2 FL plasmids and fixed at 4 days post NGF induction and immunostained for Rab5. Fire-LUTs are shown to clearly visualize IF levels. Right panel: Quantification of Rab5 fluorescence intensity normalized with the control. Bars represent the mean ± SEM of three independent experiments carried out in triplicates, and a total of 50 cells were analyzed. Statistical data analysis was performed, using the Student's *T*-test, considering statistically significant a value of $p < 0.05$ (*$p < 0.05$, **$p < 0.01$; ***$p < 0.001$). Scale bars **(A,G)** 20 μm; **(J,K,L)** 5 μm.

3, and 6 post-NGF addition in both shCREB3L2 and control-transduced cells (**Figures 4C,D**). The results indicated that total neurite length increased at D3 and D6 of NGF treatment in shCREB3L2-transduced cells relative to control cells. Likewise, a significant increase in the longest neurite length was observed at D6 in shCREB3L2-treated cells relative to control cells. Similar results were also observed in cells transiently transfected with an shRNA (named shCREB3L2 II), targeting a different sequence of CREB3L2, arguing against off-target effects (**Supplementary Figure 2**). The data indicate that CREB3L2 inhibition deregulates the neurite outgrowth during the neuronal differentiation process of PC12 cells. Furthermore, Sholl analysis was performed to analyze morphology of the neurite outgrowth (Sholl, 1953; Brown et al., 2011). To this end, five concentric shells spaced every 30 μm each were defined around the cell soma, and the number of intersections crossing the shells was quantified (**Figure 4E**). Cells expressing shCREB3L2 showed more intersections at 60 and 90 μm from the soma than control cells (**Figure 4F**). Moreover, overexpression of CREB3L2FL induced a decrease in the total neurite length and the longest neurite as well (**Figures 4G–I**). Furthermore, in shCREB3L2-treated cells, punctate structures labeled with GM130 were detected throughout the soma of the cells (**Figure 4J**), suggesting that CREB3L2 depletion induces Golgi fragmentation. Although some GM130-punctated structures were also observed in CREB3L2 overexpressing cells, this phenotype was stronger in CREB3L2 knockdown cells (**Figure 4J**).

These results were puzzling and contradicted our initial predictions. If CREB3L2 increases during NGF-induced differentiation, how does its knockdown promote a neurite outgrowth and its overexpression inhibit the same process? Are these phenotypes related to the activity of membrane trafficking pathway-related proteins? To address these questions, we evaluated PC12 differentiation after interfering with ER-Golgi or endosomal transport by over-expressing Rab1b or Rab5 constructs, respectively (Plutner et al., 1991; Bucci et al., 1992). PC12 cells were transiently transfected for 24 h and then treated with NGF for 2 and 4 days. Interestingly, overexpression of wild type Rab1b (Rab1b WT) induced the neurite outgrowth, while the dominant negative construct, Rab1b N121I (Pind et al., 1994), inhibited it (**Supplementary Figure 3**). These effects were opposite to those observed by CREB3L2 overexpression or inhibition, respectively. In contrast, the neurite outgrowth was impaired by overexpression of wild-type Rab5, whereas it was promoted by the dominant negative Rab5 construct, Rab5 S34N (**Supplementary Figure 3**; Liu et al., 2007). Rab5 phenotypes were similar to those observed after CREB3L2 inhibition and overexpression, which prompted us to examine whether CREB3L2 affects Rab5 expression. To that end, cells were transiently transfected with shScramble, shCREB3L2, pEGFP or CREB3L2FL, and the Rab5 fluorescence signal was quantified (an anti-CREB3L2 antibody was used to detect CREB3L2 overexpressing cells). Immunofluorescence analysis revealed decreased Rab5 levels in shCREB3L2-transfected cells compared with control cells (scramble shRNA) after NGF differentiation. In contrast, in CREB3L2 overexpressing cells, Rab5 fluorescence intensity was higher than in control cells (**Figures 4K,L**). Taken together, the data indicate that CREB3L2 modulates NGF-induced cell differentiation and strongly suggest that Rab5 GTPase is one of the CREB3L2 targets.

DISCUSSION

Several studies carried out in different polarized cell types have shown that the membrane trafficking pathway provides membranes needed to achieve cell polarization (Lecuit and Wieschaus, 2000; Ye et al., 2006). PC12 cells, when cultured in the absence of the nerve growth factor, are small round (about 10 μm in diameter) or polygonal-shaped cells and have very few if any neurite-like processes. NGF treatment induces a dramatic increase in cell size (Seaborn et al., 2014; **Supplementary Figure 1**). Consistent with these data, Martorana et al. (2018) have shown that NGF differentiation goes along with increased mitochondrial remodeling, involving higher levels of fission and fusion proteins. To accomplish differentiation, a massive expansion of the cell membrane occurs, and this event should be accompanied by an increase in lipid content. Several reports have already shown that NGF-induced differentiation implies higher lipid synthesis (Araki and Wurtman, 1997; Li and Wurtman, 1998), particularly of phosphatidylcholine. In this regard, an increase in StarD7, a protein implicated in the delivery of phosphatidylcholine to mitochondria, was detected in the PC12 cells after NGF addition (**Figure 1F**).

Neurons display a perinuclear or cell body-localized Golgi apparatus and small Golgi cisternae located in dendritic spines called "Golgi outposts" [GOPs, (Horton et al., 2005)]. The size and the number of GOPs are related to the differentiation stage and function of the neurons. In fact, Golgi volume and dendritic GOPs increase during neuronal development (Horton et al., 2005). In agreement with this, our results show that the differentiation of PC12 cells induced by NGF is accompanied by an increase of both the volume of the Golgi complex and the expression levels of proteins associated with the secretory pathway (**Figure 1**). Transcripts encoding for transport factors also increased. This suggests that the differentiation program induced by NGF not only induces transcription of neuronal-specific genes associated with the differentiated phenotype but also genes that encode proteins ubiquitously expressed involved in the cellular homeostatic process elicited during PC12 differentiation. Furthermore, mRNA levels analysis of the CREB3 family members showed that CREB3, CREB3L1, and CREB3L2 are co-expressed in PC12 cells. However, only CREB3L2 mRNA levels significantly increase after 6 h of NGF induction, whereas CREB3 slightly increases only after 24 h, suggesting that CREB3L2 is a member of the CREB3 family that acts as an early mediator of NGF-induced differentiation (**Figure 2**). Interestingly, CREB3L2 mRNA levels increase out of a phase with the increase of the cleaved CREB3L2 fraction (**Figures 2A,C**). Also, immunofluorescence assays reveal an increase in full-length CREB3L2 (represented by the ER pattern, **Figure 2B**). These results clearly show that CREB3L2 regulation is a complex process, involving both transcriptional and posttranslational regulation (through S1P and S2P proteases).

Differentiation in neuronal cells can be induced by an increase in intracellular concentrations of cyclic AMP (cAMP) or calcium (Sanchez et al., 2004). cAMP and calcium, in turn, activate specific signaling pathways, which ultimately lead to the activation of transcription factors and genes involved in the differentiation program. In NGF-treated PC12 cells, activation of the ERK/MAPK signaling pathway leads to the induction of a set of genes called "immediate-early genes" [IEGs, (Sheng and Greenberg, 1990)]. IEGs are activated in a rapid, robust, and transient manner, and independently of new protein synthesis (Greenberg et al., 1985). Many of these IEGs (as *c-fos*) are transcription factors required for the activation of a second set of genes-encoding proteins that may contribute to the differentiation process (Sheng and Greenberg, 1990). In PC12 cells, c-Fos is necessary for neurite elongation (Gil et al., 2004), and its mRNA levels increase as early as 15 min after NGF addition (Milbrandt, 1986). Our observations that CREB3L2 mRNA levels increase 6 h after NGF addition suggest that, in a similar manner to that of *c-fos*, the rapid response of CREB3L2 may be required during the first stages of NGF-induced differentiation. PKA and MAPK/ERK are two extensively studied signaling pathways that lead to neuritogenesis. According to our results, CREB3L2 is a downstream effector shared between these two signaling pathways (**Figure 3**).

The acquisition of the differentiated phenotype and neurite growth is accomplished by several cellular adaptations, such as membrane addition, redistribution of molecules and organelles, cytoskeleton regulators, and the activation of their associated proteins (Horton and Ehlers, 2003; Neukirchen and Bradke, 2011; Takano et al., 2015). Some of the regulators of these events are proteins associated with the membrane trafficking pathway. In this regard, our results suggest that CREB3L2 acts as a negative regulator of neuritic outgrowth (**Figure 4**). Interestingly, the suppression of TBC1D12 (a recycling endosome-resident protein) promotes neurite development in differentiated PC12 cells (Oguchi et al., 2017). Similar results were observed in a neuroblastoma cell line with the expression of p160ROCK [a Rho-associated protein kinase associated with microtubules dynamics (Hirose et al., 1998)]. In addition, a knockout of the transcription factor KLF4 enhances axon and neurite growth in retinal ganglion cells (Moore et al., 2009).

Changes in CREB3 agree with those observed in a microarray study performed on PC12 cells treated with NGF (Dijkmans et al., 2008). Although it has been described that CREB3 participates in axonal regeneration (Ying et al., 2014, 2015) and that, in astrocytes, CREB3L1 impedes axon growth and functional recovery after spinal injury (Sumida et al., 2018), many questions about the molecular mechanisms of CREB3 transcription factors in these neuronal processes remain unknown. In terms of the participation of CREB3 transcription factors in differentiation processes, our research group (Garcia et al., 2017) has previously reported the adaptation of the Golgi complex in a CREB3L1-dependent manner in rat thyroid cells incubated with TSH (thyroid stimulating hormone). It has been demonstrated that, during chondroblasts differentiation into mature chondrocytes, CREB3L2 mRNA synthesis and proteolytic activation are induced (Saito et al., 2009). Work by Al-Maskari et al. (2018) shows that, during B-cell differentiation into antibody-secreting plasma cells, not only do CREB3L2 levels increase but also its processing. Moreover, blocking S1P-mediated proteolysis prevents activated B-cells from becoming antibody-secreting cells (Al-Maskari et al., 2018).

Furthermore, morphometric analysis shows that cells expressing shCREB3L2 display a more complex neuritic outgrowth than the control cells (**Figure 4**). This can be easily linked to previous reports where the modulation of both endocytic and secretory proteins affects the complexity of the neuritic outgrowth. For example, inhibition of the small GTPase Rab11 increases dendritic arborization in hippocampal neurons (Siri et al., 2020). Also, Rab35-suppression enhances the number of neuritic processes and acts as a negative regulator during differentiation of the oligodendroglial progenitor cell line (Miyamoto et al., 2014), and the knockdown of Rab5a and b, Rab20, and Rab32 in PC12 cells promotes the neurite outgrowth (Oguchi et al., 2018). Regarding Rab5a and Rab32, *in silico* analysis reveals putative CREB3L2 response elements in their promoter regions (data not shown). In agreement with this, CREB3L2 inhibition and overexpression decreased and increased the expression of Rab5, respectively (**Figure 4**). Rab5 is a central player in the NGF-TrkA signaling pathway required for PC12 differentiation. Its activity impairs the correct neurite outgrowth through the inactivation of TrkA signaling by promoting fusion of early endosomes. This is a necessary step for their transition to late endosomes and subsequent lysosomal degradation (Rink

et al., 2005; Liu et al., 2007). Thus, the effect of CREB3L2 on the neurite outgrowth strongly suggests that it regulates Rab5 levels. This is consistent with previous evidence about the inhibitory role of Rab5 in PC12 differentiation (Liu et al., 2007) and explains the negative regulatory effect of CREB3L2 in the NGF-induced differentiation process. Moreover, Golgi fragmentation due to CREB3L2 downregulation also reflects a correlation between CREB3L2 function and membrane trafficking. Although Golgi fragmentation can be a common consequence of various processes involving cellular stress; it is also an indicator of disturbances at vesicular transport levels (Makhoul et al., 2018), suggesting that CREB3L2 could regulate the expression of other molecules involved in different steps of membrane trafficking. In this sense, the partial downregulation of CREB3L2 achieved with both shRNA sequences used could explain the mild effect observed on the Golgi phenotype. However, we cannot exclude any option, nor that it may be due to the redundancy of some functions between CREB3L2 and CREB3 or CREB3L1, or that they have completely different target genes. Our data also show that altering ER to Golgi transport, by regulating Rab1b levels or activity, affects PC12 differentiation (**Supplementary Figure 3**). In agreement, the importance of Rab1 levels and ER-Golgi transport has been previously characterized in different cellular models (Cooper et al., 2006; Tomas et al., 2012; Romero et al., 2013). Additional studies must be performed to determine the mechanisms that regulate the expression of proteins involved in different membrane transport steps. Neuronal differentiation is a remarkable process, consisting of fine tuning of inhibitory and stimulatory events exerted by a large number of proteins. Disruption of this intricate network at any level is expected to alter the outcome of the differentiating cell program. On the other hand, such a complex process does not rely on a single protein to carry out one unique function, which is why proteins belonging to the same family can be found to be redundant in their functions.

This work provides novel evidence in the field of neuronal differentiation, given that it was unknown that CREB3L2, commonly associated with ER stress, also participates in NGF-induced neuronal differentiation of PC12 cells. Further characterization of downstream targets of CREB3L2 and the other CREB3 family members is required to reveal their participation in axonal growth and neuritic processes, either in the context of development or regeneration.

DATA AVAILABILITY STATEMENT

The original contributions presented in the study are included in the article/**Supplementary Material**, further inquiries can be directed to the corresponding author.

AUTHOR CONTRIBUTIONS

LS, MFC, PDG, and CA conceived and designed the experiments. LS and MFC performed the experiments. LS, MFC, PDG, VR-S, and CA analyzed the data. PDG and VR-S contributed to reagents, materials, and analysis tools. LS, MFC, VR-S, and CA wrote the manuscript. All authors contributed to the article and approved the submitted version.

FUNDING

LS, MFC, PDG and VR-S hold/ed a CONICET fellowship. Moreover, CA is a CONICET investigator and a professor at Universidad Nacional de Córdoba. Work in the Alvarez Lab is supported by the grants PICT 2016-0042-Prestamo BID from the Ministry of Science and Technology of Argentina, SECyT-UNC (2018–2021) from Universidad Nacional de Córdoba.

ACKNOWLEDGMENTS

We thank Susana Genti-Raimondi and Graciela Panzetta-Dutari (Universidad Nacional de Córdoba, Córdoba, Argentina) for the anti-StarD7 antibody, her comments after reading the manuscript and her valuable advices for performing qRT-PCR assays; Alejandro Vilcaes (Departamento de Química Biológica Ranwel Caputto, Universidad Nacional de Córdoba, Córdoba, Argentina) and Kazunori Imaizumi (Hiroshima University, Hiroshima, Japan) for Rab5 and CREB3L2 plasmids, respectively. We also thank Cecilia Conde (Instituto de Investigación Médica Mercedes y Martín Ferreyra, INIMEC-CONICET-Universidad Nacional de Córdoba, Córdoba, Argentina) for sharing anti-Rab5 antibody and Gabriela Furlan, Laura Gatica, and Luciana Reyna for their assistance as technical managers of the different facilities of the CIBICI (CONICET), Universidad Nacional de Córdoba, Córdoba, Argentina. We are also grateful to Carlos Mas, Pilar Crespo and Cecilia Sampedro for their technical assistance with the microscope. All the microscopes used in this work belong to the "Center for Advanced Optical and Confocal Microscopy" (CIQUIBIC, INIMEC, CIBICI) – CONICET-Universidad Nacional de Córdoba, Córdoba, Argentina.

SUPPLEMENTARY MATERIAL

The Supplementary Material for this article can be found online at: https://www.frontiersin.org/articles/10.3389/fnmol.2021.650338/full#supplementary-material

Supplementary Figure 1 | NGF-differentiated PC12 cells. **(A)** Representative images of PC12 treated with NGF (100 ng/ml) during the indicated days (D2, D4, and D6). Untreated cells (D0) are considered as control. **(B)** Western blot assays performed with cell lysates obtained from PC12 cells differentiated with NGF during the indicated days. One representative blot is shown. The bar graph shows the densitometric quantification of the indicated proteins relative to the nuclear protein KAP1 (loading control). Values from untreated cells were set equal to 1. The quantification was carried out, using Image Studio analysis software. Bars represent the mean ± SEM from three independent experiments, which were analyzed, using ANOVA test, followed by Bonferroni multiple comparison post-test, considering statistically significant a value of $p < 0.05$ (*$p < 0.05$; **$p < 0.001$). Scale bar: 20 μm.

Supplementary Figure 2 | Different shRNAs, shCREB3L2 I, and shCREB3L2 II, elicit similar effects. Representative images of differentiated PC12 cells transfected with shScramble-EGFP or two independent shCREB3L2-EGFP for 48 h before NGF treatment. **(A)** Representative immunofluorescence staining of CREB3L2 in PC12 cells transfected with shScramble, shCREB3L2 I, or shCREB3L2 II (D3). Fire-LUTs are shown to clearly visualize IF levels. **(B)** Representative images of PC12 cells transduced with shScramble and shCREB3L2 II and fixed at the indicated day post NGF induction. **(C)** Quantification of the CREB3L2 fluorescence intensity normalized with the control condition (shScramble). **(D,E)** Quantification of the total neurite length and the longest neurite. Bars represent the mean ± SEM of three independent experiments carried out in triplicates, and a total of 40 cells were analyzed. Statistical data analysis was performed, using Student's *T*-test, considering statistically significant a value of $p < 0.05$ ($*p < 0.05$, $**p < 0.01$; $***p < 0.001$). Scale bar: 20 μm.

Supplementary Figure 3 | Gain- and loss-of functions of both Rab1b and Rab5, proteins associated with membrane trafficking pathway, alter the neuronal differentiation of PC12 cells. **(A)** Representative images of differentiated PC12 cells transfected with control EGFP, Rab1b WT-EGFP, or Rab1b N121I-EGFP plasmids and fixed at 4 days post NGF induction. Insets show Rab1b distribution in the cell soma. Quantification of the total neurite length **(B)** and the longest neurite **(C)**. **(D)** Representative images of differentiated PC12 cells transfected with control EGFP, Rab5 WT-EGFP, or Rab5 S34N-EGFP plasmids and fixed at 4 days post NGF induction. Quantification of the total neurite length **(E)** and the longest neurite **(F)**. Bars represent the mean ± SEM of three independent experiments carried out in triplicates, and a total of 40 cells were analyzed. Statistical data analysis was performed, using Student's *T*-test, considering statistically significant a value of $p < 0.05$ ($*p < 0.05$, $**p < 0.01$; $***p < 0.001$). Scale bar: 20 μm.

REFERENCES

Al-Maskari, M., Care, M. A., Robinson, E., Cocco, M., Tooze, R. M., and Doody, G. M. (2018). Site-1 protease function is essential for the generation of antibody secreting cells and reprogramming for secretory activity. *Sci. Rep.* 8:14338.

Angeletti, S., Rena, V., Nores, R., Fretes, R., Panzetta-Dutari, G. M., and Genti-Raimondi, S. (2008). Expression and localization of StarD7 in trophoblast cells. *Placenta* 29, 396–404. doi: 10.1016/j.placenta.2008.02.011

Araki, W., and Wurtman, R. J. (1997). Control of membrane phosphatidylcholine biosynthesis by diacylglycerol levels in neuronal cells undergoing neurite outgrowth. *Proc. Natl. Acad. Sci. U.S.A.* 94, 11946–11950. doi: 10.1073/pnas.94.22.11946

Brown, K. M., Barrionuevo, G., Canty, A. J., De Paola, V., Hirsch, J. A., Jefferis, G. S., et al. (2011). The DIADEM data sets: representative light microscopy images of neuronal morphology to advance automation of digital reconstructions. *Neuroinformatics* 9, 143–157. doi: 10.1007/s12021-010-9095-5

Bucci, C., Parton, R. G. I, Mather, H., Stunnenberg, H., Simons, K., Hoflack, B., et al. (1992). The small GTPase rab5 functions as a regulatory factor in the early endocytic pathway. *Cell* 70, 715–728. doi: 10.1016/0092-8674(92)90306-w

Chan, C. P., Kok, K. H., and Jin, D. Y. (2011). CREB3 subfamily transcription factors are not created equal: Recent insights from global analyses and animal models. *Cell Biosci.* 1:6. doi: 10.1186/2045-3701-1-6

Chung, C. G., Kwon, M. J., Jeon, K. H., Hyeon, D. Y., Han, M. H., Park, J. H. I, et al. (2017). Golgi outpost synthesis impaired by toxic polyglutamine proteins contributes to dendritic pathology in neurons. *Cell Rep.* 20, 356–369. doi: 10.1016/j.celrep.2017.06.059

Cooper, A. A., Gitler, A. D., Cashikar, A., Haynes, C. M., Hill, K. J., Bhullar, B., et al. (2006). Alpha-synuclein blocks ER-Golgi traffic and Rab1 rescues neuron loss in Parkinson's models. *Science* 313, 324–328. doi: 10.1126/science.1129462

Cowley, S., Paterson, H., Kemp, P., and Marshall, C. J. (1994). Activation of MAP kinase kinase is necessary and sufficient for PC12 differentiation and for transformation of NIH 3T3 cells. *Cell* 77, 841–852. doi: 10.1016/0092-8674(94)90133-3

Dijkmans, T. F., van Hooijdonk, L. W., Schouten, T. G., Kamphorst, J. T., Vellinga, A. C., Meerman, J. H., et al. (2008). Temporal and functional dynamics of the transcriptome during nerve growth factor-induced differentiation. *J. Neurochem.* 105, 2388–2403. doi: 10.1111/j.1471-4159.2008.05338.x

Duncia, J. V., Santella, J. B. 3rd, Higley, C. A., Pitts, W. J., Wityak, J., Frietze, W. E., et al. (1998). MEK inhibitors: the chemistry and biological activity of U0126, its analogs, and cyclization products. *Bioorganic Med. Chem. Lett.* 8, 2839–2844. doi: 10.1016/s0960-894x(98)00522-8

Durand, S., Angeletti, S., and Genti-Raimondi, S. (2004). GTT1/StarD7, a novel phosphatidylcholine transfer protein-like highly expressed in gestational trophoblastic tumour: cloning and characterization. *Placenta* 25, 37–44. doi: 10.1016/s0143-4004(03)00214-5

Fischer, I., Richter-Landsberg, C., and Safaei, R. (1991). Regulation of microtubule associated protein 2 (MAP2) expression by nerve growth factor in PC12 cells. *Exp. Cell Res.* 194, 195–201. doi: 10.1016/0014-4827(91)90354-w

Fox, R. M., and Andrew, D. J. (2015). Transcriptional regulation of secretory capacity by bZip transcription factors. *Front. Biol.* 10, 28–51. doi: 10.1007/s11515-014-1338-7

Fox, R. M., Hanlon, C. D., and Andrew, D. J. (2010). The CrebA/Creb3-like transcription factors are major and direct regulators of secretory capacity. *J. Cell Biol.* 191, 479–492. doi: 10.1083/jcb.201004062

Galbiati, F., Volonte, D., Gil, O., Zanazzi, G., Salzer, J. L., Sargiacomo, M., et al. (1998). Expression of caveolin-1 and -2 in differentiating PC12 cells and dorsal root ganglion neurons: caveolin-2 is up-regulated in response to cell injury. *Proc. Natl. Acad. Sci. U.S.A.* 95, 10257–10262. doi: 10.1073/pnas.95.17.10257

Garcia, I. A., Martinez, H. E., and Alvarez, C. (2011). Rab1b regulates COPI and COPII dynamics in mammalian cells. *Cell. Logistics* 1, 159–163. doi: 10.4161/cl.1.4.18221

Garcia, I. A., Torres Demichelis, V., Viale, D. L., Di Giusto, P., Ezhova, Y., Polishchuk, R. S., et al. (2017). CREB3L1-mediated functional and structural adaptation of the secretory pathway in hormone-stimulated thyroid cells. *J. Cell Sci.* 130, 4155–4167.

Gil, G. A., Bussolino, D. F., Portal, M. M., Alfonso Pecchio, A., Renner, M. L., Borioli, G. A., et al. (2004). c-Fos activated phospholipid synthesis is required for neurite elongation in differentiating PC12 cells. *Mol. Biol. Cell* 15, 1881–1894. doi: 10.1091/mbc.e03-09-0705

Gomez, G. A., and Daniotti, J. L. (2005). H-Ras dynamically interacts with recycling endosomes in CHO-K1 cells: involvement of Rab5 and Rab11 in the trafficking of H-Ras to this pericentriolar endocytic compartment. *J. Biol. Chem.* 280, 34997–35010. doi: 10.1074/jbc.m506256200

Greenberg, M. E., Greene, L. A., and Ziff, E. B. (1985). Nerve growth factor and epidermal growth factor induce rapid transient changes in proto-oncogene transcription in PC12 cells. *J. Biol. Chem.* 260, 14101–14110. doi: 10.1016/s0021-9258(17)38689-1

Greene, L. A., and Tischler, A. S. (1976). Establishment of a noradrenergic clonal line of rat adrenal pheochromocytoma cells which respond to nerve growth factor. *Proc. Natl. Acad. Sci. U.S.A.* 73, 2424–2428. doi: 10.1073/pnas.73.7.2424

Greenwood, M. P., Greenwood, M., Gillard, B. T., Chitra Devi, R., and Murphy, D. (2017). Regulation of cAMP responsive element binding protein 3-Like 1 (Creb3l1) expression by orphan nuclear receptor Nr4a1. *Front. Mol. Neurosci.* 10:413. doi: 10.3389/fnmol.2017.00413

He, D., Marie, C., Zhao, C., Kim, B., Wang, J., Deng, Y., et al. (2016). Chd7 cooperates with Sox10 and regulates the onset of CNS myelination and remyelination. *Nat. Neurosci.* 19, 678–689. doi: 10.1038/nn.4258

Hirose, M., Ishizaki, T., Watanabe, N., Uehata, M., Kranenburg, O., Moolenaar, W. H., et al. (1998). Molecular dissection of the Rho-associated protein kinase (p160ROCK)-regulated neurite remodeling in neuroblastoma N1E-115 cells. *J. Cell Biol.* 141, 1625–1636. doi: 10.1083/jcb.141.7.1625

Horton, A. C., and Ehlers, M. D. (2003). Neuronal polarity and trafficking. *Neuron* 40, 277–295. doi: 10.1016/s0896-6273(03)00629-9

Horton, A. C., Racz, B., Monson, E. E., Lin, A. L., Weinberg, R. J., and Ehlers, M. D. (2005). Polarized secretory trafficking directs cargo for asymmetric dendrite growth and morphogenesis. *Neuron* 48, 757–771. doi: 10.1016/j.neuron.2005.11.005

Kaplan, D. R., Martin-Zanca, D., and Parada, L. F. (1991). Tyrosine phosphorylation and tyrosine kinase activity of the trk proto-oncogene product induced by NGF. *Nature* 350, 158–160. doi: 10.1038/350158a0

Klein, R., Jing, S. Q., Nanduri, V., O'Rourke, E., and Barbacid, M. (1991). The trk proto-oncogene encodes a receptor for nerve growth factor. *Cell* 65, 189–197. doi: 10.1016/0092-8674(91)90419-y

Lecuit, T., and Wieschaus, E. (2000). Polarized insertion of new membrane from a cytoplasmic reservoir during cleavage of the Drosophila embryo. *J. Cell Biol.* 150, 849–860. doi: 10.1083/jcb.150.4.849

Li, J., and Wurtman, R. J. (1998). Nerve growth factor stimulates diacylglycerol de novo synthesis and phosphatidylinositol hydrolysis in pheochromocytoma cells. *Brain Res.* 803, 44–53. doi: 10.1016/s0006-8993(98)00595-2

Liu, J., Lamb, D., Chou, M. M., Liu, Y. J., and Li, G. (2007). Nerve growth factor-mediated neurite outgrowth via regulation of Rab5. *Mol. Biol. Cell* 18, 1375–1384. doi: 10.1091/mbc.e06-08-0725

Livak, K. J., and Schmittgen, T. D. (2001). Analysis of relative gene expression data using real-time quantitative PCR and the 2(-Delta Delta C(T)) Method. *Methods* 25, 402–408. doi: 10.1006/meth.2001.1262

MacGillavry, H. D., Cornelis, J., van der Kallen, L. R., Sassen, M. M., Verhaagen, J., Smit, A. B., et al. (2011). Genome-wide gene expression and promoter binding analysis identifies NFIL3 as a repressor of C/EBP target genes in neuronal outgrowth. *Mol. Cell. Neurosci.* 46, 460–468. doi: 10.1016/j.mcn.2010.11.011

Makhoul, C., Gosavi, P., and Gleeson, P. A. (2018). The Golgi architecture and cell sensing. *Biochem. Soc. Trans.* 46, 1063–1072. doi: 10.1042/bst20180323

Martorana, F., Gaglio, D., Bianco, M. R., Aprea, F., Virtuoso, A., Bonanomi, M., et al. (2018). Differentiation by nerve growth factor (NGF) involves mechanisms of crosstalk between energy homeostasis and mitochondrial remodeling. *Cell Death Dis.* 9:391.

McCurdy, E. P., Chung, K. M., Benitez-Agosto, C. R., and Hengst, U. (2019). Promotion of axon growth by the secreted end of a transcription factor. *Cell Rep.* 29, 363.e5–377.e5.

Milbrandt, J. (1986). Nerve growth factor rapidly induces c-fos mRNA in PC12 rat pheochromocytoma cells. *Proc. Natl. Acad. Sci. U.S.A.* 83, 4789–4793. doi: 10.1073/pnas.83.13.4789

Miyamoto, Y., Yamamori, N., Torii, T., Tanoue, A., and Yamauchi, J. (2014). Rab35, acting through ACAP2 switching off Arf6, negatively regulates oligodendrocyte differentiation and myelination. *Mol. Biol. Cell* 25, 1532–1542. doi: 10.1091/mbc.e13-10-0600

Moore, D. L., Blackmore, M. G., Hu, Y., Kaestner, K. H., Bixby, J. L., Lemmon, V. P., et al. (2009). KLF family members regulate intrinsic axon regeneration ability. *Science* 326, 298–301. doi: 10.1126/science.1175737

Murakami, T., Saito, A., Hino, S., Kondo, S., Kanemoto, S., Chihara, K., et al. (2009). Signalling mediated by the endoplasmic reticulum stress transducer OASIS is involved in bone formation. *Nat. Cell Biol.* 11, 1205–1211. doi: 10.1038/ncb1963

Neukirchen, D., and Bradke, F. (2011). Neuronal polarization and the cytoskeleton. *Semin. Dev. Biol.* 22, 825–833. doi: 10.1016/j.semcdb.2011.08.007

Oguchi, M. E., Etoh, K., and Fukuda, M. (2018). Rab20, a novel Rab small GTPase that negatively regulates neurite outgrowth of PC12 cells. *Neurosci. Lett.* 662, 324–330. doi: 10.1016/j.neulet.2017.10.056

Oguchi, M. E., Noguchi, K., and Fukuda, M. (2017). TBC1D12 is a novel Rab11-binding protein that modulates neurite outgrowth of PC12 cells. *PLoS One* 12:e0174883. doi: 10.1371/journal.pone.0174883

Okuda, H., Tatsumi, K., Horii-Hayashi, N., Morita, S., Okuda-Yamamoto, A., Imaizumi, K., et al. (2014). OASIS regulates chondroitin 6-O-sulfotransferase 1 gene transcription in the injured adult mouse cerebral cortex. *J. Neurochem.* 130, 612–625. doi: 10.1111/jnc.12736

Penney, J., Taylor, T., MacLusky, N., and Lu, R. (2018). LUMAN/CREB3 plays a dual role in stress responses as a cofactor of the glucocorticoid receptor and a regulator of secretion. *Front. Mol. Neurosci.* 11:352. doi: 10.3389/fnmol.2018.00352

Pind, S. N., Nuoffer, C., McCaffery, J. M., Plutner, H., Davidson, H. W., Farquhar, M. G., et al. (1994). Rab1 and Ca2+ are required for the fusion of carrier vesicles mediating endoplasmic reticulum to Golgi transport. *J. Cell Biol.* 125, 239–252. doi: 10.1083/jcb.125.2.239

Plutner, H., Cox, A. D., Pind, S., Khosravi-Far, R., Bourne, J. R., Schwaninger, R., et al. (1991). Rab1b regulates vesicular transport between the endoplasmic reticulum and successive Golgi compartments. *J. Cell Biol.* 115, 31–43. doi: 10.1083/jcb.115.1.31

Richter-Landsberg, C., and Jastorff, B. (1986). The role of cAMP in nerve growth factor-promoted neurite outgrowth in PC12 cells. *J. Cell Biol.* 102, 821–829. doi: 10.1083/jcb.102.3.821

Rink, J., Ghigo, E., Kalaidzidis, Y., and Zerial, M. (2005). Rab conversion as a mechanism of progression from early to late endosomes. *Cell* 122, 735–749. doi: 10.1016/j.cell.2005.06.043

Romero, N., Dumur, C. I., Martinez, H., Garcia, I. A., Monetta, P. I, Sampieri, L., et al. (2013). Rab1b overexpression modifies Golgi size and gene expression in HeLa cells and modulates the thyrotrophin response in thyroid cells in culture. *Mol. Biol. Cell* 24, 617–632. doi: 10.1091/mbc.e12-07-0530

Rottger, S., White, J., Wandall, H. H., Olivo, J. C., Stark, A., Bennett, E. P., et al. (1998). Localization of three human polypeptide GalNAc-transferases in HeLa cells suggests initiation of O-linked glycosylation throughout the Golgi apparatus. *J. Cell Sci.* 111(Pt 1), 45–60. doi: 10.1242/jcs.111.1.45

Saito, A., Hino, S., Murakami, T., Kanemoto, S., Kondo, S., Saitoh, M., et al. (2009). Regulation of endoplasmic reticulum stress response by a BBF2H7-mediated Sec23a pathway is essential for chondrogenesis. *Nat. Cell Biol.* 11, 1197–1204. doi: 10.1038/ncb1962

Saito, A., Kanemoto, S., Zhang, Y., Asada, R., Hino, K., and Imaizumi, K. (2014). Chondrocyte proliferation regulated by secreted luminal domain of ER stress transducer BBF2H7/CREB3L2. *Mol. Cell* 53, 127–139. doi: 10.1016/j.molcel.2013.11.008

Sampieri, L., Di Giusto, P., and Alvarez, C. (2019). CREB3 transcription factors: er-golgi stress transducers as hubs for cellular homeostasis. *Front. Cell Dev. Biol.* 7:123. doi: 10.3389/fcell.2019.00123

Sanchez, S., Jimenez, C., Carrera, A. C., Diaz-Nido, J., Avila, J., and Wandosell, F. (2004). A cAMP-activated pathway, including PKA and PI3K, regulates neuronal differentiation. *Neurochem. Int.* 44, 231–242. doi: 10.1016/s0197-0186(03)00150-5

Schindelin, J., Arganda-Carreras, I., Frise, E., Kaynig, V., Longair, M., Pietzsch, T., et al. (2012). Fiji: an open-source platform for biological-image analysis. *Nat. Methods* 9, 676–682. doi: 10.1038/nmeth.2019

Seaborn, T., Ravni, A., Au, R., Chow, B. K., Fournier, A., Wurtz, O., et al. (2014). Induction of serpinb1a by PACAP or NGF is required for PC12 cells survival after serum withdrawal. *J. Neurochem.* 131, 21–32. doi: 10.1111/jnc.12780

Seamon, K. B., Padgett, W., and Daly, J. W. (1981). Forskolin: unique diterpene activator of adenylate cyclase in membranes and in intact cells. *Proc. Natl. Acad. Sci. U.S.A.* 78, 3363–3367. doi: 10.1073/pnas.78.6.3363

Sheng, M., and Greenberg, M. E. (1990). The regulation and function of c-fos and other immediate early genes in the nervous system. *Neuron* 4, 477–485. doi: 10.1016/0896-6273(90)90106-p

Sholl, D. A. (1953). Dendritic organization in the neurons of the visual and motor cortices of the cat. *J. Anatomy* 87, 387–406.

Siri, S. O., Rozes-Salvador, V., de la Villarmois, E. A., Ghersi, M. S., Quassollo, G., Perez, M. F., et al. (2020). Decrease of Rab11 prevents the correct dendritic arborization, synaptic plasticity and spatial memory formation. *Biochim. Biophys. Acta Mol. Cell Res.* 1867:118735. doi: 10.1016/j.bbamcr.2020.118735

Slavin, I., Garcia, A., Monetta, P., Martinez, H., Romero, N., and Alvarez, C. (2011). Role of Rab1b in COPII dynamics and function. *Eur. J. Cell Biol.* 90, 301–311. doi: 10.1016/j.ejcb.2010.10.001

Stessin, A. M., Zippin, J. H., Kamenetsky, M., Hess, K. C., Buck, J., and Levin, L. R. (2006). Soluble adenylyl cyclase mediates nerve growth factor-induced activation of Rap1. *J. Biol. Chem.* 281, 17253–17258. doi: 10.1074/jbc.m603500200

Sumida, Y., Kamei, N., Suga, N., Ochi, M., and Adachi, N. (2018). The endoplasmic reticulum stress transducer old astrocyte specifically induced substance positively regulates glial scar formation in spinal cord injury. *Neuroreport* 29, 1443–1448. doi: 10.1097/wnr.0000000000001128

Takano, T., Xu, C., Funahashi, Y., Namba, T., and Kaibuchi, K. (2015). Neuronal polarization. *Development* 142, 2088–2093.

Tomas, M., Marin, M. P., Martinez-Alonso, E., Esteban-Pretel, G., Diaz-Ruiz, A., Vazquez-Martinez, R., et al. (2012). Alcohol induces Golgi fragmentation in differentiated PC12 cells by deregulating Rab1-dependent ER-to-Golgi transport. *Histochem. Cell Biol.* 138, 489–501. doi: 10.1007/s00418-012-0970-z

Vanhoutte, P., Nissen, J. L., Brugg, B., Gaspera, B. D., Besson, M. J., Hipskind, R. A., et al. (2001). Opposing roles of Elk-1 and its brain-specific isoform, short Elk-1, in nerve growth factor-induced PC12 differentiation. *J. Biol. Chem.* 276, 5189–5196. doi: 10.1074/jbc.m006678200

Yang, L., Na, C. L., Luo, S., Wu, D., Hogan, S., Huang, T., et al. (2017). The phosphatidylcholine transfer protein Stard7 is required for mitochondrial and epithelial cell homeostasis. *Sci. Rep.* 7:46416.

Ye, B., Zhang, Y. W., Jan, L. Y., and Jan, Y. N. (2006). The secretory pathway and neuron polarization. *J. Neurosci. : Off. J. Soc. Neurosci.* 26, 10631–10632. doi: 10.1523/jneurosci.3271-06.2006

Ying, Z., Misra, V., and Verge, V. M. (2014). Sensing nerve injury at the axonal ER: activated Luman/CREB3 serves as a novel axonally synthesized retrograde regeneration signal. *Proc. Natl. Acad. Sci. U.S.A.* 111, 16142–16147. doi: 10.1073/pnas.1407462111

Ying, Z., Zhai, R., McLean, N. A., Johnston, J. M., Misra, V., and Verge, V. M. (2015). The unfolded protein response and cholesterol biosynthesis link Luman/Creb3 to regenerative axon growth in sensory neurons. *J. Neurosci. : Off. J. Soc. Neurosci.* 35, 14557–14570. doi: 10.1523/jneurosci.0012-15.2015

Conflict of Interest: The authors declare that the research was conducted in the absence of any commercial or financial relationships that could be construed as a potential conflict of interest.

Publisher's Note: All claims expressed in this article are solely those of the authors and do not necessarily represent those of their affiliated organizations, or those of the publisher, the editors and the reviewers. Any product that may be evaluated in this article, or claim that may be made by its manufacturer, is not guaranteed or endorsed by the publisher.

frontiers in Molecular Neuroscience

MINI REVIEW
published: 31 August 2021
doi: 10.3389/fnmol.2021.717411

Estrogen Receptor β as a Candidate Regulator of Sex Differences in the Maternal Immune Activation Model of ASD

Madeline L. Arnold[1] *and Kaoru Saijo*[1,2]*

[1] Department of Molecular and Cell Biology, University of California, Berkeley, Berkeley, CA, United States, [2] Helen Wills Neuroscience Institute, University of California, Berkeley, Berkeley, CA, United States

Interestingly, more males are diagnosed with autism spectrum disorder (ASD) than females, yet the mechanism behind this difference is unclear. Genes on the sex chromosomes and differential regulation by sex steroid hormones and their receptors are both candidate mechanisms to explain this sex-dependent phenotype. Nuclear receptors (NRs) are a large family of transcription factors, including sex hormone receptors, that mediate ligand-dependent transcription and may play key roles in sex-specific regulation of immunity and brain development. Infection during pregnancy is known to increase the probability of developing ASD in humans, and a mouse model of maternal immune activation (MIA), which is induced by injecting innate immune stimulants into pregnant wild-type mice, is commonly used to study ASD. Since this model successfully recaptures the behavioral phenotypes and male bias observed in ASD, we will discuss the potential role of sex steroid hormones and their receptors, especially focusing on estrogen receptor (ER)β, in MIA and how this signaling may modulate transcription and subsequent inflammation in myeloid-lineage cells to contribute to the etiology of this neurodevelopmental disorder.

Keywords: estrogen receptor β, brain myeloid cells, maternal immune activation, autism spectrum disorder, sex differences, inflammation

OPEN ACCESS

Edited by:
Estela Maris Muñoz, CONICET Dr. Mario H. Burgos Institute of Histology and Embryology (IHEM), Argentina

Reviewed by:
Maria Julia Cambiasso, Medical Research Institute Mercedes and Martín Ferreyra (INIMEC), Argentina
Alberto Camacho-Morales, Autonomous University of Nuevo León, Mexico
Tetsushi Sadakata, Gunma University, Japan

***Correspondence:**
Kaoru Saijo
ksaijo@berkeley.edu

Specialty section:
This article was submitted to Neuroplasticity and Development, a section of the journal Frontiers in Molecular Neuroscience

Received: *30 May 2021*
Accepted: *09 August 2021*
Published: *31 August 2021*

Citation:
Arnold ML and Saijo K (2021) Estrogen Receptor β as a Candidate Regulator of Sex Differences in the Maternal Immune Activation Model of ASD. Front. Mol. Neurosci. 14:717411. doi: 10.3389/fnmol.2021.717411

INTRODUCTION

Many neurodevelopmental disorders (NDDs), such as autism spectrum disorder (ASD), attention-deficit/hyperactivity disorder (ADHD), and schizophrenia, show sex differences (Waddell and McCarthy, 2012; Hanamsagar and Bilbo, 2016; Hill, 2016; McCarthy, 2016; Bordeleau et al., 2019; May et al., 2019; Lord et al., 2020; Merikangas and Almasy, 2020); yet the mechanisms behind these observations are poorly understood. For example, it is known that males are more frequently diagnosed with ASD than females (Baron-Cohen et al., 2011; Loomes et al., 2017; Dietz et al., 2020). Several studies indicate a male to female ratio of approximately 3:1 or 4:1 in ASD, as well as sex differences in symptoms (Loomes et al., 2017; Hull et al., 2020). To explain this sex difference in ASD, several hypotheses have been proposed. One possibility is that sex chromosome gene effects contribute to ASD etiology. Indeed, mutations in many genes are known to increase the probability of ASD, and some of them, such as *FMR1*, *MeCP2*, and neuroligins 3 and 4, are on the X-chromosome (Marco and Skuse, 2006; Guy et al., 2011; Percy, 2011; Zhang et al., 2017;

Sledziowska et al., 2020; Savatt and Myers, 2021). While it will not be addressed here, excellent reviews that discuss the chromosomal contributions to sex differences in ASD can be found elsewhere (Marco and Skuse, 2006; Guy et al., 2011; Percy, 2011; Zhang et al., 2017; Sledziowska et al., 2020; Savatt and Myers, 2021). Another possible explanation for the sex differences observed in ASD is the differential regulation of sex hormones and their receptor-mediated signaling in females and males, leading to differential gene transcription. In this review, we will discuss the possibility that regulation of inflammation by sex hormone nuclear receptors (NRs) contributes to the observed sex differences in ASD.

Though both sex differences and immune involvement are well established features of ASD, mechanisms linking sex and immune factors in neurodevelopmental disorders like ASD are not as well studied. However, the importance of sex in inflammation has been demonstrated in other biological contexts. Sex-dependent inflammatory phenotypes are observed in response to innate and adaptive immune reactions as well as in acute and chronic inflammatory diseases and their animal models (Klein and Flanagan, 2016; Chamekh and Casimir, 2019; Gal-Oz et al., 2019). Males are generally more susceptible to pathogen infections (Klein, 2012; Vazquez-Martinez et al., 2018), while females are more often diagnosed with autoimmune diseases (Quintero et al., 2012; Ngo et al., 2014; Billi et al., 2019; Lasrado et al., 2020). For example, in experimental autoimmune encephalomyelitis, a mouse model of multiple sclerosis, female and male mice have differing disease courses (Constantinescu et al., 2011). Phenotypes also differ by sex in animal models of high-fat diet, which induces low grade but chronic inflammation in macrophages and disrupts homeostasis in adipose tissues, resulting in induction of metabolic syndrome (Lumeng et al., 2007; Duan et al., 2018). Male mice gain weight and display insulin resistance, while female mice are more resistant to these effects (Pettersson et al., 2012; Ingvorsen et al., 2017; Casimiro et al., 2021). These observations suggest that sex-specific factors are important in regulating inflammation.

MIA-Induced Inflammation as a Model of ASD

The maternal immune activation (MIA)-induced animal model of ASD has the potential to reveal insights about the impact of sex-specific and immune factors, and their interactions, during brain development. The MIA model was developed based on the observation that infection during pregnancy is linked to ASD (Atladottir et al., 2010; Zerbo et al., 2015; Al-Haddad et al., 2019). Outbreaks of several viruses, such rubella and influenza, have been documented to be associated with increased numbers of individuals with ASD (Zerbo et al., 2013; Shuid et al., 2021). Consistent with these findings, the MIA model uses the injection of a toll-like receptor (TLR) ligand into pregnant wild-type female mice on a specific day of gestation to induce an immune response. A commonly used ligand is polyinosinic:polycytidylic acid [Poly(I:C)], which mimics infection by double-stranded RNA viruses and triggers the TLR3-mediated innate immune response (Smith et al., 2007; Patterson, 2011). This MIA-induced ASD model displays behavioral phenotypes, including decreased sociability, increased repetitive restricted behavior, impaired learning and memory, altered levels of anxiety, and hyperactivity (Patterson, 2011; Estes and McAllister, 2016). Importantly, several groups have reported that the behavioral phenotypes in this model are only observed in male offspring (Xuan and Hampson, 2014; Coiro and Pollak, 2019; Haida et al., 2019; Keever et al., 2020; Nichols et al., 2020, preprint; **Figure 1A**). Based on these findings, MIA induction in mice is widely used to study the mechanism of ASD because it successfully recaptures behavioral phenotypes and sex-specific features observed in the disorder.

Inflammation in Fetal Myeloid-Lineage Cells Upon MIA

It is currently hypothesized that maternal cytokines are the causative factor affecting fetal brain development in the MIA-induced model of ASD (Smith et al., 2007; Choi et al., 2016). Indeed, MIA induces an adaptive immune response in mothers, particularly the activation of a subset of T helper cells (Th17 T cells) and the release of maternal cytokines such as interleukin (IL)-17, that can affect fetal brain development in mice (Choi et al., 2016). However, a few groups, including ours, have reported that MIA may also directly induce an inflammatory innate immune response in fetal myeloid cells (Onore et al., 2014; Matcovitch-Natan et al., 2016; Carlezon et al., 2019; Ben-Yehuda et al., 2020; Cui et al., 2020; Nichols et al., 2020, preprint).

Brain myeloid-lineage cells derive from primitive macrophages in the yolk sac and migrate to the brain on embryonic day (E) 9.5 in mice, after which these cells expand, migrate, and develop into microglial cells and border-associated macrophages (BAMs) (Ginhoux et al., 2010; Goldmann et al., 2016; Utz et al., 2020). These two myeloid subsets have common as well as subset-specific gene expression profiles and localize to different areas of the brain: microglia in the brain parenchyma, and BAMs in the meninges and the choroid plexus (Ginhoux et al., 2010; Goldmann et al., 2016; Mrdjen et al., 2018; Jordao et al., 2019; Van Hove et al., 2019; Utz et al., 2020). A few studies point to BAMs as a key cell type in the response to MIA in the fetal brain. Although the precise mechanism is not clear, a recent publication indicates that MIA-activated BAMs in the choroid plexus secrete the chemokine CCL2 into the fetal ventricle, resulting in enhanced local inflammation (Cui et al., 2020). Moreover, our single-cell RNA-sequencing (scRNA-seq) analysis showed that the activation of fetal BAMs in response to MIA was dependent upon fetal *Trif*, an essential signaling molecule downstream of TLR3 (Nichols et al., 2020, preprint). These findings indicate that MIA leads to fetal innate immune signaling in BAMs. Furthermore, in validating our scRNA-seq data, we found that MIA causes BAMs in the choroid plexus, but not meningeal BAMs or microglia, to have increased expression of *S100a8 and 9,* key inflammatory genes that are known to induce chemotaxis and enhance inflammation (Ehrchen et al., 2009; Cesaro et al., 2012; Cury et al., 2013; Garcia-Arias et al., 2013; Walsham and Sherwood, 2016; Nishikawa et al., 2017;

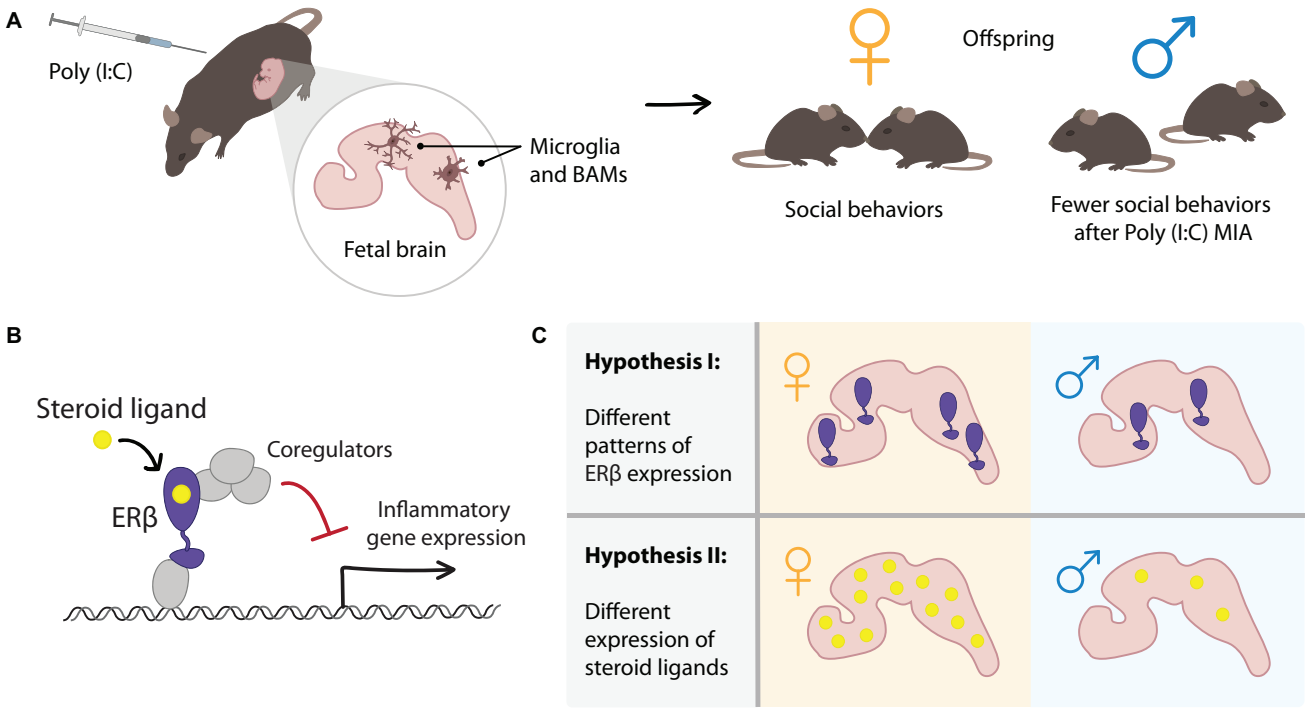

FIGURE 1 | Hypothesized role of estrogen receptor (ER)β signaling in mediating sex differences in the maternal immune activation (MIA) mouse model of ASD. **(A)** In the MIA model, polyinosinic:polycytidylic acid [Poly(I:C)] is injected into wild-type pregnant female mice at E12.5. MIA results in inflammatory signaling, including responses in myeloid-lineage cells in the fetal brain (microglia and BAMs). Offspring of Poly(I:C) treated dams display sex-specific behavioral phenotypes such as decreased social interaction in male offspring but not in female offspring. To explain the sex difference in the MIA-induced ASD mouse model, we consider sex steroid hormone nuclear receptor signaling in the fetal brain. **(B)** Mechanism of ERβ-mediated repression of inflammatory gene expression, which we previously observed in microglia. **(C)** Two hypothesized mechanisms by which sex differences in ERβ signaling in the fetal brain could contribute to the sex differences observed in the MIA model. Differential expression of (I) ERβ or (II) steroid ligands in female and male fetal brains could result in differential transcriptional responses to the MIA inflammatory stimulus.

Aranda et al., 2018; Wang et al., 2019; Silvin et al., 2020). These data suggest that inflammation in fetal myeloid cells may be involved in the development of ASD-like changes in MIA-induced fetal brains. Furthermore, it is possible that differential regulation of this inflammation may be a mechanism to explain the sex-specific phenotypes observed in this mouse model.

Expression of ERs and Sex Steroid Hormones in the Fetal Brain

Since MIA induces inflammation in brain myeloid-lineage cells, one hypothesis to explain the male bias in ASD is differing magnitude and duration of inflammation in males and females during fetal development. As we described above, in this review we will mainly discuss sex steroid NRs, especially ERβ, as potential regulators of fetal brain inflammation. We focus on ERβ because (1) ERβ is broadly expressed in mouse brain (Mitra et al., 2003; Fan et al., 2006) and (2) we previously showed that ERβ could regulate inflammation in microglial cells (Saijo et al., 2011).

So far, it is not clear whether ERα and ERβ expression in the myeloid cells of the fetal brain varies by sex. Studies have examined estrogen signaling primarily in whole brain or neuronal cells, and few have examined developmental time points prior to the neonatal period. Excellent reviews are available for overall brain expression analyses of ERα, ERβ, and enzymes required for the generation of androgens and estrogens (McCarthy, 2008; Bondesson et al., 2015). Several reports indicate that ERα, ERβ, and enzymes are present during mid-gestation. For example, ERβ expression was detected in the fetal midbrain, neuromere, hypothalamus, thalamus, and basal plate of pons at E12.5 (Fan et al., 2006), and ERα expression was observed at E16.5 in a gonadal sex dependent manner (Cisternas et al., 2015). In amygdala neuronal cultures obtained from E15 embryos, ERβ is sex-differentially regulated: lower levels of Esr2 mRNA expression were observed in females, but also sex differences in hormonal responsiveness were present, with increased Esr2 expression in response to 17β-estradiol or DHT hormonal stimulation only in females. These effects were dependent on sex chromosome complement (Cisternas et al., 2017). Activity of ERs, using an ERE-luciferase reporter, was observed in the fetal forebrain and hindbrain as early as E13.5, though no difference was detected between brains from females and males except in the P1 hindbrain (Della Torre et al., 2018). Several key enzymes involved in steroid hormone synthesis are expressed in female and male E16 fetal brain, including StAR, Cyp11a1, 5α-Reductase, and aromatase (Cisternas et al., 2015). Aromatase

is an enzyme that converts testosterone to 17β-estradiol and androstenedione to estrone. Notably, sex-dependent expression of aromatase in the developing mouse brain has been reported, which may indicate the presence of differing concentrations of ER ligands in females and males that could impact downstream signaling (Harada and Yamada, 1992; Greco and Payne, 1994; Hutchison et al., 1997; Cisternas et al., 2015; Shay et al., 2018; Sellers et al., 2020).

Little is known about the expression of sex steroid hormones in the fetal mouse brain; however, a report showed that 17β-estradiol, testosterone, and DHT were detected in the brains of fetal mice, and that these hormones may exhibit sex dimorphic expression patterns in different brain regions (Konkle and McCarthy, 2011). However, to better understand how sex steroid hormones may regulate inflammation induced by MIA, precise analysis of sex steroid hormone expression in the fetal brain will be important.

Together, these expression studies suggest that the cellular machinery for ER signaling is present in the fetal brain from a relatively early age, and that sex differences in the expression of receptors, steroid metabolizing enzymes, and hormone ligands could contribute to differential regulation by ERs in females and males. Our favorite hypothesis is that concentrations of particular ER ligands differ between females and males in such a way that MIA-induced inflammatory responses differ in magnitude or duration. For example, ligands that induce transcriptional repression of inflammatory genes via ERβ may be highly expressed in female fetal brains, leading to efficient resolution of inflammation upon MIA. The hypothetically lower expression of such repressive ERβ ligands in fetal male brains could result in larger or prolonged inflammatory responses compared to females (**Figure 1C**, Hypothesis II). A comprehensive analysis of the expression of ERs and related ligands in developing fetal mouse brains, especially comparing sex, cell type, and specific brain region, will be important in understanding the contribution of ER-mediated transcription in sex-specific brain development.

Nuclear Receptor Signaling in General

NRs are a family of transcription factors which both positively and negatively regulate transcription in response to ligand binding. Steroid hormone NRs are a class of NRs with activities that depend on endogenous small lipophilic ligands such as steroid hormones. For example, estrogen receptors (ERs) bind to estrogen response elements (essential ERE, 5'-GGTCAnnnTGACC-3') (Driscoll et al., 1998; Klinge, 2001) in gene regulatory regions to control the expression of target genes. In addition to direct DNA binding, NRs can also regulate transcription by binding to other transcription factors *in trans*. NR function depends upon the ligands that are bound to the receptor. Indeed, NRs change their conformation in response to ligand binding in order to recruit either transcriptional activator or repressor complexes (Moras and Gronemeyer, 1998; Bourguet et al., 2000; Nagy and Schwabe, 2004), and it has been proposed that ligand binding may induce post-translational changes on NRs that stabilize co-factor binding (Hammer et al., 1999; Lannigan, 2003; Pascual et al., 2005; Lalevee et al., 2010; Anbalagan et al., 2012; Helzer et al., 2015; El Hokayem et al., 2017). To carry out their transcriptional activation and repression activities, NRs recruit a wide variety of co-factors and enzymes required for modifying histones and remodeling chromatin. These factors include histone acetyltransferases, deacetylases, methyltransferases, demethylases, and chromatin remolding factors, as well as kinases, phosphatases, and ubiquitin and SUMO E3 ligases (Olefsky, 2001; Perissi and Rosenfeld, 2005; Dasgupta et al., 2014).

ERs and Their Impact on Inflammation

Various reports have suggested that sex steroid hormones and their steroid hormone nuclear receptors (NRs) may regulate inflammatory responses in innate immune cells. In particular, two estrogen receptor isoforms (ERα and ERβ) as well as the androgen receptor (AR) are well characterized sex steroid hormone NRs that are known to regulate innate immune responses (Vegeto et al., 2003; Baker et al., 2004; Suuronen et al., 2005; Harkonen and Vaananen, 2006; Sierra et al., 2008; Lai et al., 2009; Saijo et al., 2011; Kovats, 2015; Villa et al., 2015; Villa et al., 2016; Ardalan et al., 2019; Becerra-Diaz et al., 2020). We have previously reported that ERβ regulates the duration and magnitude of the inflammatory response in microglial cells (Saijo et al., 2011). ERβ binds a range of ligands, including estrogens and androgens, and specific ERβ ligands can facilitate repression of inflammation (Kuiper et al., 1997; Wu et al., 2013). See **Figure 1B** for a simplified schematic of ERβ-mediated transcriptional repression of inflammatory genes. Several reports have indicated that 17β-estradiol, a ligand for both ERα and ERβ, can regulate inflammation in myeloid-lineage cells. However, this regulation is not always clear in that some reports have suggested that ER-mediated transcription represses inflammation (Vegeto et al., 2003; Ribas et al., 2011), while others have suggested that it does not (Calippe et al., 2010; Shindo et al., 2020). While the amino acid sequences of the DNA-binding domains of these two ER isoforms are highly conserved, their ligand-binding domains (LBDs) are much less so (47% in human). Since the functions of NRs are dependent upon ligands, this lack of conservation in ER LBDs may suggest that ERα and ERβ may differ in their preferential ligands, and that binding of the same ligand to either ERα or ERβ could result in different transcriptional outputs.

Previously, we reported that ERβ represses inflammation in microglia in a ligand-dependent manner (Saijo et al., 2011). In mouse microglial cells, a subset of ligands, including the endogenous ligand 5-androsten-3β, 17β-diol (Δ5-Adiol) and the synthetic ligands Indazole-estrogen-Cl and -Br, have been shown to induce transcriptional repression of inflammation in an ERβ-dependent manner. Treatment with these repressive ligands, but not the classic ER ligand 17β-estradiol, results in the recruitment of the transcriptional corepressor CtBP (Saijo et al., 2011; **Figure 1B**). CtBP is a co-repressor platform that is known to assemble enzymes required for transcriptional repression, such as euchromatic histone-lysine N-methyltransferase 2 (EHMT2, also known as G9a), euchromatic histone-lysine N-methyltransferase 1 (EHMT1, also known as GLP), the histone deacetylases HDAC1 and 2, and lysine demethylase 1A (KDM1a, also known as LSD1) (Chinnadurai, 2002; Dcona et al., 2017). When microglial cells are stimulated with the TLR4 ligand lipopolysaccharide (LPS), ERβ binds to cFos and repressive ligands, which results in the recruitment of the CtBP complex to target genes, thus

regulating inflammation through a transrepression mechanism. Interestingly, mutations in ERβ, CtBP1/2, and HDACs have been observed in human ASD patients (Chakrabarti et al., 2009; Zettergren et al., 2013; De Rubeis et al., 2014). Although these NRs and their co-factors/binding partners are proposed to be genetic factors for ASD, we consider the possibility that these steroid hormone NRs and their ligands may exert their effects on brain development by modulating the inflammatory response to environmental immune stimuli.

CONCLUSION AND FUTURE DIRECTIONS

Endocrine disruption, such as sex hormone dyshomeostasis, during fetal brain development increases the risk of NDDs (Colborn, 2004; Schug et al., 2015; Moosa et al., 2018). Further supporting the role of sex hormone signaling in brain development, ERβ conventional knockout mice show fewer proliferating cells and more apoptotic cells in the E18.5 fetal brain (Wang et al., 2003). These observations underscore the importance of sex hormone nuclear receptor-mediated signaling during brain development in addition to the well-known role of hormone signaling in sex differentiation of the brain. Investigating the role of ER signaling in different cell types and across developmental time periods will clarify the mechanisms underlying the observed brain phenotypes after disruption of hormone signaling pathways.

Here, we have discussed the hypothesis that ERβ-mediated repression of inflammation in brain myeloid-lineage cells may contribute to the male bias observed in an MIA-induced ASD mouse model. We consider two hypotheses of how ERβ-mediated transcription may contribute to the sex-specific phenotypes in the MIA model. One is that the expression of ERβ may be different between fetal female and male brains. The other is that ERβ ligands that induce transcriptional repression may differ in fetal female and male brains (**Figure 1C**). Therefore, a precise mechanistic understanding of ERβ-mediated transcription and a thorough analysis of the expression of sex steroid hormones and their receptors in the brain may provide new insights into the sex-dependent phenotypes in ASD and other neurodevelopmental disorders.

AUTHOR CONTRIBUTIONS

MA and KS wrote the manuscript. MA made the figure. Both authors contributed to the article and approved the submitted version.

FUNDING

This material is based upon work supported by the National Science Foundation Graduate Research Fellowship Program under Grant No. DGE 1752814 and the ARCS Foundation (MA) and NIH R01HD092093 (KS).

REFERENCES

Al-Haddad, B. J. S., Jacobsson, B., Chabra, S., Modzelewska, D., Olson, E. M., Bernier, R., et al. (2019). Long-term risk of neuropsychiatric disease after exposure to infection in utero. *JAMA Psychiatry* 76, 594–602. doi: 10.1001/jamapsychiatry.2019.0029

Anbalagan, M., Huderson, B., Murphy, L., and Rowan, B. G. (2012). Post-translational modifications of nuclear receptors and human disease. *Nucl. Recept. Signal.* 10:e001.

Aranda, C. J., Ocon, B., Arredondo-Amador, M., Suarez, M. D., Zarzuelo, A., Chazin, W. J., et al. (2018). Calprotectin protects against experimental colonic inflammation in mice. *Br. J. Pharmacol.* 175, 3797–3812. doi: 10.1111/bph.14449

Ardalan, M., Chumak, T., Vexler, Z., and Mallard, C. (2019). Sex-dependent effects of perinatal inflammation on the brain: implication for neuro-psychiatric disorders. *Int. J. Mol. Sci.* 20:2270. doi: 10.3390/ijms20092270

Atladottir, H. O., Thorsen, P., Ostergaard, L., Schendel, D. E., Lemcke, S., Abdallah, M., et al. (2010). Maternal infection requiring hospitalization during pregnancy and autism spectrum disorders. *J. Autism Dev. Disord.* 40, 1423–1430. doi: 10.1007/s10803-010-1006-y

Baker, A. E., Brautigam, V. M., and Watters, J. J. (2004). Estrogen modulates microglial inflammatory mediator production via interactions with estrogen receptor beta. *Endocrinology* 145, 5021–5032. doi: 10.1210/en.2004-0619

Baron-Cohen, S., Lombardo, M. V., Auyeung, B., Ashwin, E., Chakrabarti, B., and Knickmeyer, R. (2011). Why are autism spectrum conditions more prevalent in males? *PLoS Biol.* 9:e1001081. doi: 10.1371/journal.pbio.1001081

Becerra-Diaz, M., Song, M., and Heller, N. (2020). Androgen and androgen receptors as regulators of monocyte and macrophage biology in the healthy and diseased lung. *Front. Immunol.* 11:1698. doi: 10.3389/fimmu.2020.01698

Ben-Yehuda, H., Matcovitch-Natan, O., Kertser, A., Spinrad, A., Prinz, M., Amit, I., et al. (2020). Maternal type-I interferon signaling adversely affects the microglia and the behavior of the offspring accompanied by increased sensitivity to stress. *Mol. Psychiatry* 25, 1050–1067. doi: 10.1038/s41380-019-0604-0

Billi, A. C., Kahlenberg, J. M., and Gudjonsson, J. E. (2019). Sex bias in autoimmunity. *Curr. Opin. Rheumatol.* 31, 53–61. doi: 10.1097/bor.0000000000000564

Bondesson, M., Hao, R., Lin, C. Y., Williams, C., and Gustafsson, J. A. (2015). Estrogen receptor signaling during vertebrate development. *Biochim. Biophys. Acta* 1849, 142–151. doi: 10.1016/j.bbagrm.2014.06.005

Bordeleau, M., Carrier, M., Luheshi, G. N., and Tremblay, M. E. (2019). Microglia along sex lines: from brain colonization, maturation and function, to implication in neurodevelopmental disorders. *Semin. Cell Dev. Biol.* 94, 152–163. doi: 10.1016/j.semcdb.2019.06.001

Bourguet, W., Germain, P., and Gronemeyer, H. (2000). Nuclear receptor ligand-binding domains: three-dimensional structures, molecular interactions and pharmacological implications. *Trends Pharmacol. Sci.* 21, 381–388. doi: 10.1016/s0165-6147(00)01548-0

Calippe, B., Douin-Echinard, V., Delpy, L., Laffargue, M., Lelu, K., Krust, A., et al. (2010). 17Beta-estradiol promotes TLR4-triggered proinflammatory mediator production through direct estrogen receptor alpha signaling in macrophages in vivo. *J. Immunol.* 185, 1169–1176. doi: 10.4049/jimmunol.0902383

Carlezon, W. A. Jr., Kim, W., Missig, G., Finger, B. C., Landino, S. M., Alexander, A. J., et al. (2019). Maternal and early postnatal immune activation produce sex-specific effects on autism-like behaviors and neuroimmune function in mice. *Sci. Rep.* 9:16928.

Casimiro, I., Stull, N. D., Tersey, S. A., and Mirmira, R. G. (2021). Phenotypic sexual dimorphism in response to dietary fat manipulation in C57BL/6J mice. *J. Diabetes Complications* 35:107795.

Cesaro, A., Anceriz, N., Plante, A., Page, N., Tardif, M. R., and Tessier, P. A. (2012). An inflammation loop orchestrated by S100A9 and calprotectin is critical for development of arthritis. *PLoS One* 7:e45478. doi: 10.1371/journal.pone.0045478

Chakrabarti, B., Dudbridge, F., Kent, L., Wheelwright, S., Hill-Cawthorne, G., Allison, C., et al. (2009). Genes related to sex steroids, neural growth, and social-emotional behavior are associated with autistic traits, empathy, and Asperger syndrome. *Autism Res.* 2, 157–177. doi: 10.1002/aur.80

Chamekh, M., and Casimir, G. (2019). Editorial: sexual dimorphism of the immune inflammatory response in infectious and non-infectious diseases. *Front. Immunol.* 10:107. doi: 10.3389/fimmu.2019.00107

Chinnadurai, G. (2002). CtBP, an unconventional transcriptional corepressor in development and oncogenesis. *Mol. Cell* 9, 213–224. doi: 10.1016/s1097-2765(02)00443-4

Choi, G. B., Yim, Y. S., Wong, H., Kim, S., Kim, H., Kim, S. V., et al. (2016). The maternal interleukin-17a pathway in mice promotes autism-like phenotypes in offspring. *Science* 351, 933–939. doi: 10.1126/science.aad0314

Cisternas, C. D., Cabrera Zapata, L. E., Arevalo, M. A., Garcia-Segura, L. M., and Cambiasso, M. J. (2017). Regulation of aromatase expression in the anterior amygdala of the developing mouse brain depends on ERbeta and sex chromosome complement. *Sci. Rep.* 7:5320.

Cisternas, C. D., Tome, K., Caeiro, X. E., Dadam, F. M., Garcia-Segura, L. M., and Cambiasso, M. J. (2015). Sex chromosome complement determines sex differences in aromatase expression and regulation in the stria terminalis and anterior amygdala of the developing mouse brain. *Mol. Cell. Endocrinol.* 414, 99–110. doi: 10.1016/j.mce.2015.07.027

Coiro, P., and Pollak, D. D. (2019). Sex and gender bias in the experimental neurosciences: the case of the maternal immune activation model. *Transl. Psychiatry* 9:90.

Colborn, T. (2004). Neurodevelopment and endocrine disruption. *Environ. Health Perspect.* 112, 944–949. doi: 10.1289/ehp.6601

Constantinescu, C. S., Farooqi, N., O'Brien, K., and Gran, B. (2011). Experimental autoimmune encephalomyelitis (EAE) as a model for multiple sclerosis (MS). *Br. J. Pharmacol.* 164, 1079–1106. doi: 10.1111/j.1476-5381.2011.01302.x

Cui, J., Shipley, F. B., Shannon, M. L., Alturkistani, O., Dani, N., Webb, M. D., et al. (2020). Inflammation of the embryonic choroid plexus barrier following maternal immune activation. *Dev. Cell* 55, 617–628.e6.

Cury, D. B., Mizsputen, S. J., Versolato, C., Miiji, L. O., Pereira, E., Delboni, M. A., et al. (2013). Serum calprotectin levels correlate with biochemical and histological markers of disease activity in TNBS colitis. *Cell. Immunol.* 282, 66–70. doi: 10.1016/j.cellimm.2013.04.004

Dasgupta, S., Lonard, D. M., and O'malley, B. W. (2014). Nuclear receptor coactivators: master regulators of human health and disease. *Annu. Rev. Med.* 65, 279–292. doi: 10.1146/annurev-med-051812-145316

Dcona, M. M., Morris, B. L., Ellis, K. C., and Grossman, S. R. (2017). CtBP-an emerging oncogene and novel small molecule drug target: advances in the understanding of its oncogenic action and identification of therapeutic inhibitors. *Cancer Biol. Ther.* 18, 379–391. doi: 10.1080/15384047.2017.1323586

De Rubeis, S., He, X., Goldberg, A. P., Poultney, C. S., Samocha, K., Cicek, A. E., et al. (2014). Synaptic, transcriptional and chromatin genes disrupted in autism. *Nature* 515, 209–215.

Della Torre, S., Rando, G., Meda, C., Ciana, P., Ottobrini, L., and Maggi, A. (2018). Transcriptional activity of oestrogen receptors in the course of embryo development. *J. Endocrinol.* 238, 165–176. doi: 10.1530/joe-18-0003

Dietz, P. M., Rose, C. E., Mcarthur, D., and Maenner, M. (2020). National and state estimates of adults with autism spectrum disorder. *J. Autism Dev. Disord.* 50, 4258–4266. doi: 10.1007/s10803-020-04494-4

Driscoll, M. D., Sathya, G., Muyan, M., Klinge, C. M., Hilf, R., and Bambara, R. A. (1998). Sequence requirements for estrogen receptor binding to estrogen response elements. *J. Biol. Chem.* 273, 29321–29330. doi: 10.1074/jbc.273.45.29321

Duan, Y., Zeng, L., Zheng, C., Song, B., Li, F., Kong, X., et al. (2018). Inflammatory links between high fat diets and diseases. *Front. Immunol.* 9:2649. doi: 10.3389/fimmu.2018.02649

Ehrchen, J. M., Sunderkotter, C., Foell, D., Vogl, T., and Roth, J. (2009). The endogenous Toll-like receptor 4 agonist S100A8/S100A9 (calprotectin) as innate amplifier of infection, autoimmunity, and cancer. *J. Leukoc. Biol.* 86, 557–566. doi: 10.1189/jlb.1008647

El Hokayem, J., Amadei, C., Obeid, J. P., and Nawaz, Z. (2017). Ubiquitination of nuclear receptors. *Clin. Sci.* 131, 917–934. doi: 10.1042/cs20160708

Estes, M. L., and McAllister, A. K. (2016). Maternal immune activation: implications for neuropsychiatric disorders. *Science* 353, 772–777. doi: 10.1126/science.aag3194

Fan, X., Warner, M., and Gustafsson, J. A. (2006). Estrogen receptor beta expression in the embryonic brain regulates development of calretinin-immunoreactive GABAergic interneurons. *Proc. Natl. Acad. Sci. U.S.A.* 103, 19338–19343. doi: 10.1073/pnas.0609663103

Gal-Oz, S. T., Maier, B., Yoshida, H., Seddu, K., Elbaz, N., Czysz, C., et al. (2019). ImmGen report: sexual dimorphism in the immune system transcriptome. *Nat. Commun.* 10:4295.

Garcia-Arias, M., Pascual-Salcedo, D., Ramiro, S., Ueberschlag, M. E., Jermann, T. M., Cara, C., et al. (2013). Calprotectin in rheumatoid arthritis: association with disease activity in a cross-sectional and a longitudinal cohort. *Mol. Diagn. Ther.* 17, 49–56. doi: 10.1007/s40291-013-0016-9

Ginhoux, F., Greter, M., Leboeuf, M., Nandi, S., See, P., Gokhan, S., et al. (2010). Fate mapping analysis reveals that adult microglia derive from primitive macrophages. *Science* 330, 841–845. doi: 10.1126/science.1194637

Goldmann, T., Wieghofer, P., Jordao, M. J., Prutek, F., Hagemeyer, N., Frenzel, K., et al. (2016). Origin, fate and dynamics of macrophages at central nervous system interfaces. *Nat. Immunol.* 17, 797–805. doi: 10.1038/ni.3423

Greco, T. L., and Payne, A. H. (1994). Ontogeny of expression of the genes for steroidogenic enzymes P450 side-chain cleavage, 3 beta-hydroxysteroid dehydrogenase, P450 17 alpha-hydroxylase/C17-20 lyase, and P450 aromatase in fetal mouse gonads. *Endocrinology* 135, 262–268. doi: 10.1210/endo.135.1.8013361

Guy, J., Cheval, H., Selfridge, J., and Bird, A. (2011). The role of MeCP2 in the brain. *Annu. Rev. Cell Dev. Biol.* 27, 631–652. doi: 10.1146/annurev-cellbio-092910-154121

Haida, O., Al Sagheer, T., Balbous, A., Francheteau, M., Matas, E., Soria, F., et al. (2019). Sex-dependent behavioral deficits and neuropathology in a maternal immune activation model of autism. *Transl. Psychiatry* 9:124.

Hammer, G. D., Krylova, I., Zhang, Y., Darimont, B. D., Simpson, K., Weigel, N. L., et al. (1999). Phosphorylation of the nuclear receptor SF-1 modulates cofactor recruitment: integration of hormone signaling in reproduction and stress. *Mol. Cell* 3, 521–526. doi: 10.1016/s1097-2765(00)80480-3

Hanamsagar, R., and Bilbo, S. D. (2016). Sex differences in neurodevelopmental and neurodegenerative disorders: focus on microglial function and neuroinflammation during development. *J. Steroid Biochem. Mol. Biol.* 160, 127–133. doi: 10.1016/j.jsbmb.2015.09.039

Harada, N., and Yamada, K. (1992). Ontogeny of aromatase messenger ribonucleic acid in mouse brain: fluorometrical quantitation by polymerase chain reaction. *Endocrinology* 131, 2306–2312. doi: 10.1210/endo.131.5.1425429

Harkonen, P. L., and Vaananen, H. K. (2006). Monocyte-macrophage system as a target for estrogen and selective estrogen receptor modulators. *Ann. N. Y. Acad. Sci.* 1089, 218–227. doi: 10.1196/annals.1386.045

Helzer, K. T., Hooper, C., Miyamoto, S., and Alarid, E. T. (2015). Ubiquitylation of nuclear receptors: new linkages and therapeutic implications. *J. Mol. Endocrinol.* 54, R151–R167.

Hill, R. A. (2016). Sex differences in animal models of schizophrenia shed light on the underlying pathophysiology. *Neurosci. Biobehav. Rev.* 67, 41–56. doi: 10.1016/j.neubiorev.2015.10.014

Hull, L., Petrides, K. V., and Mandy, W. (2020). The female autism phenotype and camouflaging: a narrative review. *Rev. J. Autism Dev. Disord.* 7, 306–317. doi: 10.1007/s40489-020-00197-9

Hutchison, J. B., Beyer, C., Hutchison, R. E., and Wozniak, A. (1997). Sex differences in the regulation of embryonic brain aromatase. *J. Steroid Biochem. Mol. Biol.* 61, 315–322. doi: 10.1016/s0960-0760(97)80029-5

Ingvorsen, C., Karp, N. A., and Lelliott, C. J. (2017). The role of sex and body weight on the metabolic effects of high-fat diet in C57BL/6N mice. *Nutr. Diabetes* 7:e261. doi: 10.1038/nutd.2017.6

Jordao, M. J. C., Sankowski, R., Brendecke, S. M., Sagar, Locatelli, G., Tai, Y. H., et al. (2019). Single-cell profiling identifies myeloid cell subsets with distinct fates during neuroinflammation. *Science* 363:eaat7554. doi: 10.1126/science.aat7554

Keever, M. R., Zhang, P., Bolt, C. R., Antonson, A. M., Rymut, H. E., Caputo, M. P., et al. (2020). Lasting and sex-dependent impact of maternal immune activation on molecular pathways of the Amygdala. *Front. Neurosci.* 14:774. doi: 10.3389/fnins.2020.00774

Klein, S. L. (2012). Sex influences immune responses to viruses, and efficacy of prophylaxis and treatments for viral diseases. *Bioessays* 34, 1050–1059. doi: 10.1002/bies.201200099

Klein, S. L., and Flanagan, K. L. (2016). Sex differences in immune responses. *Nat. Rev. Immunol.* 16, 626–638. doi: 10.1038/nri.2016.90

Klinge, C. M. (2001). Estrogen receptor interaction with estrogen response elements. *Nucleic Acids Res.* 29, 2905–2919. doi: 10.1093/nar/29.14.2905

Konkle, A. T., and McCarthy, M. M. (2011). Developmental time course of estradiol, testosterone, and dihydrotestosterone levels in discrete regions of male and female rat brain. *Endocrinology* 152, 223–235. doi: 10.1210/en.2010-0607

Kovats, S. (2015). Estrogen receptors regulate innate immune cells and signaling pathways. *Cell. Immunol.* 294, 63–69. doi: 10.1016/j.cellimm.2015.01.018

Kuiper, G. G., Carlsson, B., Grandien, K., Enmark, E., Haggblad, J., Nilsson, S., et al. (1997). Comparison of the ligand binding specificity and transcript tissue distribution of estrogen receptors alpha and beta. *Endocrinology* 138, 863–870. doi: 10.1210/endo.138.3.4979

Lai, J. J., Lai, K. P., Chuang, K. H., Chang, P., Yu, I. C., Lin, W. J., et al. (2009). Monocyte/macrophage androgen receptor suppresses cutaneous wound healing in mice by enhancing local TNF-alpha expression. *J. Clin. Invest.* 119, 3739–3751. doi: 10.1172/jci39335

Lalevee, S., Ferry, C., and Rochette-Egly, C. (2010). Phosphorylation control of nuclear receptors. *Methods Mol. Biol.* 647, 251–266. doi: 10.1007/978-1-60761-738-9_15

Lannigan, D. A. (2003). Estrogen receptor phosphorylation. *Steroids* 68, 1–9. doi: 10.1016/s0039-128x(02)00110-1

Lasrado, N., Jia, T., Massilamany, C., Franco, R., Illes, Z., and Reddy, J. (2020). Mechanisms of sex hormones in autoimmunity: focus on EAE. *Biol. Sex Differ.* 11:50.

Loomes, R., Hull, L., and Mandy, W. P. L. (2017). What is the male-to-female ratio in autism spectrum disorder? A systematic review and meta-analysis. *J. Am. Acad. Child Adolesc. Psychiatry* 56, 466–474. doi: 10.1016/j.jaac.2017.03.013

Lord, C., Brugha, T. S., Charman, T., Cusack, J., Dumas, G., Frazier, T., et al. (2020). Autism spectrum disorder. *Nat. Rev. Dis. Primers* 6:5.

Lumeng, C. N., Deyoung, S. M., Bodzin, J. L., and Saltiel, A. R. (2007). Increased inflammatory properties of adipose tissue macrophages recruited during diet-induced obesity. *Diabetes* 56, 16–23. doi: 10.2337/db06-1076

Marco, E. J., and Skuse, D. H. (2006). Autism-lessons from the X chromosome. *Soc. Cogn. Affect. Neurosci.* 1, 183–193. doi: 10.1093/scan/nsl028

Matcovitch-Natan, O., Winter, D. R., Giladi, A., Vargas Aguilar, S., Spinrad, A., Sarrazin, S., et al. (2016). Microglia development follows a stepwise program to regulate brain homeostasis. *Science* 353:aad8670. doi: 10.1126/science.aad8670

May, T., Adesina, I., Mcgillivray, J., and Rinehart, N. J. (2019). Sex differences in neurodevelopmental disorders. *Curr. Opin. Neurol.* 32, 622–626. doi: 10.1097/wco.0000000000000714

McCarthy, M. M. (2008). Estradiol and the developing brain. *Physiol. Rev.* 88, 91–124. doi: 10.1152/physrev.00010.2007

McCarthy, M. M. (2016). Sex differences in the developing brain as a source of inherent risk. *Dialogues Clin. Neurosci.* 18, 361–372. doi: 10.31887/dcns.2016.18.4/mmccarthy

Merikangas, A. K., and Almasy, L. (2020). Using the tools of genetic epidemiology to understand sex differences in neuropsychiatric disorders. *Genes Brain Behav.* 19:e12660.

Mitra, S. W., Hoskin, E., Yudkovitz, J., Pear, L., Wilkinson, H. A., Hayashi, S., et al. (2003). Immunolocalization of estrogen receptor beta in the mouse brain: comparison with estrogen receptor alpha. *Endocrinology* 144, 2055–2067. doi: 10.1210/en.2002-221069

Moosa, A., Shu, H., Sarachana, T., and Hu, V. W. (2018). Are endocrine disrupting compounds environmental risk factors for autism spectrum disorder? *Horm. Behav.* 101, 13–21. doi: 10.1016/j.yhbeh.2017.10.003

Moras, D., and Gronemeyer, H. (1998). The nuclear receptor ligand-binding domain: structure and function. *Curr. Opin. Cell Biol.* 10, 384–391.

Mrdjen, D., Pavlovic, A., Hartmann, F. J., Schreiner, B., Utz, S. G., Leung, B. P., et al. (2018). High-dimensional single-cell mapping of central nervous system immune cells reveals distinct myeloid subsets in health, aging, and disease. *Immunity* 48, 380–395.e6.

Nagy, L., and Schwabe, J. W. (2004). Mechanism of the nuclear receptor molecular switch. *Trends Biochem. Sci.* 29, 317–324. doi: 10.1016/j.tibs.2004.04.006

Ngo, S. T., Steyn, F. J., and Mccombe, P. A. (2014). Gender differences in autoimmune disease. *Front. Neuroendocrinol.* 35:347–369. doi: 10.1016/j.yfrne.2014.04.004

Nichols, E. K., Chuang, H.-C., Davis, M. T., Geiger, K. M., Li, R. Z., Arnold, M. L., et al. (2020). Fetal innate immunity contributes to the induction of atypical behaviors in a mouse model of maternal immune activation. *bioRxiv* [Preprint]. doi: 10.1101/2020.10.09.333815

Nishikawa, Y., Kajiura, Y., Lew, J. H., Kido, J. I., Nagata, T., and Naruishi, K. (2017). Calprotectin induces IL-6 and MCP-1 production via Toll-like receptor 4 signaling in human gingival fibroblasts. *J. Cell. Physiol.* 232, 1862–1871. doi: 10.1002/jcp.25724

Olefsky, J. M. (2001). Nuclear receptor minireview series. *J. Biol. Chem.* 276, 36863–36864. doi: 10.1074/jbc.r100047200

Onore, C. E., Schwartzer, J. J., Careaga, M., Berman, R. F., and Ashwood, P. (2014). Maternal immune activation leads to activated inflammatory macrophages in offspring. *Brain Behav. Immun.* 38, 220–226. doi: 10.1016/j.bbi.2014.02.007

Pascual, G., Fong, A. L., Ogawa, S., Gamliel, A., Li, A. C., Perissi, V., et al. (2005). A SUMOylation-dependent pathway mediates transrepression of inflammatory response genes by PPAR-gamma. *Nature* 437, 759–763. doi: 10.1038/nature03988

Patterson, P. H. (2011). Maternal infection and immune involvement in autism. *Trends Mol. Med.* 17, 389–394. doi: 10.1016/j.molmed.2011.03.001

Percy, A. K. (2011). Rett syndrome: exploring the autism link. *Arch. Neurol.* 68, 985–989. doi: 10.1001/archneurol.2011.149

Perissi, V., and Rosenfeld, M. G. (2005). Controlling nuclear receptors: the circular logic of cofactor cycles. *Nat. Rev. Mol. Cell Biol.* 6, 542–554. doi: 10.1038/nrm1680

Pettersson, U. S., Walden, T. B., Carlsson, P. O., Jansson, L., and Phillipson, M. (2012). Female mice are protected against high-fat diet induced metabolic syndrome and increase the regulatory T cell population in adipose tissue. *PLoS One* 7:e46057. doi: 10.1371/journal.pone.0046057

Quintero, O. L., Amador-Patarroyo, M. J., Montoya-Ortiz, G., Rojas-Villarraga, A., and Anaya, J. M. (2012). Autoimmune disease and gender: plausible mechanisms for the female predominance of autoimmunity. *J. Autoimmun.* 38, J109–J119.

Ribas, V., Drew, B. G., Le, J. A., Soleymani, T., Daraei, P., Sitz, D., et al. (2011). Myeloid-specific estrogen receptor alpha deficiency impairs metabolic homeostasis and accelerates atherosclerotic lesion development. *Proc. Natl. Acad. Sci. U.S.A.* 108, 16457–16462. doi: 10.1073/pnas.1104533108

Saijo, K., Collier, J. G., Li, A. C., Katzenellenbogen, J. A., and Glass, C. K. (2011). An ADIOL-ERbeta-CtBP transrepression pathway negatively regulates microglia-mediated inflammation. *Cell* 145, 584–595. doi: 10.1016/j.cell.2011.03.050

Savatt, J. M., and Myers, S. M. (2021). Genetic testing in neurodevelopmental disorders. *Front. Pediatr.* 9:526779. doi: 10.3389/fped.2021.526779

Schug, T. T., Blawas, A. M., Gray, K., Heindel, J. J., and Lawler, C. P. (2015). Elucidating the links between endocrine disruptors and neurodevelopment. *Endocrinology* 156, 1941–1951. doi: 10.1210/en.2014-1734

Sellers, K. J., Denley, M. C. S., Saito, A., Foster, E. M., Salgarella, I., Delogu, A., et al. (2020). Brain-synthesized oestrogens regulate cortical migration in a sexually divergent manner. *Eur. J. Neurosci.* 52, 2646–2663.

Shay, D. A., Vieira-Potter, V. J., and Rosenfeld, C. S. (2018). Sexually dimorphic effects of aromatase on neurobehavioral responses. *Front. Mol. Neurosci.* 11:374. doi: 10.3389/fnmol.2018.00374

Shindo, S., Chen, S. H., Gotoh, S., Yokobori, K., Hu, H., Ray, M., et al. (2020). Estrogen receptor alpha phosphorylated at Ser216 confers inflammatory function to mouse microglia. *Cell Commun. Signal.* 18:117.

Shuid, A. N., Jayusman, P. A., Shuid, N., Ismail, J., Kamal Nor, N., and Mohamed, I. N. (2021). Association between viral infections and risk of autistic disorder: an overview. *Int. J. Environ. Res. Public Health* 18:2817. doi: 10.3390/ijerph18062817

Sierra, A., Gottfried-Blackmore, A., Milner, T. A., Mcewen, B. S., and Bulloch, K. (2008). Steroid hormone receptor expression and function in microglia. *Glia* 56, 659–674. doi: 10.1002/glia.20644

Silvin, A., Chapuis, N., Dunsmore, G., Goubet, A. G., Dubuisson, A., Derosa, L., et al. (2020). Elevated calprotectin and abnormal myeloid cell subsets discriminate severe from mild COVID-19. *Cell* 182, 1401–1418.e18.

Sledziowska, M., Galloway, J., and Baudouin, S. J. (2020). Evidence for a contribution of the Nlgn3/Cyfip1/Fmr1 pathway in the pathophysiology

of autism spectrum disorders. *Neuroscience* 445, 31–41. doi: 10.1016/j.neuroscience.2019.10.011

Smith, S. E., Li, J., Garbett, K., Mirnics, K., and Patterson, P. H. (2007). Maternal immune activation alters fetal brain development through interleukin-6. *J. Neurosci.* 27, 10695–10702. doi: 10.1523/jneurosci.2178-07.2007

Suuronen, T., Nuutinen, T., Huuskonen, J., Ojala, J., Thornell, A., and Salminen, A. (2005). Anti-inflammatory effect of selective estrogen receptor modulators (SERMs) in microglial cells. *Inflamm. Res.* 54, 194–203. doi: 10.1007/s00011-005-1343-z

Utz, S. G., See, P., Mildenberger, W., Thion, M. S., Silvin, A., Lutz, M., et al. (2020). Early fate defines microglia and non-parenchymal brain macrophage development. *Cell* 181, 557–573.e18.

Van Hove, H., Martens, L., Scheyltjens, I., De Vlaminck, K., Pombo Antunes, A. R., De Prijck, S., et al. (2019). A single-cell atlas of mouse brain macrophages reveals unique transcriptional identities shaped by ontogeny and tissue environment. *Nat. Neurosci.* 22, 1021–1035. doi: 10.1038/s41593-019-0393-4

Vazquez-Martinez, E. R., Garcia-Gomez, E., Camacho-Arroyo, I., and Gonzalez-Pedrajo, B. (2018). Sexual dimorphism in bacterial infections. *Biol. Sex Differ.* 9:27.

Vegeto, E., Belcredito, S., Etteri, S., Ghisletti, S., Brusadelli, A., Meda, C., et al. (2003). Estrogen receptor-alpha mediates the brain antiinflammatory activity of estradiol. *Proc. Natl. Acad. Sci. U.S.A.* 100, 9614–9619. doi: 10.1073/pnas.1531957100

Villa, A., Rizzi, N., Vegeto, E., Ciana, P., and Maggi, A. (2015). Estrogen accelerates the resolution of inflammation in macrophagic cells. *Sci. Rep.* 5:15224.

Villa, A., Vegeto, E., Poletti, A., and Maggi, A. (2016). Estrogens, neuroinflammation, and neurodegeneration. *Endocr. Rev.* 37, 372–402. doi: 10.1210/er.2016-1007

Waddell, J., and McCarthy, M. M. (2012). Sexual differentiation of the brain and ADHD: what is a sex difference in prevalence telling us? *Curr. Top. Behav. Neurosci.* 9, 341–360. doi: 10.1007/7854_2010_114

Walsham, N. E., and Sherwood, R. A. (2016). Fecal calprotectin in inflammatory bowel disease. *Clin. Exp. Gastroenterol.* 9, 21–29. doi: 10.2147/ceg.s51902

Wang, L., Andersson, S., Warner, M., and Gustafsson, J. A. (2003). Estrogen receptor (ER)beta knockout mice reveal a role for ERbeta in migration of cortical neurons in the developing brain. *Proc. Natl. Acad. Sci. U.S.A.* 100, 703–708. doi: 10.1073/pnas.242735799

Wang, Q., Chen, W., and Lin, J. (2019). The role of calprotectin in rheumatoid arthritis. *J. Transl. Int. Med.* 7, 126–131. doi: 10.2478/jtim-2019-0026

Wu, W. F., Tan, X. J., Dai, Y. B., Krishnan, V., Warner, M., and Gustafsson, J. A. (2013). Targeting estrogen receptor beta in microglia and T cells to treat experimental autoimmune encephalomyelitis. *Proc. Natl. Acad. Sci. U.S.A.* 110, 3543–3548. doi: 10.1073/pnas.1300313110

Xuan, I. C., and Hampson, D. R. (2014). Gender-dependent effects of maternal immune activation on the behavior of mouse offspring. *PLoS One* 9:e104433. doi: 10.1371/journal.pone.0104433

Zerbo, O., Iosif, A. M., Walker, C., Ozonoff, S., Hansen, R. L., and Hertz-Picciotto, I. (2013). Is maternal influenza or fever during pregnancy associated with autism or developmental delays? Results from the CHARGE (CHildhood Autism Risks from Genetics and Environment) study. *J. Autism Dev. Disord.* 43, 25–33. doi: 10.1007/s10803-012-1540-x

Zerbo, O., Qian, Y., Yoshida, C., Grether, J. K., Van De Water, J., and Croen, L. A. (2015). Maternal infection during pregnancy and autism spectrum disorders. *J. Autism Dev. Disord.* 45, 4015–4025. doi: 10.1007/s10803-013-2016-3

Zettergren, A., Jonsson, L., Johansson, D., Melke, J., Lundstrom, S., Anckarsater, H., et al. (2013). Associations between polymorphisms in sex steroid related genes and autistic-like traits. *Psychoneuroendocrinology* 38, 2575–2584. doi: 10.1016/j.psyneuen.2013.06.004

Zhang, X., Yang, J., Li, Y., Ma, X., and Li, R. (2017). Sex chromosome abnormalities and psychiatric diseases. *Oncotarget* 8, 3969–3979. doi: 10.18632/oncotarget.13962

Author Disclaimer: Any opinions, findings, and conclusions or recommendations expressed in this material are those of the author(s) and do not necessarily reflect the views of the National Science Foundation.

Conflict of Interest: The authors declare that the research was conducted in the absence of any commercial or financial relationships that could be construed as a potential conflict of interest.

Publisher's Note: All claims expressed in this article are solely those of the authors and do not necessarily represent those of their affiliated organizations, or those of the publisher, the editors and the reviewers. Any product that may be evaluated in this article, or claim that may be made by its manufacturer, is not guaranteed or endorsed by the publisher.

frontiers in Molecular Neuroscience

ORIGINAL RESEARCH
published: 03 September 2021
doi: 10.3389/fnmol.2021.718387

Period 2: A Regulator of Multiple Tissue-Specific Circadian Functions

*Gennaro Ruggiero[1,2], Zohar Ben-Moshe Livne[3], Yair Wexler[3], Nathalie Geyer[1], Daniela Vallone[1], Yoav Gothilf[3,4] and Nicholas S. Foulkes[1]**

[1] Institute of Biological and Chemical Systems, Karlsruhe Institute of Technology, Karlsruhe, Germany, [2] Department of Physiology, Anatomy and Genetics, University of Oxford, Oxford, United Kingdom, [3] School of Neurobiology, Biochemistry and Biophysics, Faculty of Life Sciences, Tel Aviv University, Tel Aviv, Israel, [4] Sagol School of Neuroscience, Tel Aviv University, Tel Aviv, Israel

The zebrafish represents a powerful model for exploring how light regulates the circadian clock due to the direct light sensitivity of its peripheral clocks, a property that is retained even in organ cultures as well as zebrafish-derived cell lines. Light-inducible expression of the *per2* clock gene has been predicted to play a vital function in relaying light information to the core circadian clock mechanism in many organisms, including zebrafish. To directly test the contribution of *per2* to circadian clock function in zebrafish, we have generated a loss-of-function *per2* gene mutation. Our results reveal a tissue-specific role for the *per2* gene in maintaining rhythmic expression of circadian clock genes, as well as clock-controlled genes, and an impact on the rhythmic behavior of intact zebrafish larvae. Furthermore, we demonstrate that disruption of the *per2* gene impacts on the circadian regulation of the cell cycle *in vivo*. Based on these results, we hypothesize that in addition to serving as a central element of the light input pathway to the circadian clock, *per2* acts as circadian regulator of tissue-specific physiological functions in zebrafish.

Keywords: circadian clock, zebrafish, period, cell cycle, behavior, metabolism

OPEN ACCESS

Edited by:
Estela Maris Muñoz, CONICET Dr. Mario H. Burgos Institute of Histology and Embryology (IHEM), Argentina

Reviewed by:
Elise Cau, CNRS Délégation Occitanie, France
Mario Eduardo Guido, National University of Córdoba (CIQUIBIC), Argentina

****Correspondence:***
Nicholas S. Foulkes
nicholas.foulkes@kit.edu

Specialty section:
This article was submitted to Molecular Signalling and Pathways, a section of the journal Frontiers in Molecular Neuroscience

Received: *31 May 2021*
Accepted: *03 August 2021*
Published: *03 September 2021*

Citation:
Ruggiero G, Ben-Moshe Livne Z, Wexler Y, Geyer N, Vallone D, Gothilf Y and Foulkes NS (2021) Period 2: A Regulator of Multiple Tissue-Specific Circadian Functions. Front. Mol. Neurosci. 14:718387. doi: 10.3389/fnmol.2021.718387

INTRODUCTION

The circadian clock is an endogenous and self-sustaining timing mechanism present in most organisms, which evolved to anticipate daily environmental changes and thereby to coordinate physiological and behavioral adaptations (Pittendrigh, 1993). Consistent with its central coordinating role within physiology, disruption of the circadian timing system is associated with many pathological conditions (Toh et al., 2001; Turek et al., 2005; Savvidis and Koutsilieris, 2012). A vital feature of the internal clock is that external environmental signals (*zeitgebers*, primarily light, but also food and temperature changes) can regularly adjust the phase of the circadian system to ensure synchronization with the environmental day-night cycle.

In vertebrates, at the core of the molecular mechanism of the circadian clock is a series of interlocking transcription-translation feedback loops. The positive limb of these regulatory loops is constituted by the transcription factors CLOCK and BMAL, which heterodimerize, bind to E-box enhancer promoter elements and thereby activate the transcription of downstream clock target genes. These include genes which constitute the negative limb of the clock mechanism, the period (*Per*) and cryptochrome (*Cry*) genes. Following translation, the PER and CRY proteins

heterodimerize, translocate back to the nucleus, and inhibit transcriptional activation directed by CLOCK/BMAL (Partch et al., 2014). CLOCK and BMAL also regulate the expression of other, clock-controlled genes (CCGs) including the transcription factors *Rev-erbα* and *Rorα* which form a stabilizing regulatory loop within the core clock mechanism.

Over the course of vertebrate evolution, the regulatory mechanisms, as well as the anatomical organization which underlies the circadian timing system, have undergone several changes (Menaker et al., 1997). At the anatomical level, in mammals the circadian timing system is characterized by a "master" clock located in the suprachiasmatic nucleus (SCN) of the hypothalamus with multiple independent "peripheral" clocks distributed in most tissues, organs and cells. This SCN clock receives light input indirectly from the retina and is thereby synchronized with the external solar day. It subsequently relays this timing information to the peripheral clocks via a variety of endocrine and systemic cues (Schibler and Sassone-Corsi, 2002; Schibler et al., 2015). In contrast, in non-mammalian vertebrates, a directly light-entrainable circadian oscillator is distributed in multiple tissues including the pineal gland, retina, and various brain nuclei, predicting the widespread expression of photoreceptors and elements of the clock light input pathway (Fukada and Okano, 2002). An extreme independence of central clock regulation can be seen in teleost fish where all peripheral clocks can be directly light-entrained (Whitmore et al., 1998; Sassone-Corsi et al., 2000; Foulkes, 2016). At the genomic level, several clock genes have undergone duplications and probably species-specific and tissue-specific sub-functionalization. The *per* gene has three homologs in mammals and four homologs in fish, *per1a*, *per1b*, *per2,* and *per3*.

The *per2* gene has been predicted to play an important role in the photic entrainment mechanism of the circadian clock in the vertebrate circadian timing mechanism. Indeed, levels of *per1* and *per2* mRNA expression are transiently induced in response to light exposure, in the mouse SCN (Albrecht et al., 1997; Bae et al., 2001). Furthermore, in zebrafish the expression of the *per2* gene is induced robustly following direct exposure of intact larvae, isolated tissues, cells and even cell lines to light via the effect of a D-box enhancer promoter element located in the *per2* gene promoter region (Vatine et al., 2009; Mracek et al., 2012). In addition to light-entrainment, PER2 is linked with the clock mechanism itself, as the S752G PER2 mutation in humans leads to hypo-phosphorylation, PER2 stabilization, and a familial advanced sleep-phase syndrome (FASPS) phenotype (Toh et al., 2001). Via its ability to downregulate transactivation driven by the CLOCK/BMAL complex within the core clock mechanism, the PER2 protein appears to contribute to the circadian regulation of a wide range of cellular functions (Albrecht et al., 2007), including metabolism and cell cycle (Fu et al., 2002; Grimaldi et al., 2010; Gu et al., 2012).

Several studies have also pinpointed a direct role for the PER2 protein, independent of its function within the core circadian clock. Thus, in zebrafish, the PER2 protein has been implicated in the direct transcriptional regulation of the *bmal1* gene via the retinoic acid—related orphan receptor response element (RORE) binding sites in zebrafish (Wang et al., 2015). Furthermore, we have shown that light-induced expression of *per2* during early embryonic development is a prerequisite for the development of a functional circadian clock system (Ziv and Gothilf, 2006). In addition, in mouse, it has been implicated as a tumor suppressor gene (Fu et al., 2002). Therefore, current evidence points to this clock protein playing a diverse role in the dynamic control of physiological systems, including the cell cycle.

In this report, we have explored the function of the *per2* clock gene in zebrafish by generating a new *per2* knockout (KO) zebrafish line. Specifically, using TALEN technology, we introduced a truncation mutation into the zebrafish *per2* locus, and then characterized the resulting phenotype of the *per2* KO zebrafish line. We show that loss of *per2* gene function results in an abnormal pattern of rhythmic locomotor activity in *per2* KO larvae under different lighting conditions and conclude that *per2* plays an essential role in the regulation of circadian phase and amplitude of behavioral rhythms and their entrainment by light. Moreover, we demonstrate a tissue-specific function for the *per2* gene in the maintenance of rhythmic expression of core circadian clock genes and CCGs. Finally, we reveal that disruption of *per2* gene function impacts on circadian regulation of the cell cycle *in vivo*. Therefore, these results point to a pleiotropic function for the *per2* gene in circadian regulation of tissue specific function.

MATERIALS AND METHODS

Animals

Wild type (WT) and corresponding *per2* KO sibling AB strain zebrafish lines were raised at 28°C under a 14 h:10 h light/dark cycle from the hatching stage. Lights were turned on at 8:00 and turned off at 22:00 and the fish were fed twice daily. To generate embryos, male and female zebrafish were paired in the evening, and spawning occurred the next day within 1 h after lights on. For locomotor activity analysis, embryos were transferred into 48-well plates (one larva per well) during the 4th or 5th day of development and placed into the DanioVision observation chamber (Noldus Information Technology). All zebrafish procedures were approved by the Tel-Aviv University Animal Care Committee (04-18-051) and conducted in accordance with the National Council for Animal Experimentation, Ministry of Health, Israel. At the Karlsruhe Institute of Technology, all husbandry and experimental procedures were performed in accordance with European Legislation for the Protection of Animals used for Scientific Purposes (Directive 2010/63/EU), the German Animal Protection Law [May 18th, 2006 (BGBl. I S. 1206, 1313), last changed March 29th, 2017 (BGBl. I S. 626)]. Research was also approved by the Local Government of Baden-Württemberg, Karlsruhe, Germany (35-9185.81/G-131/16 and 35-9185.82/A-9/18). General license for fish maintenance and breeding: Az.: 35-9185.64.

Generation of *per2* KO Fish

Genome editing with the transcription activator-like effector nucleases (TALEN) system was used to generate *per2* KO fish, registered in the Zebrafish Model Organism Database

(ZFIN) as *per2*^{tlv02}. Specific TALENs designed to target the 2nd exon of *per2* (TALE F target sequence 5′-tcagcactactggtgtca-3′, TALE R target sequence 5′-tgaaaatcacaaattacc-3′) were obtained from Addgene (TAL3138 and TAL3139, Addgene plasmids #41312 and #41313). The TALE nuclease expression vectors were linearized with PmeI and transcribed using mMESSAGE mMACHINE T7 kit (Ambion) followed by the Poly-A tailing kit (Ambion) according to the manufacturer's protocol. Approximately 2 nl of the TALENs mRNA at concentration of 100 ng/μl each were microinjected into one-cell stage embryos (F0). The injected embryos were raised, and their progeny (F1) were fin-clipped and screened by PCR (using the primers: per2-E2-F 5′-gccagtttcgcagaaggcactg-3′, per2-I2-R 5′-agccatcaggtctcaactgtttgtca-3′) followed by T7E1 assay for identifying mutations in *per2* coding sequence. A male and female F1 fish carrying the same 8 bp deletion mutation in *per2* exon 2 (**Figure 1**) were identified by sequencing and crossed to produce homozygous KO fish (F2) and their WT siblings. The progeny of the F2 mutated homozygotes and of their WT siblings were used for behavioral analysis, raising a possibility of observing maternal effects of the mutation. However, the lack of any conclusive evidence for maternal inheritance of circadian clock function in zebrafish makes such a maternal effect unlikely (Whitmore et al., 1998).

Locomotor Activity Monitoring of Zebrafish Larvae and Statistical Analysis

Homozygous *per2* KO embryos and control embryos (progeny of WT siblings) were raised in a light- and temperature-controlled incubator under 12-h:12-h LD cycles or constant darkness at 28°C. On the 4th or 5th day of development, larvae were placed in 48-well plates in the observation chamber of the DanioVision tracking system (Noldus Information Technology) for acclimation under controlled temperature (28°C) and lighting conditions (LED; intensity of "light" and "dim light" were 1.8 W/m^2 and 0.013 W/m^2, respectively) according to the desired protocol. Starting from the 6th day of development, movement was tracked and analyzed by the EthoVision XT 11 software (Noldus Information Technology). Locomotor activity was measured across three daily cycles by the total distance moved (cm) by each larva per 10 min time-bins. All experiments were repeated independently two to four times, the results shown in **Figure 2** are of one representative experiment.

For the analysis of circadian activity under constant conditions (**Figures 2A–C**), normalization of the data was obtained by dividing each activity value by the mean activity value. Short-term trends were removed by a LOESS-smoothed 75th-percentile function (Benjamini et al., 2011) with half window widths of 3.33 h (20 sliding points) for the moving percentiles and 8.33 h (50 sliding points) for the LOESS curve. Peaks (local maxima) and troughs (local minima) in the normalized smoothed curves were used to compute the period, phase and amplitude of the circadian locomotor activity rhythms. Period was estimated as the weighted mean time difference (in hr) between each pair of consecutive peaks. Phase was estimated as the weighted mean direction [mean of circular quantities; (Jammalamadaka and SenGupta, 2001)] of peak time relative to the estimated period. Since higher amplitudes are less sensitive to noise, weight was assigned to each peak in proportion to its amplitude for estimating period and phase. The reported amplitude was defined as half the difference in normalized activity between the peak of the 2nd day of tracking and the preceding trough. Values are reported as mean ± standard error (SE). Statistical differences in period and amplitude between groups were determined by *t*-test, and statistical differences in phase were determined by Watson–Williams test for the homogeneity of means.

In an experiment with LD cycles (**Figure 2D**), smoothing was performed separately on each cycle with half window widths of 2.5 h (15 sliding points) for the moving percentiles and 4.17 h (25 sliding points) for the LOESS curve. In order to assess the difference in activity between groups under the light and dark conditions, the average distance moved (cm/10 min) was calculated for each larva separately for the light and for the dark segments. The activity values (log-transformed) of the two genotypes under the light and dark segments were compared by mixed model ANOVA.

Data plotted in **Figures 2A–D** (middle chart) is the average across larvae ± SE of the non-normalized LOESS-smoothed percentile functions, with each group consisting of 20–24 larvae.

FIGURE 1 | Above: Establishment of a TALEN-mediated *per2* KO zebrafish line. A pair of TALENs was used to target the 2nd exon of the zebrafish *per2* gene (TALEN left and right target sites are highlighted in yellow). A deletion of 8 bp (red dashes against a gray background) resulted in a frameshift mutation. **Below:** The consequent introduction of a premature stop codon and a predicted truncated PER2 protein of 160 aa compared with the 1399 aa WT protein. PER-ARNT-SIM domains (PAS, orange) and C-terminal of PAS domain (PAC, green) in the WT protein are indicated.

Gene Expression Analysis

Total RNA of zebrafish tissues was extracted using TRIzol reagent (Invitrogen) according to the manufacturer's instructions. The concentrations of RNA samples were assessed with a NanoDrop ND-1000 spectrometer (PeqLab). The quality of the RNA was determined after electrophoresis on an agarose gel to visualize the integrity of the ribosomal 28S, 18S, and 5S RNA bands. The first strand cDNA synthesis of total RNA was performed according to the manufacturer's protocol (Promega). Quantitative PCR was performed using the Step One Plus Real-Time PCR System (Applied Biosystems) and SYBR Green (Promega) master

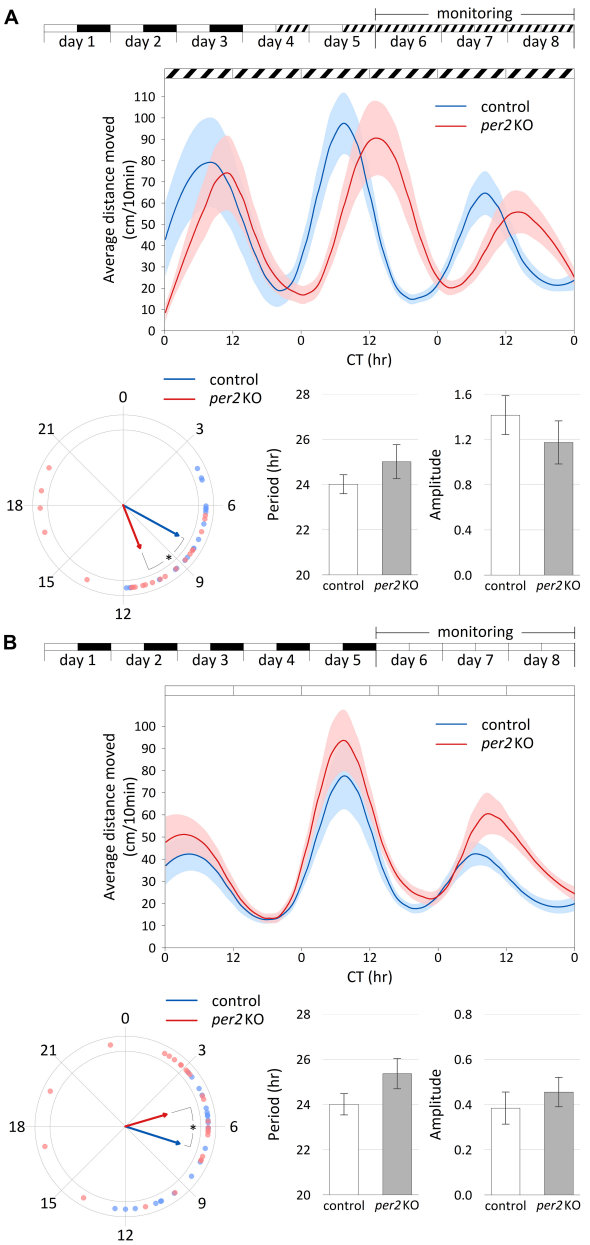

FIGURE 2 | Continued

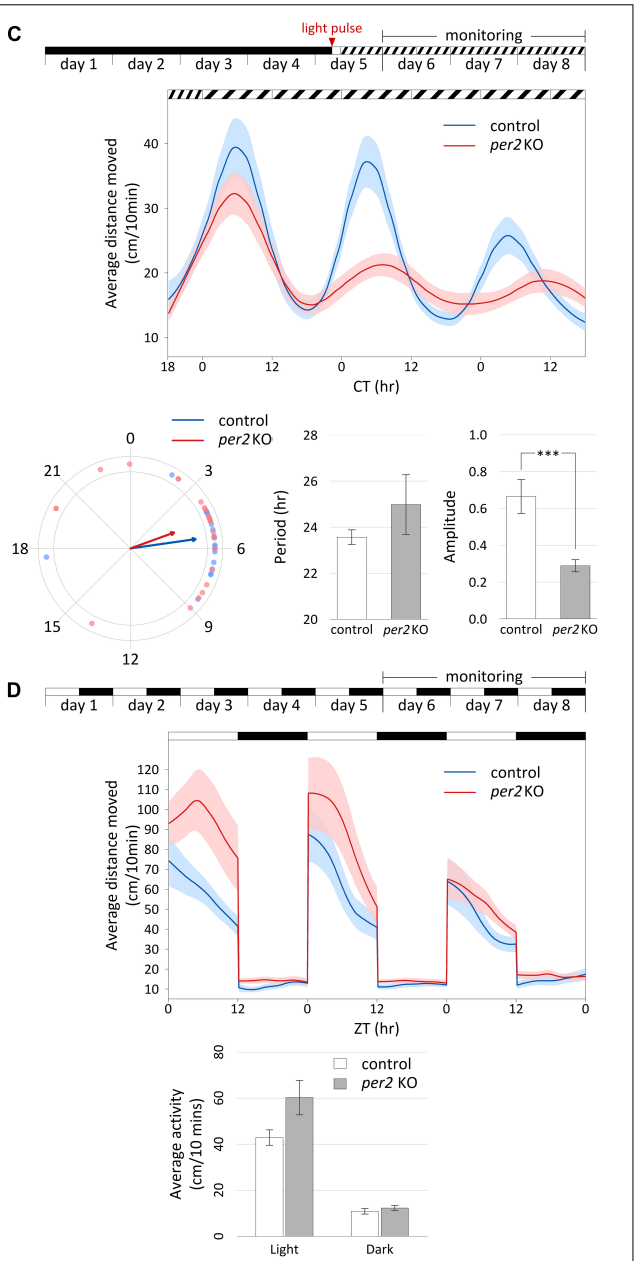

FIGURE 2 | *Per2* KO affects the phase of circadian rhythms of locomotor activity and their entrainment by light. Analysis of locomotor activity of 6–8 dpf *per2* KO and control larvae under various lighting conditions. **(A–D)** Top, experimental design of the photic treatment prior to and throughout activity monitoring. White boxes represent light, black boxes represent dark, and diagonally lined boxes represent dim light. Middle, the average distance moved (cm/10 min) is plotted on the *y*-axis and circadian time (CT) for panels **(A–C)** or *zeitgeber* time (ZT) for panel **(D)** is plotted on the *x*-axis; error bars indicate SE. **(A–C)** Bottom from left to right, comparison of average phase, period (±SE) and amplitude (±SE) between genotypes. In the circular plot of circadian phase, arrow direction represents the average phase for each genotype and the length represents the variance (longer arrow stands for low variance and vice versa). **(D)** Bottom, comparison of average activity (±SE) between genotypes throughout the light and dark segments. **(A)** Circadian rhythms of locomotor activity under DimDim, after entrainment by 3 LD cycles and 2 light-dim light (LDim) cycles; *per2* KO larvae (n = 21) display a

(Continued)

FIGURE 2 | Continued
phase delay of 2.7 h compared to control larvae ($n = 20$; $p < 0.05$ (denoted by *), Watson–Williams test). **(B)** Circadian rhythms of locomotor activity under LL, after entrainment by 5 LD cycles; *per2* KO larvae ($n = 24$) display a phase advance of 2.3 h compared to control larvae ($n = 22$; $p < 0.05$ (denoted by *), Watson–Williams test). **(C)** Circadian rhythms of locomotor activity under DimDim, after exposure to a 3-h light pulse (indicated by red arrowhead); *per2* KO larvae ($n = 23$) display a decreased amplitude of activity rhythmicity compared to control larvae ($n = 23$; $p < 0.001$ (denoted by ***), *t*-test). **(D)** Locomotor activity under LD cycles is not affected by *per2* KO; no significant difference in average activity was observed between genotypes during both the light and the dark segments ($n = 24$ *per2* KO; $n = 23$ controls).

mix according to the manufacturers' recommendations. Primer sequences are shown in **Supplementary Table 1**. The relative expression levels for each gene were calculated by the $2^{-\Delta\Delta CT}$ method and normalized using the relative expression of β-actin.

Western Blotting

Protein extracts were prepared by homogenizing sample tissues in 1X Laemmli (6% SDS, 20% glycerol, 125 mM Tris pH 6.8, 0.01% bromophenol blue, 100 mM DTT) containing a 1X cocktail of protease inhibitors (Sigma-Aldrich) buffer. The samples were electrophoresed on an SDS polyacrylamide gel and transferred to an Immun-Blot [polyvinylidene difluoride (PVDF)] membrane (Millipore) by electroblotting. Antibody incubation and washing was performed following the manufacturers' recommendations and visualization was performed by using the ECL detection system (Bio-Rad). Images were acquired and analyzed by using the Image Lab Software (Bio-Rad).

Statistical Analysis of Gene Expression

Significance in the difference in gene expression dynamics between mutants and controls was assessed via a two-way ANOVA, fitted independently for each gene in each tissue. The ANOVA model consisted of three fixed effects: genotype (*per2* KO or WT siblings), time, and their interaction genotype × time (see detailed results in **Table 1**). A significant interaction indicates an alteration in the gene's expression dynamics in the mutants. A significant genotype effect indicates a total increase or reduction in expression level in the mutants across all time points. A significant time effect indicates non-constant expression over time as would be expected in the rhythmic genes chosen in this work. *Post hoc* analysis was performed in instances of significant interaction ($p < 0.05$), comparing the two genotypes at each time point individually. *P*-values were corrected using Sidak's method. Analysis was carried out using GraphPad Prism 7.0. All estimates are expressed as means ± SD of biological or technical replicates.

RESULTS

Altered Rhythmic Locomotor Activity in *per2* Mutant Larvae

In order to directly address the function of *per2* in zebrafish, we established a TALEN-based *per2* KO fish line. An 8 bp deletion was generated in the 2nd exon of *per2*, resulting in a frameshift which is predicted to encode a truncated protein of 160 amino acids (aa) instead of the 1399 aa WT PER2 protein (**Figure 1**). Without the crucial PAS protein-protein interaction domains, this small, truncated protein is predicted to lack the normal function that involves direct interaction with other transcriptional regulatory factors. The presence of this mutation was subsequently validated by PCR and DNA sequencing in each subsequent generation of the *per2* KO line.

In order to assess the impact of this TALEN-generated mutation on clock-regulated behavioral rhythms and their entrainment by light, we initially analyzed the rhythmic locomotor activity of *per2* KO and control larvae under different photic regimes. Following entrainment by LD cycles (Cahill et al., 1998) or by exposure to a single pulse of light (Ben-Moshe et al., 2014), WT larval zebrafish display daily rhythms of locomotor activity under constant conditions with higher activity levels during the subjective daytime, a pattern that is highly reproducible amongst independently raised families.

Locomotor activity was measured in LD-entrained *per2* KO and WT control larvae that were placed under constant dim light (DimDim; **Figure 2A**) or under constant light (LL; **Figure 2B**). Under both conditions, rhythms of locomotor activity were maintained with no significant difference in period or amplitude (DimDim, periods of 24.0 ± 0.4 and 25.0 ± 0.8 and amplitudes of 1.42 ± 0.17 and 1.17 ± 0.19 for control and *per2* KO larvae, respectively; LL, periods of 24.0 ± 0.5 h and 25.4 ± 0.7 h and amplitudes of 0.38 ± 0.07 and 0.46 ± 0.07 for control and *per2* KO larvae, respectively). However, substantial phase differences between the genotypes were observed under both conditions. Interestingly, the two lighting conditions induced an opposite effect. While under DimDim, *per2* KO larvae exhibited a phase delay of 2.7 h compared to the controls, under LL, *per2* KO larvae exhibited a phase advance of 2.3 h (DimDim, phases of 7.9 ± 0.5 and 10.6 ± 0.8 for control and *per2* KO larvae, respectively; $p < 0.05$, Watson–Williams test; LL, phases of 7.2 ± 0.6 and 4.9 ± 0.8 for control and *per2* KO larvae, respectively; $p < 0.05$, Watson–Williams test). Thus, loss of *per2* function induces a differential effect on the phase of locomotor activity rhythms which depends on the lighting conditions. The results under DimDim (**Figure 2A**) agree with a previous report with a different *per2* mutant, in which *per2* mutant larvae presented an approximately 2-h phase delay and a ∼1.1-h lengthened period under constant darkness (Wang et al., 2015).

When larvae raised in constant darkness were exposed to a single 3-h light pulse on the 5th day post-fertilization (dpf) and then monitored under DimDim (**Figure 2C**), a procedure which is sufficient to trigger and set the phase of high amplitude rhythms of locomotor activity (Ben-Moshe et al., 2014), *per2* KO larvae displayed a significantly lower amplitude of activity (0.66 ± 0.09 and 0.29 ± 0.03 for control and *per2* KO larvae, respectively, $p < 0.001$, *t*-test). However, the period and phase did not change significantly (periods of 23.6 ± 0.3 h and 25.0 ± 1.3 h and phases of 5.5 ± 0.4 and 4.7 ± 0.8 for control and *per2* KO larvae, respectively). These observations reflect the predicted role of PER2 in light-entrainment and are consistent with previous findings obtained by morpholino-mediated *per2* knock-down using a similar experimental setup (Ben-Moshe et al., 2014),

TABLE 1 | Under LD conditions, the *per2* knockout alters circadian rhythms of mRNA expression in (i) CCGs in the liver, heart, fins, muscles, gut and eyes (**Figure 4**), (ii) clock-controlled genes in the heart (**Figure 5**), (iii) regulators of key physiological hepatic processes in the liver (**Figure 6**), (iv) genes encoding enzymes involved in biosynthesis of non-essential amino acids in the liver (**Figure 7**), (v) regulators of skeletal muscle myogenesis and regeneration in the muscles (**Figure 8**), and in (vi) cell-cycle regulators in the fin (**Figure 9**).

Related figure	Tissue	Gene	Two-way ANOVA results		
			Genotype	Time	Genotype × Time
Figure 3	Embryo, whole body	*per1b*	<0.001***	<0.001***	n.s
		cry1a	<0.001***	<0.001***	<0.001***
		clock1	<0.001***	<0.001***	<0.001***
Figure 4	Liver	*cry1a*	<0.05*	<0.001***	<0.001***
	Heart		<0.001***	<0.001***	<0.001***
	Brain		n.s	<0.001***	n.s
	Fin		<0.05*	<0.001***	<0.05*
	Muscle		<0.001***	<0.001***	<0.001***
	Gut		<0.05*	<0.001***	<0.001***
	Eye		<0.001***	<0.001***	<0.001***
	Liver	*clock1*	n.s	<0.001***	<0.001***
	Heart		<0.05*	<0.001***	<0.001***
	Brain		n.s	<0.001***	n.s
	Fin		n.s	<0.001***	<0.001***
	Muscle		n.s	<0.001***	<0.001***
	Gut		n.s	<0.001***	<0.001***
	Eye		n.s	<0.001***	<0.001***
Figure 5	Heart	*timp3*	<0.001***	<0.001***	<0.001***
		cox6a2	<0.001***	<0.001***	<0.001***
		mef2a	<0.001***	<0.001***	<0.001***
		smad3a	<0.001***	<0.01**	<0.01**
Figure 6	Liver	*impdh2*	<0.01**	<0.001***	<0.001***
		hnf1a	<0.001***	n.s	<0.001***
		cyp1a	<0.001***	<0.001***	<0.001***
		ppargc1b	<0.01**	<0.001***	<0.01**
Figure 7	Liver	*glu1a*	n.s	<0.001***	<0.001***
		asns	<0.001***	<0.001***	<0.001***
		gtp2l	<0.001***	< 0.001***	<0.001***
		glud1b	<0.01**	<0.001***	<0.001***
		got1	n.s	<0.001***	<0.001***
		got2a	n.s	<0.001***	<0.001***
Figure 8	Muscle	*hsf2*	<0.001***	<0.001***	<0.001***
		myf6	<0.001***	<0.001***	<0.001***
Figure 9		*cyclin A2*	<0.001***	< 0.01***	<0.001***
	Fin	*cyclin B1*	<0.001***	<0.001***	<0.001***
		p21	<0.001***	<0.001***	<0.001***

*qRT-PCR was used to measure mRNA expression levels across five time points at 6 hourly intervals. Significance in the difference in gene expression dynamics between mutants and controls was assessed via a two-way ANOVA, fitted independently for each gene in each tissue. The ANOVA model consisted of three fixed effects: genotype (per2 KO or WT siblings), time, and their interaction genotype × time. A significant interaction indicates an alteration in the gene's expression dynamics in the mutants. A significant genotype effect indicates difference in the gene's average expression between the mutants and the controls across all time points. A significant time effect was exhibited in all tissues in almost all genes, indicating unsurprisingly that the expression over time is non-constant. The exception is hnf1a in the liver (**Figure 6**), whose rhythmic expression was maintained in the mutants, but with a 12 h phase-shift. No effect of per2 knockout on the circadian rhythm was observed in whole-body mRNA expression of the CCGs per1, cry1a and clock1 in embryos (**Figure 3**), as well as expression of cry1a and clock1 in adult brains. Darker green shading donotes calculated p values of <0.001, light green shading denotes p < 0.01 and grey shading denotes p < 0.05 (***p < 0.001, **p < 0.01, *p < 0.05).*

where circadian locomotor activity rhythms were similarly disrupted by this manipulation.

Under LD cycles (**Figure 2D**), the locomotor activity patterns of *per2* KO larvae were unaltered compared to control larvae. Both groups exhibited significantly higher activity during the light phase compared to the dark phase ($p < 0.0001$, ANOVA) due to a masking effect, in which activity is mainly determined by the lighting conditions and not by the clock. No significant differences were observed between the activity of the two groups during both the light and the dark segments, an observation that does not correspond to a previously reported experiment with another *per2* mutant, where *per2* mutant larvae displayed reduced overall locomotor activity under LD conditions compared to control larvae (Wang et al., 2015).

This dissimilar outcome from two *per2* mutant lines may reflect different experimental conditions or genetic backgrounds. Overall, our analysis supports an essential role for PER2 in the regulation of circadian phase and amplitude of behavioral rhythms and their entrainment by light.

Expression of Circadian Clock Genes in *per2* Mutant Zebrafish Larvae

In order to explore the consequences of loss of *per2* function at the gene expression level, we examined the pattern of rhythmic core clock gene expression in the *per2* mutants under normal LD (12 h light-12 h dark) cycle conditions. We initially compared the dynamic mRNA expression pattern of a subset of circadian clock genes (*clock1*, *cry1a,* and *per1b*) in whole body RNA extracts of WT sibling and *per2* mutant zebrafish larvae raised under LD cycle conditions (**Figure 3**). While our results revealed a small reduction in expression levels in the mutants in the case of all 3 clock genes, the overall expression pattern for these clock genes was comparable in the WT and mutant larvae.

Tissue-Specific Regulatory Roles of *per2* in Adult Zebrafish Peripheral Tissues

Since the whole-body expression pattern of clock genes did not differ greatly between *per2* mutants and WT fish, we next tested for tissue-specific differences in the expression of clock genes. We examined the rhythmic expression of the *cry1a* and *clock1* clock genes in liver, heart, brain, fin, muscle, gut, and eyes of WT and *per2* mutant zebrafish adults maintained under LD cycle conditions (**Figure 4**). Interestingly, a change in the rhythmic profile of *clock1* and *cry1a* expression was detected in the heart, liver, gut and muscle of the *per2* mutants relative to the WT fish.

Given the observation of tissue-specific changes in the rhythmic expression of certain clock genes in our zebrafish mutant, we next performed a gene expression analysis of CCGs in *per2* KO zebrafish heart, liver, and muscle under normal LD cycle conditions, as a first step toward evaluating the possible impact of the *per2* mutation on zebrafish cardiac, hepatic and skeletal muscle physiology.

For the heart, we examined the expression of the following CCGs: *timp3,* encoding a tissue inhibitor of matrix metalloproteinases that was identified as being circadian clock regulated in the mouse heart (Durgan and Young, 2010), *mef2a* a clock controlled transcription factor involved in heart development and myofibril assembly (Wang et al., 2005, 2007), *cox6a2* a nuclear-encoded cytochrome oxidase subunit involved in mitochondrial electron transport, that shows circadian modulation in the mouse heart (Martino et al., 2004) and *smad3a*, a TGF-β signaling gene exhibiting a circadian expression pattern throughout the brain of zebrafish larvae

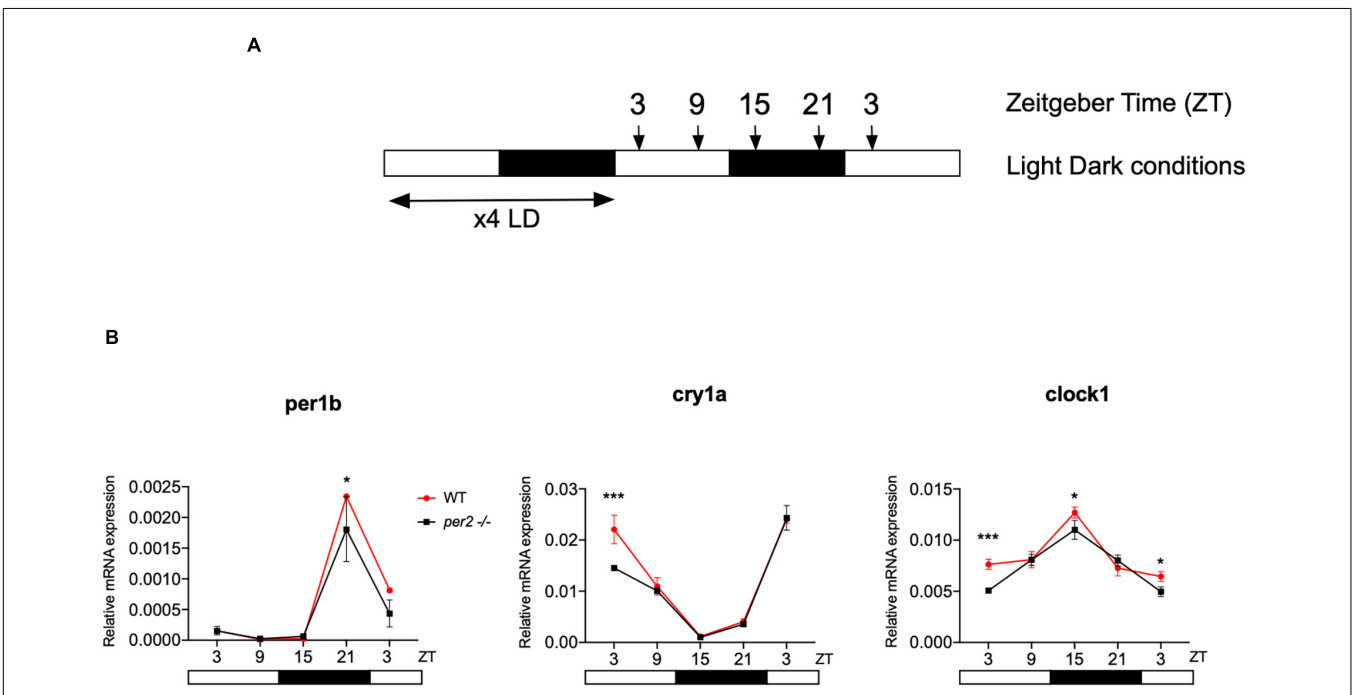

FIGURE 3 | Circadian clock gene expression analysis in *per2* KO and WT larvae. **(A)** Schematic representation of the experimental design. The horizontal bars represent the lighting conditions before and during sampling; white and black boxes indicate light and dark periods, respectively; the arrows show the sampling times. WT and *per2* mutant larvae were kept 4 dpf in LD cycle (12 h light-12 h dark) conditions. On the 5th dpf, total RNA was extracted from pools of larvae collected at 6-h intervals during a sampling window of 24 h. **(B)** qRT-PCR analysis of mRNA expression levels of the circadian clock genes (*clock1*, *cry1a*, and *per1b*) in WT and *per2* mutant larvae. Mean mRNA relative expression (n = 2–3) ± SD is plotted on the y-axis, while *zeitgeber* time (ZT) is plotted on the x-axis. ZT0 corresponds to lights-on, ZT12 to lights-off. A significant, small decrease in expression level was observed in mutants in all three genes (***$p < 0.001$, ANOVA genotype effect, **Table 1**). Asterisks represent levels of significance in comparing the two genotypes at each time point individually, corrected by Sidak's method (***$p < 0.001$, *$p < 0.05$).

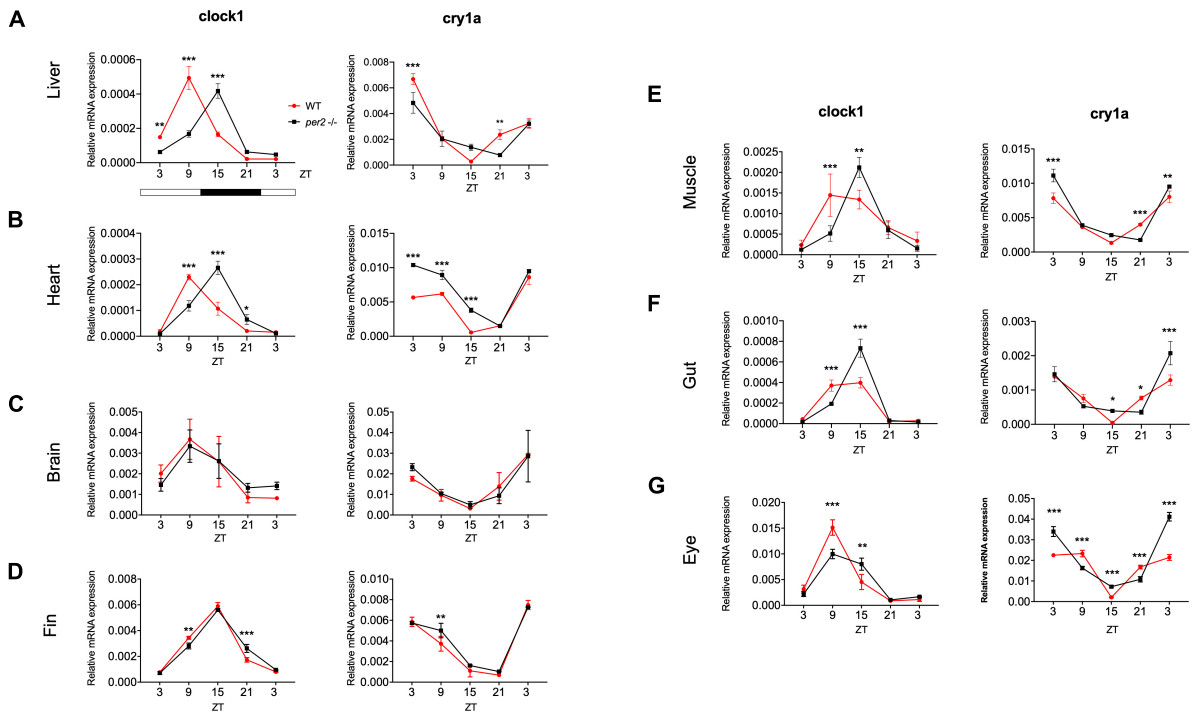

FIGURE 4 | *Per2* knockout alters rhythmic mRNA expression of the *cry1a* and *clock1* clock genes in adult zebrafish tissues. qRT-PCR analysis of expression levels of the circadian clock genes *clock1* and *cry1a* in the **(A)** liver, **(B)** heart, **(C)** brain, **(D)** fin, **(E)** muscle, **(F)** gut and **(G)** eyes of WT and *per2* mutant adult fish. Sets ($n = 3$) of 4 WT and *per2* KO fishes (each set containing two males and two females) were maintained under LD cycle (14 h light-10 h dark) conditions, tissues were dissected and pooled for RNA extraction at 6-h intervals during a sampling window of 24 h. Mean mRNA relative expression ± SD is plotted on the *y*-axis; *zeitgeber* time (ZT) is plotted on the *x*-axis. *Zeitgeber* times are indicated for each sample. ZT0 corresponds to lights-on, ZT14 to lights-off. A change in rhythm was observed for both genes in liver, heart, fin, muscle, gut, and eyes, as determined by a significant ANOVA Genotype × Time interaction effect ($p < 0.001$, see **Table 1**). For both genes, no effect was observed in the brain. Asterisks represent levels of significance in comparing the two genotypes at each time point individually, corrected by Sidak's method (***$p < 0.001$, **$p < 0.01$, *$p < 0.05$).

(Sato et al., 2012; Sloin et al., 2018; Finger et al., 2021). The circadian expression of each of these CCGs in *per2* KO heart tissue was affected, with a significant alteration of the circadian expression pattern, thus suggesting a potential involvement of *per2* in the circadian regulation of heart physiology in zebrafish (**Figure 5**). We then analyzed the expression of the *impdh2* [IMP dehydrogenase, a rate limiting enzyme in *de novo* purine synthesis (Li et al., 2013)], *cyp1a* [cytochrome P4501A, involved in detoxification (Carmona-Antoñanzas et al., 2017)], *ppargc1b* [Peroxisome proliferator-activated receptor gamma coactivator 1-beta, a transcriptional coactivator involved in multiple aspects of cellular energy metabolism (Lin et al., 2003)] and *hnf1a* [hepatocyte nuclear factor 4, alpha, involved in regulating liver-specific gene expression (Courtois et al., 1987)] genes which all encode regulators of key physiological hepatic processes and have been reported to show circadian rhythms of expression in zebrafish larvae (Li et al., 2013). The *cyp1a*, *ppargc1b,* and *hnf1a* genes all exhibited a significantly altered circadian expression pattern in the *per2* KO liver (**Figure 6**). Specifically, *cyp1a* showed a general reduction in expression levels and disrupted rhythmic expression. Furthermore, *ppargc1b* and *hnf1a* exhibited a 6 and 12 h phase delay of the rhythmic pattern, respectively. Interestingly, however, the phase of rhythmic expression of *impdh2* resembled that observed in WT liver controls, suggesting that the precise pattern of disrupted rhythmic gene expression upon loss of *per2* function differs between CCGs. Given the central role played by the circadian clock in regulating key metabolic pathways including amino acid biosynthesis (Krishnaiah et al., 2017), we next chose to test if the circadian expression of a set of CCGs encoding key or rate-limiting enzymes involved in the biosynthetic pathways for non-essential amino acids (Li et al., 2013), was affected in the *per2* KO liver. We specifically tested expression of *got1* and *got2a* (glutamic-oxaloacetic transaminase 1, and 2a) which are linked with the aspartate biosynthesis pathway), asparagine synthetase (*asns*) mediating asparagine production, glutamate dehydrogenase 1b (*glud1b*), mediating glutamate synthesis, glutamine synthetase 1a (*glu1a*), catalyzing glutamine formation and glutamic pyruvate transaminase 2-like (*gpt2l*), involved in alanine biosynthesis. Significant changes in the pattern of rhythmic expression of all six CCGs were observed in *per2* KO liver (**Figure 7**). Specifically, *gtp2l, asns,* and *got1* all displayed a reduced amplitude of rhythmic expression. Furthermore, *glud1b, asns*, *got1,* and *got2a* exhibited a phase shift of approximately 6 h, as previously observed for clock gene expression.

Expression of CCGs in the *per2* KO skeletal muscle was also tested. In particular, based on a previous study that identified putative CCGs in skeletal muscle of the zebrafish

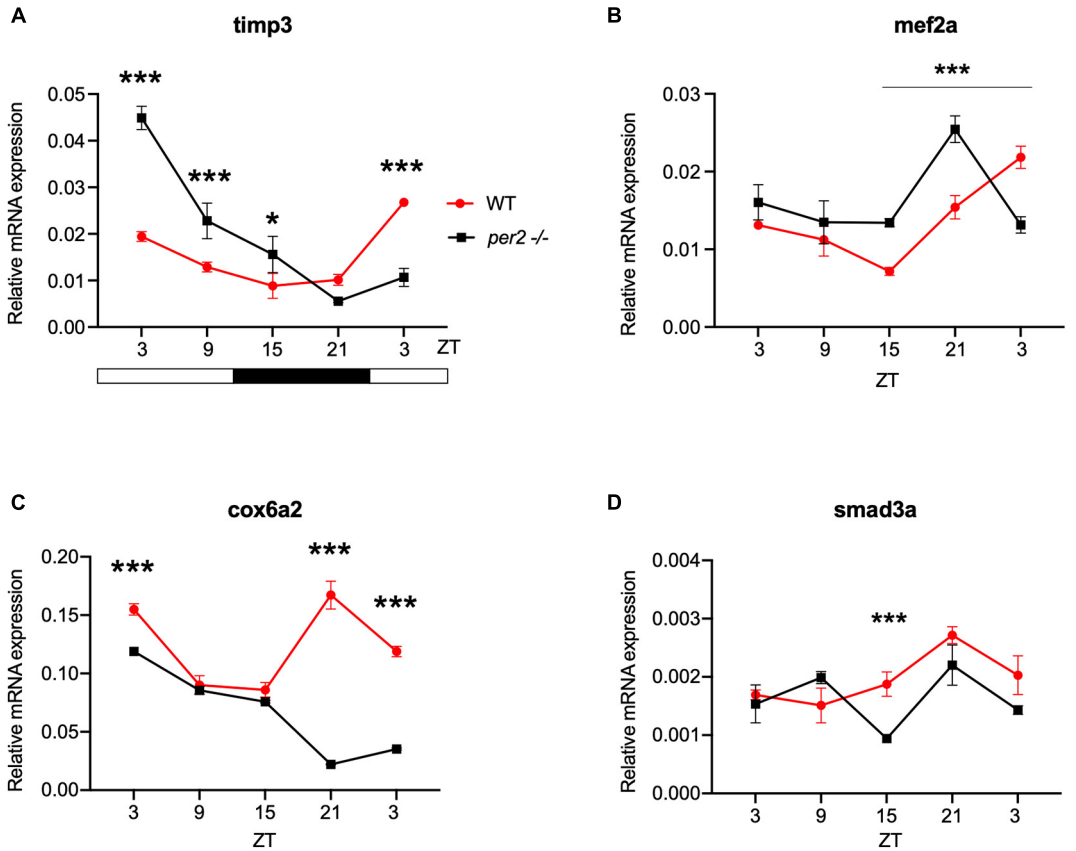

FIGURE 5 | *Per2* knockout alters the rhythmic mRNA expression of clock-controlled genes in the adult zebrafish heart. qRT-PCR analysis of expression levels of four putative CCGs **(A)** *timp3,* **(B)** *mef2a*, **(C)** *cox6a2,* and **(D)** *smad3a* in WT and *per2* KO heart tissues. Sets (n = 3) of 4 WT and *per2* KO fish (each set containing two males and two females) were maintained under LD cycle (14 h light-10 h dark) conditions, hearts were dissected and pooled for RNA extraction at 6-h intervals during a sampling window of 24 h. Mean mRNA relative expression ± SD is plotted on the *y*-axis; *zeitgeber* time (ZT) is plotted on the *x*-axis. *Zeitgeber* times are indicated for each sample. ZT0 corresponds to lights-on, ZT14 to lights-off. A change in rhythm was observed for *timp3*, *cox6a2, mef2a,* and *smad3a*, as determined by a significant ANOVA Genotype × Time interaction effect for all genes ($p < 0.01$, see **Table 1**). Asterisks represent levels of significance in comparing the two genotypes at each time point individually, corrected by Sidak's method (***$p < 0.001$, *$p < 0.05$).

(Amaral and Johnston, 2012), we tested the expression of *myf6* and *hsf2* (**Figure 8**), that play an important role during skeletal muscle myogenesis and regeneration (McArdle et al., 2006; Hinits et al., 2007; Wang et al., 2008; Chong et al., 2009; Amaral and Johnston, 2012). We revealed that both *hsf2* and *myf6* exhibited a significant alteration in their rhythmic expression pattern in *per2* KO skeletal muscle. Rhythmic *Myf6* expression showed a phase delay of 6 h that matches the phase shift observed in the expression pattern of the clock genes *cry1a* and *clock1* while *hsf2* exhibited a robust reduction of rhythm amplitude. Thus, taken together, our findings (**Figures 4–8**) implicate the *per2* gene in playing a role in circadian clock regulation in a tissue- and gene-specific manner.

Abnormal Cell Cycle Control in *per2* KO Zebrafish

Given the proposed role of *per2* as a tumor suppressor gene we next investigated the contribution of the *per2* gene to the circadian regulation of the cell cycle in zebrafish. We tested the gene expression of the clock-controlled cell cycle checkpoint regulators *cyclin A2, cyclin B1* and *p21* in WT control and *per2* KO fins sampled *in vivo*. *p21* is a potent cyclin-dependent kinase inhibitor (CKI) which functions as a regulator of cell cycle progression from G1 to S phase, while *cyclin B1* and *cyclin A2* serve as regulators of the entry into M and S phase, respectively. In all cases, in the mutant samples we observed significant changes in the rhythmic profile of gene expression with a phase delay compared to WT fin controls (**Figure 9**).

In our previous studies, we have shown that M phase progression in zebrafish adult fin tissues, is gated to occur preferentially during the dark phase as a result of circadian clock regulation (Idda et al., 2012). Therefore, we tested whether dynamic changes in the levels of M phase were affected in the *per2* KO zebrafish adult fin tissues. We used a western blot assay to quantify levels of the phospho-H3 protein, a marker of chromatin compaction associated with mitosis, in the whole fin protein extracts of the WT and *per2* KO zebrafish lines. In agreement with our previous results (Idda et al., 2012), WT fin tissues exhibited a peak of phospho-H3 protein levels around ZT16 (**Figure 10**).

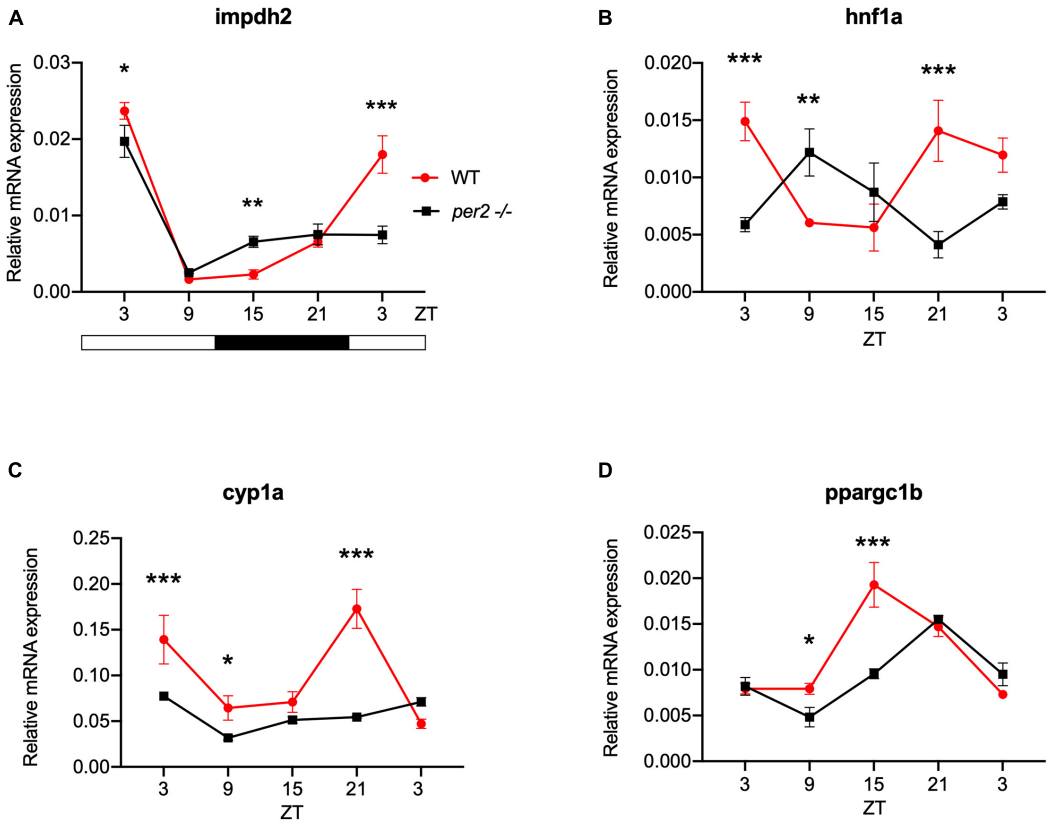

FIGURE 6 | *Per2* knockout alters the rhythmic mRNA expression of regulators of key physiological hepatic processes in the adult zebrafish liver. qRT-PCR analysis of expression levels of four CCGs **(A)** *impdh2,* **(B)** *hnf1a,* **(C)** *cyp1a,* and **(D)** *ppargc1b* in WT and *per2* KO liver. Sets of 4 WT and *per2* KO fishes (each set containing two males and two females) were maintained under LD cycle (14 h light-10 h dark) conditions, livers were dissected and pooled for RNA extraction at 6-h intervals during a sampling window of 24 h. Mean mRNA relative expression (n = 2–3) ± SD is plotted on the y-axis; *zeitgeber* time (ZT) is plotted on the x-axis. *Zeitgeber* times are indicated for each sample. ZT0 corresponds to lights-on, ZT14 to lights-off. A change in rhythm was observed for *impdh2*, *hnf1a, cyp1a* and *ppargc1b*, as determined by a significant ANOVA Genotype × Time interaction effect for all genes ($p < 0.01$, see **Table 1**). Furthermore, *hnf1a* exhibited a 12 h phase delay, and *ppargc1b* exhibited a 6 h phase delay. Asterisks represent levels of significance in comparing the two genotypes at each time point individually, corrected by Sidak's method (***$p < 0.001$, **$p < 0.01$, *$p < 0.05$).

Instead, in the *per2* KO fin tissues this peak was significantly reduced, consistent with abnormal circadian clock regulation of cell cycle progression in the *per2* KO proliferative fin tissues.

DISCUSSION

The data presented in this study point to a complex role for the *per2* gene in the circadian timing system in fish. In particular, we have demonstrated that the *per2* gene loss-of-function mutation affects rhythmic behavior of zebrafish larvae, the phase of rhythmic core clock gene expression, as well as the expression of certain CCGs in a tissue-specific manner. Finally, we reveal that loss of *per2* gene function is associated with abnormalities in the circadian regulation of the cell cycle *in vivo*.

Per2 Function Influences Clock-Controlled Behavior

The light inducible expression of the *per2* gene in the mammalian SCN as well as in the pineal gland, brain and peripheral tissues in fish point to an important role for the *per2* gene in the entrainment of the circadian clock by light. This prediction is supported here by the difference between WT and *per2* KO larvae in the amplitude and robustness of their locomotor activity rhythms in response to a 3-h light pulse. Nevertheless, the fact that the clock of *per2* KO fish is still somewhat entrained by light indicates the existence of mechanisms which compensate for the loss of *per2* gene function. It is tempting to speculate that the clock gene *cry1a* may be an element of such a mechanism. *Cry1a* is another robustly light-induced clock gene which is able to interact with other core clock proteins, such as CLOCK and BMAL (Tamai et al., 2007). In addition, we have previously shown that 1-h exposure to light is sufficient to induce the expression of several core clock genes or accessory clock genes (Ben-Moshe et al., 2014) suggesting the existence of additional compensatory factors.

In addition to light-entrainment, *per2* loss-of-function also strongly affects the phase of the locomotor activity rhythms, suggesting a role for PER2 in the clock mechanism itself. Interestingly, the effect of *per2* KO on the circadian phase is

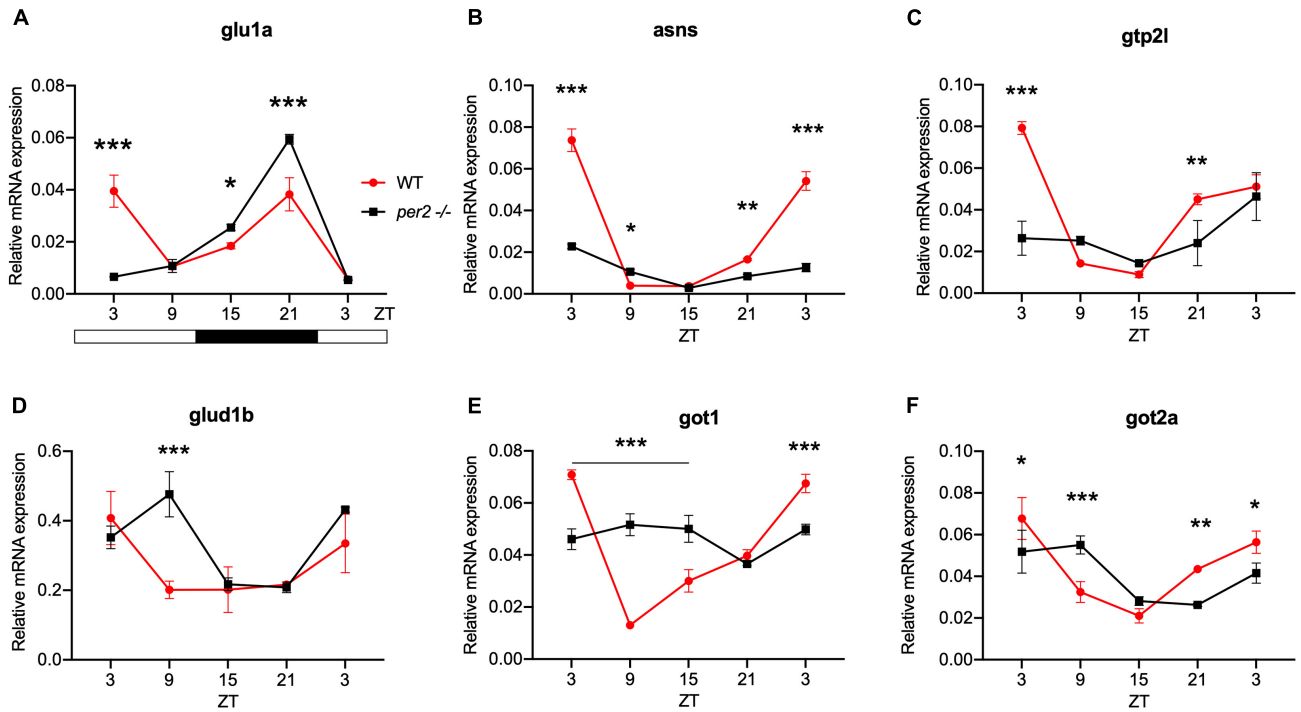

FIGURE 7 | *Per2* knockout alters the rhythmic mRNA expression of CCGs encoding key enzymes in non-essential amino acid synthesis in the adult zebrafish liver. qRT-PCR analysis of expression levels of six CCGs **(A)** *glu1a*, **(B)** *asns*, **(C)** *gpt2l* **(D)** *glud1b* **(E)** *got1,* and **(F)** *got2a* in WT and *per2* KO liver tissues as described in the legend for **Figure 6**. A change in rhythm was observed for all genes, as determined by a significant ANOVA Genotype × Time interaction effect for all genes ($p < 0.001$, see **Table 1**). Asterisks represent levels of significance in comparing the two genotypes at each time point individually, corrected by Sidak's method (***$p < 0.001$, **$p < 0.01$, *$p < 0.05$).

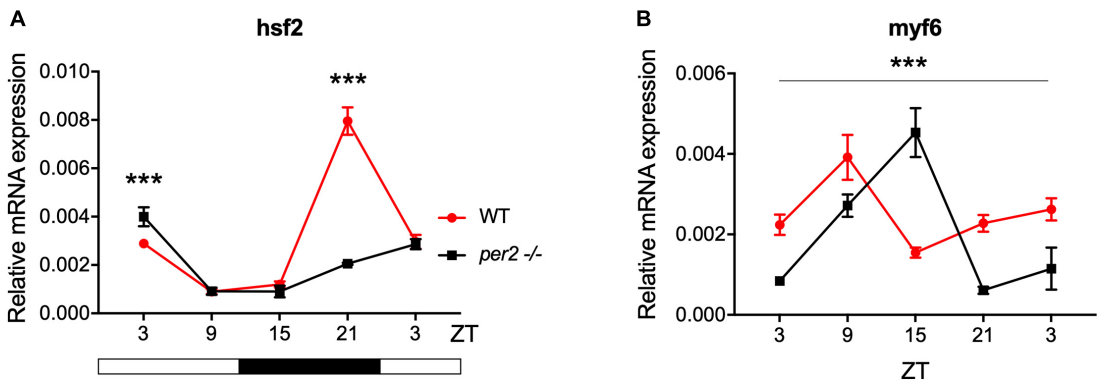

FIGURE 8 | *Per2* knockout alters the rhythmic mRNA expression of CCGs in adult zebrafish skeletal muscle. qRT-PCR analysis of expression levels of the CCGs **(A)** *hsf2* and **(B)** *myf6* in WT and *per2* KO skeletal muscle. Sets of 4 WT and *per2* KO fish (each set containing two males and two females) were maintained under LD cycle (14 h light-10 h dark) conditions, muscle tissue was dissected and pooled for RNA extraction at 6-h intervals during a sampling window of 24 h. Mean mRNA relative expression ($n = 2$–3) ± SD is plotted on the *y*-axis; *zeitgeber* time (ZT) is plotted on the *x*-axis. *Zeitgeber* times are indicated for each sample. ZT0 corresponds to lights-on, ZT14 to lights-off. A change in rhythm was observed for both CCGs, as determined by a significant ANOVA Genotype × Time interaction effect for all genes ($p < 0.001$, see **Table 1**). *myf6* exhibited a 6 h phase delay. Asterisks represent levels of significance in comparing the two genotypes at each time point individually, corrected by Sidak's method (***$p < 0.001$).

context-dependent – under constant dim-light *per2* KO led to a phase delay of 2.7 h while under constant light *per2* KO led to a phase advance of 2.3 h. Since zebrafish *per2* is a light-responsive gene, the light-dependence of *per2* KO effects may be predicted. It is tempting to speculate that the different phase shifts observed under different light intensities in the mutant might reflect accompanying differences in light-induced signal transduction in the larvae which subsequently differentially target PER2 function. Furthermore, the phase of the locomotor activity rhythms in the mutants shows a higher variability relative to WT

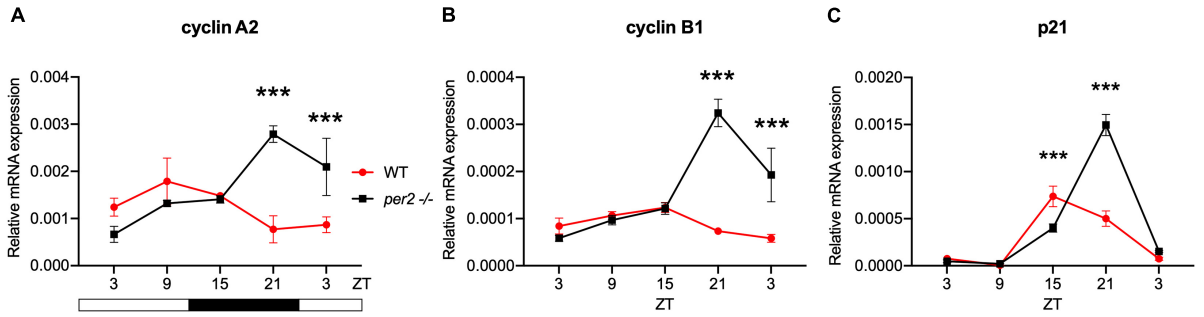

FIGURE 9 | *Per2* knockout alters the rhythmic mRNA expression of cell cycle regulator genes in adult zebrafish fin tissues. qRT-PCR analysis of expression levels of some cell cycle CCGs **(A)** *cyclin A2,* **(B)** *cyclin B1,* and **(C)** *p21* in WT and *per2* KO fin tissue. Sets of 4 WT and *per2* KO fishes (each set containing two males and two females) were maintained under LD cycle (14 h light-10 h dark) conditions, a portion of caudal fin tissue was amputated and pooled for RNA extraction at 6-h intervals during a sampling window of 24 h. Mean mRNA relative expression (n = 2–3) ± SD is plotted on the y-axis; *zeitgeber* time (ZT) is plotted on the x-axis. *Zeitgeber* times are indicated for each sample. ZT0 corresponds to lights-on, ZT14 to lights-off. A change in rhythm was observed for *cyclin A2*, *cyclin B1*, and *p21*, as determined by a significant ANOVA Genotype × Time interaction effect for all genes ($p < 0.001$, see **Table 1**). Asterisks represent levels of significance in comparing the two genotypes at each time point individually, corrected by Sidak's method (***$p < 0.001$).

controls pointing to a disruption of the entire clock system by the *per2* mutation. Thus, using rhythmic locomotor activity as a clock output we have demonstrated that *per2* is involved in both the core clock mechanism and its entrainment by light.

Per2 Regulation of Clock Gene Expression

Period proteins together with the cryptochromes are classically regarded as negative elements in the transcription translation feedback loop mechanism at the core of the circadian clock (Partch et al., 2014). However, the lack of a major effect on cycling clock gene expression in *per2* KO larvae would tend to argue against such a global role for PER2 in zebrafish. We did observe significant tissue-specific differences in the dynamic expression pattern of core clock genes in our *per2* KO fish. For example, rhythmic expression of *clock1* mRNA was affected in the liver, heart, muscle and gut of the *per2* KO, but not in other tissues. PER2 shares amino acid sequence motifs with both coactivators and corepressors of hormone receptors. For example, the mouse PER2 protein is characterized by two LXXLL motifs in both of its predicted protein–protein interaction domains (Albrecht et al., 2007). This motif is present in different coactivators which interact with nuclear receptors such as the steroid hormone receptor coactivator-1 (SRC-1) (Oñate et al., 1995). Moreover, it has been demonstrated that the PER2 protein upregulates *bmal1b* gene expression by directly binding to the Rorα nuclear receptor in zebrafish (Wang et al., 2015). Interestingly, a ROR/REV-ERB response element (RORE) has also been identified in the zebrafish *clock1* promoter, an observation that would potentially account for the dysregulation of *clock1* gene expression in certain tissues of *per2* KO adults. Thus, light-induced *per2* expression might serve to adjust the phase and amplitude of rhythmic expression of the *clock* gene. An unresolved issue remains how the observed changes in the profile and timing of *clock1* and *cry1a* mRNA expression in certain tissues does not lead to corresponding alterations in the rhythmic expression of other core clock component genes, such as *per1b* as well as other CCGs. It is tempting to speculate that the effects of PER2 are manifest in a gene-specific fashion and may reflect the different constellations of clock-regulated enhancer elements present in the promoters of various CCGs and core clock genes.

Per2 Tissue-Specific Function

The contribution of *per2* to shaping the profile of tissue specific rhythmic core clock gene expression raises the question of the extent to which the *per2* gene may also play a role in regulating tissue-specific physiology. In order to address this question, we also analyzed CCG expression in the liver, heart and muscle of the *per2* KO line. In particular, we focused attention on the expression of genes that are involved in the regulation of molecular mechanisms which underlie important physiological processes ranging from metabolism, development and maintenance of homeostasis to basic cellular processes, including cell growth and division (proliferation), cell movement (migration), controlled cell death (apoptosis) and cell differentiation. In the *per2* KO heart we observed a significant impact on the circadian expression of the *timp3, mef2a, cox6a2,* and *smad3a* genes (Wang et al., 2005, 2007; Sloin et al., 2018). Our results therefore implicate *per2* in the circadian clock-mediated regulation of various cardiac functions. This is of potential medical importance because there is a well-documented time of day-dependent increase in the sensitivity to myocardial infarction (Peckova et al., 1998) and disruption of circadian rhythms is a major contributor to heart pathophysiology (Crnko et al., 2019).

We also investigated the involvement of the *per2* gene in the circadian clock regulation of liver-specific CCGs, such as *impdh2, cyp1a, ppargc1b,* and *hnf1a* as well as genes encoding rate-limiting enzymes involved in the biosynthetic pathways for non-essential amino acids, namely *got1*, *got2a*, *asns*, *glud1b, glu1a,* and *gpt2l.* The results reveal an impact of the *per2* mutation on the rhythmic expression of many of these key metabolic regulatory-specific genes. Interestingly, the *per2* gene has already been associated with the regulation of liver-specific metabolic pathways in

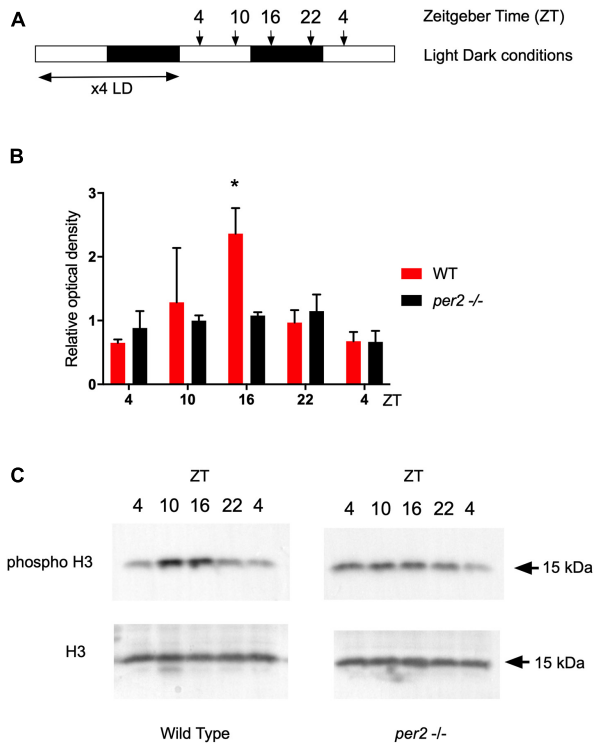

FIGURE 10 | Western blot analysis and quantification of the phospho-H3 protein in fins of the WT and *per2* KO zebrafish line. **(A)** Schematic representation of the experimental design. **(B)** Quantification of Western blot analysis of Phospho-Histone H3 (p-H3) ser10 expression level normalized to using Histone H3 (H3) as loading control. Relative optical density values for pH3-specific bands were calculated from measurements of ECL images and plotted on the *y*-axis. **(C)** Representative images of western blots obtained with pH3 and H3 specific antibodies used for the quantification in panel **(B)**. Asterisks represent levels of significance in comparing the two genotypes at each timepoint individually, corrected by Sidak's method (*$p < 0.05$).

mammals. In particular, REV-ERBα and PPARα interact with the PER2 protein in the liver to regulate the transcription of their target genes (Schmutz et al., 2010). Moreover, using *per2* KO mice, it has been shown that PER2 directly represses the nuclear receptor PPARγ, critical for adipogenesis, and hepatic insulin sensitivity (Grimaldi et al., 2010). Therefore, these previous findings together with our own CCG expression analysis support the notion that the *per2* gene plays an important role in liver physiology. We also reveal disruption of rhythmic expression of the CCGs *myf6* and *hsf2* in the *per2* KO skeletal muscle. Thus, PER2 may play an important role in the temporal coordination of the mechanisms which direct the repair of muscle damage generated during daytime-elevated locomotor activity.

Per2 Gene Function Influences Circadian Clock Regulation of the Cell Cycle

The involvement of *per2* gene function in the circadian regulation of the cell cycle has been widely demonstrated in mammals (Fu et al., 2002; Gu et al., 2012; Yang et al., 2012; Tan et al., 2015). Consistently, we observed a robust effect of the loss of *per2* gene function on the phase of rhythmic expression pattern of important cell cycle regulators, *p21, cyclin A2,* and *cyclin B1* in adult fin tissue. It is important to note that in the same tissue, rhythmic expression of clock genes is apparently normal indicating that the *per2*-regulated expression of clock-controlled cell cycle regulators in peripheral tissues may be regulated by a distinct mechanism from the transcriptional control circuits within the core circadian clock mechanism itself. Namely, the cell cycle control represents a specific, clock output function for *per2*. In the case of the *p21* gene in zebrafish, transcriptional regulation by the core clock mechanism via E-box enhancers has been shown to direct rhythmic expression (Laranjeiro et al., 2013). Furthermore, at a mechanistic level, it has already been demonstrated that the PER2 protein modulates p53 stability and transcriptional activity in normal human cells, thus affecting the gene expression of cell cycle regulators, including *p21,* in response to DNA damage in mammals (Gotoh et al., 2014). Therefore, the phase-setting effects on *p21* rhythmic expression may rely on the loss of protein-protein interaction between PER2 and p53 in the *per2* KO zebrafish line. Previously, it has been shown that M phase progression in zebrafish adult fin tissue, shows a light-entrained, circadian clock regulation (Idda et al., 2012). Our quantification of the levels of mitosis throughout the LD cycle, revealed a dampened M-phase rhythm in the *per2* KO fin tissue. The dysregulation of rhythmic M phase progression, together with the abnormal gene expression profile of *p21*, *cyclin A2,* and *cyclin B1*, indicates that *per2* may play a role in timing of the G1/S or G2/M cell cycle checkpoints. Given the impact of *per2* gene function on the regulation of the expression levels of these important cell cycle regulators, it could be anticipated that PER2 may play a key role during the early stages of zebrafish embryonic development. However, the normal early embryonic development observed in *per2* KO mutants would tend to argue against this. Instead, this observation would tend to support a hypothesis that the contribution of PER2 to cell cycle regulation is cell type-or developmental stage-specific.

In conclusion, our results suggest that the *per2* gene plays a crucial role in the circadian regulation of multiple tissue-specific cellular and physiological processes in zebrafish.

DATA AVAILABILITY STATEMENT

The raw data supporting the conclusions of this article will be made available by the authors, without undue reservation.

ETHICS STATEMENT

The animal study was reviewed and approved by the National Council for Animal Experimentation, Ministry of Health, Israel Local Government of Baden-Württemberg, Karlsruhe, Germany.

AUTHOR CONTRIBUTIONS

DV, NF, and YG designed the experiments. GR, ZB-ML, NG, and YW performed and interpreted the experiments. GR, ZB-ML,

DV, YW, YG, and NF prepared the manuscript. All authors contributed to the article and approved the submitted version.

FUNDING

This study was supported by the German-Israeli Foundation for Scientific Research and Development (GIF grant number I-1320-203.13/2015 to NF and YG) as well as the Helmholtz funding program, BIFTM (to NF, DV, and NG).

ACKNOWLEDGMENTS

We thank B. Rapp and O. Kassel for support and discussion.

SUPPLEMENTARY MATERIAL

The Supplementary Material for this article can be found online at: https://www.frontiersin.org/articles/10.3389/fnmol.2021.718387/full#supplementary-material

REFERENCES

Albrecht, U., Bordon, A., Schmutz, I., and Ripperger, J. (2007). The multiple facets of Per2. *Cold Spring Harb. Sym.* 72, 95–104. doi: 10.1101/sqb.2007.72.001

Albrecht, U., Sun, Z. S., Eichele, G., and Lee, C. C. (1997). A differential response of two putative mammalian circadian regulators, mper1 and mper2, to light. *Cell* 91, 1055–1064. doi: 10.1016/s0092-8674(00)80495-x

Amaral, I. P. G., and Johnston, I. A. (2012). Circadian expression of clock and putative clock-controlled genes in skeletal muscle of the zebrafish. *Am. J. Physiol. Regul. Integr. Comp. Physiol.* 302, R193–R206. doi: 10.1152/ajpregu.00367.2011

Bae, K., Jin, X., Maywood, E. S., Hastings, M. H., Reppert, S. M., and Weaver, D. R. (2001). Differential functions of mPer1, mPer2, and mPer3 in the SCN Circadian Clock. *Neuron* 30, 525–536. doi: 10.1016/s0896-6273(01)00302-6

Benjamini, Y., Fonio, E., Galili, T., Havkin, G. Z., and Golani, I. (2011). Quantifying the buildup in extent and complexity of free exploration in mice. *Proc. Natl. Acad. Sci.* 108, 15580–15587. doi: 10.1073/pnas.1014837108

Ben-Moshe, Z., Alon, S., Mracek, P., Faigenbloom, L., Tovin, A., Vatine, G. D., et al. (2014). The light-induced transcriptome of the zebrafish pineal gland reveals complex regulation of the circadian clockwork by light. *Nucleic Acids Res.* 42, 3750–3767. doi: 10.1093/nar/gkt1359

Cahill, G. M., Hurd, M. W., and Batchelor, M. M. (1998). Circadian rhythmicity in the locomotor activity of larval zebrafish. *Neuroreport* 9, 3445–3449. doi: 10.1097/00001756-199810260-00020

Carmona-Antoñanzas, G., Santi, M., Migaud, H., and Vera, L. M. (2017). Light- and clock-control of genes involved in detoxification. *Chronobiol. Int.* 34, 1–16. doi: 10.1080/07420528.2017.1336172

Chong, S. W., Korzh, V., and Jiang, Y. J. (2009). Myogenesis and molecules—insights from zebrafish Danio rerio. *J. Fish Biol.* 74, 1693–1755. doi: 10.1111/j.1095-8649.2009.02174.x

Courtois, G., Morgan, J., Campbell, L., Fourel, G., and Crabtree, G. (1987). Interaction of a liver-specific nuclear factor with the fibrinogen and alpha 1-antitrypsin promoters. *Science* 238, 688–692. doi: 10.1126/science.3499668

Crnko, S., Pré, B. C. D., Sluijter, J. P. G., and Laake, L. W. V. (2019). Circadian rhythms and the molecular clock in cardiovascular biology and disease. *Nat. Rev. Cardiol.* 16, 437–447. doi: 10.1038/s41569-019-0167-4

Durgan, D. J., and Young, M. E. (2010). The cardiomyocyte circadian clock. *Circ. Res.* 106, 647–658. doi: 10.1161/circresaha.109.209957

Finger, A.-M., Jäschke, S., del Olmo, M., Hurwitz, R., Granada, A. E., Herzel, H., et al. (2021). Intercellular coupling between peripheral circadian oscillators by TGF-β signaling. *Sci. Adv.* 7:eabg5174. doi: 10.1126/sciadv.abg5174

Foulkes, N. S. (2016). *Genetics, Genomics and Phenomics of Fish*. Amsterdam: Elsevier Inc.

Fu, L., Pelicano, H., Liu, J., Huang, P., and Lee, C. C. (2002). The circadian gene period2 Plays an important role in tumor suppression and DNA Damage Response In Vivo. *Cell* 111, 41–50. doi: 10.1016/s0092-8674(02)00961-3

Fukada, Y., and Okano, T. (2002). Circadian clock system in the pineal gland. *Mol. Neurobiol.* 25, 19–30. doi: 10.1385/mn:25:1:019

Gotoh, T., Vila-Caballer, M., Santos, C. S., Liu, J., Yang, J., and Finkielstein, C. V. (2014). The circadian factor Period 2 modulates p53 stability and transcriptional activity in unstressed cells. *Mol. Biol. Cell.* 25, 3081–3093. doi: 10.1091/mbc.e14-05-0993

Grimaldi, B., Bellet, M. M., Katada, S., Astarita, G., Hirayama, J., Amin, R. H., et al. (2010). PER2 controls lipid metabolism by direct regulation of PPARγ. *Cell. Metab.* 12, 509–520. doi: 10.1016/j.cmet.2010.10.005

Gu, X., Xing, L., Shi, G., Liu, Z., Wang, X., Qu, Z., et al. (2012). The circadian mutation PER2S662G is linked to cell cycle progression and tumorigenesis. *Cell. Death Differ.* 19, 397–405. doi: 10.1038/cdd.2011.103

Hinits, Y., Osborn, D. P. S., Carvajal, J. J., Rigby, P. W. J., and Hughes, S. M. (2007). Mrf4 (myf6) is dynamically expressed in differentiated zebrafish skeletal muscle. *Gene. Expr. Patterns* 7, 738–745. doi: 10.1016/j.modgep.2007.06.003

Idda, M. L., Kage, E., Lopez-Olmeda, J. F., Mracek, P., Foulkes, N. S., and Vallone, D. (2012). Circadian timing of injury-induced cell proliferation in Zebrafish. *PLoS One* 7:e34203. doi: 10.1371/journal.pone.0034203

Jammalamadaka, S. R., and SenGupta, A. (2001). *Topics in Circular Statistics*. Singapore: World Scientific Publishing Co Pte Ltd.

Krishnaiah, S. Y., Wu, G., Altman, B. J., Growe, J., Rhoades, S. D., Coldren, F., et al. (2017). Clock regulation of metabolites reveals coupling between transcription and metabolism. *Cell. Metab.* 25, 961–974. doi: 10.1016/j.cmet.2017.03.019

Laranjeiro, R., Laranjeiro, R., Tamai, T. K., Peyric, E., Peyric, E., Krusche, P., et al. (2013). Cyclin-dependent kinase inhibitor p20 controls circadian cell-cycle timing. *Proc. Natl. Acad. Sci. U.S.A.* 110, 6835–6840. doi: 10.1073/pnas.1217912110

Li, Y., Li, G., Wang, H., Du, J., and Yan, J. (2013). Analysis of a gene regulatory cascade mediating circadian rhythm in zebrafish. *Plos Comput .Biol.* 9:e1002940. doi: 10.1371/journal.pcbi.1002940

Lin, J., Tarr, P. T., Yang, R., Rhee, J., Puigserver, P., Newgard, C. B., et al. (2003). PGC-1β in the regulation of hepatic glucose and energy metabolism*. *J. Biol. Chem.* 278, 30843–30848. doi: 10.1074/jbc.m303643200

Martino, T., Arab, S., Straume, M., Belsham, D. D., Tata, N., Cai, F., et al. (2004). Day/night rhythms in gene expression of the normal murine heart. *J. Mol. Med.* 82, 256–264. doi: 10.1007/s00109-003-0520-1

McArdle, A., Broome, C. S., Kayani, A. C., Tully, M. D., Close, G. L., Vasilaki, A., et al. (2006). HSF expression in skeletal muscle during myogenesis: Implications for failed regeneration in old mice. *Exp. Gerontol.* 41, 497–500. doi: 10.1016/j.exger.2006.02.002

Menaker, M., Moreira, L. F., and Tosini, G. (1997). Evolution of circadian organization in vertebrates. *Braz. J. Med. Biol. Res.* 30, 305–313. doi: 10.1590/s0100-879x1997000300003

Mracek, P., Santoriello, C., Idda, M. L., Pagano, C., Ben-Moshe, Z., Gothilf, Y., et al. (2012). Regulation of per and cry genes reveals a central role for the D-Box enhancer in light-dependent gene expression. *PLoS One* 7:e51278. doi: 10.1371/journal.pone.0051278

Oñate, S. A., Tsai, S. Y., Tsai, M.-J., and O'Malley, B. W. (1995). Sequence and characterization of a coactivator for the steroid hormone receptor superfamily. *Science* 270, 1354–1357. doi: 10.1126/science.270.5240.1354

Partch, C. L., Green, C. B., and Takahashi, J. S. (2014). Molecular architecture of the mammalian circadian clock. *Trends Cell Biol.* 24, 90–99. doi: 10.1016/j.tcb.2013.07.002

Peckova, M., Fahrenbruch, C. E., Cobb, L. A., and Hallstrom, A. P. (1998). Circadian variations in the occurrence of cardiac arrests. *Circulation* 98, 31–39. doi: 10.1161/01.cir.98.1.31

Pittendrigh, C. S. (1993). Temporal organization: reflections of a Darwinian clock-watcher. *Annu. Rev. Physiol.* 55, 16–54. doi: 10.1146/annurev.ph.55.030193.000313

Sassone-Corsi, P., Foulkes, N. S., and Whitmore, D. (2000). Light acts directly on organs and cells in culture to set the vertebrate circadian clock. *Nature* 404, 87–91. doi: 10.1038/35003589

Sato, F., Sato, H., Jin, D., Bhawal, U. K., Wu, Y., Noshiro, M., et al. (2012). Smad3 and Snail show circadian expression in human gingival fibroblasts, human mesenchymal stem cell, and in mouse liver. *Biochem. Bioph. Res. Co.* 419, 441–446. doi: 10.1016/j.bbrc.2012.02.076

Savvidis, C., and Koutsilieris, M. (2012). Circadian rhythm disruption in cancer biology. *Mol. Med.* 18, 1249–1260. doi: 10.2119/molmed.2012.00077

Schibler, U., Gotic, I., Saini, C., Gos, P., Curie, T., Emmenegger, Y., et al. (2015). Clock-Talk: Interactions between central and peripheral circadian oscillators in mammals. *Cold Spring Harb. Symp. Quant. Biol.* 80, 223–232. doi: 10.1101/sqb.2015.80.027490

Schibler, U., and Sassone-Corsi, P. (2002). A web of circadian pacemakers. *Cell* 111, 919–922. doi: 10.1016/s0092-8674(02)01225-4

Schmutz, I., Ripperger, J. A., Baeriswyl-Aebischer, S., and Albrecht, U. (2010). The mammalian clock component PERIOD2 coordinates circadian output by interaction with nuclear receptors. *Gene Dev.* 24, 345–357. doi: 10.1101/gad.564110

Sloin, H. E., Ruggiero, G., Rubinstein, A., Storz, S. S., Foulkes, N. S., and Gothilf, Y. (2018). Interactions between the circadian clock and TGF-β signaling pathway in zebrafish. *PloS One* 13:e0199777. doi: 10.1371/journal.pone.0199777

Tamai, T. K., Young, L. C., and Whitmore, D. (2007). Light signaling to the zebrafish circadian clock by Cryptochrome 1a. *Proc. Natl. Acad. Sci.* 104, 14712–14717. doi: 10.1073/pnas.0704588104

Tan, X.-M., Ye, H., Yang, K., Chen, D., Wang, Q.-Q., Tang, H., et al. (2015). Circadian variations of clock gene Per2 and cell cycle genes in different stages of carcinogenesis in golden hamster buccal mucosa. *Sci. Rep. UK* 5:9997. doi: 10.1038/srep09997

Toh, K. L., Jones, C. R., He, Y., Eide, E. J., Hinz, W. A., Virshup, D. M., et al. (2001). An hPer2 phosphorylation site mutation in familial advanced sleep phase syndrome. *Science* 291, 1040–1043. doi: 10.1126/science.1057499

Turek, F. W., Joshu, C., Kohsaka, A., Lin, E., Ivanova, G., McDearmon, E., et al. (2005). Obesity and metabolic syndrome in circadian clock mutant mice. *Science* 308, 1043–1045. doi: 10.1126/science.1108750

Vatine, G., Vallone, D., Appelbaum, L., Mracek, P., Ben-Moshe, Z., Lahiri, K., et al. (2009). Light directs zebrafish period2 expression via Conserved D and E Boxes. *PLoS Biol.* 7:e1000223. doi: 10.1371/journal.pbio.1000223

Wang, M., Zhong, Z., Zhong, Y., Zhang, W., and Wang, H. (2015). The zebrafish period2 protein positively regulates the circadian clock through mediation of retinoic acid receptor (RAR)-related orphan receptor α (Rorα). *J. Biol. Chem.* 290, 4367–4382. doi: 10.1074/jbc.m114.605022

Wang, Y., Li, C., Lee, G., Tsay, H., Tsai, H., and Chen, Y. (2008). Inactivation of zebrafish mrf4 leads to myofibril misalignment and motor axon growth disorganization. *Dev. Dynam.* 237, 1043–1050. doi: 10.1002/dvdy.21478

Wang, Y.-X., Qian, L.-X., Liu, D., Yao, L.-L., Jiang, Q., Yu, Z., et al. (2007). Bone morphogenetic protein-2 acts upstream of myocyte-specific enhancer factor 2a to control embryonic cardiac contractility. *Cardiovasc. Res.* 74, 290–303. doi: 10.1016/j.cardiores.2007.02.007

Wang, Y.-X., Qian, L.-X., Yu, Z., Jiang, Q., Dong, Y.-X., Liu, X.-F., et al. (2005). Requirements of myocyte-specific enhancer factor 2A in zebrafish cardiac contractility. *FEBS Lett.* 579, 4843–4850. doi: 10.1016/j.febslet.2005.07.068

Whitmore, D., Foulkes, N. S., Strähle, U., and Sassone-Corsi, P. (1998). Zebrafish Clock rhythmic expression reveals independent peripheral circadian oscillators. *Nat. Neurosci.* 1, 701–707. doi: 10.1038/3703

Yang, X., He, X., Yang, Z., and Jabbari, E. (2012). Mammalian PER2 regulates AKT activation and DNA damage response. *Biochem. Cell. Biol.* 90, 675–682. doi: 10.1139/o2012-025

Ziv, L., and Gothilf, Y. (2006). Circadian time-keeping during early stages of development. *Proc. Natl. Acad. Sci. U.S.A.* 103, 4146–4151. doi: 10.1073/pnas.0600571103

Conflict of Interest: The authors declare that the research was conducted in the absence of any commercial or financial relationships that could be construed as a potential conflict of interest.

Publisher's Note: All claims expressed in this article are solely those of the authors and do not necessarily represent those of their affiliated organizations, or those of the publisher, the editors and the reviewers. Any product that may be evaluated in this article, or claim that may be made by its manufacturer, is not guaranteed or endorsed by the publisher.

Advantages of publishing in Frontiers

OPEN ACCESS
Articles are free to read for greatest visibility and readership

FAST PUBLICATION
Around 90 days from submission to decision

HIGH QUALITY PEER-REVIEW
Rigorous, collaborative, and constructive peer-review

TRANSPARENT PEER-REVIEW
Editors and reviewers acknowledged by name on published articles

Frontiers
Avenue du Tribunal-Fédéral 34
1005 Lausanne | Switzerland

Visit us: www.frontiersin.org
Contact us: frontiersin.org/about/contact

REPRODUCIBILITY OF RESEARCH
Support open data and methods to enhance research reproducibility

DIGITAL PUBLISHING
Articles designed for optimal readership across devices

FOLLOW US
@frontiersin

IMPACT METRICS
Advanced article metrics track visibility across digital media

EXTENSIVE PROMOTION
Marketing and promotion of impactful research

LOOP RESEARCH NETWORK
Our network increases your article's readership